



HAL
open science

Design methodology for sustainable IoT systems

Ernesto Quisbert-Trujillo

► **To cite this version:**

Ernesto Quisbert-Trujillo. Design methodology for sustainable IoT systems. Micro and nanotechnologies/Microelectronics. Université Grenoble Alpes [2020-..], 2022. English. NNT : 2022GRALT068 . tel-03923927

HAL Id: tel-03923927

<https://theses.hal.science/tel-03923927>

Submitted on 5 Jan 2023

HAL is a multi-disciplinary open access archive for the deposit and dissemination of scientific research documents, whether they are published or not. The documents may come from teaching and research institutions in France or abroad, or from public or private research centers.

L'archive ouverte pluridisciplinaire **HAL**, est destinée au dépôt et à la diffusion de documents scientifiques de niveau recherche, publiés ou non, émanant des établissements d'enseignement et de recherche français ou étrangers, des laboratoires publics ou privés.

THÈSE

Pour obtenir le grade de

DOCTEUR DE L'UNIVERSITÉ GRENOBLE ALPES

École doctorale : EEATS - Electronique, Electrotechnique, Automatique, Traitement du Signal (EEATS)

Spécialité : Nano électronique et Nano technologies

Unité de recherche : CEA/LETI

Méthodologie de conception pour les systèmes IoT durables

Design methodology for sustainable IoT systems

Présentée par :

Ernesto QUISBERT-TRUJILLO

Direction de thèse :

Thomas ERNST

CEA LETI, CEA

Directeur de thèse

Karine SAMUEL

PROFESSEURE DES UNIVERSITES, Université Grenoble Alpes

Co-directrice de thèse

Elise MONNIER

CEA Grenoble

Co-encadrant de thèse

Rapporteurs :

Nicolas PERRY

PROFESSEUR, ENSAM CER BORDEAUX-TALENCE

Jean-Pierre RASKIN

PROFESSEUR, Université Catholique de Louvain

Thèse soutenue publiquement le **26 septembre 2022**, devant le jury composé de :

Nicolas PERRY

PROFESSEUR, ENSAM CER BORDEAUX-TALENCE

Rapporteur

Ian O'CONNOR

PROFESSEUR DES UNIVERSITES, Ecole Centrale de Lyon

Examinateur

Blandine AGERON

PROFESSEUR DES UNIVERSITES, UNIVERSITE GRENOBLE ALPES

Présidente

Jean-Pierre RASKIN

PROFESSEUR, Université Catholique de Louvain

Rapporteur

Invités :

Elise Monnier

INGENIEUR HDR, CEA - Liten

Thomas Ernst

DOCTEUR EN SCIENCES, CEA - Leti



To my family

Acknowledgements

First of all, I would like to acknowledge the support of the French National Research Agency and particularly, the program "Investissements d'avenir" (ANR-15-IDEX-02).

To the entire family of the "NEED for IoT" project, I simply express my total gratitude.

I would also like to thank all the staff of the System Division (DSYS) of CEA-Leti, especially Maxime Gallardo, whose ecological awareness and scientific rigor never ceases to amaze me. Also, I am very grateful to Thomas Ernst, Karine Evrard Samuel, Elise Monnier and Emmanuelle Cor. Without them, this work would not have been possible.

I am also very indebted to the whole family of the *Centre d'Etudes et de Recherches Appliquées à la Gestion* (CERAG), and to Youla Morfouli and Blandine Ageron; their critical regarding and sharp judgments were very helpful.

Content

Acknowledgements.....	3
List of figures.....	7
List of tables	14
Glossary.....	16
Abbreviations	16
Metals and chemical substances	18
Institutions.....	18
Résumé	20
Abstract.....	25
Introduction	27
Chapter 1. Fundamentals of Internet of Things, potential impacts and trends	29
Overview	29
1. Definitions and concepts.....	29
1.1. IoT Systems, sensor systems and other systems.....	29
1.2. Fundamentals on computer networking in the context of IoT systems.....	33
2. Potential impacts of IoT systems	34
2.1. Resources depletion	34
2.2. Embodied emissions and energy of IoT systems.....	34
2.3. Energy consumption of IoT systems	34
3. Promising yet segregated or discrepant initiatives	36
3.1. Green-IoT	36
3.1.1. What is wrong with Green-IoT and other use-oriented approaches?.....	36
3.2. Self-powered IoT devices and intermittent computing.....	37
3.2.1. What is wrong with self-powered systems and intermittent computing?	38
3.3. Less-material-oriented solutions and potential drawbacks	39
3.4. End-of-Life Oriented solutions and potential drawbacks	40
4. Research questions	41
Chapter 2. Fundamentals of Data-driven design for sustainable IoT systems	42
Overview	42
1. Data operational stages and relevant aspects regarding sensor system design	42
1.1. Data acquisition	42
1.2. Data processing.....	43
1.3. Data storage.....	44
1.4. Data transmission.....	45
2. Functional analysis and right-provisioning design.....	45
2.1. Functions and capacities of electronic components.....	46
3. Dataflow issues in IoT Systems and common solutions	49
4. Dataflow design and information science theory for IoT systems.....	50
5. Data- and Information-driven design	52
5.1. Relevance of data- and information-driven design for technical design.....	52
5.2. Relevance of data- and information-driven design for sustainable design.....	54
5.3. Relevance of data- and information-driven design for context sensing.....	55
6. Conclusions	56
Chapter 3. State-of-Art of environmental studies and eco-design methods for IoT systems	57
Overview	57
1. Life Cycle Assessment and environmental studies of IoT systems	57

1.1.	Fundamentals of Life Cycle Assessment.....	57
1.2.	LCA studies of IoT systems	60
1.3.	Summary of key aspects and shortcomings of LCA studies of IoT systems	77
2.	New Product Development process, Eco-design and eco-design tools for IoT systems	78
2.1.	Fundamentals of eco-design and New Product Development Process	78
2.2.	Instruments for the design and eco design of IoT systems	80
2.3.	Summary of design and eco-design instruments for IoT systems.....	93
Chapter 4:	Proposition of the methodology.....	94
Overview		94
1.	Qualitative research	94
2.	Building a design methodology for sustainable IoT systems	98
2.1.	Physical features	99
2.2.	Circularity features.....	102
2.3.	Technical features	109
2.4.	Data flow	111
3.	Proposed methodology for sustainable IoT systems	113
3.1.	Framework for eco design.....	113
3.2.	Framework for impact estimation	114
4.	Proposed Implementations of the frameworks	115
4.1.	LCA Implementation for the framework for eco design.....	115
4.2.	Cross-typed lifecycle modeling implementation for the framework for impact estimation	118
5.	Positioning of the methodology	119
Chapter 5:	Case studies.....	123
Overview		123
1.	Case study “Smart metering”.....	123
1.1.	Some basic principles on local/remote transmissions and environmental implications	125
1.2.	Implementation of the framework for impact estimation: Theoretical impact estimation of the use phase of the case study “Smart metering”	131
1.3.	Implementation of the framework for impact estimation: environmental assessment of the use-phase of the case study “Smart metering” from empirical tracking of data flow	137
1.4.	Recommendations for the case study “Smart metering”	142
2.	Case study “Smart monitoring”	146
2.1.	Implementation of the framework for eco design.....	146
3.	Guidelines.....	179
Conclusion		182
Overview		182
1.	Findings	182
2.	Limits	183
3.	Further research	184
4.	Final words	185
Annexes		186
1.	GNU-radio companion implementation for the Lora sniffer A	186
2.	Data traffic in the local equipment of the case study “Smart metering”	187
3.	Data traffic between the local and mutualized infrastructure of the case study “Smart metering”	188
4.	Bill of Materials of the EH sensor system in its memory-based version (referential design)	190
5.	Bill of Materials of the EH sensor system in its BLE-based version.....	191
6.	Variations of the PCB area according to the design sets of the memory-based version	192

7.	Material content shares of the studied voltage comparators	193
8.	Material content shares of the studied microcontrollers	194
9.	Material content shares of the studied NFC-EEPROM memories	196
10.	Material content shares of the unique type of Voltage Detector	198
11.	Material content shares of the SoC component of the BLE module	199
12.	Recycled material content from waste flows of design set 8	200
13.	Recycled material content from waste flows of design set 20	206
14.	Materials, components and other aspects excluded from the LCA implementation (case study “Smart monitoring”).....	212
15.	Summary of LCA studies of sensors, sensor systems, partial IoT systems and full IoT systems	213
16.	Design methodology and questionnaires used in the qualitative research.....	216
	References	223

List of figures

Figure 1.1. The basic architecture of an IoT system	19
Figure 1.2. A typical sensor system architecture	31
Figure 1.3. Basic model of the network architecture of IoT systems	32
Figure 1.4. The referential OSI model	33
Figure 1.5a. Primary energy demand of 45 nm flash memories	34
Figure 1.5b Primary energy footprint of IoT-specialized electronic components	34
Figure 1.6a. Estimated electricity needs of data centers in the context of Industrial IoT	35
Figure 1.6b. Estimated electricity needs of data centers considering the Industrial IoT and the end of the Moore's law	35
Figure 1.7a. The "Think before Talk" approach for green-IoT	36
Figure 1.7b. The "Race to Sleep" approach for green-IoT	36
Figure 1.7c. The "Sleep as possible" approach for green-IoT	36
Figure 1.8. Basic architecture of and Energy Harvesting (EH) System	37
Figure 1.9a. The basic mechanism of intermittent computing	37
Figure 1.9b. An intermittent design for an EH system	37
Figure 1.10. Intermittent operating schema of Hibernus++	39
Figure 1.11a. High integration level of a sensor system. Version open-source (V0), optimized (V1) and full-integrated (V2)	39
Figure 1.11b. GWP per footprint (Kg/cm ²) comparison of V0, V1 and V2	39
Figure 1.12. Technological capitalization of the stablished form factors in DRAM memories	40
Figure 1.13a. Relative impacts per life cycle phase of a modular smartphone (Fairphone 3)	40
Figure 1.13b. Relative impacts of modularity	40
Figure 1.13c. GWP impact per year use of modular smartphones	40
Figure 1.14. Net losses of metals per period of use of repaired smartphones VS new smartphones	41
Figure 2.1. Main data operation stages of a sensor system	42
Figure 2.2a. ADC conversion of a 10V wave with a 3 bits resolution	42
Figure 2.2b. A sampling rate of 1 Hz	42
Figure 2.3. Hardware resources of modern MCUs for sensor systems	43
Figure 2.4a. A photograph of a SoC die after processing of the third level of metal	44
Figure 2.4b. SiP for Apple Watch series 4	44
Figure 2.5a. Write endurance VS write time for different types of memories	44
Figure 2.5b. Specifications of a FeRAM-memory-based MCU oriented to EH systems	44
Figure 2.6. Power Consumption VS Distance range for different wireless technology used in IoT systems	45
Figure 2.7. The basic elements of an octopus diagram	46
Figure 2.8. The provisioning slack of right-provisioning design	46
Figure 2.9. A hypothetical right-provisioned IoT device for video monitoring	46
Figure 2.10a. Data rate generation of different sensor applications and suitable communication technology	47
Figure 2.10b. Required MCU specifications to fully process sensors data	47
Figure 2.10c. Required MCU specifications to encrypt and transmit data	48
Figure 2.11a. Execution time comparison of four IoT microprocessor configurations	48
Figure 2.11b. Energy consumption comparison of four IoT microprocessor configurations	49

Figure 2.11c. Performance comparison of four IoT microprocessor configurations	49
Figure 2.11d. Efficiency comparison of four IoT microprocessor configurations	49
Figure 2.12a. An instance of data aggregation: temporal correlation.....	50
Figure 2.12b. An instance of data aggregation: Spatial correlation	50
Figure 2.13a. Relative impacts of an IoT system (in four design versions).....	50
Figure 2.13b. The deployment of the IoT system (baseline).....	50
Figure 2.14a. Eco-design method for optimization of ICT services.....	51
Figure 2.14b. Rationale of Information Science canon.	51
Figure 2.15a. A float-switch-based IoT system oriented to measure the liquid level of a recipient	52
Figure 2.15b. An ultrasonic-based IoT system oriented to measure the liquid level of a recipient	52
Figure 2.16. A Sport-service-oriented IoT system for smart training.....	53
Figure 2.17a. A solar-, battery-based IoT system for urban garbage collection.....	54
Figure 2.17b. Impact comparison of a daily transmission versus an hourly transmission design	54
Figure 2.18a. A typical EH system.....	55
Figure 2.18b. An alternative EH system using context sensing	55
Figure 2.18c. Walking and running activities detected by an EH system using context sensing	55
Figure 2.19a. An accelerometer-base sensor system.....	55
Figure 2.19b. An EH sensor system based on context-sensing.....	55
Figure 2.20a. Accuracy of a EH system using context sensing (CEE estimation during walking).....	55
Figure 2.20b. Accuracy of a EH system using context sensing (CEE estimation during running).....	55
Figure 3.1. Fundamental steps for conducting a LCA study.....	57
Figure 3.2. An example of a product system framed in its system boundary.....	58
Figure 3.3. A full IoT system for glass waste-collection.....	60
Figure 3.4. Environmental impact of the IoT system with a daily and hourly frequency transmission rate.....	61
Figure 3.5. Effects of mutualizing local and Telecom infrastructure along 24 similar services.....	61
Figure 3.6. A basic schematic of a textile-based IoT system.....	62
Figure 3.7a. Baseline Ecocost impact results of a textile-based IoT system (Scenario A and B).....	62
Figure 3.7b. Power dissipation decrease from reducing the reference flow of a textile-based IoT system.....	62
Figure 3.8. Environmental impact of a WSN oriented to optimizing the urban garbage collection of a city.....	63
Figure 3.9. Energy consumption share of communication tasks of sensors systems and repeaters.....	63
Figure 3.10. Impact comparison (baseline design), alternative 1 and alternative 2.....	63
Figure 3.11. Environmental impact of a glass collection IoT system.....	65
Figure 3.12. Impact comparison of the current state and IoT-based systems for truck tires monitoring.....	66
Figure 3.13. Difference in impact between IoT scenario and current state by impact categories.....	67
Figure 3.14a. Service latency VS number of terminal nodes simulation results of an IoT system	68
Figure 3.14b. Estimations of the overall power consumption VS number of terminal nodes.....	68
Figure 3.14c. Estimated emissions from non-renewable energy sources used to power fog and cloud computing.....	68
Figure 3.14d. Estimated emissions from renewable energy sources used to power fog and cloud computing.....	68
Figure 3.15a. Impact comparison of a WSN-based system and a regular system for municipal garbage collection	69
Figure 3.15b. RMD Impact estimation of the life cycle of a WSN-based system for municipal garbage collection.....	69
Figure 3.16. RMD and GW impact contribution of sensors systems, repeaters and gateway.....	70

Figure 3.17a. The product system boundary of an energy monitor version	70
Figure 3.17b. The product system boundary of a multifunctional HEMS	70
Figure 3.17c. The product system boundary of a Zigbee-based energy management system	70
Figure 3.18a. Endpoint Carbon footprint impact of a Philips HUE occupancy sensor	72
Figure 3.18b. Endpoint Carbon footprint impact of a Google Home mini home connected assistant	72
Figure 3.18c. Endpoint Carbon footprint impact of a DJI MAVIC mini light weight drone	72
Figure 3.18d. Endpoint Carbon footprint impact of a smart watch from Apple and Garmin	72
Figure 3.19. Basic schematic of the electronic design of a ACL and SDT sensor systems	72
Figure 3.20. Basic schematics of the ECD and PS components	72
Figure 3.21. Impact results of an ACL sensor system	73
Figure 3.22. Impact results of a SDT sensor system	73
Figure 3.23. Impact comparison of the default design of a ACL sensor system and its redesign	74
Figure 3.24a. A sensor system for prognostic health monitoring of structures	74
Figure 3.24b. GWP impact of the production of a sensor system for prognostic health monitoring of structures	74
Figure 3.25. Essential components of the “Vibe-ing” system for providing vibration health therapy	75
Figure 3.26a. Ecocost impact of the life cycle phases of the “vibe-ing” system	75
Figure 3.26b. Ecocost impact details of the production phase of the “vibe-ing” system	75
Figure 3.26c. Ecocost impact details of the electronic components of the “vibe-ing” system	75
Figure 3.26d. Ecocost impact details of the materials in the Elektrisola textile wire	75
Figure 3.27a. Basic schematic of the paper-based electrochemical sensor oriented to detect bacteria in water	76
Figure 3.27b. Cross-sectional view of the paper-based electrochemical sensor	76
Figure 3.28. Embodied energy and carbon footprint of the materials and manufacturing processes	77
Figure 3.29. Generic environmental aspects taken into account in a typical product development process	79
Figure 3.30. Technical overview of IoT systems according to the ITU standard Y.2060	80
Figure 3.31. IoT reference model according to the ITU standard Y.2060	80
Figure 3.32. An adapted version of the FG M2M ITU deliverable oriented to the M2M support layer	81
Figure 3.33. An adaptation of the classical architecture for IoT systems	84
Figure 3.34. Layered-diagram for the embed software system development	85
Figure 3.35. Methodology based on the analysis of an object, functionalities and added value	85
Figure 3.36. Representation of a dynamic WSN system	86
Figure 3.37. Impact estimation methodology for WSN systems	87
Figure 3.38. Methodology for the optimization of services through WSNs	88
Figure 3.39. Adapted version of the rationale information science framework	89
Figure 3.40. Hierarchical IoT systems framework	89
Figure 3.41a. Simulated WSN topology for numerical experiments (low network density)	90
Figure 3.41b. Number of repeaters required for different network densities	90
Figure 3.42. Network lifetime comparison for the hierarchical topology and the hybrid topology	90
Figure 3.43. Representation of an IoT device in terms of its functional blocks and linked HSLs	90
Figure 3.44a. An example of a hardware impact profile for a complex IoT device type	91
Figure 3.44b. Impact obtained by considering hardware impact profiles	91
Figure 3.45. Simple description of a mechatronic device and its ecological impact	92

Figure 4.1. A representation of the current design workflow of IoT systems	97
Figure 4.2. Placing potential eco-design steps into the current design workflow of IoT systems	98
Figure 4.3. Use of the Bill of Attributes (BoA) and the Bill of Materials (BoM) for impact estimation	99
Figure 4.4. GWP100 impact contribution of the manufacturing phase of a smartphone	100
Figure 4.5a. Regression model for the environmental impact of gold-wired BGA components	101
Figure 4.5b. Regression model for the environmental impact of copper-wired BGA components	101
Figure 4.6a. Embodied energy demand of 45nm flash memories with different packaging technologies	101
Figure 4.6b. Embodied energy demand of 57nm DRAM memories with different packaging technologies	101
Figure 4.7. Embodied energy of 130 nm microprocessors	101
Figure 4.8a. A basic PCB layout design guidelines for Area Array Package components	102
Figure 4.8b. An Area Array Package component (WLCSP).....	102
Figure 4.9. Relationship between dilution of metals in ore and 2004 price ranges for refined metals	103
Figure 4.10a. Adapted Sherwood Plot for metals dilution in waste automobiles	104
Figure 4.10b. Adapted Sherwood Plot for metals dilution in disassembled automobile parts	104
Figure 4.11. Adapted Sherwood Plot for metals dilution in WPCBs	104
Figure 4.12. Metal net loss relative to BAU content of a new smartphone VS a repaired smartphone	105
Figure 4.13. Indium and Yttrium metal flows relative to new Smartphone content (BAU)	105
Figure 4.14a. A typical thermal reflow profile schema for assembly or disassembly components	106
Figure 4.14b. Different reflow profiles applied in disassembly experiments	106
Figure 4.14c. Bridging defects in solder balls in two of six BGA memories	106
Figure 4.15a. Excessive warpage resulting in shorted solder balls (bridging).....	106
Figure 4.15b. Experimental warpage obtained for a PBGA 35 x 35 mm2 component	106
Figure 4.16a. Mean effect plots of specific features (on the maximal warpage of PBGA components	107
Figure 4.16b. p values from an ANOVA test applied to the maximal warpage (FEA simulations).....	107
Figure 4.17. Intact and deformed solder balls whose IC package suffered a critical warpage	107
Figure 4.18. Critical warpages of different BGA components.....	108
Figure 4.19a. Disbonding types of a gull-wing-typed IC component and a BGA component.....	108
Figure 4.19b. Counts of different disbonding types in disassembly experiments.....	108
Figure 4.20a. Optimal preheat temperature to achieve high disassembling rates in WPCBs	109
Figure 4.20b. Maximal temperature to achieve high disassembling rates in WPCBs	109
Figure 4.20c. Optimal incubation time to achieve high disassembling rates in WPCBs	109
Figure 4.21a. Base failure rate of tantalum capacitors in function of temperature	110
Figure 4.21b. Safe writing cycling operating conditions of an EEPROM memory	110
Figure 4.22a. Main program execution of Hibernus++	110
Figure 4.22b. Technical features of NVM memories including writing endurances	110
Figure 4.23a. Lifetime estimations of an IoT device transmitting different data sizes every 100 seconds	112
Figure 4.23b. Lifetime estimations of an IoT device transmitting different data sizes every 1 second	112
Figure 4.24. Influence of data size on the lifetime of devices using modern wireless technology	112
Figure 4.25. The proposed approach for impact estimation and eco-design of IoT systems	113
Figure 4.26. Proposed framework for eco design	114
Figure 4.27. Proposed framework for impact estimation	115

Figure 4.28. Suggested LCA Implementation for the framework for eco design	115
Figure 4.29. Detailed process modeling of the manufacturing life cycle phase of an IoT device.....	116
Figure 4.30. Suggested E-o-L implementation for the framework for eco design.....	117
Figure 4.31. Shredding and electrostatic / magnetic separation processes applied to WEEE.....	118
Figure 4.32. Suggested cross-typed life cycle modeling implementation for the framework for impact estimation.....	118
Figure 4.33. Positioning of the proposed methodology (with respect to its integration in the NPD process).....	120
Figure 4.34. Positioning of the proposed methodology (with respect to its eco-design intention).....	121
Figure 5.1a. The electronic card of the pulse emitter of the case study “Smart metering”.....	123
Figure 5.1b. The possible induction generator used in the case study “Smart metering”.....	123
Figure 5.2a. The resin-flooded sensor system of the case study “Smart metering”.....	124
Figure 5.2b. Electronic card of the sensor system of the case study “Smart metering”.....	124
Figure 5.3a. Top-side of the electronic card of the gateway of the case study “Smart metering”.....	124
Figure 5.3b. Bottom-side of the electronic card of the gateway of the case study “Smart metering”.....	124
Figure 5.4. A basic deployment of the full IoT system of the case study “Smart metering”.....	125
Figure 5.5a. Illustration of a frequency band splitted into multiple channels	125
Figure 5.5b. A bandwidth defined around a frequency channel.....	126
Figure 5.6. Theoretical example of a binary data sequence transmitted by LoRa.....	126
Figure 5.7. Relative time at which a symbol is transmitted at different Spreading Factors in a defined bandwidth.....	126
Figure 5.8. Bitrate VS Energy consumption/ Time on air relation in LoRa-Based communications.....	127
Figure 5.9. Headers and footers added to a frame payload in a LoRa protocol stack.....	128
Figure 5.10. TCP/IP model contrasted to the OSI referential model.....	129
Figure 5.11a. TCP header format.....	129
Figure 5.11b. IP Header format	129
Figure 5.11c. 802.11 header format.....	129
Figure 5.12. The three basic steps of a TCP three-way handshake mechanism.....	130
Figure 5.13. The three basic steps of a TCP teardown mechanism.....	130
Figure 5.14. Cross-typed lifecycle modeling for the case study “Smart metering”.....	132
Figure 5.15. Packet exchange between the local and mutualized infrastructure.....	133
Figure 5.16. Assumed schema for the sleep and transmission states of the flowmeter.....	136
Figure 5.17. GW impact of the case study “Smart metering” (worst, regular and best scenarios).....	137
Figure 5.18. Experimental network deployment of the IoT system of the case study “Smart metering”.....	138
Figure 5.19a. The Sniffer used for the LoRa traffic of the case study “Smart metering”.....	138
Figure 5.19b. An example of a LoRa transmission captured by the sniffer.....	138
Figure 5.20. LoRa traffic between the flow meter and the gateway.....	139
Figure 5.21. Data traffic between the gateway and the cloud server.....	140
Figure 5.22. Local and internet traffic of the IoT system of the case study “Smart metering”.....	141
Figure 5.23a. GW impacts of the case study “Smart metering” (empirical estimation).....	142
Figure 5.23b. Internet traffic for sending counts.....	142
Figure 5.23c. Internet traffic for consulting water consumption.....	142
Figure 5.24a. The coverage area of a gateway covering perfectly an area of 1 km ²	144
Figure 5.24b. Maximal area covered by one gateway according to the manufacturer.....	144

Figure 5.24c. Coverage shortcomings of one gateway in an area of 1.6 x 1.6 km or 2,56 km ²	144
Figure 5.24d. Network deployment for assuring full connectivity of an area of 2,56 km ²	144
Figure 5.25. Modern piezoelectric buzzer	147
Figure 5.26a. A cylinder made by a piezoelectric ceramic material embedded into an object	147
Figure 5.26b. Piezoelectric effect	147
Figure 5.27. Simplified representation of intermittent functioning (case study “smart monitoring”)	148
Figure 5.28. Example of an interpreted high- and a low-intensity use of an object	148
Figure 5.29. The essential raw data, information, and knowledge of the case study “Smart monitoring”	149
Figure 5.30. Illustration of the essential raw data of the case study “Smart monitoring”	149
Figure 5.31. First alternative of data manipulation and information design	149
Figure 5.32. Second alternative of data manipulation and information design	150
Figure 5.33. Basic electronic design of the NFC-memory-based version of the EH sensor system	151
Figure 5.34. Basic electronic design of the BLE-based version of the EH sensor system	153
Figure 5.35. Standard IPC-7351B applied to the land pattern of three SMD electronic components	154
Figure 5.36. Relative AD impacts of all design sets for the NFC-memory-based version	155
Figure 5.37a. Detailed AD impact contributors of the worst design alternative (Set 12)	156
Figure 5.37b. Detailed AD impact contributors of the best design alternative (Set 20)	156
Figure 5.38a. Absolute AD impact of the worst design alternative (set 12)	157
Figure 5.38b. Absolute AD impact of the best design alternative (set 20)	157
Figure 5.39a. Relative AD impacts of design set 1 and 18	159
Figure 5.39b. Absolute impacts of the electronic design of set 1	159
Figure 5.39c. Absolute impacts of the electronic design of set 18	159
Figure 5.40a. AD impact distributions of set 1 (default uncertainty)	160
Figure 5.40b. AD impact distributions of set 18 (default uncertainty)	160
Figure 5.41. Overlapped distributions of AD impacts of set 1 and set 18	160
Figure 5.42. AD impact distribution of design of set 18 outperforming that one of set 1 (gold content variation)	161
Figure 5.43. AD impact distribution of design of set 18 outperforming that one of set 1 (several variations)	161
Figure 5.44. Relative GW impact of all design sets for the NFC-memory-based version	163
Figure 5.45a. Detailed GW impact contributors of the worst design alternative (Set 6)	163
Figure 5.45b. Detailed GW impact contributors of the best design alternative (Set 14)	163
Figure 5.46a. Absolute GW impact of the worst alternative (set 6)	164
Figure 5.46b. Absolute GW impact of the best alternative (set 14)	164
Figure 5.47a. Relative GW impacts of set 12 and Set 20	165
Figure 5.47b. Absolute GW impact of set 12	165
Figure 5.47c. Absolute GW impact of set 20	165
Figure 5.48a. GW impact distribution of the design of set 12, with a sample of potential TFBGA-typed microcontrollers with different variations in the material content shares of their subparts, getting worse to the point of being an inconvenient design compared with the design of set 20	166
Figure 5.48b. GW impact distribution of the design of set 20, with a sample of potential WLCSP36-typed microcontrollers with different variations in their internal die area ratios, outperforming that one of set 12	166
Figure 5.49. AD and GW relative impacts of the respective worst and best design sets, contrasted with the AD and GW relative impacts of the referential design set of the NFC-memory-based version	167
Figure 5.50a. Cross section view showing the basic subparts of a BGA-typed component	168

Figure 5.50b. Cross section view showing the basic subparts of a CSP-typed component	168
Figure 5.51. Cross section view of a BGA and CSP components	169
Figure 5.52a. Arrangement of three SMD electronic components under the IPC1753B standard	169
Figure 5.52b. Arrangement of three SMD electronic components under the IPC1753C standard	169
Figure 5.53a. Recalling of the intermittent routines for the NFC-memory-based version	170
Figure 5.53b. Actual organization of the memory blocks of the studied EEPROM memory	170
Figure 5.54a. GW Impact distribution (writing rate variation with a very low use intensity of the object)	171
Figure 5.54b. GW Impact distribution (writing rate variation with a low use intensity of the object)	171
Figure 5.54c. GW Impact distribution (writing rate variation with a moderate use intensity of the object)	172
Figure 5.54d. GW Impact distribution (writing rate variation with a high use intensity of the object)	172
Figure 5.55. Relative impact of the life cycle of the BLE version and the NFC-memory-based version	173
Figure 5.56a. AD and GW impact contributors of the BLE version	173
Figure 5.56b. Detailed impact contributors of the BLE module (BlueNRG2)	173
Figure 5.57. Recall of the EoL LCA modeling proposed in the framework for eco design	174
Figure 5.58a. Impact distribution of the random values of the studied features (F1-F4) showing the probability that the AD impact of the lifecycle of Set 8 is greater than that one of set 20	175
Figure 5.58b. Impact distribution of the random values of the studied features (F1-F4) showing the probability that the GW impact of the lifecycle of set 20 is greater than that one of set 8	175
Figure 5.59a. Relative AD and GW impacts of set 8 and set 20, both with a best recycling scenario	176
Figure 5.59b. Relative AD and GW impacts of set 8 (reuse scenario) and set 20 (best recycling scenario)	176
Figure 5.60a. Relative AD Impact comparison of the worst, regular and best recycling scenarios of set 8	177
Figure 5.60b. Relative AD Impact comparison of the worst, regular and best recycling scenarios of set 20	177
Figure 5.61a. Relative GW Impacts of the worst, regular and best recycling scenarios of set 8	178
Figure 5.61b. Relative GW Impacts of the worst, regular and best recycling scenarios of set 20	178

List of tables

Table 1.1. Classification of sensor types	30
Table 1.2. Some approaches close to IoT systems	32
Table 1.3. Some techniques for Green-IoT	36
Table 1.4. Harvested power density ranges according to the main energy sources	38
Table 2.1. Atmega328 MCU execution times and number of cycles for data processing and transmission	47
Table 2.2. IoT microprocessor configurations for sensor computing	48
Table 2.3. Common functions and representative computational kernels	48
Table 2.4. Design of sensor systems and edge devices providing sufficient resources	53
Table 2.5. Edge and cloud computing allocation and temporary storage design	54
Table 3.1. Characterization factors for the GW impact category	60
Table 3.2. Elements considered in the LCA study of an IoT-based glass collection system	64
Table 3.3. Aspect considered for modeling the energy requirements of an IoT system	65
Table 3.4. Number of tires estimated under a manual and an IoT-based checking system	66
Table 3.5. Partial construction of an average use scenario of a smart fridge	67
Table 3.6. Data generation rate and associated impacts for some functions of smart fridges	67
Table 3.7. Impact comparison of the use of a regular fridge and a smart fridge	68
Table 3.8. CED results and Ecocost impacts of the life cycle of the four HEMS versions	71
Table 3.9. Highest impact contributors of sensor systems belonging to an ILS IoT system	71
Table 3.10. Materials and energy used in the fabrication of 1000 paper-based sensors	76
Table 3.11. Guidelines oriented to reduce the impact of the B-o-L of sensor and sensor systems	82
Table 3.12. Guidelines oriented to reduce the impact of the use and E-o-L life cycle phases of sensor systems	83
Table 3.13. Analysis of an object and the potential added-value of an IoT	85
Table 3.14. Relevant aspects and critical questions for smart JMK objects	85
Table 3.15. Appropriated design for integrating connectivity and smartness to JMK objects	86
Table 3.16. Some examples of hardware resources classified by HSLs and functional blocks	91
Table 3.17. Description of the methodology consisting of a mix of indicators	91
Table 4.1. Adapted results of the first part of the qualitative research	95
Table 4.2. Adapted results of the second part of the qualitative research	96
Table 4.3. Material content share in one ton of WPCBs	103
Table 4.4. Power needs of specific SoC communication interfaces	111
Table 4.5. Lifetime estimation of different IoT devices	113
Table 4.6. Transfer coefficients of the important content to the metal and residue fractions	118
Table 5.1. Maximum LoRa payload according to different Spreading Factors	127
Table 5.2. Capacities of key technical features of electronic components of the case study “Smart metering”	131
Table 5.3. Three hypothetical scenarios of the data traffic of the case study “Smart metering”	134
Table 5.4. Estimated impact of the case study “Smart metering” under the worst, regular and best scenario	135
Table 5.5. Empirical Internet traffic captured from the regular and user-driver operations	141
Table 5.6. Real internet traffic of the case study “Smart metering”	141
Table 5.7. Estimated impact of the case study “Smart metering” considering local and internet traffic	142

Table 5.8. Estimation of the maximal lifetime of one 9V Li-ion battery (gray cells) used by the flowmeter.....	144
Table 5.9. Criteria of electronic component selection for the referential design set (set 13).....	146
Table 5.10. Combinations or “sets” for the design of the memory-based version.....	154
Table 5.11. Results of the elementary flow and sensibility analysis of the worst and best design sets (AD category).....	157
Table 5.12. Summary of relevant material content in design set 1 and 18.....	158
Table 5.13. Impact relevance of materials and their absolute and relative contents in set 1 and set 18.....	158
Table 5.14. Proposed variations for different material content shares in set 18.....	161
Table 5.15. Material quantities of electronic components’ subparts of set 18.....	162
Table 5.16. Recommended variations to improve the design of set 18 facing up to the design of set 1.....	162
Table 5.17. Results of the elementary flow and sensibility analysis of the worst and best design sets (GW category).....	164
Table 5.18. Relevant material content shares and internal die area ratios of set 20 and set 12.....	165
Table 5.19. Proposed variations for set 20 and set 12.....	166
Table 5.20. Variations that alternative WLCSP-typed microcontrollers should pursue to improve the design of set 20 over the design of set 12; and limits in the gold and silver content shares in wires and solder balls of alternative TFBGA-typed microcontrollers should respect at most, in order to keep the convenient design of set 12 in relation to the design of set 20.....	167
Table 5.21. Physical attributes of the memories of the referential set 13 and alternative set 14.....	168
Table 5.22. Empirical writing rate values obtained from different use intensities of the object.....	171
Table 5.23. Current and threshold values of the studied circularity features of the TFBGA64-typed microcontroller below which bridging does not occur.....	175
Table 5.24. Gold and silver recovery rates of the different recycling scenarios of set 8.....	176
Table 5.25. Gold and silver recovery rates of the different recycling scenarios of set 20.....	176

Glossary

Abbreviations

AA	Air Acidification
ACL	Anticounterfeit Label
ADC	Analog-to-Digital Converter
ADP	Abiotic Resource Depletion Potential
ADR	Adaptive Data rate Routine
AES	Advanced Encryption Standard
ANOVA	Analysis of Variance
AT	Air Toxicity
BAU	Business As Usual
BGA	Ball Grid Array
BLE	Bluetooth Low Energy
BoA	Bill of Attributes
B-o-L	Beginning of Life
BoM	Bill of Materials
bps	bits per second
CCP	Capture Compare Pulse
CED	Cumulative Energy Demand
CEE	Calorie Expenditure Estimation
CF	Characterization Factor
CoAP	Constrained Application Protocol
CPU	Central Process Unit
CR	Coding Rate
CRC	Cyclic Redundancy Check
CSP	Chip Scale Package
CTE	Coefficient Thermal Expansion
DAC	Digital-to-Analog Converter
DfE	Design for Environment
DfR	Design for Recyclability
DfD	Design for Disassembly
DIKW	Data Information Knowledge Wisdom
DNS	Domain Name System
DRAM	Dynamic Random Access Memory
ECD	Electrochromic Display
ED	Energy Depletion
EEPROM	Electrically-Erasable Programmable Rear-Only Memory
EH	Energy Harvesting
E-o-L	End of Life
EP	Energy for Production steps
EPEAT	Electronic Product Environmental Assessment Tool Label
EPU	Energy for the Product Usage
FAST	Function Analysis System Technique
FEA	Finite Element Analysis
FeRAM	Ferroelectric Random Access Memory
FIR	Finite Impulse Response
FFT	Fast Fourier Transform
GB	Gigabyte
GHG	Greenhouse gas emissions
GHz	Gigahertz
GPIO	General Purpose Input/Output
GPU	Graphic Processing Unit
GSM	Global System for Mobile communications
GWP	Global Warming Potential
HCI	Human Computer Interaction
HEMS	Home Energy Management System
HSL	Hardware Specification Level
HTTP	Hypertext Transfer Protocol
HWP	Hazardous Waste Production
Hz	Hertz
IAP	Internet Access Point
IC	Integrated Circuit
ICT	Information and Communication Technologies
ILP	Instruction Level Parallelism
ILS	Intelligent Lighting System
IP	Internet Protocol
ISP	Internet Service Provider
ITU	International Telecommunications Union
IoT	Internet of Things
Kg/inh	Kilograms per inhabitant
kHz	Kilohertz
kWh	Kilowatts per Hour
LCA	Life Cycle Assessment

LCI	Life Cycle Inventory
LCIA	Life Cycle Impact Assessment
LPWA	Low-Power Wide-Area
LoRaWAN	Long Range Wide Area Network
LTE	Long-Term Evolution
LR-WPAN	Low-Rate Wireless Personal Area Network
M2M	Machine-to-Machine
MAC	Media Access Control
MAPE	Mean Absolute Percentage Error
Mbps	Megabit per second
MCU	Microcontroller Unit
MEMS	Microelectromechanical Systems
MFA	Material Flow Analysis
MHz	Megahertz
MIC	Message Integrity Control
MPU	Microprocessor Unit
MRAM	Magnetic Random Access Memory
NB-IoT	Narrowband IoT
NFC	Near Field Communication
NIC	Network Interface Controller
NPD	New Product Development
NVM	Non-Volatile Memory
OD	Ozone Depletion
OSI	Open System Interconnection model
PBGA	Plastic Ball Grid Array
PCB	Printed Circuit Board
PCM	Phase Change Memory
PDU	Protocol Data Unit
POC	Photochemical Oxidation
ProTox	Process Toxicity Screening
PS	Piezo-based
PSS	Product Service System
PWM	Pulse Width Modulation
QoS	Quality of Service
RAM	Random Access Memory
REACH	Registration, Evaluation, Authorization and Restriction of Chemical Directive
ReRAM	Resistive Random Access Memory
RFID	Radio-Frequency Identification
RoHS	Restriction of Hazardous Substances Directive
ROM	Read Only Memory
RPI	Recycling Potential Indicator
RMD	Raw Material Depletion
RTL-SDR	RTL2832U-based Software-Defined-Radio bundle
RWP	Residual WEEE Production
Rx	Power consumption for receiving data wirelessly
SADT	Structured Analysis and Design Technique
SDG	Sustainable and Development Goals
SDT	Shock-Detection-Tag
SF	Spreading Factor
SiP	System-in-Package
SNR	Signal-to-Noise Ratio
SoC	System-on-Chip
SPI	Serial Peripheral Interface
STT-RAM	Spin-Transfer-Torque Random Access Memory
t	Teardown mechanism
TCP	Transport Control Protocol
TCP/IP	Transport Control Protocol / Internet Protocol
ths	Three-way handshake mechanism
TLP	Thread Level Parallelism
TPI	Toxic Potential Indicator
TRL	Technology Readiness Level
TSOP	Thin Small Outline Packaging
TSSOP	Thin Shrink Small Outline Packaging
TWh	Terawatts per Hour
Tx	Power consumption for transmitting data wirelessly
UDP	User Datagram Protocol
URL	Uniform Resource Locator
VC	Voltage Comparator
VD	Voltage Detector
WD	Water Depletion
WDT	Watchdog Timer
WE	Water Eutrophication
WEEE	Waste from Electrical and Electronic Equipment
WLCSF	Wafer Level Chip Scale Packaging
WPCB	Waste Printed Circuit Board
WT	Water Toxicity

Metals and chemical substances

Ag	Silver
Al	Aluminum
Al ₂ O ₃	Aluminum Oxide
Ar	Argon
Au	Gold
C ₄ F ₈	Octafluorocyclobutane
CH ₄	Methane
CHF ₃	Trifluoromethane Fluoroform
CO ₂	Dioxide Carbone
Cr	Chrome
Cu	Copper
Fe	Iron
Ga	Gallium
Ge	Germanium
H ₂	Hydrogen
H ₂ O ₂	Hydrogen Peroxide
H ₂ SO ₄	Sulfuric Acid
H ₃ PO ₄	Phosphoric Acid
He	Helium
Hg	Mercury
In	Indium
IPA	Isopropyl Alcohol
Mn	Manganese
Mo	Molybdenum
N ₂	Dinitrogen
NF ₃	Nitrogen Trifluoride
NH ₃	Ammonia
Ni	Nickel
HF	Hydrogen Fluoride
HNO ₃	Nitric Acid
Pb	Lead
Pd	Palladium
Pt	Platinum
Sb	Antimony
Sn	Tin
Ti	Titanium
V	Vanadium
W	Tungsten
Y	Yttrium
Zn	Zinc

Institutions

CEA-Leti	Commissariat à l'Energie Atomique et aux Energies Alternatives (Laboratoire d'Electronique et de Technologie de l'Information)
DSYS	System Division

“If I had an hour to solve a problem I'd spend 55 minutes thinking about the problem and five minutes thinking about solutions.”

A. Einstein

Résumé

L'adoption accélérée de l'Internet des objets (IoT) dans nos sociétés modernes a généré une production accrue des dispositifs connectés, et en même temps une augmentation significative des flux de données. C'est la raison pour laquelle, la communauté scientifique s'inquiète de plus en plus de l'impact environnemental de ce secteur, et de l'utilisation appropriée des ressources de fabrication des dispositifs. Par exemple, le platine (un matériel jugé critique) est hautement demandé pour la construction des mémoires modernes, car celles-ci sont considérées comme des éléments indispensables pour la performance et la manipulation des données produites par le système de capteurs, les serveurs et également par les Technologies de l'information et de la communication (TIC). De même, il convient mentionner que, d'ici quelques années, il faudra environ 17 fois plus d'énergie secondaire pour produire des circuits intégrés qu'il n'en fallait en 2016. Et que, malgré les développements technologiques dans les semi-conducteurs ayant permis de concevoir des systèmes plus efficaces ; les résultats des études dans le domaine montrent qu'à moyen et long terme, ces avancées ralentiront voire s'arrêteront complètement, entraînant ainsi une augmentation de la consommation d'énergie secondaire sans précédent, en raison du traitement de données qui ne cesse pas d'augmenter.

Face à la crise environnementale, l'intérêt du milieu scientifique se concentre sur trois aspects importants : (a) mesurer l'impact environnemental lié au développement des systèmes IoT, (b) proposer des outils destinés à réduire ces impacts, notamment dans les premières étapes de conception, (c) et finalement proposer solutions innovantes.

- a) Concernant le premier point, la littérature montre qu'une grande partie des recherches mettent en évidence l'importance des dispositifs locaux (capteurs, systèmes de capteurs et dispositifs périphériques « *edge* »), mais l'architecture complète des systèmes IoT (équipements locaux, réseaux de communication et serveurs distants) est très peu envisagée. En effet, les travaux qui visent à estimer l'impact environnemental de ces architectures indiquent, en général, un impact moindre sur l'infrastructure mutualisée. Il est important de noter, que ces recherches admettent certaines limitations importantes dans les méthodes d'estimation, c'est le cas des simplifications (par exemple, en ce qui concerne les capacités des dispositifs locaux) et/ou également montrent de la difficulté à extrapoler les résultats qui seraient exclusifs à des cas d'étude spécifiques. De plus, on a constaté que dans les analyses de cycle de vie (ACV) il existe une absence insidieuse en ce qui concerne l'étude des flux de référence (identification correcte et définition) lequel devrait être construit sur la base du flux de données présent dans un système. En rapport aux systèmes IoT partiels, la littérature montre que la production et les remplacements de nœuds ont un impact environnemental significatif, mais les détails, tels que les raisons qui entraînent cet impact sont négligés. De la même façon, les études réalisées sur le périmètre des systèmes de capteurs attribuent des impacts environnementaux importants à certains matériaux pour la fabrication de composants électroniques, en particulier les cartes électroniques, circuits intègres, et autres composants. Le peu d'intérêt porté sur ces derniers sujets dans la littérature limite l'évaluation adéquate des impacts environnementaux, et par conséquent, l'écoconception des systèmes IoT également.
- b) En ce qui concerne le deuxième point, les outils de conception et d'écoconception de systèmes IoT proposés par la littérature, présentent certaines défaillances, ce qui entrave considérablement leur application dans le développement de nouveaux dispositifs. En effet, les normes disponibles sont orientées vers le développement technique et non écologique, les guides d'écoconception sont très limités dans l'étape de conception et peu détaillés en ce qui concerne la sélection de composants et de technologies. En outre, les méthodologies d'écoconception ne précisent pas les techniques de conception électronique des équipements locaux. Par ailleurs, les outils d'écoconception mentionnés précédemment se concentrent dans la plupart des cas uniquement sur quelques aspects

de certaines phases du cycle de vie des dispositifs, notamment sur la consommation d'énergie dans la phase d'utilisation des systèmes IoT ou de l'empreinte carbone dans la fabrication des dispositifs. De plus, une faible partie de ces travaux font peu référence à l'infrastructure complète du système IoT.

- c) Finalement, le troisième point, les approches qui proposent des solutions dites innovantes, telles que le « *Green IoT* », les systèmes de récupération d'énergie, la computation intermittente, l'intégration de systèmes, le packaging avancé ou la conception modulaire, ont démontré qu'il y a possibilité de réduire l'impact environnemental. Cependant, ces approches peuvent être sources de dommages collatéraux. En effet, le « *Green IoT* » promeut souvent des techniques et procédures destinées à réduire la consommation énergétique des systèmes IoT, sans tenir compte des ressources supplémentaires (conceptions électroniques plus complexes ou réseaux de capteurs plus denses) qui garantissent la qualité de service des transmissions locales. En ce qui concerne les systèmes de récupération d'énergie, cette approche présente une limite par rapport aux composants électroniques dits fondamentaux, car ceux-ci peuvent se dégrader rapidement dans un contexte de fonctionnement intermittent. Certains travaux en rapport à l'intégration de systèmes et au packaging avancé montrent que de ces techniques, peuvent découler des avantages considérables en ce qui concerne les dispositifs hautement intégrés. Principalement, en ce qui concerne la simplification « *back-end* » de certains composants actifs, qui peuvent également augmenter la quantité de dioxyde de carbone (CO₂) émise par densité fonctionnelle au stade de la fabrication (c'est-à-dire plus de CO₂ émis par cm² produit). En matière de conception modulaire, les avantages écologiques présentés par cette approche ne sont effectifs que si les dispositifs sont réparés et préservés à moyen terme. De la même manière, on observera une perte potentielle de matériaux à faible recyclabilité fonctionnelle qui sont présents dans certains modules avec un haut taux de remplacement, par exemple l'Yttrium et l'Indium dans les écrans de smartphones.

Ainsi, les recherches menées dans le domaine de l'écoconception de systèmes IoT et leur impact environnemental font face à des défis considérables au cours de la décennie à venir. En effet, ils présentent des inconvénients majeurs, tels que l'inexistence de données ACV, dans certaines phases du cycle de vie ou de l'architecture complète de systèmes IoT, notamment pour l'infrastructure mutualisée. De même, selon une recherche qualitative réalisée au sein des équipes de conception de la Direction des Systèmes du CEA-Leti, il a été constaté que l'application exhaustive des études ACV n'est pas toujours faisable. En effet, il requiert des efforts considérables qui sont liés à la disponibilité de temps des concepteurs, ingénieurs et managers. Il a été également observé qu'ils n'ont pas seulement besoin d'un outil simple et pratique d'évaluation des impacts environnementaux et d'écoconception facilitant la prise de décisions, mais, aussi d'un outil qui s'adapte subtilement au processus du développement de nouveaux prototypes.

C'est dans ce contexte que, cette thèse répondra à deux questions de recherche. D'abord, comment les concepteurs peuvent-ils estimer l'impact environnemental de l'architecture entière de systèmes IoT? Ensuite, comment peuvent-ils minimiser cet impact au travers d'une méthodologie pratique de conception inscrite dans le processus de développement de nouveaux prototypes ?

Ce travail s'articule autour de l'idée, qu'à partir de l'organisation et de la collecte efficace de données brutes en une application IoT, il est possible d'obtenir de l'information substantielle. Ainsi, à partir d'une analyse fonctionnelle, il est possible de concevoir un flux de référence essentiel d'un système IoT.

Dans ce sens, ce travail sera développé sur la base de deux points de réflexion. Premièrement, il énonce deux concepts éminents et indissociables « *fonction-capacité* » présents dans les composants électroniques et exécutés dans différentes phases opératives de données. À partir de ces deux concepts, ce travail a construit un **outil-cadre d'évaluation d'impact environnemental**, *a contrario* de ce que la littérature propose par rapport aux outils d'évaluation. Ce cadre met en évidence les éléments essentiels

de l'architecture complète des systèmes IoT, et fait également référence à ses interactions, facilitant une estimation rapide et adéquate du flux de référence réel d'un système IoT. Deuxièmement, il fait référence à l'idée de « *dispositifs bien approvisionnés* ». À l'aide de ce critère, ce travail propose un **outil-cadre original d'écoconception** inscrit dans le processus de développement de prototypes. Il guide la sélection de composants adéquats sous trois critères interdépendants : physique, technique et circulaire, à partir d'un pas préliminaire de conception de flux de données et d'information.

Sur la base de ces deux nouveaux outils-cadres, qui en même temps se complètent, ce travail présente une méthodologie unique d'éco-innovation facile à appliquer à partir des informations disponibles aux concepteurs (tel que des *datasheets* ou des déclarations de matériaux). Cette méthodologie a été implémentée en deux parties.

Dans la première partie, l'outil-cadre d'évaluation d'impact environnemental a été implémenté à un modèle transversal de cycle de vie, selon une approche « *Bottom-up* », afin de dévoiler les flux de références complets. Cette implémentation a été illustrée par une étude de cas du système IoT complet destinée à surveiller la consommation d'eau dans une zone définie. Le but était de réaliser deux types d'évaluations, dans la phase d'usage du cycle de vie. D'un côté, une *estimation théorique* de flux de référence et un calcul de l'impact environnemental à long terme. Et de l'autre côté, une *estimation empirique* de flux de référence et un calcul de l'impact réel à partir de l'analyse du trafic global de données, tenant compte des aspects endogènes et exogènes (lesquels affectent les transmissions locales). Ces deux estimations (théorique et empirique) ont été effectuées sur la base des divers critères techniques, sous trois scénarios (pessimiste, typique, optimiste). Les résultats montrent que dans *l'estimation théorique*, l'impact environnemental est d'environ 5 Kg CO₂-eq émis sur deux années d'opération continue du système. Dans *l'estimation empirique*, l'impact est de plus de 6 Kg CO₂-eq émis pour la même période d'usage. L'augmentation de l'impact environnemental de ce dernier est dû à un volume plus grand du trafic de données non-locales par rapport au volume qui a été calculé par l'estimation théorique.

Dans la deuxième partie, l'outil-cadre d'écoconception a été implémenté en deux étapes. La première est considérée comme une étape préliminaire de l'identification de composants électroniques et implique la conception de flux de données. Cette étape est appliquée sur la base du cadre universel de sciences de l'information « *Rationale of information Science* » et dans leur analyse ont été identifiées deux types de versions. Une version est basée sur la Communication en champ proche ou « *Near-Field Communication* » (NFC) et considère 24 variantes à partir de la combinaison de 2 types de comparateurs de voltage, 4 types de microcontrôleurs et 3 types de mémoires; l'autre version est basée sur la technologie Bluetooth (BLE). La deuxième étape est adaptée au travers d'un modèle d'*analyse de cycle de vie ACV* bien détaillé, elle implique l'évaluation de composants électroniques conformément aux critères interdépendants introduits précédemment.

L'implémentation de l'outil-cadre d'écoconception écologique a été illustré par l'étude de cas d'un prototype de système de capteurs autonomes qui fait partie d'un système IoT orienté à surveiller le taux d'usage d'un objet. Cette étude a été développée au sein de la Direction des Systèmes de CEA-Leti, dans le but de réaliser une évaluation comparative structurée en trois aspects: d'une part, une *évaluation technique* destinée à comparer l'impact environnemental de la version BLE avec celui de la version NFC, d'autre part, une évaluation physique et une évaluation circulaire destinées à comparer certaines variantes de la version NFC. Ces évaluations sont expliquées dans les paragraphes ci-dessous:

- Une évaluation physique a été réalisée sous le critère de réchauffement climatique (GW) et a constaté deux aspects. Premièrement, parmi les 24 variantes conçues, la pire des variantes a été construite par des circuits intégrés avec des grandes puces et une carte électronique avec une surface plus large. Cette dernière est directement affectée par le « *land pattern* » de certains types de composants électroniques. Deuxièmement, la présence d'or et d'argent dans les sub-parties des

composants électroniques contribue marginalement à l'impact GW. Ainsi, dans le cadre de ces deux derniers aspects, une première analyse de Monte Carlo a été effectuée, celui-ci montre qu'une réduction moindre d'or ou d'argent peut être un facteur déterminant, au moment d'élaborer des conceptions écologiques. Par ailleurs, afin de réduire l'impact environnemental des variantes avec de microcontrôleurs du type WLCSP, il est nécessaire de considérer des composants avec un ratio surface puce / mase IC bien réduit.

- Une autre évaluation physique qui a été effectuée sous le critère d'épuisement des ressources abiotiques (AD) a constaté deux aspects importants. Premièrement, parmi les 24 variantes conçues, la pire des variantes a été construite par des circuits intégrés composés en grande partie de fils d'or. De plus, un quart des dommages de l'ensemble des impacts environnementaux est occasionnée par de significantes quantités d'argent, de cuivre et d'étain en différentes sub-parties du microcontrôleur TFBGA. Deuxièmement, les dommages des différents types de boîtiers peuvent varier significativement en fonction des matériaux avec lesquels ils sont construits. En effet, la quantité d'un matériel peut être déterminant selon la « *relevance d'impact* » de ce matériel dans une « *catégorie d'impact environnemental* ». C'est dans ce contexte, qu'une deuxième analyse Monte-Carlo a été réalisée. Elle a démontré qu'il existait une amélioration dans la conception écologique des cartes électroniques dans la catégorie d'impact AD, lorsqu'il y a une réduction des quantités des matériaux avec une haute relevance d'impact, ou lorsqu'il y a une réduction minimale des quantités significatives de matériaux avec faible relevance d'impact.
- L'évaluation technique est réalisée en comparant le cycle de vie de deux versions, la version BLE et la version NFC. La première ne réalise aucun enregistrement de données dans une mémoire, elle les envoie directement aux téléphones mobiles. Au contraire, la deuxième (NFC) avant de les exporter par lots, les enregistre dans une mémoire (écriture). La démarche de cette dernière prend en compte le taux de vieillissement des blocs de la mémoire (en fonction de la fréquence de l'écriture), lequel est proportionnel au taux d'usage de l'objet de cas d'étude. C'est la raison pour laquelle, au moment d'analyser l'évaluation technique, la préférence d'usage des utilisateurs (BLE ou NFC) joue un rôle important. En effet, à une haute intensité d'usage, l'intensité des enregistrements dans la mémoire seront plus importants, donc plus la mémoire se dégrade, augmentant ainsi la possibilité de remplacement du dispositif (prototype). Partant de ce constat, une troisième analyse Monte-Carlo a été réalisée, afin de comparer les deux versions, il a été observé que dans un contexte de faible utilisation de l'objet, une augmentation substantielle de la fréquence d'écriture n'affecte pas la fiabilité des mémoires de la version NFC et donc assure son avantage environnemental par rapport à la version BLE. Cependant, dans un contexte d'utilisation modérée de l'objet avec une augmentation substantielle de la fréquence d'écriture, ou dans un contexte d'utilisation intensive de l'objet avec une augmentation modérée de la fréquence d'écriture, dans les deux cas il y aura une dégradation importante de la mémoire et par conséquent le remplacement du dispositif avant de satisfaire son unité fonctionnelle.
- L'évaluation circulaire a été réalisée sur la base de deux types analyses. D'une part, une analyse Monte Carlo qui tient compte des attributs circulaires de composants du type BGA, tels que la taille du boîtier, l'épaisseur du « *compound* » et du substrat ; le diamètre et le « *solder bump pitch* » des pins. Cette analyse a montré que, dans la phase de sélection des composants, la probabilité de succès de séparer et réutiliser les microcontrôleurs BGA, augmente si les concepteurs priorisent les tailles de boîtiers petits, et également des *solder bump pitches* larges. Mais, il est important de remarquer que d'après cette analyse, les boîtiers extrêmement petits peuvent également entraver la séparation thermique. D'autre part, il a également été effectué une analyse comparative d'impact environnemental de deux variantes hétérogènes de la version NFC dans le contexte du recyclage. Dans cette analyse, on tient compte d'un attribut circulaire, la taille du boîtier, et suggère que la

séparation manuelle des composants plastiques de la carte électronique, et la séparation mécanique de ses grands composants, peuvent offrir des bénéfices, mais seulement si on effectue un traitement correct des résidus non électroniques et si ses composants séparés contiennent une quantité significative de métaux cibles.

Après avoir réalisé une analyse exhaustive et implémenté les deux outils-cadres dans les deux cas, cités précédemment, ce travail propose des recommandations qui sont traduites en 22 guides de conception. Ces directives doivent être adoptées, raffinées et complétées à d'autres études, sous une approche critique et globale, en utilisant la méthodologie présentée dans ce travail de manière continue, cohérente et automatisée, notamment avec l'adaptation des systèmes d'information.

Mots clés : Internet of Things, IoT, Technologies de l'information et de la communication, TIC, écoconception, éco innovation, Analyse de Cycle de Vie, ACV, Computation Intermittente, Systèmes IoT, Systèmes de capteurs, Systèmes de récupération d'Energie, Green IoT.

Abstract

The accelerated adoption of the Internet of Things by our modern societies has increased significantly the production of connected devices in recent years. In the face of the potential impacts of this tendency, researchers put more efforts on measuring the environmental impact of IoT systems, proposing tools to reduce this impact and offering innovative solutions.

However, Life Cycle Assessment (LCA) literature focused on IoT systems shows that few authors cover the full architecture. In the scope of partial systems, some authors point out significant impacts from the production and replacement of nodes, without giving more details in terms of electronic design. Moreover, it is observed a lack of, or a poor definition of reference flows, which, according with evidence found in certain studies, should be built on the basis of the data flow present in a system. On the other hand, the eco design tools found in literature suffer from shortcomings and some of the most innovating solutions —such as green-IoT, energy harvesting systems or intermittent computing — are projected promising, but also can cause collateral damage. Besides of all this, the research on impact estimation struggles with the absence of LCA data, and practice of eco design is hampered by the impracticability of applying exhaustive LCA modeling, within the typical design workflow of devices.

It is in this context that this thesis aims to build a practical design methodology oriented to estimate the environmental impact of full IoT systems, and minimize this impact from the early steps of the development of new prototypes. To achieve this goal, this work starts from the idea that substantial information for an IoT application can be obtained from the efficient collection and organization of sufficient, yet meaningful raw data. In this manner, this thesis is developed on the basis of two points of reflection. The first one establishes two inexorable and indissociable concepts “**function-capacity**” that facilitate the definition of reference flows. Based on that, a **framework for impact estimation** is built. The second one promotes the approach of “**right-provisioned-devices**” that guides the selection of suitable components under three interdependent criteria (physical, technical and circular), considering a preliminary design step of data and information flow. Based on that, another **framework for eco design** is built. Both frameworks complement each other and compose a unique methodology for the eco innovation of IoT systems, applicable from basic information available to designers.

In this work, this methodology has been implemented and illustrated in two parts. Firstly, the framework for impact estimation was implemented by a bottom-up, transversal life cycle model, which aims to illustrate the theoretical and empirical estimation of the reference flow and long-term impact of an IoT system oriented to smart metering. By taken into account technical criteria and endogenous and exogenous aspects that affects transmissions, the empirical estimate shows a greater impact than that one obtained from the theoretical estimate, which is explained by a greater volume of data traffic between local and cloud infrastructure.

Secondly, the framework for eco design was implemented and illustrated by a preliminary design step of data and information flow of a prototype of a self-powered EH sensor system developed at the System Division of CEA-Leti; and by a LCA-based evaluation step, that involves two of its versions. In this sense, a physical-based analysis reveals the influence of the codependence of PCB surfaces and land patterns of electronic components on global warming, the significant contribution of ICs’ die surfaces to this impact category (especially those belonging to the CSP technology), and the marginal, yet decisive contribution of gold and silver. For the AD impact category, it was observed the central role of gold, silver, copper and tin for impact estimation and eco design, all in function of their quantities and their impact relevance (aspects that are capital when evaluating different technologies of packaging).

Within the intermittent functioning of the prototype (which belongs to an IoT system oriented to monitor the usage rate of an object), a technical-based analysis showed that in a context of low use, a substantial increase in the writing frequency does not affect the reliability of the NFC-version’s memory (ensuring

an environmental advantage against the BLE-version). However, in a context of moderate use of the object with a substantial increase in the writing frequency, or in a context of intensive use of the object with a moderate increase in the writing frequency, the probability of degrading the memory and consequently replacing the device before satisfying its functional unit augment considerably.

Finally, a circular-based analysis showed that BGA components with small packages (mainly) and large solder bump pitches (additionally) are more likely to avoid bridging effects (one of the causes that interfere with their reuse), but very small packages can also interfere with the process of thermal separation. This circular-based analysis also suggests that the manual separation of the plastic components, and the mechanical separation of big electronic components, can both generate significantly benefits, but only if a proper treatment of non-electronic residues is applied, and if separate components contain significant amounts of target metals.

These and other findings are synthetized into 22 guidelines that must be adopted with a critical and global approach. That is, they should be challenged, refined or complemented in the context of other case studies; and by using the proposed methodology in a continuous, coherent and automated manner, particularly with the adaptation of Information Systems.

Keywords: Internet of Things, IoT, Information and Communication Technology, ICT, Eco design, Eco innovation, Life Cycle Assessment, LCA, Intermittent computing, IoT systems, sensor systems, Energy Harvesting systems, green-IoT.

Introduction

The ongoing information age shapes our modern societies and paves the way to prosperity. In last decades, we have witnessed an accelerated progress from the development of Information and Communications Technologies (ICT), and specific advancements in modern semiconductors, materials, web scale analytics and Artificial Intelligence. At the same time, the fifth- and the upcoming sixth-generation technologies presage a more connected world supporting colossal communications between sophisticated devices.

In this context, the Internet of Things (IoT) emerges as one of the millstones of this bright reality. Only in 2018, the World Economic Forum found that 84% of more than 600 IoT worldwide projects support or have the potential to support 17 Sustainable Development Goals (SDG) including industry, innovation and infrastructure (SDG 9), sustainable cities and communities (SDG 11), affordable and clean energy (SDG 7), responsible production and consumption (SDG 12) and good health and well-being (SDG 3) [193]. What is more, from wearable and implantable devices to complex systems inside vehicles, the IoT has the potential to bring more than \$11 trillion of benefits, contributing with more than 11% to the global economy by the end of 2025 [1].

An evidence of this direction is the steady growth of IoT devices in last years. Estimations shows that, in 2020, the number of IoT devices overcame the number of humans and exceeded the regular electronic fleet by an approximate factor of 1,2 [2]. Others believe that in 2023, there will be 1,8 IoT-based connections for each member of the global population [194]. However, at the same time, there is an increasing concern that this rapid and uncontrollable expansion of IoT systems leads several ecological problems related to resource depletion, climate change and waste.

In last decades, global extraction of essential metals for electronics and sensors such as copper has increased by a constant annual rate of 3% and it is expected a historic production record of 50 Mt/year in 2050, followed by a drastic decrease due to degradation on the quantity and quality of ores [3]. The global warming damage could be also significant, not only in the manufacturing phase of IoT and edge devices, but also in their use phases, assuming that they depends on mutualized infrastructure to work. As a matter of example, charging a smartphone in France contributes with only 0,3% of GHG emissions of its life cycle, but this contribution increase rapidly to 50% when mutualized infrastructures allowing multiple services (internet and datacenters) are included [4]. In the same way, researches expect similar impacts from IoT systems [6], according to sensor complexity and data application typology (i.e.: imaging).

In addition to this, there is a significant asymmetry between WEEE growth and circularity. Currently, research and industry are confronted not only to low collection rates but also to inner design challenges related to disassembly issues. In 2018, Western European countries have not achieved the 85% WEEE collection target, probably due to several reasons including dissipation of waste flows in the environment (approximately 1,4 Kg per inhabitant (Kg/inh) of WEEE would be landfilled or incinerated), or informal WEEE flows (0,5 to 1,4 Kg/inh of WEEE would ended up in illegal flows) [195]. From the collected share, current technology falls short to separate efficiently components from waste electronic cards for recovering strategic metals such as gold, silver, copper, bismuth and tin [196].

All these issues reveals the unsustainable condition of IoT and the urge of change. At this moment, more than a hundred of solutions among standards, guidelines and customized eco-design tools were proposed to deal with the environmental load of electronics and recently, scientific communities started to focus their efforts to solve the impact of IoT devices, but, in general, all these efforts are either difficult to apply throughout the existing product development process or they are simply segregated or discordant. On the other hand, encouraging approaches oriented to specific IoT issues such as energy consumption and waste are found in specialized literature but, with some exceptions, they are devoid of a global and lifecycle perspectives.

It is in this context that this thesis emerges. It aims to build a simplified yet holistic methodology that not only facilitates sustainability of IoT systems, based on the integral environmental impact assessment of full IoT system and the ecological design of IoT prototypes, both feasible from the available information that a designer usually has; but also guide, complement and harmonize future research in promising domains. This objective is particularly challenging because, contrary to regular electronics, An IoT system facilitates human-to-human, human-to-machine and machine-to-machine (M2M) interactions by heterogeneous networks of local and edge devices; and mutualized infrastructure. Specifically, sensors or sensor systems embedded in regular objects captures raw data from environment, which is later processed or resending by intermediate devices toward remote servers.

On the other hand, while this thesis is read, less than 1% of data generated by more than 30000 sensors in an oil ring is used [1] and sound sensors in Barcelona transmit raw data of noise pollution every minute [5]. Are the design of these IoT systems over- or under-sized? With this doubt in mind, the starting point of this research is recognizing data as the distinctive added value that establish referential flows; and as a design-driver of sustainable IoT systems. More specifically, the main presumptions being tested throughout this research is that (1) the appropriate analysis of data collection and flow reveals crucial aspects for accurate impact estimation, and for appropriate design alternatives for sustainable IoT prototypes; and that (2) such alternatives must be evaluated with a physical, technical, circular and lifecycle perspectives.

Consider, for example, exploiting the implicit information from voltage outputs data of a wearable piezoelectric harvester to estimate the amount of calories expended instead of using accelerometers, during specific human activities. With a Mean Absolute Percentage Error of 0,12 when walking and 0,16 when running, Lan, G. et al. [7] not only demonstrate that this is totally possible, but also put in evidence the potential of data, information and knowledge for sustainable IoT systems. Like this work, many other similar contributions proliferate around the world in the promising fields of data context sensing, Energy Harvesting (EH) systems, or intermittent computing but, what is the environmental and computational loads to implement such initiatives?

Within this work, these doubts, together with fundamental challenges and tendencies such as design priorities and tradeoffs, computing offloading and electronic component interdependency are addressed. In addition, principal difficulties in impact estimation are considered and appropriate ways to integrate sustainability in the typical design workflow of IoT prototyping are explored. This is done with the collaboration of the System Division (DSYS) of the research institute CEA-Leti, and in the context of two case studies, that involves an energy-harvesting prototype and a commercial IoT system. The result is a referential methodology that is positioned as an eco-innovation tool that surmount the very often lack of information and laborious nature of Life Cycle Assessment (LCA) in the prototyping phase of IoT systems.

The next chapters are oriented to answer the main interrogation: How can one estimate the potential impact of an IoT system and how can one minimize this impact by an efficient and practical design methodology?

Chapter 1 explores the fundamental concepts of IoT systems, their potential impacts and the recent initiatives for their sustainability; aspects that all together reveal the inner research questions. Chapter 2 addresses these questions by understanding the fundamental role of data and information for the impact estimation and design of IoT systems. Chapter 3 present a critical and exhaustive review of the State of Art of impact estimation and eco-design of IoT systems. From the knowledge gaps identified in this chapter, a fieldwork on designers' needs and the structured analysis of data design flow, specific capacities and attributes of electronic components, chapter 4 builds, proposes and positions a design methodology composed of two frameworks. Chapter 5 illustrate the use of this methodology and put in evidence its usefulness by generating 22 guidelines from the examination of two case studies. Chapter 6 recall the main findings, limits and further perspectives identified so far and concludes this work.

Chapter 1. Fundamentals of Internet of Things, potential impacts and trends

Overview

This chapter presents some fundamental concepts of Internet of things and establishes a common language for the development of the following chapters (section 1). Then, the section 2 presents a short reflection on the potential impacts of IoT systems to highlight the urgency of change. Finally, section 3 provides a brief, yet reasoning analysis of the benefits and shortcoming of current initiatives so that two research questions related to the main interrogation of this work can be established at the end.

1. Definitions and concepts

1.1. IoT Systems, sensor systems and other systems

The generic term “Internet of Things” does not benefit from a clear definition because certain visionaries and earlier technologies coined the term along the years. For example, long before that the first allusions about “linking a company’s supply chain to the internet” were made by Kevin Ashton in 1999 [206]; Mark Weiser [207-208] had already been talking about “ubiquitous computing” or “ubiquitous computing”, to refer to the way of allowing regular things benefit from the low-cost and computer miniaturization tendency, evidenced in 1990.

Considering that an embedded-, sensor-based electronic device can connect to remote servers by means of edge devices and internet, a more specific term of “IoT systems” is proposed by Serpanos, D. & Wolf, M. [197]. Normally, IoT systems are specific-oriented application products that figure among the most sophisticated Information and Communication Technologies (ICT). It could be defined as “a global infrastructure for the information society, enabling advanced services by interconnecting things — physical or virtual objects— based on existing and evolving interoperable information and communication technologies” [82].

An IoT system is composed of a local infrastructure (equipment of one or more end-devices, edge-devices and, optionally, fog-devices) and a mutualized infrastructure (telecom equipment and cloud resources). Figure 1.1 depicts these elements and their interactions in a basic architecture.

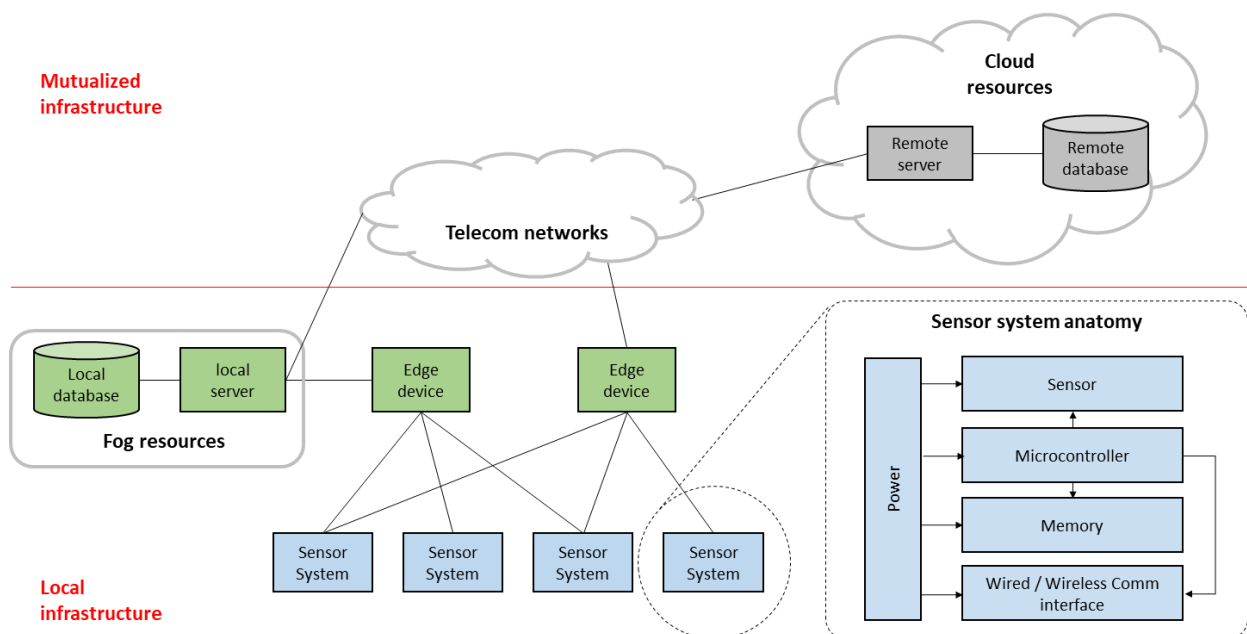


Figure 1.1. The basic architecture of an IoT System composed of the local and mutualized infrastructure. It includes, for example, sensor systems as end-devices, a local server and database as fog resources, and a remote server and database as cloud resources.

In Figure 1.1, an end-device could be a sensor component, an actuator or a sensor system. A sensor is an electronic component (EC) able to measure diverse phenomena from environment by a transduction process, and through specific techniques [198]. Conversely, actuators receive some type of control signal

(electric or digital) that triggers a physical effect [153]. Table 1.1 provides a classification of sensor types, built from the descriptions and details found in the comprehensive review conducted by McGrath, M. J., & Scanail, C. N. [198].

	Sensor type	Description	off-the-shelf sensors	Details
Contactless	Mechanical	Mechanical sensors measure changes in a device or materials as the result of an input that cause a mechanical deformation [209].	Microelectromechanical systems (MEMS)	Consist of mechanical microstructures all integrated into a same silicon chip. They integrate electric and mechanical elements, such as sensor and actuators on a very small scale [153].
			Accelerometers	Piezo-resistive accelerometers consist of resistive materials bonded to a cantilever beam that bends under the influence of acceleration.
			Gyroscopes	Gyroscope sensors use vibrating mechanical elements (proof-mass) to sense rotation based on the transfer of energy. Tuning fork gyroscopes contains a pair of masses that are driven to oscillate with equal amplitude but in opposite directions.
	Optical	Optical sensors work by detecting waves or photons of light. They operated by measuring a change in light intensity related to light emission or absorption by a quantity of interest.	Photodetectors	Photodetectors are based on the principle of photoconductivity, where the target material changes its conductivity in the presence or absence of light.
			Infrared	Active infrared sensors employs an infrared light source, which project a beam of light that is detected at a separate detector. Passive infrared sensors rely on detected heat from objects.
			Fiber optic	Fiber optic sensors use multimode fibers with large core diameters, coated with materials that respond to changes in strain, temperature or humidity.
			Interferometers	Interferometers use a light source (i.e., laser LED) and two single fibers. The light is split and coupled into both of the fibers. The quantity being measured modulates the phase of the optical signal.
Contact or contactless	Semiconductor	Semiconductor sensors modify the n- and/or p-structures to measures different phenomena.	Gas sensors	Gas sensors have a porous sensing layer made in thick-film metal oxide semiconductor layer such as SnO ₂ or tungsten trioxide, and a sensor base.
			Temperature sensors	Temperature sensors are based on the change of voltage across a p-n junction, which exhibits strong thermal dependence.
			Magnetic sensors	Hall-effect sensors consist of a thin layer of p- or n-type semiconductor material that carries a continuous current. They measure the voltage difference across the intensity of a magnetic field applied perpendicularly to the direction of the current flow.
Contactless	Electrochemical	Electrochemical sensors are composed of a sensing or working electrode and a reference and counter electrode. These electrodes are placed in contact with liquids or solid electrolytes to monitor different chemical properties (e.g., pH levels).	Potentiometric sensors	Potentiometric sensors measure difference in voltage between the working electrode and a reference electrode.
			Amperometric sensors	Amperometric sensors measure changes in current. The potential of the working electrode is maintained at a fixed value and the current is measured at a time basis.
			Coulometric	Coulometric sensors measure the quantity of electricity in coulombs by holding a working electrode at a constant potential and measuring the current that flows through an attached circuit.
			Conductometric sensors	They operates on the principle that electrical conductivity can change in the presence or absence of some chemical species.
Sample removal	Biosensors	Biosensors use biochemical mechanisms to identify an analyte of interest in samples.	Transducers for biosensors	Transducers for biosensors convert the biological activity —sensed by a bio receptor— into a quantifiable signal (For example changes in conductivity during enzymatic redox reactions).

Table 1.1. Classification of sensor types. According to McGrath, M. J., & Scanail, C. N. [198], sensors can measure quantities of interest in three ways: contact or non-contact with the quantity of interest; or sample removal.

On the other hand, a sensor system is a limited-resource device, composed of a sensor component, a microcontroller unit (MCU), a memory, a communication interface and a power subsystem, all integrated fully or partially in a same Printed Circuit Board (PCB) (see the sensor system anatomy showed in figure 1.1). It transforms the measured quantities obtained by its sensor component into data, and it could extend its capacities by augmented resources such as different wireless technologies, memories, or additional sensors and electronic components. Figure 1.2 shows a typical architecture of modern sensor systems.

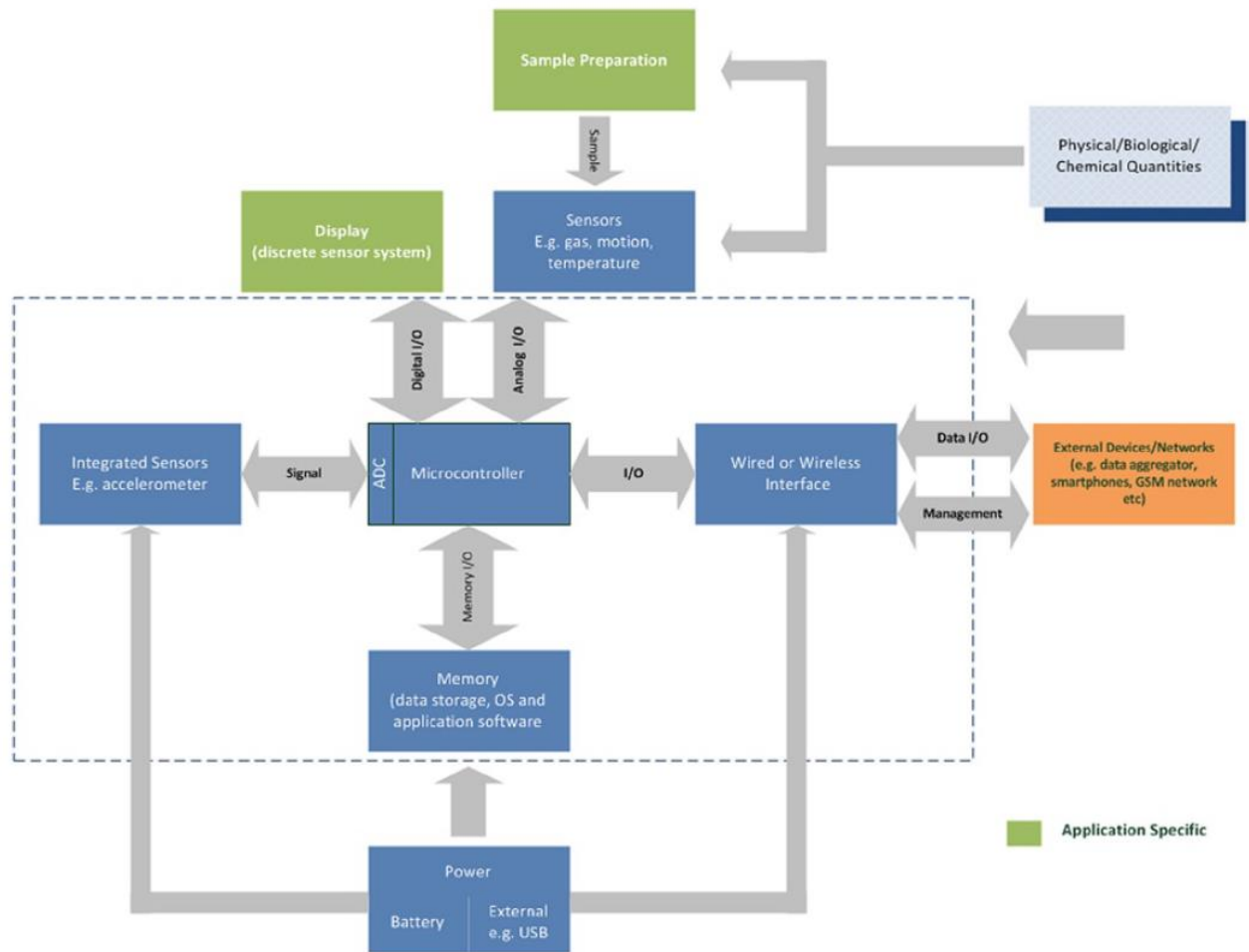


Figure 1.2. A typical sensor system architecture (blue boxes). A “signal” from the environment is measured by a sensor component (e.g., the force caused by a change in motion sensed by an accelerometer) and further transformed into a digital/analogic signal or data by the MCU (specifically, by its Analogic-to-Digital (ADC) converter). This digital/analogic signal or data flows physically by the Inputs/Outputs (I/O) peripherals of the MCU and other electronic components. Figure extracted from [198].

An electronic component can be classified as a passive component or an active component. A well-extended definition of passive components (e.g., capacitors or resistors) says that it is an electronic device that requires nothing but alternating current to functioning; it is not capable of power gain and is not a source of energy [219]. Active components, on the other hand (e.g., semiconductor diodes, Integrated Circuits (IC), unipolar and bipolar transistors, etc.) have analog electronic filters able to amplify a signal or produce a power gain (they do this because their source of energy are separated from the electrical signal) [220].

On the other hand, an edge device is an extended-resource device (i.e.: a lithium-battery-based gateway, an internet relay or a smartphone), which mainly provides high-level connectivity between sensor systems and the rest of the IoT system; and optionally, performs some computations. In contrast, a fog device is a nearby resource at the edge network (e.g., a local server or database) that performs different operations of a full or partial IoT system. The core concept of a fog resource or fog computing in an IoT system is that some network devices handle some services of the cloud infrastructure, enabling massive traffic and high readiness by processing requests closer to where the data is generated [203]. On the other hand, cloud computing is a model for enabling ubiquitous, convenient, on-demand network access to a shared pool of configurable computing resources (e.g., servers, storage and services) that can be rapidly provisioned and released with minimal effort [204]. In this sense, a cloud resource (e.g., a cloud server) is a powerful-, multiservice-server provided by a database system [197].

The telecom network showed in figure 1.1 can be further organized into different sub-networks. In fact, the International Telecommunication Union (ITU) establishes a basic model composed of an IoT area network, an access network and a core network (figure 1.3).

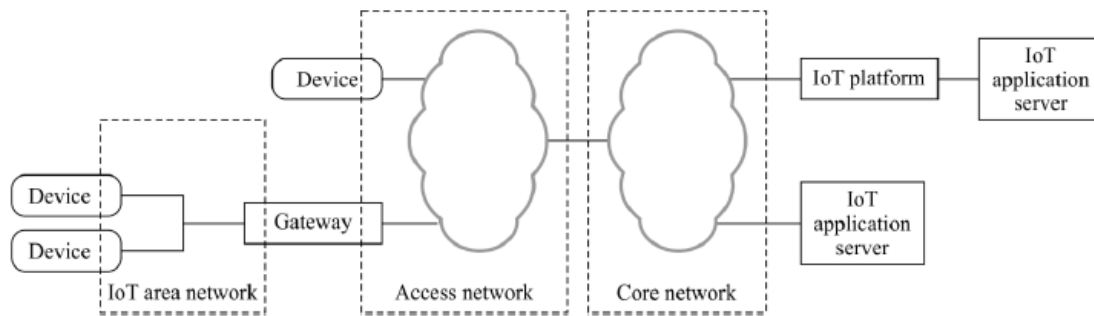


Figure 1.3. Basic model of the network architecture of IoT systems. Figure extracted from [217].

In this way, this institution provides the following standard definitions [217]:

- The IoT area network is a network of devices for the IoT and gateways interconnected through local connections.
- The access network connects access technology (such as a radio access network) to the core network [218]. For example, a gateway—that is, any Internet Access Point (IAP) device, such as an internet box— may also belong to the access network because it “interconnects the devices with the core network”.
- The core network is a portion of the delivery system composed of networks, systems equipment and infrastructures, connecting the service providers—the cloud resources—to the access network. For example, the Internet Protocol (IP) core network—that is, the Internet Service Provider (ISP) equipment which forms the regional, national and global networks [12]— can be considered as the core network because it “connects the service provider domain (i.e.; IoT application servers) to the access network”.

In this thesis, the access and core networks, together with the cloud resources are understood generally as the “mutualized infrastructure” but, when necessary, distinctions will be made.

Having established a unique language from the definitions above, table 1.2 provides a brief description of some approaches close to IoT systems that, although possess some of the features mentioned before, they might not be considered as such.

Approach	Description	Example	Why it could not be considered as an IoT system
Wireless Sensor Networks (WSN)	In the interpretation of Bonvoisin et al. [61], a WSN links together electronic devices that cooperates for obtaining and providing information about a system, by the monitoring of one of its relevant phenomenon [211].	A WSN oriented to monitoring the content level of a recipient, working with centralized gateways and a local server.	A WSN may or may not be considered an IoT system. While WSNs can operate locally (only with end- and edge devices); IoT systems need to work with mutualized infrastructures (i.e., internet and cloud servers). Indeed, IoT is not only a local infrastructure, but a global infrastructure to connect things through interoperable underlying communication networks [84].
Pervasive or ubiquitous computing	"Pervasive computing uses small, battery-powered, wireless computing and sensing devices embedded in our environment to provide contextual information to new types of applications" [212].	A Home Energy Management System (HEMS) of embedded controllers oriented to manage the energy usage of home devices [214]	In some cases, pervasive computing and IoT could be used interchangeably, as long as Internet connection in both approaches does exist. However, pervasive computing might be more oriented to Human Computer Interaction (HCI) issues—on making the connected things disappear from human attention; while IoT focuses more on connecting devices [215].
Mechatronics	"Mechatronics is the result of applying Information Systems to physical systems [...] The physical system consists of mechanical, electrical and computer systems as well as actuators, sensors and real-time interfacing" [213].	A car with an Electronic Traction System (ETS) that uses individual wheel-speed sensors to detect when wheels slip.	A mechatronic system belongs to a third level of intelligence: "physical products with embedded sensors, memory and data processing capabilities" [216]. To gain the status of IoT system, identification and communication capabilities must be added it [108].

Table 1.2. Some approaches close to IoT systems.

1.2. Fundamentals on computer networking in the context of IoT systems

From figure 1.1 and the later definitions, the connectivity-nature of all devices is evidenced. Indeed, any IoT device is a piece of computer equipment with the mandatory capability of communication; and the additional capabilities of sensing, actuation, data capture, data storage and data processing [82]. In broadly terms, for two or more computer devices communicate, common languages or “protocols” are needed. Typically, computer protocols deals with connection initialization, negotiation, data formatting, error detection/correction and connection termination tasks [156]. In order to address these functions and reduce the design complexity of computer networks, one use layered-based models (protocol hierarchies) and “protocol stacks”, which are lists of specific protocols used by a certain system (one protocol per layer) [210]. In this line, the Open System Interconnection (OSI) model provides a referential framework to facilitate communication between network systems based on seven layers: the application, presentation, session, transport, network, data link and physical layers (Figure 1.4).

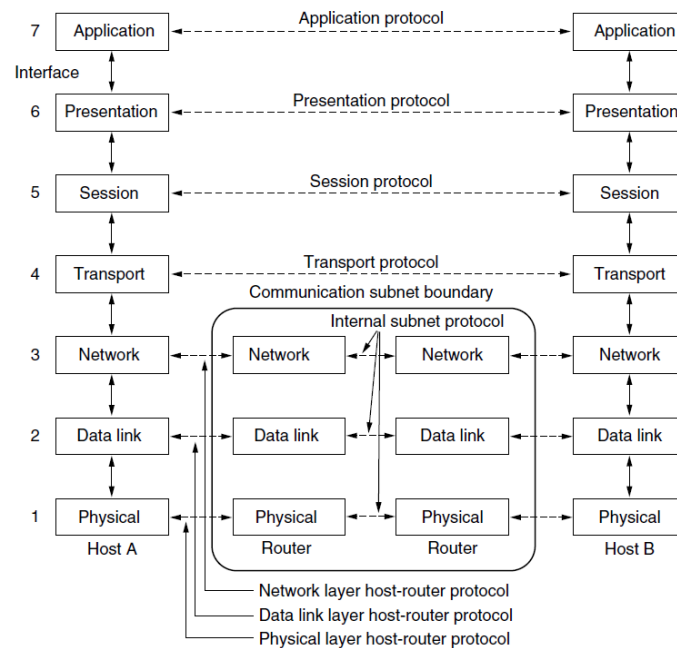


Figure 1.4. The layered-based protocol hierarchy and the protocol stack (dotted lines) of the OSI model. It shows a simple communication schema between host A and host B, both belonging to two different computer networks. Figure extracted and adapted from [210].

In a simple communication from host A (the left down-flow), a protocol in every layer adds headers and footers to the data application, generating an aggregated message with a “protocol overhead” (accumulated headers and footers), which flows by an interface (primitive operations and services between layers). In the network layer, this message becomes a complete Protocol Data Unit (PDU) — often called a “packet”, which is further organized in frames by the Data link layer, according to the carry capacity of the physical means. When the packet reaches the host B, the corresponding footers and headers in every layer are interpreted by a homologue protocol, so that the data application can be used in the application layer of host B (right up-flow).

Because end devices in IoT systems exchange information in challenging contexts (variable distance ranges, energy-constrained designs, different frequency bands and network topologies, etc.), specific technologies and protocols were developed to addresses the complexity of wireless communication in the network, link and physical layers of the local infrastructure. Among the common protocols applied to the extended 802.15.4 access technology, one can mention the Zigbee, Zigbee IP, 6LoWPAN, ISA100.11a, WirelessHART, and Thread protocols. For the Low-Power Wide-Area (LPWA) technology, one can instance the Narrowband IoT (NB-IoT) and Long Range Wide Area Network (LoRaWAN) protocols. In the case of the application, presentation, session and transport layers, one can identified the Constrained Application Protocol (CoAP) and the Message Queuing Telemetry Transport (MQTT) protocol. The former is based on the User Datagram Protocol (UDP) and the latter on the

Transmission Control Protocol (TCP); both are protocols used not only in IoT systems but also in computer networking in general.

2. Potential impacts of IoT systems

2.1. Resources depletion

The evidenced growth of sensors, sensor systems, internet networks and cloud infrastructures in recent years, together with the potential increase of ICT data in the short term, arise concerns related to depletion and criticality of specific materials. For example, in 2017, an approximate share of 8% of the global primary production of platinum (part of critical material list recognized by the European Union [205]), was attributed to the electronic sector (Ceramic capacitors, hard disks and memories) [199-200]. Considering a very low recycling rate of this metal in Waste Electrical and Electronic Equipment (WEEE) flows (from 0% to 5% according to Graedel, T. E., et al [221]), and its significant losses in manufacturing reported by Palomino, A. et al [201], it is expected not only a rapid decline of natural deposits but also supply chain disruptions, especially for ramping memory technologies. This crisis would be imminent in the case of production of Ferroelectric Random-Access Memories (FeRAM), **because of incremental data generation rates of ICT in further years**, as warned by Ku, A. Y. et al [202]. To understand why, the reader should consider his estimates in the material intensity of the platinum used only in the control gate subcomponent of these memories, that would amount to 236 metric tons per Zetabyte (Mt/ZB) against to an insufficient annual production of 172 Mt in 2016 (without counting losses in manufacturing, and considering an estimate of 163 ZB/day by 2025, according to Reinsel, D. et al [222]).

2.2. Embodied emissions and energy of IoT systems

On the other hand, the primary energy used for the manufacturing of electronic components in sensor systems depends on several features such as package size or package technology, which require more-in-deep analysis. A comprehensive study conducted by Das, S., & Mao, E. [8] showed, for example, that a same packaging technology might have different energy demands according to the number of pins of flash memories (see Figure 1.5a). Based on the global market forecasts of specific IoT ICs (sensors, MEMS, connectivity ICs, and processor ICs), these authors estimate that the total primary energy demanded for manufacturing IoT-specialized components will increase from 2 exajoules (EJ) in 2016 to 35 EJ in 2025 (Fig. 1.5b) (This estimation does not include the energy required by the internet and cloud infrastructure).

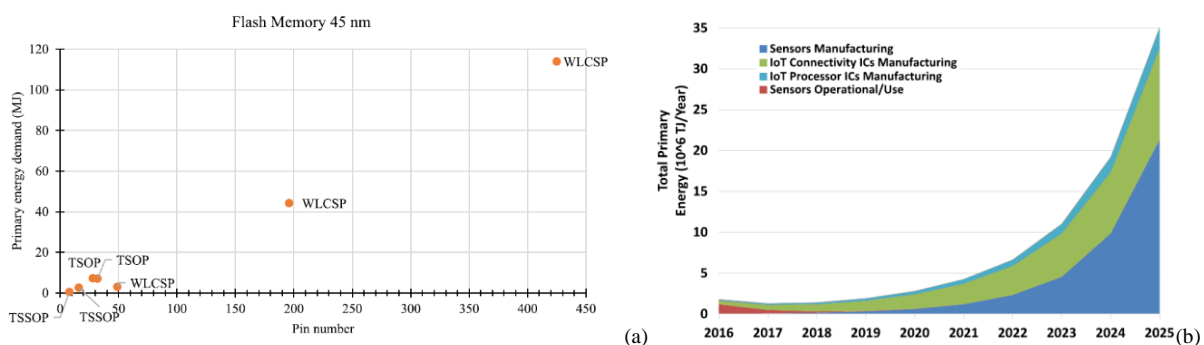


Figure 1.5. (a) Primary energy demand of 45 nm flash memories with different number of pins and packaging technologies (Wafer Level Chip Scale Packaging (WLCSP), Thin Small Outline Packaging (TSOP) and Think Shrink Small Outline Packaging (TSSOP)). (b) Primary energy footprint of IoT-specialized electronic components (sensors, MEMS and connectivity / processor ICs). The decreasing energy needs in operational stages would correspond to a constant improvement Kilowatt/hour, per year, per chip (kWh/year/chip). Figures extracted and adapted from [8].

2.3. Energy consumption of IoT systems

In 2012, the electricity consumption of the global ICT fleet was estimated at 920 Terawatts/hour (TWh) [223-224] causing an estimate of 530 Mt of CO₂ [225] (with one third of this damage attributed to end-devices, one third to telecommunication networks and one third to data centers). Nowadays, estimations shows a moderate and controlled increase in electricity needs, mainly thanks to efficient innovations in technology. For example, Masanet, E. et al. [226] reported a low increase of only 6% in total electricity consumption of data centers between 2010 and 2018. According to Koot, M., & Wijnhoven, F. [227],

this improvement is due to efficient data processing, cooling and uninterrupted power supplies. Moreover, these authors argue that during the next 10 years, and regardless of the significant increase in both consumer and business workloads, the energy consumption of data centers will be constant, thanks to technological innovations. Figure 1.6a provides one of their simulation-based sensibility analysis, in which it is found that a projected electricity demand of only 364 TWh will be enough to cover the climbing industrial IoT in 2030.

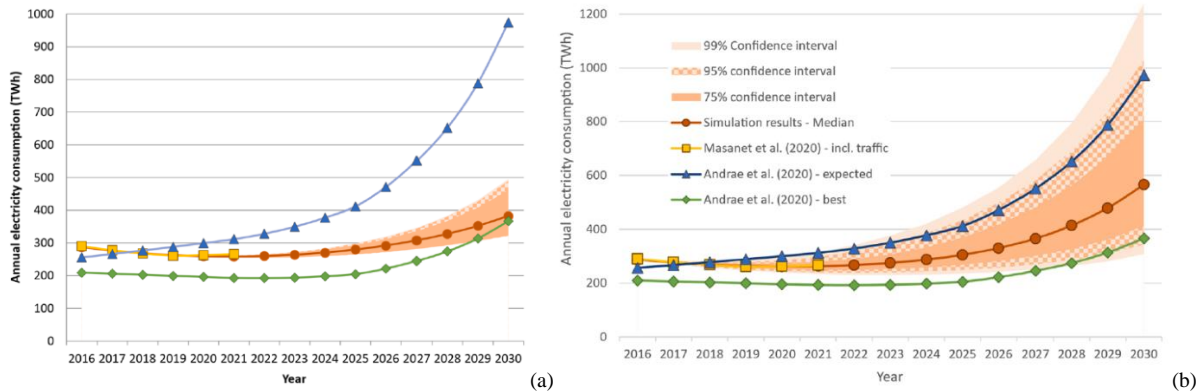


Figure 1.6. Monte Carlo-based, sensitivity analysis (10000 runs, including confidence intervals of 75%, 95% and 99%) of Electricity needs of data centers, considering (a) the climbing advent of industrial IoT and (b) Effect of both Industrial IoT and end of the Moore’s law on data center electricity consumption. Figures extracted and adapted from [227]. The legend is applied for both figures and the referential studies are available in Masanet, E. et al [226] and Andrae et al [228-231].

However, they also believe that these favorable circumstances may rapidly decay in the mid- and long-term, as the computing efficiency rate (twice every two years, as established by the Moore’s law) slow down or totally stop in next years. With this concern in mind and by considering a declining trend of the Moore’s law (from an efficiency-increase rate of 25% in 2016 to 0% in 2030), they conducted another analysis in the context of industrial IoT, **this time finding a significant augmentation of the data centers’ electricity needs going up to 752 TWh in 2030** (figure 1.6b).

Unfortunately, there are few studies like this one that estimate the energy consumption of IoT systems at a global perspective. Instead, there is a growing body of literature that warn the urge of a holistic, life-cycle perspective for estimating the impacts of global ICT [9]. Within this posture, a particular challenge is considering the global energy used in the operational phase of an ICT product [10] which often depends strongly on the application and use. The scarce research oriented to these aspects attempt to estimate the electricity consumption per data size (kWh per Gigabyte (GB)) of datacenters and internet infrastructure (core and access network). For example, based on empirical data Malmudin, J. et al [11] found that the electricity consumption of an efficient video-streaming datacenter is around of 0.01 kWh/GB. Moreover, Aslan, J. et al. [12] estimate a value of 0,06 kWh/GB of electricity intensity of a fixed-line Internet transmission network in Sweden in 2015. Interestingly, three years before, the former authors concluded that the manufacturing and operational phases of end-user equipment, enterprise networks, data centers and access networks (in that order) contributes significantly to the global carbon foot of ICT [163]; clarifying that, the energy use and embodied carbon footprint per data transmitted can be used as intensity metrics in environmental studies of IP core networks but, in the case of end-user equipment, a use-time basis is more relevant, because the energy consumption and the carbon footprint impact is not to the same extend related to transmit data volume.

In this line, Belkhir, L., & Elmeligi, A. [6] projected a respective contribution of 31, 24 and 45% of user-devices, networks and data centers to the total GHG footprint of ICT, and recommend more vigilance for the sector, **especially regarding the growth of IoT** and crypto concurrencies. With this respect, tendencies to ubiquitous computing and constant miniaturization of sensor systems may lead to significant data generation rates, **relocating computing intensity load to mutualized infrastructure** as it is warned by Köhler, A., & Erdmann, L. [15] and reported in the work of Gossart, C. [16].

Having recognized some of the potential impact of IoT systems, the next section present a number of discrepant yet promising approaches and solutions.

3. Promising yet segregated or discrepant initiatives

3.1.Green-IoT

Green-IoT is a recent, use-oriented perspective focused on reducing the impact of IoT systems in the use phase. According to Shaikh, F. K. et al. [18] and Arshad, R. et al. [99], Green IoT is defined as the energy efficient procedures adopted by IoT systems, oriented to reduce the environmental impact of existing applications and services, or the environmental impact of IoT systems themselves. Consider, for example, the set of practical green-IoT techniques summarized by Zhu, C. et al [17] applied on strategical sensor-based and IoT contexts (Table 1.3. present a brief view, as a matter of illustration).

Context	techniques
WSN	1) Make sensor nodes only work when necessary, while spending the rest of their lifetime in a sleep mode 2) Radio optimization techniques (transmission power control, modulation optimization, etc.) 3) Energy-efficient routing techniques (e.g., cluster architecture, multipath routing, node mobility, etc.)
Cloud computing	1) Power-saving Virtual Machine (VM) techniques (VM consolidation, migration, placement and allocation) 2) Energy-efficient resource allocation mechanisms (e.g., auction-based and gossip-based resource allocation)
M2M	1) Smart adjustment of transmission power 2) Efficient communication protocols (routing protocols)
Data centers	1) Dynamic power management techniques (e.g., Turboboost, vSphere) 2) Energy-aware routing algorithms to consolidate traffic flows
ICT	1) Minimize the length of data path 2) Advanced communication techniques (e.g., Multiple Input - Multiple output (MIMO))

Table 1.3. Some techniques for green Wireless Sensor Networks (WSN), green Cloud Computing, green Machine-to-Machine (M2M), green Data centers and green-IoT proposed by Zhu, C. et al [17].

3.1.1. What is wrong with Green-IoT and other use-oriented approaches?

Although practical, Zhu, C. et al. warn that some of the techniques showed in table 1.3 would be eclipsed, for example, by the extra resources needed to guarantee high Quality of Service (QoS¹), or by the extra energy to cover additional complexity. Moreover, they advocate for (1) a reasoning design of green-IoT, tackled from an overall system energy consumption perspective and (2) a better understood of different characteristic of IoT applications (together with their service requirement). This recommendations gain more sense in particular, yet common situations. For example, benefits and drawbacks of the technique “make sensor nodes only work when necessary, while spending the rest of their lifetime in a sleep mode” would depend on (1) the density of a sensor network and the transmission-receiving power configurations; and (2) the additional resources for switching between modes (as showed in the paragraph below).

In general, researchers focused on reducing the energy consumption of sensor systems aim to develop reliable self-powered devices or avoid overconsumption of batteries. In this sense, a large and growing body of literature has investigated the management of hardware resource to avoid futile tasks in sensor systems. For example, Callebaut, G. et al. [19] propose a simple and potential approach known as “Think before talk”, “race to sleep” and “sleep as much as possible” for long range-communication, battery-based sensor networks (Figure 1.7).

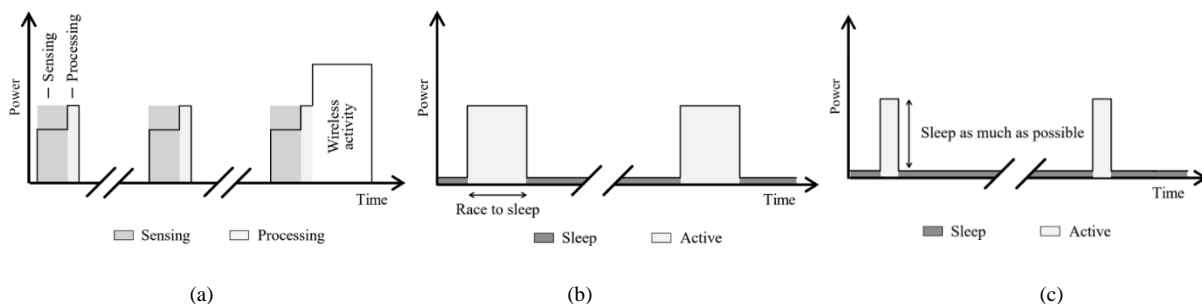


Figure 1.7. (a) “Think before talk” approach (requires validation of sensor measurements and data preprocessing before transmitting). (b) “Race to sleep” approach, (c) “sleeps as possible” approach (Figure extracted and adapted from [19]). Because computing is a less-energy-demanding task than transmitting (wireless activity), data manipulation of these three approaches aim to preprocess and send the minimal and substantial data to edge devices.

¹ Quality of Service or (QoS) refers to the capability of a network or networks to provide better service to selected network traffic over various technologies [106]. Specifically, it refers to concrete metrics such as packet loss rate that determine the quality of communication.

Unfortunately, this kind of approach would be very complex to implement, and it may highly depend on the application type. In addition, environmental gains would be seriously compromised, if the sleep-active switching-modes require additional low dropout voltage regulators, as the authors admit.

3.2. Self-powered IoT devices and intermittent computing

An alternative to energy-saving approaches is using Energy Harvesting (EH) sensor systems and intermittent computing; in general, both initiatives aim to simplify the electronic design and solve the problem of overconsumption of batteries. By definition, an energy harvesting system collects the environmental energy and converts it into electricity [20]. It is usually composed of an energy transducer, used to convert ambient energy into electrical energy; a rectifier, and a main capacitor for energy management and storage. A voltage regulator is generally present too as a sort of control subsystem for adapting the voltage level to requirements of the powered device. An optional energy storage element and a load—the main electronic of the application—are also key components. Figure 1.8 shows a basic architecture of an energy harvesting system. The key feature of energy harvesting system for IoT systems is that a transducer can be used to not only convert one type of energy into another, but also detect a physical phenomenon.

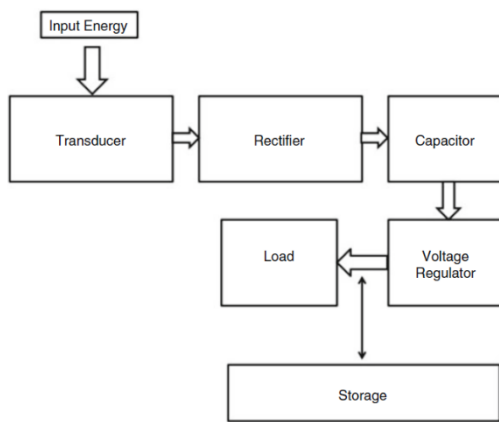


Figure 1.8. Basic architecture of an Energy Harvesting (EH) system (Extracted from [20]).

EH systems depends on available energy from environment. Because of that, modern EH sensor systems work under the principle of intermittent computing. An intermittent computing device is characterized by short periods of program execution, interrupted by continuous reboots [21]. Figure 1.9 shows the basic mechanism of an intermittent computing device together with a practical application for EH systems.

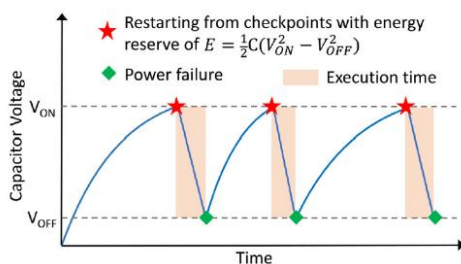
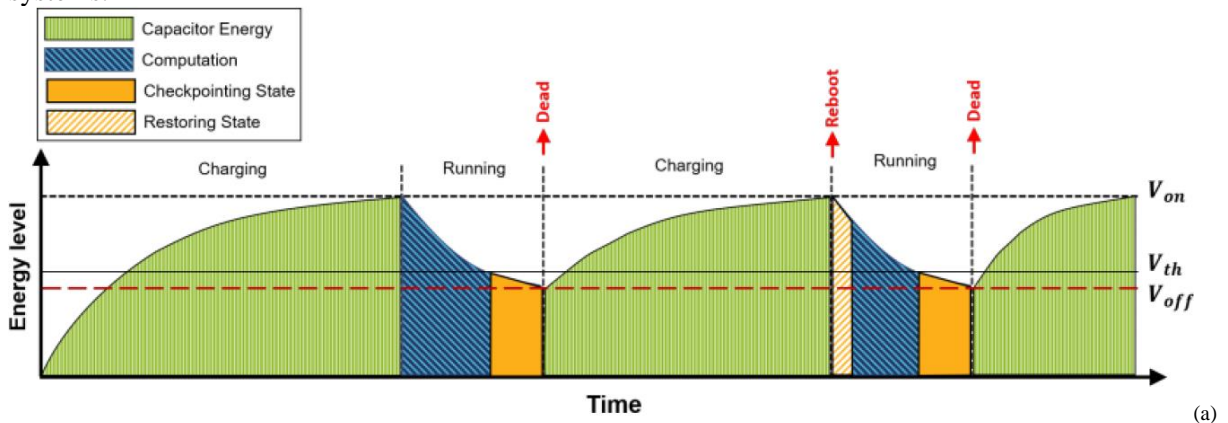


Figure 1.9. (a) The basic mechanism of intermittent computing (Extracted from [22]). (b) An intermittent design for an EH system (E = Energy, C = capacitance of the main capacitor (Adapted from [23])).

In figure 1.9a, the EH system collects and stores energy from the environment in the main capacitor until a superior threshold of voltage (V_{ON}) is achieved; and provides energy for program execution until energy level drops down to an inferior threshold of voltage (V_{th}). From then on, the remaining energy is used for making a checkpoint of the program states and variables before the EH system shuts down at V_{off} . When V_{ON} is reached again, the EH system restore the previous program states and variables and the cycle repeats. Because EH systems provides nanowatt-to-microwatt energy ranges (table 1.4), running a program to completion is impossible and in-memory checkpointing strategies are crucial to avoid inconsistencies, performance and reliability issues such as violation of atomicity and event program crashes [21].

Energy source	Category	Harvested power density	Sensor		MCU		Wireless transceiver			
			component	Power cons. (mW)	component	Power cons. (active mW)	component	power cons. (mW in Tx)	data rate (Mb/s)	Range (m)
GSM/3G/4G	Radio frequency	0,1 μ W/cm ² [20]								
WiFi	Radio frequency	1 μ W/cm ² [20]								
Human	Vibration/motion	4 [a] - 1800 μ W/cm ² [232]	Smoke alarm - DSW98A [232]	0,108	EM6603* [232]	0,0054	Bluetooth class 2 [8]	1,075	50	40
					EM6605* [232]	0,012	Bluetooth class 2 [8]	1,075	50	40
Industry	Temperature	10 μ W/cm ² [20]								
Indoor	Light	6 [b] - 10 μ W/cm ² [20]								
Human	Temperature	25 μ W/cm ² [20]			EM6605* [232]	0,012				
Thermoelectric	10°C gradient	40 μ W/cm ² [232]								
Industry	Vibration/motion	100 μ W/cm ² [20]	Light sensor - SFH5711 [232]	0,09						
Piezoelectric	Shoe inserts	330 μ W/cm ² [232]	Smoke alarm - DSW98A [232]	0,108						
Vibration	Microwave oven	0,01 - 0,1 mW/cm ² [232]	Light sensor - SFH5711 [232]	0,09						
Outdoor	Light (cloudy day)	0,15 mW/cm ² [232]	Smoke alarm - DSW98A [232]	0,108						
Indoors	Light (desk lamp < 60W)	0,57 mW/cm ² [232]	Proximity - SFH7741 [232]	0,21						
			Optical switch - SFH7740 [232]	0,21						
			Light sensor - ISL29011 [232]	0,27						
			Temperature sensor - STCN75 [232]	0,4						
Outdoor	Light (sunny day)	10 [a] - 15 mW/cm ² [232]	Light sensor - TSL2550 [232]	1,155	PIC16F877** [232]	1,8	Bluetooth class 3 [8]	0,8	50	10
			Accelerometer - ADXL202JE [232]	2,4	MC68HC05PV8A** [232]	4,4	ZigBee [8]	0,31	2	20
			Humidity/temper - SHT 11 [232]	2,75	AT90LS8535** [232]	15				
			Barometric Pressure - MS55ER [232]	3	ATmega163L** [232]	15				
			Touch sensor - QST108KT6 [232]	7						
			Strain gauge - SG-LINK(1000 Ω) [232]	9						

Table 1.4. Harvested power density ranges according to the main energy sources used by EH sensor systems. They are arranged by the typical power consumption of the most energy-intensity components of a sensor system load (Sensor, MCU and wireless transceiver components) in their maximal power needs. * 4bit, ** 8bit.

3.2.1. What is wrong with self-powered systems and intermittent computing?

Bearing in mind the harvested power densities (the estimated harvested power per cm² of a harvesting device) and the maximal power consumption requirements of some of the most energy-intensity components in table 1.4, one notices that almost all energy sources are insufficient to run continuously the main components of a sensor system at the same time (with the exception of solar-based EH sensor systems, but only in optimal conditions). Therefore, intermittent design, with checkpointing routines in Non-Volatile Memories (NVM) are necessary in most of the time. The problem is that, checkpointing schemes may exhaust writing cycles (the number of time that a memory block can be overwritten) of internal memories at a very fast pace, as Daulby, T. et al [24] argue. To defend their posture, they demonstrated that the lifetime spans of Spin-Transfer-Torque, Magnetic RAM memories (STT-MRAM) and Resistive RAM memories (ReRAM) are seriously reduced to less than 5 days, when a writing pace of 0,4 seconds (or, in other words, interruptions of 0,4 seconds) within a well-famous intermittent scheme called Hibernus++ [138] (figure 1.10) is applied.

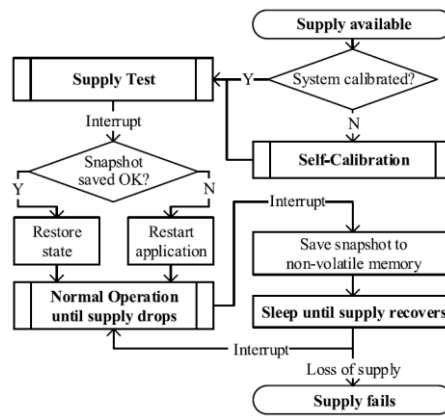


Figure 1.10. Intermittent operating schema of Hibernus++. Figure extracted from [138]. Low energy provokes an interruption and an overwrite (a “Save snapshot to non-volatile memory” step) in a memory block.

3.3. Less-material-oriented solutions and potential drawbacks

The perspective of “Do more with less” has also attracted the attention of researchers in recent years. For instance, Wagner, E. et al. [26] presented an environmental analysis of three full-integrated versions of a WSN sensor system prototype, with the aim of demonstrating the ecological benefits of miniaturization and function integration. Although less impacts are evidenced in high integrated prototypes (a reduction of 89% in the total Global Warming Potential (GWP), obtained by a reduced design (version V1, showed in figure 1.11a)), the authors warn potential conflicts through miniaturization (e.g., on recycling) leading to resource dissipation, and recommend further efforts to tackle this aspect. Moreover, a GWP per footprint comparison (Kg/cm^2) of the three versions shows that the GWP impact increase with the functional density, as figure 1.11b suggests (in other words, the environmental gains of using less active components and connections is eclipsed by the inclusion of more sophisticated packaging process that leads to higher concentration of impacts per surface unit).

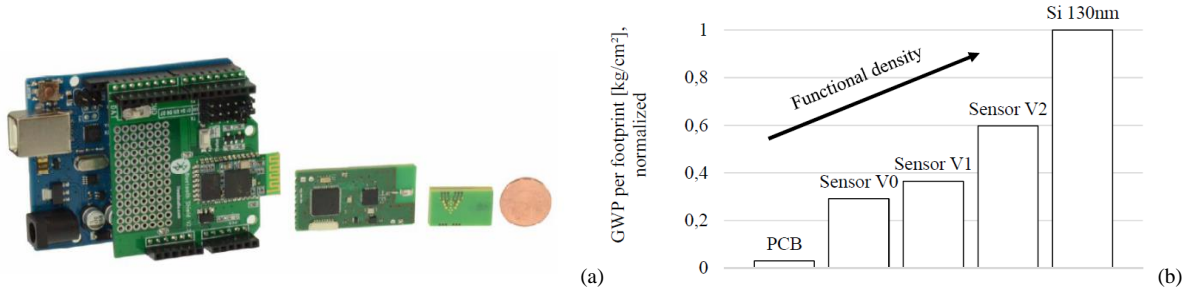


Figure 1.11. (a) High integration level of a sensor system. From left to right: V0 (customized open source solution), V1 (optimized design consisting of an implementation of selected functionalities, layouts and interfaces), V2 (full-integrated design consisting of advanced packaging through mixed-technology embedding of passives and active components). (b) GWP per footprint comparison (Kg/cm^2) of V0, V1 and V2; normalized to the impacts of an active microelectronic die (Si 130nm) and compared to a piece of an unpopulated PCB area. Figures extracted from [26].

In this line, Kasulaitis, B. et al. [114] advocates for a deep understanding of user-demanded functionality to achieve real impact reductions in a “doing more with less” perspective, and denounce a sort of technological capitalization within the established form factors in the semiconductor sector (see figure 1.12). This means that, in recent years, electronic component manufacturers tends to add more efficiency but keep the typical packaging sizes; leading to a dematerialization utopia, and technical-oversized designs of sensor systems.

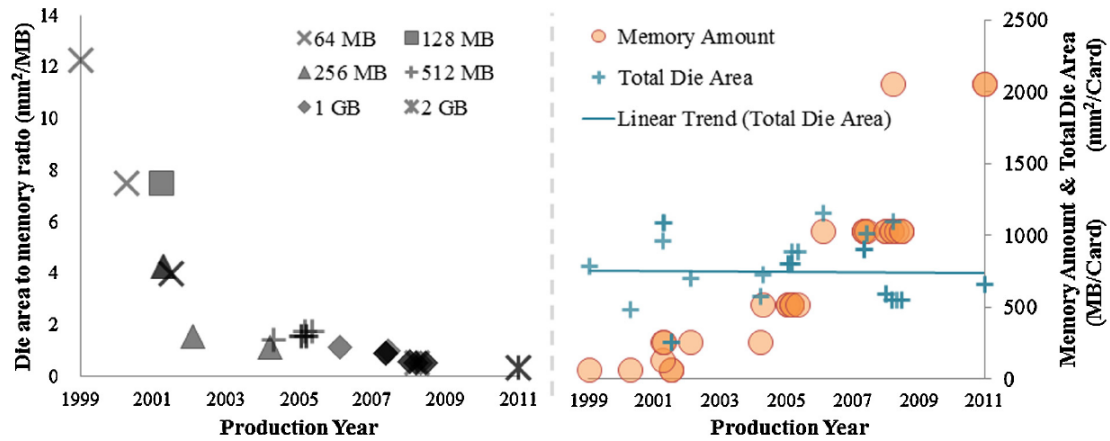


Figure 1.12. Technological capitalization of the established form-factors (typical packaging sizes in the sector) in DRAM memories. It shows that the gains in functional capacity (die area per function, left axis) are counteracted by increasing memory amount contained in each DRAM component (right axis). As a result, total DRAM die area per component is relatively constant (linear trend). Darker markers indicates multiple occurrences of the same combination. Figure extracted from [114].

3.4. End-of-Life Oriented solutions and potential drawbacks

Despite of the potential benefits from circular strategies, little was proposed for the specific field of IoT systems. Instead, researches oriented their efforts to circularity of smartphones —an edge device, normally used as an internet gateway for sensor systems. In 2020, Proske, M. et al. [28] reported significant benefits on resources preservation from repairing modular smartphones (figure 1.13a). Nevertheless, they explain that the significant impacts in the production phase is caused by a more complex core module (figure 1.13b), and clarify that potential benefits (up to 42% of GWP damage drop per year) would be expected only if modular smartphones are used for at least 7 years (assuming reparations in which faulty modules are replaced by new ones (repair scenario A) or faulty modules are repaired at board-level (repair scenario B)).

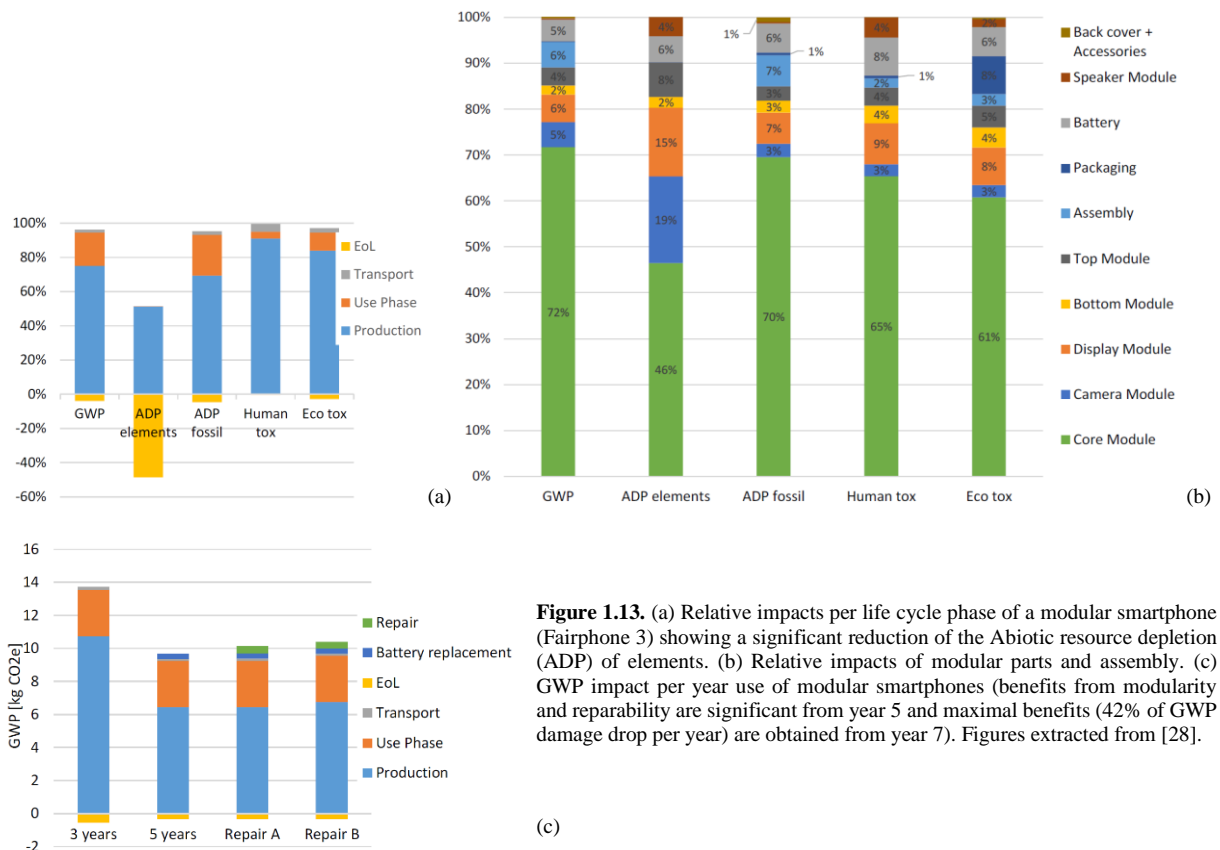


Figure 1.13. (a) Relative impacts per life cycle phase of a modular smartphone (Fairphone 3) showing a significant reduction of the Abiotic resource depletion (ADP) of elements. (b) Relative impacts of modular parts and assembly. (c) GWP impact per year use of modular smartphones (benefits from modularity and reparability are significant from year 5 and maximal benefits (42% of GWP damage drop per year) are obtained from year 7). Figures extracted from [28].

In this same line, a Material Flow Analysis (MFA) conducted by Söderman, M. L., & André, H. [112] demonstrates that losses of several metals can be reduced moderately when smartphones are repaired, with the exception of Indium (In) and Yttrium (Y), two metals whose losses increase in +9%, as it is showed in figure 1.14. This is explained by the fact that (1) Indium- and Yttrium-rich screens are the most replaced parts in repairing operations (that is, damaged screens are discarded and reemplaced constantly), (2) the lack of functional recycling of Indium and Yttrium in discarded screens and smartphones and (3) a short lifetime extension of repaired smartphones.

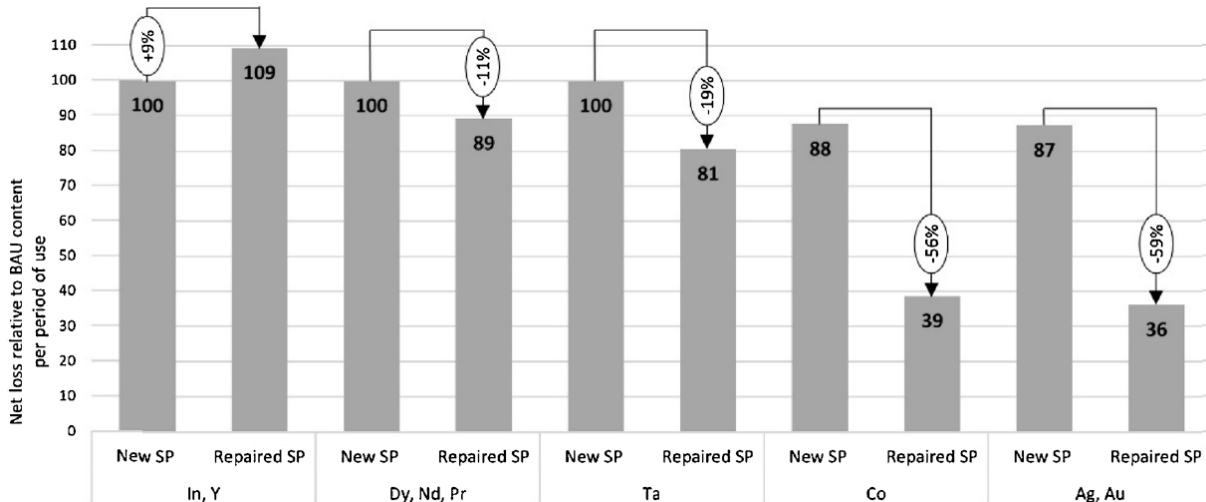


Figure 1.14. Net losses of metals of a repaired smartphone (repaired SP) relative to Business As Usual (BAU) product content (new smartphone (New SP)) per period of use. Figure extracted from [112].

4. Research questions

The uncontrolled increase of IoT devices and data that may pose stress not only to our environment (as suggested in section 2.3) but also to our resources (as seen in section 2.1), and the potential problems derived from green-IoT (section 3.1.1), EH systems and intermittent computing (section 3.2.1), and other interesting solutions (section 3.3 and 3.4); both reveal the difficulty of the main interrogation stated in the introduction section, and force its breakdown in the following research questions:

- **Research question 1:** How a designer can consider data flow within an IoT system in order to harmonize and reduce the potential impacts of promising initiatives?
- **Research question 2:** How a designer can disclose, measure and integrate key environmental aspects to the typical design of sensor systems and edge devices (local devices) in a practical, efficient and comprehensive way?

Chapter 2. Fundamentals of Data-driven design for sustainable IoT systems

Overview

This chapter is organized in five sections that shape the main approach for addressing the research questions presented in chapter 1. The first section dissects the data operational stages in IoT systems and infers essential aspects to be considered for sustainable design. The second section elucidates the concept of functional analysis in engineering design so that key functions in each data operational stages of IoT systems can be recognized. Based on that, this section recognizes the strong relationship between functions and capacities of electronic components and reveals the importance of right-provisioned design. On the other hand, the third section explores the data flow of a large-scaled IoT system to realize the prospective data volume magnitude in our current information age, contrasted with available data processing techniques; and the fourth section provides an example of the influence of data flow in sustainable IoT systems. The fifth Section concludes this chapter by presenting a Data-, information-driven design approach, based on supporting literature and on all the key aspects seen so far. All the findings of these sections will guide the literature review in chapter 3, and will help to build a design methodology for sustainable IoT Systems in chapter 4.

1. Data operational stages and relevant aspects regarding sensor system design

In general, the main operational stages of a sensor system include a data acquisition phase, a data processing phase (or pre-processing phase), a data storage phase and a data transmission phase [30]. Figure 2.1 shows these steps together with their possible interactions.

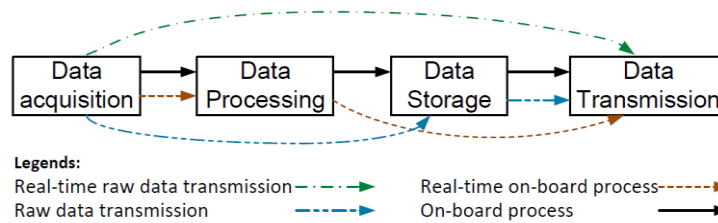


Figure 2.1. Main data operation stages of a sensor system. It could involve other devices and mutualized infrastructure. For sensor systems, the first and the last stages are present in all applications while the second and the third stages may or may not exist, depending on the data flow design of the application, available resources, etc. Figure extracted from [30].

In an on-board process, data is collected, processed and transmitted by the sensor system. A real-time on-board process usually involves some preprocessing routines over raw data while in a raw data transmission, bunch of raw data are saved in memory and transmitted periodically. A real-time raw data transmission describes scenarios where external sensor components are connected to the rest of a sensor system by physical means (i.e.: wired temperature probes).

1.1. Data acquisition

Data acquisition refers to collecting data from a number of analogue resources and converting it to digital form, suitable for transmission to a computation device [31]. One of the essential components of data acquisition is an Analog-to-Digital Converter (ADC) and alternatively, yet less commonly, a Digital-to-Analog Converter (DAC). Both converters use a reference voltage. The process of converting analog signals into digital formats involves two steps: quantifying (representing the continuous values of an analog signal using a set of discrete values) and codifying (representing discrete values by bit sequences) [32]. Figure 2.2a shows the Analog-to-Digital conversion of a 10V wave with a 3 bits sequence resolution.

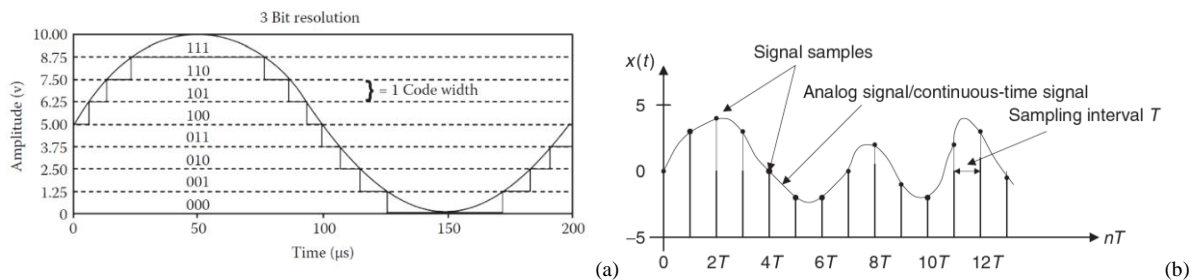


Figure 2.2. (a) ADC conversion of a 10V wave with a 3 bits sequence resolution [32]. The number of bit sequences determines the number of possible discrete values of the conversion, and the ADC resolution level. (b) A sampling rate of 1 Hz for an analog signal (1 signal sample per 1 Sec, assuming $T = 1\text{sec}$) [33].

One of the important aspects to consider in design the data collection step is the relationship between ADC capacities and the appropriated sampling rate of the application. A sampling rate is the number of digital samples that are obtained from an analog signal in one second and is commonly measured in Hertz (Hz) (see Figure 2.2 b). High accuracy applications (such as sound- or image-based applications) require high sampling rates and high resolutions. Unfortunately, the higher the sampling rate, the more volume of data generated.

1.2.Data processing

Data processing refers to the preliminary or main processing, storing or pre-transmission tasks over raw data. MCUs are fundamental components in this operational stage. Figure 2.3, shows some of the essential resources of modern MCUs that allows data processing tasks.

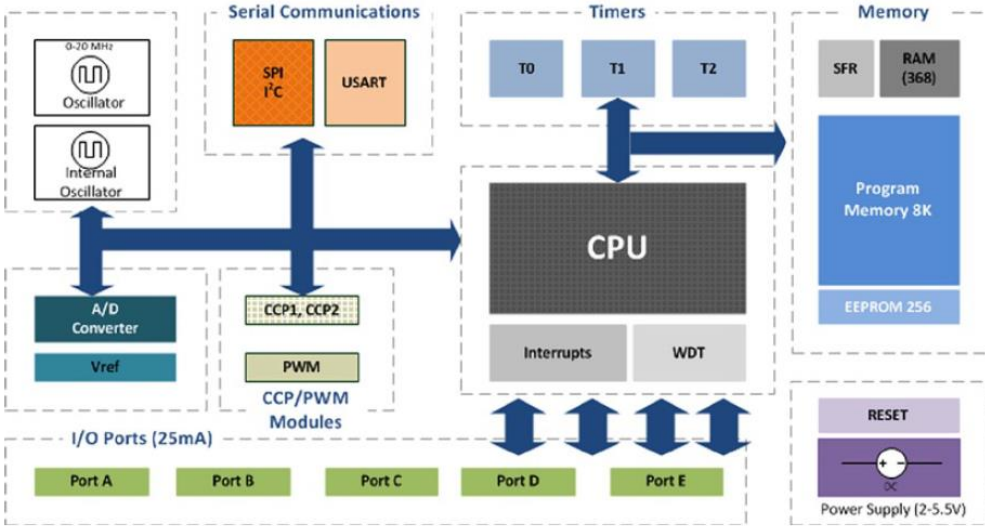


Figure 2.3. Hardware resources of modern MCUs for sensor systems [198]. Important aspects of all these elements are summarized in the three paragraphs below, according to the descriptions provided by the authors.

The Central Process Unit (CPU) or microprocessor makes calculations in a period of time (processor speed/frequency) and with a certain quantity of energy. As microprocessors work concurrently, interrupts (software- or hardware-based calls) are needed, to stop the normal execution of a program periodically. In this sense, microprocessors also use Watchdog Timers (WDT) to ensure that a program does not get trapped in an inconsistent state. On the other hand, ADC conversion (A/D) processes may require additional calculations such as filtering and signal isolation; or waveform modulations (which is usually performed by Capture Compare Pulse (CPP) and Pulse Width Modulated (PWM) modules).

Serial communications are bus-typed synchronous (i.e.: I²C or Serial Peripheral Interfaces (SPI)) or asynchronous (i.e.: RS232/RS485) interfaces that communicate MCUs with other components of a sensor system (such as wireless communication modules or external memories). Additionally, Input/Output (I/O) ports facilitates full connectivity and may include General Purpose Input/Output (GPIO) programmable pins to act as input interfaces for sensor data, or as output interfaces to control external components.

Timers are commonly used to generate precise time delays by counting fixed intervals of time, or to act as a real-time clocks, or to initiate specific events (e.g., interruptions). In this sense, internal oscillators use quartz crystal to generate precise, stable time pulses and generate time signals. Also, microcontrollers usually integrate crystal-based Real Time clocks (RTC) to keep accurate time. Finally, internal MCU's memories store program codes, raw or processed data of the application in NVM memories. Common NVM technology includes some emerging non-volatile RAM, ROM, Flash and EEPROM memories (described later in the next section).

In a sensor system, MCUs coexist with other electronic components within the main PCB. However, emerging technologies such as System-in-package (SiP) or System-On-Chip (SoC) tends to integrate all or some of these components in a single package or chip. SoC integrates ICs with different functions

such as CPU, GPU (Graphic Processing Unit), memory, etc. into a single chip for a system or a subsystem, while SiP uses packaging technology to integrate dissimilar chips with different materials and functions, and from different design houses, foundries, wafer sizes, features sizes and companies into a single package [34]. Figure 2.4 illustrated the difference between a SoC and SiP products.

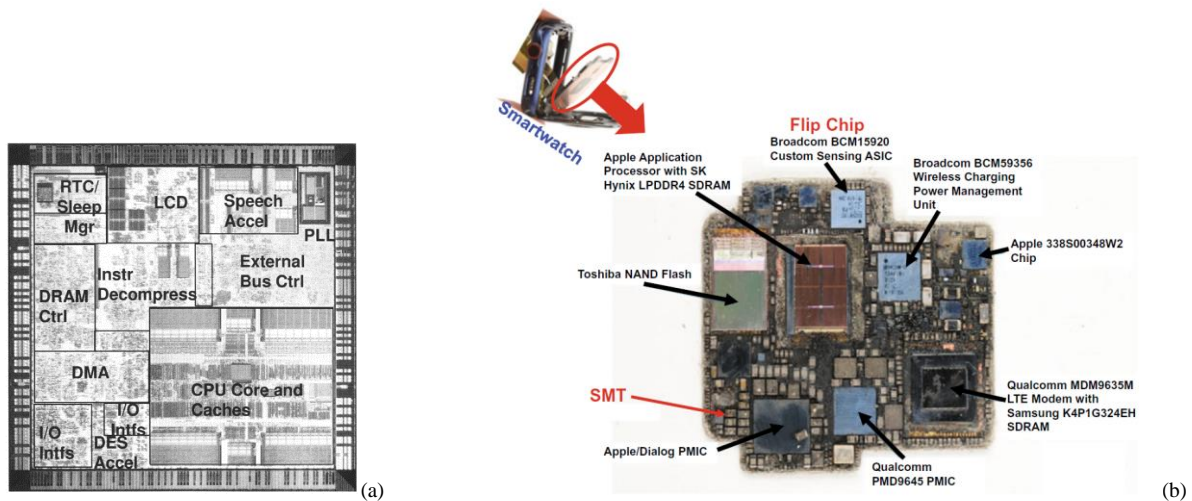


Figure 2.4. (a) A photograph of a SoC die after processing of the third level metallization. (b) SiP for Apple Watch series 4. Both figures were extracted from [35]

Such integration degree may avoid additional components and related materials, but would lead to an increase of damage with an increase of functional density, as seen in the section 3.3 of chapter 1. On the other hand, several studies in the context of IoT [26], [73-75], attribute significant environmental loads to semiconductors. This is the reason why selection of right-provisioned MCU is of paramount importance, as it will be further evidenced in section 2.

1.3.Data storage

Data storage refers exclusively to the storage of data application and usually use additional memories. Basic rewriteable NVM types consists of Flash and EEPROM memories and some of the emerging technologies includes Magnetic Random Access Memories (MRAM), Resistive Random Access Memories (ReRAM or RRAM), Phase Change Memories (PCM) and Ferroelectric Random Access Memories (FeRAM). Typical Flash memories are low-cost devices with moderate and high storage capacity. They are faster in writing but slower in erasing routines and suffer from fast degradation. On the contrary, EEPROM memories have high endurance and, in general, they are faster than Flash memories but more expensive, with low storage capacity. Emerging memory technologies have emerged precisely to overcome these and other shortcomings. Some of the most relevant features of NVMs are the writing cycle time and the writing endurance rate [36]. Designer of sensor systems usually considers these two aspects, together with cost, memory densities and other requirements and constraints of IoT systems (See Figure 2.5).

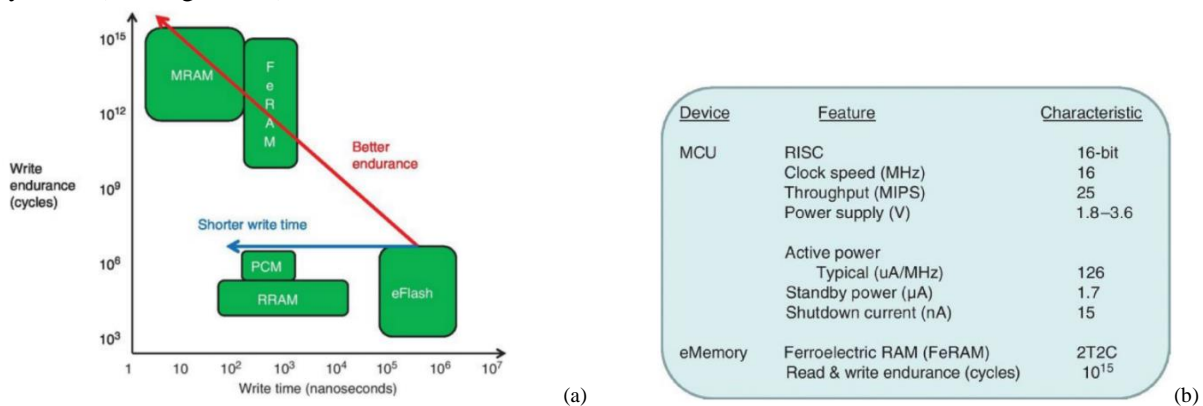


Figure 2.5. (a) Write endurance versus write time for different types of memories. (b) A 2-transistor-2-capacitor-based (2T2C) embedded FeRAM memory for a commercial ultralow power MCU oriented to EH systems. Both figures are extracted from [36].

Bad decisions on write endurance criteria may lead to the early replacement of a device due to writing-reading errors, as it will be further discussed on chapter 4.

1.4.Data transmission

Data transmission refers to specific tasks oriented to transmitting raw data or refined data to edge, fog or cloud resources. To do this, wireless, and less common wired means are used; and several technologies, together with technical and networking aspects are taken into account. For example, figure 2.6 compares different wireless technologies, on the basis of two technical aspects (i.e.; Power-consumption and data rate) and a network aspect (distance range).

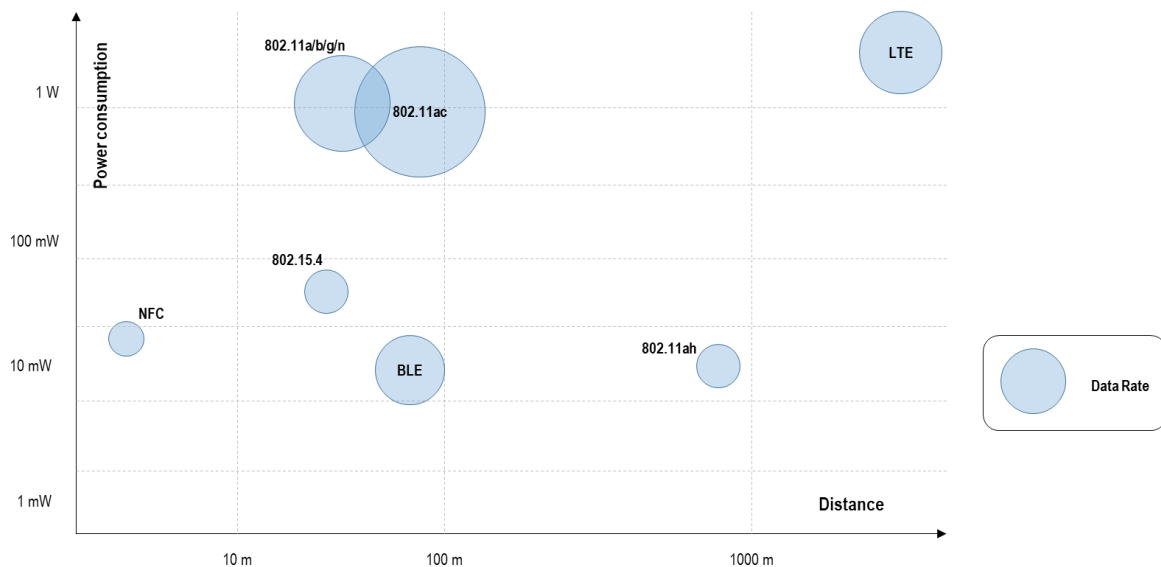


Figure 2.6. Power Consumption versus Distance range for different wireless technology used in IoT systems: Near Field Communication (NFC), 802.11a/b/g/n (WiFi), 802.11ac (WiFi 5), WiFi 802.11ah (WiFi HaLow), 802.15.4 (Low-Rate Wireless Personal Area Networks (LR-WPANs) such as Zigbee), Bluetooth Low Energy (BLE) and Long-Term Evolution (LTE) wireless broadband communication technology (i.e.: GSM, 4G, 5G). Figure adapted from [37].

The data rate can be seen as the speed at which two computer devices, over a link or channel, transfer data. On the other hand, the required power to do that may vary according to several parameters, depending of the selected transmission channel. In wireless communication, three of the many parameters that affects significantly the power consumption of a wireless interface are its power consumption for transmitting (Tx), the power consumption for hearing a channel and receiving a transmission (Rx), and also the period of time within these actions are executed (usually called Active, Idle and Sleep states).

Thus, for this operational stage, fundamental questions in design includes which communication technology select (according to several criteria such as data rates, Tx and Rx power consumption, or distance ranges) , and what tradeoffs between quality of service (QoS) and energy consumption; or between on-board processing and computing offloading should be made [30]. Answers to these questions may extremely affect the environmental impact of and IoT system as is further explained in section 5.

2. Functional analysis and right-provisioning design

The idea of function and functional analysis in design are widespread and there is no seminal definitions in literature. However, a generally accepted notion found in engineering manuals and textbooks says that a function is an action made by a product, expressed by a goal to be achieved. In general, there are three types of functions: main functions (essential functions of a product that justify its creation, for example “monitor water consumption”), complementary functions (supporting functions related to main functions, for example “connect to internet”) and constraint functions (for example “RoHS certified”). On the other hand, a functional analysis aims to summary, characterize, order, rank and weight the functions of a product. Some of the classic tools to conduct a functional analysis are octopus diagrams,

Function-Analysis-System-Techniques (FAST), and Structured Analysis Design Techniques (SADT). Figure 2.7 illustrate an octopus diagram.

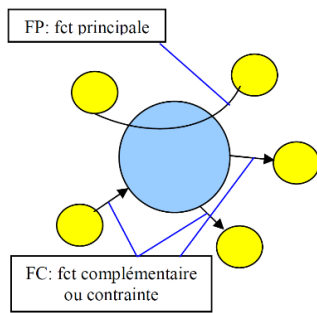


Figure 2.7. The basic elements of an octopus diagram. The blue circle represents the product and the yellow circles external elements of its operational environment. Links passing through the product represent main functions (FP) and directional links represent complementary, and constraint functions (FC). Figure extracted from [233].

The outcomes of the functional analysis is saved in a list of specifications that may or may not contain technical details. In the context of IoT systems; all sensors, sensor systems, edge and cloud devices should be designed to cover these specifications with the right-provisioned resources. A right-provisioned device is a neither under- nor over-provisioned device that executes specific functions [38]. Figure 2.8 shows the idea behind right-provisioning design, which involves allowing for some kind of “provisioning slack”.

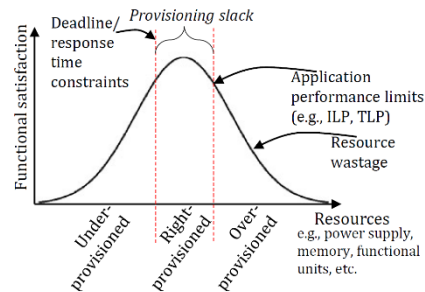


Figure 2.8. The provisioning slack of right-provisioning design. Figure extracted from [38].

In figure 2.8, a device is under-provisioned when is unable to satisfy the application’s functional requirements such as deadlines or response time constraints. On the contrary, a device may be over-provisioned with out-of-order execution resources if, for example, the application has limited Instruction Level Parallelism (ILP) and the application’s instructions execute necessarily in order [39]. Sometimes over-provisioned resources could be leveraged for other applications while in other cases; they are simple wasted [38].

2.1.Functions and capacities of electronic components

The development of a right-provisioned IoT devices would start from an exhaustive functional analysis, which should be decomposed in specific tasks-functions within each data operational stage of a specific application. This would dictate later critical specifications to take into account for design (figure 2.9).

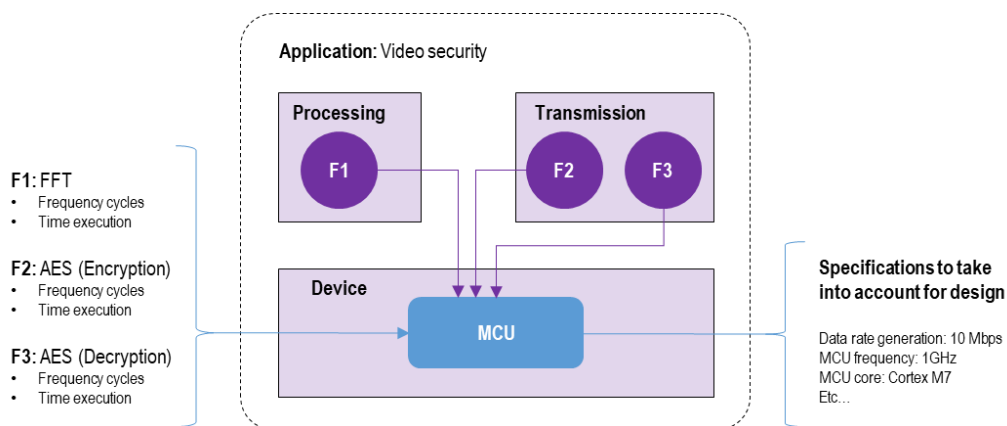
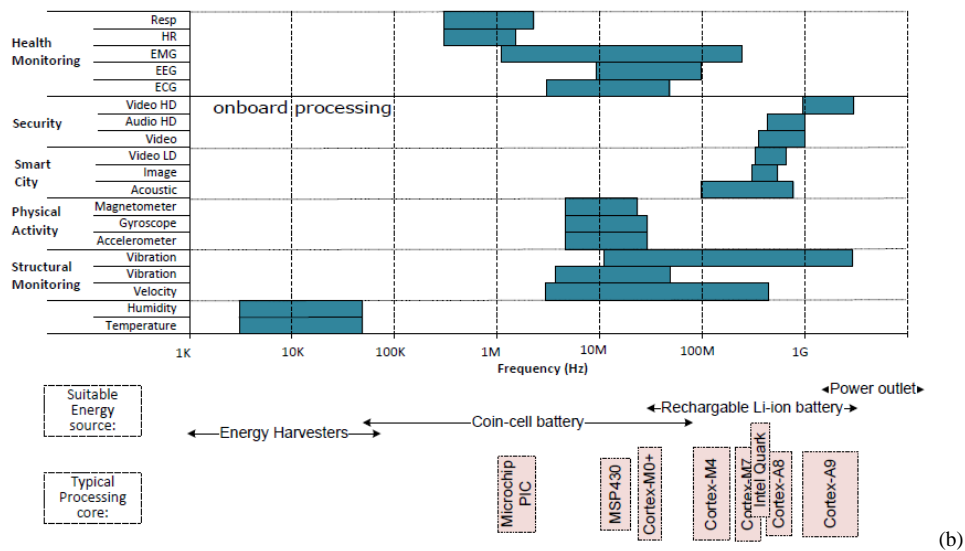
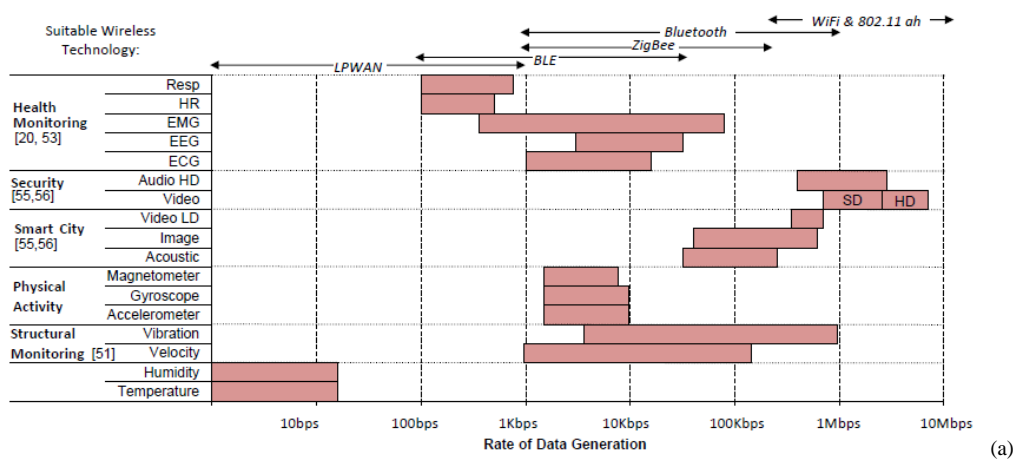


Figure 2.9. An instance of a hypothetical right-provisioned IoT device from the analysis of specific functions in the data processing stage (for example Fast Fourier Transform (FFT)) and data transmission stage (for example Advanced Encryption Standard (AES) encryption/decryption), of the application “Video surveillance”. It assumes a device composed of only one component (MCU) and it considers the typical functions (F1, F2 and F3), parameters (e.g., Frequency cycles, time execution) and specifications suggested in [30]. The figure summarizes the key idea of right-provisioned electronic components found in current literature (blue elements) and adds the suggested idea of right-provisioned IoT Devices in terms of functions and data operational stages (purple elements).

This postulate was partially, and implicitly assumed but only for electronic components. For example, based on the typical data resolution and sampling rates of common applications presented in previous work [40-41]; and on experimental data of Central Process Unit (CPU) cycles and execution times seen in specific functions (operations) of a commercial microcontroller oriented to sensor systems (see table 2.1), Samie, F. et al. [30] derived the maximal data rate generation and the minimal MCU frequencies to consider in different IoT applications (Figure 2.10).

Operation	Exe. time [μs]	# of cycles	Code Size [B]	
FFT (256 p)	18	586	3850	
FIR	1492	23872	1750	
AES	Enc	18.25	292	3666
	Dec	22.75	364	
CRC	3.75	60	500	

Table 2.1. Atmega328 MCU execution times and number of cycles for typical data processing functions on raw data (FFT and Finite Impulse Response (FIR)); and data transmission operations (Advanced Encryption Standard (AES) and Cyclic Redundancy Check (CRC)).
Table extracted from [30].



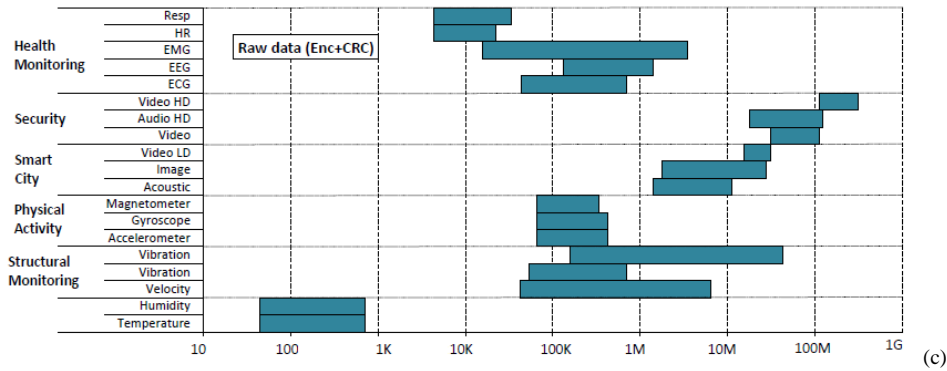


Figure 2.10. (a) Data rate generation of different sensor applications and suitable communication technology. (b) Required MCU frequency to fully process sensors raw data together with their typical power source and suitable microprocessor cores. (c) Required MCU frequency to encrypt and transmit data. All figures were extracted from [30].

For their part, Adegbija, T. et al. [42] present a set of four high-level microarchitecture configurations for sensor computing, on the basis of processing power and four kinds of commercial microprocessors (MCU configurations, as showed in table 2.2).

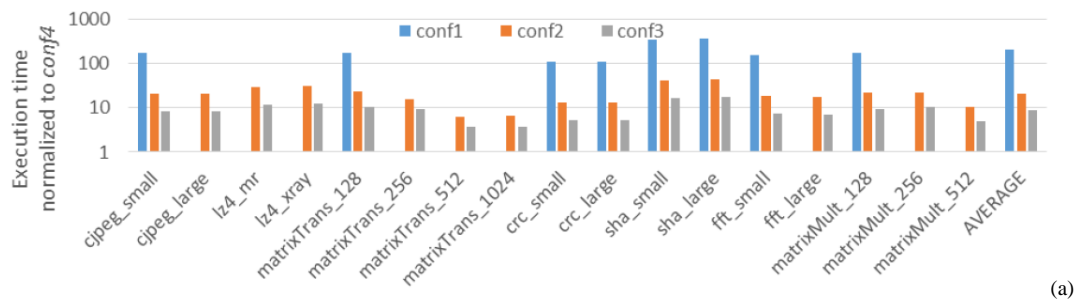
	Config1	Config2	Config3	Config4
Sample CPU	ARM Cortex M4	Intel Quark	ARM Cortex A7	ARM Cortex A15
Frequency	48 MHz	400 MHz	1 GHz	1.9 GHz
Number of cores	1	1	4	4
Pipeline stages	3	5	8	15
Cache	None	None	32KB I/D L1, 1MB L2	32KB I/D L1, 2MB L2
Memory	512KB flash	2GB RAM	2GB RAM support	1TB RAM support
Execution	In-order	In-order	In-order	Out-of-order

Table 2.2. IoT microprocessor configurations for sensor computing. The configuration 1 (config1) represents a low-power and low-performance MCU, the configuration 2 (config2); a recently-developed IoT targeted CPU, the configuration 3 (config3); a mid-range CPU and configuration 4 (config4); a high-end, high-performance embedded system CPU. Table extracted from [42].

Based on this classification, on a six-step design method that includes seven key functions (including sensing, communication, image processing, compressions, security and fault tolerance) and on typical computational kernels (atomic, basic processing tasks presented in table 2.3), Adegbija, T. et al. [39] conducted a simulation-based, comparative study on the basis of four criteria: execution time, energy consumption, performance and efficiency (see figure 2.11).

Application function	Benchmarks	Benchmark description
Sensing	<i>matrixTrans</i> (<i>_128</i> , <i>_256</i> , <i>_512</i> , <i>_1024</i>)	Dense matrix transpose of $n \times n$ matrix
Communications	<i>fft</i> (<i>_small</i> and <i>_large</i>)	Fast Fourier Transform (FFT)
Image processing	<i>matrixMult</i> (<i>_128</i> , <i>_256</i> , <i>_512</i>)	Dense matrix multiplication of $n \times n$ matrix
Lossy compression	<i>jpeg</i> (<i>_small</i> and <i>_large</i>)	Joint Photographic Experts Group (JPEG) compression
Lossless compression	<i>lz4</i> (<i>_mr</i> and <i>_xray</i>)	Lossless data compression
Security	<i>sha</i> (<i>_small</i> and <i>_large</i>)	Secure hash algorithm
Fault tolerance	<i>crc</i> (<i>_small</i> and <i>_large</i>)	Cyclic redundancy check

Table 2.3. Common IoT Application functions and representative computational kernels for comparison (benchmarks). Table extracted from [39]



(a)

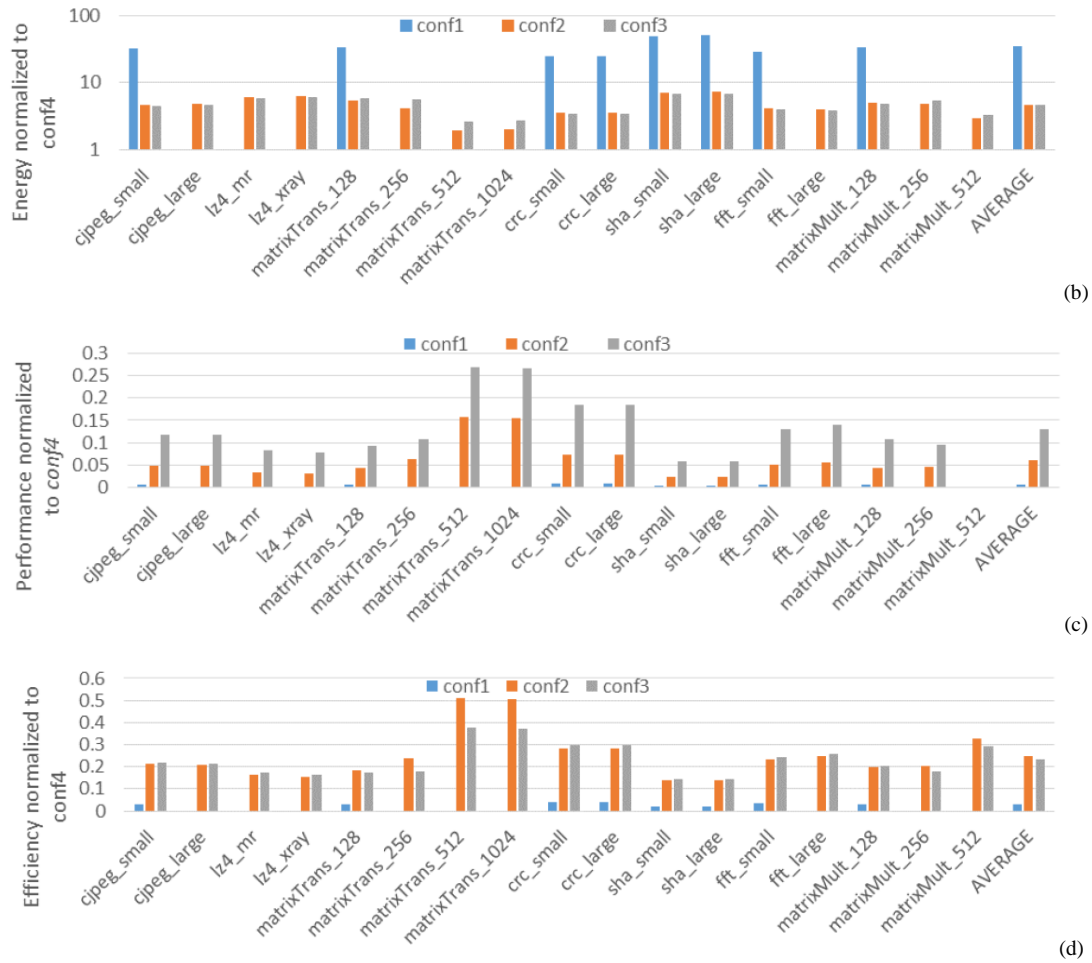


Figure 2.11. Comparison of four configurations (conf1, 2, 3, 4) of commercial IoT microprocessors on the basis of computational kernels and four criteria: (a) Execution time. (b) Energy consumption. (c) Performance (in Giga Operations Per Second (GOPS)). (d) Efficiency (in GOPS per Watt (GOPS / W)). Conf4 is the base configuration for comparisons due to its high resource availability. All figures are extracted from [39].

In this way, the authors found that compared to conf4; conf1, conf2 and conf3 increased the average execution time by a factor of 202x, 23x, and 9x (figure 2.11a); and increased the energy consumption by a factor of 35x, 4.6x, and 4.7x respectively (figure 2.11b). Conf4 had the lowest energy consumption because of its significant reduction in execution time. For performance, their results show that conf1, conf2, and conf3 degraded the performance by a factor of 171x, 17x, and 8x (figure 2.11c). For efficiency, conf1 degraded the degree of effectiveness by a factor of 33x. Conf2 and conf3 degraded the efficiency by a factor of 4x (figure 2.11d). On the other hand, the authors clarify that the significant benefits from conf4 are only viable in systems that are not energy-constrained (e.g., MCUs that are constantly connected to a power source) and conclude, interestingly, that key aspects like clock frequency and execution order, together with input data size, are of a paramount importance for the design of IoT microprocessors.

So far, the evidence shows that the appropriated analysis of functions, involved specifications and tradeoffs of available capacities (i.e.; configurations) of electronic components along the data operational stages allows the design of right-provisioned sensor systems. The further interactions of these right-provisioned sensor systems with the rest of the edge, fog and cloud devices compose the global dataflow design of IoT system.

3. Dataflow issues in IoT Systems and common solutions

In the last years, the growing deployment of sensor systems and the increasingly consumer demands for high-performance IoT applications involving acquisition and transmission of complex data have posed significant bandwidth and latency challenges [42]. In this context, the mutualized infrastructures face particular problems including scalability, energy consumption and availability [30] that force rethinking

data management in IoT systems. For example, from an experimental study based on a data collection platform called Sentilo [42-43] that centralized data from more than 1800 sensor devices in a region of Barcelona, researchers estimated a total data generation rate of 8GB per day [5], and advocated for clear and stable long-term data management solutions if whole coverage of the city were envisioned (which means a colossal deployment of more than 320M of sensor devices). Such management solutions could be oriented to reduce the data transfer volume by reducing transmission frequencies or applying specific data manipulation preprocessing techniques in edge devices and fog resources (e.g., data aggregation, data compression or approximate computing).

Data aggregation consists of combining and summarizing the data coming from different sources in order to eliminate redundancy and minimize transmissions [45]. Figure 2.12 show two typical data aggregation scenarios applied on raw sensor data (temporal and spatial correlations).

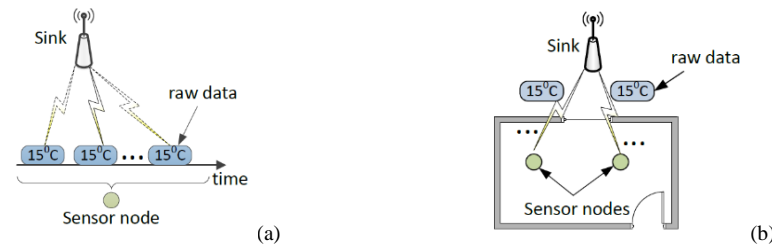


Figure 2.12. (a) Temporal correlation: raw data value of one or more sensor systems normally keep constant in a specific period. (b) Spatial correlation: raw data values of nearby sensor systems is often similar. Both figures are extracted from [46].

Aggregating data is about computing-memory intensity algorithms involving mathematical computations (addition, minimum, maximum, mean, etc.) or energy-expensive complex routines such as fusion vector data like video streams from multiple sources [42]. In the same way, data compression and approximate computing techniques are two energy-intensive techniques. The former removes statistically redundant data in order to present concisely data, and the latter allows non-exact, inaccurate results for resilient applications that can produce outputs of sufficient quality, despite some imprecise computations [42, 47].

Although approximate computing and data aggregation and compression may reduce significantly the data transfer volume of IoT systems, such techniques demand more energy and higher capacities locally. Unfortunately, IoT device makers tend to address these issues by developing more complex and unnecessary over-provisioned products, which usually results in impact transfers to manufacturing phases and/or complications on the redesign of low-energy-oriented devices.

4. Dataflow design and information science theory for IoT systems

In a sustainable IoT system, tasks in all data operational stages depend not only on the available resources of electronic components, but also on specific aspects of the information that is required by the application. For example, Bonvoisin, J. et al. [10] reconsidered the needed information of an IoT system oriented to urban garbage collection application (here called service), and demonstrated significant impact reductions based on hardware, data and information redesign (Figure 2.13).

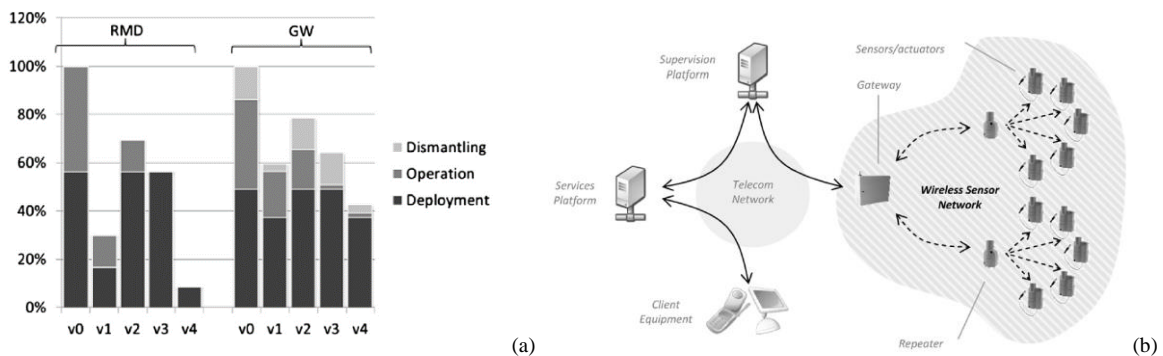


Figure 2.13. (a) Raw Material Depletion (RMD) and Global Warming (GW) impacts comparison of an IoT system baseline (V0), a hardware level eco-designed version (V1), a hearing-sensibility eco-designed version (V2), an information eco-designed version (V3) and a combination of all alternatives (V4). (b) The deployment of the IoT system baseline. Both figures are extracted from [10].

In figure 2.13a, V0 represents the impacts of the baseline design of an IoT system that adapt truck routes in function of the waste containers levels in the city of Grenoble (France). In this baseline design, a battery-based sensor system is embedded into a garbage container and it is isolated with resin. Also, 40% of its energy consumption is due to overhearing (hearing message not intended to reach it) increasing its potential replacement in a period of 10 years (because of its drained battery). V1 represents an alternative design in which the isolation resin is replaced by hermetic insulation, facilitating the reuse or recyclability of embedded sensor systems. V2 suggests auto-reducing the hearing sensibility so that a sensor system be able to hear and understand only 95% of messages sent by its neighbors. V3 proposes using the average fill rate of containers in order to adapt the message transmission frequency of sensor systems (if the container level is below 50%, the sensor calculates the expected time at which the level should reach 50%. Above 50%, new and more frequent measurements are planned, based on historical data and simple calculations). V4 combines V1, V2 and V3.

V1 can lead to a recovery of 85% of raw materials in end-of-life phases of sensor systems and brings a reduction of 40% in the GWP damage if applying repairing or remanufacturing strategies. V2 reduces the RMD and GWP impacts in 31% and 21% respectively because sensors decrease their energy consumption and increase their batteries lifetime. V3 leads to low data traffic and energy consumption by sensors, which contributes to a reduction of 44% and 36% for the RMD and GWP impacts respectively (there are no device replacements in this alternative).

In this study, V2 and V3 design alternatives were obtained from applying a specialized ICT service design framework that involves rethinking the appropriateness of data and information in an information eco-design step (figure 2.14a). This framework was developed on the basis of a rationale of Information Science, which is showed in figure 2.14b.

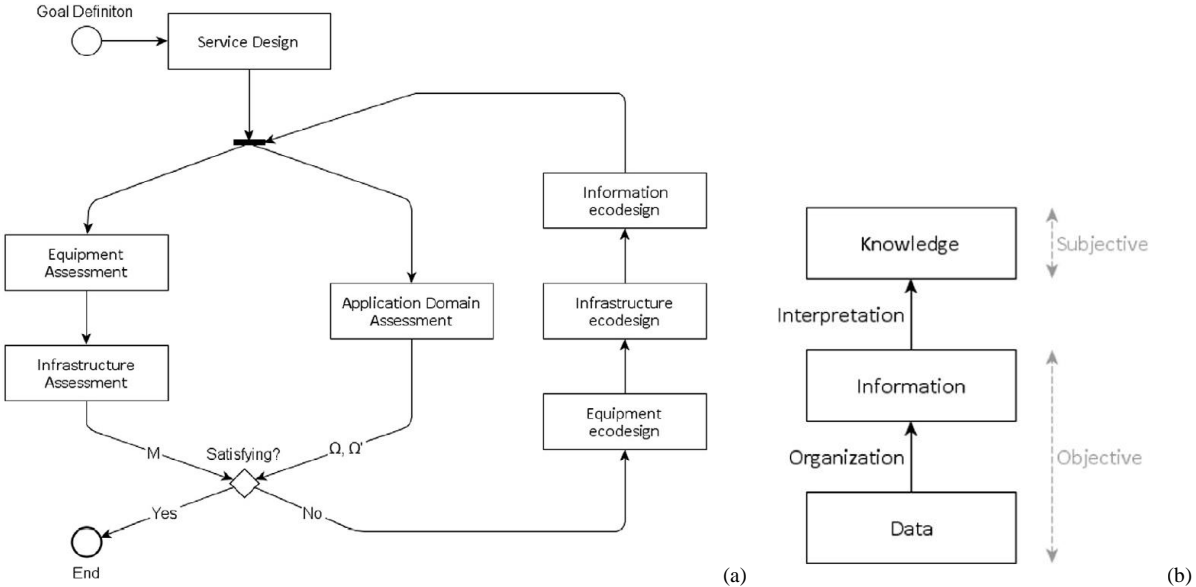


Figure 2.14. (a) Eco-design method for optimization of ICT services. (b) Rationale of Information Science canon. Both figures are extracted from [10]

In figure 2.14b, the data, information and knowledge structural canon refers to the widespread Data Information Knowledge Wisdom (DIKW) pyramidal model of information science. Although there exist many definition for each of the elements of this model in literature; here, data could be defined as a sensory stimuli, which we perceive by our senses —or sensor components, and information is just organized data that infers facts, figures and other forms of meaningful representations that are used to enhance the understanding of something [49]. In figure 2.14b, while data and information are objectives elements, knowledge depends on a human or machine interpretation. In the next sections, the subjacent data, information and knowledge structure of IoT systems is disclosed, together with its central role in technical and ecological design.

5. Data- and Information-driven design

As it is mentioned early in chapter 1, raw data of IoT systems is perceived by sensor components through a transduction step, either by direct contact with the object in which the phenomena is produced (i.e.: liquid, gases, human body, etc.) or indirect contact (i.e.: passive infrared) or sample removal [198]. Depending on the way by which this data is collected and organized, essential yet substantial information can be obtained. For example, consider a float-switch-based and an ultrasonic-based IoT systems for liquid content level monitoring, both depicted in figure 2.15.

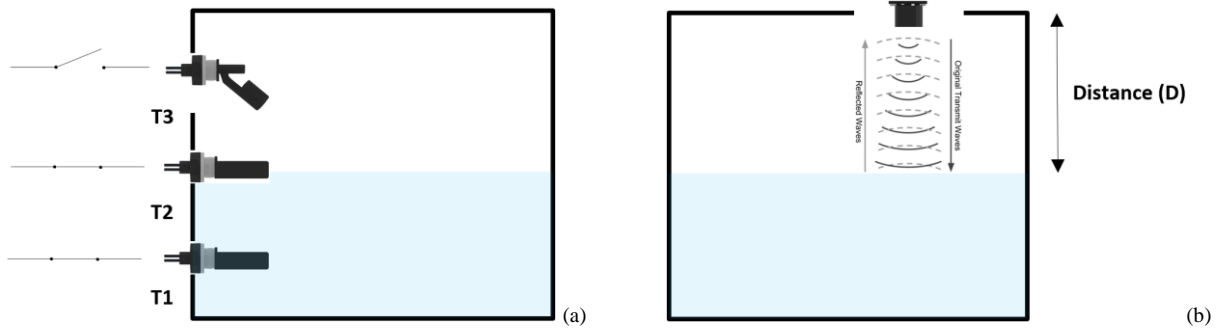


Figure 2.15. (a) A float-switch-based IoT system. (b) An ultrasonic-based IoT system. Both systems are oriented to measure the liquid level of a recipient.

The float-switch-based IoT system uses floats that raise or lower, opening or closing circuits, as the liquid level raises or lowers. On the other hand, the ultrasonic-based IoT system uses ultrasonic sensors like that one in figure 2.15b, which are piezoelectric-based components that work by emitting and receiving ultrasonic waves. Essential information of both systems can be obtained from the organization of raw data: in the float-switch-based IoT system, time (T3) can be estimated from historical data (T1 and T2) while in the ultrasonic-based IoT system, the same information can be obtained approximately by considering the Distance (D) as a function of the time it takes for the waves to reflect back (time of flight):

$$Distance (D) = \frac{Speed\ of\ sound\ in\ Air * Time\ of\ flight}{2} \quad (2.1)$$

Obviously, both systems have their advantages and disadvantages and selecting one over the other will depend on the functional analysis of the system adapted to different data operational stages, its requirements and the application type (here, point level measurement versus continuous level measurement). For example, for the float-switch-based system described in figure 2.15a, an electronic design based on an open collector circuit with a pull-up resistor may be sufficient to storage the counts of electrical signals, later interpreted as the liquid level of the recipient. In contrast, the ultrasonic-based system (figure 2.15b) may require embedding the computation of equation 2.1 into the microprocessor of an ultrasonic sensor component.

5.1.Relevance of data- and information-driven design for technical design

There is evidence showing that only a thoughtful analysis on essential data and information allows a correct design of IoT systems. For example, by considering the acceleration of gravity and the rotation angular velocity (essential Data) of MEMS sensors (accelerometer and gyroscope), Ishida, K. [50] obtained essential information (user motions) for an IoT system oriented to smart training. Specifically, he developed a sport-service-oriented IoT system based on an analysis phase for skills and a service phase for training of a complex sport (skateboarding) (Figure 2.16). In the analysis phase, high-sampling-rate data needs to be collected from wearable sensors. The raw data collected in this phase is later sent to a cloud server, which evaluates important indexes such as motion amplitude or counter-motion (basic information). On the contrary, in the service phase, low-sampling-rate data is processed on the wearable sensors or other edges devices, based on evaluation indexes already obtained in the analysis phase.

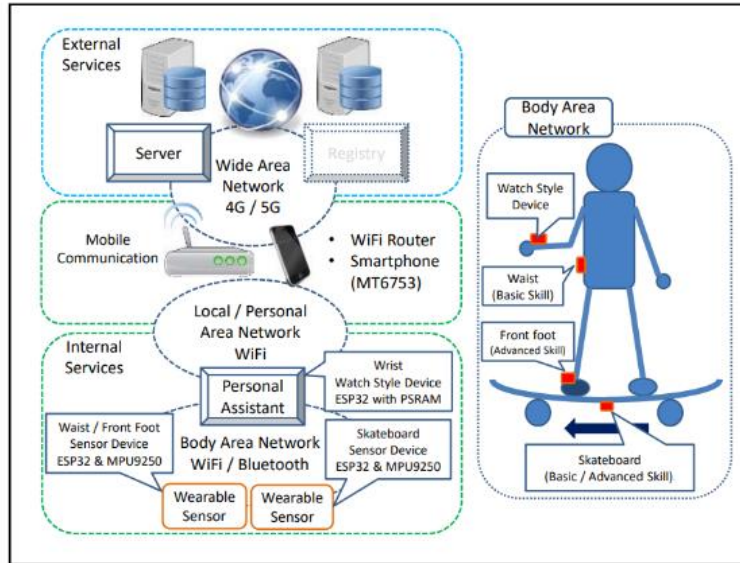


Figure 2.16. A Sport-service-oriented IoT system for skill analysis and skill acquisition and improvement of skateboarding [50]. The IoT system provides service for two specific techniques: Swing and lean motions (basic skills) and flipping the board (advanced technique).

As showed in Table 2.4, the proposed data- and information-design would mobilize only the sufficient resources and reveals two aspects. Firstly, it determines (1) where the computing load will be placed (edge or cloud computing), accordingly to the data generation rates and computation complexity (see table 2.5); and (2) the use of additional resources such as SD memories (temporary storage).

Secondly, it demonstrates the relevance of functions and capacities of electronic components. For example, the electronic design of the proposed IoT system highly depends on the data transfer rate capacities of available technology (i.e.: WiFi in the case of the analysis phase and Bluetooth in the case of the service phase); and on specific features of raw data (such as sample rates of the inertial sensors, transfer rates of UDP/Bluetooth packets, maximum number of Bluetooth connections, and the needed sampling rates for different sport techniques (50Hz for basic skills and 200Hz for advanced skills)).

	Basic Skill	Advanced Skill
Necessary sampling rate for wearable sensor	50-Hz ESP32 with MPU9250 (100 Hz) is suitable.	100-Hz to 200-Hz ESP32 with MPU9250 (100 Hz) might not show a clear difference between successful and failed cases.
Analysis Phase	WiFi router is applicable. ESP32 and MT6735 are also applicable for sending multiple data readings in a UDP packet. Bluetooth is not applicable.	WiFi router, ESP32, and MT6735 are applicable for sending multiple data readings in a UDP packet. Bluetooth is not applicable.
Service Phase	WiFi router is applicable for handling three indexes (i.e., amplitude, periodicity, and counter-motion). Bluetooth is applicable for two indexes (i.e., amplitude and periodicity).	WiFi router is applicable for finding difference between successful and failed cases at 10 milliseconds. Bluetooth is not applicable.

Table 2.4. Design of sensor systems and edge devices providing sufficient resources for the sport-service-oriented IoT system. Table extracted from [50]. To gain an idea of the power consumption of Bluetooth and WiFi, the reader can consult the figure 2.6 in section 1.4.

	Analysis Phase	Service Phase
WAN transfer rate	High: Raw data	Low: summary
Temporary storage	Not required	Required
Computation complexity	Low on edge High on cloud	High on edge Low on cloud

Table 2.5. Edge and cloud computing allocation (computation complexity) and temporary storage design based on data transfer rates and information in the analysis and service phases (motion amplitude and counter motion). Table extracted from [50].

5.2.Relevance of data- and information-driven design for sustainable design

There is also evidence showing that abundant data affects negatively the ecological design of IoT systems, providing insignificant contributions to information requirements. For example, Lelah, A. et al. [51] reported a respective increase of 62%, 27%, 24% and 17% in the Energy Depletion (ED), GWP, Hazardous Waste Production (HWP) and Air Toxicity (AT) impacts categories of a garbage-collection IoT System when increasing data transmission frequency of sensor systems from 1 to 24 transmissions per day (see figure 2.17b).

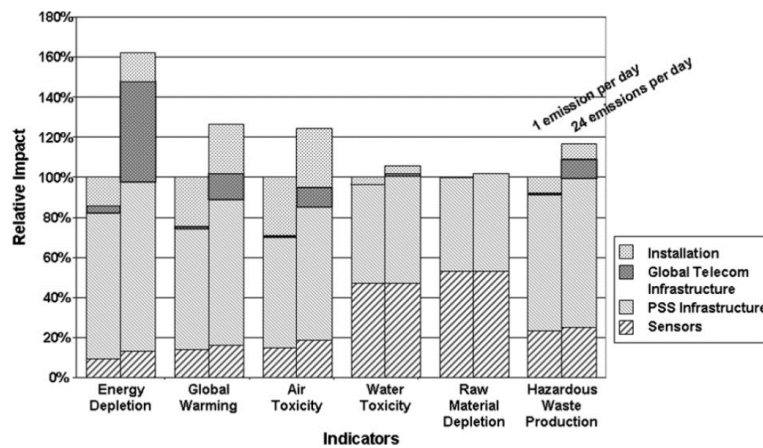
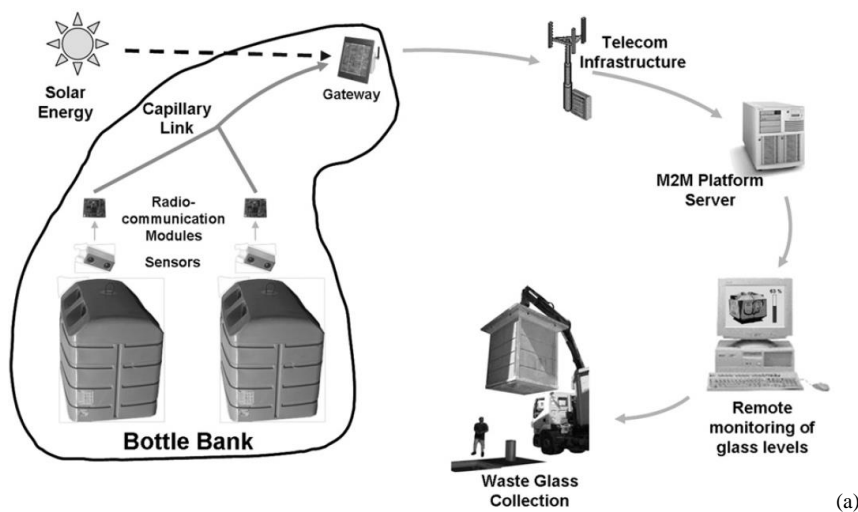


Figure 2.17. (a) A solar-, battery-based IoT system for urban garbage collection. (b) Impact comparison of a daily transmission versus an hourly transmission design. Both figures were extracted from [51].

Such impacts are explained by the increase in size of the photovoltaic cells, cases and accumulators of gateways; and the battery and case scale up of sensor nodes to support additional transmissions. Not surprisingly, the authors advocate for more attention for data dimensioning needs in early design stages of IoT systems.

5.3.Relevance of data- and information-driven design for context sensing

On the other hand, the concept of data- and information-driven design are fundamental aspects for energy harvesting systems and context-sensing design. Context sensing refers to the detection of a wide variety of contexts (e.g., kinetic activity) by reusing energy harvesting patterns [23]; for example the voltage signals (See figure 2.18).

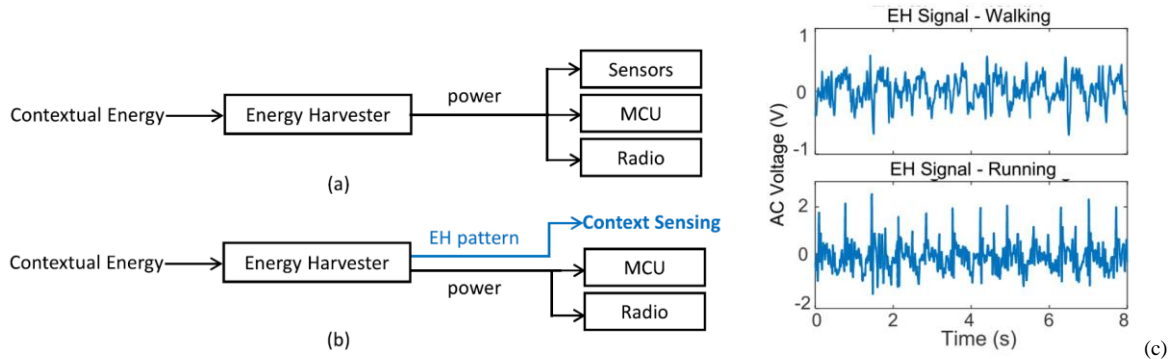


Figure 2.18. (a) A typical EH system. The energy consumption of sensors significantly affects the operation lifetime of the system. (b) An EH system using context sensing. The charging and discharging pattern of the energy harvester (i.e.: voltage variations in the main capacitor) detects a variety of contexts as it showed in figure (c). Figures extracted from [23].

Meaningful Information obtained from context sensing depends on sober data, and the appropriated way to organize this data. As a matter of example, a study conducted by Lan, G. et al. [7] compares the human Calorie Expenditure Estimation (CEE, expressed in Kj / Min) provided by a typical accelerometer-based sensor system (Figure 2.19a) with the CEE provided by an EH sensor system based on context-sensing (Figure 2.19b).

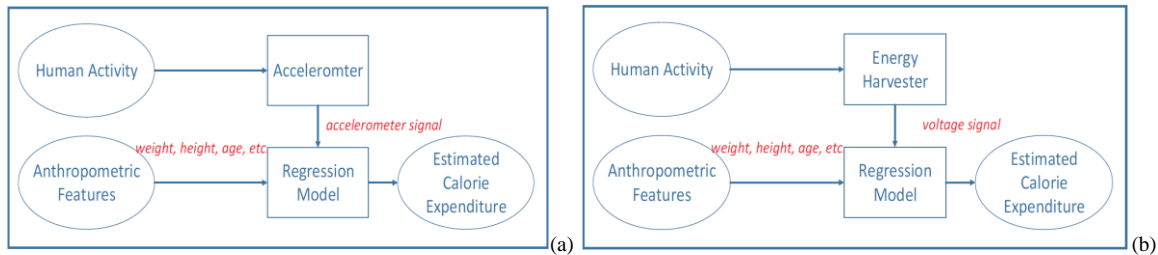


Figure 2.19. (a) Accelerometer-base sensor system. The CEE is based on the work of Chen, K. Y., & Sun, M. [54] whose use a regression model composed of accelerometer signals x, y and z; and anthropometric data of user. (b) EH sensor system based on context-sensing. The regression model of this system is composed of the anthropometric data of the user and the output AC voltage signals from the transducer.

By organizing the signal voltage variations with the anthropometric features of the user (weight, height and age) in a regression model, the context-sensing-based EH sensor system obtains the CEE average (information) with a Mean Absolute Percentage Error (MAPE) of 0,12 for walking and 0,16 for running (compared with the typical accelerometer-based sensor system). Figure 2.20 shows the accuracy of both systems.

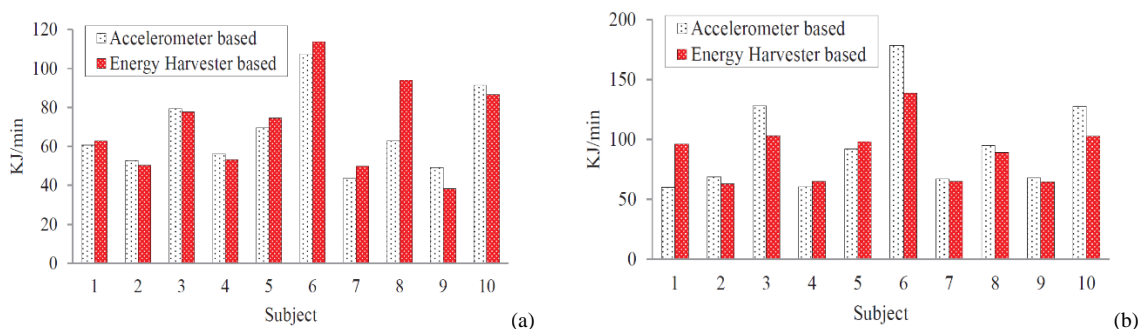


Figure 2.20. Comparison of the CEE of ten subjects provided by an accelerometer-based EH sensor system VS the average CEE provided by an EH sensor system using context-sensing. (a) For walking. (b) For running. Both figures are extracted from [7].

As showed, context-sensing would allow for more sober, ecological devices with acceptable accuracy based on essential data and information. In the example above, although authors do not mentioned it, dispensing with a MEMS accelerometer would mean an environmental saving of 147g CO₂-eq, as it is suggested in [55]. In this line, Ma, D. et al. [23] also conclude that context-sensing allows potential replacement of energy-intensive sensor components such as accelerometers and gyroscopes, reducing impacts of sensor systems in use phases.

6. Conclusions

By recalling the main interrogation of this work: “How can one estimate the potential impact of an IoT system and how can minimize this impact by an efficient and practical design methodology?”; and the research question 1 that it involves: “How a designer can consider data flow within an IoT system in order to harmonize and reduce the potential impacts of promising initiatives?”, one observe in the related literature that:

- From the performance perspective, some techniques such as data aggregation, compression or approximate computing were proposed to reduce bandwidth and latency problems of modern IoT systems; such initiatives would help to reduce indirectly the environmental impact of the mutualized infrastructure of IoT systems but would also demand more energy-intensity computation in the local infrastructure.
- From the environmental perspective, there is evidence that suggest that a sober yet effective right-provisioned IoT system would depend not only on its available resources but also on specific aspects of the information that is required by its application (i.e.; appropriateness and quantity); and on the ways that this information is obtained. However, although there exist pioneer work showing the relevance of these aspects and innovative ways to gains meaningful information from raw data (i.e.; context-sensing), no methods nor detailed tools to apply these approaches systematically in the design workflow of full IoT systems were found in literature.

Thus, the following insights for addressing the aforementioned shortcomings in next chapters can be stated for now:

- Firstly, as a phenomenon can be captured and acknowledged by different methods (as seen in chapter 1, table 1.1), the kind of raw data that an IoT designer chose, as well as the way by which such data is collected and organized into information is of a paramount of importance for sustainable design of IoT systems.
- Secondly, the transitions from raw data to information and from information to knowledge depend on local, edge and cloud resources. The analysis and design of such transitions help to establish the referential flow for impact estimation and eco-design of multiple devices in an IoT system.
- Finally, a right-provisioned device is designed according to the capacities of its electronic components, which are related to specific functions supporting acquisition, processing, storing and transmission tasks.

These insights will frame the state of art of chapter 3 and help to construct the proposed methodology in chapter 4.

Chapter 3. State-of-Art of environmental studies and eco-design methods for IoT systems

Overview

Dealing with the research questions seen in chapter 1 requires the revision of two primary aspects in literature: (1) the representative studies regarding impact estimation of IoT systems and (2) the potential methodologies and current tools oriented to their eco-design. In this chapter, the first aspect will be preceded by a review of the fundamental concepts of the Life Cycle Assessment (LCA) methodology. This permits gaining a better understanding not only of the main findings (i.e.; big impact contributors) and usual solutions; but also of the methodological shortcomings (i.e.; underestimation of dataflow and ambiguous reference flows), common difficulties, and general lack of LCA data observed in literature. For the second aspect, this chapter begins with important definitions and concepts regarding eco-design, and a brief description of the stages inside the New Product Development (NPD) procedure. This allows to assimilate the pioneer work revealing the relevance of data as an eco-design driver on the one hand, and the limitations, the convergence, complementary and discrepancies of current eco-design instruments for sensor-based systems on the other hand. Both parts identify relevant work related the two research questions stated before, and explain key findings in a structured manner to facilitate, together with the outcomes of chapter 2, the proposition of a design methodology in chapter 4.

1. Life Cycle Assessment and environmental studies of IoT systems

1.1. Fundamentals of Life Cycle Assessment

In order to facilitate the review and interpretation of representative LCA studies of sensors, sensor-based systems and IoT systems, the definition and description of some essential concepts of Life cycle Assessment found in the ISO 14040 standard [56] are summarized in the following subsections.

1.1.1. Life Cycle Assessment procedure

Life Cycle Assessment (LCA) is a standard quantification method that facilitates the estimation of multiple impact categories related to a product. Specifically, a LCA study considers several life cycle phases (i.e.; extraction and acquisition of raw materials, production, use and waste treatments), including all the energy and additional materials, products and emissions involved in these phases. By this perspective, the transfer of potential impacts between life cycle phases, impact categories, or particular processes can be identified and avoided. The steps for conducting a LCA study are presented in figure 3.1.

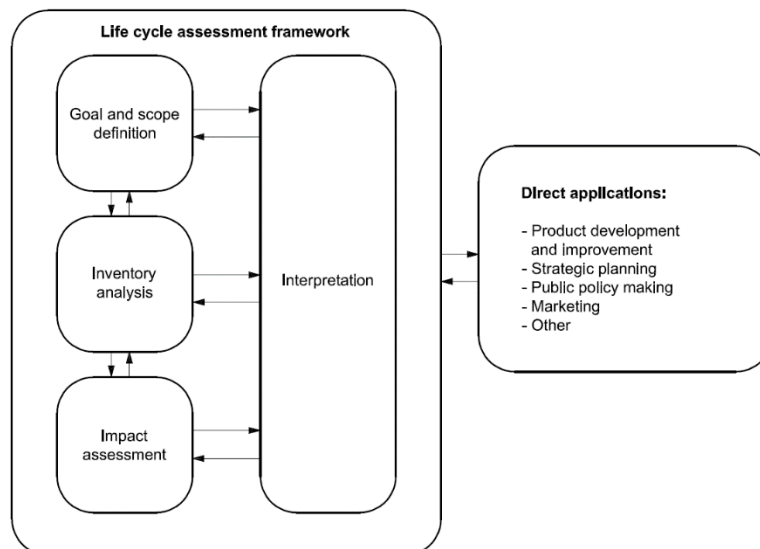


Figure 3.1. Fundamental steps for conducting a LCA study. Figure extracted from [56].

1.1.1.1. Goal and scope

The goal must define clearly the intended application of the study because it will frame the further steps of the methodology. The goal may be showing the environmental impact of a product based on an individual or comparison analysis, evaluating it based on a norm or a standard, evaluating its redesign alternatives, or facilitating the construction of ecological policies around it. On the other hand, the scope definition or the system boundary includes the limits of the product system and the level of details of the environmental assessment.

i) Product system

A product system refers to the life cycle model of a product in terms of unit processes; and elementary, product and intermediate flows (figure 3.2).

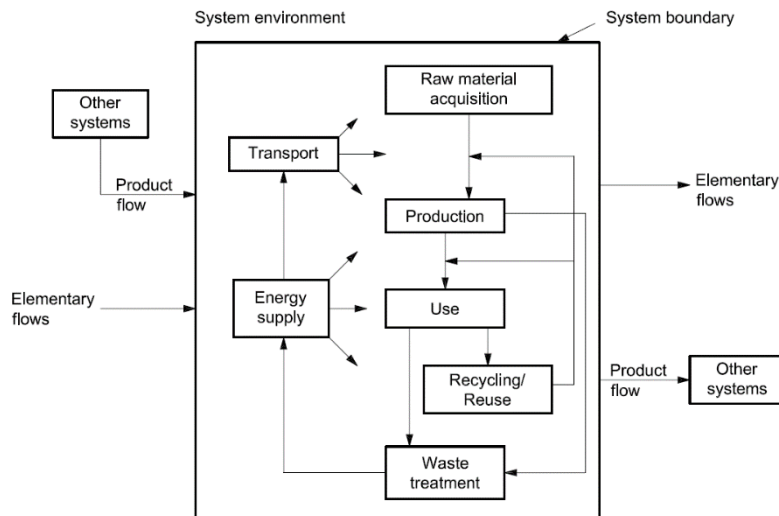


Figure 3.2. An example of a product system framed in its system boundary. It includes typical unit processes (inner small boxes); and elementary, intermediate and product flows. Notice that a product system can be linked to other product systems by product flows. Figure extracted from [56].

A unit process is the smallest element considered in the life cycle inventory analysis for which input and output data is quantified. An elementary flow represents material or energy entering a product system that has been drawn from the environment without previous human transformation; or material / energy leaving a product system that is released into the environment without subsequent human transformation. A product flow represents products entering from, or leaving to another product system. Intermediate flows (flows within a system boundary) represent product, material or energy occurring between unit processes.

ii) Functional unit

A product may perform one or many functions. The functional unit defines the quantification of selected function or functions in a LCA study and guide the definition of a product system. More specifically, it quantifies the performance characteristics of a product to provide a reference to which the inputs and outputs are related. This reference is necessary to ensure comparability of results. Comparability of LCA results is particularly critical when different product systems and when different versions of a product system are being assessed; the functional unit ensure that such comparisons are made on a common basis. In this sense, it is important to determine the reference flow in each product system, or in each version of a product system being compared.

iii) Reference flow

The reference flow is the quantity of product systems, material, energy, or even additional products needed to fulfill the functional unit as it is expressed. A common example provided in the ISO 14040 standard [56] illustrates perfectly the relevance of defining clearly the functional unit and the reference flow of a product. This example presents the specific function “drying hands” which can be performed by two different product systems: a paper towel or an electrical air-dryer. For these two systems, the selected functional unit is the same —drying an identical number of pairs of hands; whereas their reference flows could be very different (the average paper mass for the former and the average volume of hot air for the latter). In this sense, notice that, for both product systems, it is possible to compile different input inventories (i.e.: quantity of paper or electricity) and outputs (i.e.: quantity of waste paper or electronic waste).

1.1.1.2. Inventory analysis and Impact Assessment

The inventory analysis step involves the description and the data collection processes needed to model a product system, according to the functional unit evaluated by a LCA study. It includes the calculation procedures to quantify relevant inputs and outputs of a product system and its outcome catalogues the flows crossing the system boundary. The Impact Assessment step consists of applying a Life Cycle Impact Assessment (LCIA) method to estimate the environmental impacts of a product system by

associating the outcome of the inventory analysis with specific impact categories and impact characterization factors (usually according to Equation 3.1²).

$$I_c = \sum_i^n (m_i \times CF_{c,i}) \quad (3.1)$$

Where:

I_c = Impact estimation of an Impact Category (c) resulting from the input or output flow of n substances

m_i = Mass of a substance (i) found in the inventory analysis outcome

$CF_{c,i}$ = Characterization factor of the impact category (c) applied to a substance (i)

There exist LCIA methods that cover several impact categories in common impact groups (midpoint methods) and other LCIA methods that provide additionally unique impact indicators (endpoint methods), usually by applying weighting procedures. Typically, These procedures consists of two steps: (1) multiplying the LCIA results with normalization factors that represent the overall inventory of a reference (for example an average citizen) and (2) multiplying these normalized results with a set of weighting factors, that indicate the different relevance that different impact categories, or areas of protection may have [234]. All these indicators are reported and interpreted in the last step of the LCA methodology (Interpretation).

1.1.2. Characterization factors and environmental impact categories

A characterization factor is a factor derived from a characterization model used to convert one instance of the inventory analysis outcome to a common unit to compute an impact category indicator. An impact category indicator is a quantifiable representation of an impact category that represent an environmental issue. For example, to compute the impact of the environmental issue “abiotic resource depletion” of a specific raw material used by a product system, certain characterization models (included in LCIA methods such as CML-IA [235] and Anthropogenic stock extended Abiotic Depletion Potential (AADP)) construct a characterization factor by contrast the run-out rate of this resource with the run-out rate of a reference resource (equation 3.2).

$$ADP_i = \frac{\frac{DR_i}{(R_i)^2}}{\frac{DR_{sb}}{(R_{sb})^2}} \quad (3.2)$$

Where:

ADP_i = Characterization factor for the impact category Abiotic Resource Depletion Potential (ADP) of the resource (i).

R_i = Available ore stocks of the resource i

DR_i = Extraction rate of the resource i

R_{sb} = Available ore stock of a reference resource (Antimony)

DR_{sb} = Extraction rate of the reference resource

In equation 3.2, the run-out rate of both resources could be expressed as the ratio between their extractions rate and their available ore stocks, and the characterization factor of the resource (i) could be expressed in terms of the reference source (kg Sb-eq). Notice that equation 3.2 is framed in function of the rarity of the resource or, in other words, it concerns a particular feature of inputs flows in the inventory analysis outcome. Regarding the output flows, characterization factors could be also constructed by considering impact equivalences between specific output flows affecting specific impact categories, for example “Global Warming Potential” (table 3.1).

² According to Guinée et al. 2002 [57].

		Characterization factors (Equivalence) for GWP in 100-year time horizon	
Emission (Output flow)	Formula	IPCC AR4 Report [58]	IPCC AR5 Report [59]
Carbon dioxide	CO ₂	1	1
Methane	CH ₄	25	28
Nitrous oxide	N ₂ O	298	265

Table 3.1. Characterization factors for the impact category Global Warming Potential (GWP) in a 100-year horizon. Here, the common unit is expressed in terms of CO₂ mass equivalence. For example, emitting of 1gram of methane is equivalent to emitting 25 or 28 grams of CO₂ (CO₂ g-eq). Both substance contribute to the GWP impact category.

1.2. LCA studies of IoT systems

With an emerging number of publications [10, 26, 60-61, 72-77, 240], the impact estimation of sensors and sensor systems has attracted the interest of LCA communities in recent years. On the other hand, the impact estimation of full IoT systems gains more adepts [51, 69, 71, 143, 227, 236], as the number of publications showing the impacts not only of sensor systems but also of edge computing and mutualized infrastructure increases at a moderate pace. The next sections will detail these studies from a perspective of data and information flows, as fundamental instruments for defining the reference flow for environmental impact assessment; and later, from a structural perspective: LCA studies of full IoT systems (with an special emphasis on impact estimation of transmitting and processing data over the internet and cloud servers) and partial IoT systems (including edges devices, sensor systems and sensor components). Each of these sections provides useful aspects for the next chapter.

1.2.1. LCA studies of IoT systems reveling the importance of data and information for establishing reference flows

According to the conclusions of previous chapter, the functional unit of an IoT system could be defined as the production of information, which depends on the collection and the unique way to treat specific types of raw data. In this sense, two IoT systems with a common functional unit may have different reference flows —different sensors, sensor systems, mutualized infrastructure or even different energy consumption patterns— depending on the way by which data is transformed into information.

With this in mind, dimensioning differently the needs of data may originate different reference flows and impact results, as Lelah et al. [51] point out. In their cost-benefit LCA-based study, they describe a baseline version of an IoT system oriented to optimize the glass collection service system of a city, providing information of glass-level-content of bins once a day (Figure 3.3).

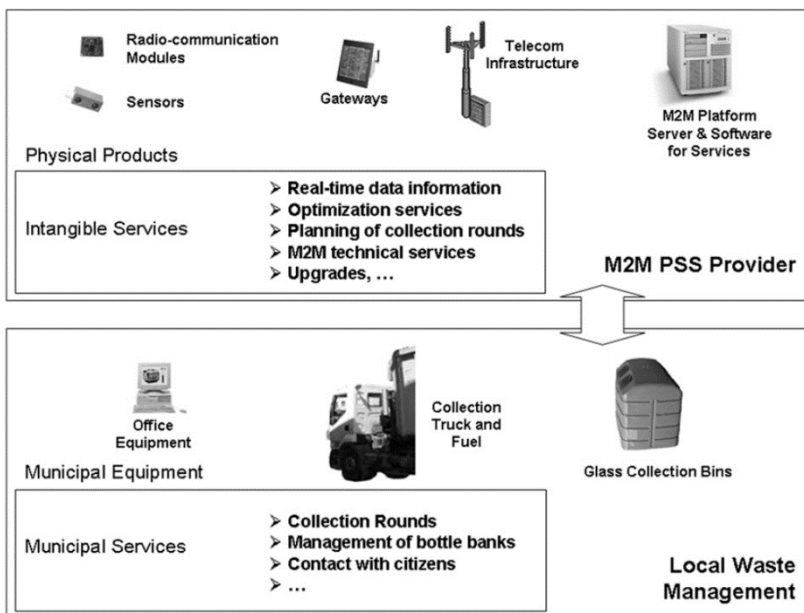


Figure 3.3. A full IoT system for glass waste-collection. Authors organized the IoT system in elements that belongs to the optimization service system (M2M and Product Service System (PSS) provider) and elements that belong to the regular service system (Local waste management). The scope of the LCA study covers only the M2M PSS Provider system. Figure extracted from [51].

The baseline version is composed of a network of sensors systems, which are placed in waste bins and communicate with nearby solar-powered gateways by a low power radiofrequency protocol (Wavenis). This IoT system use the gateways to send the information to the global telecom infrastructure by Global System Mobile (GSM) communication in order to centralize data and generate information in a cloud server (M2M platform). This information is later presented to the end user though regular computers (PC). The gateways, the M2M platform and the PC elements compose the Product Service System (PSS) of the system.

Thus, under these conditions, this LCA study (that does not indicate explicitly its reference flow) demonstrate the influence of different data transmission frequencies on (1) the reference flow in terms of additional resources in local devices, and energy consumption in mutualized infrastructure; and (2) on the environmental impacts of the entire IoT system. Starting from its functional unit defined as “collecting waste glass in the Voiron County (France) during ten years”, this study considered changing the baseline design of the data transmission frequency (in which each sensor system transmits content-level data of containers once a day) to an hourly frequency (each sensor system executes 24 transmissions per day), with the aim of reducing the danger of overflowing bins. This change would modify the reference flow of the baseline version because capacities of current equipment would be scaled-up (bigger photovoltaic cells, accumulators and casings for gateways, and augmented batteries and casing of sensors systems); contributing to a significant increase of environmental impacts in almost all categories. Especially, it is observed an increase of 62% for the Energy depletion and an increase of 27% for the global warming impact categories (figure 3.4).

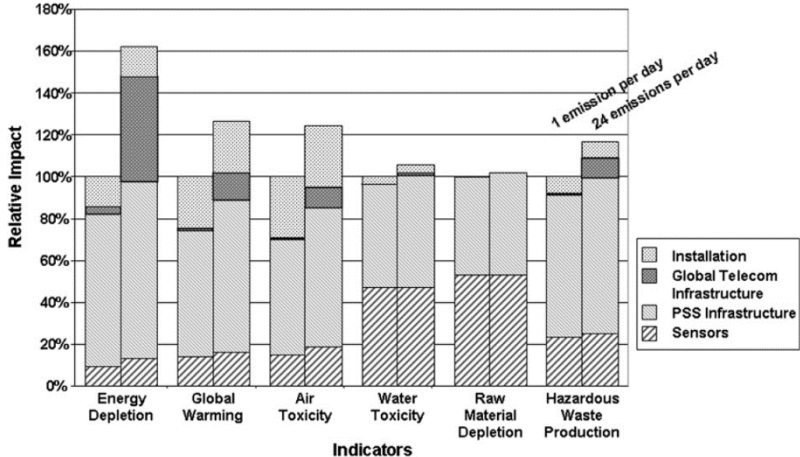


Figure 3.4. Environmental impact of the IoT system with a daily and hourly frequency transmission rate. Figures extracted from [51].

Interestingly, the second impact contributor of the hourly data transmission design is the global telecom infrastructure (with a corresponding impact contribution of 31% and 10% for the Energy Depletion and the Global Warming impact categories). Regarding these results, the authors propose allocating 24 similar IoT applications in the local equipment (PSS system) and the mutualized infrastructure (Global Telecom Infrastructure). In this way, the impact would be 1/24 for each service separately. The impact evaluation of this hypothetical scenario reveals a drastic reduction of almost 45% and 31% for the Raw Material Depletion and Global Warming impacts categories respectively (Figure 3.5).

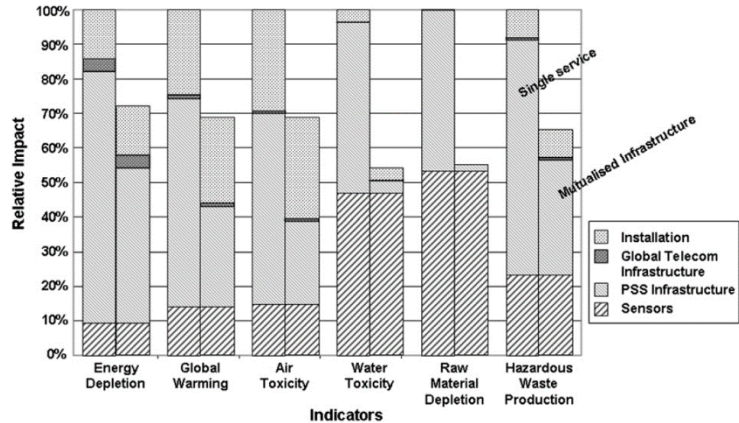


Figure 3.5. Effects of mutualizing local and Telecom infrastructure along 24 similar services. Figure extracted from [51].

Another LCA study conducted by Köhler, A. R. et al. [60] shows that a reduction of the data sampling resolution of a textile-based IoT system induces a proportional reduction on its reference flow in terms of required material and energy. With two different scenarios involving two functional units: “energy management and safety for an elderly person home for 20 years (sensing floor size 30 m²)” (scenario A), and “Presence monitoring for a lecture room for 20 years (sensing floor size 4 m²)” (scenario B), the system boundary of this LCA study describes a partial IoT system composed of a transceiver and capacitive proximity sensors grouped in microelectronic modules distributed in a floor area (figure 3.6).

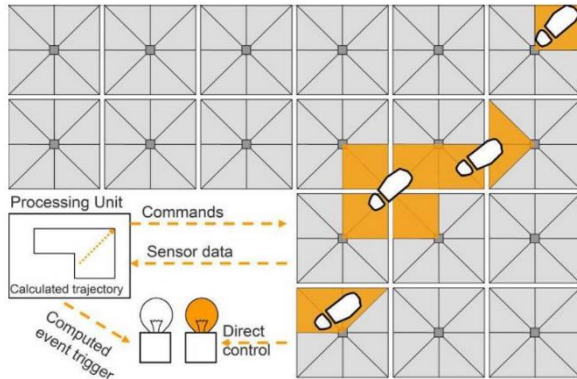


Figure 3.6. A basic schematic of a textile-based IoT system. Inside the floor underlay, proximity sensors are installed in conductive textile-based triangular areas (Polyester fleece). Eight sensors are connected to a microelectronic module, which communicates with a transceiver wirelessly (in 868 MHz frequency). Figure extracted from [60].

Baseline endpoint Ecocost impact results for scenario A and scenario B amounts to more to 700 Euros and 200 Euros respectively (Figure 3.7a). As much of these impacts are explained by a continuous power dissipation along the use phase of the microelectronic modules, authors propose reducing the sensing floor’s spatial resolution from 4 to 2 modules per square meter (motivated by the low-data-resolution needs of both scenarios). Figure 3.7b shows the power saving from this modification on the reference flow, together with some alternative settings on the data operational stages of the IoT system: switching off the radio receiver of the sensor modules (sub scenario 2), putting the MCU in sleep mode when capacitance measurement and data transmission are not required (sub scenario 3); and reducing the frequency of measurements (sampling rate) from 10Hz down to 2Hz to prolong sleeping states (sub scenario 4).

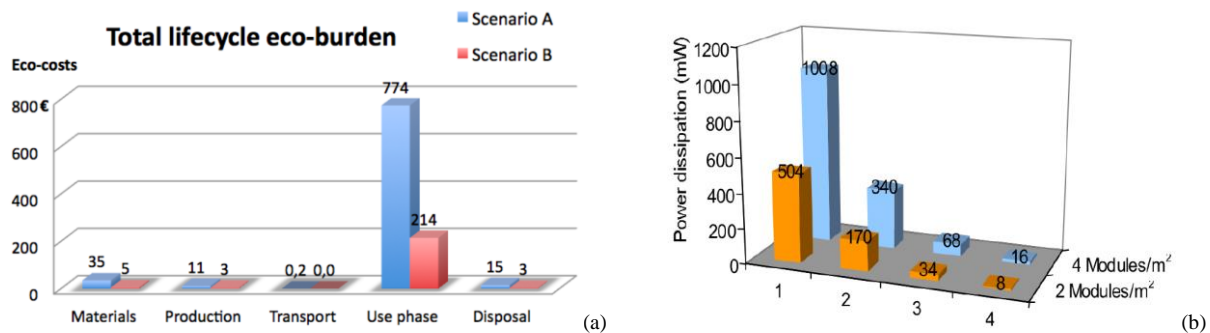


Figure 3.7. (a) Baseline Ecocost impact results of a textile-based IoT system (Scenario A and B). Manufacturing (materials and production) of microelectronic modules contributes only with 4.9% in scenario A, and with 3.6% in scenario B. (b) Power dissipation decrease from reducing the sensing floor’s spatial resolution from 4 to 2 microelectronic modules per m². Figures in sub scenario 1 show the power dissipation of the IoT system without additional settings. Figures extracted from [60].

Unfortunately, in spite of the evident benefits (a reduction on the power dissipation of more than 66%, 93% and 98% for sub scenarios 2, 3 and 4 respectively), the authors of this study do not provide further details about the implementation of the aforementioned settings.

On the other hand, the reference flow of IoT systems may include significant replacements of local devices too, depending on the functional unit and operational conditions in data transmission stages. For example, in a complementary LCA study conducted by Bonvoisin, J. et al. [61], the functional unit “centralized ten-year hourly provision of glass level values for all waste containers in Grenoble (France)” mobilizes the deployment of 288 sensor systems, all of them replaced approximately once during ten years because of battery lifetime limitations (7.5 years). In the same period, it is also required installing 72 repeaters whose replacements amount to 156 devices, mainly due to their limited battery

lifetimes of 4 years. The impact contribution of such context would range from 63% to 83% for sensors systems, and from 15% to 35% for repeaters in different impact categories (Figure 3.8).

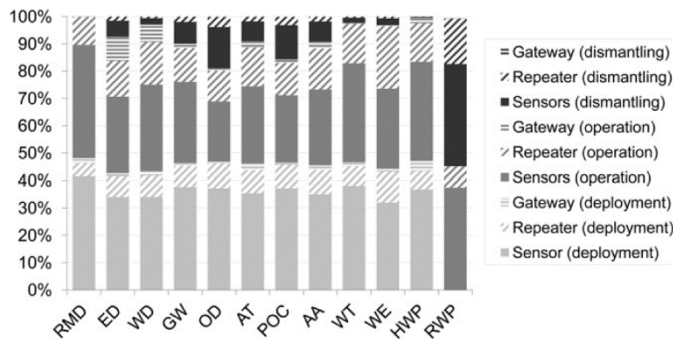


Figure 3.8. Environmental impact of a WSN oriented to optimizing the urban garbage collection of a city. Raw Material Depletion (RMD), Energy Depletion (ED) Water Depletion (WD), Global Warming (GW), Ozone Depletion (OD), Air Toxicity (AT), Photochemical Oxidation (POC), Air Acidification (AA), Water Toxicity (WT), Water Eutrophication (WE), Hazardous Waste Production (HWP), Residual WEEE Production (RWP). Figure extracted from [61].

Much of these impacts are explained by the early replacement of sensor systems and repeaters, whose batteries drain quickly due to energy-intensive communication tasks. For example, in the case of sensors, 40% of the energy consumed is attributed to overhearing and 28% to radio bandwidth scanning (see figure 3.9). In the case of repeaters, the energy consumption is distributed between overhearing (30%) and communication (64%).

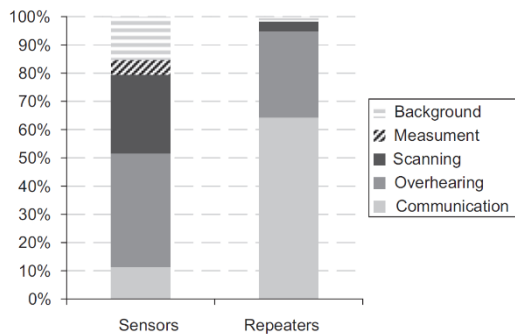


Figure 3.9. Energy consumption share of communication tasks of sensors systems and repeaters. Figure extracted from [61].

Overhearing would be produced by certain factors such as the data rate generation of the network and the hearing sensibility of receivers. Because very high levels of sensibility produce overhearing and very low levels degrades the quality of communication, the authors of this study propose restricting the hearing sensibility of each sensor system to the strict necessary as a first redesign alternative (Alternative 1). Specifically, they propose decreasing the hearing sensibility of each sensor system so that the probability of successful reception of messages achieve 95%. Based on this alternative, they also propose doubling the battery capacity of repeaters (Alternative 2). Figure 3.10 shows the environmental saves of both strategies.

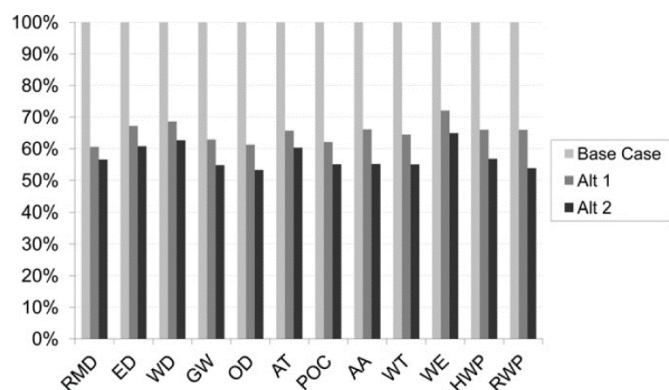


Figure 3.10. Comparison of impacts for the baseline design; and alternative 1 (Alt 1) and alternative 2 (Alt 2) redesign options. Figure extracted from [61].

In figure 3.10, the environmental saves of the redesign alternative 1 are explained by a reduction of 10% in the energy consumption of sensor systems, which extends the lifetime of their batteries and avoid replacements. However, in this scenario, repeaters consumes more energy than before because of poorer communication links and they are more often replaced (188 replacements instead of 156). In this sense, scaling-up their battery capacities (Alternative 2) leads to less replacements (73 instead of 188) and

environmental saving compensations with respect to the first redesign alternative (from 4% for RMD to 12% for RWP impact categories).

- As observed, in this section Lelah, A. et al. [51] and Bonvoisin J. et al. [61] show respectively clear increments and reductions of environmental impacts from modifications in reference flows, which is the result of direct changes in the data intensity, addressed by IoT systems. Specially, redesign alternative 1 proposed by Bonvoisin J. et al. [61] shows that a little degradation in data quality (5% of messages lost) can influence positively and/or negatively the impact of IoT systems (i.e.: less replacement of sensor systems but more repeaters to support poorer communication links). On the other hand, Köhler, A. R. et al. [60] shows that considering data requirements according to IoT application types may lead to drastic reductions on reference flows (in terms of number of devices and energy).
- However, although this evidence shows that variations in reference flows from data manipulation should be analyzed before conducting LCA studies; all authors in this section do not recognize explicitly the relevance of this previous step.
- In this sense, in this work it is acknowledged the relevance of a preliminary analysis of data (its requirements, meaning, manipulation and flow) and the derived information from it; and the next chapter will aim to construct a novel design methodology that explicitly integrates this preliminary analysis to better define or redefine the reference flow of IoT systems.

1.2.2. LCA studies of full IoT systems and impact estimation of mutualized infrastructures

Estimating the impact related to the use of cloud servers and mutualized networks of IoT systems is challenging. As a starting point, one can consider the work carried out in the broader field of ICT for gaining understanding of the inner complexity of mutualized infrastructures and later apply this knowledge to the literature review of full IoT systems.

According to Malmodin, J. et al. [62], the available literature of impact estimation of mutualized infrastructure in ICT products and services presents a dichotomy between environmental studies based on economic and environmental data (that is later allocated to specific ICT sectors) [63], and environmental studies based on the analysis of specific ICT products or services (that are later related to generic ICT sectors) [64]. These approaches are usually known as “top-down” and “bottom-up” approaches respectively.

In the context of IoT systems, top-down LCA literature includes the aforementioned study conducted by Lelah, A. et al. [51]. This study uses data from a French telecom operator to allocate the necessary energy for running the GSM and internet communication. Table 3.2 presents some aspects and a description of the operational phase of these elements.

Element	Description	Life cycle phase considered in the study		
		Manufacturing	Transportation	Use
GSM	Local network (sensor & gateways) ↔ Telecom network	No	No	Electricity grid only
Internet	Telecom network ↔ M2M platform	No	No	Electricity grid only
M2M Platform (cloud server)	Server, rack, air cooling	Electricity grid only	Yes	Electricity grid only
Internet	M2M platform ↔ Collection service	No	No	Electricity grid only
PC end-user	PC at the collection service	Electricity grid only	Yes	Electricity grid only

Table 3.2. Elements considered in the LCA study of an IoT-based glass collection system presented by Lelah, A. et al. [51].

Basically, this study calculates the energy consumption part of the GSM and internet infrastructure by dividing the total energy use of the telecom infrastructure (during the use phase) into running the facilities and actual communication. Then, parts were allocated to specific services such as telephony and internet; and finally the estimated impact of the energy allocated to particular communication such as GSM and internet involved in the IoT application was calculated according to the number and types

of subscriptions concerned. In this way, the estimated impacts summarized in figure 3.11 suggest little damage attributed to the use of mutualized infrastructure of the IoT system (far less than 10% in the Energy Depletion impact category).

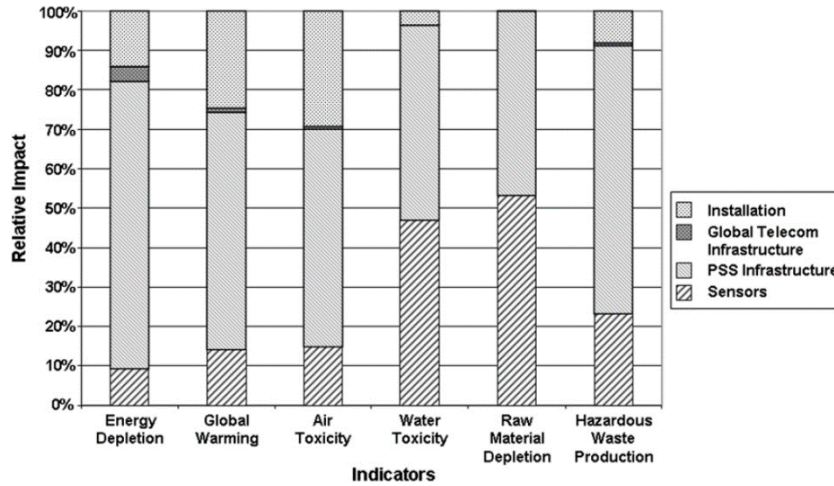


Figure 3.11. Environmental impact of the glass collection IoT system presented by Lelah, A. et al. [51] for sensors systems transmitting once a day. The mutualized infrastructure (Global Telecom Infrastructure) includes the GSM and internet communication. The M2M platform (cloud server) is not included into the Global Telecom Infrastructure but into the PSS infrastructure.

On the other hand, a distinctive characteristic of bottom-up LCA studies oriented to ICT products and services [11], [62], [65-68], [237] is the common method used to calculate the energy consumption of mutualized infrastructure involved in use phases, which consist on estimating the electricity required by cloud servers and telecom networks for processing data generated on the local side (kWh per Gigabyte generated).

This approach is applied in a bottom-up LCA study of an IoT system oriented to monitoring the use of truck tires [69]. It considers an energy used per data volume ratio (kWh / GB) to calculate the global impact of the system. Table 3.3 and equations 3.3 and 3.4 show the aspects considered in this study for modeling the energy requirements of mutualized infrastructure (cloud servers and internet 4G connection).

	Data flow and assumptions	How total was calculated	Unit
Energy requirements data collection by sensors	1 W typical power *	1 / 1000 [kW] * total hours of tire use [h]	kWh
Gateway energy requirements for data transmission	Sends data every 2 minutes via 4G LTE network *	Equation 3.3	kWh
Cloud-side energy requirements	Sends data every 2 minutes * 4 bytes per transfer **	Equation 3.4	kWh

Table 3.3. Aspect considered for modeling the energy requirements of an IoT system oriented to monitoring the use of truck tires. (*) Technical data from de IoT system manufacturer. (**) Estimations by authors. Adapted from [69].

$$G_E = \frac{1 \text{ transfer}}{2 \text{ min}} \times \frac{4 \text{ Bytes}}{\text{transfer}} \times \frac{10^{-9} \text{ GB}}{\text{Byte}} \times \frac{0,3 \text{ kWh}}{\text{GB}} \times \text{Total minutes of tire use [min]} \quad (3.3)$$

$$E_{\text{Cloud}} = \frac{B_d \cdot D}{3600} \times \left(E_T + 1,5 \frac{P_{st,SR}}{C_{st,SR}} \right) + 2B_d \frac{1,5 P_{SD}}{B_{SD}} [W] \cdot \text{Total hours of tire use [h]} \quad (3.4)$$

Where:

G_E = Energy consumption of the gateway for data transimission

E_{Cloud} = Energy consumption of the cloud server

$P_{st,SR}$ = Power required by a content server, estimated to 0,225 kW

$C_{st,SR}$ = Capacity of the content server estimated to 800 Mbits per second

P_{SD} = Power required by the hard disk arrays, estimated to 4,9 kW

B_{SD} = Capacity of the hard disk arrays, estimated to 604,8 Tbits

B_d = Number of bits transfered per second

D = Number of downloads/uploads per hour

E_T = Cloud side energy needed to transfer 1 bit, estimated 2,7 $\mu\text{J}/\text{bit}$

For developing equation 3.3, Ingemarsdotter, E., et al [69] uses the ratio of 0,3 kWh / GB for internet 4G connections reported in [67]; as well as the cloud-side energy needed to transfer 1 bit (2,7 $\mu\text{J}/\text{bit}$), and the estimated power required by a content server and hard disk arrays (0,225 and 4,9 kW respectively), all reported in [70]. The capacity of the content server (800 Mbits/s) and the capacity of the hard disk arrays (604,8 Tbits) in equation 3.3 comes from this latter reference too.

The purpose of the study is contrasting the benefits provided by the IoT system (reduction in fuel consumption, extension of the lifetime and retreading of tires) with its associated impact: manufacturing of piezoelectric-based sensor systems, gateways and RFID tags; and energy consumption for data transmission through internet, and treatment by cloud servers. Together with additional inventory analysis including the tires and treat production, the drive distance before tire exchange, and the fuel consumption of trucks; the authors found that monitoring the wearing rate of tires through the IoT system gives a 4% lower weighted life cycle impact than the current state, explained by a reduction of tires used by a tractor/semi-trailer truck along 2×10^6 km (table 3.4).

	Number of tires	
	Current state	IoT scenario
New tires	4,9	3,6
One time retreaded tires	3,1	2,5
Two time retreaded tires	2	1,8
Three time retreaded tires	1,2	1,2
Total number of tires	11,2	9,1

Table 3.4. Number of tires under the current state scenario (manual checking of tires every 8 weeks) and the IoT scenario (constant smart checking). The functional unit is “enabling a tractor/semi-trailer (10-tires-tracted) truck to drive 2×10^6 Km”. Adapted from [69].

According to the authors, this reported benefit may vary based on variations in tires and trucks (i.e.; rolling resistance of tires, type of truck, etc.) and to a lesser extent on the weight of the sensor systems and gateways. Moreover, the production of these devices and, specially, the required energy for using the mutualized infrastructures involved in the operational phase of the IoT system (“IoT Energy use data transmission 4G” and “IoT energy use cloud”) would not contribute significantly to the impacts as the objects do (“abrasion” or “manufacturing” of tires, and “fuel” for trucks) (Figure 3.12).

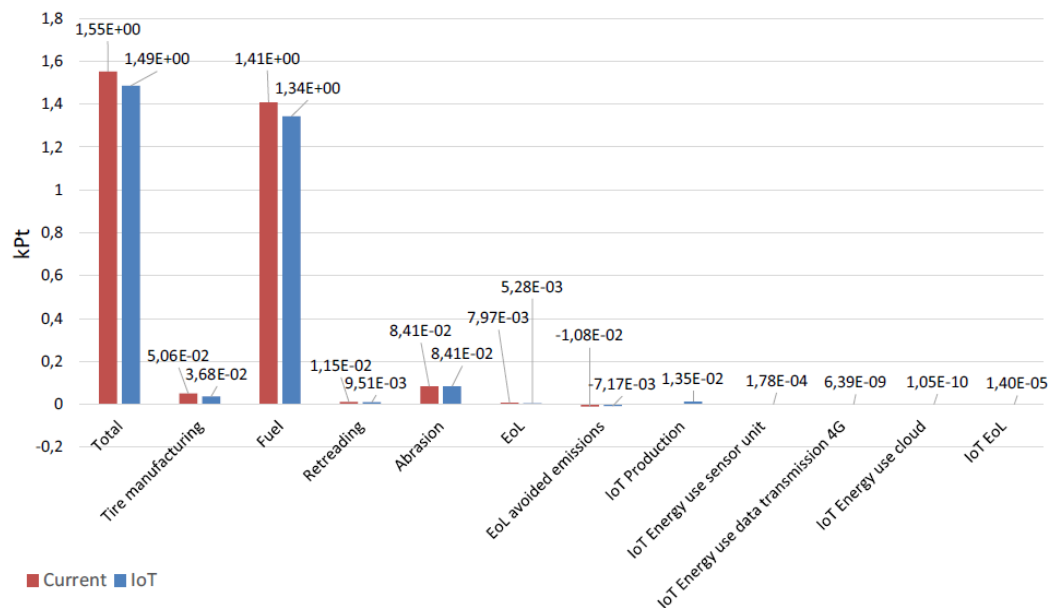


Figure 3.12. Impact comparison of the current state and IoT-based systems for truck tires monitoring. It presents results according to weighted single scores of impact (kPt) of the LCIA method ReCiPe 2016 (total and per life cycle phases for the current state and IoT-based scenario) [69]. The manufacturing phase of mutualized infrastructure is not taken into account.

However, this conclusion must be interpreted prudently since the weighted impact of producing and using the IoT-based system could be underestimated. Indeed, if one considers the difference in impact between the current state and the IoT scenario by categories (figure 3.13), one observe that using the IoT-based system can be counterproductive for certain impact types (in freshwater eutrophication and toxicity, marine ecotoxicity, and Human non-carcinogenic toxicity).

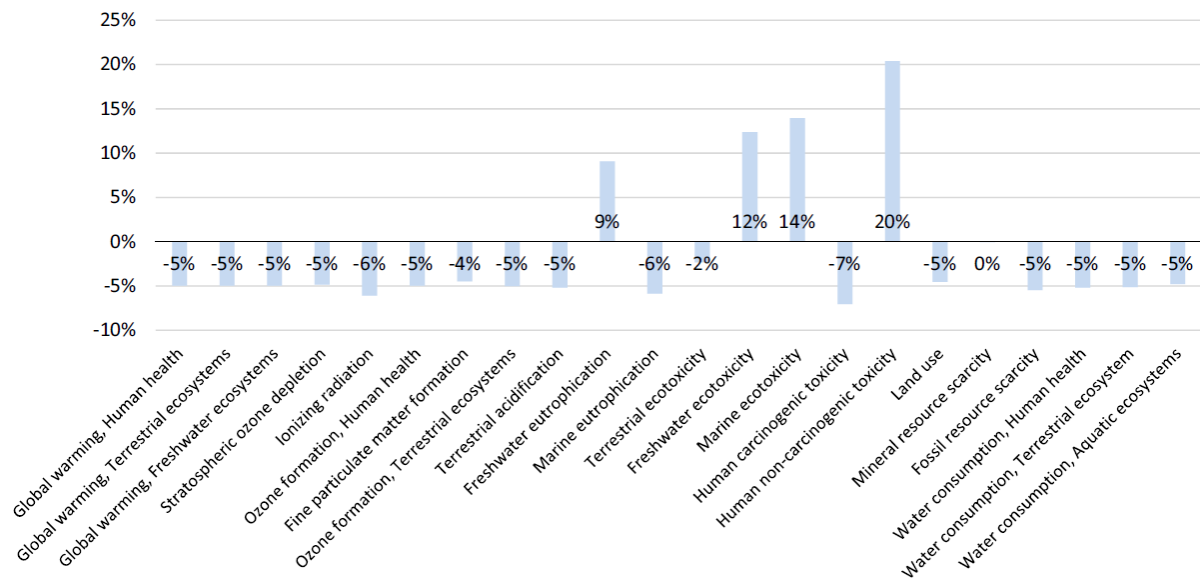


Figure 3.13. Difference in impact between the current state and the IoT scenario, by impact categories (as percent of current state impact). Figure extracted from [69].

Unfortunately, the authors do not provide detailed results in terms of the different phases of the life cycle of the IoT system (including the use of mutualized infrastructure) and further interpretations are not possible.

Dekoninck, E., & Barbaccia, F. [71] for their part, present a bottom-up LCA study of an IoT system based on the amount of data generated from a smart fridge. In this cost-benefit study, the authors focused on the ten-year use-phase impacts comparison of a regular fridge versus a smart fridge within four scenarios (average use of the normal fridge; and least, average, and intensive use of the smart fridge). For estimating the use of local and mutualized infrastructure in the case of the smart fridge, the construction of the average use scenario was based on surveys and literature (Table 3.5), and the least and intensive use scenarios were derived hypothetically from it. Table 3.6 shows the estimated data generation for the different smart functions and their associated impacts derived from Malmodin, J. et al. [11], and table 3.7 shows the carbon footprint comparison of the four scenarios.

Smart functions	Frequency (per week)	Source
Look inside remotely	3	Surveys
Browse internet	3	Lit. review

Table 3.5. Partial construction of average use scenario of a smart fridge concerning the functions that involves the use of local and mutualized resources. Adapted from [71].

Smart functions	Data use (GB/hr)	Impact*
Look inside remotely	0,6	2,1x10 ⁻⁵ Kg CO ₂ -eq / photo
Internet browse	0,6	1,48 Kg CO ₂ -eq / GB
App use (3G connection)	0,4	2,77 Kg CO ₂ -eq / GB

Table 3.6. Data generation rate and associated impacts for some smart functions. (*) Derived from literature. Adapted from [71].

System Stage	Normal fridge	Smart fridge		
		Least use	Average use	Intensive use
Product use	2400	2500	4200	8000
Fridge	2438	2438	2438	2438
Screen		39	72	132
Cameras		3	3	2
Speakers			16	44
Internet			1657	5396
Grocery shopping	10700	10700	10300	7600
Brick 1 mortar	10700	10700	9400	
Grocery shopping (Online)			920	7600
Loading groceries into fridge	55	55	55	55
Use the app			220	500
Food wasted	9800	9800	6800	3900
Opening door during week	140	140	130	110
Total	36233	36375	36211	35777

Table 3.7. Impact comparison of the four scenarios expressed in CO₂ kg-eq terms. Adapted from [71].

Unfortunately, although this study reveals interesting reductions on the global impact for the average and intensive use scenarios on the one hand, and an augmented contribution of the internet use in the intensive use scenario (approximately 15%) on the other; it is not clear the way by which the authors computes these results from the provided data generation rate per smart functions (according to table 3.6) and the use frequency of these smart functions (according to table 3.5).

Alternatively, Sarkar, S. et al. [143] conducted a simulation-based, comparative analysis of impacts of cloud and fog computing in the context of IoT. Based on a mathematical model of the service latency (computation and transmission delays) of different-sized IoT systems composed of several devices (terminal nodes); they estimated the power consumption of fog and cloud computing under specific data operational stages (data forwarding, computation, storage and transmission) (Figure 3.14b); and concluded that, for numerous latency-sensitive applications, fog computing outperforms cloud computing, both in terms of provisioned QoS and ecological benefits (Figure 3.14c-d).

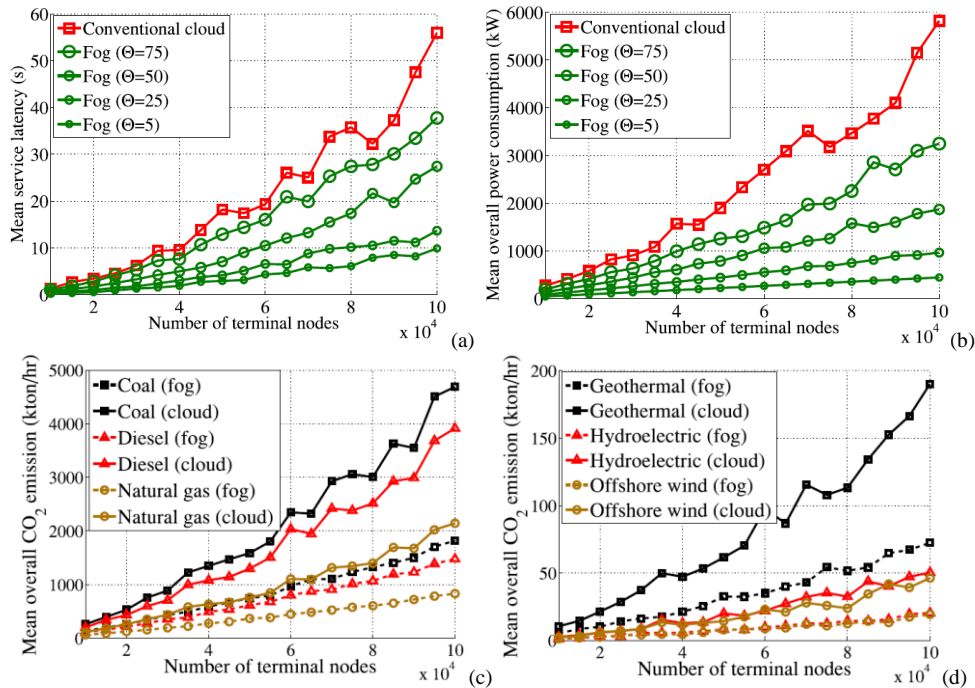


Figure 3.14. (a) Service latency VS number of terminal nodes simulation results and (b) Overall power consumption (including power consumption for data forwarding, computation and transmission) VS number of terminal nodes. Θ represents the ratio of the total bytes transmitted to the fog computing tier to the number of bytes referred to the cloud computing tier. (c) and (d) shows the total CO₂ emissions for non-renewable and renewable energy sources respectively (according to the CO₂ emission rates found in [239]). All figures were extracted from [143].

Motivated by these results, the authors eventually justify fog computing as an improved, eco-friendly platform compared to cloud computing and announce future work based on fog computing prototypes to support real-time implementations.

- As observed, in this section, the top-down LCA study presented by Lelah, A. et al. [51] shows that the use of the French telecom infrastructure does not contribute significantly to the global impact of IoT systems (on a daily data transmission basis). If one compare their results with results provided by Ingemarsdotter, E. et al. [69], one could conclude preliminary that impact from energy consumption of mutualized infrastructures is negligible.
- In the latter work, however, the impact contribution of the mutualized infrastructure cannot be distinguished, nor can its results be generalized to IoT systems (the authors clarify that their results may vary in other data-intensive contexts). Furthermore, the second bottom-up LCA study presented by Dekoninck, E., & Barbaccia, F. [71] shows a non-negligible impact contribution of around 15% attributed to the intense use of internet, an impact whose survey-based calculations would not be clear.
- Finally, although interesting, the work of Sarkar S. et al [143] relies in several assumptions on terminal nodes such as self-awareness-geo-spatial location capabilities, that would not reflect the reality of modern, energy-constrained IoT systems.
- In this sense one can neither conclude whether the impact coming from the use of mutualized infrastructure of IoT systems is negligible or not (regardless of the method used for estimating the energy needs), nor extrapolate results presented in this section to other studies due to the case-by case nature of the literature.
- The next chapter will try to propose a generic and transparent method that easily models the generation of data and calculates approximately the global impact of heterogeneous IoT systems.

1.2.3. LCA studies of partial IoT systems (sensor systems and edge/fog devices)

The environmental study of partial IoT systems is usually carried out in a context of cost-benefit comparisons of specific IoT applications. For example, the aforementioned work carried out by Bonvoisin, J. et al. [10] presents a comparison of benefits and environmental impacts of using a WSN (composed of content-level sensors systems, repeaters and gateways) for optimizing the routes of municipal garbage collectors of a city.

Specifically, the results of this study show a reduction of 25% in the Global Warming (GW) potential thanks to the optimization of the collector truck routes (-19% of travelled distance), less containers to collect (41% more full containers treated) and fuel savings (-26% less diesel consumption). However, these environmental savings are eclipsed by a significant increase of impacts in the Resource Material Depletion (RMD) impact category (figure 3.15a), which would be explained by the deployment and replacements of numerous off-ground sensors systems in the operational period of ten years (figure 3.15b).

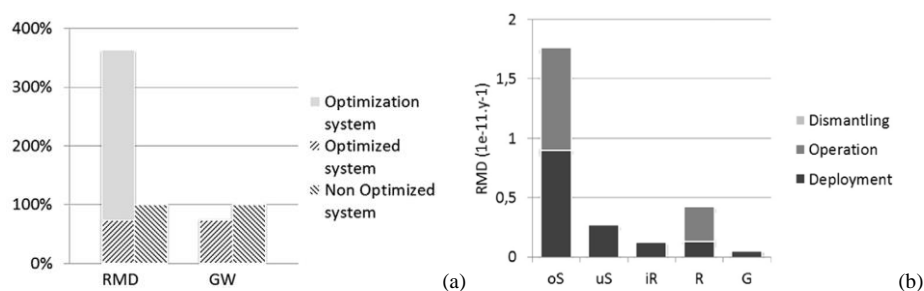


Figure 3.15. (a) Impact comparison of the optimized system for municipal garbage collection including the WSN (optimization system, composed of sensor systems, repeaters and gateways) and the regular garbage collection service (Non-optimized system). (b) RMD Impact estimation of the deployment, operation and dismantling phases of the WSN (oS = off-ground sensor systems, uS = Underground sensor systems, iR = intermediary repeaters, R = Repeaters, G = Gateways). Figures extracted from [10].

The impact on the deployment and operational stages of the WSN is explained not only by the rapid extinction of the battery of the off-ground sensor systems that causes numerous replacements, but also by the use of raw materials and emissions in the manufacturing phase of deployed all sensor systems, repeaters and gateways. Specifically, the RMD impact is distributed between the manufacturing phases of the gateways' battery and the electronic components of sensor systems and repeaters; and the GW impact comes mainly from their mechanical parts (casing and resins) (figure 3.16).

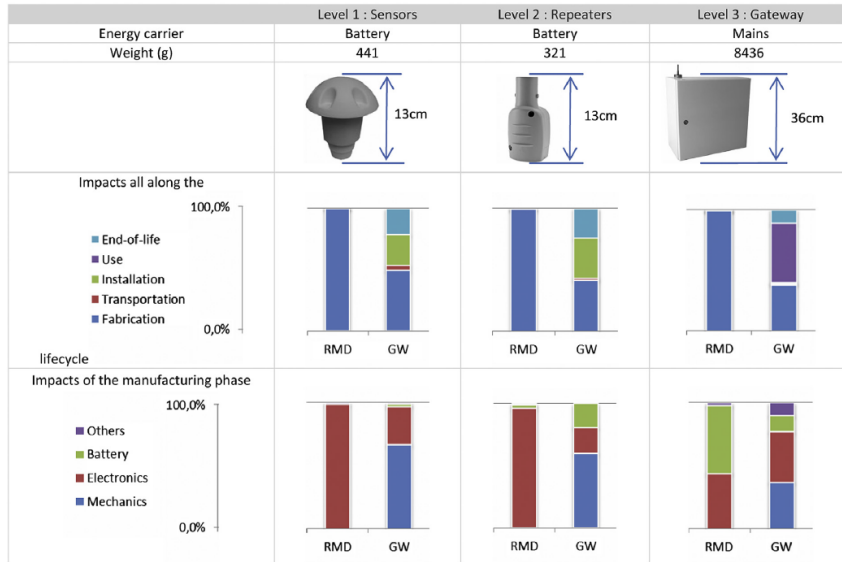


Figure 3.16. RMD and GW impact contribution of sensors systems, repeaters and gateway. (An auxiliary battery equips the gateway and its average power consumption is 6,6 Watts). Figure extracted from [10].

Another cost-benefit study provides a comprehensive review of the ecological efficiency of Home Energy Management System (HEMS) in four versions [72]. The first version consists of an energy monitor composed of a sensor, a transmission unit and a display (Figure 3.17a). The second version consists of an “old” multifunctional HEMS composed of an 8” LCD touchscreen, two sensors (gas and electricity) with two data transmission units, an adapter and repeaters (Figure 3.17b). The third version consists of a “new” multifunctional HEMS composed of a 7” LCD-touchscreen, switching adapters, wiring displays to the heater, and no-additional WiFi router. The fourth version consists of an energy management system made up of individual plugs in a zigbee mesh network (Figure 3.17c).

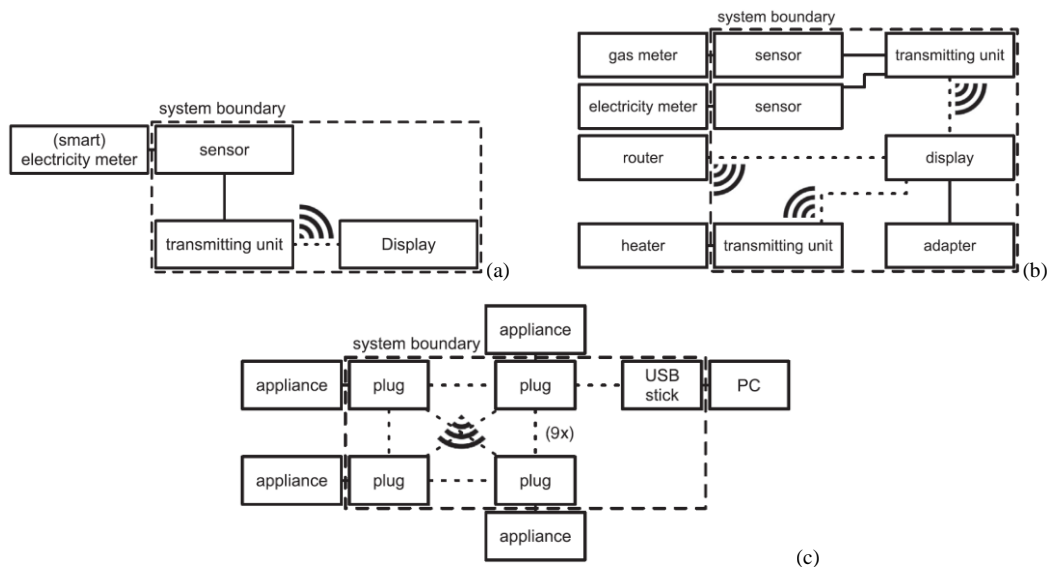


Figure 3.17. The product system boundaries of (a) the energy monitor version, (b) the multifunctional HEMS and (c) the Zigbee-based, energy management system. All figures are extracted from [72].

This cradle-to-grave study combines a Cumulative Energy Demand (CED) analysis with an Ecocost LCA-based analysis to determine whether the amount of energy saved by each of the four HEMS versions exceeds the energy required to produce, use and dispose them in eight different scenarios.

Results show (1) that the total impact depends on the type of HEMS, and (2) an approximate impact reduction of 45% from reducing the energy consumption (to 44 kWh) and the number and size of the components of the multifunctional HEMS version (see detailed results of the “new” HEMS version in table 3.8). Unfortunately, authors do not give further details about these interesting findings.

	Energy monitor	Multif. HEMS (old)	Multif. HEMS (new)	Energy management device
CED prod+disp	231 MJ	1535 MJ	1176 MJ	1285 MJ
CED use phase	534 MJ	5493 MJ	2676 MJ	2639 MJ
Total CED	765 MJ	7028 MJ	3852 MJ	3924 MJ
Eco-costs prod+disp	€4	€34	€26	€25
Eco-costs use phase	€5	€48	€23	€23
Total eco-costs	€9	€82	€49	€48

Table 3.8. Cumulative Energy Demand (CED) results and Ecocost impacts for production, use and disposal of the four HEMS versions, calculated over 5 years. Table extracted from [72].

- As observed in their cost benefit study, Bonvoisin, J. et al. [10] shows minor benefits and significant impacts from using IoT systems. Unfortunately, although this great difference is explained by the replacements of sensor systems and repeaters, and more specifically by their electronic components, authors does not provide further details. This lack of detailed results regarding electronic composition is also observed in the work of Van Dam, S. S. et al. [72].
- In this sense, in the next chapter a methodology will be designed to facilitate the transparent impact evaluation of local devices based on electronic components.

1.2.4. LCA studies of partial IoT systems (sensor systems and sensor components)

The LCA literature oriented exclusively to sensor systems identifies specific electronic components with high contributions in different environmental impact categories. For example, in an LCA comparative study of sensor systems belonging to an Intelligent Lighting IoT System (ILS) for buildings, Dubberley, M. et al. [73] found that the PCB and the integrated circuits components contribute significantly to several impacts categories. In addition, it was concluded that the sensors systems’ batteries has large impacts on Ozone depletion and Acidification; and moderate impacts on human health (Carcinogenicity) and Photochemical smog. Table 3.9 synthetize these results together with the impacts of other less relevant electronic components.

	Acidification	Eco toxicity	Eutrophication	Fossil fuel Depletion	Global Warming	Carcinogenicity	Non carcinogenicity	Ozone depletion	Photochemical smog
Ballast transformer (Inductor Cu)	25,7%								
Ballast transformer (Inductor Si steel)							2,4%		
Integrated circuits (ballast)		4,0%		24,6%					
Integrated circuits (sensor systems)		7,9%	32,4%	49,1%	27,2%	18,7%	3,7%		6,4%
Li Battery (sensor systems)	37,8%		25,2%		18,0%	28,8%		94,3%	13,0%
Paint (ballast)								1,8%	
PCB (sensor systems)	32,8%	82,8%	25,7%	15,6%	29,7%	40,7%	87,6%	2,8%	70,8%

Table 3.9. Highest (red), second highest (orange) and third highest (green) impact contributors of sensor systems belonging to an ILS IoT system. Adapted from [73].

As table 3.9 shows, the prevalent contributors in almost all categories are the IC components, the PCB and the battery. In this sense, authors suggest prioritizing the size reduction of the PCB and electronic circuits in redesign stages, mainly by functions simplifications of each component. It is also proposed replacing the battery with a connection to the ballast (which converts the building's AC electricity to DC and steps down the voltage), and minimizing the use of plastic in the housing of the sensor systems. Unfortunately, impact estimations of these initiatives are unavailable.

In another LCA study [74], it was also concluded that the PCB and the IC components contribute significantly to the environmental impact of different sensor systems, depending on their complexity (figure 3.18).

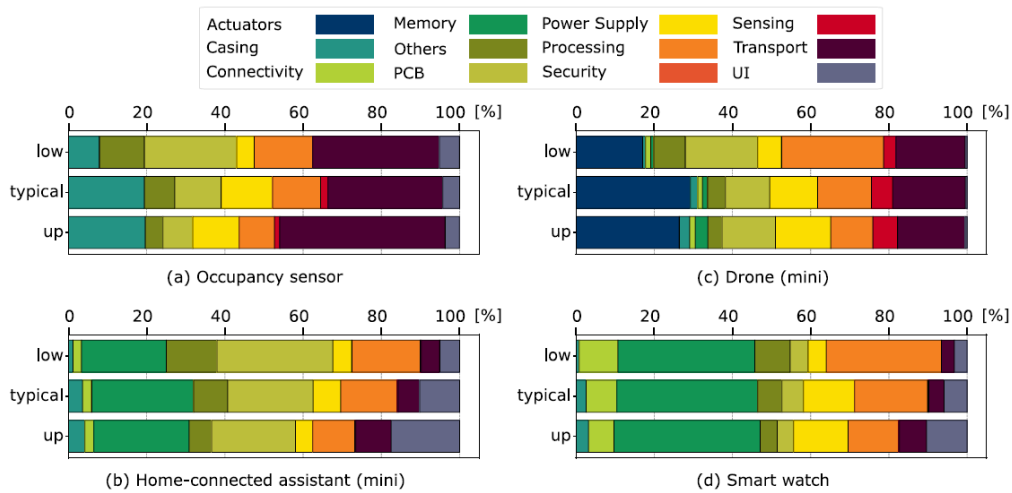


Figure 3.18. Endpoint Carbon footprint impact of (a) a Philips HUE occupancy sensor, (b) a Google Home mini home connected assistant, (c) a DJI MAVIC mini light weight drone and (d) a smart watch from Apple and Garmin. The LCA functional unit of all these IoT devices is defined as “production and transport to the use location of a single device”. Figures adapted from [74].

Indeed, if only impacts of production are taken into account, all types of sensor systems present relevant impacts from either the PCB component (i.e.; occupancy sensor or Home connected assistant) or certain integrated circuit components (i.e.: the memory for the home-connected assistant and the smart watch). Beside of this, it is also observed a persistent contribution of microcontrollers (processing components) in all types of sensor systems and, interestingly; and special contributors such as casing parts in occupancy sensors and actuators in drones.

In another LCA study [75], it is observed that significant environmental loads can be also identified in specific components subparts made by specific materials. Specifically, in this cradle-to-grave LCA study that introduce an anticounterfeit label (ACL) sensor system based on electrochromic display (ECD) and a piezo-based (PS) shock-detection-tag sensor system (SDT) (figure 3.19-3.20), it is observed that much of the environmental impact can be attributed to the production of NFC chip and Radio-Frequency Identification (RFID) antenna components.

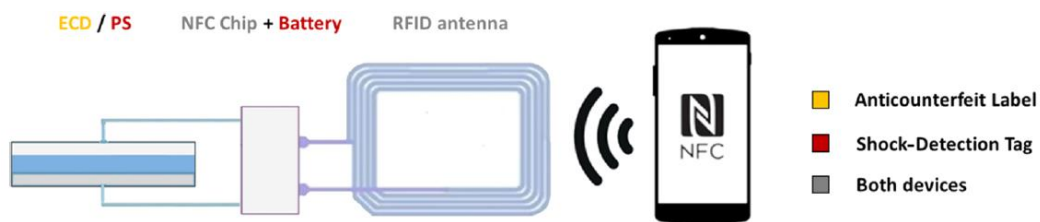


Figure 3.19. Basic schematic of the electronic design of the ACL and SDT sensor systems. The ACL is attached to a product to enable authentication during its transportation and storage. The SDT detects and record damages in goods when exposed to shocks, falls, or vibrations during transportation. Figure extracted from [75].

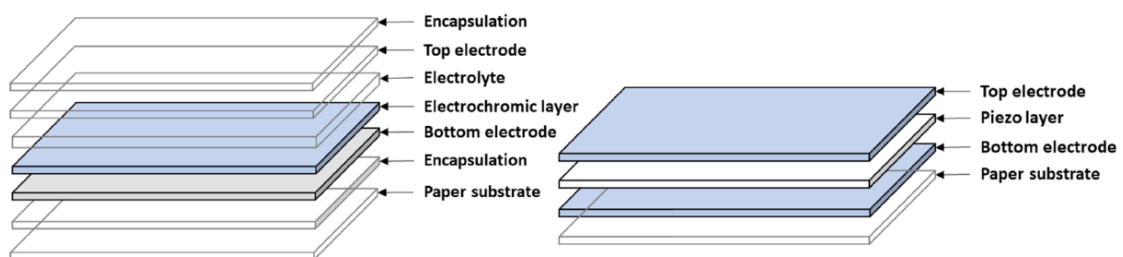


Figure 3.20. Basic schematics of the ECD and PS components. The ACL sensor system uses the changes of color of the ECD display induced by a redox reaction in the electrochromic material. The SDT sensor system uses piezoelectric materials embedded in the PS component, which generates electrical charges whenever a mechanical stress is produced. Figure extracted from [75].

By considering that both sensor systems use either microparticle- or nanoparticle-based silver ink for the construction of the RFID antenna, which is printed on paper substrate together with the ECD and PS subparts, Figure 3.21 and figure 3.22 show the impact contribution of this component in both sensor systems, which ranges from more than 20% to almost 100% in different impact categories.

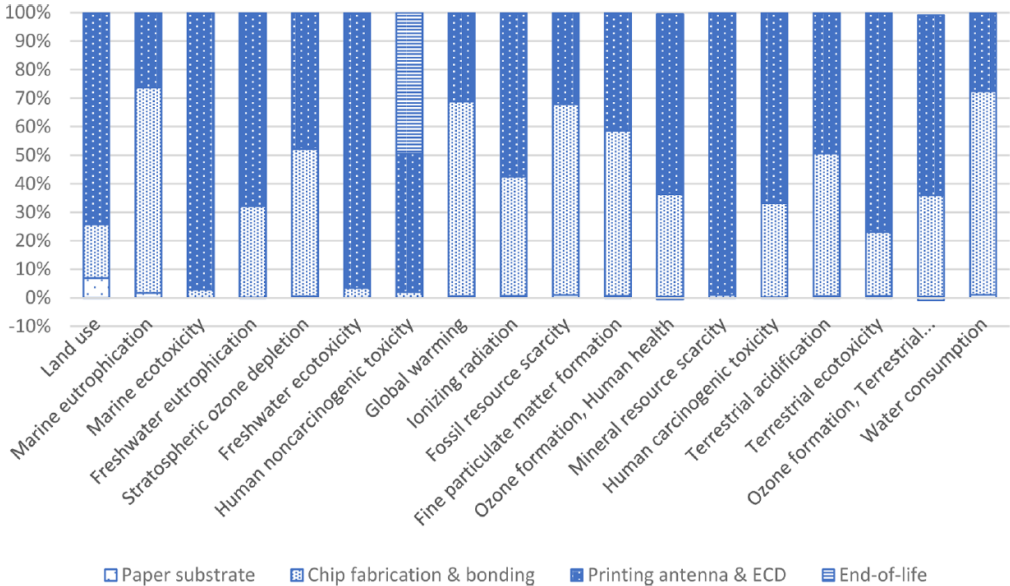


Figure 3.21. Impact results of the ACL sensor system. the functional unit is defined as “producing at least 20 times visible chromaticity change after receiving a 13,56 MHz signal (from the smartphone) over a period of 2 years”. For this, a single ACL sensor system is defined as the reference flow. Figure extracted from [75].

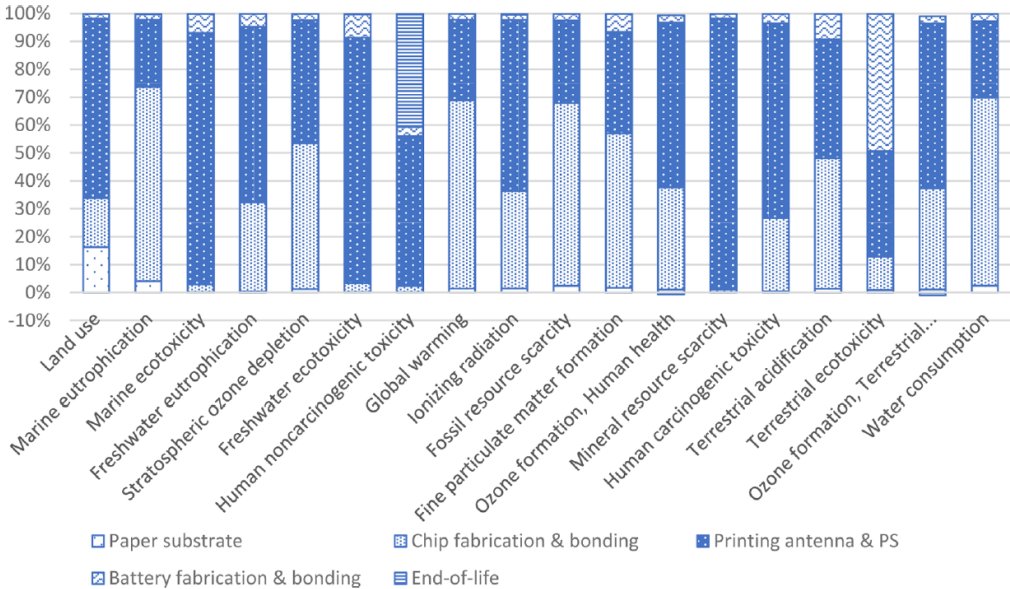


Figure 3.22. Impact results of the SDT sensor system. the functional unit is defined as “detecting and recording any frequency above 13,56 MHz over the product’s transportation, translating into a voltage signal readable by a smartphone”. For this, a single SDT sensor system is defined as the reference flow. Figure extracted from [75].

As observed, the silver content in the RFID antenna component leads to different impact contributions in all categories, especially in the mineral resource scarcity. Regarding these results, two main redesign strategies were proposed: (1) reduce the amount of silver in the antenna through the use of flexography printing of silver nanoparticles and (2) replace the silver ink with copper nanoparticles by using screening-printing techniques. Apart from alleviating the ecological burden in the resource scarcity category (with mineral resources savings ranging from 60% to 90%), these alternatives contribute to an combined impact reduction of 64% and 85% respectively in toxicity (terrestrial, marine and freshwater) and human health (carcinogenic and non-carcinogenic impact categories) (see figure 3.23).

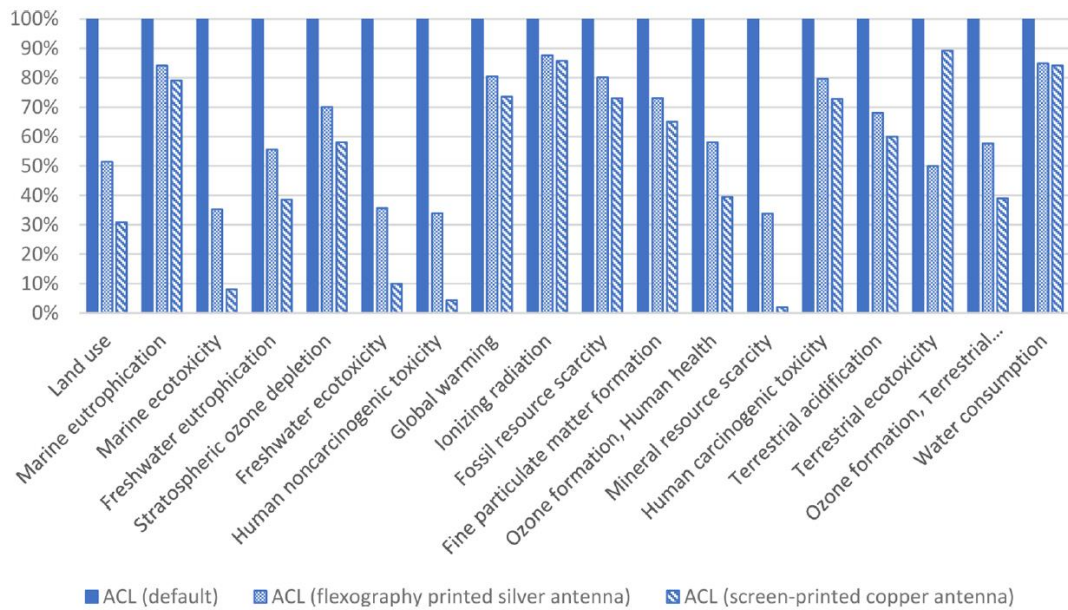


Figure 3.23. Impact comparison of the default design of the ACL sensor system and its redesign based on flexography printing silver ink and screening printing copper ink. Results are almost similar for the SDT sensor system. Figure extracted from [75].

On the other hand, Wagner, E. et al. [26] identified significant impacts in active components in different versions of a sensor system for prognostic health monitoring of structures (figure 3.24b).

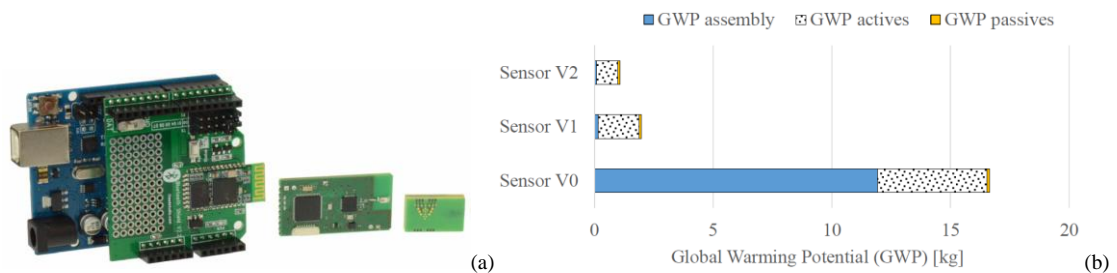


Figure 3.24. (a) A sensor system for prognostic health monitoring of structures. From left to right: Version 0 (V0) of the sensor system (customized Arduino Uno version), V1 (lean, customized system version), V2 (full integrated advance packaging version). (b) GWP impact of the production of the three versions. Figures extracted from [26].

Indeed, while much of the environmental impact of the open source version (V0) is allocated to the assembly of 41 components (including 11 active components), connectors, large and less densely populated PCB areas and large electronic components (Big dual-inline-package processors); much of the environmental impact of the lean, customized version (V1) is allocated almost exclusively to active components (a MSP 430 microcontroller, a CC2520 transceiver and three types of sensors) (figure 3.24b). In addition, this study concludes that the environmental savings of the full integrated version (V2) are attributed to the avoidance of back-end production processes of integrated circuits (incorporation of lead frames, gold connections, molding compounds and die attach).

In the context of sensor components, LCA literature shows that impacts are mainly attributed to the use of specific materials. For example, in a LCA study [76] of a wearable self-care health actuator described in figure 3.25, it is showed that the impact is attributed, to a greater extent, to the use of large amounts of silver in the production of a special textile wire (Elektrisola wire) and, to a lesser extent, to the production of the PCB component (figure 3.26).

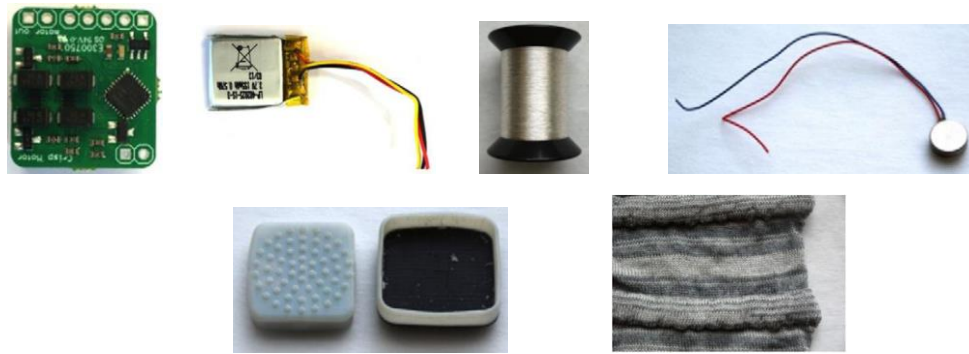


Figure 3.25. Essential components of the “Vibe-ing” system for providing vibration health therapy. From left to right (top): Motor printed circuit board, 2000mAh 3.7V battery, Elektrisola textile wire and DC Vibration motor. Bottom: Casing shells (left) and textile body (right). The casing shells accommodate the DC vibration motor, which reacts to capacity touches or specific therapy programs. Figures extracted from [76].

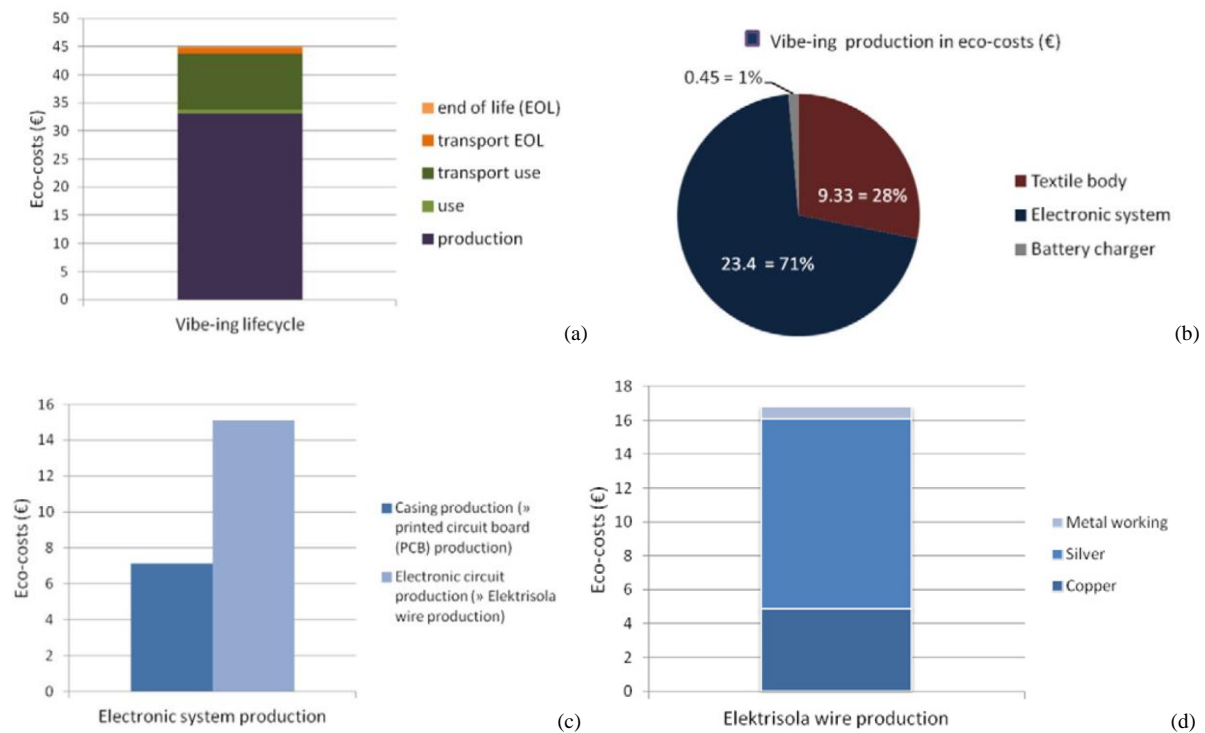


Figure 3.26. LCA results for the “vibe-ing” system. (a) Ecocost impact of the life cycle phases, (b) impact contribution in the production phase, (c) impact contribution of the electronic system and (d) impact of specific materials in the Elektrisola textile wire. Figures extracted from [76].

Based on these results, the authors propose (1) the use of an alternative version of the textile wire with high copper content or (2) reduce the use of the current silver-based wire by 75%. Option 1 would generate an impact reduction of 45%, with the potential risk of affecting the final appearance of the garment (copper has a different coloration than silver). On the other hand, option 2 would reduce the impact in more than 50%, with the risk of compromising communication and connections between the different modules of the system.

In this line, another comparative study conducted by Le Brun, G. & Raskin, J. P. [77], shows the ecological advantages of using promising and eco-friendly materials in innovative sensors for specific applications. Specifically, this study shows that the environmental impact of using paper-based

electrochemical sensors (figure 3.27) would be much lower than the impact of using regular silicon-based biosensors for water quality detection.

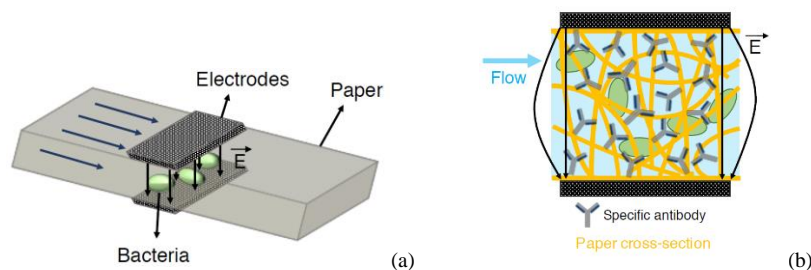


Figure 3.27. (a) Basic schematic of the paper-based electrochemical sensor oriented to detect bacteria in water. The water sample is guided through the paper by natural capillarity. Electrodes on the paper surface sense the paper volume and electrical impedance is used as a volume detection mean to probe the dielectric changes of the system corresponding to bacteria presence. (b) Cross-sectional view of the sensor.

Antibody bio receptors are required in the device to specifically detect bacteria cells. Figures adapted from [77].

With a functional unit defined as “performing 1000 water quality measurements in terms of pathogen presence” that includes an equivalent reference flow of 1000 single-use sensors, the author compares the environmental impact of Silicon-PDMS microfluidic (Si-PDMS) sensors and Carbon NanoTubes / Aluminum microfluidic Paper-based Electrochemical Devices (CNT- μ PED and Al- μ PED). Based on the material composition and energy consumption in the manufacturing phases of this three types (table 3.10) and in literature [238], they show that CNT- μ PED sensor type contributes the less to the Embodied energy and carbon footprint loads (figure 3.28).

Material (in Kg) or Energy (in kWh)	CNT- μ PEDs	Al- μ PEDs	Si-PDMS
Electricity	2,25	390	226
Paper	16	16	
CNTs	0,04		
Water	22		
Surfactant	0,9		
Al		0,15	0,003
Ar		6,03	0,27
N ₂		3,465	88,75
H ₂		0,225	0,01
He		0,405	0,018
Ag		0,2	
HNO ₃		0,2	
Ethanol		0,2	
Formaldehyde		0,02	
Wafer			0,08
Al ₂ O ₃			0,001
PDMS			1,5
H ₂ O ₂			4,6
H ₂ SO ₄			16
TMAH			0,02
Ethyl Lactate			0,186
HDMS			0,154
C ₄ F ₈			0,003
CHF ₃			0,001
CH ₄			2,5
NF ₃			0,06
NH ₃			0,11
HF			4,6
IPA			12
H ₃ PO ₄			12
Total	38,94	26,90	142,87

Table 3.10. Materials and energy used in the fabrication of 1000 paper-based sensors (CNT- μ PEDs and Al- μ PEDs) and 1000 Si-PDMS sensors. Adapted from [77]. The electrodes of the paper-based sensors are made of carbon nanotubes-based aqueous conductive inks on different paper substrates.

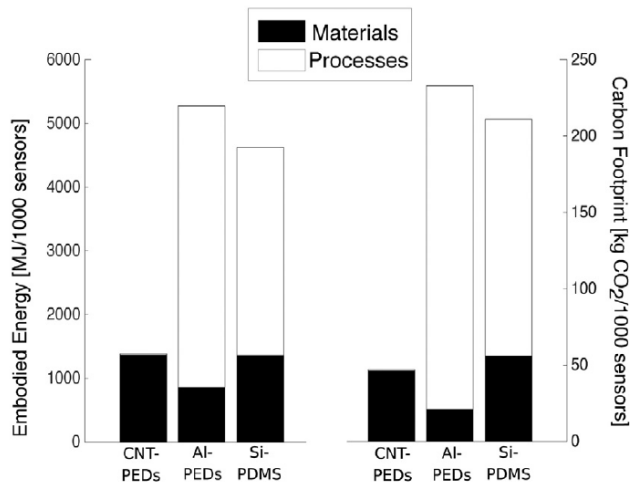


Figure 3.28. Embodied energy and carbon footprint of the materials and manufacturing processes of 1000 CNT- μ PEDs, Al- μ PEDs and Si-PDMS sensors. The specific embodied energy and carbon footprint of each material and energy supply are available in [238]. Figure extracted from [77].

- In this section, Dubberley, M. et al. [73] and Pirson, T. et al. [74] reveal the significant contribution of PCBs, integrated circuits and other components to the environmental impact of IoT devices and Glogic, E. et al. [75] suggest that impact of specific components would be explained to the use of specific materials (i.e.: silver). Furthermore, Wagner, E. et al. [26] even point out specific subparts in back-end production processes of active components with high impact potentials.
- In this sense, some authors propose substitution-, or reduction-innovative techniques without delving into the technical or commercial viability of these modifications (for example, Van der Velden, N. et al. [76] warn that a poorer concentration of silver, or a rich concentration of copper in specialized wirings could affect the internal connectivity or the final appearance of E-wearables respectively). On the other hand, all the authors do not analyze whether or not these modifications affect other life cycle stages of IoT devices (i.e.: use and end of life).
- In this sense, in the next chapter a lifecycle framework will be proposed to estimate the potential impacts of replacing or modifying electronic components, as well as to facilitate the integration an interdependency analysis of such changes in redesign stages of IoT devices.

1.3. Summary of key aspects and shortcomings of LCA studies of IoT systems

Annex 15 provides a synthesis of all LCA studies presented so far together with some additional aspects that are worth mentioning. From it, it can be observed —regardless of the system boundaries and the limited results that some authors provide— that significant impacts are attributed mostly to sensor systems and, specifically, to inner electronic components (such as PCB, electronic circuits and batteries). These electronic components would be made with unfavorable materials (silver, copper, silicone, etc). In this sense, specific redesign strategies suggest replacing and reducing certain materials; or decreasing the number of sensor systems in IoT systems, depending on their operational contexts and functional units.

Significant impacts are also attributed to the energy consumption of sensor systems in the operational stage of IoT systems. This is related to the required number of local devices for covering functional units on the one hand, and to energy consumption patterns on the other hand. The redesign strategies proposed in this sense vary from a resource managing perspective (mutualizing edge devices for enabling different applications; or prolonging sleep states) to a hardware perspective (i.e. : increase the capacity of the batteries) to avoid early replacements. In this context, although some authors demonstrate the relevance of the reference flow for obtaining accurate impact results, much of the LCA literature suffer from either ambiguous or nonexistent definitions of reference flows. In addition to this, reference flows of all LCA studies are not defined on the basis of essential resources oriented to collect, process and transmit data and information.

On the other hand, although most of the studies attempt to address the complete life cycle of IoT systems, the impact estimation of certain stages falls short due to specific problems related to lack of data, the difficulty of life-cycle-phase modeling, or uncertainties. For example, in the study carried out by Glogic, E. et al. [75], the modeling of the end-of-life phase of both devices (the ACL and SDT sensor systems) presents several simplifications and uncertainties associated to assumptions in the landfilling scenario (related to inclusion of paper fractions) and recycling rates of paper substrates that would depend on the use location of the devices. In this line, Lelah, A. et al [51] do not take into account the end-of-life modeling for two reasons: the lack of a consistent E-o-L database and the difficulty of modeling realistic maintenance scenarios for wireless sensor networks. In this manner, their work would be extended to the E-o-L of the sensor systems one year later, but using an independent methodology (ReSICLED [78]). In this extended work [61], they would justify this decision due to the lack of environmental data on E-o-L processing techniques in databases.

This problem of missing data is also recurrent for other life cycle phases of IoT systems such as manufacturing and, specifically, the use phase; where the lack or scarcity of data related to mutualized infrastructure (telecoms) forces researchers to limit the system boundaries of their studies to local devices to avoid interpretation problems on results (as in the case of the LCA study presented by Lelah, A. et al. [51]). In this sense, certain authors recommend improving the availability of comprehensive and updated LCI databases related to the manufacturing process of sensor systems (i.e.: typical materials or sub-assemblies) [60], investing more efforts to deal with uncertainties during LCA analysis [61], and including the use of networks and cloud resources in the operational phase of IoT systems within LCA system boundaries [61], [71], [74].

However, although a comprehensive impact estimation of the entire life cycle of an IoT system is essential to avoid impact transfers not only between different impacts but also between different life cycles [79], Wagner, E. et al. [26] warn that the exhaustive application of a LCA analysis in the early design of sensor systems could become inefficient, because designers are faced additionally with further decisions and challenges in different contexts (e.g., choosing the suitable antenna and the optimal protocol for specific communication tasks or solve radio frequency interference problems and high energy consumption).

2. New Product Development process, Eco-design and eco-design tools for IoT systems

2.1. Fundamentals of eco-design and New Product Development Process

In order to better explain the particularities and contribution of current tools for sustainable IoT systems, the definition of eco-design, as well as a brief description of its implementation on the New Product Development (NPD) process, found in the ISO standard 14062 [80] and the ISO standard 14006 [81], are synthesized and presented in the following sections.

2.1.1. Eco design

The integration of environmental aspects into the design and development process of a product, by considering its entire lifecycle could be termed as eco-design. An environmental aspect is any element of an organization's activities, product or services that can interact with the environment (surroundings in which an organization operates, including air, water, land, resources, flora and fauna, humans and their interrelations). Eco-design may include aspects related to environmental aspects in general (i.e.; Design for Environment (DfE)) or aspects that concern specific processes in specific lifecycle phases (e.g., Design for Recyclability (DfR) or Design for Disassembly (DfD)) but, in general, for electronics, it aims to reduce emissions and the quantity of direct and indirect resources; and avoid toxicity [113].

2.1.2. New Product development Process

New Product Development (NPD) is a sequential process that considers a product idea from planning to market launch. For this, several aspects such as business strategies, marketing considerations, research methods and design are taken into account. The NPD process is applied for new products, as well as for improvements or modifications to existing products or services. Figure 3.29 shows the typical steps in NPD together with the common environmental aspects considered for eco design.

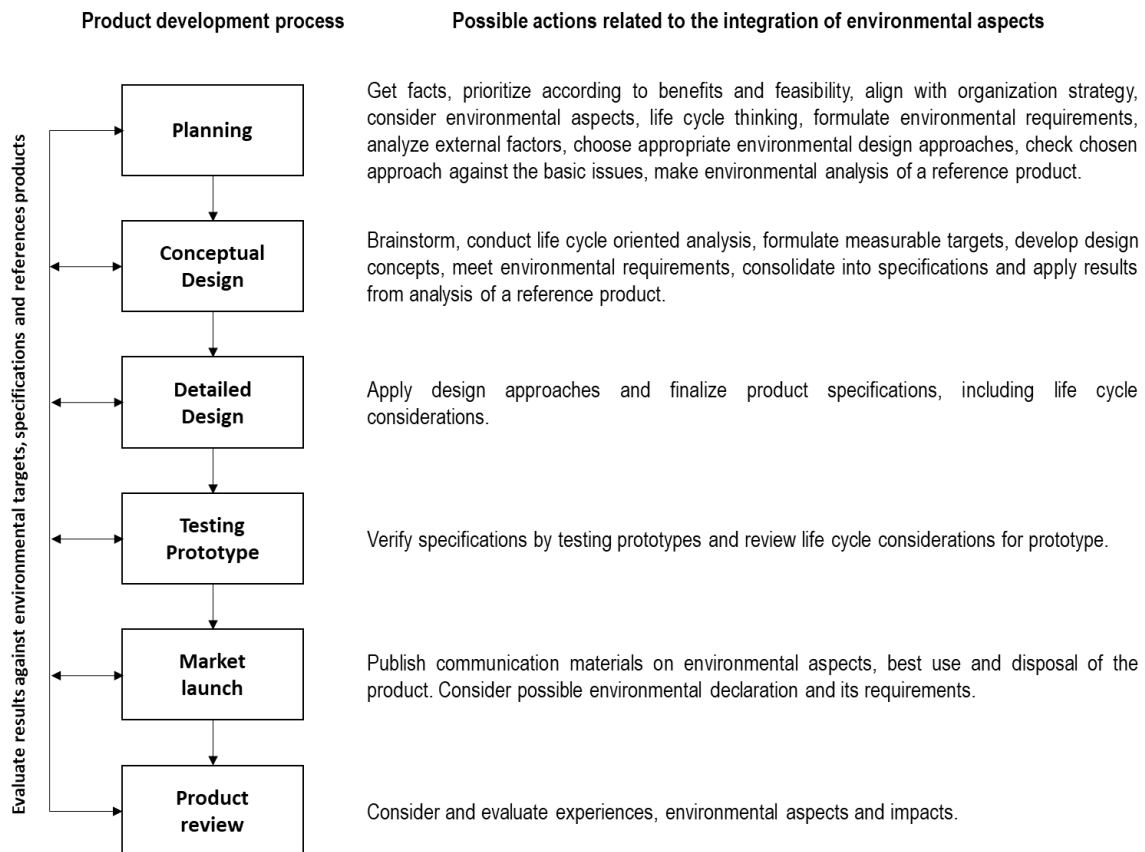


Figure 3.29. Generic environmental aspects taken into account in a typical product development process. Figure adapted from [80].

In figure 3.29, the introduction of environmental aspects into early phases of the NPD process facilitates more flexibility for considering specific demands (i.e.: environmental directives) together with other requirements. (i.e.: technical specifications). The planning stage includes the planning and formulation of requirements applied to the product by considering the available time and budget. This step can start by an analysis of external factors with significant influence on the product such as the client's expectations and requirements, environmental demands (such as ensuring resources optimization and human health, or reducing hazardous substances, emissions and waste) and internal factors (such as availability of components, subcomponents, and materials).

The conceptual design stage aims to cover the requirements defined in the planning stage. In this phase, the design ideas and the identified requirements gives indications of the environmental objectives related to the product, which are addressed by different tools such as guidelines, checklists or manuals. These tools can be generic or customized for an organization and its products. The conceptual design stage generates technical and environmental specifications that are later addressed in the detailed design stage. A detailed design has specific information related to the product, its life cycle, and its potential environmental impacts.

In the testing prototype stage, the construction and tests of prototypes facilitates the evaluation of the detailed design by comparing it with environmental targets and other specifications. Different technical tests related to material properties, use wearing, functions, quality and lifespan of specific elements, processes and components could be performed at different levels before or during the evaluation of prototypes. In the same line, different properties and environmental aspects such as usage modes, mass, disassembly, recycling potential, energy and material consumption efficiency can be evaluated in this NPD stage.

Finally, the market lunch phase puts the product in the market through the presentation and the communication of its environmental features and advantages; and the product review phase aims to

verify whether the product respond or not to the expectations of the organization or customers (i.e.: expectations including the product and its environmental performance).

2.2. Instruments for the design and eco design of IoT systems

This section presents the current instruments that facilitate the design and eco-design of IoT systems as follows: Firstly, it presents the current standards that facilitate essential definitions and frameworks for the regular design of IoT systems and then the emerging standards that frames the design of IoT systems to ensure the technical and ecological development in specific domains. Then, it presents the general guidelines in different life cycle phases of IoT systems. Finally, it presents specific tools applied in different stages of the NPD process of sensor systems and IoT systems. Each of the following sections ends with a synthesis in terms of advantages, disadvantages, shortcomings, contribution, and difficulty of application in the NPD process.

2.2.1. Standards

In the technical area, the International Telecommunications Union (ITU) published the seminal standard Y.2060 [82] that provides a technical overview of IoT systems (figure 3.30), and a reference model composed of four main layers: the application layer, the support layer, the network layer and the device layer (see figure 3.31).

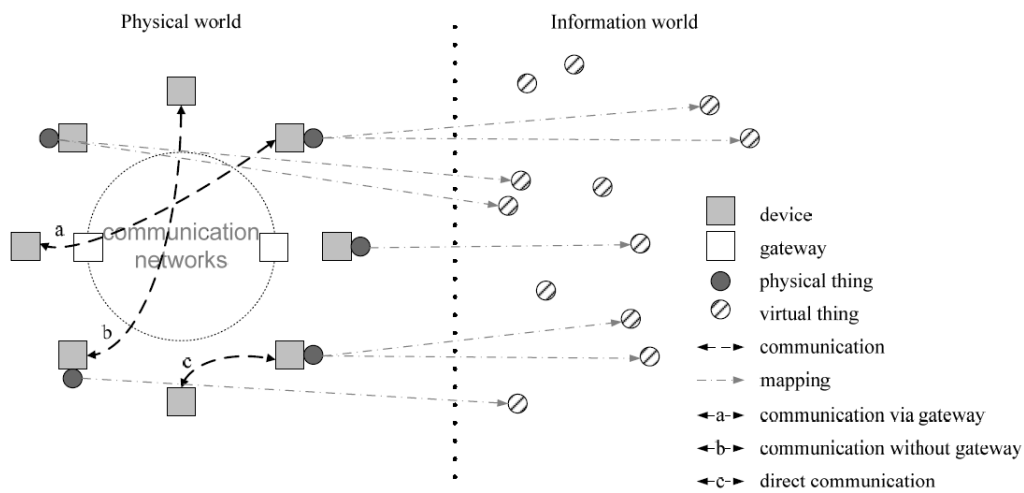


Figure 3.30. Technical overview of IoT systems according to the ITU standard Y.2060 [82]. A device can be understood as a sensor system, and a gateway as an edge device. A physical thing can be represented in the information world through one or more virtual things (mapping), but disassociations may be possible. Although only physical interactions (communication between devices) are depicted here, information interactions (exchanges between virtual things) are possible.

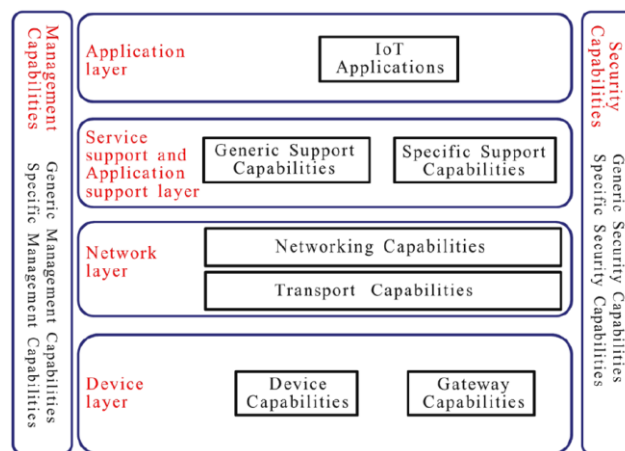


Figure 3.31. IoT reference model according to the ITU standard Y.2060 [82]. The complementary management and security layers are related to common capabilities for resource management and security of sensor systems (i.e. software update or authentication).

As observed in figure 3.31, the Service Support / Application Support layer is categorized into generic capabilities that every IoT system must meet and specific capabilities oriented to particular applications. On the other hand, while the network layer differentiates the needed network capabilities to connect things (for example, access control or routing) from the basic data transport capabilities (connectivity and control management information); the device layer makes a distinction between the required capabilities of sensor systems (i.e.: Ad-hoc networking and sleeping-, awaking-states) and Internet gateways (i.e.: multiple interface support or protocol conversion).

Future publications use this referential model to define specific requirements in other domains such as M2M and smart sustainable buildings. The M2M ITU Focus group (FG M2M) [83] establishes, for example, the specific and essential capabilities for sensor systems (i.e.: device identification, naming, discovery and registration capabilities) and the support layer (i.e.: diagnostics, fault recovery and device group management capabilities) to ensure resilient connectivity (figure 3.32).

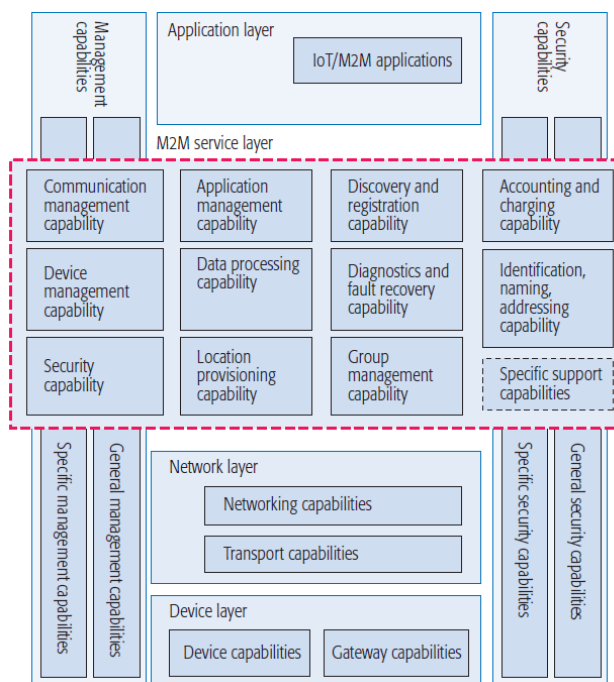


Figure 3.32. An adapted version of the FG M2M ITU deliverable oriented to the M2M support layer (service). Due to the lack of human intervention in the context of M2M, specific capabilities such as discovery and registration in sensor systems and support layer are essential. Figure extracted from [84].

The work done in the M2M focus group is later harmonized with other domains including common recommendations for IoT (Y.2066) [85], edge computing (Y.4208)[86] and internet gateways (Y.2067)[87]. This study group includes also the ITU-T L.1370 recommendations [88] that establishes the needed services (support capacities), data, functional features and technical requirements for enabling sustainable smart buildings. The following list presents some of the technical features that every of the mandatory sensor systems (energy consumption meters, flowmeter for water consumption, fire, flooding carbon oxide detectors, air quality and pollution sensors systems) of a smart building should have:

- An IoT device should include a processor with at least two cores of at least 1 Ghz processing speed.
- An IoT device should include a low-latency and solid-state drive mass memory up to 8 Gb.
- An IoT device should provide wireless local area network connectivity by at least two protocols and by at least one interface (i.e.: 3G, 4G, etc).
- An IoT device should provide wired local area network connectivity by at least two protocols and by at least one interface (i.e.: Ethernet).

- An IoT device should provide specific frameworks for third-parties application and service deployment (i.e.: Java OSGI framework).

- As observed, all standards presented in this section could facilitate the identification of external factors related to the operational context of IoT systems in generic contexts or particular domains. In this sense, the IoT referential model presented in the standard Y.2060 [82] could be used as a starting point in the planning stage of the NPD process of IoT systems.
- In the detailed design stage, the recommendation for supporting sustainable building [ITU-T L.1370] could facilitate the identification of minimal technical specifications in this particular context.
- However, the use of these standards are very limited because they are not oriented to the environmental design of the IoT systems themselves. For example, they are not effective in the conceptual design stage because they do not provide environmental targets in the life cycle phases of sensors systems or mutualized infrastructure.
- In the next chapter, one will attempt to (1) benefit from the abstractions they provide (especially IoT referential model) and (2) extend these abstractions for the eco-design of IoT systems itself.

2.2.2. Guidelines

Beginning of Life (B-o-L) Guidelines are scarce and oriented mainly to the manufacturing of sensor systems or sensor components. For example, Zhu, C. et al. [17] propose reducing the size of RFID tags to decrease the amount of non-biodegradable materials and Gurova, O. et al. [89] compile a series of guidelines found in literature related to raw materials and production process of smart wearables, which do not differ much from guidelines found in the sector of electronics. Table 3.11 presents some of the guidelines found in these works that could have an influence in early design, within the NPD process of IoT systems.

Author	Guidelines
Zhu, C. et al. [17]	1. Reduce the sizes of RFID tags to decrease the amount of non-degradable material used in manufacturing.
Gurova, O. et al. [89]	1. Avoid alloys that are difficult to separate at the end of life of a product [90]. 2. Avoid dangerous plastics and consider safer, biodegradable alternatives [91]. 3. Consider new materials for circuits that can be disassembled (i.e.: Use thermoplastic substrates and novel adhesive systems for bonding dielectric layers and component attachment [92]) 4. Use components that are certified as less harmful (Reach and RoHS) [93-94] 5. Optimize the design to use less energy in production (i.e.: by designing more efficient cooling) [95] 6. Use existing production platforms that benefits from scale instead of buying production equipment [96] 7. Consider shifting or replacing parts, if these parts contains rare earth elements (REEs), and use parts made by plentiful raw materials [97].

Table 3.11. Summary of guidelines oriented to reduce the impact of the B-o-L of sensor and sensor systems.

Guidelines related to the use phase of IoT systems are more focused on reducing the energy consumption of sensor systems. For example, Zhu, C. et al. [17] presents a series of guidelines for the low energy consumption of RFID tags, wireless sensor networks, cloud computing, M2M, data centers and generic ICT. Gurova, O. et al. [89] continue its synthesis of guidelines now related to the use of low energy consumption for smart wearables. Nivethitha, V. and Aghila, G. [98] propose guidelines for efficient and resilient edge computing design. Arshad, R. et al. [99] and Bonvoisin, J. et al. [10] for their parts, argue for more efforts in finding the just-enough quantity and quality of data with the appropriate computing placing. On the other hand, the End of Life (E-o-L) phase is only covered by Gurova, O. et al. [89] in the context of smart wearables. Some of these guidelines with potential influence on the technical and eco-design of IoT systems are presented in table 3.12.

	Author	Guidelines
Use Phase	Zhu, C. et al. [17]	<ol style="list-style-type: none"> 1. Develop energy-efficient algorithms and protocols for optimizing tag estimation, adjusting transmission power level dynamically, avoiding tag collision, overhearing, etc. 2. Make sensor systems only work when necessary (and switching to sleep mode as soon as possible). 3. Analyze energy depletion patterns and use energy harvesting mechanism. 4. Use radio optimization techniques (i.e.: transmission power control, directional antennas, etc.). 5. Use data reduction mechanisms (i.e.: data aggregation, adaptive sampling, etc.). 6. Use energy-efficient routing techniques (i.e.: cluster techniques multipath routing, node mobility). 7. Use Power-saving virtual machine techniques (i.e.: consolidation, migration, placement, etc.). 8. Use energy-efficient allocation algorithms (i.e.: auction-based resource allocation, gossip-based resource allocation). 9. Adjust the transmission power (to the minimal necessary level). 10. Design efficient communication protocols (i.e.: routing protocols). 11. Use renewable or green source of energy for data centers and efficient dynamic power-management technologies (i.e.: Turboboost, vSphere) and energy-efficient hardware (i.e.: Dynamic Voltage and Frequency Scaling (DVFS)) 12. Send only data that are needed (i.e.: predictive data delivery). 13. Minimize length of data and wireless path (routing schemes and cooperative relaying). 14. Use advance communication techniques (i.e.: multiple-input multiple-output).
	Gurova, O. et al. [89]	<ol style="list-style-type: none"> 1. Consider registering with ecolabels (i.e.: Energy star [100] EPEAT [101]) 2. Take into account not only local but also remote energy use of backbone infrastructure and cloud servers [6]. 3. During product design, decisions of whether computation or storage happening on-device or remotely have to be considered concerning energy efficiency.
	Nivethitha, V. and Aghila, G. [98]	<ol style="list-style-type: none"> 1. Architecture should be adaptive and elastic (with respect to growth of users, data traffic or data size) without compromising performance [102]. 2. Treat servers as disposable resources [102]. 3. The computational element should be made available near to the users/data source.
	Arshad, R. et al. [99]	<ol style="list-style-type: none"> 1. Reduce the network size (by efficient placement of sensor systems or ingenious routing mechanisms). 2. Use selective sensing (collect only data that is required in a particular situation). 3. Find intelligent trade-offs (according to particular scenarios) between processing or transmit data to save energy like compressive sensing [103] and data fusion.
	Bonvoisin, J. et al [10]	<ol style="list-style-type: none"> 1. Interpret data as soon as possible in the transmission chain in order to send light and high-level information instead of heavy low-level data. 2. Find the device coverage that minimize the number of devices deployed. 3. Reduce the power consumption in the idle state to a minimum.
E-o-L Phase	Gurova, O. et al. [89]	<ol style="list-style-type: none"> 1. Use Design for Disassembly (DfD) approach, enhancing recyclability of ICT [104]. 2. Apply techniques that will allow separation of materials [105].

Table 3.12. Summary of guidelines oriented to reduce the impact of the use and E-o-L life cycle phases of sensor systems.

- As observed, this section present some energy-efficiency guidelines that could be used as a starting point to establish measurable targets in the conceptual planning stage. For example, the guidelines “minimize length of data and wireless path” proposed by Zhu, C. et al. [17] forces designer to establish concrete sampling rates or minimal QoS thresholds depending of the IoT application and its operational context.
- However, the usefulness of all the guidelines presented in this section is limited concerning further decisions in the detailed design stage of the product development process. For example, they fall short on the selection of specific technologies and technical specifications.
- Moreover, many guidelines have already been proposed in the literature. Since applying them all in an IoT system would be difficult or impractical, a method to evaluate their significance, according to the context and the requirements of applications, is needed.

- By taking into account all these aspects, and by considering the findings of section 1.2, in the next chapter one will study more carefully some guidelines concerning data and information flows for the construction of a design methodology. A special attention will be given also to guidelines concerning modifications on the physical attributes of devices and electronics components too, as the relevance of these aspects was clearly highlighted in previous sections.
- On the other hand, the proposed methodology in the following chapter will aim, among other aspects, to evaluate the appropriateness and efficiency of existing guidelines.

2.2.3. Design and eco design methodologies for IoT systems

In the context of typical design of IoT systems, Chakravarthi, V. S. [107] adapts the three-layer classical architecture for IoT systems into a basic framework (Figure 3.33) and uses it to describe specific aspects of IoT devices, which could be aligned with certain stages of the product development process of IoT systems.

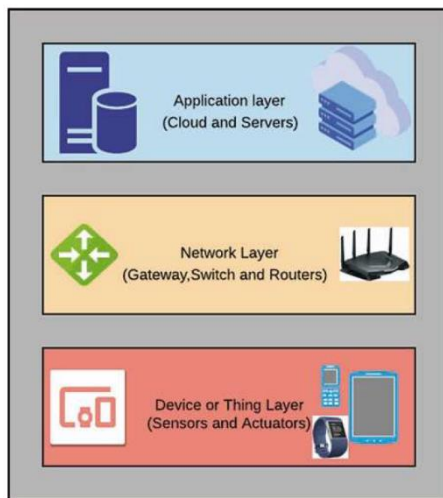


Figure 3.33. An adaptation of the classical architecture for IoT systems proposed by Chakravarthi, V. S. [107]. According to this author, the cloud element in the application layer is used not only for data processing tasks but also for controlling, configuring and triggering events at devices that belong to the network layer.

With this basic framework (which recall to some extent to the IoT referential model found in the ITU-T standard Y.2060 [82]), the author highlights the relevance of well defining—in her words, the “problem definition” of the IoT application. This could be understood as the establishment of essential requirements identified by specific questions. For example, in the context of an IoT application oriented to monitoring human-body temperature, relevant requirements could arise by answering the questions “what is the accuracy needed?” or “what should be the maximum form factor of the device”. As observed, this process could be aligned with the planning stage of the NPD process of IoT systems.

This author shows later that answer of these questions could lead to spot concrete technologies with particular specifications. For example, by considering a high accuracy level for human-body temperature monitoring, IR-based temperature sensors could be chosen, and specific quality ranges (i.e.: 0,3-0,6 °C) could be established. Based on this, specific electronic components could be selected preliminary and evaluated according to their features and capacities. With respect to the NPD process, these aspects could be related to the conceptual and detailed stages.

Finally, the author suggests that a proof-of-concept development could be carried out by considering (1) A Software development Environment (guided by 4 basic sequential elements depicted in figure 3.34), and some considerations regarding the PCB (The programmability limits of the processor or processors, the Input / Output interfaces of electronic components and standard bus interfaces). As observed, these aspects could be aligned with the testing and prototyping stage of the NPD process of IoT systems.

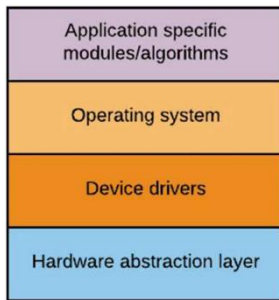


Figure 3.34. Layered-diagram for the embed software system development proposed by Chakravarthi, V. S. [107]. The hardware abstraction layer (HAL) provides basic software functions called boot loader. The device drivers may work through HAL functions or directly. The operating system allows sequential or virtual concurrency execution of functional tasks. Figure extracted from [107].

Heinis, T. et al. [108] for their part, propose a methodology composed of three parts: the analysis of the physical object (the object that will benefit from the IoT application), the analysis of data processing functions, and the analysis of the added value resulting from data processing (see figure 3.35).

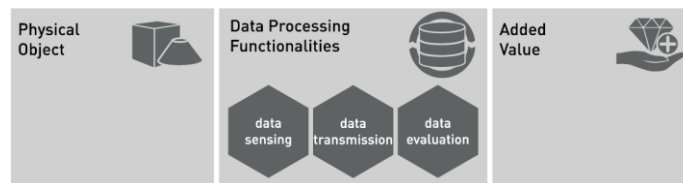


Figure 3.35. Proposed methodology based on the analysis of a physical object, data processing functionalities and added value. Figure extracted from [108].

Starting from the definition of the physical object, this methodology consists firstly on defining the user and the benefits that he or she will receive from an IoT application (the added value of the IoT system). For example, Table 3.13 shows this analysis in the context a case study (a mechatronic device), expressing the potential added value of the IoT application by user stories or Voice of Customer (VoC) instances.

Definitions	
Physical objects	<p>Object: Jarvis Mechatronic Kit (JMK) Purpose: Project-based engineering education Definition: A mechatronic object is a physical product with embedded sensors, memory and data processing capabilities. It lacks of identification and communication capabilities. Potential IoT application: Integrate connectivity and smartness to the JMK prototype.</p>
Potential added Value	<p>"As a student, I want to reflect on my prototyping activities with the JMK and compare it to others in order to accelerate my learning progress" "As an educator and researcher, I Want to compare the performance of students with their mechatronics prototyping activities to check for correlations" "As the developer of JMK, I want to see how the product is used and when it fails in order to improve it"</p>

Table 3.13. Analysis of the object and the potential added value of integrating an IoT system to it. As observed, the added value depends on the type of user. Adapted from [108].

From this analysis, generic but relevant aspects of the design of data processing functionalities are considered (like those shown in table 3.14), and then essential and specific technical aspects for the development of a prototype are identified (see table 3.15).

	Relevant aspects	Critical questions
Added value	User orientation, value meaning Data security, privacy	Who is the user addressed with the IoT application? How does he benefit from it? How to avoid drawbacks on added value due to unsecure data or privacy?
Data processing functionalities	Integral VS add-on solution Data sensing Data transmission Data evaluation	How do the data processing functionalities influence the physical object? What kind of data needs to be sensed? What is the approach to get the data? How is the data communicated? How is an internet connection established? Where is the data collected? How is it evaluated to derive meaning?

Table 3.14. Relevant aspects and critical questions for the main subtasks of aggregating connectivity and smartness to the JMK object. Adapted from [108].

Thing features	Variable	Data to be collected (Measured signal - wiretapped)	Signal manipulation	Signal reading
DC-Motor	Direction Speed Torque	Digital state (High / Low) PWM (duty cycle, 5000Hz) Analogue voltage (525mV per amp)	None — 2nd order RC filter — ADC — — ADC —	GPIO using polling SPI SPI
Servo motor	Position	PWM (duty cycle, 50Hz)	— 2nd order RC filter — ADC —	SPI
Stepper motor	Direction steps	Digital state (High / Low) Digital impulses (Low)	None None	GPIO using polling GPIO using interrupts (edge detection)
Solenoids	Activation state	Digital state (High / Low)	None	GPIO using polling
Thing	Smart thing (IoT system integration)			

Table 3.15. Appropriated techniques and technologies from integrating connectivity and smartness to a JMK object oriented to educators. Adapted from [108].

Notice that answers to questions in table 3.14 depends on the added value of a specific type of user, which later shapes the specificities of table 3.15. For example, to follow the activities of the engineering students (added value oriented to educators and researchers), the IoT system must sense the activities of the JMK's actuators (DC, servo, stepper motors and solenoids). From this, the most appropriate techniques and technologies to collect specific data (i.e.: direction, speed and torque for the DC motor) are identified. Interestingly, after applying this methodology, its authors found that design decisions are interdependent (concretely, they found that early decisions in the design of data processing subtasks limits future decisions due to choices compatibility).

In the context of eco-design of IoT systems, the limited literature of sensors, sensor systems and IoT systems can be classified into two approaches: an approach oriented to the potential impact reduction by data flow analysis and resources management; and an approach oriented to the evaluation and planned reduction of impacts from hardware redesign. The aforementioned work of Bonvoisin, J. et al. [61] falls into the first category. With the conviction that a WSN composed of numerous sensor systems manifest complex behavior depending on specific functions and particular contexts, they proposed defining a WSN as a dynamic system, where the life cycle of a device must be clearly differentiated from the life cycle of the node that it represents (see figure 3.36).

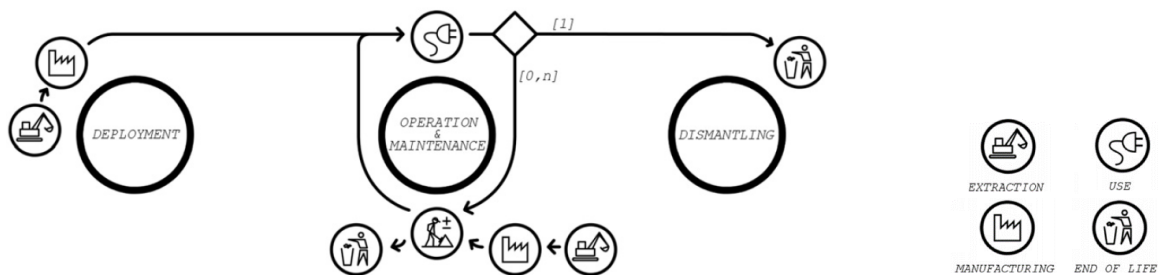


Figure 3.36. Representation of a dynamic WSN system according to Bonvoisin, J. et al [61]. Notice that the installation of a new device and the removal of the replaced one match in a common activity, represented by the roadwork pictogram.

In figure 3.36, the device life cycle is defined by four main life cycle phases (extraction of raw materials, manufacturing, use and end of life). The node life cycle is defined by the deployment stage (the device is installed), the operation and maintenance stage (the device is used and replaced n times until the end of life of the entire WSN), and the dismantling stage. Notice that the extraction of raw materials and manufacturing life cycle phases of the first device coincides with the extraction of raw materials and manufacturing stage of the first node that it represents in the system; and that the end of life phase of the last used device coincides with the dismantling stage of the last node, where the whole network is dismantled. In this way, the estimated impact of the WSN is established with the help of equation (3.5).

$$I = \sum_{n \in \Omega} (DEP_n + (N_n \times REP_n + CON_n + MAI_n) + DIS_n) \quad (3.5)$$

Where:

I = Overall impact of the network

Ω = Collection of all nodes in the network

DEP_n = Impact of the node n during the deployment phase

N_n = Number of time that a device materializing a node is replaced

REP_n = impact of the replacement device (raw materials, manufacturing, end of life)

CON_n = Grid electricity consumed by all devices in operational phase (if battery based devices, this is equal to 0)

MAI_n = Impact of maintenance interventions on all devices materializing the node n

DIS_n = Impact of the node n during the dismanteling phase

Notice that the power consumption of a device in the operational phase combines two factors: power (which can be determined deterministically by the designers) and lifetime (which, in the case of a battery-based device, is determined by its energy consumption linked to its activities). In this way, the following impact estimation methodology based on four components is established (figure 3.37).

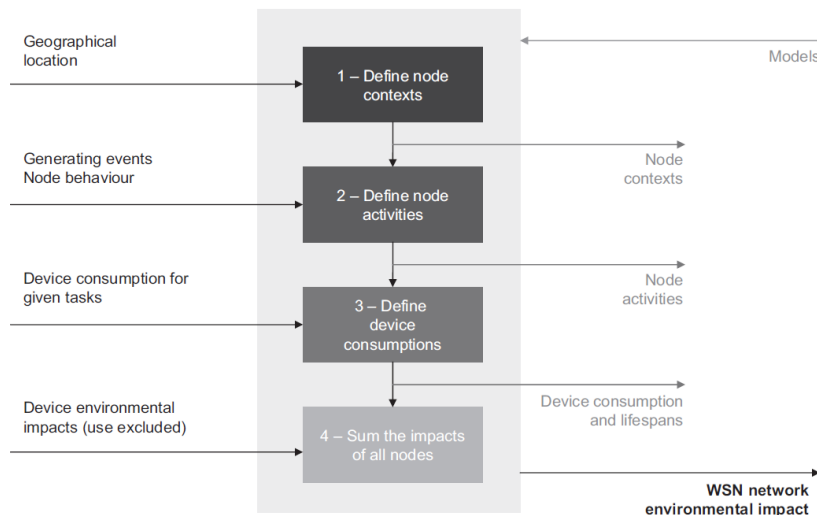


Figure 3.37. Impact estimation methodology proposed by Bonvoisin, J. et al. [61] for estimating the impacts of WSNs. The implementation of this methodology would depend on the network being examined.

In figure 3.37, the definition of the context refers to defining the neighborhood of each node, which would consist of considering the geographic location and the communication range between nodes. The second step tries to define the activities of a node by considering the reactions of the system as events that generate communication (for example, a request from the application server for a measurement at a particular node). The third step “Define device consumptions” consist of determining the power required for all activities of a device and the time that these activities takes, as explained above. Finally, the step four consists of calculating the total impact by equation (3.5).

A subsequent methodology presented by the same authors [10] may fall into the group of data-driven methodologies too. This methodology proposes estimating the environmental impact and facilitating the eco-design of WSNs at three levels of analysis: equipment, infrastructure and information (Figure 3.38).

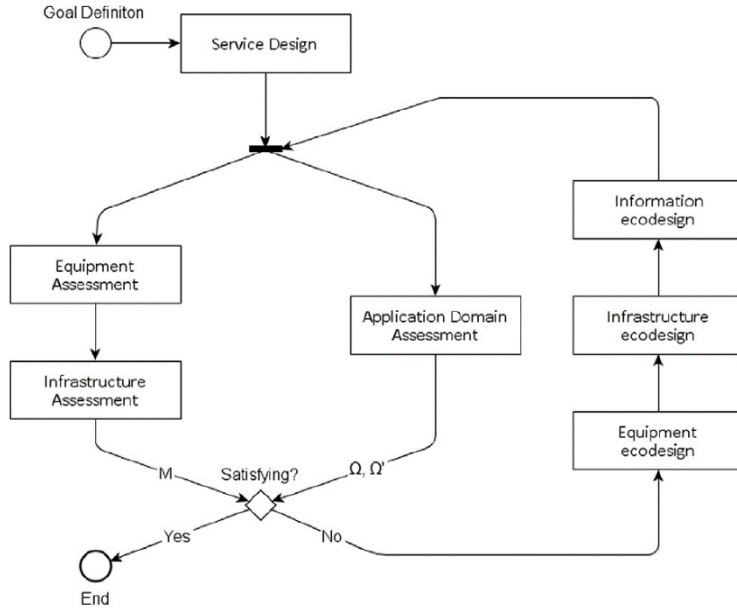


Figure 3.38. Methodology for the optimization of services through WSNs proposed by Bonvoisin, J. et al. [10]. M represents the total impact of the WSN equipment and infrastructure; Ω represents the impacts of a regular version of a service and Ω' represents the reduced impact of an WSN-based version of the service. This methodology was applied to the optimization of urban waste collection.

In figure 3.38, the goal definition step establishes the impact categories to be taken into account with their respective weights (equation 3.6).

$$W = \sum_{i=0}^n W_i * (\omega_i, \omega'_i + m_i) \quad (3.6)$$

Where:

n = Number of impact categories taken into account

W_i = Weighting function of an impact category

ω_i, ω'_i and m_i are the respective impacts of Ω, Ω' and M on an impact category

Depending on the goal of the designer —avoiding impact transfers ($W = 0$) or reducing impacts of a specific category ($W < 0$), the condition that would end the iterative process of eco-design is established.

The equipment assessment step corresponds to the evaluation of the life cycle of a device and the infrastructure assessment step corresponds to the evaluation of the life cycle of all the nodes in the network over a period of time, as established in the former methodology [61], previously described. On the other hand, the application domain assessment step corresponds to the evaluation of impacts of a traditional service (Ω), and the estimation of using the WSN-based optimized-version of this service (Ω'). For example, in the case study presented by the authors, the impact of the traditional garbage collection system and the benefits of the implementation of the WSN are determined on the basis of the reduced distance in kilometers and fuel savings.

The most interesting contribution of this methodology is the information eco-design step, which refers to reducing the reference flow (the use of infrastructure and equipment) through a prior analysis of the data flow in the network (i.e.; volume, geographic location, criticality and temporality); and the appropriate information that would generate the minimum computational load on the local and mutualized infrastructure. When they applied this methodology, this step was carried out by applying the well-known rationale information science framework (figure 3.39) but other similar frameworks could be used.

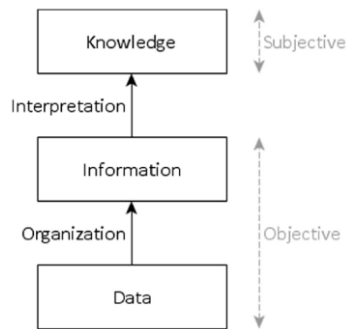


Figure 3.39. Adapted version of the rationale information science framework used in [10].

Interestingly, although the case study shows relevant impacts attributed to electronic components of sensor systems and repeaters (see figure 3.16), the authors claim that further impact reduction on this aspect is impossible, convinced by the idea that energy consumption of these devices is already be quite optimized.

With a more technical approach oriented exclusively to reducing energy consumption, Huang, J. et al. [109] proposes a scheme for the massive deployment of sensors systems and edge devices in IoT systems. Their methodology is composed of a hierarchical scheme (figure 3.40), and a mixed algorithm oriented to reduce the energy consumption of sensor systems and the number of Edges devices (Relay nodes) in an IoT system.

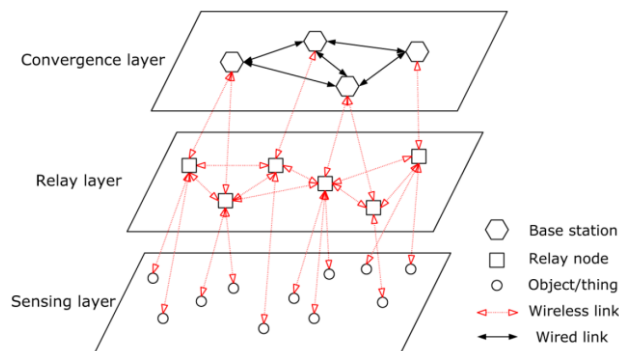


Figure 3.40. Hierarchical IoT systems framework proposed by Huang, J. et al. [109]. In the relay and convergence layers, two or more devices can communicate with each other. The base stations are oriented to internet connection and the object/thing components represent objects equipped with sensor systems.

The hierarchical scheme in figure 3.40 recalls in some extent the technical overview of IoT systems presented in the standard Y.2060 [82] and the layered architecture proposed by Chakravarthi, V. S. [107], with the difference that the sensor systems in the sensing layer cannot communicate with each other (in order to save power and balance the computational load).

The algorithm, on the other hand, seeks to find the minimal distance between repeaters and sensor systems. It establishes a connection graph between repeaters and base stations in a first stage; and calculate the minimal energy consumption by applying a Steiner tree algorithm in a second stage. The authors apply this methodology to a WSN deployment simulation in an area of 100 x 100 m² (figure 3.41a) and conclude that (1) the minimum number of repeaters (RNs) increase with the size of the network, (2) the number of repeaters reduces with larger communication radii (R), and (3) the minimum number of repeaters is affected by the density of the global network (figure 3.41b).

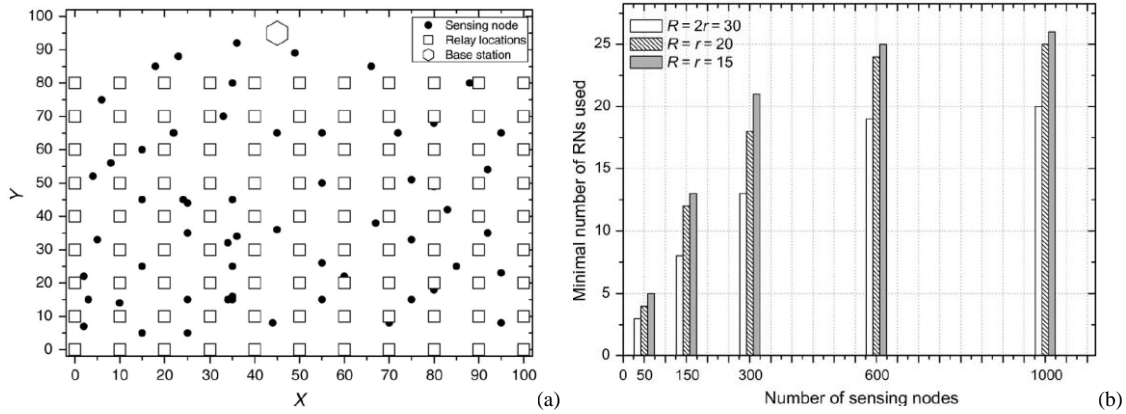


Figure 3.41. (a) Simulated WSN topology for numerical experiments (low network density). (b) Number of repeaters required for different network densities (50, 150, 300, 600 and 1000 sensor nodes with different communication radii (R)). Figure extracted from [109].

To demonstrate the efficiency of the proposed hierarchical scheme, the authors compare the energy consumption of the optimized hierarchical topology with a non-hierarchical (hybrid) topology, where neighboring sensor systems can communicate with each other. The results are showed in figures 3.42 in terms of lifetime of the networks.

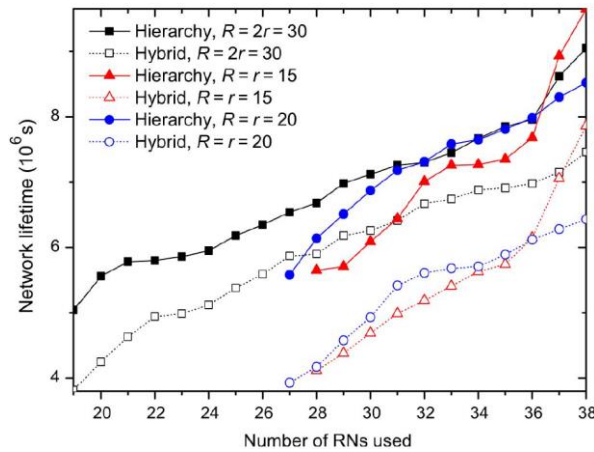


Figure 3.42. Network lifetime comparison for the hierarchical topology and the hybrid topology. In a hybrid schema, the sensor systems near to relay nodes are overloaded and consumes more energy that bordering sensor systems. Figure extracted from [109].

Regarding the methodologies oriented to the evaluation and planned reduction of impacts from hardware redesign, Pirson, T. et al. [74] proposes a parametric framework based on hardware profiles, Hardware Specification Levels (HSLs) and functional blocks to estimate the cradle-to-gate impact of IoT devices. In this framework (figure 3.43), a functional block brings together components that perform a specific function (which would recall directly the typical architecture of sensor systems seen in chapter 1, and indirectly the operational stages of sensor systems seen in chapter 2). Also, a HSL would provide a hardware-resource profile oriented to a specific functional block (Table 3.16 shows some examples of these resources categorized by specific HSLs). Impact estimation is applied on these hardware-resources to obtain hardware impact profiles characterized by different HSLs related to specific functional blocks (figure 3.44).

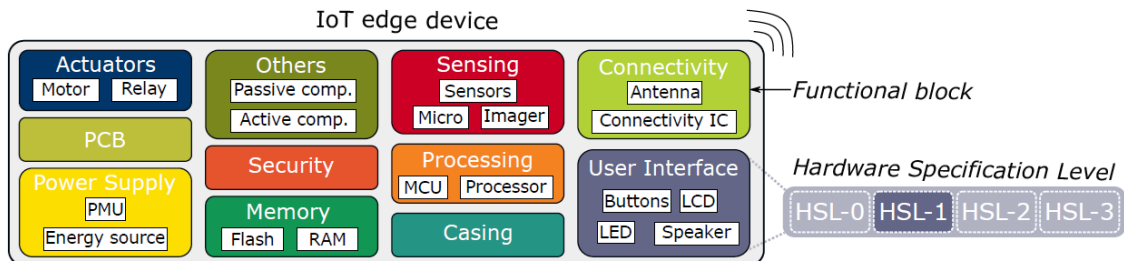


Figure 3.43. Representation of an IoT device in terms of its functional blocks and linked HSLs. Figure extracted from [74].

Functional block	Definition	Hardware Specification Levels (HSLs)			
		HSL 0	HSL 1	HSL 2	HSL - 3
Connectivity	Components which are involved in data transmission	Printed antenna (PCB)	Connectivity IC (c) (5 / 10 / 20 mm ²)	Connectivity IC (d) (20 / 30 / 45 mm ²)	Connectivity IC (d) (45 / 50 / 60 mm ²)
Memory	Components that storage data	Flash RAM (Embedded in processing)	DRAM (g) (32 / 128 / 512 MB)	DRAM (g) (0.5 / 1 / 2 GB)	DRAM (g) (0.5 / 1 / 2 GB) (31.5 / 61.5 / 123.1 mm ²)
Power supply	Energy source and energy management	Miniature coil (2 / 3 / 4)	Coil cell Li-Po	Li-on battery (i) (10 / 50 / 100 g)	Radial capacitor (0 / 1 / 2)
Processing	Components involve in data processing and control tasks	MCU (c) (5 / 10 / 17 mm ²)	Auxiliary MCU (c) (5 / 10 / 17 mm ²)	Application processor (e) (50 / 60 / 75 mm ²)	Application processor (e) (75 / 100 / 125 mm ²)
Sensing	Components involving in measuring physical quantities from environment	No sensor	microphone (0.05 / 0.1 / 0.2g)	Multiple sensors (a) (0 / 3 / 5 mm ²)	Single CMOS imager (b) (8 / 30 / 58 mm ²)

Table 3.16. Some examples of hardware resources (low / typical / upper) classified by HSLs and some functional blocks. (a: CMOS 0.25 μ m, b: CMOS 0.13 μ m, c: CMOS 90nm, d: CMOS 22nm, e: CMOS 14nm, g: DRAM 57nm, i: Data from [74]). LCA is applied for each resource of each HSL. Adapted from [74]).

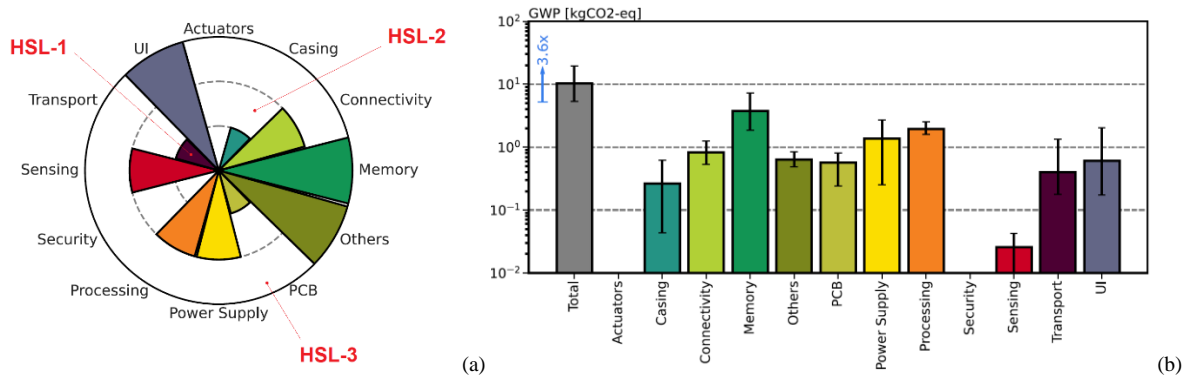


Figure 3.44. (a) An example of a hardware impact profile for a complex IoT device type (Smart watch). (b) The resulting impact obtained by the proposed framework for the hardware impact profile seen in (a). Figures adapted from [74].

In figure 3.44b, the total impact is given by the sum of the carbon footprint contributions for a given hardware profile. In this way, different combinations of HSLs in different functional blocks generate unique impacts attributed to specific types of IoT devices. For example, the total impact of a simple device with simple functionalities such as an occupancy sensor is relatively low (1,4 kg CO₂-eq) in relation to a complex device with multiple functionalities (i.e.: a connected home assistant, that generates a maximum impact of 23,4 Kg CO₂-eq).

On the other hand, Middendorf, A. et al. [110] report that LCA studies are normally made at the review stage (post-design stage) of the product development process and highlight the absence of design tools aimed at integrating environmental analysis to early stages. With this in mind, they propose a methodology consisting of a mix of indicators (grouped in a tool called EE-toolbox [111]) deployed in three parts for the eco-design of mechatronics (Table 3.17).

	Stage	Tool / Methodology	Indicator	Description
Part I	Stage 1a: Based on product Material content	EE-Toolbox [111]	Toxic Potential Indicator (TPI) Recycling Potential Indicator (RPI) Energy Intensity (Erm)	Toxicity based on product content Sustainability of product contents for specific recycling paths Energy intensity based on raw materials
	Stage 1b: Base on product information		Energy for the product Usage (EPU)	
Part II	Stage 2: Based on Specific Process Data		Process Toxicity Screening (ProTox) Energy for Production steps (EP)	Toxicity indicator for process oriented material flows and Related Energy Production steps
Part III	Stage 3: With further LCI data	LCA		

Table 3.17. Description of the methodology consisting of a mix of indicators proposed by Middendorf, A. et al. [110].

The first part consists of evaluating a mechatronic device based on the material content and its energy consumption in the use phase. The second part evaluates the device on the basis of specific data of manufacturing processes and toxicity. The third part would be oriented to a more detailed analysis whenever LCI data is available (suggested by the authors, but not included in the methodology). For illustration, the part I of this methodology is applied to the environmental evaluation of a mechatronic robot composed of image sensors, a main and a secondary PCBs, a data processing unit, an energy accumulator, a motor-gearbox-combination, drive chains and casing (figure 3.45).

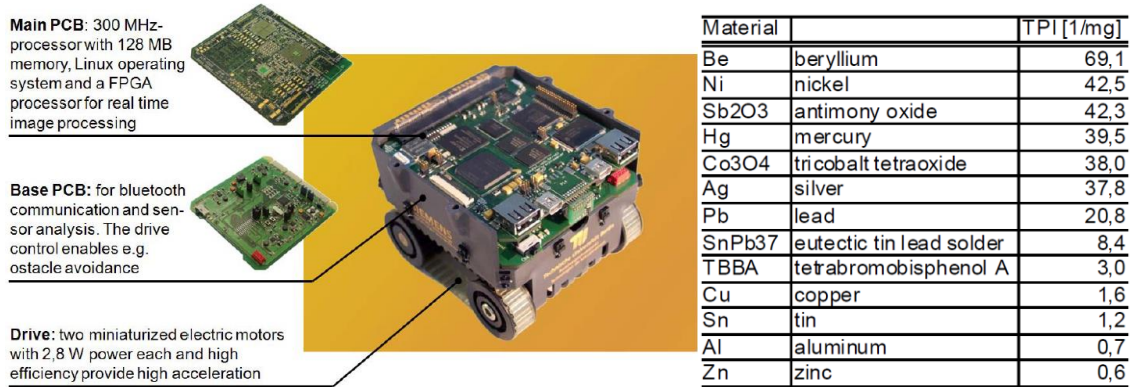


Figure 3.45. Simple description of the mechatronic device analyzed in Middendorf, A. et al. [110] and its ecological impact in terms of its raw materials and their respective TPI indicators (scaled from 1 to 100).

To illustrate the integration of the environmental design (here, on the basis of TPI indicators) to the NPD process, the authors consider replacing the rigid epoxy FR4 material of the main PCB (with an impact of 1.1 TPI / mg) by polyamide (with a TPI impact equal to Zero). This strategy would further reduce the overall weight of the device but would also increase its price by a factor of 5x.

- In the context of regular design of IoT systems, Chakravarthi, V. S. [107] makes more explicit the basic architecture and the product development process stages of IoT systems by concrete examples and Heinis, T. et al. [108] realize that early decisions in the conceptual design stage (i.e.: selection of specific technologies) influence further steps in the detailed design stage.
- Unfortunately, although one could say that both works make a comprehensible review of relevant aspects within the NPD process, it is evident that both methodologies are limited to the technical design of IoT systems.
- In the context of eco-design of IoT systems, Bonvoisin, J. et al. [61] contribute significantly to the eco-design of WSNs by making explicit the distinction between sensor systems and the nodes they represent; and their subsequent work [10] is capital because it recognizes the fundamental, driving role of data and information for eco-design of WSNs.
- However, although the former considers the impact assessment of manufacturing phases of sensor systems and nodes and the latter includes an equipment assessment step, both works do not give more details on how one can redesign sensor devices, when further iterations of the proposed methodologies occur. In addition, the application of these methodologies within the product development process is not clear and they would not include mutualized infrastructure.
- On the other hand, although Huang, J. et al. [109], Pirson, T. et al. [74] and Middendorf, A. et al. [110] propose promising methodologies whose application into the NPD process of IoT systems could vary according to designers' needs, they fall short because they are focused on single life cycle phases of IoT systems.

- Furthermore, any methodology presented in this section (with the exception of the methodology proposed by Bonvoisin, J. et al. [10]) considers the impact estimation of full IoT systems (local and mutualized infrastructure).
- In the next chapter, the previous concepts of data-information design will be extended in a novel methodology for sustainable IoT systems, which will include a detailed life cycle eco-design procedure for devices, electronic components and energy consumption. This methodology will also benefit from some aspects of the reference frameworks seen so far and will be integrated explicitly into the product development process of full IoT systems.

2.3. Summary of design and eco-design instruments for IoT systems

As observed in this section, Bonvoisin, J. et al. [10] recalls that the eco-design of WSNs should not be limited to physical devices, but extended to data and information design. More precisely, they are in favour of starting the eco-design process by reflecting on the essential information that an WSN needs; which would later reduce the energy consumption and the number of end- and edge-devices. This would be possible by questioning the information required by the application and collecting only the essential data for it. They illustrates this idea clearly when considering a system oriented to monitoring a phenomenon; in this context, it is not necessary to send data for normal behavior, but only for anomalies. The authors of certain guidelines indirectly share this perspective (i.e.: the guideline “Use selective sensing (collect only data that is required in a particular situation)” proposed by Arshad, R. et al. [99]).

On the other hand, the contributions of certain authors are complementary. For example, the guidelines “Find the device coverage which minimize the number of devices deployed” proposed by Bonvoisin, J. et al. [10], “Reduce the network size by efficient placement of sensor systems or ingenious routing mechanisms” proposed by Arshad, R. et al. [99]; and the methodology presented by Huang, J. et al. [109] complement each other. In addition to this, the conclusions generated by the latter resemble the conclusions presented by Bonvoisin, J. et al. [61] regarding the premature battery depletion of sensor systems due to overhearing and intense data traffic.

On the other hand, the energy-based methodology proposed by Huang, J. et al. [109] could be completed with the lifecycle-based methodology presented by Bonvoisin, J. et al. [61] (where not only the entire life cycle of a device is taken into account, but also the life cycle of the node which it represents). However, there are also certain postures that could distance these last two works. For example, while Huang, J. et al. [109] highlights the importance of increasing the number of repeaters and their communication range to extend the lifetime of IoT systems, Bonvoisin, J. et al. [61] advocates for reducing the number of all devices through the analysis of data flow and information; and the search of appropriate communication ranges between devices.

Another aspect that stand out in literature is the lack of pragmatism of certain standards and guidelines. For example, the guideline “The computational element should be made available near to the user / data source” proposed by Nivethitha, V. and Aghila, G. [98] and the recommendation “An IoT devices should include a processor with at least two cores of 1Ghz processing speed” included in the ITU-T L.1370 recommendation would not simply apply to energy-constrained sensor systems (i.e.: self-powered sensors systems) or inaccessible devices (devices whose changing batteries is difficult).

On the other hand, certain non-Life-cycle methodologies such as those proposed by Heinis, T. et al. [108], Huang, J. et al. [109] and Middendorf, A. et al. [110] must be used judiciously in order to avoid impact transfers. Finally, it is also envisaged that authors of certain LCA-based methodologies extend their study boundaries beyond the life cycle of local devices in further works. Beside of all this, it is also important to highlight that all authors cited in this section generally report the lack of environmental data regarding IoT devices, IoT systems and electronics in general.

Chapter 4: Proposition of the methodology

Overview

From a qualitative research revealing the current workflow and needs of design teams, this chapter presents two frameworks oriented to solve the research questions 1 and 2 stated in chapter 1. Both frameworks address the issues found so far in literature and are built by a reasonable and structured analysis based on electronic components to avoid impacts transfers, and ensure proper impact estimation and eco-design of full IoT systems. The next sections present this analysis, which reveals the significance of specific types of attributes, functions and capacities of electronic components for the eco design of local equipment and the practical impact estimation of mutualized infrastructure. The proposed frameworks then recall the essential elements to be considered for integrating ecological aspects into the planning, conceptual / detailed design and prototyping stages of the NPD process of IoT systems, facilitates the construction or evaluation of sharp guidelines, and compose a methodology covering the essential needs and expectations of designers and project leaders. At the end, a suggested implementation for both frameworks is presented, and the full methodology is positioned with respect to other contributions.

1. Qualitative research

To guarantee the adoption of the new eco-design methodology that will be proposed in this thesis and its proper integration into the NPD process, a qualitative research was carried out in two parts, with the participation of project leaders and IoT designers of the System Department (DSYS) of CEA-Leti. The first part aims to understand their usual design workflow in five steps, and the second part investigates their needs, expectations and attempts (if any) to integrate environmental aspects into real projects. Tables 4.1 and 4.2 summarize the relevant findings of these two parts respectively (for a more detailed description of the methodology used for this qualitative investigation, as well as the research instruments used, see Annex 16).

How can you design a rapid IoT prototype ready for demonstration in 5 steps?						
IoT application	Participant	Step 1	Step 2	Step 3	Step 4	Step 5
Medical monitoring	Participant 1 (IoT designer)	Define the architecture of the complete system Define the means of information transfer Multisensor device Data recovery relay Data storage element Information interface	Design the multisensor device Sensor test	Building up the complete information chain	Integration of the multisensor device to the information chain	Preparation of a demonstration
Sport monitoring	Participant 2 (IoT designer)	Design a sensor system (sensor, memory, battery or EHS and wireless interface)	Embed the sensor system into the object (skateboard)	Collecting statistics of data sport	Build up a machine learning algorithm	Recyclability evaluation of the sensor system
	Participant 3 (Project leader)	Identify technical specifications together with the client	State of art of the available technology in the context of sport monitoring	Technology comparison in the context of the specifications	Develop a hardware prototype (TRL4 level) and implement the software in the MCU	Laboratory tests On field tests
	Participant 4 (IoT designer)	Interviews with the client and end-users to find the right concept	Identify the functional and technical requirements in a priority way	Select the electronic components of a prototype that cover these requirements Design the architecture Define the data management strategy Estimate energy consumption and, if necessary redesign	Build a hardware prototype	Test the prototype and obtain the end-user feedback
	Participant 5 (IoT designer)	Brainstorming of crucial variables of the sport activity and client validation	Define the suitable sensor components considering additional aspects such as Robustness, minimal integration and energy consumption	Define energy supply, data flow and processing, computing placing (edge or cloud) and user interface	Design and build a prototype Develop a database and obtain data from athletes	Redesign if necessary considering extending more services

Table 4.1. Adapted results of the first part of the qualitative research. Some answers were shorted and translated from French to English.

In Table 4.1, it can be seen that both, project leaders and IoT designers generally begin the design process of IoT devices with a functional analysis based on customer requirements. Also, there is a tacit attention to the IoT architecture (local and mutualized infrastructure) and to the data flow within it, but after the conceptual design (usually in a third or fourth step, after the selection of electronic components). On the other hand, although the questionnaires of this part did not address the eco design topic, only one participant (participant 2) considered that an analysis on recyclability should be carried out in the final design stage (step 5). This would confirm the tendency to apply eco-design procedures late in the product development process, as it is reported in the literature.

Participant	a. What is your knowledge about eco-design?	b. Did you propose eco-design initiatives in your projects?	c. What do you expect from an eco-design tool and what would be the main barriers for its implementation?
Participant 1 (Lead project)	Little	Little: only research on EoL treatment.	A tool that reduces the use of rare materials A tool that takes into account recycling (disassembly) A tool that takes into account reparability (replacement of pieces/components) A tool that takes into account supply chains of materials
Participant 2 (Lead project)	Poor knowledge: We started to integrate knowledge on eco-design for electronic system design.	Non	A tool oriented to environmental impact assessment and eco-design
Participant 3 (Lead project)	Life cycle Analysis and eco-design are a step for reducing environmental impact of all kind of products (textile, IoT, etc.).	Yes, in one project proposal. Main barriers: funding.	General guidelines. Define clearly wording: LCA, eco-design, circular economy and associate methodology.
Participant 4 (IoT designer)	None	Non	knowing the country of origin of products/components/materials or elements and their associated impacts
Participant 5 (IoT designer)	Reduce the power consumption, the number of components, the size of the PCB, use components that have the lowest environmental footprint.	Non	Two tools would be interesting: One guide of components selection based on big families and their associated impact. One tool for calculation of the global impact of the electronic card from the bill of materials.
Participant 6 (Lead project)	General notions about eco design.	We try to minimize global energy consumption and limit critical material (not specified) Main barriers lack of time or budget.	simplicity, maybe by using archetype cases in order to quickly notice important points applying eco design without too much changing current work procedures
Participant 7 (IoT designer)	Only knowledge about material and energy requirements in mechanical fabrication processes.	Non	Quick to use (i.e.: present clear "design rules" instead of conducting exhaustive LCA). Facilitate "design rules" addressing 80% of the sustainability improvement on all designs instead of address 100% of sustainable improvements of few designs.
Participant 8 (IoT designer)	Only ideas: reparability, recyclability, optimization of the energy consumption	Sometimes questioning the usefulness Store less data in the long-term. Main barrier: lack of eco-design willingness from clients	A tool that helps to identify and to repair the failures of components or devices A tool that documents these failures (and their reparation procedures) and facilitates the sharing of knowledge A tool that shows the ecological gains of new designs as added value
Participant 9 (IoT designer)	Basic notions of eco design. Knowledge on several guidelines for efficient, reusable, or clean programming code.	Tried to deliver efficient software code for projects. Tried to apply good coding practices.	A tool that takes into account bill of materials, energy consumption, CO ₂ emissions at use and data flow (especially in the processing case). In the software case, I expect to have an idea of where the processing should take place to mitigate the environmental impact of the system.

Table 4.2. Adapted results of part two of the qualitative research. Some answers were shorted and translated from French to English.

In table 4.2, it is observed that most of the participants have basic notions of eco-design and some of them would even identify some aspects of it in the context of electronic design. For example, participant 5 already considers specific components (i.e.: PCB) with specific physical characteristics (ie: size) to be analyzed, and participant 9 already considers good practices for programming and management of edge or cloud resources for data processing.

In conclusion, in the typical design flow of IoT systems (results from part one of the qualitative research), it was found that 3 of the 5 participants start with an analysis of the customer needs and application requirements. Between steps two and three, there is no clear design procedures: while some participants consider searching and comparing the most appropriate electronic components for the requirements identified in step 1, others consider analyzing other preliminary aspects such as identifying functional and technical requirements; or analyzing the flow and processing of data through the IoT architecture, together with energy consumption. In step 4, the design and development of a prototype are considered mainly, and the development of system software (e.g., development of the MCU's embedded software, databases and Artificial Intelligence algorithms) additionally. Step 5 would be oriented to obtain the customer feedback by conducting demonstrations and laboratory / field tests.

Thus, the current workflow of design team could be synthesized according to the NPD stages suggested in figure 4.1.

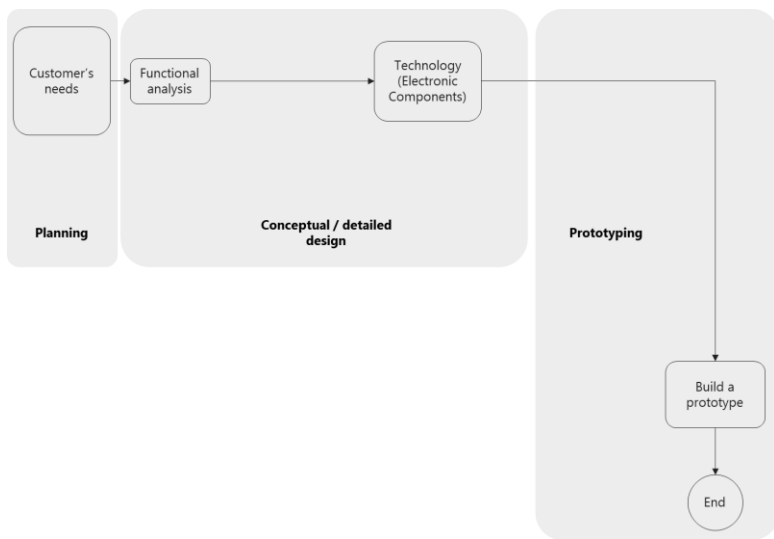


Figure 4.1. A representation of the current design workflow of IoT systems embedded into a suggested NPD process (gray boxes). The planning stage would consist of collecting and analyzing the customer requirements. Activities in the conceptual and detailed stages would range from conducting technical and functional analysis to selecting and comparing electronic components. The prototyping stage would be oriented to developing prototypes (mainly) and conducting tests (secondary).

On the other hand, the results of part two of the qualitative research show an awareness of general aspects (i.e.: life cycle thinking) and specific strategies of eco-design (reparability, recyclability, reduction of energy consumption, of materials, of components, etc.). In this context, some initiatives (independent research, Project proposals, etc.) would have been carried out, but with limited effectiveness due to limited resources (time and economical investment). Concerning the expectations of an eco-design methodology for IoT systems, project leaders and designers would need a methodology that:

- Facilitate design decisions (by using guidelines, classical use cases, type or families of components, and design rules).
- Be simple, fast and non-exhaustive; oriented to the estimation of impacts and eco-design but without disturbing the current design workflow.
- Consider materials, energy and emissions in the production phase and the use phase.
- Consider the quantities and origins of materials; and facilitate device circularity.

While the first requirement can be understood as a preliminary step helping the decision making processes (a step that could be placed before the selection process of electronic components), the last two requirements can be seen as an evaluation step oriented to devices and / or full systems (a step that could be placed before the development of prototypes). Figure 4.2 provides a synthesis of this preliminary interpretation.

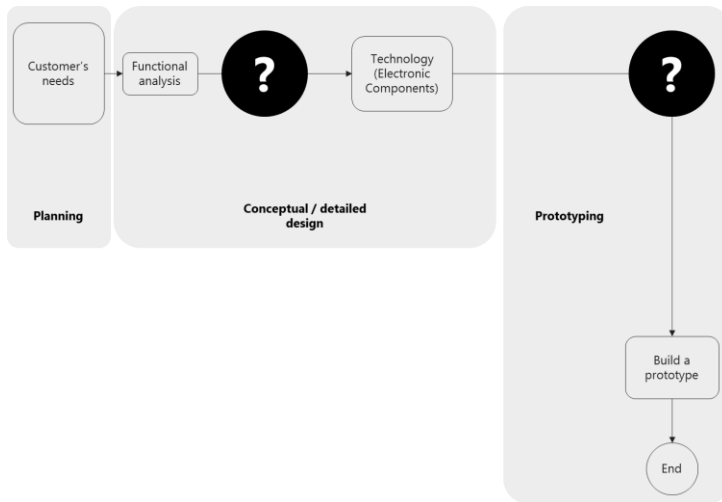


Figure 4.2. Placing potential eco-design steps into the current design workflow of IoT systems for integrating ecological aspects into the NPD process.

2. Building a design methodology for sustainable IoT systems

To solve the research question 1: "How a designer can consider data flow within an IoT system in order to harmonize and reduce the potential impacts of promising initiatives?", from chapter 2, it has been established that:

- A physical phenomenon can be sensed and acknowledged in different ways, and that the information produced by an IoT system depends on the transformation of raw data throughout its data operational stages.
- A right-provisioned device would be one whose electronic components cover specific functions with sufficient capacities.

To solve the research question 2: "How a designer can disclose, measure and integrate key environmental aspects to the typical design of sensor systems and edge devices (local devices) in a practical and efficient way so that to develop sustainable IoT systems?", from Chapter 3, it was established that an appropriate eco-design methodology of IoT systems should:

- Include a preliminary analysis of data and its flow, since the way by which it is manipulated to become useful information determines the reference flow of full IoT systems.
- Include a transparent and detailed analysis of electronic components (especially ICs and PCBs), including their critical characteristics with high influence on environmental evaluations (such as content of certain materials); and on the electronic design of local devices (e.g., interdependence of components), under a lifecycle perspective.

Apart from this, in previous chapters it was also observed that:

- There are generic standards and frameworks for the design of IoT systems that could be aligned with early NPD stages (for typical and environmental applications). However, there are not standards nor frameworks for the eco-design of IoT systems themselves.
- There are some guidelines that, although they also can be aligned with certain stages of the NPD, they offer, unfortunately, generic, limited, impractical and sometimes contradictory solutions.
- Capital work revealing the importance of data and information for eco-design of WSN do not give further instruments to redesign the electronic composition of sensor devices, nor its integration into the NPD is clear, nor its scope include mutualized infrastructures.
- In general, Current eco-design tool do not consider mutualized infrastructures and certain tool would be concentrated only in specific aspects (i.e.; in specific life cycle phases).
- The impact assessment of mutualized infrastructures is ambiguous and the impact related to the energy consumption of local and edge devices is significant.
- Much of the environmental data necessary for impact assessment is not available or difficult to calculate.

Bearing in mind these aspects, the following sections develop a structured analysis on certain electronic components to study

- Their critical characteristics that influence the most the environmental impacts (section 2.1) and savings (section 2.2) of IoT system.
- Their potential influence on reference flows (section 2.3).
- Their capacities to collect meaningful raw data and process substantial information with the sufficient resources (section 2.4).

The goal is gathering the necessary knowledge to build a practical, yet comprehensive eco-design methodology that can (1) cover the most essential needs of design teams reported in section 1, (2) be applied to the any IoT project from the electronic design of local devices to the appropriated impact estimation of mutualized infrastructure, (3) be integrated in the current the NPD process of IoT systems and (4) overcome the eventual lack of LCA data.

However, before starting, it should be clarified that this analysis is developed on the basis of some prominent clues found in literature, that orient the attention to some primary features of electronic components for eco-design (physical, technical and circular features), with the aim of abstracting some relevant aspects from it and guiding the construction of a reasonable and complete design methodology for IoT systems. Beside of that, the following sections tries to harmonize the insights from previous chapters to the research questions of this thesis (e.g., impacts of materials in electronic components affecting the environmental loads and eco design of local equipment; or data rates of wireless IC affecting not only the lifetime of sensor systems but also the network traffic and the estimated impact of mutualized infrastructure of IoT systems). Finally, although the sections below are developed on the basis of literature related to consumer electronics and ICT, they do not intend to cover, for any reason, an exhaustive treatise on these fields.

2.1.Physical features

The analysis of physical features of electronic components and devices is capital for this work. For example, one observed in chapter 3 that disparate impacts can be obtain not only from the use of different materials oriented to the same function (i.e.: copper and silver), but also from their quantities. In this sense, considering physical features involving these and other potential aspects may facilitate significantly the impact estimation of local equipment of IoT systems and consequently their eco-design.

The environmental impact of a product is understood not only on terms of its resources consumption and emissions involved in its production, use and disposal, but also on terms of its intrinsic attributes (e.g., materials, dimensions, etc.) summarized in its Bill of Materials (BoM); and in its Bill of Attributes (BoA), which is a generalization that categorize the impact contribution of each of its components or subcomponents [114].

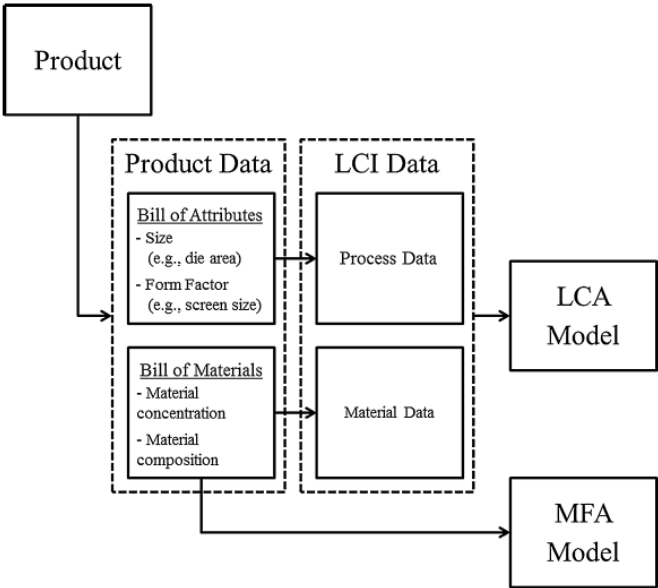


Figure 4.3. Use of the Bill of Attributes (BoA) and the Bill of Materials (BoM) for LCA and MFA analysis. Figure extracted from [114].

For example, while the BoM facilitates material flow data for MFA analysis and provides quantitative information for the LCI step in LCA studies, the BoA organizes the information of the BoM into physical characteristics and processes to estimate the environmental impact of components and / or specific subcomponents of products (figure 4.3).

In this sense, and considering the role of the BoA in the context of the sustainable electronics, a considerable amount of evidence shows the significant contribution of the front-end manufacturing process of ICs to the environmental impact of ICT products, which can be expressed through the area of ICs' dies. For example, the front-end production of ICs in a smartphone represent approximately 42% of the total impact of its manufacturing phase (Figure 4.4). This impact is usually explained by the die surfaces of ICs (approximately 2,2 kg CO₂-eq, corresponding to a total die area of 7,3 cm² according to Andrae & Andersen [247]).

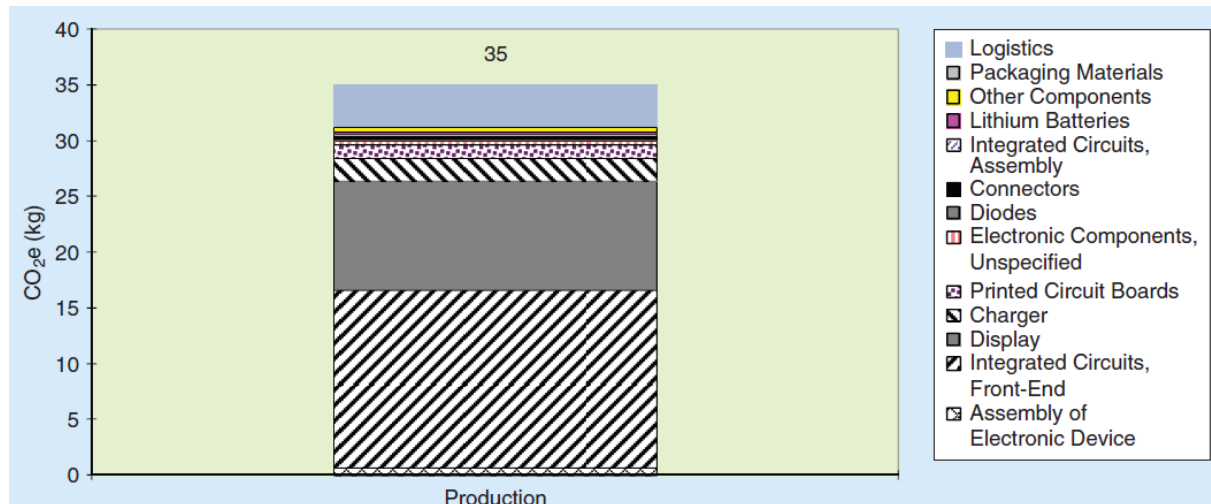


Figure 4.4. GWP100 impact contribution in the manufacturing phase of a smartphone according to Andrae & Andersen [247].

Thus, different methods oriented to measuring the die surface of ICs in electronics were proposed recently and show the capital importance of this physical attribute for the environmental impact of modern electronics. Consider, for example, the work conducted by Kasulaitis, B. V. et al. [114] in which different techniques oriented to estimate the die areas of different ICT products were presented and dissected exhaustively (from destructive and visual approaches (i.e.: grinding or X-ray imaging), to estimations based on ratios involving additional attributes of ICs and other components (e.g., the area and weight of IC packages, the area of PCBs, etc.). However, beside the technique, the authors of this work concludes, like implicitly others [246], that small differences in die areas affect significantly the results of environmental evaluations of ICT products.

On the other hand, other studies demonstrate the significant impact not only of dies but also of certain materials present in specific subcomponents of ICs. For example, Andrae & Andersen [116] identified significant impacts from the gold-plated solder balls of Ball Grid Array (BGA) components, and Kuo, C. H. et al. [117] report a great impact of gold content not only in wires of BGA components, but also in wires of Flip Chip (FC) and Lead-Frame-based (LF) components. Moreover, they found a positive correlation between the environmental impact, the packet volume and the number of pins of BGA components; and proposed two regression models based on these physical attributes (Figure 4.5).

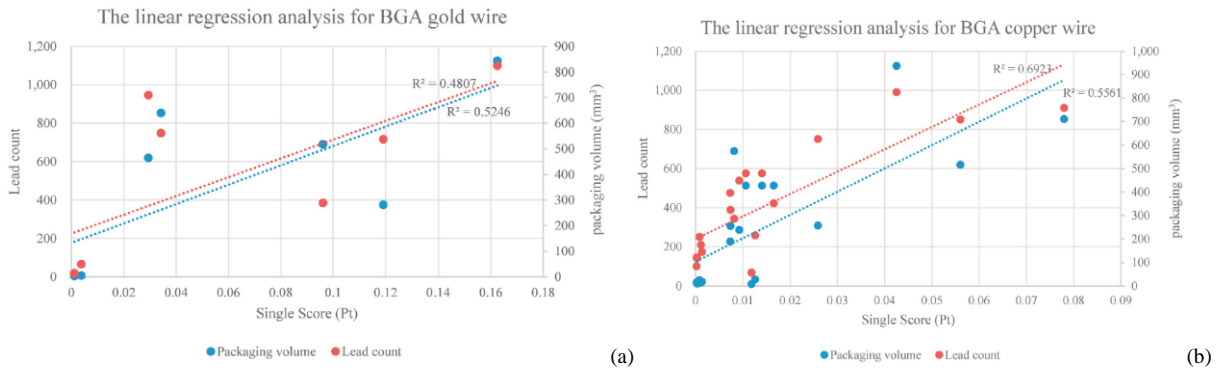


Figure 4.5. Regression model for the environmental impact (single score Pt) of BGA components based on the number of pins (lead count) and the volume of the package. (a) For gold-wiring version, (b) for a copper-wiring version. Figures extracted from [117].

Das, S. & Mao, E. [8] for their parts, are also oriented in this direction by revealing, by means of a comparative LCI analysis, a positive correlation between the number of pins and the embodied energy demand (MJ / Chip) of different ICs (Figure 4.6).

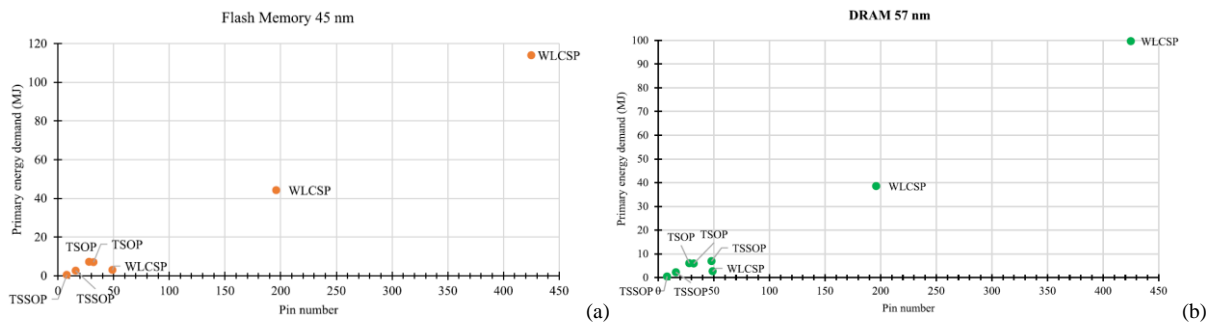


Figure 4.6. Embodied energy demand of (a) 45nm flash memories and (b) 57nm DRAM memories. Both with different packaging technologies. For the acronyms, consult the glossary. Figures extracted from [8].

Consequently, in principle, to reduce the embodied emissions and primary energy of IoT devices one should (1) meticulously quantify ICs’ die surfaces and reduce them as much as possible when selecting electronic components and (2) discriminate electronic components on the basis of individual physical attributes such as the number of pins or the size of packages. While point 1 will be approached in the next chapter, point 2 presents some underlying difficulties, as it could be intuited by inspecting figure 4.7.

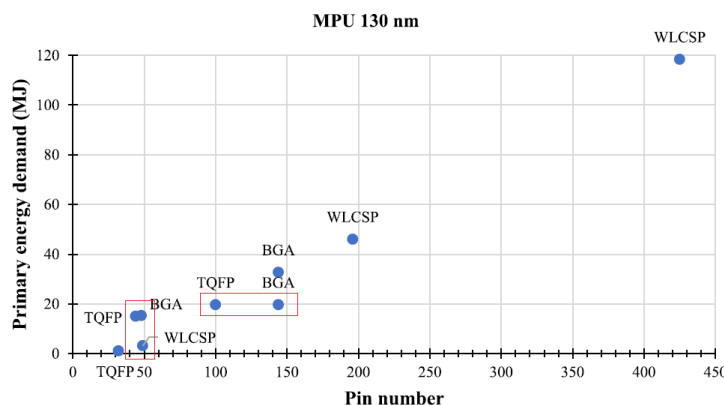


Figure 4.7. Embodied energy of 130 nm microprocessors (MPU) with different packaging technology and different number of pins. Figure adapted from [8].

Indeed, if IoT designers base their decisions on the number of pins exclusively, they (1) might believe reduce the impact of an IoT device by choosing a 100-pin TQFP component instead of a 150-pin BGA component; and (2) make no difference between a BGA and WLCSP component with the same number

of pins (e.g., 50 pins). However, they might be wrong, as these technologies cannot be evaluated only from the point of view of a single physical attribute (as it is showed in figure 4.7). For example, the advantage of the 50-pin WLCSP component over the equal-pin BGA component in figure 4.7 could be explained by the additional impact of using a PCB-typed substrate on the BGA component, or by using more ecological materials (e.g., copper) in its Under Bump Metallurgy (UBM) subparts, compared to the lead frame or wires subparts of a TQFP component with almost the same number of pins.

Furthermore, decision-making in eco-design can become even more complicated when analyzing certain physical features of electronic components in the context of the general electronic design. For example, Andrae & Andersen [116] warns that, although WLCSP components show clear ecological advantages at an individual level compared to other components with different packaging technologies, they would not be convenient at a system level, since they would require the use of more PCB layers (figure 4.8a) due to their pin densities (pins number per package mass) (figure 4.8b).

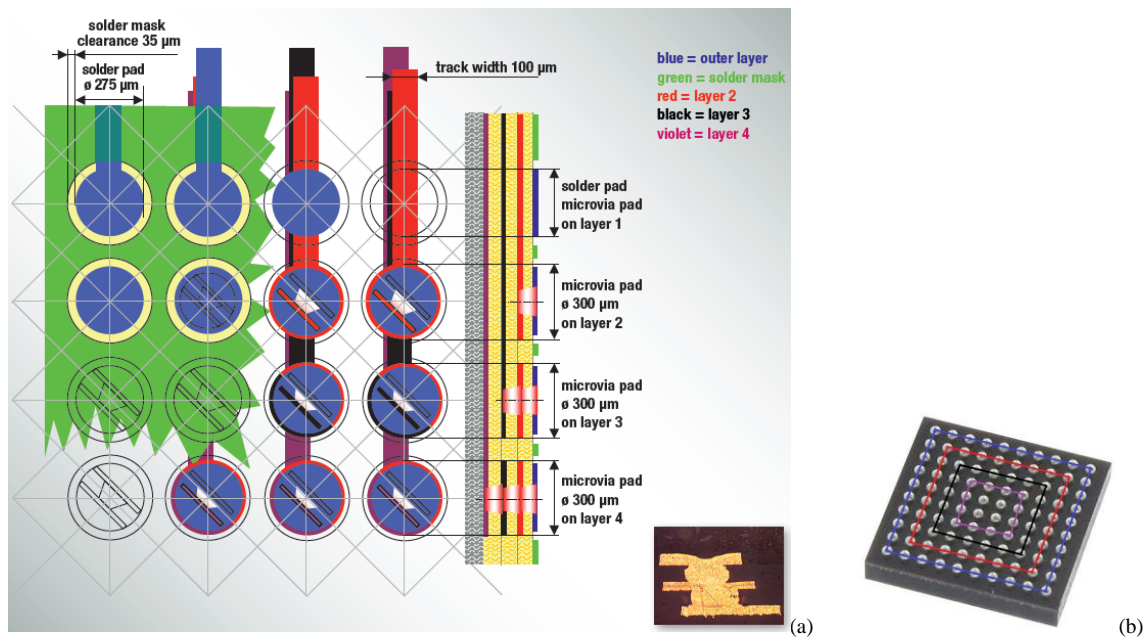


Figure 4.8. (a) Basic PCB layout design guidelines for Area Array Package components according to [118]. (b) An Area Array Package component (WLCSP). The number of PCB layers would increase proportionally to the number of pin arrays of the WLCSP component (from the outer array (blue one) to the inner array (violet one)).

- Therefore, the estimation of the potential impacts and the eco-design of an IoT device would be framed, among other aspects, both by physical characteristics of its electronic components (eg, number of pins, dimensions, mass, specific materials, etc.), and by the influence of these characteristics over other components and the rest of the electronic design (interdependency).

2.2.Circularity features

As the reported impact of producing sensor systems is high (see section 1.2.3 and 1.2.4 of chapter 3), studying the features of electronic components and devices that partially or fully avoid (or increase) such impact is fundamental in this work. As a matter of example, the reader may recall from chapter 1 the potential drawbacks of full systems integration affecting recyclability because of resource dissipation. By taking into account this and others potential aspects, one can construct a more reasoned yet practical methodology for impact estimation and eco-design of IoT systems.

The application of circular strategies on electronic components reduce the impact of local devices. However, Söderman & André [112] put designers on guard against the potential risk of strictly applying these strategies without first analyzing certain aspects. For example, Bovea, M. D. et al. [119] shows that repairing electronic cards of small electronic devices such as hand blenders causes more environmental impacts than replacing them (regardless of their age); and agrees with Pini, M. et al. [120] by concluding that repairing is convenient depending on the parts to be replaced; and with Lu, B. et al. [121] by concluding that a reuse strategy is suitable only for certain components, but not for entire

devices. Below, two of the most common circular approaches of consumer electronics; the recycling of devices and the reuse of electronic components will be explored in more detail, under the lens of specific features.

2.2.1. Circularity features affecting recyclability

Recycling Waste Printed Circuit Boards (WPCBs) would reduce significantly the amount of emissions, waste and above all, raw materials involved in the production of IoT devices. Indeed, WPCBs contain important shares of copper, gold and silver (table 4.3), which could be recovered with known techniques (e.g., by metallurgical or chemical processes). However, for the recycling of these metals to be economically viable (that is, in basic terms, so that the amount recovered of these metals from electronic waste exceeds the amount that would be obtained from natural deposits) it is basically necessary to reach certain dilution levels of these metals in electronic scrap (e.g., more than 400 grams in one ton or 400 ppm in the case of gold³), which is possible only through a design that facilitates the separation of specific parts rich in these materials.

Composition (%)	Bare PCB	ECs	Total (populated PCB)
Sn	10.12	3.20	6.0
Pb	3.20	0.68	1.7
Cu	21.62	13.80	19.9
Fe	0.21	19.49	11.8
Al	1.36	6.91	4.7
Zn	0.056	5.66	3.4
Ni	0.036	0.65	0.4
Cr	0.027	0.53	0.3
Cd (g t ⁻¹)	0.53	14.45	8.9
Au (g t ⁻¹)		40.76	24.4
Ag (g t ⁻¹)	194.91	112.68	145.7

Table 4.3. Material content share in one ton of WPCBs. Abundant materials are expressed in percentages, and precious and toxic materials (such as Cd, Au and Ag) are expressed in ppm. Table adapted by Kaya, M. [128].

Indeed, an efficient separation would increase the gold concentration per ton of separated ICs scrap or the silver concentration per ton of bare WPCBs as shown in table 4.3; recovering more resources in recycling processes and obtaining more economic benefits than if we treated them without prior separation. This is understood by analyzing the relationship between the dilution of metals in natural ore and their refining prices (Figure 4.9); and it could be illustrated by comparing the recycling of a whole car (Figure 4.10a) versus the recycling of its separated parts (figure 4.10b).

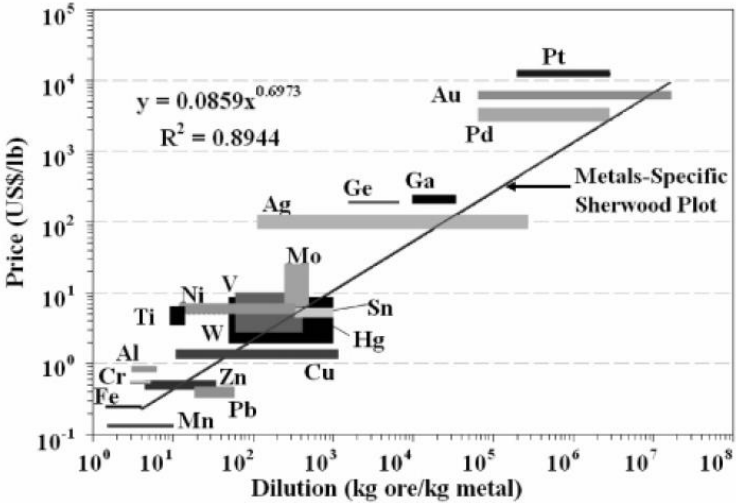


Figure 4.9. Relationship between dilution of metals in ore (the width of the bar) and 2004 price ranges (the height of the bar) for refined metals, with dilutions ranging from the lowest ore grade being mined (the rightmost side of the bars) to the highest (the leftmost side of the bars). The metal-specific Sherwood Plot is a regression line fitted to the average 2004 refined metal prices and the lowest profitable ore grades. Metals whose dilution and refining prices are placed above the line are profitable exploited. Figure extracted from [129].

³ E-scrap (PCBs, laptop and handheld computers, and some mobile phones) has gold contents range from 100 to 400 ppm; and High value e-scrap (Circuit boards from main frames, some mobile phones, ICs and MLCCs) has contents above 400 ppm [130].

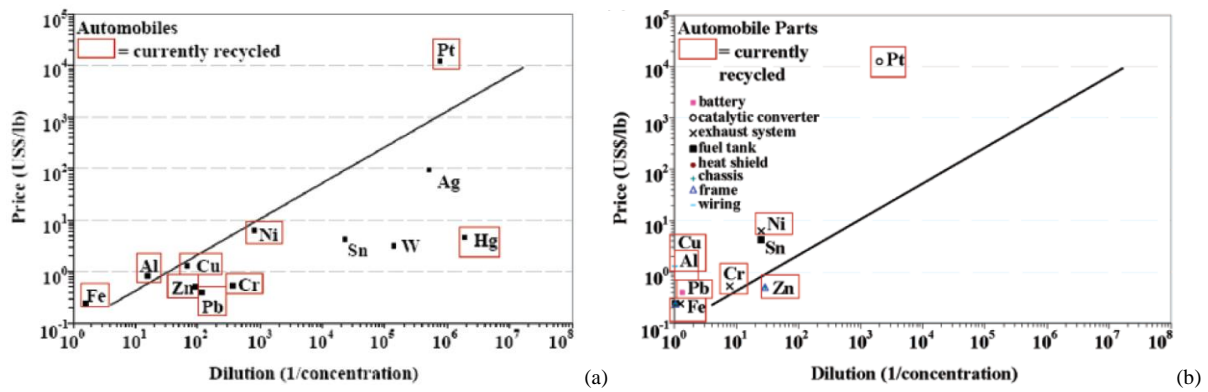


Figure 4.10. Adapted Sherwood Plots for (a) metals dilution in waste automobiles in relation to recycling price. (b) Metal dilution in disassembled automobile parts in relation to recycling price. Both figures were extracted from [129].

If one contrast the dilution of different metals in ores and their refining prices shown in figure 4.9; with their dilutions in waste automobiles in figure 4.10a, and in dismantled parts (figure 4.10b); A considerable increase in the concentration and profitability from recycling can be noticed when efficient separation of homogeneous parts of products is applied. This aspect is of paramount importance and could explain the reason by which many metals present in WPCBs are not currently recycled (Figure 4.11).

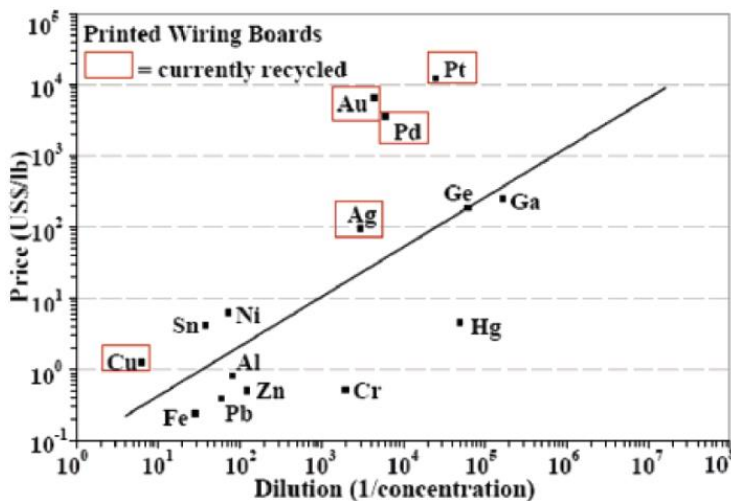


Figure 4.11. Adapted Sherwood Plot for metals dilution in WPCBs in relation to recycling price. Figure extracted from [129].

Furthermore, the low concentration and separability of specific metals in WPCBs would not only prevent their recycling (although their extraction and refinement prices would be similar to their recycling prices, as seen for germanium⁴ in figure 4.11), but also make difficult the recovery and purification of other metals. Indeed, according to Söderman & André [112], unlike metals with high functional recyclability⁵ (gold, silver, palladium and cobalt), other metals with non-functional recyclability⁶ are ignored at an industrial level and are simply dissipated into the environment. To illustrate their posture, they present the material flow analysis of repaired smartphones, demonstrating a loss of more than 9% for Indium and Yttrium (Figure 4.12).

⁴ Germanium content in electronic products is extremely low; for example, less than 0.001 grs in a smartphone according to Bookhagen, B. et al. [131].

⁵ Functional recyclability: term coined by Guinée et al. [132] that defines the recovery of metals or metal alloys that are returned to the raw material production processes through separation and classification procedures.

⁶ Non-Functional recyclability: part of recycling in which a metal is collected with old scrap, normally considered as an impurity in the recuperation process of other metals or alloys (for example, small amounts of copper in recycled iron that are incorporated into the carbon steel recovery process) [133].

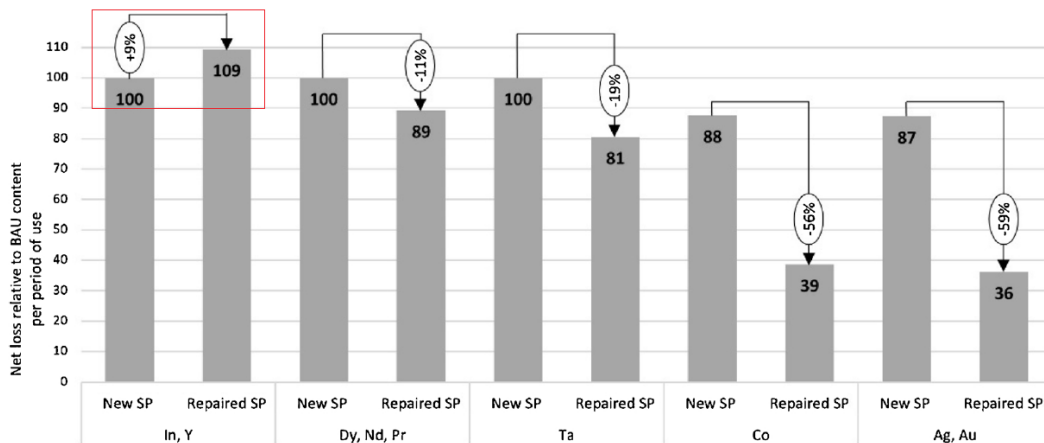


Figure 4.12. Metal net loss relative to Business as Usual (BAU) content of a new smartphone (SP) (shorter lifetime and recycling) VS a repaired smartphone (repaired SP). Figure adapted from [112].

This loss would be explained by the constant replacement of broken screens, rich in Indium and Yttrium (non-functional-recyclable metals) in almost all repairs, on the one hand; and by the usual short lifetime extension of repaired smartphones on the other hand (see figure 4.13).

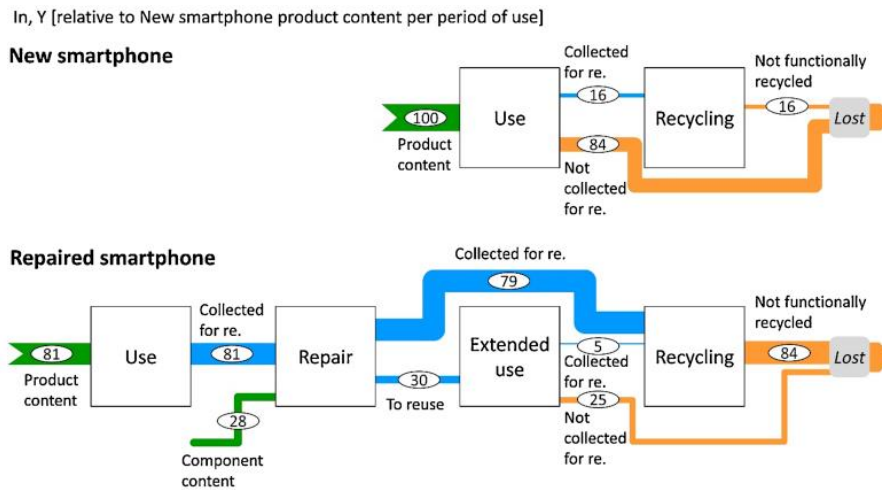


Figure 4.13. Indium and Yttrium metal flows relative to new Smartphone content (BAU) per period of use from gate-to-grave. The additional quantities of Indium and yttrium in replacement screens (bottom figure) are depicted as “Component content”. Figure extracted from [112].

2.2.2. Circularity features affecting re-use

The reuse of electronic components faces reliability constraints. Fortunately, the scientific community is beginning to consider the importance of this aspect for the sustainability of electronics and new studies demonstrate the reliability of reusing electronic components obtained through thermal disassembly processes. For example, in an experimental study conducted by Sitek, J. et al. [122], six BGA memories were extracted from, and reassembled to electronic cards applying several cycles of different thermal reflow profiles (figure 4.14a-b); and then subjected to a visual inspection and functional test in order to check their integrity and operational reliability. While only two memories presented a common defect known as bridging⁷ in their solder balls in the visual inspection (figure 4.14c); all memories, after reballing corrections, passed the functional test (consisting on reading their stored data test using a specific algorithm).

⁷ Bridging is a condition in which the adjacent solder balls of Area Array Package components (e.g., BGA components, WLCSP, etc.) come into contact and form a solder bridge.

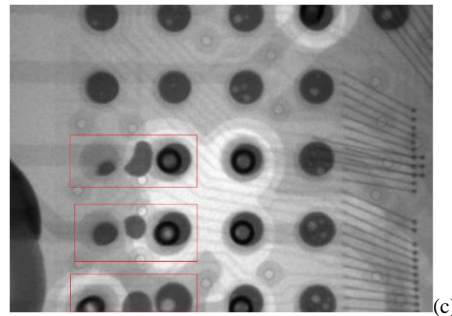
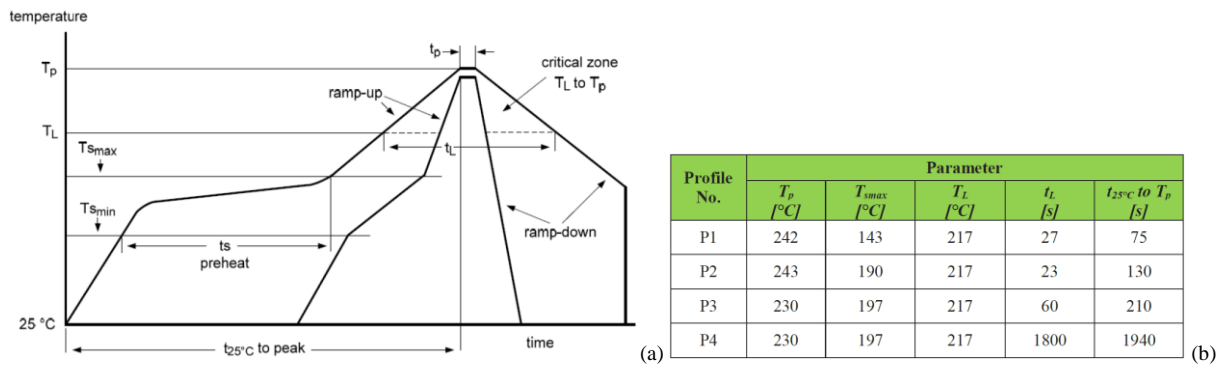


Figure 4.14. (a) A typical thermal reflow profile schema for assembly or disassembly electronic components [123]. (b) Different reflow profiles applied in disassembly experiments in [122]. (c) Bridging defects in solder balls in two of six BGA memories: the one was exposed to 3 thermal cycles under profile 2 (P2) and the other to 9 cycles under profile 4 (P4). Figures b and c were extracted from [122].

In this way, the authors of this study conclude that the thermal resistance of BGA memories goes beyond what is established in their datasheets; and explain that their reliability for reusing would be conditioned only to the bridging effect, which would be produced by the mechanical force applied when extracting the components from PCBs (e.g., manually lifted). Although this study offers solid evidence regarding the reliability of reusing BGA components (once solving the bridging defect through a process called reballing), the causes for which its authors explain the bridging defects in thermal separation processes should be questioned. Indeed, more research is needed in this regard and the scientific community is providing more and more information about the phenomenon. For example, there is a growing body of evidence suggesting that the bridging defect is related to the deformation (warpage) that a component suffers under thermal stress (Figure 4.15a), which is intensified by some physical attributes.

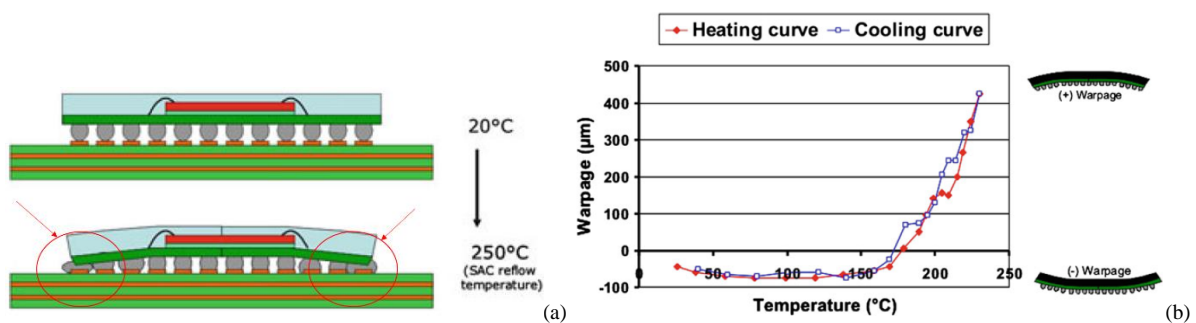


Figure 4.15. (a) Excessive warpage resulting in shorted solder balls (bridging). (b) Experimental warpage (downward and upward bending) obtained for a PBGA 35 x 35 mm² component according to Grossmann & Zardini [124]. Both figure were extracted from this work.

Indeed, one of the main causes of warpage is attributed to the difference in the Coefficients of Thermal Expansion (CTE) of the different materials that compose the homogeneous internal parts of ICs that, under thermal stress, exert different mechanical forces causing deformations in the packages. Thus, high temperatures that exceed the solder melting point would cause extreme deformations, like those shown in figure 4.15b; and shorted solder balls (bridging), like those shown in figure 4.15a [124]. Beside of that, the warpage effect would be also intensified by other physical attributes of ICs such as the size of the package and the molding compound thickness [124-125]; and the substrate thickness and the solder bump pitch [125].

Regarding these last attributes, another study conducted by Kang, J. S. [125] examines their levels of influence on the warpage of different Plastic Ball Grid Array (PBGA) components (Figure 4.16). By using 16 combinations of different form factor values for the solder bump pitch —feature or factor 1 (F1), package size (F2), compound thickness (F3) and substrate thickness (F4) in Finite Element Analysis (FEA), this study obtains the maximal deformations (W_{max}) of four commercial PBGA components, which are subsequently analyzed by an Analysis of Variance (ANOVA) test to determine the level of significance of each of the aforementioned attributes.

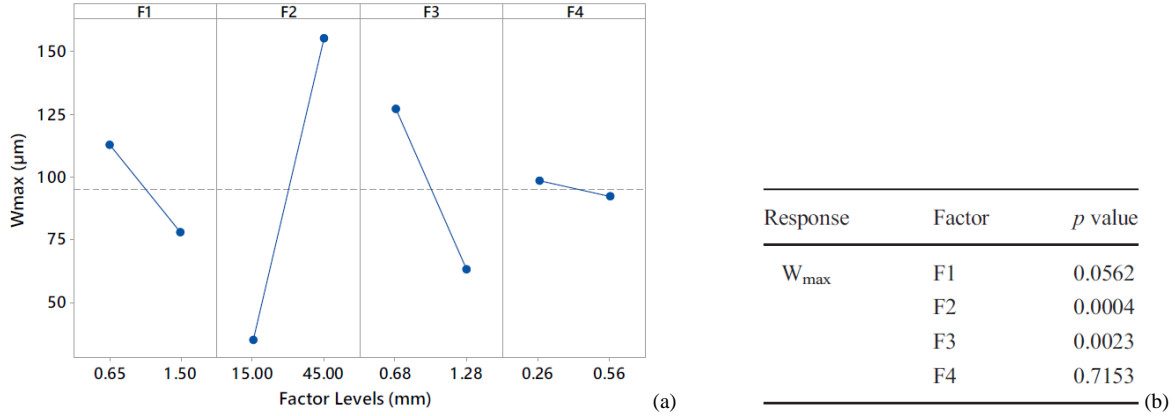


Figure 4.16. (a) Mean effect plots of specific features (F1-F4) on the maximal warpage (in μm) of four commercial PBGA components according to Kang, J. S. [125]. The dotted horizontal line depicts an intact component and the left and right number in each factor represent its lowest and highest values. (b) p values from an ANOVA test applied to the maximal warpage (W_{max}) obtained from 16 FEA simulations. The smaller the p value of a physical factor, the more its significance for warpage.

In this way, the authors conclude that the most influential features are (in order of importance) the size of the package (F2), the molding compound thickness (F3), the solder bump pitch (F1) and the substrate thickness (F4). From this, they construct a regression model for the maximal warpage (W_{max}) prediction of PBGA components (equation 4.1).

$$W_{max} = 12 - 80,7 F1 + 9,29 F2 - 44,4 F3 + 88,7 F1F3 - 3,532 F2F3 - 0,92 F2F4 - 1,597 F1F2F3 \quad (4.1)$$

Returning to the premise that the warpage effect triggers bridging, another study held by Grossmann & Zardini [124] demonstrate the influence of critical warpages, the volume of the solder balls and the distance between them (the solder bump pitch) on the bridging defects of BGA components (figure 4.17).

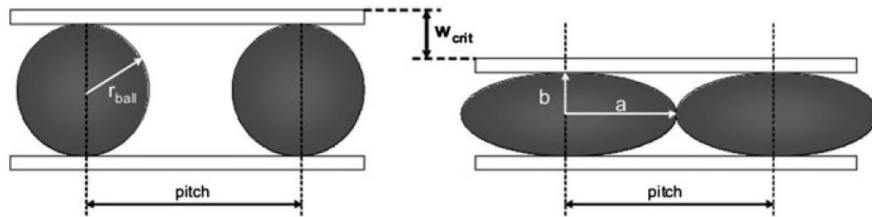


Figure 4.17. Intact solder balls spheres (left) separated by a “solder bump pitch” distance; and deformed solder balls ellipsoids (right) whose IC package suffered a critical warpage (W_{crit}). Figure extracted from [124]

Indeed, in normal conditions, the solder balls have sphere forms with radius (r_{ball}) and volume (V_{sphere}), which are later deformed by a critical warpage (W_{crit}) in compressed ellipsoids with volume ($V_{ellipsoid}$) causing bridging. More specifically, according to Grossmann & Zardini [124], as the critical warpage at which the two adjacent ellipsoids in figure 4.17 touch each other is achieved only when a is equal to half of the solder bump pitch, and b to r_{ball} minus half of the W_{crit} (equation 4.2); and as the volume of a deformed ellipsoid ($V_{ellipsoid}$ in equation 4.3) is equal to the volume of a perfect sphere (V_{sphere} in equation 4.4), the critical warpage (W_{crit}) at which adjacent solder balls do not touch is given by equation 4.5 as follows.

$$a = \frac{pitch}{2} \rightarrow b = r_{ball} - \frac{W_{crit}}{2} \quad (4.2)$$

$$V_{ellipsoid} = \frac{4\pi}{3} a^2 b = \frac{4\pi}{3} \left(\frac{pitch}{2}\right)^2 \left(r_{ball} - \frac{W_{crit}}{2}\right) \quad (4.3)$$

$$V_{sphere} = \frac{4\pi}{3} r_{ball}^3 \quad (4.4)$$

$$W_{crit} = Ball\ diameter \times \left(1 - \left(\frac{Ball\ diameter}{pitch}\right)^2\right) \quad (4.5)$$

Thus, by taking into account the diameter of the solder balls (which is equal to 2 times their radius) and the solder bump pitch, these authors obtain analytically the critical warpages of different BGA components (figure 4.18); that are only 40 μ m higher than the empirical warpage values seen in figure 4.15b.

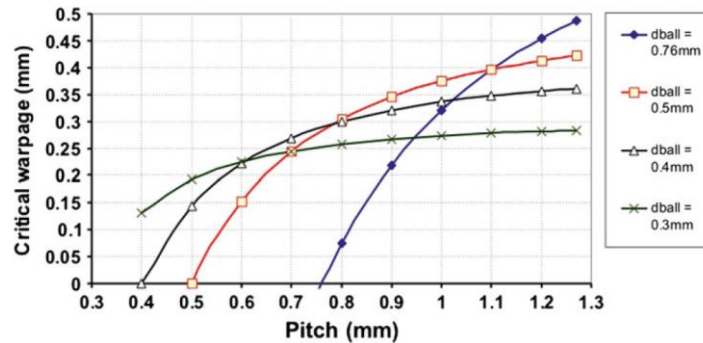


Figure 4.18. Estimated critical warpages of different BGA components depending on the diameter of their solder balls (*dball*) and the distance of their solder bump pitches. Figure extracted from [124].

On the other hand, low temperatures in desoldering processes may avoid warpage and bridging effects, but provoke other issues that would harm the reuse of electronic components. About it, for example, Layiding, W. et al. [126] demonstrate empirically that low temperatures in thermal separation processes cause disbonding damages on the pins of different electronic components (Figure 4.19). These damages (e.g., bending in lead-typed components and bonding breaks, especially in BGA components) could be explained by premature separation of electronic components before the solder melts (usually due to lower-temperature reflow profiles).

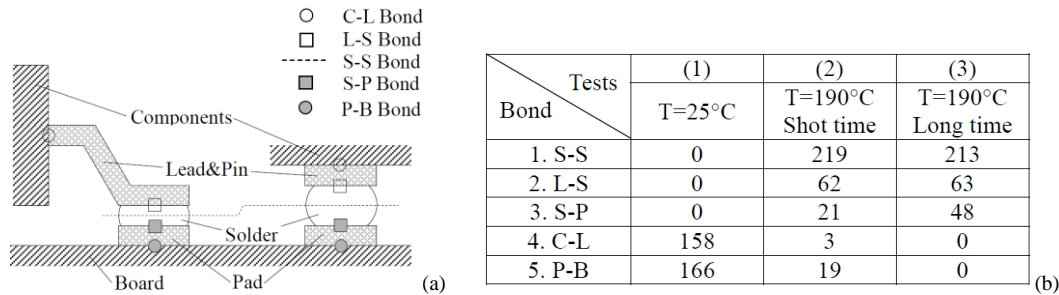


Figure 4.19. (a) Disbonding types of a gull-wing-typed IC component (left) and a BGA component (right). A common damage occurs when a lead or a solder ball breaks from a component (C-L bond breaks). (b) Counts of different disbonding types of BGA components in disassembly tests profiles experiments (1), (2) and (3). Both figures were extracted from [126].

Therefore, to minimize damages and achieve only good separations (i.e.: Solder-Solder (S-S), Lead-Solder (L-S) or Solder-Pad (S-P) disbonding types), it would be necessary that the WPCB be heated to temperatures above the melting point for long enough, but avoiding extreme temperatures that trigger warpages (consider, for example, the disassembly conditions or experiment 3 in figure 4.19b, in which any C-L break occurs).

Regarding the optimal conditions for thermal disassembly, Chen, M. et al. [127] obtained high disassembly rates (the ratio of the number of intact, separated components to the total components in WPCBs) under specific conditions of preheat temperature, maximum temperature and incubation time (figures 4.20a-c). By applying an automatic heated-air disassembling equipment on 13 different types of WPCBs, they concluded, interestingly, that small components (side length < 3mm) are the

components with the lowest probability to be successfully separated (with a disassembly rate range from 40 to 50%).

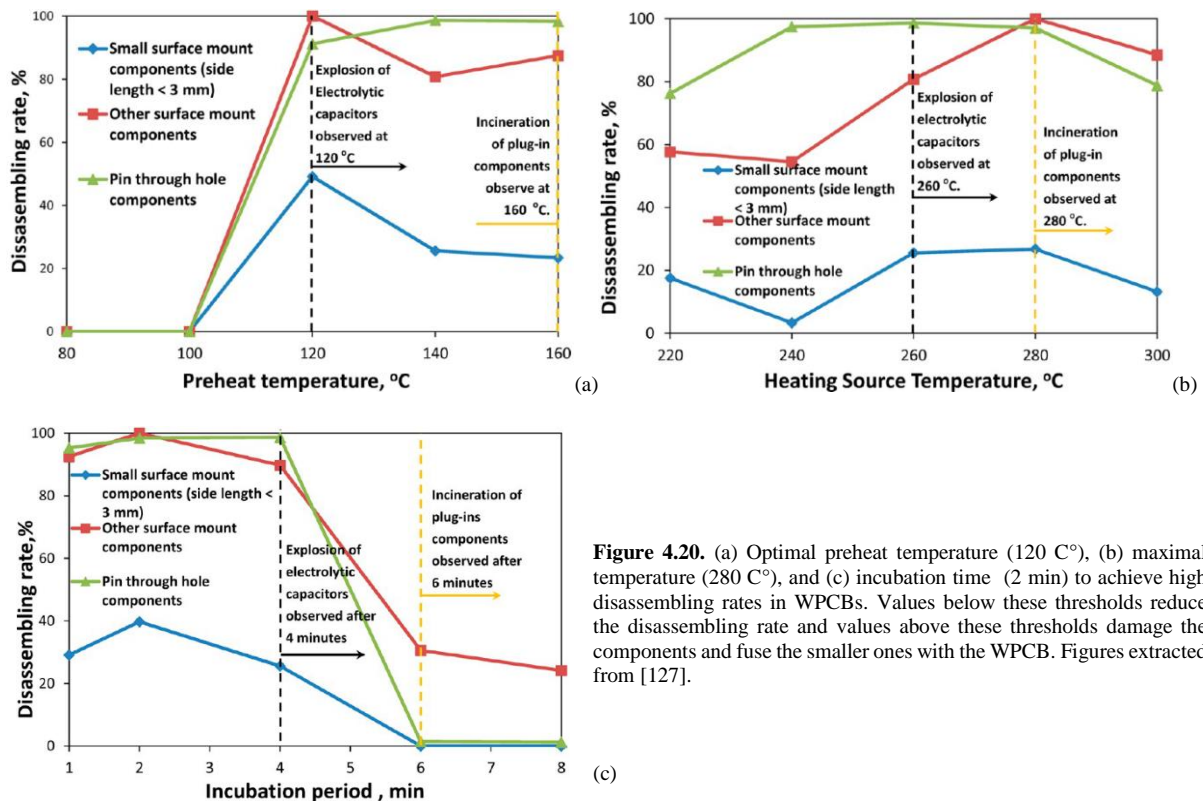


Figure 4.20. (a) Optimal preheat temperature (120 °C), (b) maximal temperature (280 °C), and (c) incubation time (2 min) to achieve high disassembling rates in WPCBs. Values below these thresholds reduce the disassembling rate and values above these thresholds damage the components and fuse the smaller ones with the WPCB. Figures extracted from [127].

- In the light of all the previous works, it could be stated that the estimation of the potential impacts, or benefits of circular strategies (like recycling) applied to IoT devices would be framed, among other aspects, by (1) individual features of electronic components (for example, the content of specific materials in components subparts), (2) interdependent features (similar service times between components (as seen for screens of smartphones); and even (3) external factors such as a correct design oriented to easy separation, or refining prices of raw materials.
- On the other hand, the benefits of other circular strategies (like reusing) applied to electronic components would be limited by reliability, which is also conditioned by specific features (e.g., size of the component, specific dimensions of the pins, types packaging technology, etc.), and by external factors in disassembly processes (e.g., the appropriate desoldering temperature).

2.3. Technical features

Understanding the influence of technical features on the data operational stages and the reference flow of IoT systems is critical for their impact estimation and right-provisioned design. For example, one observed the crucial role of writing cycles of memories for the lifetime of modern intermittent system (chapter 1, section 3.2.1), or the primary purpose of collecting and treating meaningful raw data in chapter 2 (section 4 and 5), together with the essential features of electronic component to do it (section 1). This section aims to aware the reader the relevance of this kind of features and invites him or her to consider them under different operational contexts.

As seen in the work of Bonvoisin et al. [61], the environmental impact of a network of sensor devices will depend on the operational lifetime of each of the nodes that composes the network. In this sense, the failure rate⁸ of each electronic component that shapes a sensor device linked to a network node will necessarily depend on its operational time, on the one hand; and on environmental conditions (e.g.,

⁸ Considering a failure as an important variation of the nominal value of an operating parameter; for example, capacitance in capacitors or reading errors in memories.

ambient temperature, pressure, humidity, radiation or mechanical stress) and operational conditions (e.g., functional loads such as current, power dissipation and voltage) on the other hand [134]. For example, under normal conditions, electronic components generally have a very low failure rate; but degradations in functionalities arise as these conditions change over time (figure 4.21).

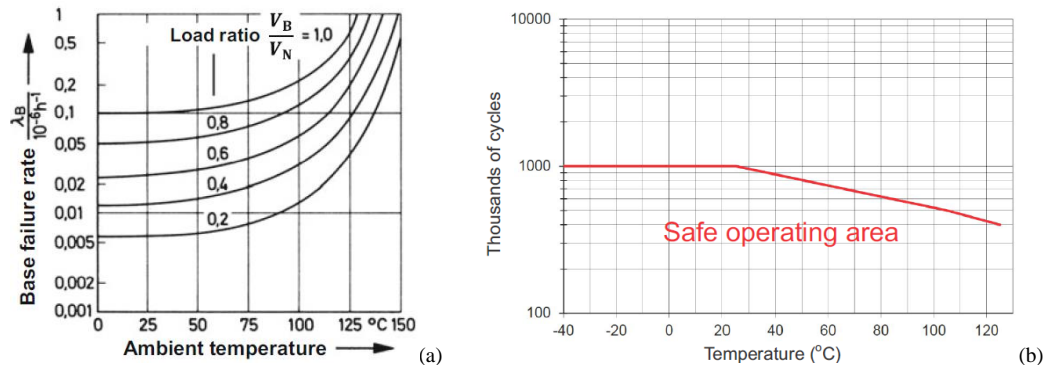


Figure 4.21. (a) Base failure rate λ_B (ratio of number of failures to number of test units in time (h)) of tantalum capacitors in function of temperature [135]. (b) Safe writing cycling operating conditions (per byte) VS temperature of an EEPROM memory [136].

Indeed, one of these conditions is ambient temperature, which universally affects all electronic components without exception. For example, it can be seen how a progressive increase in ambient temperature increases exponentially the failure rate of tantalum capacitors in figure 4.21a; or reduces the lifetime (in terms of writing cycles) of EEPROM IC memories in figure 4.21b. These aspects, together with other more technical factors, may affect the reference flow of IoT systems (i.e.; in terms of failure devices) and are of paramount important for their eco design.

For example, the failure rate (mainly linked to use intensity and additionally affected by ambient temperature) of memories become a relevant aspect for the eco-design of intermittent EH sensor systems. In these devices, as seen in chapter 1, the states of the program execution must be saved continuously in a NVM memory (a routine known as check pointing) every time the accumulated energy is nearly exhausted, and restored each time there is sufficient energy for reinitializing the main processor [137]. Depending on a variety of operating conditions, such as the complexity of the program execution or the frequency by which an EH sensor system accumulates and depletes energy, these checkpoints can quickly wear out the writing cycles available in main memory.

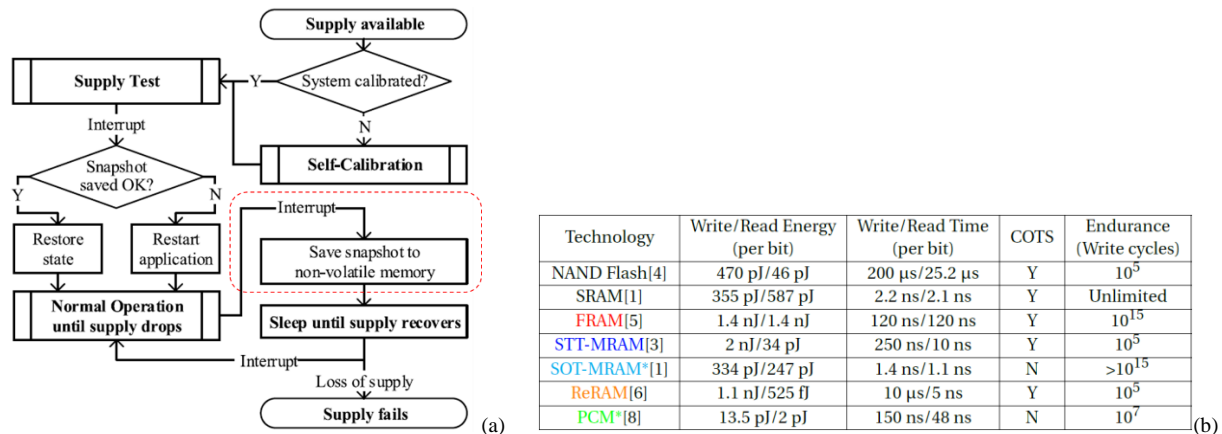


Figure 4.22. (a) Main program execution of Hibernus++ (a well-known main operating algorithm for EH intermittent systems proposed by Balsamo, D. et al. [138]). Interruptions after the normal execution step (“Normal operation until supply drops”) trigger check pointing routines (“save snapshot to non-volatile memory”). (b) Technical features of NVM memories including writing endurance [24].

Consider, for example, the work of Daulby, T. et al. [24] who study the lifetime of a Seiko smart watch, executing a well-known algorithm for EH intermittent systems (Hibernus++) with FRAM, STT-RAM and ReRAM memories. Assuming a check pointing frequency of 2,5Hz (interruptions of 0,4 seconds, figure 4.22a) and normal ambient temperature, they show that FRAM memories (with an approximate

write cycle rate greater than 10^{15} per memory block) guarantee an approximate device's lifetime of 6,37 Million years, while STT-MRAM or ReRAM memories (both with a write cycle rate of only 10^5), only 4,63 days.

Furthermore, in addition to the environmental conditions and writing cycles, other technical attributes, such as the granularity and density of memories (according to Colin, A. [137]), as well as the energy and time required in writing and reading operations (according to Daulby, T. et al [24] and Colin A. [137]) would complicate the design and eco-design of sensor systems, especially in contexts of constricting energy and / or applications with high readiness requirements (to have an approximate order of magnitude of this technical features in eco-design of IoT devices, see figure 4.22b).

- Consequently, the technical features of electronic components play an important role in the accurate definition of reference flows and impact estimation of IoT systems; and in the ecological design of sensor systems (especially in the use phase).
- The performance of these technical features depends, among other aspects, on operational conditions such as the use intensity of a component, and/or external factors such as environmental conditions (e.g., ambient temperature).
- By taking into account these and other technical features of different electronic components of an IoT device, together with their probable incompatibilities and their possible tradeoffs, one can guarantee a more appropriate functional and ecological design.

2.4.Data flow

Understanding how and under what conditions raw data is generated, converted and delivered is capital for answering the main interrogation reported in this work and solve its related research questions. From chapter 3 (section 1.2.1), for example, it was established that the data volume transmitted from local to mutualized infrastructures (in terms of sampling rate, size and frequency) affects enormously the reference flow and, consequently, the impact of IoT systems. This section aims to extend the study of these aspects under the lens of certain electronic components, some technical features, and specific technologies.

Das, S. & Mao, E. [8] show that design decisions when selecting sensor components should be guided through an analysis of the type of signal, range and data resolution they generate, and Morin, E. et al. [139] show, for their parts, that the lifetime of an IoT device —in terms of the depletion rate of its available energy (13.5 Kj corresponding to two AAA batteries), is drastically conditioned not only by the energy needs in the data transmission (Tx) and receiving (Rx) activities, or in idle and sleep states; but also by a combination of additional factors linked to data manipulation and quality, including the data size required by the application, the data rate, and even the distance range at which its communication interface operates in relation to another device (see table 4.4 and Figure 4.23).

	Power	P_Tx (mW)	P_Rx (mW)	P_Idle (mW)	P_Sleep (μW)
802.11 PSM	G2M5477	699.6	170	66	13.2
	RTX4100	1050	350	9.1	9.45
	MAX2830	699.6	204.6	92.4	66
	STM SPWF01SA	1135	346.5	85.8	141.9
BLE	nRF51822	37.2	42.3	13.2	7.8
	BLE112	97.2	90	27.4	3.24
	BlueNRG	31.7	29	7.104	6.4
802.15.4	GreenNet	25.024	19.26	7.104	5.76
	SmartMeshIP	24.11	20.87	4.67	4.32
	TelosB	76	79	41	15

Table 4.4. Power needs for transmission, reception, idle and sleep states of specific SoC communication interfaces. Adapted from [139].

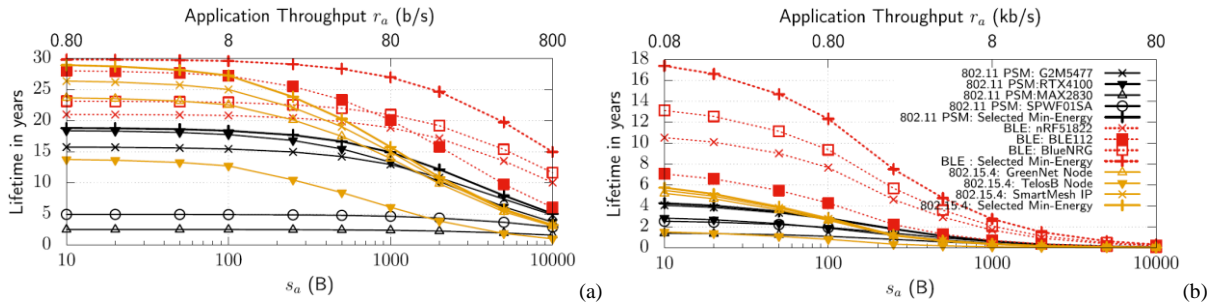


Figure 4.23. (a) Lifetime estimations of an IoT device transmitting different data sizes (S_a , in bytes B) every 100 seconds (low data rates), and (b) every 1 second (high data rates). The legend is applied for both figures, which were adapted from [139].

Indeed, Figure 4.23a shows, for example, that many of the components with high-energy consumption for transmitting and receiving data are more efficient than the component with the lowest energy consumption in this activities (see column Tx and Rx for the SoC component Telos B in table 4.4). This phenomenon, only evident in low data rate conditions, is explained by the power consumption of the sleep state of the Telos B component, higher than that of the other components (except for MAX2830 and STM SPWF01SA components). On the other hand, in figure 4.23b it can also be seen that the gap between all components of the 802.11PSM and 802.15.4 standards (the latter containing the Telos B component) is narrowing, in a context of intense data traffic (transmissions every 1 second). The authors explain that, while the power consumption of the sleep state becomes an important technical attribute for the lifetime of a device with low activity (transmitting at low data rates, such as those in figure 4.23a), The energy needs for transmitting and receiving data become relevant for a busy device communicating at high data rates.

What’s more, they demonstrate the influence of data size on the lifetime of devices using modern wireless technology; in figure 4.24, it is observed that with very low data rates (1 transmission per day), Sigfox and LoRa technologies consume more energy as data size increases, reducing drastically the lifetime of an IoT device. This is explained by the large amount of energy required to transmit over long distances, the significant data fragmentation and the protocol overhead; all distinctive features of these technologies.

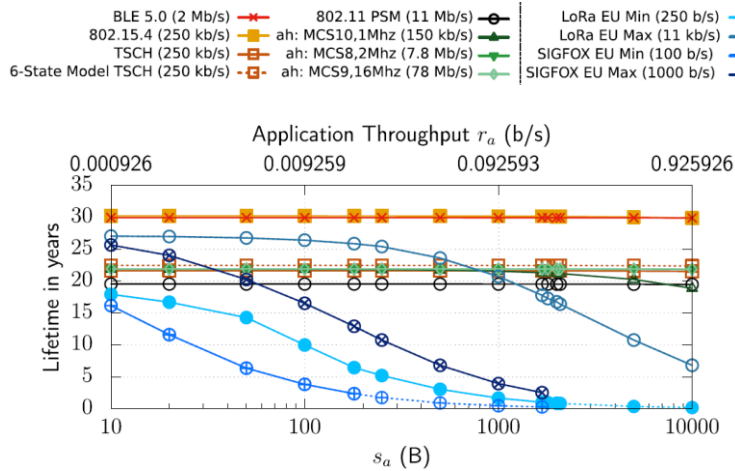


Figure 4.24. Different data sizes (S_a , in bytes B) transmitted in fragmented packets per day. As Sigfox and LoRa handle only small packets, these technologies significantly fragment large data sizes in small, numerous messages, resulting in additional energy consumption for transmission and protocol overhead. Figure taken from [139].

In this manner, by taking into account all these aspects, these authors generate a reference table of approximate lifetime of different IoT devices, operating with two AAA batteries under different technologies and specific operational conditions, to facilitate the selection of the most appropriate technology depending on the data flow and data quality requirements of specific IoT applications (Table 4.5).

Application (s_a/t_a)	BLE	802.15.4	TSCH	802.11 PSM	802.11ah 8_2	SIGFOX 1%	LoRa 1%
Audio streaming G.711 (80 B/10 ms)	~ 90 days	15 days	21 days	15 days	5 days	0	0
Heart rate monitor (50 B/1 s)	10.5 years	5 years	5.5 years	3 years	1 year	0	0
Temperature sensing (50 B/100 s)	23.5 years	23 years	20.5 years	8 years	9 years	0	1 year
Snow level metering (50 B/day)	24 years	24 years	20.5 years	8 years	10 years	21 years	27 years

Table 4.5. Lifetime estimation of different IoT devices under certain applications, in terms of data rate (S_a / T_a), and considering a clock drift of 40 ppm, a packet error rate of 20%, and the maximum European available rates. Table extracted from [139].

- In this sense, the appropriate impact estimation of full IoT systems and the eco-design of IoT devices would be guided, initially, by the type and generation of data originated in the sensor components of sensor systems. Having a clear idea of how an IoT system demands and uses this data later, to transform it into useful information, together with understanding the technical and operational context in which this data will be transmitted, would facilitate the selection of more suitable electronic components on the basis of its technical features.

3. Proposed methodology for sustainable IoT systems

Alternatively, this thesis advocates for a more thoughtful design of data, information, and knowledge for right-provisioned, sustainable IoT systems.

From chapter 2, it was evidenced the potential of IoT systems for generating massive data (as observed in the experimental work of Sinaeepourfard, A. et al. [5]), with the implicit risk of increasing damage from the production and/or the use of devices with extended capacities (as demonstrated by Lelah, A. et al. [51]). By considering this, and by taking into account the conclusions of the previous sections 2.4 of this chapter, this thesis advocates for a more reasoned design of data and information for right-provisioned, sustainable IoT systems (figure 4.25).

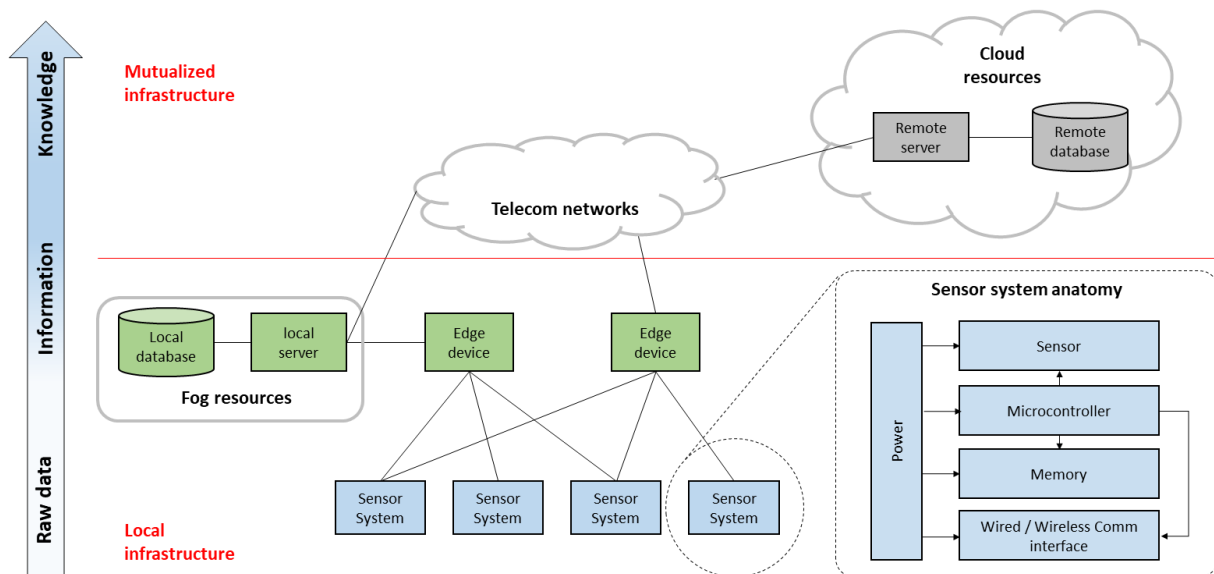


Figure 4.25. The proposed approach for impact estimation and eco-design of IoT systems, making explicitly the design of data and information flows (data-information-knowledge design) along the full IoT architecture.

In this sense, and by considering the results of the qualitative research presented before, the contributions of section 2.2 of chapter 3, and the conclusions of sections 2.1, 2.2, and 2.3 of this chapter; a novel methodology for the eco-design of IoT systems consisting of two frameworks is proposed below.

3.1. Framework for eco design

The first framework (figure 4.26), aims to reduce the ecological impact of IoT systems through a preliminary analysis of raw data (e.g., type of signals, quantity, etc.), its flow and its planned transformation from the study of customer requirements (customer's needs). This step would help to identify the computational load on the mutualized infrastructure, on the one hand, and the right-provisioned electronic components to construct local devices on the other. Subsequently, certain

parameters of specific environmental, physical, and technical attributes of these electronic components should be considered for rapid LCA impact analysis, sensitivity analysis, or uncertainty tests.

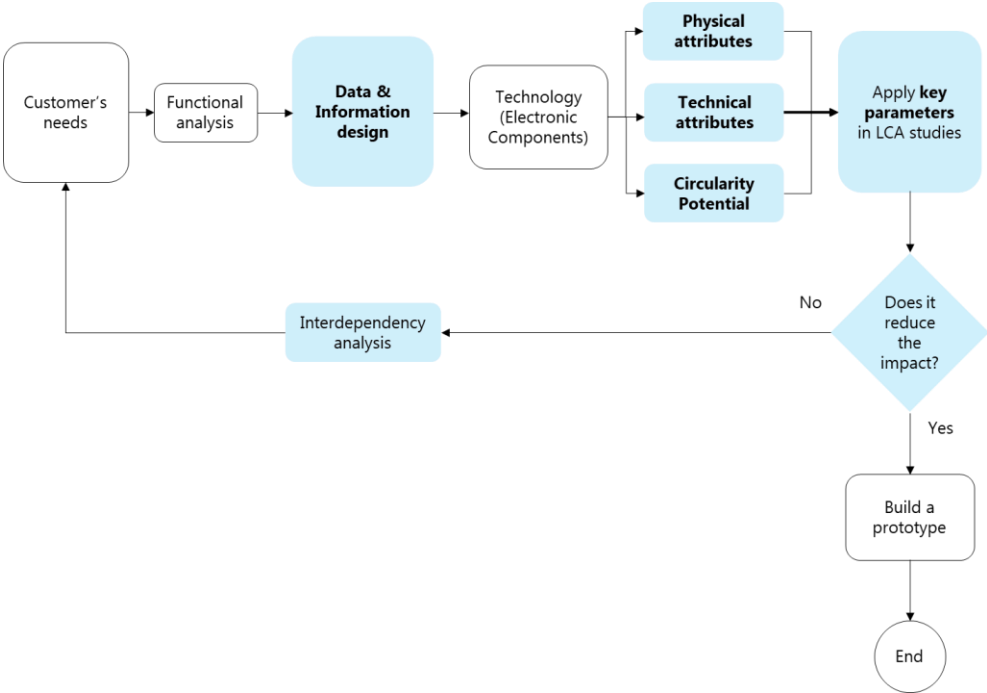


Figure 4.26. Framework for the integration of ecological aspects in the NPD process of local IoT devices. The white boxes show the usual design workflow of IoT devices revealed by the qualitative study of section 1 and the blue boxes show the integration of ecological aspects.

In this framework, if the impact does not reduce, the replacement of the most problematic components should be considered in a new design iteration, previously analyzing their interdependence with the rest of the electronic design (i.e.: interdependencies of technical features) and in the ecological design (i.e.: impact transfers in different lifecycle phases). Once the impact is reduced, designers can move on to the prototyping stage. This framework could work simultaneously and, with the support of the framework for impact estimation described below (framework for the global impact estimation of IoT system).

3.2. Framework for impact estimation

This framework is built from the basic three-layered architecture of IoT systems (sensing-, edge- and cloud-layers) seen on different works [86], [107], [140-143]; together with a novel representation of electronic components of local devices and their interactions. In this framework (figure 4.27), one or more devices (D) compose the sensing and edge layers. Each of these devices is composed of one or more electronic components (C), which fulfill specific functions of the data operational stages of an IoT system through specific capacities (FC) (a specific value of a technical parameter). Such Function-Capacity association allows identifying the reference flow of a full IoT system and facilitates its lifecycle modeling.

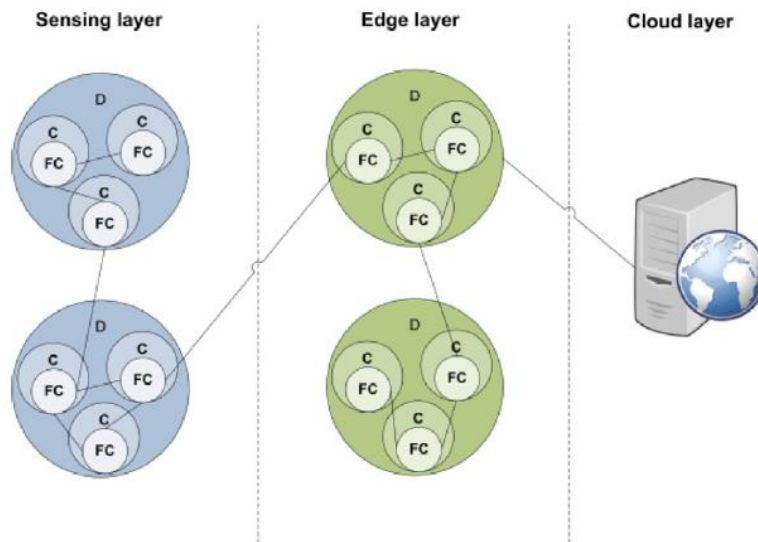


Figure 4.27. Framework for the global impact estimation of IoT systems. Each component (C) of a device (D) in a layer contributes directly or indirectly to a data operational stage function by a specific capacity (FC) linked to a technical attribute.

Build on the basis of the most relevant findings seen before, these two frameworks recall the essential elements in eco-design (framework for eco design), and global impact estimation (framework for impact estimation) to avoid potential impact transfers in local devices and facilitate the rapid but appropriate environmental assessment of full IoT systems respectively. Therefore, both frameworks are complementary and compose a compound methodology oriented to facilitate the construction of concrete LCA implementations and more effective eco-design guidelines, as it will be demonstrated in next chapter.

4. Proposed Implementations of the frameworks

On the basis of these frameworks, specific implementations for environmental analysis and eco-design can be built, according to the available resources and goals of design teams. For example, designers can study different combinations of electronic components with different features and parameters through the framework for eco design; or observe the long-term impact of data, flowing along the local and mutualized infrastructures through the framework for impact estimation. Two implementations oriented to this suggested goals are proposed below and are illustrated by two case studies in the next chapter.

4.1.LCA Implementation for the framework for eco design

In the framework for eco design, the data & information design step could be implemented by using the rationale information science scheme showed in figure 3.39 of chapter 3; and the remain steps by a suggested LCA model considering physical, technical and environmental attributes of electronic components, for the corresponding manufacturing, use and E-o-L phases of local devices (figure 4.28).

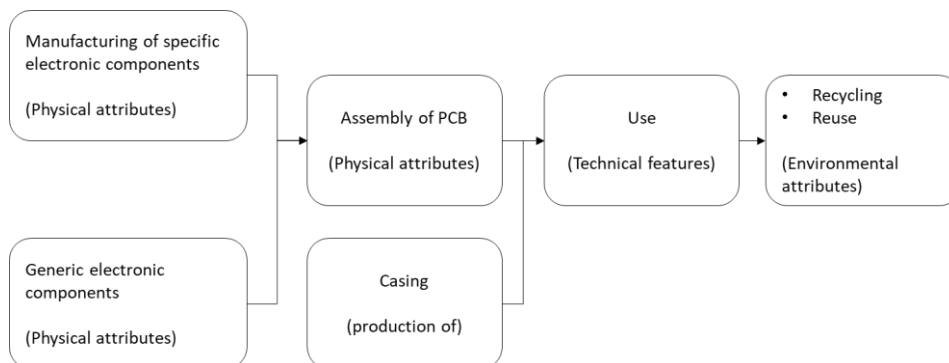


Figure 4.28. Suggested LCA Implementation for the framework for eco design. Life cycle phases may consider specific and/or generic electronic components. Designers should define the attributes and the related parameters of those that would be further dissected in specific analysis (e.g., sensibility or uncertainty analysis) according to their goals. This implementation considers the inclusion of other non-electronic components (i.e.: casings) and specific manufacturing processes (e.g., Assembly of the electronic card) of local devices. For the E-o-L modeling, this implementation considers recycling and reusing.

For sensitivity or uncertainty analysis in the manufacturing phase, the materials of ICs; and the PCB, die and ICs packages areas are considered according to the schema below.

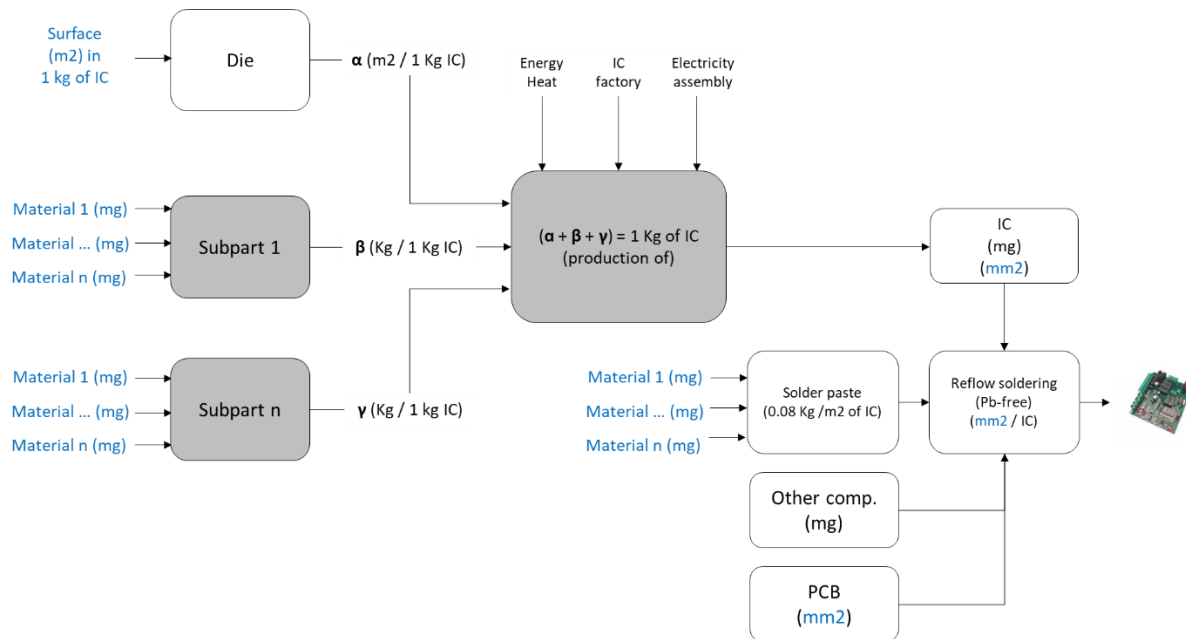


Figure 4.29. Detailed process modeling of the manufacturing life cycle phase of an IoT device (including assembly of the electronic card). Production of specific ICs is normalized to 1 kg, and blue text inputs are values of suggested attributes that should be applied in further sensibility or uncertainty analysis.

As small differences in estimated die areas of ICs would provokes large impacts of ICT products [114], this implementation includes a detailed modeling of internal die areas, which considers the footprint area of the component (A_{IC}) and the share of the processed wafer (S_{IC}) in the total packaged IC weight (W_{IC}). These physical attributes are used to obtain the die area to package mass ratio of the IC component (area-mass ratio) according to equation 4.6, which is found in the LCI methodology of the Ecoinvent database (Hischier, R. et al. [174]).

$$A_d = \frac{A_{IC}}{W_{IC}} \times S_{IC} \quad (4.6)$$

Where:

A_d = Area of the internal die (in m^2 , normalized to the production of 1 Kg of the studied IC)

A_{IC} = Footprint area of the studied IC (in m^2)

W_{IC} = Weight of the studied IC (in Kg)

S_{IC} = Share of the processed wafer in the total IC weight (in %)

In figure 4.29, the white processes could be modeled from known LCA databases (e.g., Ecoinvent) and gray customized process from the material declarations and production reports of electronic components provided by manufacturers. In this implementation, energy heat, electricity consumption and IC factory infrastructure used for the production of 1 kg of ICs could be taken from Ecoinvent literature [144] (493 MJ, 668,6 kWh and 2×10^{-8} units of factory infrastructure respectively). Notice that a subpart represents a homogeneous subcomponent of a specific IC (e.g., lead frame, wires, die attach, etc.), unable to be further separated manually or mechanically. On the other hand, for the use phase, designers can consider, for example, the energy consumption; and the time and use intensity of specific electronic components (e.g., communication interfaces and memories).

Finally, the E-o-L phase of the proposed implementation may consider key attributes affecting the recycling and reuse of electronic components according to the basic waste flow described in figure 4.30.

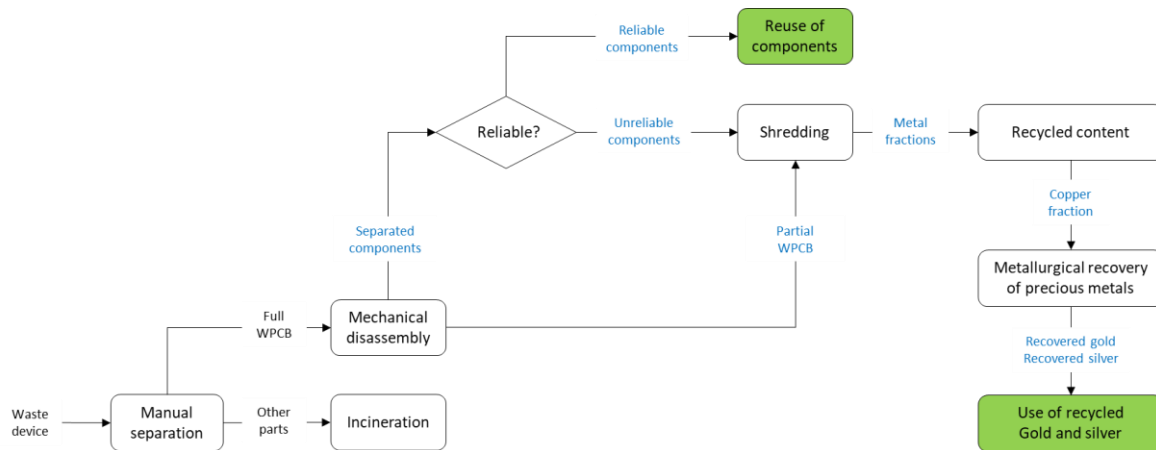


Figure 4.30. Suggested E-o-L implementation for the framework for eco design showing the best scenario for waste IoT devices. The manual separation process generates the waste flow “full WPCB” which will be treated with mechanical disassembly (e.g., thermal desoldering), generating two waste flows: intact components that are successfully separated from WPCBs and partial WPCBs with components that were not extracted. The recycling process “Metallurgical recovery of precious metals” uses copper metal fractions from shredding process.

It is composed of the minimal steps for recycling precious metals from waste devices and a reliability test for reusing electronic components. This reliability test may involve visual inspection or functional test such as those conducted by Sitek, J. et al. [122]; or analytical estimations of specific situations that decrease the reliability of recovered components (e.g., critical warpages and bridging), by taking into account circularity attributes of electronic components such as package sizes or pins dimensions, as seen in section 2.2. Green processes in figure 4.30 depict environmental benefits, which could be discounted from calculated impacts (avoiding manufacturing of electronic components or recovery of precious metals). Blue texts represent waste flows whose quantities may vary according to specific attributes of electronic components that affect the disassembly rate of WPCBs (e.g., length of the sizes of electronic components, as shown in Chen, M. et al. [127]). All attributes mentioned so far should be further applied in sensitivity or uncertainty analysis.

In the proposed EoL implementation, the recycling process may include the following waste scenarios:

- Worst: The full device goes to shredding process (not shown in figure 4.30).
- Regular: Before shredding process, the electronic card is separated manually from other device parts (e.g., plastic casings) and it is recycled entirely (not shown in figure 4.30)
- Best: Before shredding process, the electronic card is separated manually from other device parts (e.g., plastic casings) and it is recycled together with some electronic components that were not disassembled successfully (Intact separated components that fail reliability tests may be recycled separately too).

Notice that the metal fraction flows increase from the worst to the best recycling scenarios above and, for simplicity, in this implementation other non-electronic parts (e.g., casings parts) are incinerated. To determine the exact metal fractions obtained from shredding processes and the amount of precious metals recovered from it, one can use the basic shredding and separation schemes for electronic products proposed by Huisman et al. [145] (figure 4.31); and the estimated recovery percentage of gold and silver from the separated copper fraction (table 4.6).

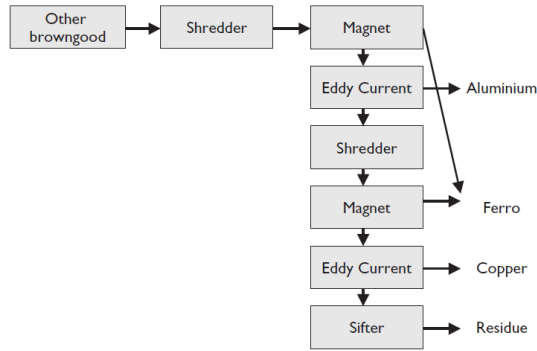


Figure 4.31. Shredding and electrostatic / magnetic separation processes applied to WEEE (brown goods). After shredding, three metal fractions (Aluminum, Ferro, Copper) and Residue waste streams are obtained. Figure extracted from [145].

[%]	Ferro	Aluminium	Copper	Residue
Aluminium	0.50%	82.58%	4.92%	12.00%
Copper	0.94%	5.00%	78.21%	15.85%
Ferro	95.00%	1.00%	1.00%	3.00%
Glass	0.56%	0.56%	10.00%	88.89%
Plastics	1.21%	0.50%	10.00%	88.29%
Ag	0.99%	0.99%	84.92%	13.10%
Au	0.99%	0.99%	80.00%	18.02%
Pb	1.18%	1.18%	80.00%	17.65%
Others	0.69%	0.67%	35.29%	63.35%

Table 4.6. Transfer coefficients of the important content to the metal and residue fractions. Adaptation by Hischier, R. et al. [146]. It shows the mean recovery percentage of specific metals from metal fractions obtained by shredding process (Ferro, Aluminum or Copper).

4.2. Cross-typed lifecycle modeling implementation for the framework for impact estimation

From the framework for impact estimation, it can be deduced that every electronic component contributes (through the execution of specific functions, and within its capacities) not only to the functional unit, but also to the environmental impact of an entire IoT system. On the other hand, Wellsandt, S. et al. [147] recall that the increasingly complexity of products and services (such as IoT applications based on multiple devices) require a multiple lifecycle modeling approach, in which impacts from every element is correctly represented. By considering the former aspect and by applying the latter approach to the electronic components of local equipment (representing common processes — functions on data or raw information— in which they interact); the following cross-typed, multiple life cycle model is proposed for the implementation of the framework for impact estimation (figure 4.32).

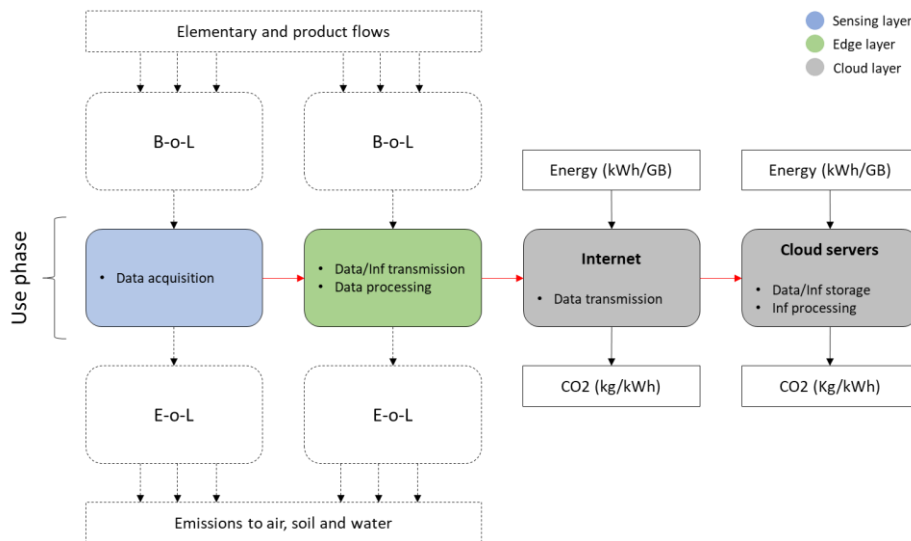


Figure 4.32. Suggested cross-typed life cycle modeling implementation for the framework for impact estimation of full IoT systems. Blue and green boxes represent one or many sensing and edge devices respectively. Black arrows represent physical flows (i.e.: raw materials, energy, supplies or intermediate products flows) and red arrows represent data flow generated by specific functions in the data operational stages of an IoT system (the common process in which electronic components interact). Modeling or impacts of dotted elements may or may not be simplified.

Indeed, these common processes are specific functions of the data operational stages seen in section 1 of chapter 2 but with a system level perspective. They are linked to specific capacities of electronic components (FC relationships in the framework for impact estimation), and define the reference flow of the IoT system. In this sense, the proposed implementation could represent, for example, the most basic interaction in which a sensor component of a sensor system collects raw data (data acquisition function in the blue process) at a specific sampling rate, that will be later treated by a specific electronic component (e.g., a MCU) of an edge device to obtain information (data processing function in the green process). This information could be later transmitted (information transmission) to mutualized infrastructures by a specific communication interface of the edge device (e.g., through a LoRa or a BLE modules) at a specific data rate.

In figure 4.32, although all data operational stages are possible in a sensing or edge device, the suggested implementation simplifies the use phase modeling by abstracting the essential functions —within the data operational stages— that characterize every layer.

Furthermore, notice that:

- An important distinction is made between data and information in edge devices, as they could simply retransmit data to mutualized infrastructures or transform data into information, depending of their available resources (e.g., abundant energy from Li-ion batteries or powerful computing available in fog servers).
- Cloud servers may store data apart from information for further use.
- Although the lifecycle modeling of electronic components of sensing and edge devices may include processes for their B-o-L and E-o-L phases (the dotted elements in figure 4.32), modeling of the internet and cloud servers are strictly limited to the use phase for simplicity. This is due to the current difficulties of determining the precise reference flow in the cloud layer (in terms of the exact number of network devices in the access and core networks and cloud servers).

In the proposed implementation, it could be assumed a bottom-up approach to calculate the impact of transmitting and processing data in the internet and cloud infrastructures, based on data generation of local devices. The environmental impacts of the dotted lifecycle phases (B-o-L and E-o-L) of electronic components in figure 4.32 could be also simplified (by assumptions) or aggregated to the total impact by using reported LCA results in literature (for example, by using reported LCA results of a similar electronic component in the simplified lifecycle phase(s)), provided that such impacts are compatible with the rest of the implementation (i.e.: same impact categories and indicators).

5. Positioning of the methodology

To position the proposed methodology with respect to the other methodologies seen in chapter 3, its contribution and its area of action within the NPD process of IoT systems is established (Figure 4.33). Its position regarding its specific eco-design intention is also recognized in figure 4.34. In both cases, its level of difficulty for its application is presented in terms of the required investment in time and effort for data collection. This is done by placing the State-of-Art and the proposed methodology in the eco-design-tools taxonomy proposed by Bovea & Pérez-Belis [148], with a variant that indicates their main approach (LCA or non-LCA), and their scope regarding the full IoT architecture (the sensing, edge and cloud layers). The benefits of the proposed methodology reported in this section will be demonstrated in the next chapter.

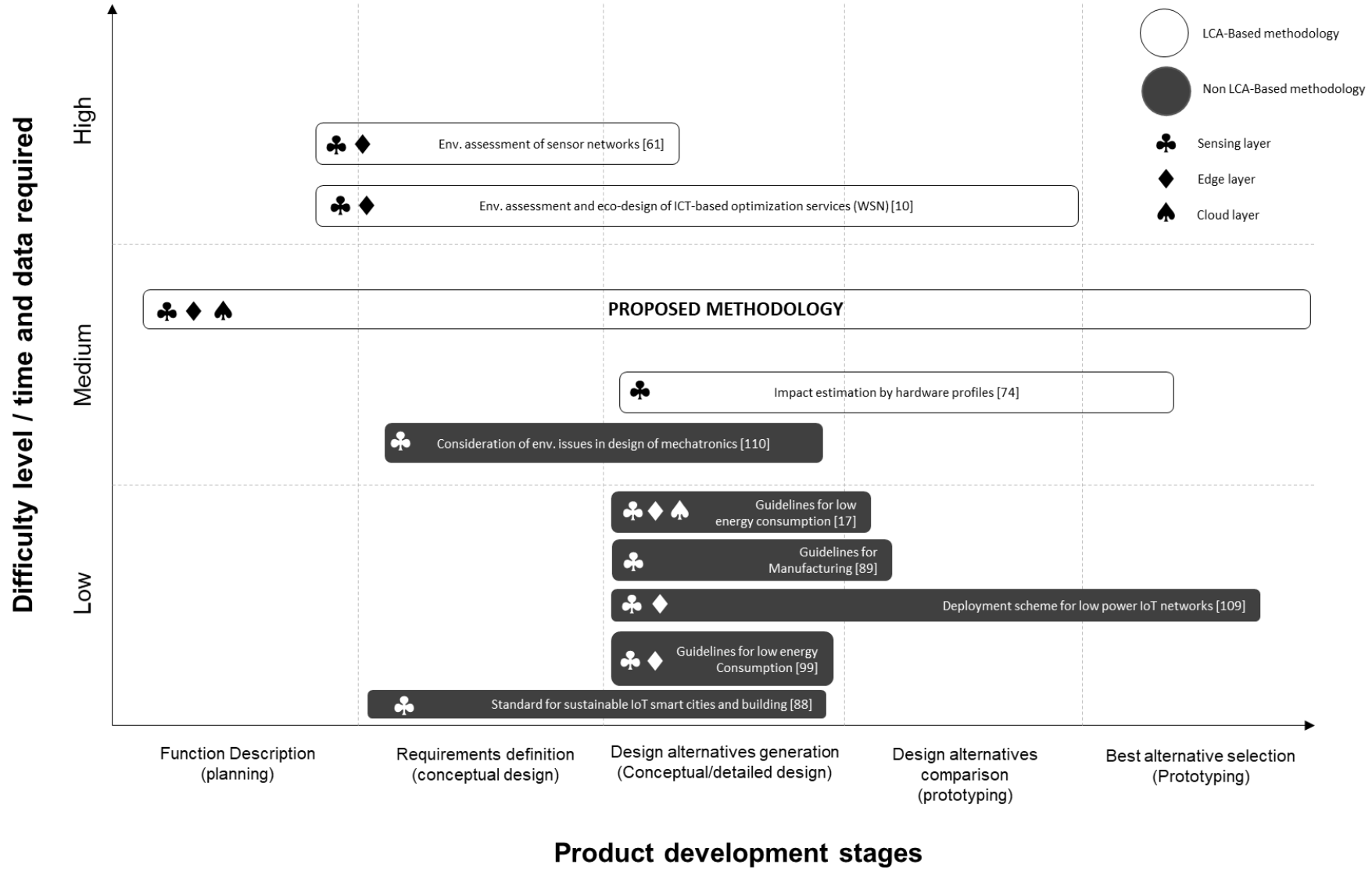


Figure 4.33. Positioning of the proposed methodology with respect to its integration in the NPD process (From planning to prototyping) and its level of difficulty for its application.

In figure 4.33, the proposed methodology is integrated smoothly into the typical NPD process of IoT systems by implementing a preliminary step of data and information flow analysis before the selection of electronic components of local devices. The result of this analysis is adapted to the requirements generated by a functional analysis; unlike the standards [88] and the impact assessment [61] and eco-design [61],[10] methodologies found in the state-of-art. The proposed methodology also generates more specific design alternatives that can be later evaluated and compared on the basis of specific aspects of the electronic components of local devices (i.e.: technical, physical and circularity attributes); and on the basis of data and information flows along the entire lifecycle of complete IoT systems, unlike other methodologies [10], [74], [109-110]; and guides [89], [17], [99] found in literature. Thus, under an iterative workflow, the proposed methodology would identify the best design alternatives for the prototyping of local devices and the deployment of mutualized resources. However, its implementation would require a moderate effort from IoT designers (especially in pilot phases) to recognize the proper type and quantity of data for specific applications; and/or certain physical, technical and circularity characteristics of specific electronic components. This investment in time and effort could be recovered in the short and medium term depending on the continuous and documented use of the proposed methodology (i.e. : with its automation through an information system).

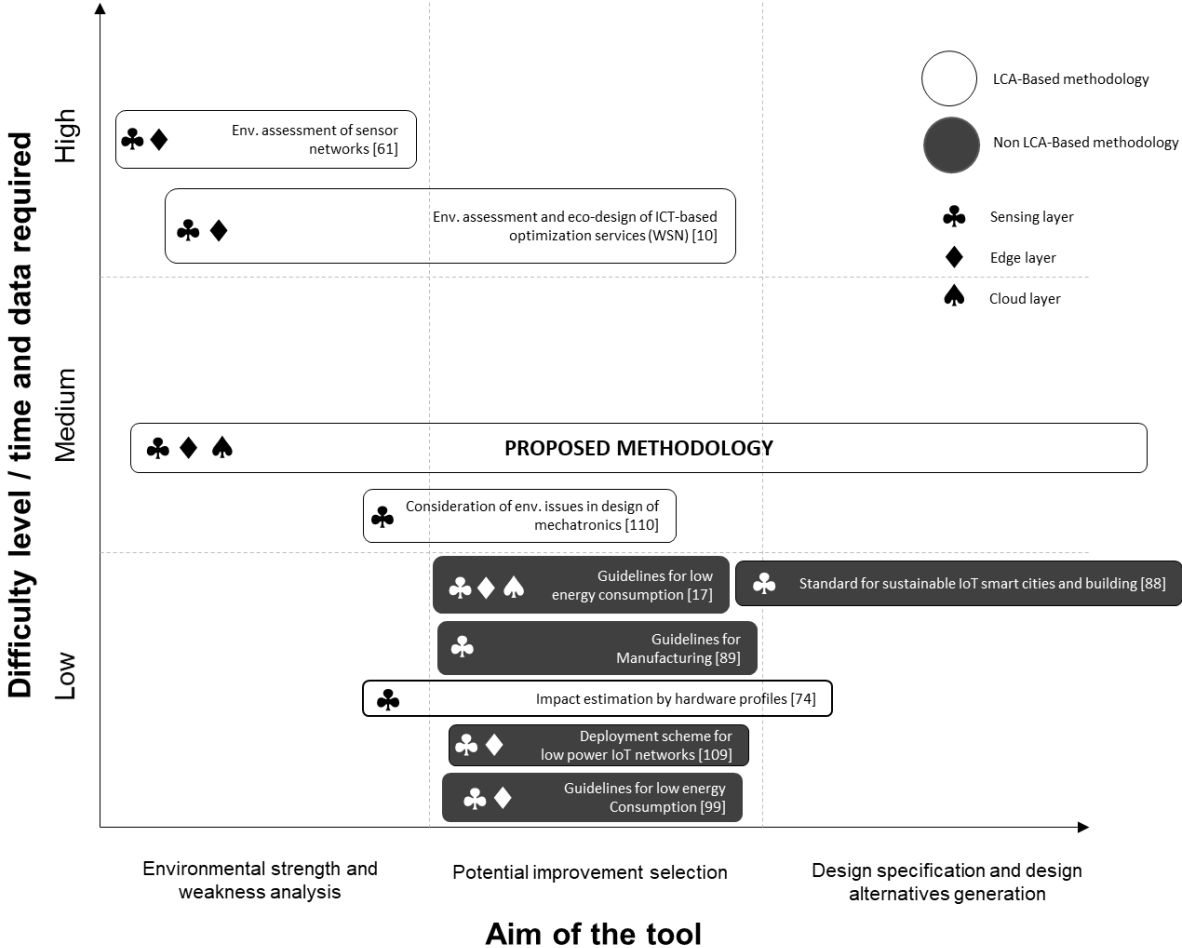


Figure 4.34. Positioning of the proposed methodology with respect to its eco-design intention and its level of difficulty for its implementation.

In figure 4.34, unlike the generic guidelines [89], [17], [99] and standards [88] found in the literature, the proposed methodology aims to facilitate not only the construction of more specific guidelines oriented to the proper selection of electronic components based on concrete attributes, but also the recognition of inefficient guidelines and weak design (e.g., over- or under-provisioned electronic components) according to specific functions within the data operational stages of IoT systems. This last aspect is fundamental for the definition of reference flows and generation of design alternatives, never seen before in other works ([61] or [10]). However, its implementation would require an investment of time and effort a little higher than the application of standards and generic guides, especially in the first design iterations of specific projects. These efforts would be related to the collection of descriptive and technical information of electronic components, easily found in basic documentation (e.g., datasheets, material declarations, product environmental profiles, etc.). However, such labor would be also simplified in the long term through the automation of the proposed methodology.

Chapter 5: Case studies

Overview

This chapter presents two case studies to illustrate the application of the proposed methodology by employing the two implementations seen in the previous chapter. One implementation aims to estimate the long-term impacts of data, which flows along the local and mutualized resources of a mature IoT system. The other implementation aims to evaluate different alternatives for the electronic design of a self-powered, intermittent sensor system. In this sense, this chapter is organized in three main sections. The first section offers a detailed description of the first case study —“smart metering” of water consumption; and presents the implementation of a cross-typed lifecycle modeling of its local and mutualized equipment in terms of functions in specific data operational stages and electronic components capacities. This allows estimating the total volume of data generated by the entire IoT system, so that its appropriated LCI can be built and its long-term impact can be estimated. Thereupon, this result is contrasted with the impact estimated from the real data traffic portrait of the deployed IoT system. After this section, the reader will realize the relevance of the function-component-capacity relationship, and will be able to conceive quick calculations of impacts coming from the use phase of mutualized devices, considering the data generation and transmission capacities of specific electronic components of local devices.

The second section offers a detailed description of the second case study —“smart monitoring” of an object’s deterioration. It focuses entirely on a prototype and presents a LCA implementation that evaluates two design versions and three types of electronic components (voltage comparators, MCUs, and NFC-EEPROM memories) on the basis of two data flow strategies and several features. After this section, the reader will fix in mind the essential and undissociated concepts for conducting efficient eco-design, not only for reducing impacts in the manufacturing phase of IoT devices (by appropriate electronic and data design), but also for identifying inefficient design that compromise the environmental performance of and IoT system in the use and EoL life cycle phases (for example due to under- or over-provisioned components, unfavorable components for reusing or recyclability, etc.). At the end of each section, key findings and specific recommendations —from the evaluation of existing guidelines when possible— are given for both case studies.

The third section synthesizes these outcomes through the construction of sharp guidelines, which must be complemented by other ones that will emerge progressively with the continuous use of the design frameworks of the proposed methodology, in the context of other case studies.

1. Case study “Smart metering”

This case study describes a mature IoT system oriented to smart metering, commercialized to track water consumption in domestic environments (it was chosen because of collaborations between CEA-Leti and the manufacturer Solem on part of this system for further evolutions). Its local infrastructure is composed of a sensor system [149] equipped by an inductive pulse emitter [150], and a LoRa/Internet gateway [152]. The inductive pulse emitter is isolated from the sensor system and its manufacturer (bmeters) is different from that one of the sensor system and the gateway (Solem). The inductive pulse emitter is a battery-powered device flooded in transparent resin to resist humidity and it plays the role of the sensor component in the IoT system. It is wired to the sensor system and, although it is difficult to determine its specific method for generating pulses (technical documentation is unavailable and visual inspection of the bottom side of the electronic card is not possible); in this work one assumes that it generates pulses by the bank of low voltage capacitors found in its electronic card (Figure 5.1a), which would store energy and discharge it into an inductor, in a hypothetical closing switch schema, as that one showed in figure 5.1b.

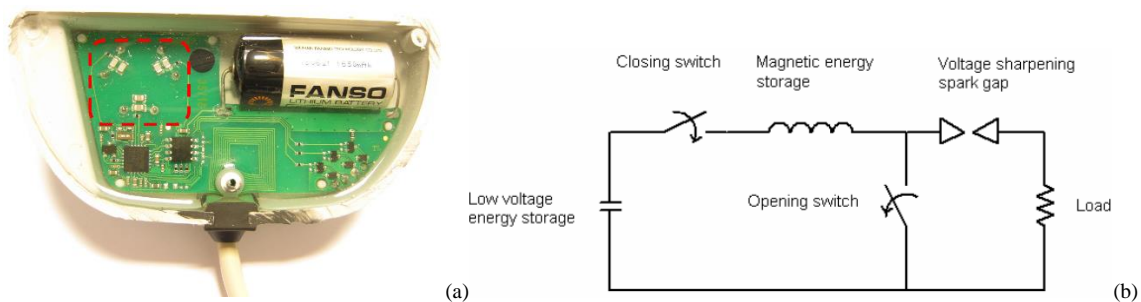


Figure 5.1. (a) The electronic card of the pulse emitter showing the bank of capacitors (red frame), which would be used in a closing switching schema to generate a pulse. (b) The possible induction generator used in the pulse emitter of case study “Smart metering” (figure extracted from [152]).

The sensor system is a battery-powered device that has to be located no more than 30 meters from the pulse emitter to minimize malfunctioning or imprecise metering. It is protected from humidity by an opaque resin (figure 5.2a) and it is mainly equipped with a RN2384 LoRa module [160] and a Bluetooth module [162] (figure 5.2b). As observed in figure 5.2b, the electronic card lacks of an MCU and memory components, which makes one hypothesizing that the device uses at least a microprocessor (embedded in the SoC component of the LoRa or Bluetooth modules) to manage at least processing and transmissions tasks; and at least an embedded memory to keep metering configuration settings.

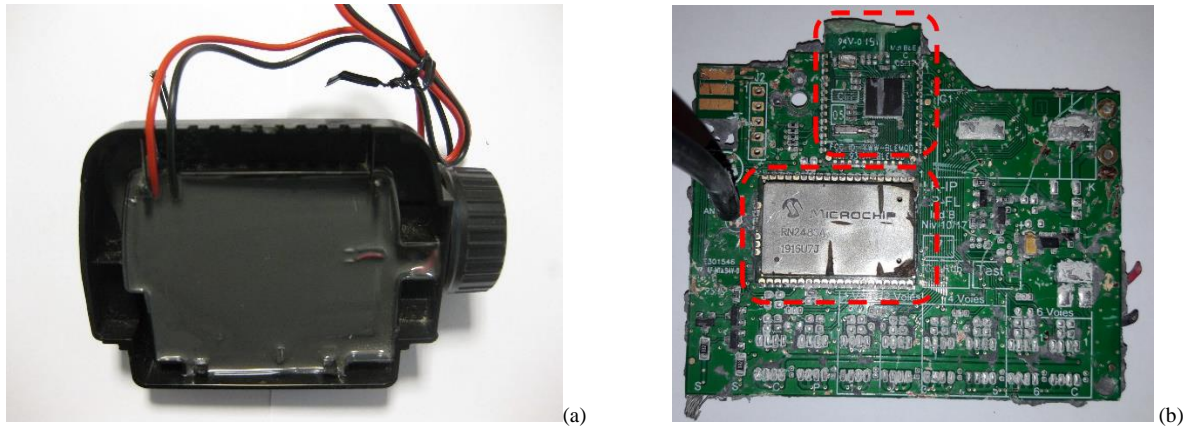


Figure 5.2. (a) The resin-flooded sensor system. (b) Electronic card of the sensor system (with its Bluetooth module in top and its LoRa module in bottom).

On the other hand, the gateway is a device powered by the electric grid and play the role of the edge device of the IoT system. It is mainly equipped with the same LoRa and Bluetooth modules of the sensor system, a WiFi ESP8266EX module [161], an ARM Microcontroller and a Flash memory (figure 5.3). According to the manufacturer, this device can centralize data of at most 25 sensor system devices, and it must be placed to a maximal distance (range) of 800 meters from them (in a star topology).

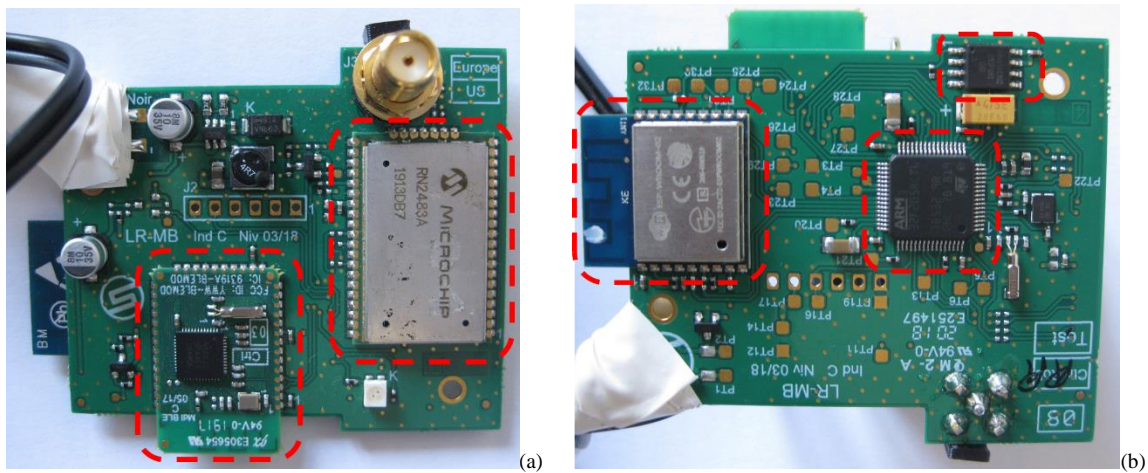


Figure 5.3. Electronic card of the gateway. (a) Top-side showing its Bluetooth module (left) and its LoRa module (right). (b) Bottom-side showing its WiFi module (left), its microcontroller (right bottom) and its flash memory component (right top).

The most basic functioning of the IoT system of the case study is described as follows. The inductive pulse emitter is attached to a conventional jet meter and sends electrical signals (pulses) to the sensor system whenever the inductive interface of the jet meter indicates water consumption. In this sense, the sensor system plays the role of a flowmeter, tracking the electrical signals generated by the inductive pulse emitter. Periodically, this flowmeter communicates with the gateway wirelessly using LoRa technology. On the other hand, the gateway communicates with the cloud server by an Internet Access Point (IAP) device (e.g., an internet modem) via its WiFi module. Figure 5.4 shows a basic deployment of the IoT system in term of the proposed framework for impact estimation (layers, devices (D) and components (C)).

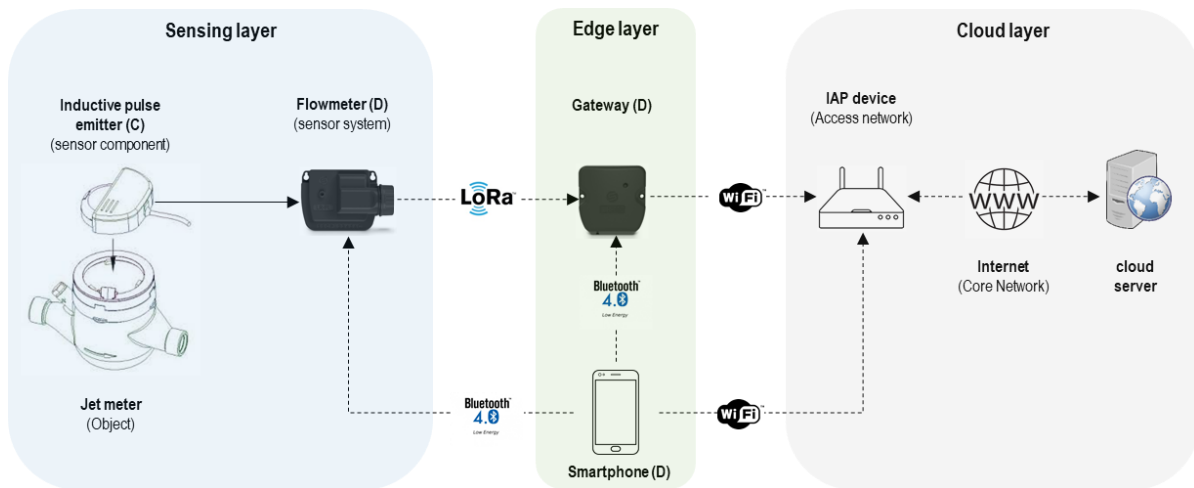


Figure 5.4. A basic deployment of the full IoT system of the case study “Smart metering” in terms of the proposed framework for impact estimation (Solid and dotted arrows indicate wired and wireless communication respectively). According to Aslan, J. et al [12] and to the standardized network architecture of IoT systems seen in the section 1.1 of chapter 1, the IAP device would belong to the cloud layer because it interconnects the local devices with Internet Service Providers (ISPs) and internet core networks.

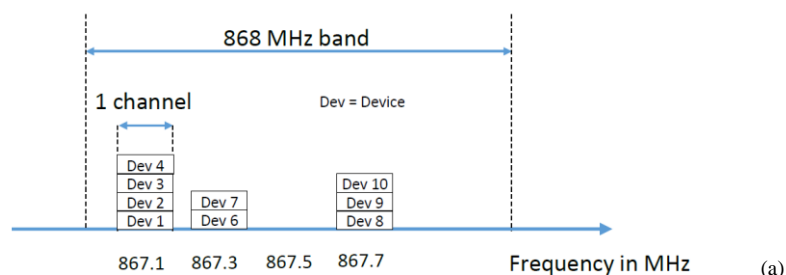
According to technical documentation, periodic, LoRa-based transmissions between the flowmeter and the gateway occur every 3 minutes. The flowmeter, meanwhile, transform the tracked signals (raw data) into information (count of pulses), which is saved every 15 minutes. In this way, it is believed that the gateway accumulates the periodic LoRa packets transmitted by the flowmeter and update the cloud server every 15 minutes, to keep synchronized the water consumption statistics in the local and the cloud sides. On the other hand, the smartphone establish Bluetooth connections with the flowmeter and the gateway to either set/modify their initial configurations (e.g., security settings and sampling rate accuracy) or consult water consumption locally. Consultations and metering configuration changes can be also held through the online user’s dashboard, available in cloud server (mySolem.com). Section 1.2 and 1.3 adapts the implementation of the framework for impact estimation to estimate theoretically and empirically the data flow within this IoT system and from that, the reference flow and impact of its use phase in the long-term.

1.1. Some basic principles on local/remote transmissions and environmental implications

To follow sections 1.2 and 1.3 of this chapter and understand the implementation of the framework for impact estimation in terms of the function-capacity relationships of the electronic components included in the case study “smart metering”; the next sections provide a basic, yet useful explanation of how LoRa- and Internet-based communications occur, extending the fundamental concepts given in section 1.2 of chapter 1.

1.1.1. LoRa modulation

In its more basic definition, LoRa is a modulation technique optimized for long-range, low-power-consumption communications in IoT environments [153]. In Europe, this modulation technique uses the 433 MHz, 868 MHz or 2.4GHz frequency bands to provide wireless communication. A frequency band is the physical mean by which data signals travel through the air and it can be subdivided in frequency channels (figure 5.5a), that have a defined capacity or bandwidth (figure 5.5b).



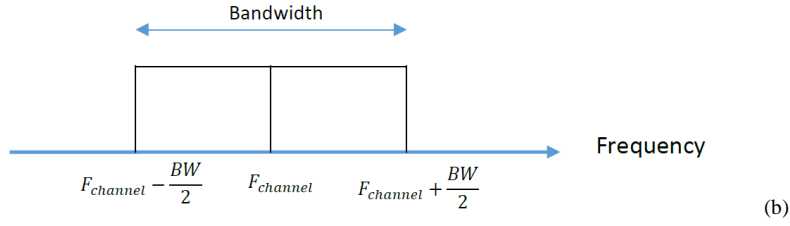


Figure 5.5. (a) Illustration of a frequency band split into multiple channels. (b) A bandwidth (BW) defined around a frequency channel ($F_{channel}$). Both figures were extracted from [154].

On the other hand, a LoRa modulator takes data and transform it into a “symbol” or “chirp” that, in simple words, is nothing more than a piece of data that can be transmitted sequentially in a defined bandwidth. To better understand this concept, consider the time-frequency graph (spectrogram) presented in figure 5.6, which is an adapted example of LoRa symbols transmissions that can be found in Montagny, S. [154].

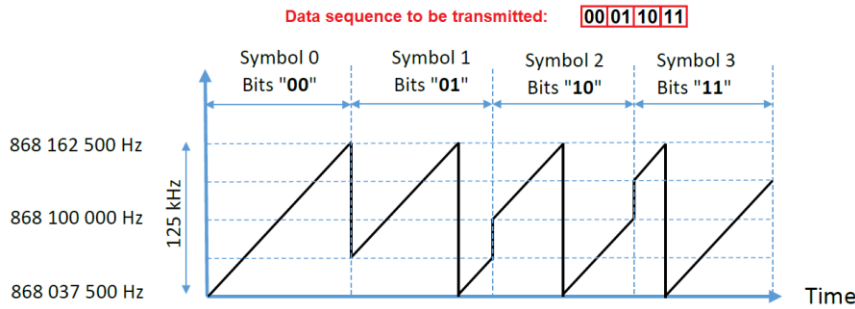


Figure 5.6. Theoretical example of a binary data sequence “00011011” modulated under a Spreading Factor 2 (4 symbols or chirps), and transmitted under a 125 kHz bandwidth in the 868.1 MHz frequency channel. Figure Adapted from [154].

As observed, a data sequence is “divided” into symbols according to a defined number of bits. The number of bits transmitted per symbol is known as the Spreading Factor (SF). As the reader may notice, the time at which a sized-defined symbol is transmitted (T_{symbol}) depends on the Spreading Factor and the Bandwidth, as illustrated in figure 5.7 and clarified in equation 5.1.

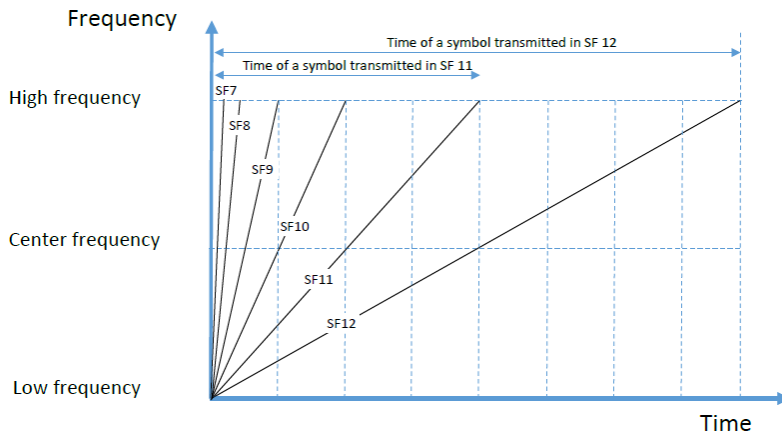


Figure 5.7. Relative time at which a symbol is transmitted at different Spreading Factors in a defined bandwidth (T_{symbol}). Figure extracted from [154].

$$T_{symbol} = \frac{2^{SF}}{Bandwidth} \quad (5.1)$$

Where:

T_{symbol} = the time at which a symbol is transmitted through a defined Spreading Factor and a bandwidth

2^{SF} = Number of symbols of a data sequence defined by a Spreading Factor

In this way, the time at which an entire data sequence composed of several symbols is transmitted from a LoRa transceiver to a LoRa gateway (Time on Air) is determined by the product between the number of symbols (n_{symbol}) and T_{symbol} (equation 5.2).

$$Time\ on\ air = n_{symbol} \times T_{symbol} \quad (5.2)$$

On the other hand, since each symbol consists on a number of bits determined by the SF, the rate at which a data sequence is encoded (Bitrate) is given by:

$$Bitrate = SF \times \frac{Bandwidth}{2^{SF}} \quad (5.3)$$

Thus, in a determined bandwidth, the higher the Spreading Factor (SF), the higher the Time on Air and the lower the Bitrate, which means the more the transceiver of the LoRa modulator works, consuming energy. This is one of the several reasons by which the LoRa protocol implements an Adaptive Data rate Routine (ADR) in LoRa gateways. ADR allows regulating automatically the SF value in the LoRa gateway as well as the power output of the transceiver according to certain factors such as the receiving sensibility, the minimal Signal-to-Noise Ratio (SNR), and the packet loss estimation. All this parameters are highly affected by the distance at which the LoRa modulator (the transceiver) and the gateway are placed, as observed in Figure 5.8).

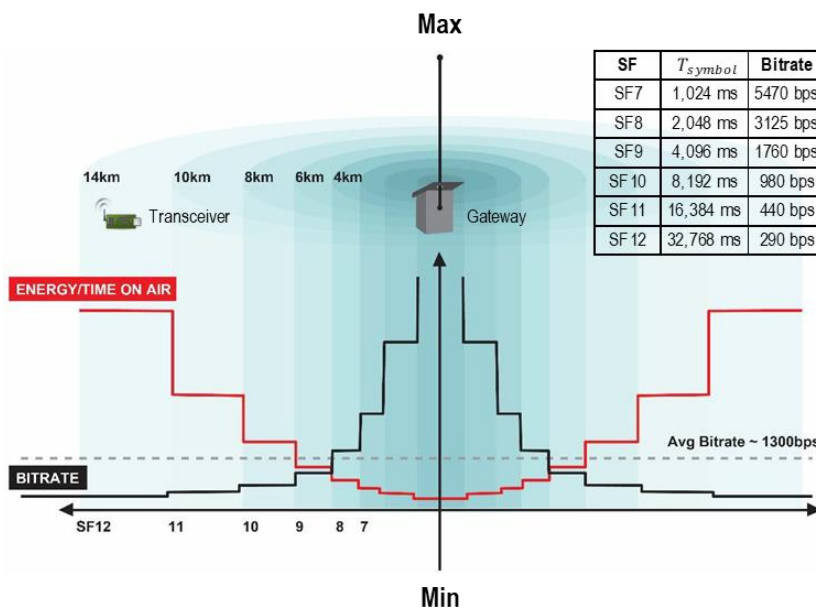


Figure 5.8. Bitrate VS Energy consumption/ Time on air. The dimensionless vertical axis may represent maximal or minimal values for the time on air of a data sequence (which depends on n_{symbol} and T_{symbol}); or the bitrate (in bits per second (bps)) in a determined bandwidth (for example consider the values for a 125kHz bandwidth in the provided table). Figure adapted from [155].

Indeed, as the distance increase, the established link between a LoRa transceiver and a LoRa gateway degrades (long distance may increase the signal-to-noise ratio or the packet loss rate). This force the LoRa gateway to regulate the Spreading Factor to high values to assure quality in transmissions, which means fewer data encoded per second, extending the time on air of a data sequence. In this sense, limiting the size of data sequences —or in other words, the data of the application— is a paramount of importance. Table 5.1 gives the maximum data application size that a LoRa packet can carry in a 125MHz bandwidth, according to a given SF related to a distance range, together with the affected bitrate.

Spreading factor	Bandwidth	Data application (payload)	Bitrate	Range
SF12	125 kHz	51 Bytes	290 bps	14 Km
SF11	125 kHz	51 Bytes	440 bps	11 Km
SF10	125 kHz	51 Bytes	980 bps	8 Km
SF9	125 kHz	115 Bytes	1760 bps	6 Km
SF8	125 kHz	242 Bytes	3125 bps	4 Km
SF7	125 kHz	242 Bytes	5470 bps	2 Km
SF7	250 kHz	242 Bytes	11000 bps	2 Km

Table 5.1. Maximum data application size (payload, in bytes) that a LoRa packet can carry according to different Spreading Factors in a 125 MHz bandwidth (the affected bitrate and the maximal distance range are also provided).

1.1.2. LoRa protocol stack and data frames

The concept of data payload introduced by table 5.1 refers to one of the elements that the structure of a LoRa packet has. As seen in chapter 1, a packet is a complete Protocol Data Unit (PDU) that includes additional header- and footer- information from all layers of a protocol stack [156]. In the case of LoRa, the headers and footers are added and appended respectively to the data application (frame Payload), according to the LoRa protocol stack showed in Figure 5.9.

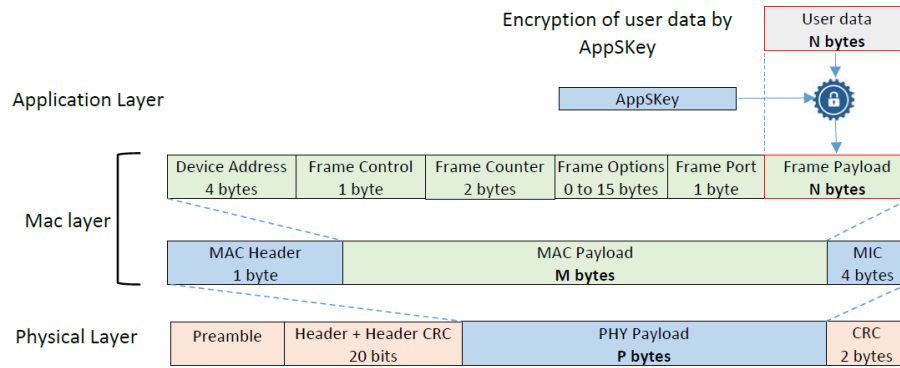


Figure 5.9. Headers and footers added to a frame payload in a LoRa protocol stack. Figure extracted from [154].

In figure 5.9, the Frame Payload contains the data application, which is encrypted and may vary in size, depending on the application, the SF and the bandwidth (see table 5.1). The Media Access Control (MAC) Layer adds to the Frame Payload, a MAC header indicating the type of message; a device address field, and a frame header (control, counter, and option port flags). The MAC layer also appends a Message Integrity Control (MIC) to be authenticated by the receiving device. In the Physical layer, the preamble field adds typically 8 supplementary symbols to maintain the receiver device synchronized; and an optional header that indicates the size of data and the coding rate (CR) of the LoRa packet. The Physical Layer also appends a Check Redundancy Cycle (CRC) field to allow detecting errors in the LoRa packet, which becomes a LoRa data frame ready to be sent through the physical mean of transmission. By considering all these additional elements, the maximal size of a LoRa data frame would be estimated as follows:

$$Max\ Lora\ data\ frame\ size = Preamble + Phy_{HF} + MAC_{HF} + Frame_H + Frame_{payload} \quad (5.4)$$

Where:

$Preamble = 8\ symbols\ (variable)$

$Phy_{HF} = maximal\ number\ of\ bytes\ added\ by\ the\ Headers\ and\ Footers\ of\ the\ Physical\ layer\ (5\ Bytes)$

$MAC_{HF} = maximal\ number\ of\ bytes\ added\ by\ the\ Headers\ and\ Footers\ of\ the\ MAC\ layer\ (5\ Bytes)$

$Frame_H = maximal\ number\ of\ bytes\ adds\ by\ the\ frame\ Header\ (23\ Bytes)$

$Frame_{payload} = number\ of\ bytes\ of\ the\ data\ application\ (variable)$

For example, in a LoRa connection established between two devices, with a maximal data payload defined by a Spreading Factor of 7, and in a bandwidth of 125 MHz, the total size of a LoRa packet would be:

$$Max\ Lora\ data\ frame\ size = 7\ bytes + 5\ Bytes + 5\ Bytes + 23\ Bytes + 242\ Bytes = 282\ Bytes$$

1.1.3. TCP/IP Protocol stack and data frames

In basic terms, The Transport Control Protocol / Internet Protocol (TCP/IP) model provides networking to enable seamless interoperability across media and computing hardware platforms [157]. It simplifies the Application, Presentation and session layers of the referential OSI model seen in chapter 1, into one layer called the Application Layer. It also simplifies the Data Link and Physical layers into one layer known as the Network Access layer. Figure 5.10 provides a contrasted view between the OSI referential model and the TCP/IP model, together with the typical protocols used in each layer of a TCP/IP protocol stack.

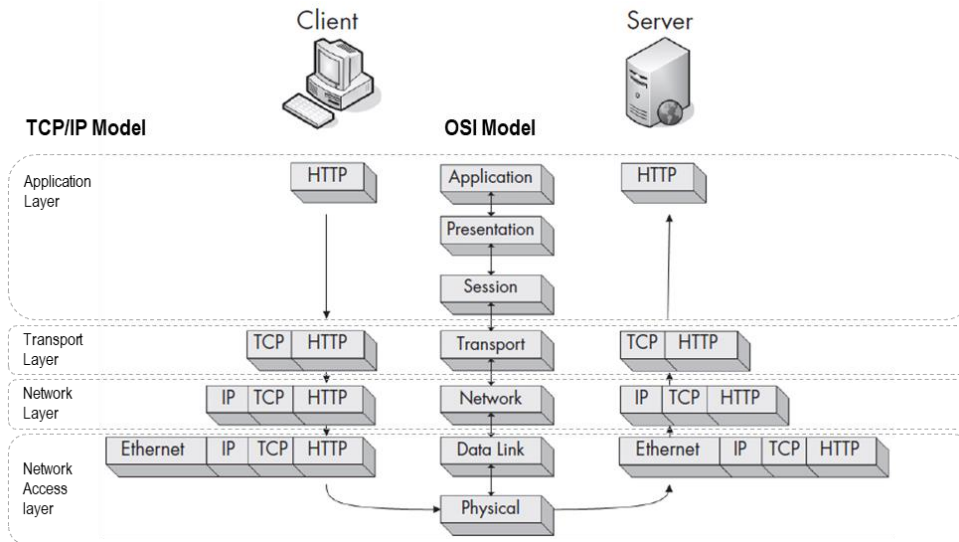


Figure 5.10. Application, Transport, Network, and Network access layers of the TCP/IP model contrasted to the OSI referential model showing a one-way transmission from a client to a server. The Network Access layer facilitates wired (Ethernet) or wireless communication depending on the physical mean of transmission. Adapted from [156].

In the application layer, the TCP/IP protocol stack usually uses the Hypertext Transfer Protocol (HTTP) to transmit a packet. The HTTP protocol is oriented to facilitate data sharing in distributed, collaborative, hypermedia information systems [158]. It includes the user data (frame payload), whose size may vary depending on the attended application. HTTP uses two request types that indicate the kind of action that a transmitting device wants to perform with a cloud server; a POST request to upload user data to the cloud server or a GET request to download data from the cloud server (after responding any of these requests, the cloud server sends an acknowledgement-typed message to the transmitting device).

In the transport layer, the TCP/IP protocol stack adds a TCP header with a maximal size of 160 bits (20 Bytes) to the HTTP frame to ensure data delivery and provide end-to-end reliability for data reliability or error recovery (figure 5.11a). Later, the Network layer adds to it an IP header (figure 5.11b) with a maximal size of 20 bytes to allow communication between remote networks. At the end, the Network access layer adds information about the physical address (e.g., MAC address) to identify devices in a physical transmission mean (e.g., wired / wireless environments). Figure 5.11c provides a generic 802.11 header format with a maximal size of 30 Bytes in the context of wireless communication.

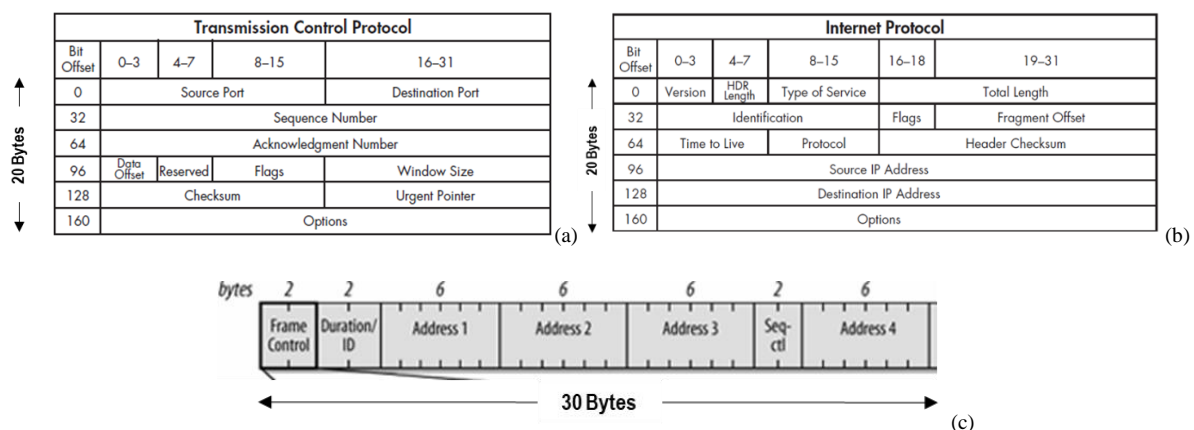


Figure 5.11. TCP (a), IP (b), and 802.11 (c) header formats. Figure a and b were adapted from [154] and figure c was extracted from [159].

Thus, the total size of a TCP/IP data frame could be estimated as follows:

$$Max\ TCP\ IP\ data\ frame\ size = MAC_H + IP_H + TCP_H + Frame_{Payload} \quad (5.5)$$

Where:

MAC_H = maximal number of bytes added by the Header of the Network Access Layer (MAC addresses) (30 Bytes)

IP_H = maximal number of bytes adds by the IP Header (20 Bytes)

$TCP_H = \text{maximal number of bytes adds by the TCP Header (20 Bytes)}$

$Frame_{payload} = \text{number of bytes of the data application (variable)}$

For example, the total size of a TCP/IP data frame whose contains a data payload of 1410 bytes may be:

$Max\ TCP\ IP\ data\ frame\ size = 30\ Bytes + 20\ Bytes + 20\ Bytes + 1410\ Bytes = 1480\ Bytes$

1.1.4. A Simple data transmission event with TCP/IP

Although computer communications are more complex than the schemes described below, they describe ones of the basic networking mechanisms that allow a basic and reliable data transfer between two devices, which is capital for this work.

1.1.4.1. TCP three-way handshake mechanism

The three-way handshake (ths) is a mechanism that allows a transmitting device know if a receiving device is available and ready to process incoming data. It establishes and assures a reliable connection before and during data transmission and it is composed of three basic and sequential steps (Figure 5.12).

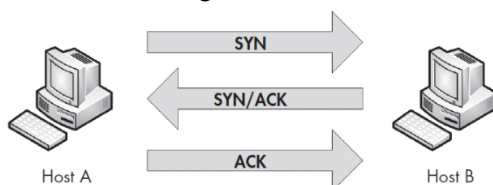


Figure 5.12. The three basic steps of a TCP three-way handshake (ths) mechanism. Figure extracted from [156].

1. **Synchronization (SYN):** the transmitting device (Host A) sends a TCP packet with a synchronization request (SYN) that includes an initial sequence number to the target device (Host B), demanding connection establishment. This TCP packet is empty, but includes its header together with the ones of lower layers (those of the network and network access layers).
2. **Synchronization / Acknowledgement (SYN / ACK):** The target device (B) responds to this request by sending another TCP packet with a SYN and ACK responses containing its initial sequence number and an acknowledgement number respectively. This TCP packet is empty, but includes its header together with the ones of lower layers.
3. **Acknowledgement (ACK):** The transmitting device (A) sends to the target device (B) a last empty TCP packet with and acknowledgement number.

Consequently, the maximal number of bytes in a TCP three-way handshake mechanism would amount to 210 bytes, which correspond to 3 empty packets containing TCP, IP and MAC headers with their maximal size (20, 20 and 30 Bytes respectively, according to figure 5.11), including SYN, SYN/ACK, and ACK request and responses. After this mechanism, both devices have all the necessary information to start and exchange data transmissions reliably.

1.1.4.2. TCP teardown mechanism

When the full data transfer from device A to device B is completed, another mechanism to close the established connection begins. This mechanism is called TCP teardown and it is composed by three sequential steps (Figure 5.13).

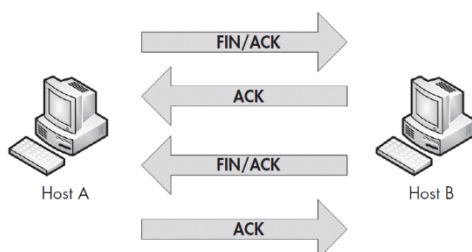


Figure 5.13. The three basic steps of a TCP teardown mechanism. Figure extracted from [156].

1. **End transmission request and acknowledgement (FIN / ACK):** the transmitting device (A) send to the target device (B) an empty TCP packet with an end request (FIN) and an acknowledgement number ACK.

2. **Acknowledgements (ACK) and End transmission confirmation (FIN / ACK):** the target B responds with another acknowledgement (ACK), and sends to transmitting device (A) an empty TCP packet with a FIN response and an acknowledgment number ACK.
3. **Acknowledgement (ACK):** Finally, the transmitting device (A) sends to the target device (B) a last empty TCP packet with a closing acknowledgement number (ACK).

Consequently, the number of bytes in a TCP teardown mechanism would amount to 280 bytes, which correspond to 4 empty packets containing TCP, IP and MAC headers with FIN/ACK and ACK requests and responses.

1.2. Implementation of the framework for impact estimation: Theoretical impact estimation of the use phase of the case study “Smart metering”

The previous section 1.1, as well as the technical aspects seen in its subsections permit the construction of the table 5.2 according to the framework for impact estimation presented in the previous chapter (section 4.2), in the context of a one-way transmission from local devices to the cloud infrastructure of the case study.

Device (D)	Electronic component (C)	Data operational stages	Function	Capacity related to the function (FC)	
Inductive pulse emitter	Capacitors and inductors	Data collection	Generating pulses	Maximal Sampling rate*	10 Pulses per Sec
Flow controller	LoRa module	Data processing	Counting pulses	Maximal Sampling rate*	10 Pulses per Sec
				current consumption sleep mode*	0,0016 mA
		Information transmission	Sending count	Maximal data payload in 800m (SF7, 125 MHz)**	242 Bytes
				current consumption transmit mode*	44,5 mA
Gateway	LoRa Module	Information reception	Receiving counts	Maximal data payload received in 800m (SF7, 125 MHz)**	1410 Bytes
	Microcontroller	Information processing	Preparing TCP/IP packet	Unknown	Unknown
	WiFi module	Information retransmission	Resending counts	Maximal data frame size**	1480 Bytes

Table 5.2. Theoretical capacities of key technical features of electronic components for building the reference flow in the use-phase of the IoT system of the case study “Smart metering”. *Technical data provided by manufacturers (available in references). ** Deducted or estimated from technical documentation.

For consistency with the proposed framework, Table 5.2 presents the sensing devices in light-blue lines and edge devices in light-green lines; and the function column shows only those essential tasks assumed in different data operational stages described in chapter 2. Due to the lack of documentation about the data design of the IoT system and because of the inductive pulse emitter and the flow meter come from different manufacturers, it is not possible to confirm whether the maximal sampling rate showed in table 5.2 is an effort to adapt the inductive pulse emitter to the electronic design of the flowmeter, or it is an effort to adapt the flowmeter to the optimal sampling rate of the pulse emitter, to assure a lifespan of 10 years suggested in its datasheet. Here, this maximal sampling rate is attributed to both devices. It is also assumed that, in sleep mode, the flowmeter uses the microprocessor of its LoRa module to count the pulses generated by the inductive pulse emitter. Moreover, because the manufacturer recommends a maximal distance of 800 meters between the flowmeter and the gateway, it is assumed that the flowmeter and the gateway are design to run with a spreading factor 7 (according to figure 5.8), allowing a maximal data payload of 242 Bytes for LoRa transmissions (according to table 5.1). It is assumed that LoRa transmissions happen in a 125 kHz bandwidth.

On the other hand, the maximal data payload received by the LoRa module of the gateway is presumed to be 1410 Bytes, which corresponds to 5 complete accumulated LoRa packets in 15 minutes (including LoRa protocol headers and footers as defined in equation 5.4 and assuming that the gateway do not modify these packets sent by the flowmeter). In the gateway, It is assumed that its microcontroller add to these 1410 bytes the TCP/IP and MAC headers, obtaining a final packet of 1480 bytes (according equation 5.5), that is sent to the cloud server via its WiFi module (every 15 minutes, assuming a simultaneous synchronization updating of the flowmeter and the cloud server). Figure 5.14 schematizes these aspects in the terms of the proposed crossed-typed, life cycle modeling implementation of the framework for impact estimation, seen in previous chapter.

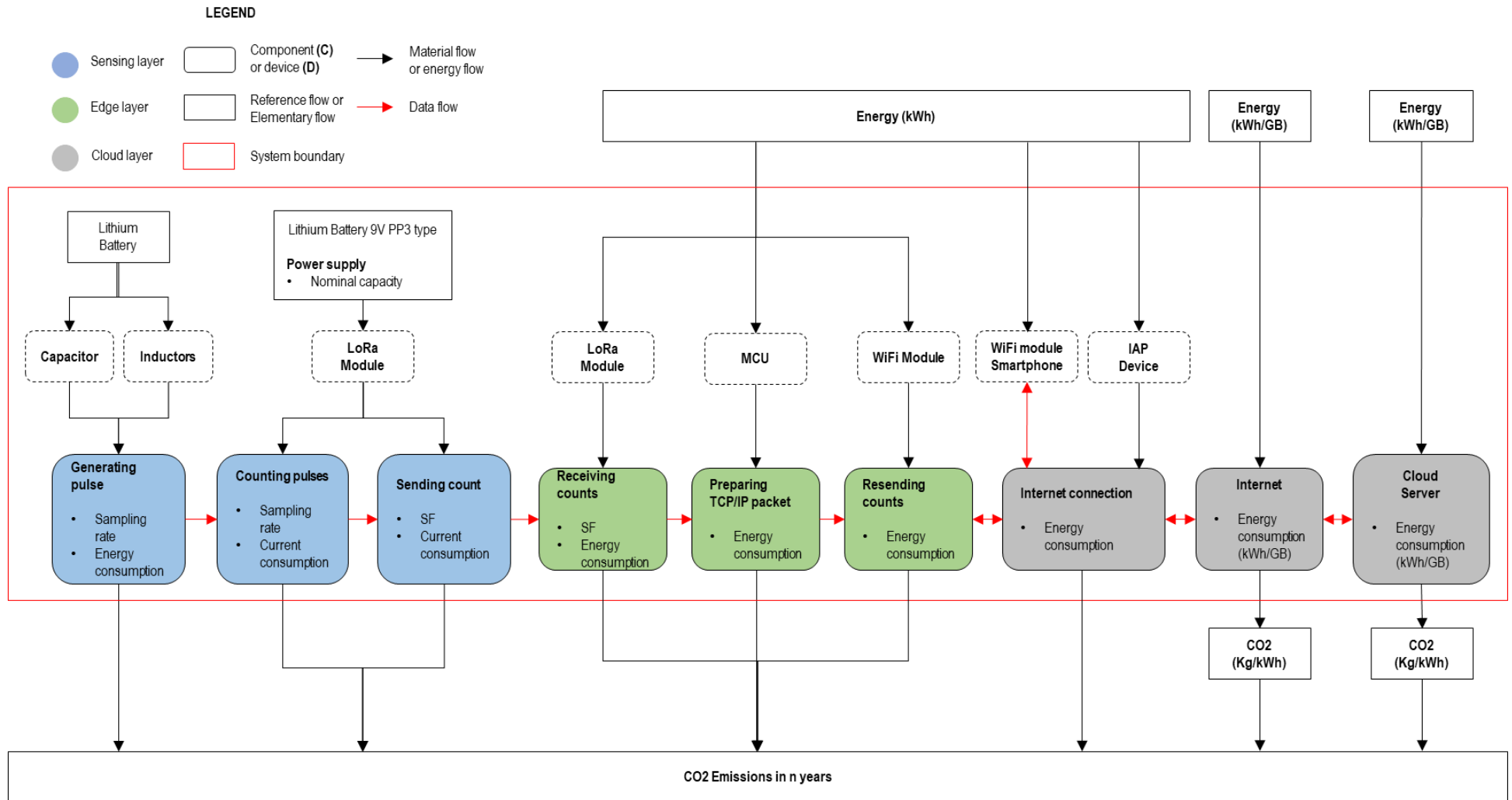


Figure 5.14. Cross-typed lifecycle modeling for the case study “Smart metering” in the use phase (implementation of the framework for impact estimation). Notice that, although the two batteries for the corresponding inductive pulse emitter and flowmeter may be considered as electronic components (Power supply), here it is considered as reference flows whose quantities depend on the number of batteries needed to power both devices in a period of time. Because this analysis is oriented to estimate the impact of the case study in the use phase, the elements allowing the operational functioning of the system (the dotted elements) are depicted, but their BoL and EoL impacts are not taken into account.

Figure 5.14 shows only those electronic components involved in the data operational stages functions stated in table 5.2, together with the energy source for each device or layer. This model helps to estimate the GW impact of the IoT system in the use phase in terms of energy used per function. In the case of the inductive pulse emitter, the impact of generating pulses is directly related to the number of batteries used for this purpose. In the same way, the impact of counting the pulses and sending the counts in the flowmeter is related to the number of batteries needed to execute these tasks in a sleep and transmit mode, respectively. In the case of the gateway, the impact of updating the cloud server is directly related to its energy needs and the kind of source (electric grid supply). Finally, the impact of using the cloud server, as well as the access network (IAP device) and the internet core network is related to the energy needed to process and transmit a specific amount of data respectively (in kWh per GB).

On the other hand, although one-way transmissions from the gateway to the cloud server are believed in theory; in practice, there exists round-trip transmissions to establish a reliable connection between both devices (depicted by the double-sided red arrows in figure 5.14). These round-trip transmissions concern the three-way handshake and teardown TCP and acknowledgement mechanisms mentioned before and they are also present between the smartphone and the cloud server, to allow online consultations of water consumption. Figure 5.15 shows the theoretical TCP/IP packets transiting along the internet and cloud infrastructure of the IoT system of the case study.

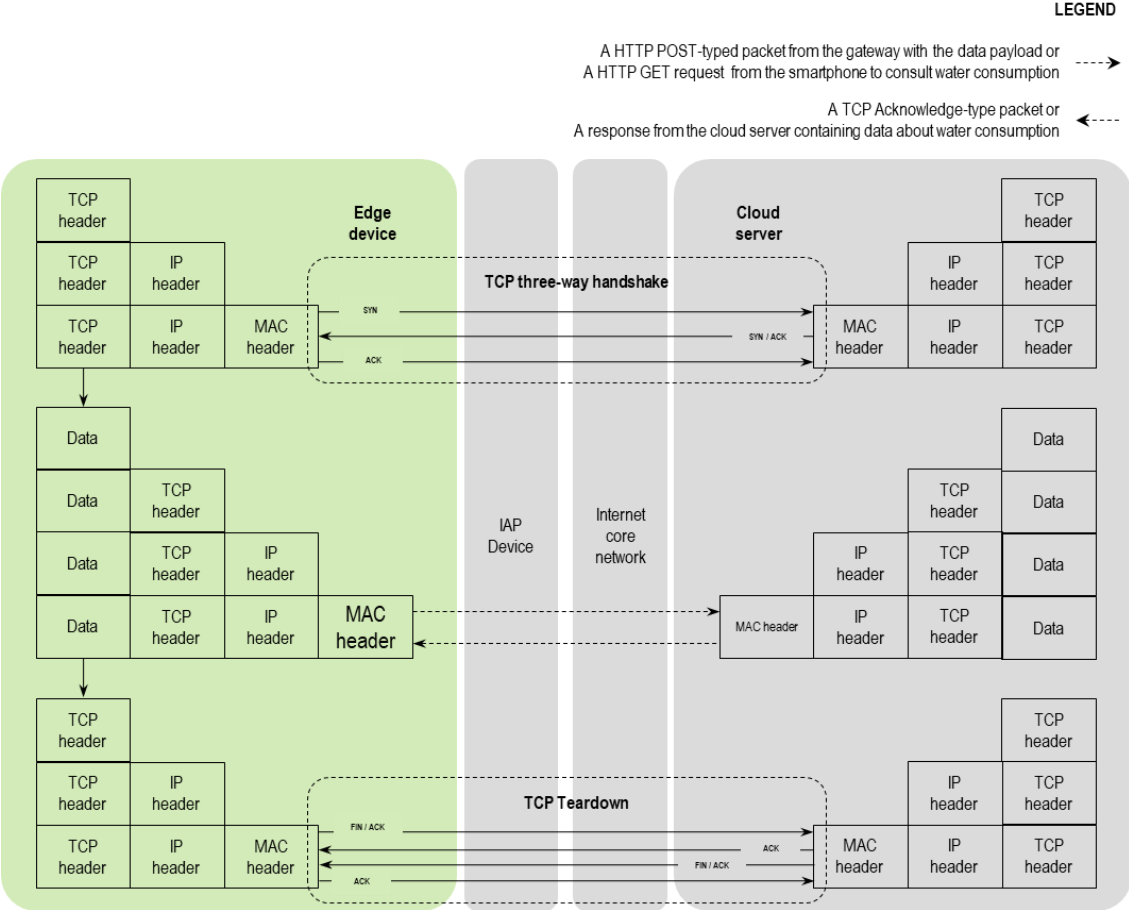


Figure 5.15. Theoretical TCP/IP packets (horizontal arrows) in a single transmission between an edge device (flowmeter or smartphone) and the cloud server. In the top, the TCP/IP three-way handshake mechanism. In the middle, the actual packets sent to the cloud server (an typical HTTP POST request, within the regular operation of the IoT system; or a HTTP GET request from a smartphone to the cloud server). In the bottom, the TCP teardown mechanism.

In this way, if one assumes the functional unit “**facilitating the hourly monitoring of water consumption of an area of 1 Km², during 2 years**”, the total data circulating in the internet infrastructure and cloud server can be organized into three scenarios: a worst scenario in which the maximal data payload of 5 accumulated LoRa packets is resend constantly (242 Bytes per LoRa packet, which together with all the protocol overheads makes TCP/IP packets of 1480 bytes, as explained

before), a regular scenario assuming the median data payload (121 bytes, resulting in TCP/IP packets of 875 bytes) and a best scenario assuming a minimal data payload (1 byte, resulting in TCP/IP packets of 275 bytes).

(sender ↔ receiver)	Function	Transmissions events	Packets	Data traffic (GB)		
				Worst scenario (1480 Bytes)	Regular scenario (875 Bytes)	Best scenario (275 Bytes)
Gateway ↔ Cloud server (GC)	Resending counts	70066	630594	0,1331	0,0891	0,0499
Smartphone ↔ Cloud server (SC)	Hourly consultations	17520	157680	0,0103		
			Total	0,1434	0,0994	0,0602

Table 5.3. Three hypothetical scenarios of the data traffic of the case study “Smart metering” in 2 years. Every scenario assumes a variable data payload per LoRa packet, which is accumulated together with other 4 packets, as it is explained in above.

In table 5.3, the number of packets involved in the resending of counts are obtained by considering the number of transmissions events established between the gateway and the cloud server according to equation 5.6.

$$P_{GC} = P_{GC_{ths}} + P_{HTTP_{post}} + P_{HTTP_{ACK}} + P_{GC_t} \quad (5.6)$$

Where:

P_{GC} = Number of packets circulating between the gateway and the cloud server in two years

$P_{GC_{ths}}$ = Number of packets in a TCP threeway handshake multiplied by the number of transmissions events

$P_{HTTP_{post}}$ = Number of packets needed to upload data multiplied by the number of transmissions events

$P_{HTTP_{ACK}}$ = Number of acknowledgement typed packets sent by the cloud server

P_{GC_t} = Number of packets in a TCP teardown multiplied by the number of transmissions events

Assuming a frequency of four transmissions events established every hour (one every 15 minutes), the number of transmission events between the gateway and the cloud server amounts to 70066 in two years. In each of this transmissions events, TCP three-way handshake and teardown mechanisms happen before and after sending one HTTP packet ($P_{HTTP_{post}}$), oriented to upload data to the cloud server. According to the message exchange chart in figure 5.15, these mechanisms generates 3 and 4 additional packets for $P_{GC_{ths}}$ and P_{GC_t} respectively. Thus, $P_{GC_{ths}}$ amounts to 210198 packets (70066 transmission events multiplied by 3 TCP threeway handshake packets) and P_{GC_t} to 280264 packets (70066 transmission events multiplied by 4 TCP teardown packets). On the other hand, both $P_{HTTP_{post}}$ and $P_{HTTP_{ACK}}$ amount to 70066 packets (70066 transmission events multiplied by 1 HTTP packet for the post request and the acknowledgement respectively).

Similarly, the number of TCP/IP packets involved in an online consultation of water consumption is obtained by considering the number of transmissions events established between the smartphone and the cloud server according to equation 5.7.

$$P_{SC} = P_{SC_{ths}} + P_{HTTP_{get}} + P_{HTTP_{response}} + P_{SC_t} \quad (5.7)$$

Where:

P_{SC} = Number of packets circulating between the Smartphone and the Cloud server in two years

$P_{SC_{ths}}$ = Number of packets in a TCP threeway handshake multiplied by the number of transmissions events

$P_{HTTP_{get}}$ = Number of packets needed to send a water consumption request to the cloud server

$P_{HTTP_{response}}$ = Number of packets needed to response a water consumption request

P_{SC_t} = Number of packets in a TCP teardown multiplied by the number of transmissions events

Assuming a frequency of 24 transmissions events per day (one every 1 hour), the number of transmission events established between the Smartphone and the Cloud server amounts to 17520 in two years. In each

of this transmissions events, it is assumed that only one packet for a water consumption request ($P_{HTTP_{get}}$) and one packet for the response ($P_{HTTP_{response}}$) are needed. As in the case of regular operation, the online consultation of water consumption includes 3 additional packets for the TCP three-way handshake mechanism and 4 additional packets for the TCP teardown mechanism. In this way, the total data traffic for the case study in a specific scenario (last line of table 5.3) includes the total data generated to resend the pulse counts from the gateway to the cloud server ($Data_{GC}$) plus the total data generated to consult water consumption from a smartphone to the cloud server ($Data_{SC}$). Both parts are estimated according to equation 5.8 and 5.9 respectively:

$$Data_{GC} = (P_{GC_{ths}} \times 210 \text{ Bytes}) + (P_{HTTP_{post}} \times Bytes_{scenario}) + (P_{GC_t} \times 280 \text{ Bytes}) \quad (5.8)$$

$$Data_{SC} = (P_{SC_{ths}} \times 210 \text{ Bytes}) + (P_{HTTP_{get}} \times 1 \text{ Byte}) + (P_{HTTP_{response}} \times 1 \text{ Byte}) + (P_{SC_t} \times 280 \text{ Bytes}) \quad (5.9)$$

Where:

$Bytes_{scenario}$ = total bytes of accumulated LoRa transmissions under a specific scenario, according to table 5.3

In both equations, the constants of 210 Bytes and 280 Bytes correspond to the maximal number of bytes generated by a TCP three-way handshake and teardown mechanisms respectively, as seen in sections 1.1.4.1 and 1.1.4.2. On the other hand, $Bytes_{scenario}$ in equation (5.8) correspond to the total number of bytes to be sent from the gateway to the cloud server, which varies according to the data payload in a LoRa transmission. For example, for the worst scenario, it was assumed that every LoRa packet has the maximal data payload for the specific Spreading Factor of 7 and bandwidth 125 kHz (242 bytes, according to table 5.1) plus the LoRa protocol headers (40 Bytes, according to equation 5.4). This gives LoRa Packets of 282 Bytes which are sent (1 every 3 minutes) and accumulated in the gateway (5 every 15 min). Assuming no modifications on them, it is believed that the gateway resent these grouped LoRa packets (5 times 282 Bytes = 1410 Bytes) to the cloud server by adding them a TCP, IP and MAC headers (30, 20, and 20 bytes respectively), giving a total HTTP post packet of 1480 Bytes. In this same line, the regular scenario would involve an assumed LoRa data payload of 121 Bytes (a median value), and the best scenario 1 Byte (an assumed, minimal value), both give a total of 875 and 275 Bytes HTTP post packets to be sent every quarter hour.

➤ Thus, by considering the studied functions and key capacities of electronic devices and electronic components seen in table 5.2, the life-cycle modeling implementation seen in figure 5.14, and the theoretical data traffic obtained in table 5.3; the impact of the use phase of case study amounts approximately to 5,72, 5,48 and 5,47 Kg CO₂-eq for the worst, regular and best scenarios respectively, according to the reference flow detailed in table 5.4.

Device	Electronic component	Functions	Capacity*		Reference flow			Impact (Kg CO ₂ -eq)**		
			Feature	Value	Worst	Regular	Best	Worst	Regular	Best
Pulse emitter	Capacitors & inductors	Generating pulses	Maximal sampling rate	10 Pulse / sec	1 Li-ion battery			0,0382		
	Li-ion Battery	Power supply	Typical capacity	1650 mAh						
Flow meter	LoRa module	Counting pulses	Current consumption sleep mode	0,0016 mA	2 Li-ion 9V Batteries	1 Li-on 9V Battery	1 Li-on 9V Battery	0,458	0,229	0,229
			Bitrate (SF7, 125 KHz)	5470 bps						
		Sending counts	Current consumption Transmission mode	44,5 mA						
	Li-ion 9V Battery	Power supply	Typical capacity	1200 mAh						
Gateway	LoRa module	Receiving counts	Energy consumption	0,006 kW	105,12 kWh			5,150		
	WiFi module	Preparing TCP/IP packets Resending counts								
Smartphone	WiFi module	Hourly consultations of water consumption	Energy consumption (sending in 700 kB /sec)	1629 mW	0,50 kWh			0,045		
			Energy consumption (Receiving)	1375 mW						
Internet & Access networks			Energy consumption	0,15 kWh / GB	0,0215 kWh	0,0149 kWh	0,0090 kWh	0,017	0,012	0,007
Cloud server			Energy consumption	0,14 kWh / GB	0,0201 kWh	0,0139 kWh	0,0084 kWh	0,016	0,011	0,007
					Total			5,7235	5,4846	5,4758

Table 5.4. Estimated impact of the use phase of the case study “Smart metering” under the worst, regular and best scenario. *data available in respective technical documentation or literature found in previous and reference sections. **According to CML-IA 2001 LCIA method (Global warming 100a).

To understand the reference flow and the impact columns in table 5.4, consider the following aspects. Firstly, it is believed that only 1 Li-ion battery is needed for running the pulse emitter under 10 pulse per sec in the three scenarios (as suggested by manufacturer, whose claims a lifetime of 10 years under regular conditions of usage). On the other hand, it is assumed that the number of batteries required by the flowmeter would depend on the current consumption and the time of its operational states (sleep and transmitting). The later aspect depends at the same time on the bitrate of its LoRa module working under a Spreading Factor of 7 in a bandwidth of 125 kHz. To explain this idea, consider figure 5.16.

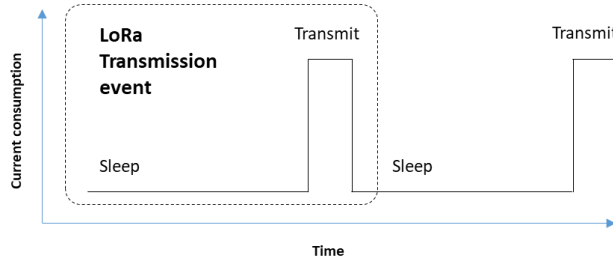


Figure 5.16. Assumed schema for the sleep and transmission states of the flowmeter during one LoRa transmission event.

In figure 5.16, a LoRa transmission event involves a sleep and a transmission state. As a LoRa transmission happens every 3 minutes (or 180 seconds, according to the technical documentation of the flowmeter), the time at which the flow meter is in transmission (t_{trans}) and sleep mode (t_{sleep}) during a LoRa transmission event depends on the bitrate capacity of the LoRa module, according to equation 5.10 and 5.11.

$$t_{trans} = \frac{PS_{LoRa}}{BR_{SF}} \quad (5.10)$$

$$t_{sleep} = 180 \text{ secs} - t_{trans} \quad (5.11)$$

Where:

PS_{LoRa} = Size of a LoRa Packet (in bits)

BR_{SF} = Bitrate capacity of the LoRa module of the flowmeter in a specific Spreading Factor and bandwidth

Thus, if one transform t_{trans} and t_{sleep} in hours, the number of batteries required by the flow meter (B_{fm}) working in a specific scenario is given by:

$$B_{fm} = (BLT_{trans} \times t_{trans} \times TTE_{LoRa}) + (BLT_{sleep} \times t_{sleep} \times TTE_{LoRa}) \quad (5.12)$$

Where:

BLT_{trans} = Battery Life Time factor for transmission mode (in battery per hour)

BLT_{sleep} = Battery Life Time factor for sleep mode (in battery per hour)

TTE_{LoRa} = Total number of LoRa Transmission Events in two years

To obtain the Battery Life Time factors for the sleep and transmission states, one divide the nominal capacity of a Li-ion 9V battery (mAh) by the current consumption of both states respectively, all multiplied by a performance efficiency of the battery, that considers its natural discharging rate. For example, to obtain the Battery Life Time factor for the transmission mode of the specific LoRa module of the flowmeter, one consider 95% of nominal capacity of a battery (to include natural discharging rate of 5%) and the current consumption of 44,5 mA for the transmission state in the following way:

$$BLT_{trans} = \left(\frac{1200 \text{ mAh}}{44,5 \text{ mA}} \right) \times 95\% = 25,6 \text{ h} \text{ or } 1 \text{ battery for } 25,6 \text{ hours in continuous transmission state}$$

Secondly, the total electricity needed for dealing with the internet traffic in each scenario is obtained by multiplying the total data traffic found in table 5.3 by electricity to gigabyte (kWh/GB) ratios for the internet core networks and data centers, available in literature. In this work, one uses a 0,15 kWh/GB ratio for the Access and Internet core networks, which considers the median value between the proposed ratios found in Malmodin, J. et al. [163] and Krug, L. et al [164]; and the 0,14 kWh/GB ratio for the

cloud infrastructure, proposed by Andrae, A. S., & Edler, T. [165], who collected and analyzed several works oriented to estimate the energy needs of data centers.

Finally, for the smartphone side, one considers the energy required for powering its WiFi module in the transmitting and receiving mode (0,001629 and 0,001375 kW respectively, according to Perrucci, G.P. et al. [166]) multiplied by the total time that the WiFi module is in these correspondent modes (it is assumed that the user turns on the WiFi function of his or her phone during one minute to consult his or her water consumption, which is equal to 292 hours during 2 years). The power output of the battery is assumed to 95%.

In this manner, the impact column of table 5.4 shows the impact of a one-cell-based Li-ion battery for the inductive pulse emitter (Production of one Li-ion battery cell (GLO)), and the impact of a six-cell-based Li-ion battery, in the case of the flowmeter. For calculations, one consider the impact of producing a dry cell Li-ion battery (6,7675 Kg CO₂-eq 100a, according to the CML-IA 2001 LCIA method); and the weight of a battery cell, assuming that a typical six-cell-based battery of 9V weights 33,9 grams (so one cell = 33,9 / 6 = 5,65 grams or 0,00565 kg)). The impacts of the gateway and smartphone consider the electricity mix in France (Market for electricity, medium voltage (FR)) and the impacts of the cloud server as well as the internet and access networks (including the IAP device) take into account an international electricity mix (Market for electricity, medium voltage (GLO)). The LCIA methodology used is CML-IA 2001 (Global warming 100a). Figure 5.17, shows the relative impacts for the three studied scenarios.

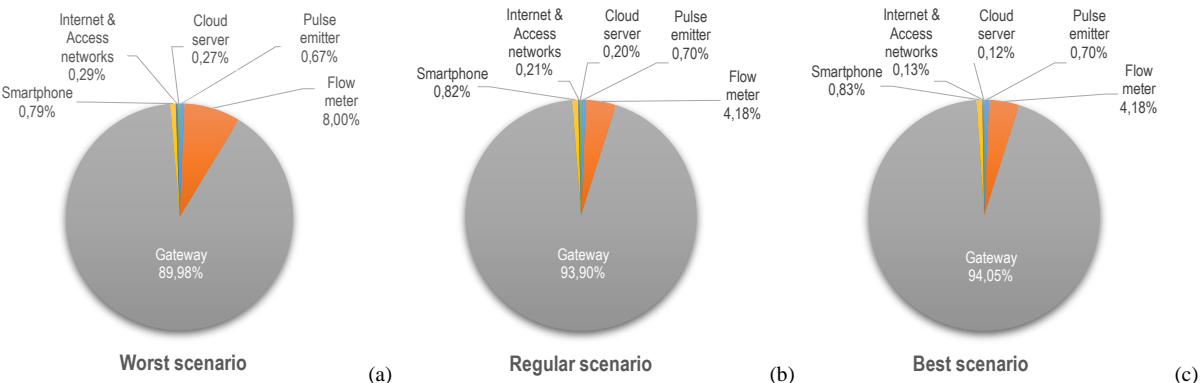


Figure 5.17. Relative GW impact results of the use phase of the case study “Smart metering” under a worst scenario (transmitting a HTTP post packet of 1480 Bytes containing 5 accumulated LoRa of 282 Bytes) (a), a regular scenario (875 Bytes containing 5 LoRa packets of 161 Bytes) (b), and a best scenario (275 Bytes containing 5 LoRa packets of 41 Bytes) (c).

1.3.Implementation of the framework for impact estimation: environmental assessment of the use-phase of the case study “Smart metering” from empirical tracking of data flow

This section present an experimental analysis of the data flow within the case study “Smart metering”. It aims to contrast the theoretical results obtained in the previous section and provide insights for evaluating the use-phase impact of an IoT system in more detail by following the framework for impact estimation, and the packet exchange seen in the respective figures 5.14 and 5.15.

1.3.1. Experimental settings and methodology

To do this, a packet traffic analysis is carry out by implanting two network analyzers (sniffers) equipped with specialized software, according to the schema below.

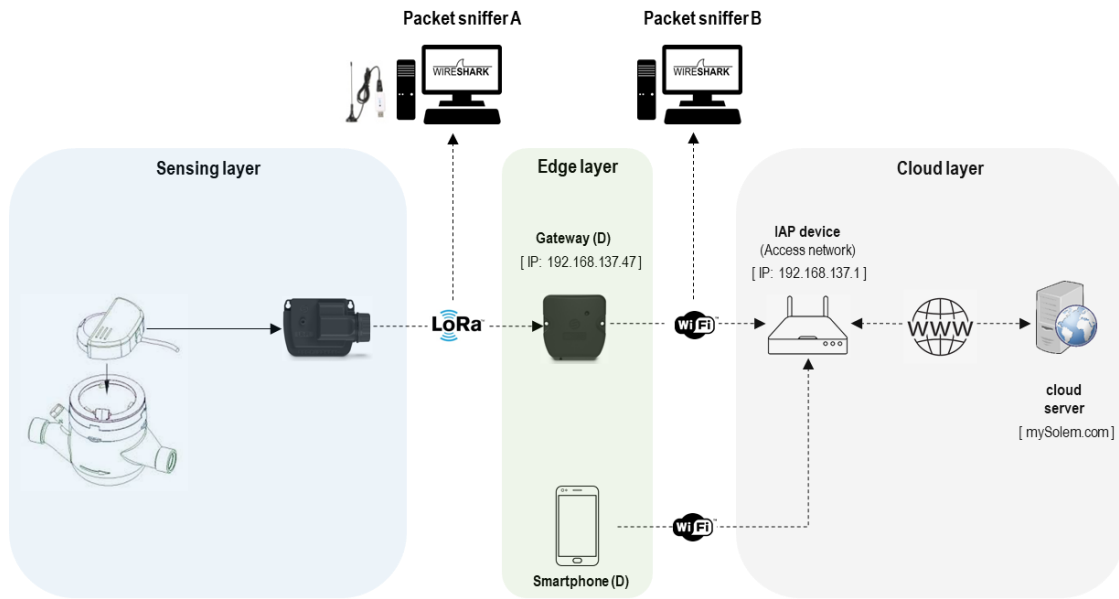


Figure 5.18. Experimental network deployment of the IoT system of the case study “Smart metering” including packet sniffers A and B. The IP addresses and domain name (mySolem.com) of the devices involved in the internet data traffic are showed. According to Aslan, J. et al [12] and to the standardized network architecture of IoT systems seen in the section 1.1 of chapter 1, the IAP device would belong to the cloud layer because it interconnects the local devices with Internet Service Providers (ISPs) and internet core networks.

A packet traffic analysis refers to the technique of capturing and interpreting live data as it flows along different segments of a network, and a sniffer is a hardware/software tool used to capture and analyze raw network data going across a physical transmission mean [156]. In figure 5.18, a Wireshark-based sniffer (packet sniffer A) equipped with a RTL2832U-based Software-Defined-Radio (RTL-SDR) bundle (figure 5.19a) and GNU-radio companion software running in a Linux PC is placed between the flowmeter and the gateway to capture and analyze LoRa transmissions of both devices. A specific GNU-radio companion model based on gr-lora implementation [167] was developed to allow the RTL-SDR device intercept LoRa Transmissions (details available in Annex 1).

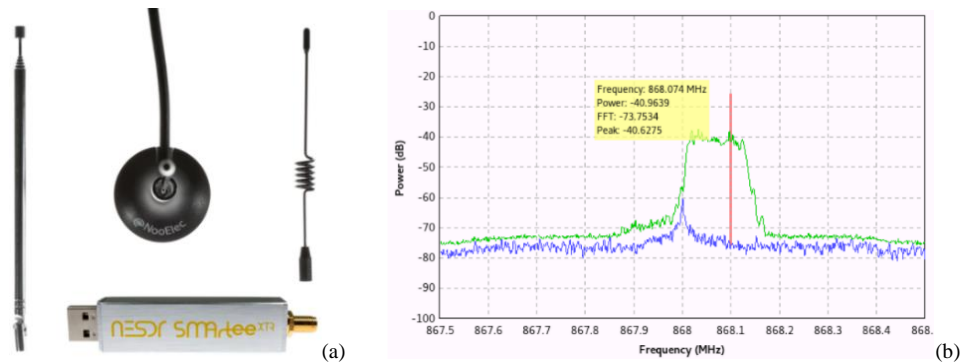


Figure 5.19. (a) The RTL2832U-based Software Defined Radio (RTL-SDR) USB bundle used for the LoRa traffic analysis in this work (Datasheet available in [168]). (b) An example of a LoRa transmission in the 868.1 MHz frequency captured by a RTL-SDR bundle and the gr-lora GNU-radio implementation.

The second packet sniffer B in figure 5.18, is a Wireshark-based sniffer using the wireless Network Interface Controller (NIC) of a desktop PC (in promiscuous mode) running in windows 7. It was implanted between the gateway and the IAP device to capture and analyze WiFi transmissions intended to the cloud server. In figure 5.18, the distance between the flow meter and the gateway is 4 meters.

1.3.2. Experimental Procedure

The experimental network described above operated approximately 10 hours (from 11h40 to 22h20) in which regular water consumption was emulated by applying compressed air to the jet meter. During this time, hourly consultation of water consumption were made, by acceding the cloud server via a smartphone equipped with a WiFi module. Sniffer A and B were initialized before the starting up the

network. To capture the LoRa packets, the GNU-Radio companion model considered a spreading factor of 7, a frequency band of 868 MHz hearing in three frequency channels, and a bandwidth of 125kHz. The LoRa packets were intercept by the RTL-RDS bundle and broken down into User Datagram Protocol (UDP) packets, which were reoriented to the Wireshark interface by the ports 40868, 40869 and 40870 of sniffer A (one for every frequency channel). In the data traffic reported by sniffer B, specific Wireshark filters were applied to obtain every packet circulating between the gateway and the cloud server (Annex 3 presents an extract of the filtered data traffic between the gateway and the cloud server).

1.3.3. Results

Figure 5.20 shows a sample of the last LoRa transmissions between the flow meter and the gateway in minute resolution (from 21h06 to 22h06).

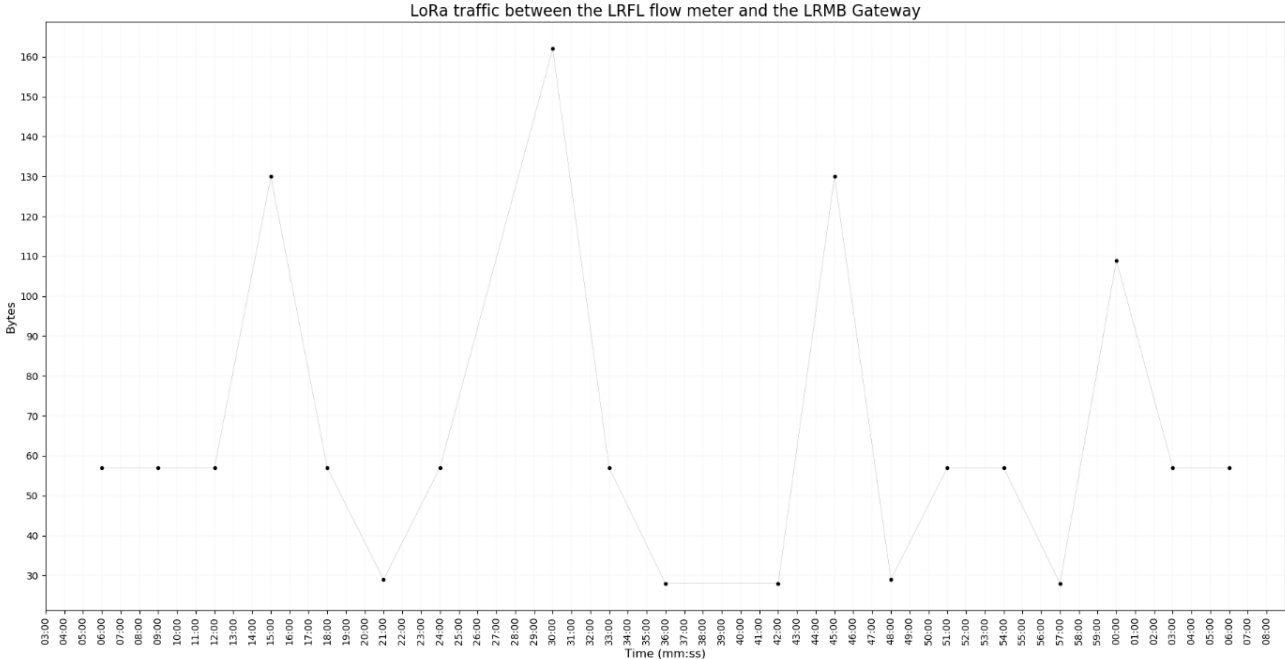


Figure 5.20. LoRa traffic between the flow meter and the gateway (excluding UDP headers, from 21h06 to 22h06, minute resolution). Each point represent the aggregate data size of LoRa transmissions in one minute.

As observed, transmissions between both devices occurs every 3 minutes as stated by the manufacturer (with some exceptions, in which packet loss is assumed) and, besides some outliers, it could be said that the typical size of LoRa packets is 57 Bytes (as it is documented in annex 2). Under this condition, there is consistent evidence that reality is close to the best scenario described in section 1.2, in which the size of a LoRa packet was assumed 41 Bytes (1 byte of data payload + 40 bytes of LoRa headers, according to equation 5.4).

On the other hand, figure 5.21 shows a sample of the data traffic per second generated from the gateway to the cloud server occurred in approximately two minutes (from 21:58:03 to 21:59:51).

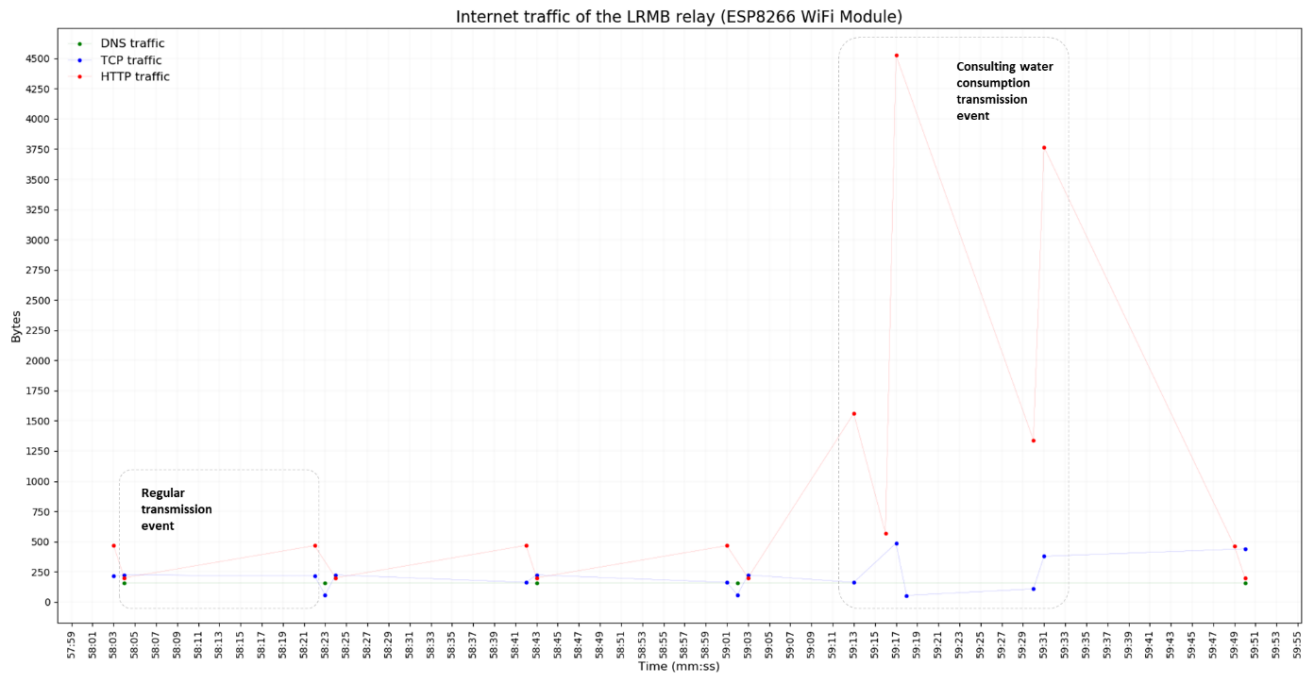


Figure 5.21. Data traffic between the gateway and the cloud server (from 21:58:03 to 21:59:51) in second resolution. Each point represent the aggregate data size of DNS, TCP and HTTP transmissions occurred in one second.

Contrary to the assumptions stated in previous section, figure 5.21 shows that, in normal conditions, the transmission events between the gateway and the cloud server —transmissions events that includes TCP three-way handshake / teardown routines and HTTP post requests— occurs every 18 seconds approximately. The mean TCP three-way handshake traffic (SYN, SYN/ACK or ACK type messages indistinctly) and the mean TCP teardown traffic (FIN, FIN/ACK or ACK typed-messages indistinctly) range from 54 to 58 bytes, which would indicate that the TCP, IP or MAC headers do not include certain optional fields showed in figure 5.11.

Moreover, the HTTP traffic —traffic that contains POST request packets with data application— is fixed to 200 Bytes, which would suggest that the gateway transform the incoming LoRa packets into formatted packets with constant size. Another important aspect to be mentioned is that the cloud server generates HTTP timeout requests of almost 468 bytes before starting a TCP teardown routine. A timeout request (HTTP code 408) allows a server announce and close an unused connection and its continuous presence after uploading an acknowledging the data application would indicates that the gateway waits for this request to start a TCP teardown routine. On the other hand, the Intensive HTTP traffic observed in figure 5.21 from 21h59m13s to 21h59m31s during a water consultation request via the cloud server (by acceding the user dashboard at www.mySolem.com) would suggest extra transmissions events in which the server demands additional data from the gateway (data that probably differs from counts). This generates high volumes of data that seems to be fragmented on packets of less than 800 Bytes, as it is observed in annex 3).

Finally, it can be observed recurrent Domain Name System (DNS) packets too. DNS is an upper-layer protocol in charge of finding the IP address from a Uniform Resource Locator (URL), in this case www.mySolem.com. When a device need to find and save the IP address of a remote server from an URL, it sends a *query request* to a DNS server —in the cloud, which sends the response information in a *query response* [156]. This operation takes place usually in early connections and the recurrent presence of DNS requests (with a mean size of 71 bytes) and DNS responses (each with approximately 87 bytes) in the regular operation of the case study (sending counts every 18 secs) would suggest that the gateway do not keep in memory the IP address of the cloud server (generating extra traffic in mutualized infrastructures).

To visualize all these aspects, figure 5.22 shows the LoRa, DNS, TCP and HTTP traffic of the case study during the full experiment (approximately 10 hours).

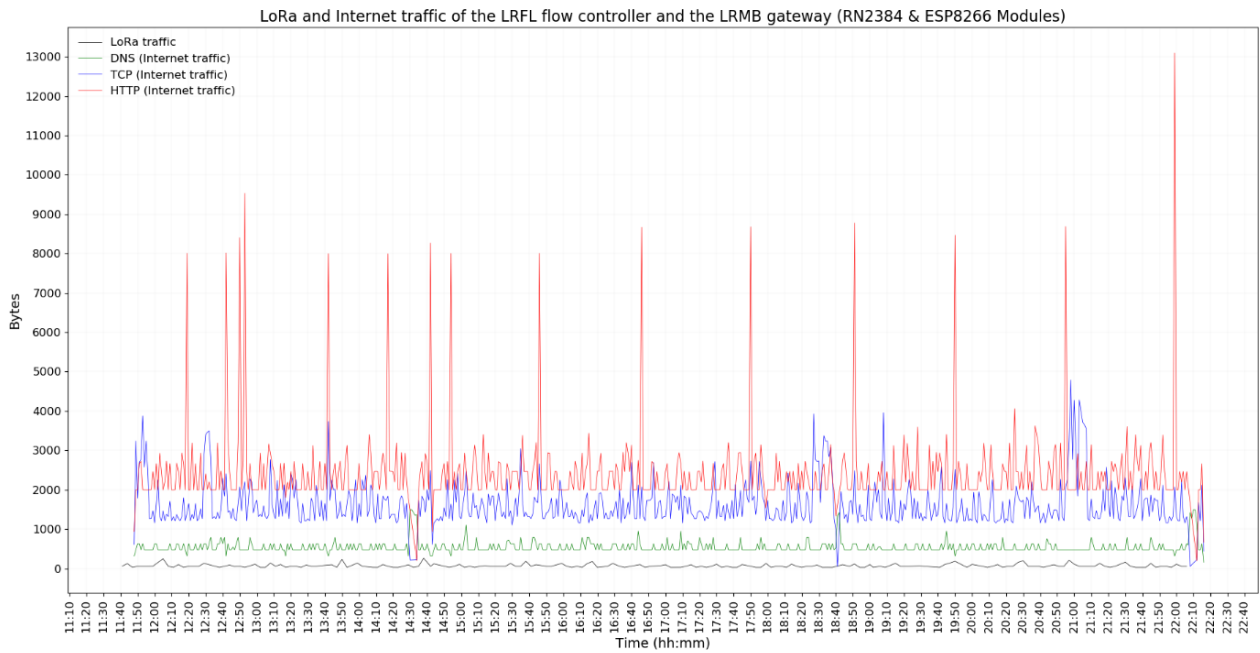


Figure 5.22. Local and internet traffic of the IoT system of the case study “Smart metering” (from 11h50 to 22h20, minute resolution). Each peak represents the aggregated data size of respective LoRa, DNS, TCP and HTTP transmissions in one Minute and every high peak depicts a hourly user consultation through the cloud server.

Under these conditions, a new impact estimation of the use-phase of the case study can be performed, according to table 5.5, 5.6 and 5.7 below.

Transmission events	Packet type	# of Packets	Approximate size packet (Bytes)
Gateway ↔ Cloud server (GC)	DNS Request	1	71
	DNS Response	1	87
	TCP ths	3	58
	HTTP post GC	1	200
	TCP Ack	1	54
	HTTP Request timeout (408)	1	468
Smartphone ↔ Cloud server (SC)	TCP t	4	58
	TCP ths	3	58
	HTTP post GC	7	787
	HTTP OK (200)	1	572
	HTTP GET	1	71
	HTTP response	1	71
	TCP t	4	58

Table 5.5. Empirical Internet traffic captured from the regular operation of the IoT system (Gateway ↔ Cloud server (GC)) and from the online consultation of water consumption (Smartphone ↔ Cloud server (SC)) in terms of number of packets and real data size. The gray cells show the new traffic revealed in the data traffic analysis of the network.

(sender ↔ receiver)	Function	Transmissions events	Packets	Internet Data traffic (GB)
Gateway ↔ Cloud server (GC)	Resending counts (every 18 sec)	3503888	42046656	4,197
Smartphone ↔ Cloud server (SC)	Hourly consultations of water consumption	17520	297840	0,108
			Total	4,305

Table 5.6. Real internet traffic of the case study “Smart metering” in 2 years.

Device	Electronic component	Functions	Capacity*		Reference flow	Impact (Kg CO ₂ -eq)**
			Feature	Value		
Pulse emitter	Capacitors & inductors	Generating pulses	Maximal sampling rate	10 Pulse / sec	1 Li-ion battery	0,0382
	Li-ion Battery	Power supply	Nominal capacity	1650 mAh		
Flow meter	LoRa module	Counting pulses	Current consumption sleep mode	0,0016 mA	1 Li-ion 9V Batteries	0,229
			Sending count	Bitrate (SF7, 125 KHz)		
		Current consumption Transmission mode		44,5 mA		
	Li-ion 9V Battery	Power supply	Nominal capacity	1200 mAh		
Gateway	LoRa module	Receiving counts	Energy consumption	0,006 kW	105,12 kWh	5,150
	WiFi module	Preparing TCP/IP packet				
		Resending counts				
Smartphone	WiFi module	Hourly consultations of water consumption	Energy consumption (sending in 700 kB /sec)	1629 mW	0,501 kWh	0,045
			Energy consumption (Receiving)	1375 mW	0,423 kWh	
Internet			Energy consumption	0,15 kWh / GB	0,6457 kWh	0,500
Cloud server			Energy consumption	0,14 kWh / GB	0,6027 kWh	0,467
					Total	6,4296

Table 5.7. Estimated impact of case studied A considering experimental data of local and internet traffic. *data available in respective technical documentation found in the reference section. ** According to CML-IA 2001 LCIA method (Global warming 100a).

➤ By considering a data size of 41 Bytes for LoRa packets, it is only necessary 1 Li-ion 9V battery for local transmissions (according to equation 5.12) and the impact of the rest of the local equipment is the same. However, there is an evident increase of the impacts related to the internet infrastructure and cloud server (figure 5.23a). This is explained mainly by the new data traffic observed between the gateway and the cloud server in the normal (sending counts) and the water consumption operations (figure 5.23b and 5.23c respectively). As a result, the total impact of the system increases by 17,42% (approximately to 6,43 Kg CO₂-eq) with respect to the theoretical estimation of the best scenario seen in section 1.2).

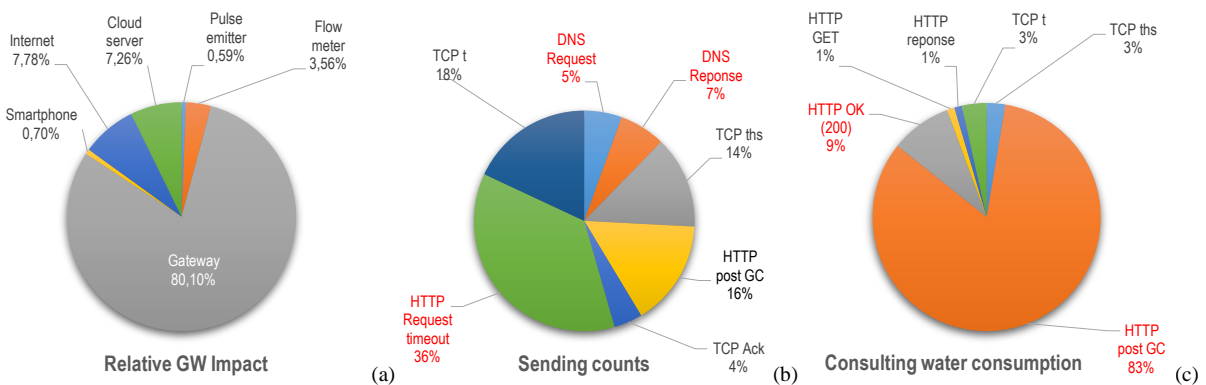


Figure 5.23. (a) Relative GW impacts of the IoT system of the case study “Smart metering” in the use phase. (b) Internet traffic for sending counts (regular operation state of the IoT system). (c) Internet traffic for consulting water consumption. Figure b and c are depicted in terms of data traffic and types of packets generated during 2 years.

1.4.Recommendations for the case study “Smart metering”

According to the estimations made in section 1.2 and the evidence presented in the previous section, the uncontestable priority for the redesign of the IoT system of the case study Smart metering should be considering an alternative source of renewable energy for the gateway, as it contributes the most to the impact of the IoT system in the use phase. However, if this change is adopted, it must be accompanied by a redesign of the data flow, which need to be oriented to cover only the necessary transmissions with sufficient quality, depending on the context of use. Indeed, although the data traffic in the internet infrastructure and the cloud server does not provoke the biggest impacts (according to both, the theoretical and experimental estimations), it contributes indirectly to the impact of the gateway, since this device is in charge of treating all this traffic exclusively (the fabricant do not report additional

functionalities). In other words, the data traffic affects directly the load and energy needs of the gateway and, indirectly, its impact.

- Thus, the potential guideline “Analyze energy depletion patterns and use energy harvesting mechanisms” [17] gains more relevance in this case, and an urgent redesign action in this sense would be analyzing the reasons behind the high frequency of transmission events so that designers can reduce it (by remodeling the data flow, whenever manufacturers disclose further information). Beside of this, there is additional work to do to avoid (1) unnecessary internet traffic in each transmission event (i.e.; DNS traffic) and (2) unnecessary internet traffic for closing a transmission event (HTTP timeout requests).

The first aspect may be solved by keeping in memory the IP address of the cloud server and triggering an auxiliary mechanism to obtain it, whenever its IP address changes. The second aspect could be addressed by forcing the gateway starting a TCP teardown routine immediately after uploading the data application (after sending a HTTP post request), preventing the server from sending timeout requests.

- In this line, a drastic yet interesting solution would be using User Datagram Protocol (UDP) to sending the counts instead of using TCP/IP and HTTP. UDP is a connectionless protocol oriented to speed and not to reliability (a packet may not be delivered, delivered twice or in the wrong order). Bearing in mind the data simplicity and the redundant nature of the transmissions between the gateway and the cloud server in regular operating conditions (sending counts); UDP should be considered to alleviate not only the traffic load for stablishing connections (i.e.; by avoiding TCP three-way handshake loads) but also the heavy load for closing them (i.e., avoiding TCP teardown and HTTP timeout loads). However, this would depend on the reliability and security requirements of the application.

The impact of the internet infrastructure and the cloud server could be reduced too if data aggregation or reduction techniques were applied in the gateway, whenever an online consultation of water consumption happens. Indeed, although knowing the specific content circulating in the big peaks of figure 5.22 is not possible (with the available information sources reviewed in this work), one knows that either other data beside counts is sent, or accumulated information are sent, or both.

- In this sense, simplifications in whatever of these potential contents may be very beneficial, provided that designer proceed with caution, as the synthesis or reduction of data or information could require more energy in the gateway’s side. In this sense, the potential guideline “Use data reduction mechanisms” [17] could be adopted by designers, as long as they also challenge their solutions, in the light of the guideline “During product design, decisions of whether computation or storage happening on-device or remotely have to be considered concerning energy efficiency” [89].

On the other hand, it is intriguing to see that the manufacturer suggests a maximal distance range of 800 meters between the flowmeter and the gateway, when the LoRa technology offers longer communication ranges (from 2 km to 14 km, depending to the Spreading Factor). Although revealing the reasons why the manufacturer suggests this distance is beyond the scope of this work, it is believed that some probable reasons is assuring reliability and maximizing the lifetime of the flowmeters’ batteries (by avoiding long transmission periods, as it was seen and explained in section 1.1.1). However, this would cause a greater environmental impact, since the number of gateways deployed in a network could rapidly increase, depending on their positions and especially on the extension of the studied area, as shown in Figure 5.24c and 5.24d.

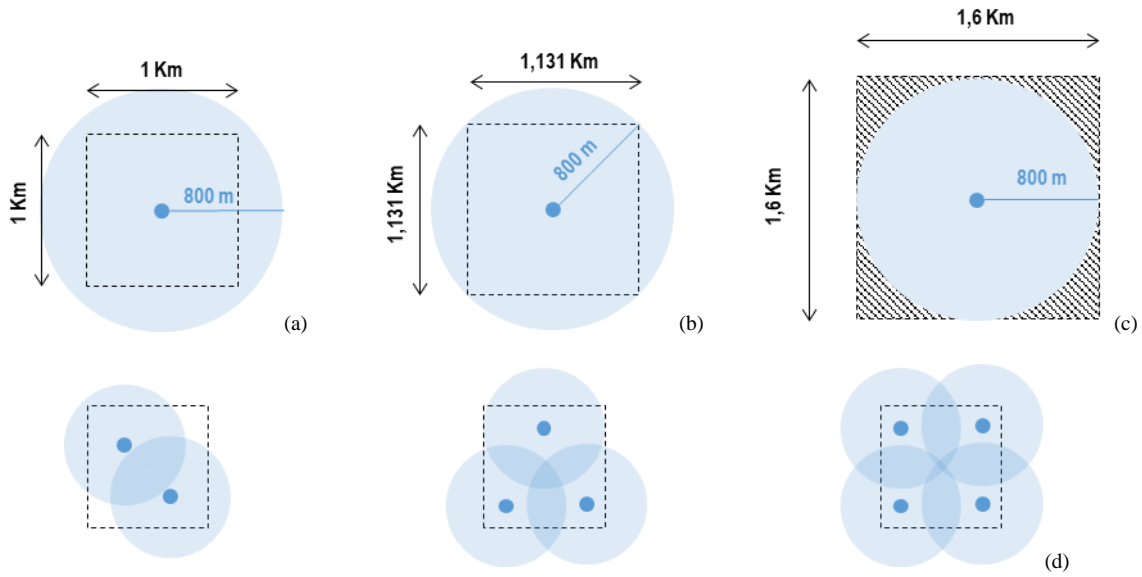


Figure 5.24. (a) The coverage area of a gateway (the central point) covering perfectly an area of 1 km² (as defined by the functional unit). (b) Maximal area (1.28 km²) covered by one gateway, according to the manufacturer (the diagonal of the squared area is equal to the diameter of the maximal coverage area supported by a gateway, that is, 2 times 800 meters or 1,6 km). (c) coverage shortcomings of one gateway in an area of 1,6 x 1,6 km or 2,56 km² (the shadow spots). (d) Possible network deployment for assuring full connectivity for an area of 2,56 km², if the designer follows the recommendation of the manufacturer (two gateways would be insufficient and four would be too much). Figure a-c is in scale 1:50000, figure d in scale 1:100000.

Indeed, although the study of the manufacturing phase of the local equipment was not addressed in previous sections, it can be observed in figure 5.24d that, to guarantee the coverage of a larger area (i.e.; 2,56 km²), a minimal deployment of three gateways is required. However, this does not necessarily have to be so. From the operational point of view, the experimental results show that the flowmeter does not generate significant volumes of data (i.e.; 57 Bytes per LoRa transmission); by considering that this load was perfectly managed by one gateway in a SF of 7 (as evidenced in experiments), there is no reason to think that a gateway could not provide the same level of reliability for longer distance ranges for years, as estimations in table 5.8 suggest.

Distance range	SF	Bandwidth	Bitrate		In a transmission event		In two years		B_{fm} (in 2 years)	Lifetime of one 9V battery (years)
			in bits / s	in Bytes / s	t_{trans} (s)	t_{sleep} (s)	t_{trans} (h)	t_{sleep} (h)		
2 Km	SF7	250 kHz	11000	1375	0,041	179,96	4	17513	0,18	10,98
2 Km	SF7	125 kHz	5470	684	0,083	179,92	8	17509	0,34	5,86
4 Km	SF8	125 kHz	3125	391	0,146	179,85	14	17502	0,58	3,45
6 Km	SF9	125 kHz	1760	220	0,259	179,74	25	17491	1,01	1,98
8 Km	SF10	125 kHz	980	123	0,465	179,53	45	17471	1,79	1,12
11 Km	SF11	125 kHz	440	55	1,036	178,96	101	17416	3,96	0,50
14 Km	SF12	125 kHz	290	36	1,572	178,43	153	17364	6,00	0,33

Table 5.8. Estimation of the maximal lifetime of one 9V Li-ion battery (gray cells) used by the flowmeter for transmitting periodic LoRa packets of 57 Bytes, under different Spreading Factors, distance ranges and bandwidths. The light blue line shows the technical features and calculations for the conditions taken in the experimental procedure described in sections 1.3.1 and 1.3.2. Descriptions of the Total number of LoRa Transmission Event (TTE_{LoRa}), and calculation procedures for the time elapsed in the different states of the LoRa transceiver of the flowmeter (t_{trans} , t_{sleep}), and the number of batteries that it requires (B_{fm}) are available in equations 5.10, 5.11 and 5.12 respectively.

As observed, the current IoT system can potentially support LoRa transmissions in a range of 2 km for more than 5 years and, in the best scenario, for more than 10 years, if a bandwidth of 250 kHz is rather considered.

- However, although promising, this suggestion should be taken into account with caution as more variables influencing the quality of LoRa transmission between the flowmeter and the gateway may exist (further research and estimations should be conducted, as long as documentation about the design of the flowmeter, gateway or the dataflow between them is publicly available). An useful guideline to consider in this context would be “Reduce the network size” [99], which could be complemented by the guideline “find the device coverage that minimize the number of device deployed” [10].

On the other hand, the recommendation of replacing the battery-powered design of the flowmeter by another self-powered or even hybrid-powered design could be interesting in specific contexts. For example, a designer should prioritize a self-powered design in a context that involves extended areas (11 or 14 km), since under these conditions, a single battery would cover the operation of the IoT system only for less than 1 year (according to the last column of table 5.8). On the contrary, focusing on a self-powered design in an operational context involving short distance ranges (2 or 4 Km) would provide only marginal benefits (one would avoid changing batteries every 5 or 3 years) or worse; one could transfer impacts from the use-phase to the manufacturing phase of the flowmeter (depending on the complexity of its self-powered design).

Finally, although the Bluetooth functionality was not addressed in this study, it is believed that the use of the Bluetooth modules of the flowmeter and the gateway would not be frequent, as the main purpose of this component is providing first configuration settings on these devices. Indeed, a strong hypothesis is that once the full IoT is deployed; configuration changes would be done through the user's dashboard in the cloud server most of the time. Similarly, for the water consultation locally (by connecting a smartphone to the flowmeter or the gateway via Bluetooth), it is very likely that the end-user tends to consult his or her water consumption directly by internet as this method is more practical than getting around close to several and/or distant flowmeters. In this way, this latter belief gains even more sense from an environmental point of view, if one considers the additional impact generated by traveling long distances in extended areas (i.e.; cultivatable lands).

- If all these hypotheses are confirmed, designers should consider removing the Bluetooth module for further design and facilitating a wired-typed connection design for initial configurations of both devices. This option needs further research in terms of additional impacts and potential gains in comparative studies (e.g., Bluetooth VS USB ports) by considering physical, technical and circularity attributes of the alternatives (e.g., materials, additional passive components, additional energy consumption or other drivers and barriers affecting ecological design and circular strategies).

2. Case study “Smart monitoring”

The case study “Smart monitoring” consists of a prototype of an EH sensor system developed at the System Division (DSYS) of CEA-Leti. The Technology Readiness Level (TRL) of maturity of this prototype is level 6 (proof of concept validated in relevant environment) and it is currently in the stage 4 (testing) of the Product development process. The specific application of the IoT system to which it belongs is confidential. However, for the purpose of this work, suffice it to say that the end-user of this IoT system needs to keep track of the wearing rate of an ordinary object without affecting its employment and in a full autonomous way. The DSYS design teams are in charge of the design of the electronic card of the EH sensor system, and partner firms are in charge of developing all the additional parts of the device, such as plastic chassis and cases that allow embedding the device into the object. These partners are also in charge of the edge- and cloud-side software design. Depending on the design of the EH sensor system, the edge device could be a modern smartphone equipped with NFC or BLE technologies. The cloud infrastructure consist on a regular remote server.

From the aforementioned end-user need, a functional analysis identifies two main functions:

- Function 1: Recovering energy from the environment
- Function 2: Presenting statistical data of the usage rate of the object.

From these two functions, and from the data design step later described in section 2.1.1, the DSYS engineers have developed two versions of the EH sensor system device; a memory-based version and a BLE-based version. Annex 4 provides a list of the electronic components (Bill of Materials or BoM) that shapes the memory-based version. This BoM becomes the referential electronic design for further LCA comparison in this work and it is referred to from now on as set 13. Table 5.9 presents a description of the relevant criteria, selection ranges and minimal capacities (related to data operational stage functions) of some principal electronic components that were taken into account for the development of set 13.

Electronic component	Criteria			
	Wholesale price	Size	Energy consumption	Capacities
Microcontroller	From 0,6 to 3,06 €	From 9 to 49 mm2	Active mode: 163 μ A/MHz Stop mode: 1 μ A	RAM > 8 KB Flash > 32 KB Frequency: 32 KHz ADC: 12-bit ADC 1,14Msps
Voltage detectors	From 0,13 to 1,63 €		From 0,5 to 0,55 μ A	
Voltage comparator	From 0,299 to 0,819 €		From 0,3 to 1,5 μ A (@ 25 C°)	
Capacitor 1210		Height < 2,5 mm		Capacitance: 10 μ F

Table 5.9. Criteria of electronic component selection for the referential design set (set 13).

In this case study, reducing the load of the system by selecting the less energy-demanding component is crucial because the capacity of the EH sensor system to recovery energy is minimal. Moreover, the size of every electronic component is relevant since that will influence the final size of the PCB and, consequently the final size of the device, whose need to be embedded into the object. On the other hand, the price is also important, since mass production of the EH sensor system is planned.

2.1.Implementation of the framework for eco design

In the context of the case study “Smart monitoring”, the implementation of the proposed methodology through the framework for eco design (seen in chapter 4, section 4.1) is developed in two parts: Section 2.1.1 describes the design of data and information originated in the EH sensor system and section 2.1.2, 2.1.3 and 2.1.4; the sequential analysis of key parameters of electronic components, which will be applied on a LCA-based specific analysis to reveal sharp recommendations for the eco-design of the EH sensor system device.

2.1.1. Data and information design

This section presents an analysis on data and the ways that it can be further transformed and exploited within the IoT system of the case study. Specifically, this analysis is conducted under the Rationale of

Information Science framework seen in chapter 2 (section 4) and chapter 3 (section 2.2.3) by consider (1) the type of meaningful data that can be collected and (2) the type of meaningful information that can be extracted from it so that it can be later interpreted as the use wearing degree of the object. This analysis is described in two steps as follows.

Step 1: Finding meaningful data

The object of the case study “Smart monitoring” is constantly deformed during its use and energy can be harvested from this mechanical stress, by using an embedded piezoelectric ceramic-based transducer (figure 5.25), as it is explained in figure 5.26.

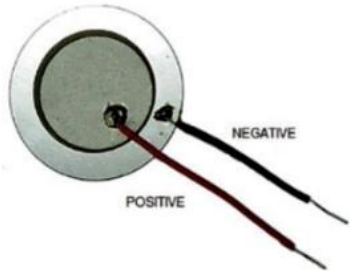


Figure 5.25. Modern piezo electronic buzzer with an in-between piezoelectric ceramic material that recover energy from mechanical stress (e.g., compression, deformation, etc.).

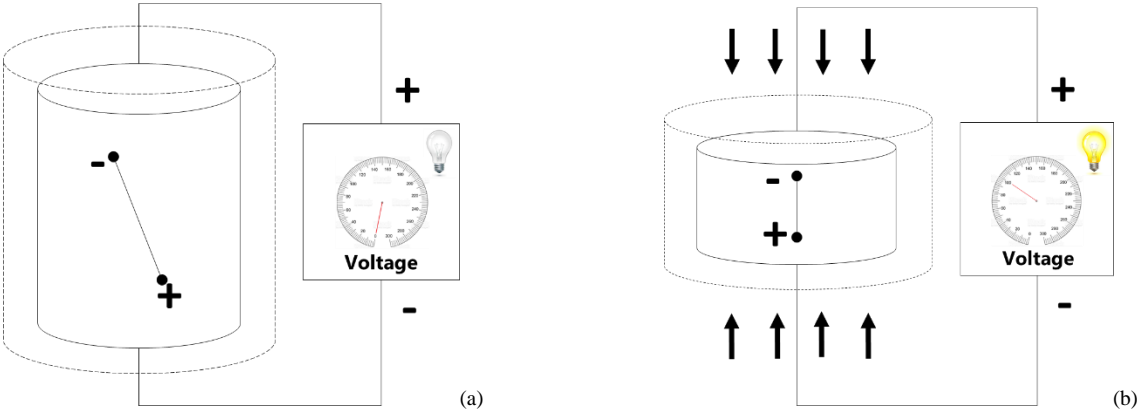


Figure 5.26. (a) A cylinder made by a piezoelectric ceramic material embedded into an object (the outer, dotted cylinder). Piezoelectric ceramics may be seen as a mass of minute crystallites with dipoles randomly oriented (one showed here, for simplicity). (b) Deformation stress on the object and the piezoelectric material (in this case compression) causes a change in dipole orientation so that a voltage appears between electrodes. Figures adapted and simplified from [169].

In the context of the case study “Smart monitoring”, this recovered energy can be accumulated and stored in a main capacitor, which —depending on the intensity and frequency of deformations— supply energy intermittently to the sensor system (as showed in figure 5.27); making the device fully autonomous.

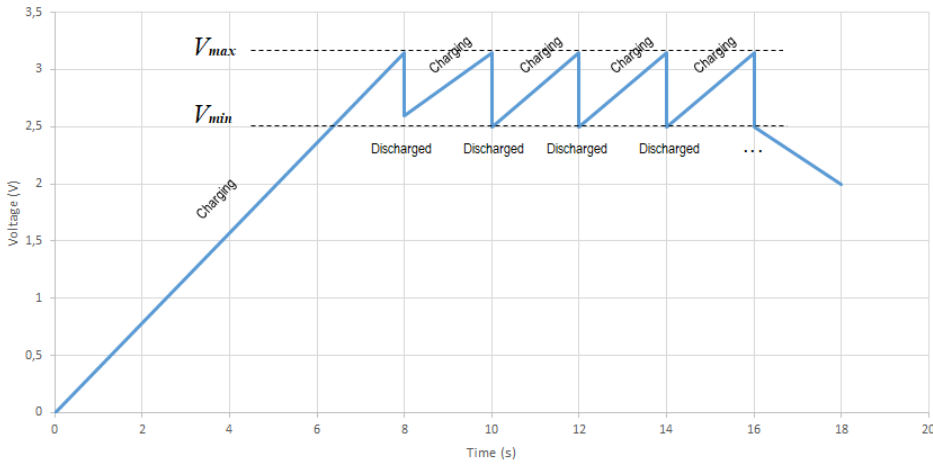


Figure 5.27. Simplified representation of the intermittent power supply schema of the EH sensor system of the case study “Smart monitoring”. When a maximal stored voltage threshold (V_{max}) is achieved, the system uses the available energy to run the program of the sensor system. When the system depletes the available energy until a minimal voltage threshold (V_{min}), the sensor system stops to consume energy, enters to a sleep mode, and a new charging cycle begins.

Step 2: Exploiting meaningful data into useful information (Data and information design)

As deduced from figure 5.27, the frequency at which the main capacitor charges and discharges energy in a period of use of the object is proportional to the mean power generated by the system, as expressed by equation 5.13.

$$\bar{P}_\alpha = P_s + \left(\frac{NE_{\alpha n}}{T_\alpha} \times \Delta_E \right) \quad (5.13)$$

Where:

\bar{P}_α = mean power generated by the system in a period of use α

P_s = Power consumption of the device in Standby state (constant)

$NE_{\alpha n}$ = Number of charging\Discharging cycles (n) of the main capacitor in a period of use α

T_α = Time elapsed in a period of use α

$$\Delta_E = \frac{\text{Capacitance of the main capacitor} \times (V_{max}^2 - V_{min}^2)}{2}$$

In this sense, large and small power mean values could be interpreted as high- and low-intensity use rates of the object respectively, as it is illustrated in figure 5.28.

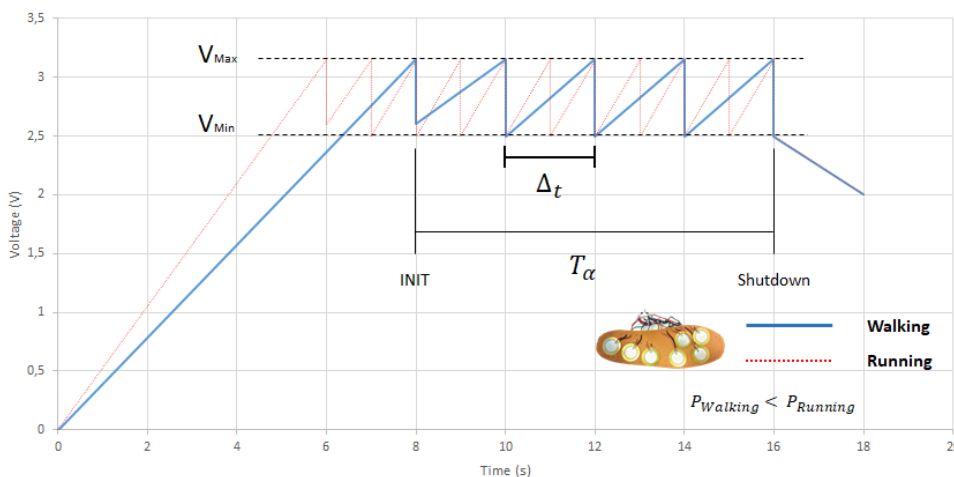


Figure 5.28. Example of an interpreted high-intensity use (Running) and a low-intensity use (walking) of an object (for example a sole) under deformation stress, in terms of their mean power values ($P_{walking}$ and $P_{running}$ respectively). The mean power values are obtained from the number of charging\discharging cycles n of a main capacitor (4 for walking, 8 for running, as is depicted by the respective voltage peaks above) and the elapsed time in a period of use (T_α).

In ideal conditions, the frequency of charging\discharging cycles of the main capacitor is constant, but in real conditions, it is variable (in the example above, walking and running schemas may be mixed in normal use). Consequently, T_α can only be estimated by aggregating the time elapsed in each of the charging\discharging cycles that occur between the initialization of the system (INIT) and the device shutdown. In this sense, the differentials of time (Δ_t) for each of the n charging\discharging cycles, and

the number of these cycles in a period α (NE_{α_n}) become the essential, meaningful raw data of the IoT system of the case study “Smart monitoring”. These raw data is used to calculate the time elapsed (T_α) and consequently the mean power (\bar{P}_α); which at the same time becomes the useful information to be interpreted as the mean wear of the object in a period of use of the object, according to Figure 5.29.

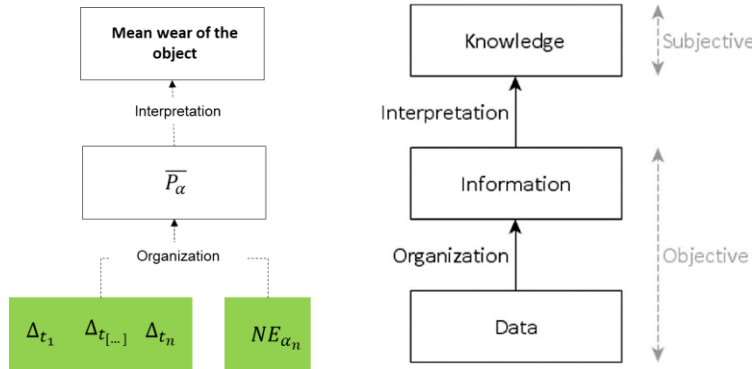


Figure 5.29. The essential raw data, information, and knowledge of the IoT system of the case study “Smart monitoring” (left), contrasted with the rationale Information Science framework reviewed in previous chapters (right). Notice that, while Δ_t and NE_{α_n} are raw data exclusively collected in the sensing layer (green boxes), their organization and further interpretation can be made in the sensing, edge or even cloud layers.

With this in mind, the manipulation of the essential raw data (data collection and storage) and the generation of information (data processing) for further interpretation could be designed in two ways. In a first alternative, only the differentials of time in each charging cycle (Δ_t) and counts of these cycles (NE_{α_n}) could be collected and saved in different blocks of a NVM memory in the sensor system, so that they can be further organized in an edge device to obtain T_α , and \bar{P}_α , as it is illustrated in figure 5.30 and 5.31.

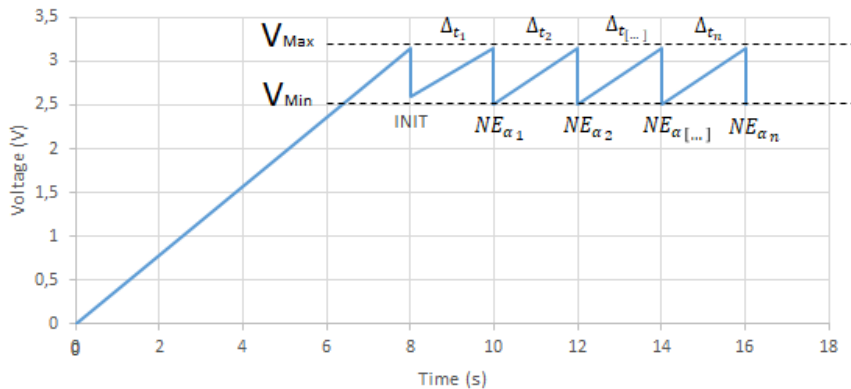


Figure 5.30. Illustration of the essential raw data for the intermittent functioning of the EH sensor system of the case study “Smart monitoring”.

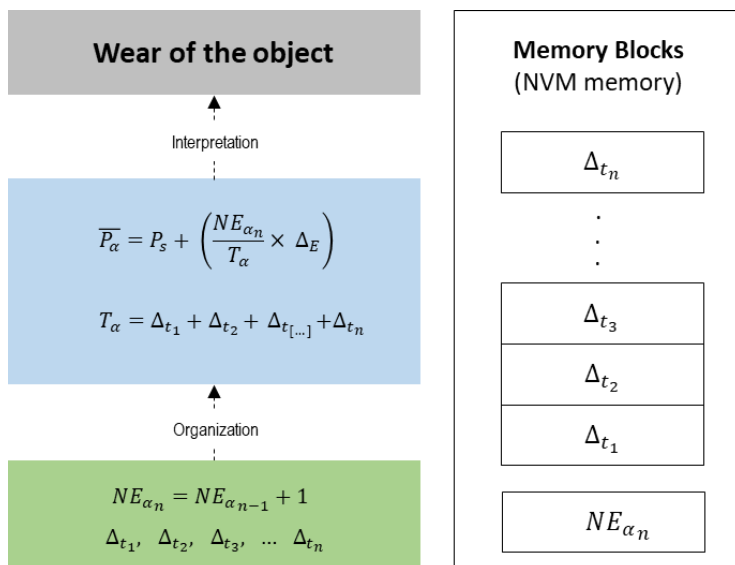


Figure 5.31. First alternative of data manipulation and information design for the IoT system of the case study “Smart monitoring”. The user starts using the object at time = 0 s, and the main program initializes (INIT) the system and saves respectively the counts NE_{α_n} and differential times Δ_{t_i} in a fix and sequential blocks of a NVM memory, using the accumulated energy in the main capacitor, whenever the V_{max} threshold is achieved. Notice that, in this schema, organization of the raw data (computing of T_α and \bar{P}_α) happens exclusively in the edge layer (blue box).

In a second alternative, the value of T_{α_n} and NE_{α_n} are updated constantly by aggregation of the individual values of Δ_t in each charging\discharging cycle and the last registered count $NE_{\alpha_{n-1}}$ respectively. For this, only four memory blocks of a NVM memory are used, as is illustrated in figure 5.32.

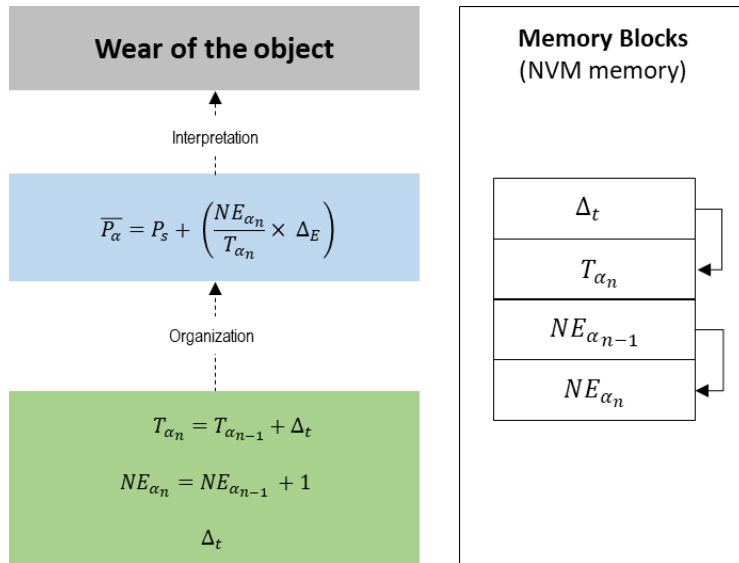


Figure 5.32. Second alternative of data manipulation and information design for the IoT system of the case study “Smart monitoring”. The user starts using the object at time = 0 s and the main program initializes (INIT) the system and updates constantly the values of Δ_t , T_{α_n} , $NE_{\alpha_{n-1}}$ and NE_{α_n} in four fixed blocks of a NVM memory, using the accumulated energy of the main capacitor, whenever the V_{max} threshold is achieved. When the system initializes for the first time, values of T_{α_n} and NE_{α_n} are zero. When the system wake-up for the second time, data is not reset, but continue to be incremented. Notice that, in this schema, organization of part of the raw data (computing of T_{α_n}) happens in the sensing layer (green box).

From the two design alternatives described above, the following design aspects arise:

- The first alternative could make use of all available blocks of a memory, and the risk of over flooding is high.
- In the first alternative, the memory density and the reading speed may or may not be crucial, depending on the readiness requirements of the application.
- High readiness can be assured from the second alternative (only 4 memory blocks need to be read), but it may (or may not) drain the recommended number of writing cycles per block of a memory component.

To deal with these aspects, two versions of the EH sensor system were developed in the DSYS division of CEA-Leti: an NFC, memory-based version working under the second alternative and an alternative Bluetooth-Low-Energy (BLE) version. The next section provides a complete description of the electronic design of both versions.

2.1.2. Electronic component alternatives according to the data and information design

The central approach of the memory-based version is using the accumulated energy of the EH sensor system to write Δ_t , T_{α_n} , NE_{α_n} and $NE_{\alpha_{n-1}}$ directly in an EEPROM memory. This EEPROM memory would be embedded into a System on Chip (SoC) device equipped with NFC technology. On field tests show that this version has high readiness and there is no risk of over flooding the memory, since data would be uploaded constantly (according to the data design alternative 2, described in figure 5.32). This version describes a typical energy harvesting subsystem as like as the one showed in the figure 1.8 of chapter 1, in charge of powering a microcontroller and a NFC-EEPROM memory. Figure 5.33 shows the basic electronic design and operation in terms of the framework for impact estimation (IoT system layers, devices, components, functions and capacities) and physical and data flows.

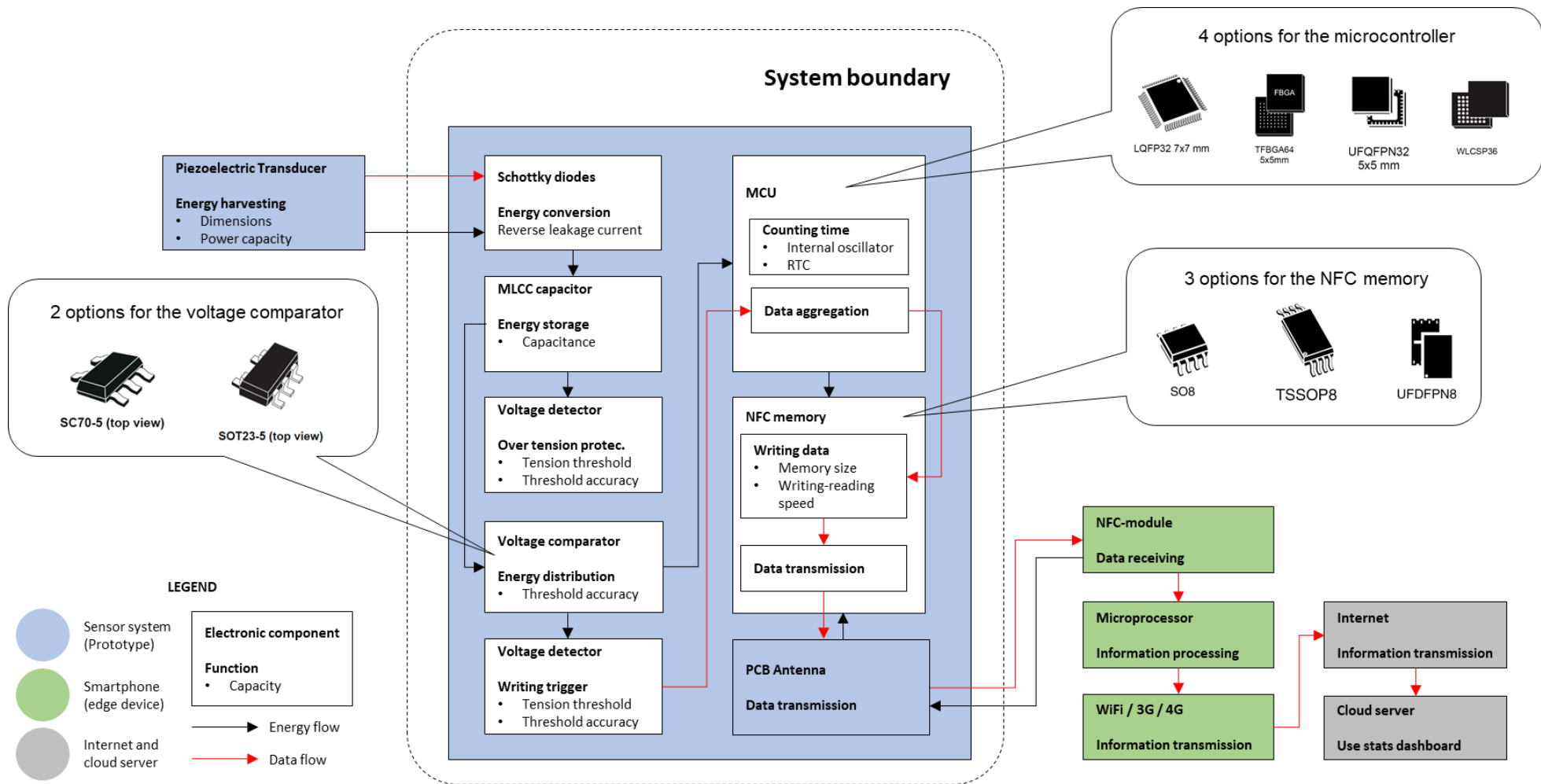


Figure 5.33. Basic electronic design of the NFC-memory-based version of the EH sensor system in terms of the proposed framework for impact estimation. The black arrows depicts energy flows and the red arrows, data flow. The image shows the system boundary applied for the LCA modeling that will be described in next sections. Each component shows the critical function(s) that it provides, together with the critical capacity for it.

Basically, in this version the main capacitor accumulates energy from a piezoelectric transducer and provides energy to execute a writing cycle of the four aforementioned values whenever a maximal voltage threshold is achieved. Specifically, a voltage comparator (VC) authorizes the distribution of the available energy to the microcontroller and to the bottom voltage detector (VD) showed in figure 5.33. The red arrow between them represents a data flow, because the microcontroller consider the time at which it is awakened by the voltage detector (writing trigger function). In this way, the microcontroller aggregates this time (Δ_t) and a count (+1) to the corresponding previous values ($T_{\alpha_{n-1}}$ and $NE_{\alpha_{n-1}}$ respectively, saved in the EEPROM-NFC memory). After this, a new charging cycle begins.

Because of their fundamental roles observed in figure 5.33, 2 voltage comparator types (SC70-5 and SOT23-5 [170]) 4 microcontroller types (LQFP32, TFBGA64, UFQFPN32 and WLCSP36 [171]) and 3 NFC-EEPROM memory types (TSSOP8, UFDFPN8 and SO8 [172]) were considered to illustrate the further eco-design steps in the context of the framework for eco design of the proposed methodology, and challenge the referential design presented before (set 13). These components were selected according to their functions and critical capacities in relation to the data flow showed in figure 5.33.

Figure 5.33 also shows the functioning of the edge and cloud resources. For the edge side, a smartphone collects T_{α_n} and NE_{α_n} from the NFC memory whenever it is closed enough to the EH sensor system device (the black arrow indicates that the smartphone provides additional energy to the NFC memory to do this via the antenna on the PCB). From T_{α_n} and NE_{α_n} , the processor of the smartphone computes \bar{P}_α . This information is further interpreted as the mean object's intensity use on the cloud server side.

On the other hand, the BLE-based version derives from the NFC-memory-based version. It describes the same EH subsystem with the difference that in this version, the accumulated energy is used to power a BLE module instead to a microcontroller (the bottom voltage detector is kept and its works identically as from the NFC-memory-based version). The central approach of this version is sending the raw data generated in an i^{th} charging\discharging cycle (Δ_{t_i} and NE_{α_i}) directly to the smartphone via Bluetooth, instead of save it in a memory. On field tests show that this version would also have high readiness and reliability. Figure 5.34 shows its basic electronic design and operation under the terms of the framework for impact estimation (components, functions and capacities and IoT layers).

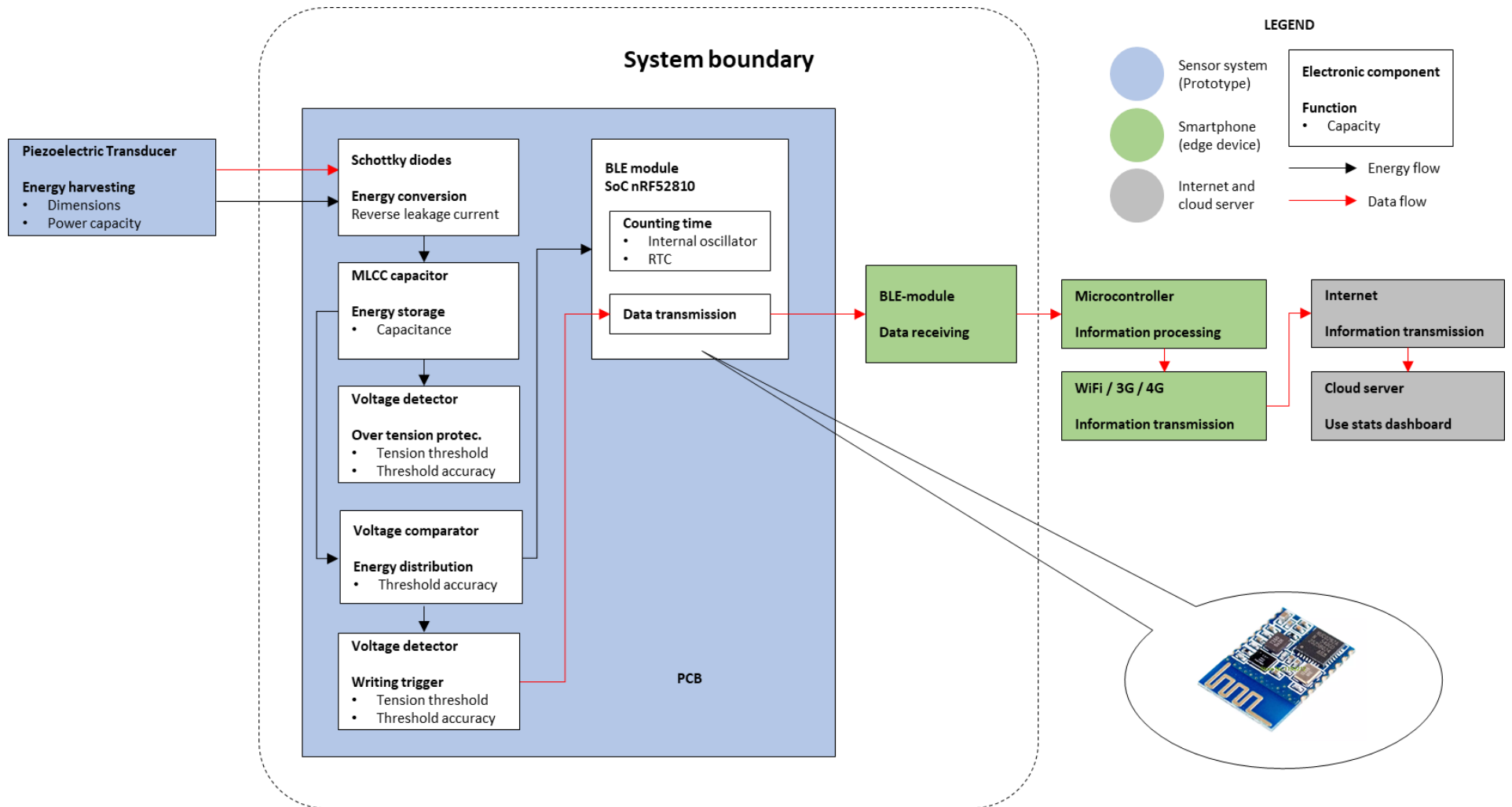


Figure 5.34. Basic electronic design of the BLE-based version of the EH sensor system in terms of the proposed framework for impact estimation. The black arrows depict energy flows and the red arrows data flow. The image shows the system boundary applied for the LCA modeling that will be described in next sections. Each component shows the critical function(s) that it provides, together with the critical capacity for it.

Figure 5.34 shows almost the similar energy and data flows seen as for the NFC-memory-based version with the difference that raw data (Δt_i and NE_{α_i}) is sent directly to the smartphone via the Bluetooth interface of the SoC component of the BLE module (there is not protocol overhead, because data application is embedded in a BLE advertising packet, as Morin, E. et al [139] recommend). In the edge side, the smartphone uses its BLE module to receive this data, in order to obtain $\overline{P_{\alpha}}$, information that is later interpreted as the mean intensity use of the object in the cloud side. Annex 5 provides a detailed description of the electronic design (BoM) of this BLE-based version.

2.1.3. Evaluation of electronic component alternatives through physical attributes

By considering that only one type of IC for specific functions should be selected and combined to shape the electronic design of the NFC-memory version showed in figure 5.33 (one type of voltage comparator for energy distribution, one type of MCU for counting time and aggregation, and one type of NFC EEPROM memory for data writing and transmission); 24 possible combinations or electronic design sets (including the referential set 13) were identified. Table 5.10 shows all these possible alternatives.

Set 1	Set 2	Set 3	Set 4	Set 5	Set 6	Set 7	Set 8	Set 9	Set 10	Set 11	Set 12	Set 13	Set 14	Set 15	Set 16	Set 17	Set 18	Set 19	Set 20	Set 21	Set 22	Set 23	Set 24	Component	
1	1	1	0	0	0	1	1	1	0	0	0	1	1	1	0	0	0	1	1	1	0	0	0	VC SC70-5	Voltage comparators
0	0	0	1	1	1	0	0	0	1	1	1	0	0	0	1	1	1	0	0	0	1	1	1	VC SOT23-5	
1	1	1	1	1	1	0	0	0	0	0	0	0	0	0	0	0	0	0	0	0	0	0	0	LQFP32	MCUs
0	0	0	0	0	0	1	1	1	1	1	1	0	0	0	0	0	0	0	0	0	0	0	0	TFBGA64	
0	0	0	0	0	0	0	0	0	0	0	0	1	1	1	1	1	1	0	0	0	0	0	0	UFQFPN32	
0	0	0	0	0	0	0	0	0	0	0	0	0	0	0	0	0	0	1	1	1	1	1	1	WLCSP36	
1	0	0	1	0	0	1	0	0	1	0	0	1	0	0	1	0	0	1	0	0	1	0	0	TSSOP8	EEPROM Memories
0	1	0	0	1	0	0	1	0	0	1	0	0	1	0	0	1	0	0	1	0	0	1	0	UFDFPN8	
0	0	1	0	0	1	0	0	1	0	0	1	0	0	1	0	0	1	0	0	1	0	0	1	SO8	

Table 5.10. All possible electronic component combinations or “sets” for the design of the NFC-memory-based version. A “1” indicates that a specific electronic component (line) was selected for that particular electronic design set (column). The referential design set (set 13) is marked in gray.

Because of this diversity, the evaluation of design alternatives though physical attributes will be led in the context of the NFC-memory-based version. The following section shows how to conduct this analysis on alternative electronic components in two ways: it studies the influence of materials on the Abiotic Depletion (AD) impact category on the one hand, and the influence of physical features (i.e.; surface areas of internal dies), interdependencies (i.e., PCBs area variation according to IC land patterns), and materials on the Global Warming (GW) impact category on the other. For this, the LCA implementation suggested in the section 4.1 of the previous chapter is applied by taking into account the following aspects.

Firstly, from the reference electronic design (Set 13), one establishes a referential PCB size (704 mm^2) and derives its size variation for the other design combinations presented in table 5.10, based on the surface (landing pattern) of the electronic components that compose such combinations. For simplicity and illustrative purposes, the standard IPC-7351B [173] in this most penalizing mode (0,5 mm) is taken into account for determining the area that every electronic component under study will occupied in the electronic card. This standard is applied on them, by considering their land patterns or PCB footprints including all their pins, as is showed in figure 5.35.

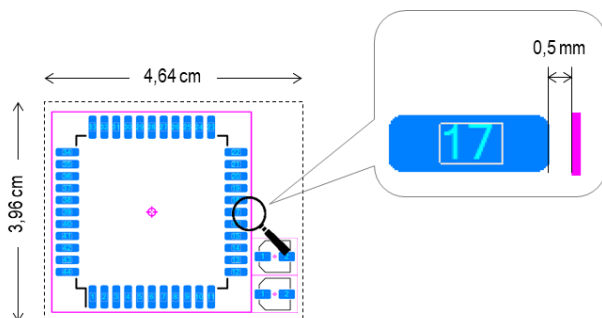


Figure 5.35. Standard IPC-7351B (the purple perimeter, that leaves a free space of 0,5 mm in its most penalizing version), applied to the land pattern (PCB footprint) of three SMD electronic components in a PCB instance of 3,96 cm x 4,64 cm. The standard allows keeping minimal distances among components in the PCB surface to avoid production fails in reflow soldering processes (Annex 6 provides all the PCB size variation in function of the combined electronic components proposed in table 5.10).

Notice that the PCB size is considered for the impact contribution analysis in the GW category, but not in the AD category. This is for practicality reasons: since all design combinations and versions used the same kind of PCB (a six-layered FR4 type), impact contribution analysis by elementary flows is

unproductive (impact difference would be explained uniquely by material quantities in PCBs—which is directly proportional to their dimensions— but not by their material variety. In this sense, the reader will find a complete description of the material composition of all electronic components under study from annex 7 to 9. (For the material composition of the invariable components (e.g., passive components), he or she should consult the correspond Ecoinvent process modeling used in this work [174]).

Secondly, The LCA model implementation proposed in previous chapter is applied in SimaPro using the Ecoinvent V3.6 LCA database. In this line, electronic components under analysis are modeled in detailed, according to the proposed manufacturing lifecycle model of figure 4.26 of chapter 4, and the rest of the electronic components are modeled from default Ecoinvent processes. The assembly step (including the solder paste, energy and assembly facilities) is modeled on the basis of electronic components surfaces. Because of its significant contribution to all design sets and versions, the detailed LCA modeling of the SOT23-5 typed voltage detector (VD SOT23-5) [175] is also applied, although it contributes the same to all versions (this is an invariable component). Full material declaration and further impact analysis of this component is provided in annex 10.

Thirdly, For the impact assessment, the CML-IA LCIA methodology is used, considering only two impact categories: Global Warming potential in a period of 100-year (GW-a100) and Abiotic Depletion (AD) (following the research methodology of the reported work of Bonvoisin, J. et al. [10], who found contrasted behaviors of both impact categories in the context of ICT products.

Finally, the functional unit defined for the specific analysis of physical attributes of electronic components considers the production of the EHS sensor system (in different design sets), whereas the functional unit for specific analysis of technical and circularity attributes adds the use and the EoL phases of the device. On the other hand, as the design combination involves variations only on three component types (voltage comparators, microcontrollers and memories), detailed impact contribution including all components in an electronic design is given only in initial impact results and / or when necessary (i.e.: in comparison analysis of different versions, but not in comparison of different design combination or sets).

2.1.3.1. Importance of materials and physical attributes for the AD impact category

Figure 5.36 shows the relative AD impact of all possible design sets for the NFC-memory-based version.

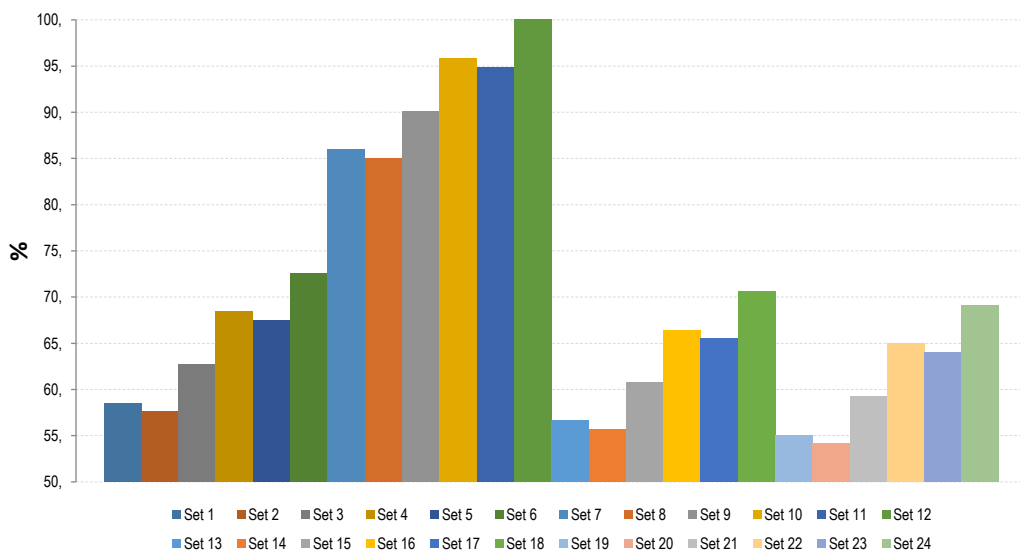


Figure 5.36. Relative AD impacts of all design sets for the NFC-memory-based version (24 combinations). The functional unit is defined as “production of one EHS sensor system device in its NFC-memory-based version”

For the AD impact category, the best and the worst design alternatives are set 20 and set 12 respectively (the latter with an impact of more than 45% with respect to the former, as showed in figure 5.36). A detailed inspection of the impact contribution of the interchangeable components of set 12 (figure 5.37a) shows that the biggest contributors are its TFBGA64-typed microcontroller and its SOT23-5 typed voltage comparator (VC SOT23-5). Both with an approximate impact of more than 31% and 12% respectively.

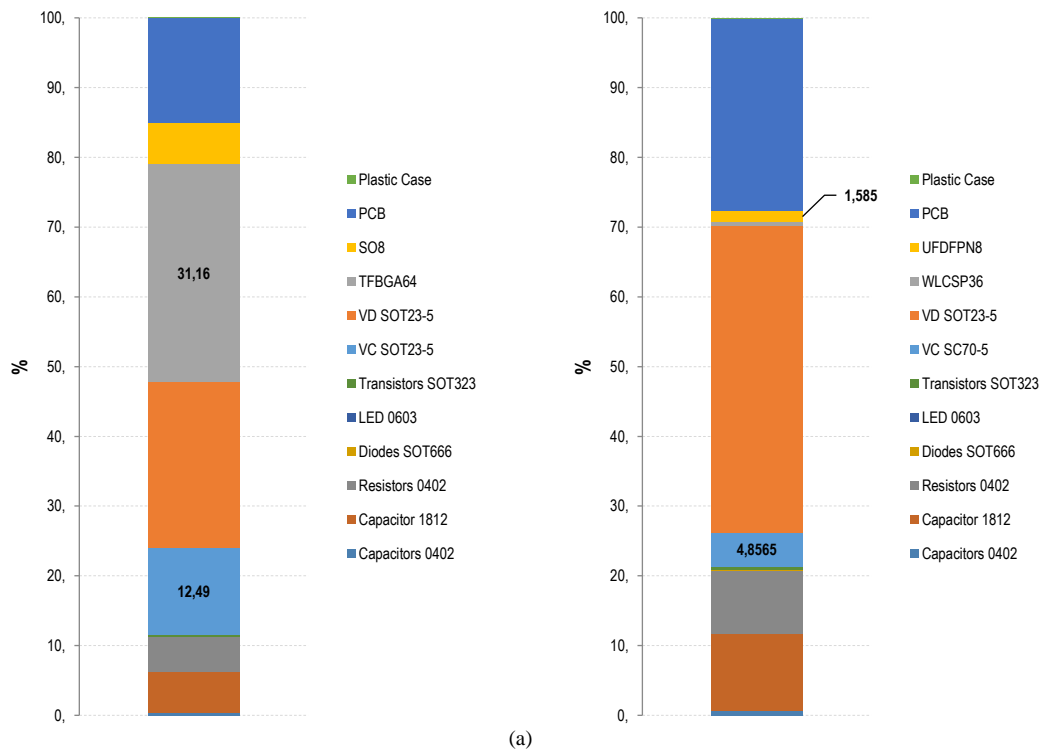


Figure 5.37. Detailed AD impact contributors of (a) the worst design alternative (Set 12), and (b) the best design alternative (Set 20). Notice that electronic components are specified by packaging type.

Moreover, an initial elementary flow analysis on raw material extractions on these electronic components reveals that the impact is mainly explained by the presence of gold in wires (0,351 mg in the case of the TFBGA64-typed microcontroller and 0,157 mg in the case of the SOT23-5 typed voltage comparator).

On the other hand, the convenient design of set 20 (whose impact contributors are detailed in figure 5.37b) is mainly explained by the relative low presence of (1) gold in the wires of its SC70-5 typed voltage comparator (0,033 mg); and (2) silver in the die attach of its UDFPN-typed memory (1,108 mg), which only contribute respectively with less than 5% and 2% to the total AD impact of the set. Furthermore, the environmental performance of Set 20 would be also explained by the null presence of neither gold nor silver in its WLCSP-typed MCU component (of which the predominant material is copper).

To better understand the relevance of these later aspects and their potential for eco-design of IoT devices, and with the aim to spot further unfavorable materials in homogeneous electronic components subparts, an iterative examination on set 12 and set 20 is conducted as follows. Firstly, an elementary flow analysis is conducted to identify and remove materials with high impacts on both sets. Secondly, an impact comparison of these modified sets is done; if the impact gap between the best and the worst sets disappears, it means that all relevant substances in specific electronic components' subparts were identified; otherwise, an individual elementary flow analysis on modified sets is relaunched another iteration restart (sensitivity analysis). Figure 5.38 shows the absolute impact of both sets as a reference for this combined analysis, and Table 5.11 shows its results, starting from the elimination of gold (iteration 0) in different subparts of electronic components of both sets.

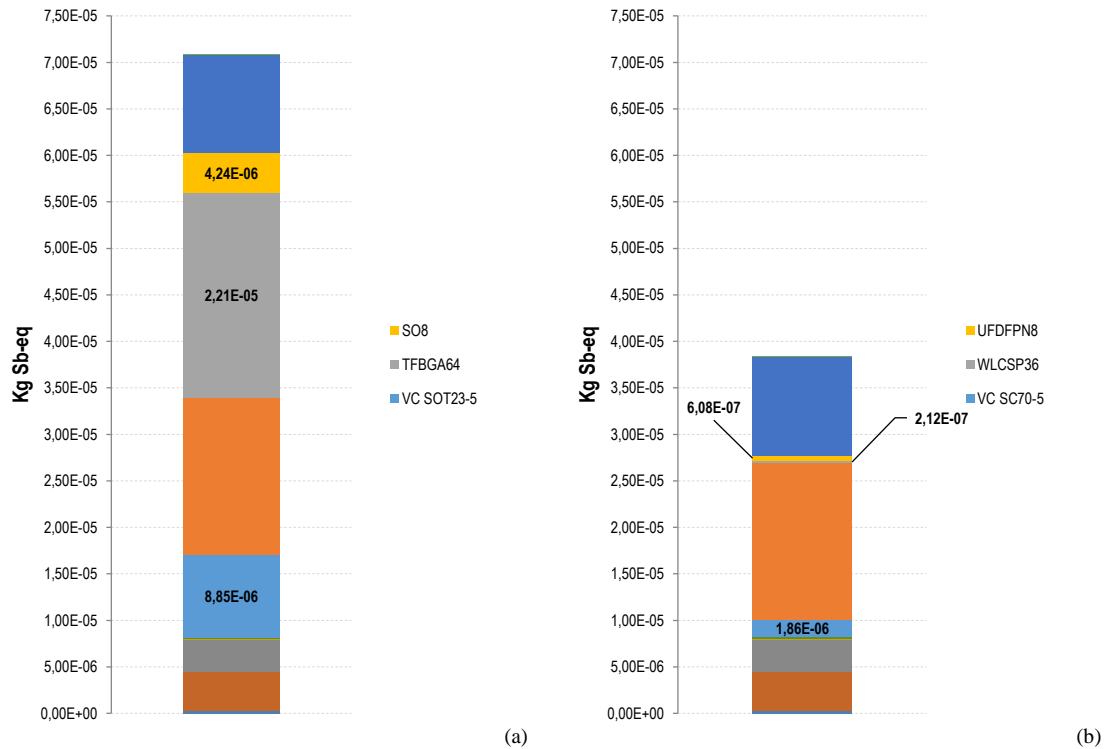


Figure 5.38. Absolute AD impacts of set 12 (a) and set 20 (b).

Iteration	Element	Set 12				Set 20			
		Electronic component	Subpart	Abs impact (Kg Sb-eq)	mass in IC (mg)	mass in IC (mg)	Abs impact (Kg Sb-eq)	Subpart	Electronic component
0	Gold 6,7E-4% in ore	VC SOT23-5	Wires	2,07E-06	0,157	0,033	4,34E-07	Wires	VC SC70-5
			Lead frame	1,31E-08	0,001				
		TFBGA64	Wires	4,62E-06	0,351				
			Substrate	2,76E-07	0,021				
		SO8	Wires	8,16E-07	0,062				
1	Silver 4,2E-3% in ore	VC SOT23-5	Die Attach	1,10E-08	0,057	0,016	3,08E-08	Lead frame	VC SC70-5
			Die Attach	4,02E-07	2,085				
		TFBGA64	Solder Balls	1,54E-08	0,08	0,014	2,70E-09	Solder Balls	WLCSP36
			Die Attach	1,78E-07	0,925	1,108	2,13E-07	Die Attach	
2	Copper 0,99% in sulfide	VC SOT23-5	Lead frame	1,62E-09	6,651	2,829	6,88E-10	Lead frame	VC SC70-5
			Substrate	2,57E-09	10,586				
		TFBGA64	Solder Balls	8,03E-12	0,033	0,018	4,38E-12	Solder Balls	WLCSP36
						0,003	7,29E-13	RDL Target	
						0,062	1,51E-11	RDL Anode	
						0,002	4,86E-13	UBM Target	
		SO8	UBM Anode			0,073	1,77E-11	UBM Anode	UFDFPN8
			Lead frame	5,92E-09	24,347	2,918	7,09E-10	Lead frame	
3	Tin	TFBGA64	Wires			0,018	4,38E-12	Wires	WLCSP36
			Solder Balls	1,23E-07	6,513	1,146	2,17E-08	Solder Balls	

Table 5.11. Results of the combined analysis (Elementary flow and sensibility analysis) to find the elements that influence the most to the AD impact results of set 12 and set 20. For simplicity, only high concentrations in ore in the mixed market of metals is shown. After iteration 3, high contents of other materials in common components for both sets (i.e., Palladium in ceramic capacitors and resistors) appear. Because these components are invariable in all sets, their materials influences are not presented in this comparative table.

In table 5.11, the presence of gold in the wires and substrate, silver in the die attach and solder balls, tin in the solder balls and copper in the substrate and solder balls of the TFBGA-type MCU of set 12 provoke almost 25% of its absolute impact ($5,44 \times 10^{-6}$ of the $2,21 \times 10^{-5}$ Kg Sb-eq impact presented in figure 5.38a); and almost the same share (23,73%) can be obtained for the SOT23-5 typed voltage

comparator ($2,10 \times 10^{-06}$ of the $8,85 \times 10^{-06}$ Kg Sb-eq impact) whose wires are rich in gold and lead frame in copper.

On the other hand, notice the confronting-styled presentation of table 5.11 to contrast these and other electronic components' subparts of both sets. The central columns permits discerning the following relevant aspects of electronic components in the context of physical properties. Firstly, dissimilar packaging technology may generate significant differences, depending on the impact relevance of materials from which they are made. For example, while TFBGA64-typed MCUs uses typically unfavorable materials such as gold and silver in wires and die attaching subparts respectively, WLCSP-typed MCUs uses convenient materials such as copper in distinctive and massive subparts (DRL and UBM subparts). Secondly, the quantity of a material in an electronic component subpart may or may not be determinant for eco-design, depending on the impact relevance of this material for a particular impact category.

Although this later aspect may be evident when selecting simple design alternatives (those options in which differences lie only on a single component); the application of this clue may become very hard, special when one consider contradictory alternatives and / or heterogeneous electronic design (mixed electronic card with different electronic components for each of the functions identified). Consider, for example, the material content of set 1 and set 18 presented on Table 5.12.

Subparts	Materials	Set 1	Set 18	Set 1	Set 18	Set 1	Set 18
		VC SC70-5 (Mass mg)	VC SOT23-5 (Mass mg)	LQFP32 (Mass mg)	UFQFPN32 (Mass mg)	TSSOP8 (Mass mg)	SO8 (Mass mg)
Die attach	Silver		0,057	0,643	0,198		0,925
	Palladium		0,001				
Lead frame Coating	Palladium					0,002	0,007
	Gold					0,002	0,003
Lead frame	Copper	2,829	6,651	51,148	24,288	14,147	24,347
	Palladium	0,003	0,007				
	Silver	0,016		3,528	1,701		
	Gold		0,001				
Wires	Silver			0,289	0,188		
	Gold	0,033	0,157			0,019	0,062
Anode Ball	Tin			1,209	1,659		
Solder (mm2)	Tin	2,97	4,64	51,84	26,01	13,95	20

Table 5.12. Summary of relevant material content (according to elementary flow analysis) in set 1 and set 18. Convenient and inconvenient material quantities of corresponding subparts of confronting components are marked in green and red respectively.

As observed, choosing between a TSSOP8- and a SO8-typed memory is not difficult (the latter use more materials in more quantities than the former). Moreover, the SC70-5 typed voltage comparator belonging to set 1 would be convenient because the quantities of palladium and copper of its lead frame and gold in its wires (all marked in green) are less than the quantities of the corresponding subparts of the SOT23-5 typed voltage comparator in set 18 (marked in red). However, the lead frame of the SC70-5 typed voltage comparator contains silver whereas the other does not. On the other hand, contents of silver and copper in the die attach and lead frame; and silver in the wires of the UFQFPN32-typed microcontroller component of set 18 are fairly less than those of the LQFP32-typed microcontroller component of set 1. Under these conditions, it is difficult to say at a glance what design alternative (set 1 or set 18) is the best and only a further analysis considering not only the impact relevance of materials but also its quantities in the global design is required, to facilitate further decision making (table 5.13).

Material	Impact CF (Kg Sb-eq)	Total in Set 1 (mg)	Total in Set 18 (mg)	Set1	Set18
Gold	52,043	0,054	0,223	1,00	4,13
Silver	1,184	4,476	3,069	1,46	1,00
Palladium	0,571	0,005	0,015	1,00	3
Copper	0,016	68,124	55,286	1,23	1,00
Tin	0,001	1,209	1,659	1,00	1,37

Table 5.13. Impact relevance of materials (in terms of Impact Characterization Factors (CF) of the CML-IA LCIA method) and their absolute and relative contents in set 1 and set 18 (middle and rightmost columns) to be consider for knowing which of the two sets is the best. The lowest content for each material is taken as the content reference (1,00).

Indeed, by observing the high relevance of gold, and its dominant presence in set 18 (4 times more than set 1), it could be concluded that the AD impacts of set18 overcomes those of set 1, (Regardless the

superior content of silver and copper in Set1). This intuition is confirmed by calculating and comparing the relative impact for both sets in SimaPro (figure 5.39a).

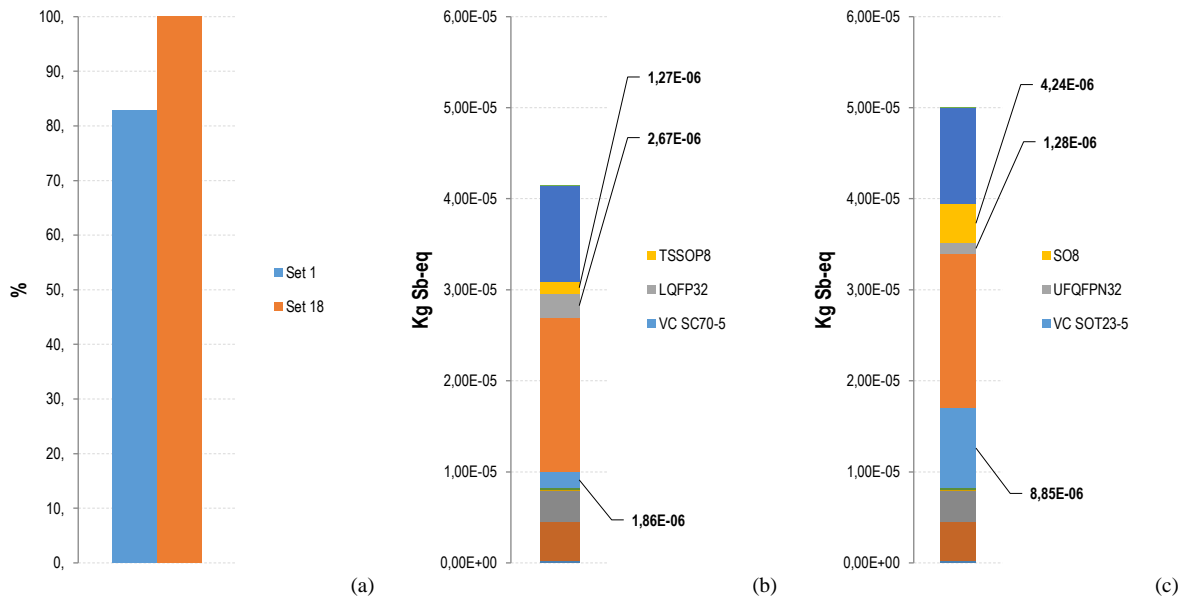


Figure 5.39. (a) Relative AD impacts of set 1 and Set 18. (b) Absolute impacts of the electronic design of set 1. (c) Absolute impacts of the electronic design of set 18. Notice not only the superior impact of the S08-typed memory and the SOT23-5 typed voltage comparator of set 18, but also the impact of the LQFP32-type MCU component of set 1, caused by the silver and copper contents in its lead frame.

However, this conclusion is only valid as long as the gold content of the S08-typed memory and the SOT23-5 typed voltage comparator overcome that of the corresponding TSSOP8-typed memory and the SC70-5 typed voltage comparator; or as long as the silver content in the SC70-5 typed voltage comparator or the LQFP32-typed microcontroller of set 1 does not increase (consider, for example, the impact of silver in the LQFP32 MCU component showed in figure 5.39b). This analysis could get even more complex yet interesting, if one consider more electronic components with different subparts made with more materials (e.g., copper, palladium, tin, etc), in different quantities and with different impact relevance.

In this work, this material-based analysis on electronic components' subparts is further extended to a parametric uncertainty analysis to find at which extended, quantities of different materials may vary until (1) benefits from an optimal design alternative disappears or (2) a worst design enhance to a referential. Bearing this in mind, and in regard of the insights found so far in the context of this case study; this parametric-uncertainly analysis is firstly conducted only on the gold content in the wires of the SOT23-5 typed voltage comparator of set 18, and secondly on other relevant material contents in different subparts of other electronic components altogether. The goal is showing at which extend quantities of this materials may vary until enhanced environmental profile of set 18 with respect of set 1 disappears.

2.1.3.1.1. Analysis of material content shares influence on AD impacts

The proposed uncertainty analysis is conducted with Monte Carlo test by proving different material content share variabilities in several electronic components' subparts. However, before seeing the results from this study, consider figures 5.40 and 5.41 to gain understanding of the mechanism of analysis employed in this section, as well as in next sections. Assuming the gold content percentage in wires of 0,96% of the studied SOT23-5 typed voltage comparator (according to annex 7b) as the typical gold content share in wires of SOT23-5 typed voltage comparators, and a null variation of this share in a sample of different SOT23-5 typed voltage comparators, selected for completing the design of set 18 (defaults conditions); AD impacts of set 18 never enhance to the degree of those of set 1 (Figure 5.40a-b).

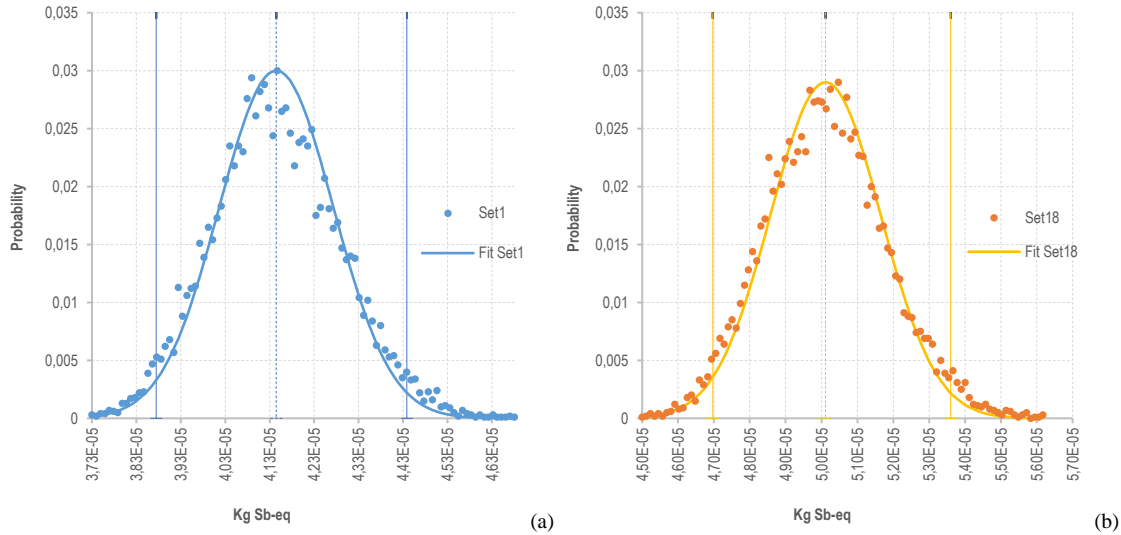


Figure 5.40. AD impact distributions of (a) set 1 and (b) set 18 obtained by separated Monte Carlo tests, including only default uncertain variables in Ecoinvent processes (Data points were fitted to Gaussian function by minimizing the Root of Sum of Squares error (RSS)). Both results show the probability of obtaining the calculated impact of both sets presented in figures 5.39b-c under default conditions. Henceforth, the dotted line depicts the assumed mean impact of sets and the two solid lines represents an interval of confidence of 95%.

Indeed, the probability at which both sets have the same impact—for example 4.50×10^{-05} Kg Sb-eq—is null. Now consider a sample of different SOT23-5 voltage comparators whose gold content shares in wires vary slightly from the mean share content of 0,96% (e.g., with a standard deviation (σ) of 0,005%), holding all their others physical attributes such as their other materials or their total packaging weights constant (*ceteris paribus*). With a 95% of confidence, figure 5.41 shows that under these conditions, there exists an increased likelihood that both sets have the same impact (e.g., 4.35×10^{-05} Kg Sb-eq); in the overlapping area generated by their confidence intervals.

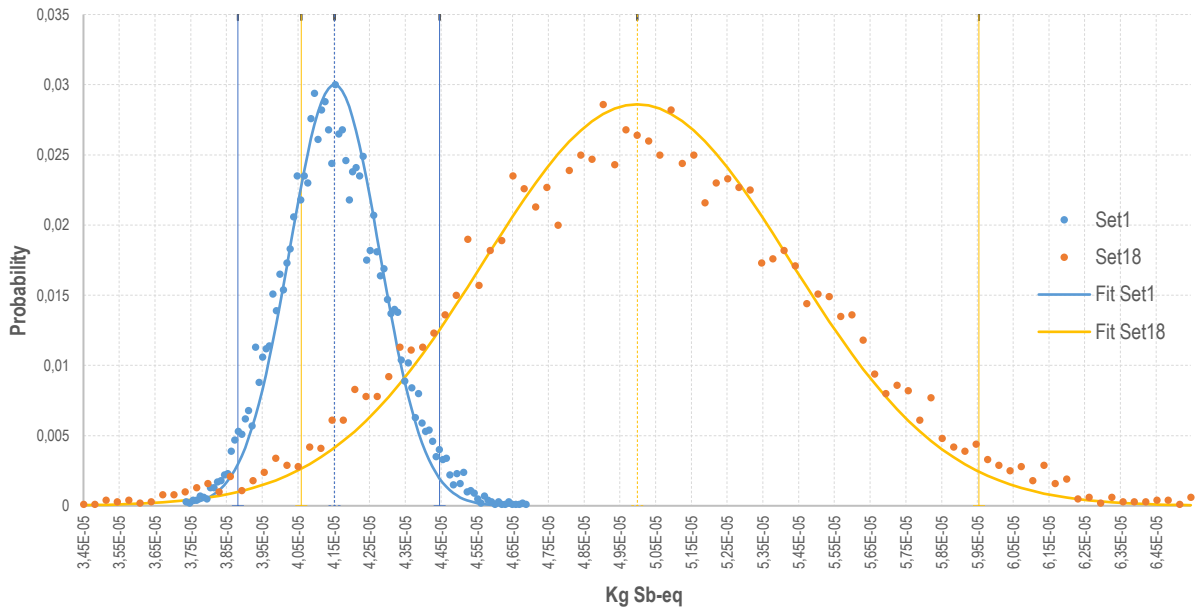


Figure 5.41. Overlapped distributions of AD impacts of set 1 and set 18 (the latter with a little variability of gold content share in wires of its SOT23-5 typed voltage comparator (standard deviation of the gold content share = 0,005%)); showing a likelihood of almost 0,01 that both sets have the same impact (4.35×10^{-05} Kg Sb-eq) with 95% of confidence.

Note that the Monte Carlo test of both sets in figure 5.41 were conducted individually and its interpretation should be taken with prudence. However, it illustrates very well the effects of physical features and their variations on the AD impacts of a design (i.e.; variations in the material content shares on specific components subparts). Figure 5.42 shows a simultaneous Monte Carlo test for both sets with the aforementioned variability on the gold content share of wires ($\sigma = 0,005\%$) of the SOT23-5 typed voltage comparator of set 18. Yet this time, impact calculation of both sets runs side by side and the probability that the design of set 18 outperforms (or not) that one of set 1 is calculated instead (in other words, each Monte Carlo run calculates the impact difference between set 1 and set 18 (impacts of set 1 minus impacts of set 18)); if these differences are all (or almost all) positive, it would indicate high

probability that design of set 18 enhances design of set 1). This is the way by which uncertainty is examined from now on in this work.

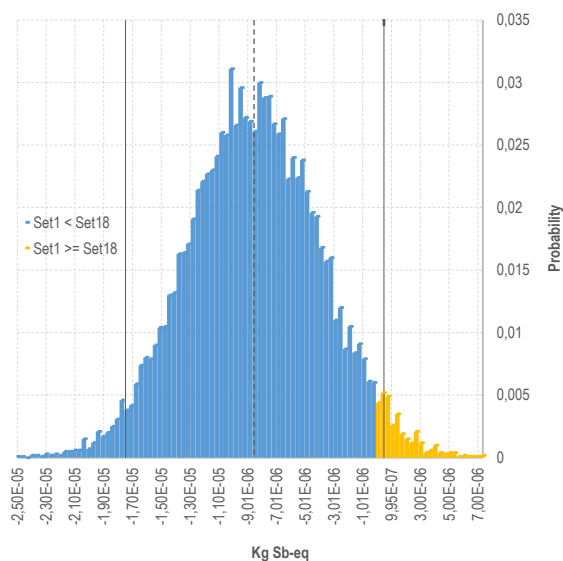


Figure 5.42. AD impact distribution of set 18 outperforming that of set 1 with 95% of confidence (Orange area).

Figure 5.42 shows a little probability that design of set 18 —with a sample of potential SOT23-5 typed voltage comparators with a mean gold content share of 0,96% in wires and a variability of $\sigma = 0,005\%$ — outperforms that one of set 1 (the differences between the AD impacts of design of set 1 and set 18 are mostly negative). Concretely, that means that an alternative SOT23-5 typed voltage comparator, whose gold content share of wires is less than 0,955% (0,005% less than a typical gold content share of wires of 0.96%) will, *ceteris paribus*, rise the chances of design of set 18 to outperform design of set 1.

Although promising, the later variation does not allow design of set 18 to achieve high probabilities to outperform design of set 1, at least with a 95% of certainty. Figure 5.43 shows the chances of set 18 to outperform set 1, considering combined variations on content shares not only of gold, but also of silver, palladium, Tin and copper in selected subparts of its electronic components (see table 5.14); they were chosen according to the relevance and high contents of their materials, as showed by the red cells in table 5.15.

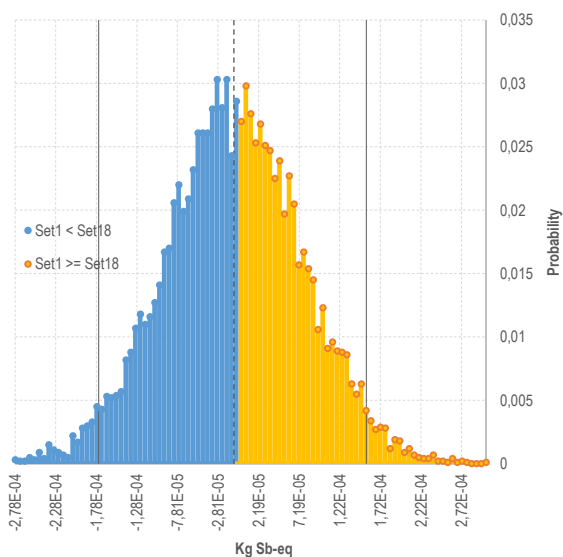


Figure 5.43. AD impact distribution of set 18 (with samples of potential SOT23-5 typed voltage comparators, UFQFPN32-typed microcontrollers and SO8-typed memories, with different variations in the material content share of their subparts) outperforming that of set 1, with 95% of confidence (Orange area, showing the probability that AD impacts of set 1 overcome those of set 18). The probability distribution was obtained by Monte Carlo test on the variations proposed in table 5.14 (10000 test iterations).

Electronic component	subpart	Material	% in IC (consider as the mean shares)	variations (SD)
VC SOT23-5	Wires	Gold	0,96%	0,042%
	Lead frame	Palladium	0,04%	0,013%
UFQFPN32	Anode Ball	Tin	3,38%	0,002%
	Lead frame	Copper	49,49%	0,012%
SO8	Die Attach	Silver	1,16%	0,046%
	Lead frame Coat	Palladium	0,01%	0,005%

Table 5.14. Proposed variations for different material content shares in subparts of electronic components of set 18. The variations were obtained by trial and error tests, considering the dispersion (standard variation (SD)) of material content shares in relation to typical mean values (in this work, assuming the reported content shares seen in annexes 7 to 9 as the typical mean values).

Subparts	Materials	Set 18		
		VC SOT23-5 (Weight mg)	UFQFPN32 (Weight mg)	SO8 (Weight mg)
Die attach	Silver	0,1	0,2	0,9
Lead frame coating	Palladium			0,01
Lead frame	Copper	6,7	24,3	24,3
	Palladium	0,01		
Wires	Gold	0,16		0,06
Anode Ball	Tin		1,7	

Table 5.15. Material quantities of electronic components' subparts of set 18. The red cells show the highest content of a material among all the common subparts of the different electronic components studied in set 18, or material content that is presented only in one electronic component. They were selected for applying the material content share variations showed in table 5.14.

As observed in table 5.14 and 5.15, by using electronic components with small content share variations on materials with high relevance in set 18 (e.g., gold in the wires of the SOT23-5 typed voltage comparator, or silver in the die attach of the SO8-typed memory); and very low content share variations on materials with low relevance, but with high contents in set 18 (e.g., copper in the lead frames of the UFQFPN32-typed MCU), designers can be sure, with 95% of confidence, that design of set 18 have almost the same chances (45,87%) of having the same impact of design of set 1, as it is showed in figure 5.43.

Concretely, this means that designers wanting to improve set 18 should look for alternative SOT23-5 typed voltage detectors, UFQFPN32-typed MCUs, and SO8-typed memories with similar attributes that those of the studied electronic component (i.e.; similar in the majority of their materials, similar in their total weight, etc.); but different with respect of the material content shares of certain of their subparts, as it is suggested in Table 5.16.

Electronic component	subpart	Material	Eco-design targets (With respect to initial content shares)
VC SOT23-5	Wires	Gold	Less than 0,919%
	Lead frame	Palladium	Less than 0,027%
UFQFPN32	Anode Ball	Tin	Less than 3,378%
	Lead frame	Copper	Less than 49,475%
SO8	Die Attach	Silver	Less than 1,110%
	Lead frame Coat	Palladium	Less than 0,004%

Table 5.16. Recommended variations that alternative SOT23-5 typed voltage comparators, UFQFPN32-typed microcontroller and SO8-typed memories should pursue to improve the design of set 18 facing up to the design of set 1. The eco-design targets were obtained by subtracting the proposed variations in table 5.14 (the standard variation values) from the typical material content shares (The reported content shares seen in annexes 7 to 9).

2.1.3.2. Importance of materials and physical attributes for the GW impact category

For illustration purposes and because the significant relevance of the PCB in the GW impacts of ICT devices, evidenced in literature; the following analysis consider the land patterns of the studied electronic components to observe the size variations and the GW impacts of the PCB component of the different design sets seen previously. This analysis focuses on the internal die of the studied electronic components too, as different works in literature point out the significant contribution of this subpart to the final GW impact of ICT devices. This is done by using the LCA implementation proposed in previous chapter (section 4.1), which contains a method to find the surface of the internal die, based on the Ecoinvent methodology. Figure 5.44 shows the results of this analysis (the relative GW impacts of all possible design set combinations of the memory-based version with different PCB sizes).

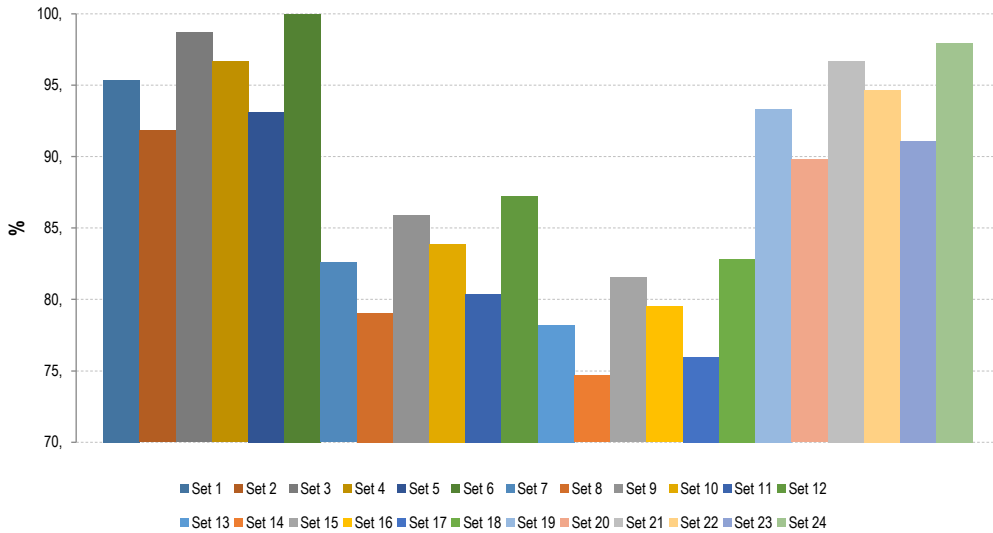


Figure 5.44. Relative GW impact of all design sets for the NFC-memory-based version (24 combinations) with a variable PCB component. The functional unit is defined as “production of one EHS sensor system device in its memory-based version”

This time, for the GW impact category, the best and the worst design alternatives are set 14 and set 6 respectively (the latter with a relative impact of more than 25% with respect to the former, as showed in figure 5.44). A detailed inspection of impacts of set 6 in figure 5.45a shows that its biggest impact contributors are its PCB, its LQFP32-typed microcontroller and its SO8-typed memory components (With an approximate impact contribution of more than 46%, 24% and 8% respectively).

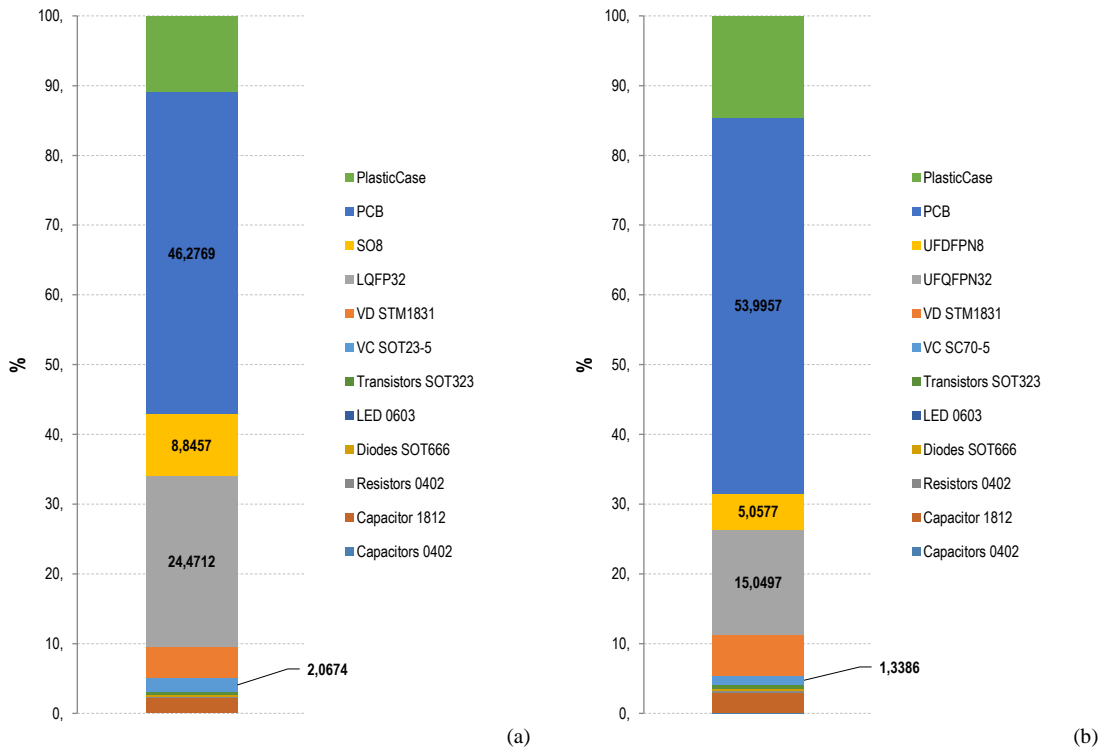


Figure 5.45. Detailed GW impact contributors of (a) the worst design alternative (Set 6), and (b) the best design alternative (Set 14). Notice that electronic components are specified by packaging type.

While the land patterns of these electronic components, together with that one of the SOT23-5 typed voltage comparator, increase the PCB size of set 6 in approximately 11,8% (786,81 mm², with respect to the PCB size of the referential design of set 13 (704 mm²)); the land patterns of the SC70-5 typed voltage comparator, the UFQFPN32-typed MCU and the UFDFPN8-typed memory reduce the PCB size of the design set 14 in almost 2,7% (685,55 mm²). Such variations explain to some extent the impact gap between set 6 and set 14 (Figure 5.46).

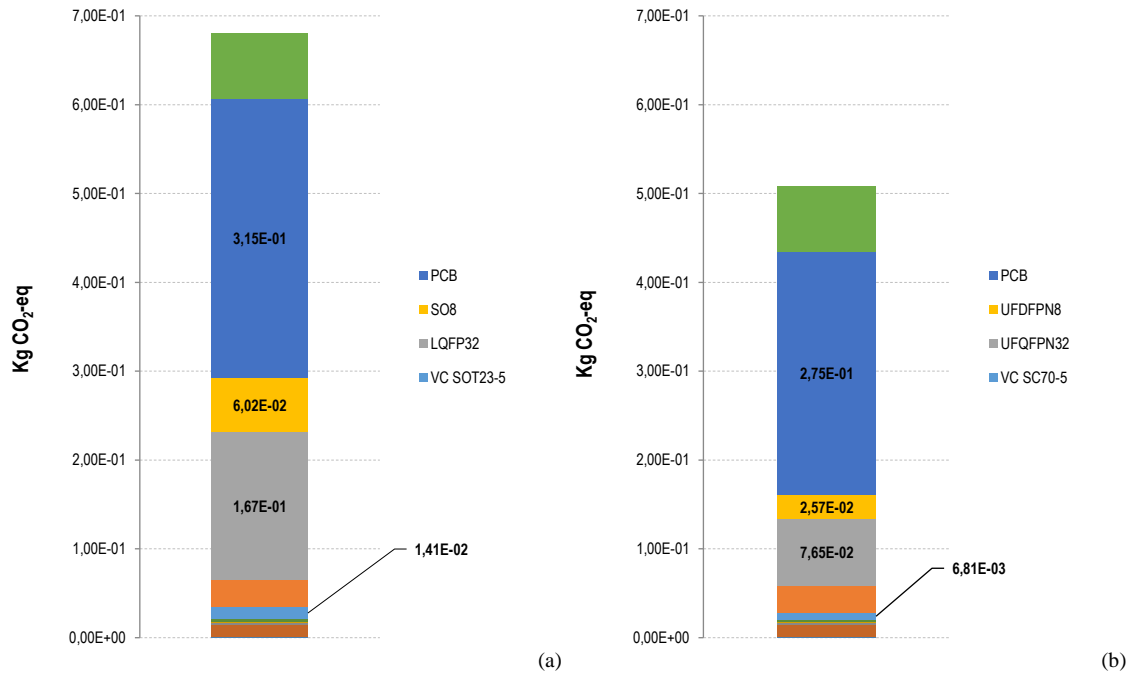


Figure 5.46. Absolute GW impact of set 6 (a) and set 14 (b).

Besides of this, an initial analysis on the relevant emissions involved in the production of electronic components of set 6 shows that another of its big impact contributors is the internal die of its LQFP32-typed microcontroller (with an absolute impact of $5,40 \times 10^{-02}$ Kg CO₂-eq, according to table 5.17). From these findings, the iterative analysis seen previously in section 2.1.3.1 is applied again to reveal further impact contributors for the GW impact category, but this time, focusing on the relevant emissions (CO₂ and CH₄) generated in specific production processes of the studied components of set 6 and set 14. Table 5.17 shows the results of this analysis.

Iteration	Process	Set 6					Set 14				
		Electronic component	Subpart	Abs impact CH ₄ (Kg CO ₂ -eq)	Abs impact CO ₂	Weight (mg) or area	Weight (mg) or area	Abs impact CO ₂	Abs impact CH ₄ (Kg CO ₂ -eq)	Subpart	Electronic component
1	Wafer production	VC SOT23-5	Die (mm2)	1,64E-04	2,05E-03	0,072	0,088	2,51E-03	2,02E-04	Die (mm2)	VC SC70-5
		LQFP32	Die (mm2)	4,33E-03	5,40E-02	1,885	1,527	4,19E-02	3,36E-03	Die (mm2)	UFQFPN32
	SO8	Die (mm2)	9,72E-04	1,21E-02	0,425	0,500	1,42E-02	1,14E-03	Die (mm2)	UFDFPN8	
	Electricity	PCB	PCB (mm2)	1,48E-02	1,71E-01	787	686	1,49E-01	1,29E-02	PCB (mm2)	PCB
2	Gold	VC SOT23-5	Wires	1,22E-04	2,21E-03	0,157	0,033	4,65E-04	2,56E-05	Wires	VC SC70-5
			Lead frame	7,73E-07	1,41E-05	0,001					
		SO8	Wires	4,80E-05	8,73E-04	0,062					UFDFPN8
			Lead frame coat	2,35E-06	4,28E-05	0,003					
3	Silver	VC SOT23-5	Die Attach	1,73E-07	4,47E-06	0,057					
							0,016	4,64E-06	3,63E-07	Lead frame	VC SC70-5
		LQFP32	Die Attach	1,46E-05	1,86E-04	0,643	0,198	5,74E-05	4,49E-06	Die attach	
			Lead frame	8,00E-05	1,02E-03	3,528	1,701	4,93E-04	3,86E-05	Lead frame	UFQFPN32
			Wires	6,55E-06	8,38E-5	0,289	0,188	5,45E-05	4,26E-06	Wires	
SO8	Die Attach	2,10E-05	2,68E-04	0,925	1,108	3,21E-04	2,51E-05	Die attach	UFDFPN8		

Table 5.17. Results of the combined analysis (Elementary flow and sensibility analysis) showing the big GW impact contributors of set 6 and set 14, according to the CO₂ and CH₄ emissions involved in the production processes of the studied electronic components or subparts. For simplicity, mixed market (GLO) for gold, silver, electricity and wafer production is showed.

As observed in table 5.17, the main GW impact contributors of sets are attributed to the electricity (mixed market for medium voltage) used for the PCB production and for the wafer production of internal dies. Mixed markets for gold and silver used in several electronic components subparts appear too, but this time, their contributions to the total GW impacts of both sets are marginal. However, notice that gold is a decisive substance when internal dies in confronted IC components are almost identical. For example, the great GW impact difference between the SO8- and the UFDFPN-typed memories (both with an absolute GW impact of $6,02 \times 10^{-02}$ and $2,57 \times 10^{-02}$ Kg CO₂-eq respectively, as showed in figure 5.46a-b); is explained by the exclusive presence of gold in the former, and not by the surface of its internal die (which differs from that one of the latter only in a factor of 1,17, as observed in table 5.17). In the case of silver, observe how its low content in the lead frame of the SC70-5 typed voltage comparator (0,016 mg) generates a reduced total impact of $6,81 \times 10^{-03}$ Kg CO₂-eq, compared to the

impact caused by the silver content (0,057 mg) in the die attach of the SC70-5 typed voltage comparator (1,41 x 10⁻⁰² Kg CO₂-eq according to figure 5.46a). Notice that both components have internal die sizes almost identical (different only in a factor of 1,22).

With the aim of applying these findings in heterogeneous electronic designs (mixed electronic cards with different electronic components for each of the functions identified), the next section presents an analysis on the die surfaces; and the gold and silver contents variability of different electronics components proposed for set 12 and set 20. However, before starting with this, consider first some useful aspects of these sets detailed in table 5.18 and figure 5.47.

Subparts	Materials	Set 20	Set 12	Set 20	Set 12	Set 20	Set 12
		VC SC70-5 (Mass mg)	VC SOT23-5 (Mass mg)	WLCSP36 (Mass mg)	TFBGA64 (Mass mg)	UFDFPN8 (Mass mg)	SO8 (Mass mg)
Die	Die area (mm ² / mg)	0,015	0,004	0,952	0,030	0,031	0,005
Wires	Gold (Au)	0,55%	0,96%		0,548%		0,078%
Solder balls	Silver (Ag)			0,24%	0,125%		

Table 5.18. Relevant material content shares and internal die area to weight ratios of the studied electronic components' subparts of set 20 and set 12. The red cells mark the highest internal die surface ratios or material content shares among all the common subparts of the different electronic components studied in both sets. They were selected for suffering further variations in the analysis presented in the next section (table 5.19).

By bearing in mind that the land patterns of the electronic components of set 12 increase the PCB size in 2,36% (720,6 mm², with respect to the PCB size of the referential set 13 (704 mm²)), and that the land patterns of the electronic components of set 20 reduces the PCB size in almost 6% (662,5 mm²) on the one hand and, considering that the die area ratios of all the electronic components of set 20 overcome those of set 12 (specially that one of the WLCSP36 MCU component, as showed in table 5.18) on the other hand; one cannot deduct at a first glance which set outperforms the other and further impact calculations are required (Figure 5.47).

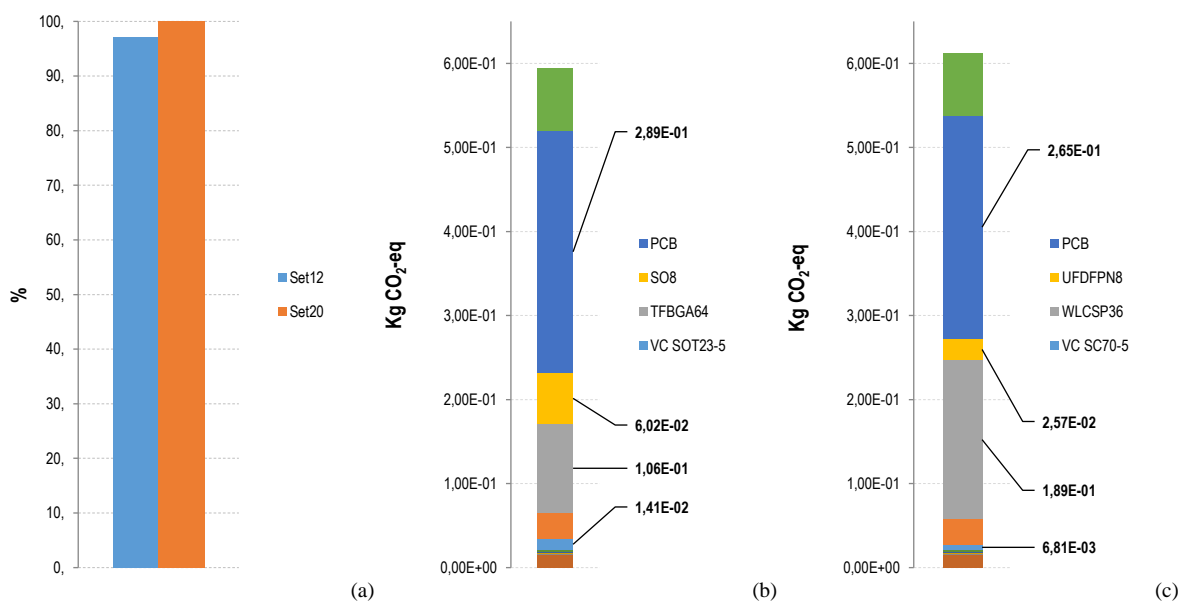


Figure 5.47. (a) Relative GW impacts of set 12 and Set 20. (b) Absolute GW impact of set 12. (c) Absolute GW impact of set 20.

The figure 5.47 shows that the impact of the larger PCB in set 12 (figure 5.47b) is counterbalanced by the impact of the internal die of the WLCSP-typed microcontroller in set 20 (figure 5.47c), making the GW impacts of both sets almost identical (figure 5.47a). As observed, the large die area ratio of the WLCSP-typed Microcontroller component (0.952 mm² per mg) makes the design of set 20 slightly unfavorable with respect to the design of set 12 (in despite of its reduced PCB size). Moreover, the relative gains of set 12 could be easy lost, if one consider disadvantageous variations in the quantity of gold in the wires, and silver in the solder balls of its TFBGA-typed microcontroller component (both substance with a share of 0,548% and 0,125% respectively, according to table 5.18 and annex 8b). In

this way, a two-part uncertainty analysis is conducted in the next section to find (1) at which extend the content of gold and silver in wires and solder balls of alternative TFBGA-typed microcontrollers for set 12 may vary, until its favorable design disappears and (2) at which extend the internal die area ratio in the WLCSP-typed microcontroller may reduce, so that the design of set 20 enhance to the degree of set 12.

2.1.3.2.1. Analysis of material content shares and die area influence on GW impacts

As stated before, this analysis is conducted in two parts. The first part considers gold and silver content uncertainties in wires and solder balls of the TFBGA-typed microcontroller component of set 12 and the second part considers a variation in the area-mass ratio of the internal die of the WLCSP-Typed microcontroller component of set 20. Variations of the aforementioned features are summarized in table 5.19 and effects of applying them are shown in figure 5.48.

Electronic component	Subparts	Physical features	Internal die are ratio or material content share (mean)	Variations (SD)
WLCSP36	Die (ratio mm ² / mg of IC)	Area	0,952	0,1
TFBGA64	Wires	Gold	0,548%	0,5%
	Solder balls	Silver	0,125%	1,0%

Table 5.19. Proposed variations for different internal die area ratios of WLCSP-Typed microcontrollers of set 20, and variations of material content shares of TFBGA-Typed microcontrollers for set 12. The variations were obtained by trial and error tests, considering a data dispersion (standard variation) in relation to a typical mean value (here assuming the reported values in annexes 8b and 8d).

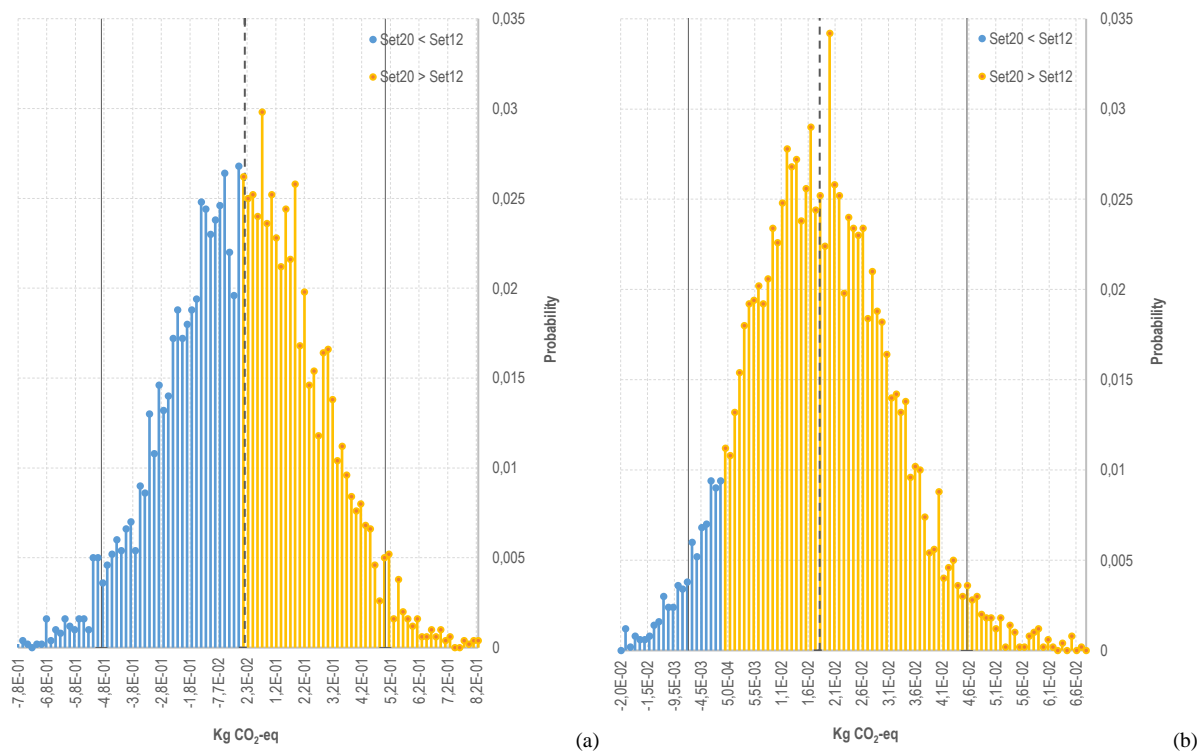


Figure 5.48. (a) GW impact distribution of the design of set 12, with a sample of potential TFBGA-typed microcontrollers with different variations in the material content shares of their subparts, getting worse to the point of being an inconvenient design compared with the design of set 20 (blue area). (b) GW impact distribution of the design of set 20, with a sample of potential WLCSP36-typed microcontrollers with different variations in their internal die area ratios, outperforming that one of set 12 (blue area). The probability distributions were obtained by Monte Carlo test (10000 test iterations) applied with the proposed variations of typical values showed in table 5.19.

Figure 5.48a shows high probabilities (almost 50%), that the slight advantage of the design of set 12 may be compromised if the gold content share in the wires and the silver content share in the solder balls of its TFBGA-typed microcontroller component increase to 1,048% and 1,125% respectively (with 95% of confidence). Moreover, Figure 5.48b shows a little, yet promising probability (more than 8%) that the design of the set 20 outperforms that one of set 12, if its area-mass ratio die ratio reduce only in 10% (0,852 mm² per mg). These aspects can be adapted in eco-design targets that designers need to look for in the context of the case study “Smart monitoring” (table 5.20); but always being cautious that other physical attributes such as the total weight and the land patterns of the alternative components, or the size of the PCB do not change or do not vary much (*ceteris paribus*).

Electronic component	Subparts	Physical features	Eco-design targets (With respect to initial die area ratios or content shares)
WLCSP36	Die (ratio mm ² / mg of IC)	Area	Less than 0,852
TFBGA64	Wires	Gold	At most 1,048%
	Solder balls	Silver	At most 1,125%

Table 5.20. Variations that alternative WLCSP-typed microcontrollers should pursue to improve the design of set 20 over the design of set 12; and limits in the gold and silver content shares in wires and solder balls of alternative TFBGA-typed microcontrollers should respect at most, in order to keep the convenient design of set 12 in relation to the design of set 20. The eco-design target for the die area ratio of the WLCSP36-typed MCU component was obtained by subtracting the proposed variations in table 5.19 (the standard variation values) from the typical die area ratio of the component (detailed in annex 8d). The eco-design target for the gold and silver content shares were obtained by adding the proposed variations in table 5.19 (the standard variation values) to the typical material content shares presented in table 5.19 and found in annex 8b.

2.1.3.3. Recommendations for the case study “Smart monitoring” in the context of physical attributes

The analysis of materials and physical attributes facilitates partially the decision making process and/or the establishment of eco-design targets. As observed in previous sections, two components may do the same function with the same performance, but their materials and physical attributes may provokes very different results. This is due to few yet key variations that designer should look for sensibility analysis whenever the information of these attributes is available.

In the context of the case study “Smart monitoring”, designers should explore these aspects in relevant design sets, confront their advantages and disadvantages, and find a good balance of both. For instance, figure 5.49 contrasts the worst and best design sets for the AD and the GW impact categories with the referential design of this case study (set 13).

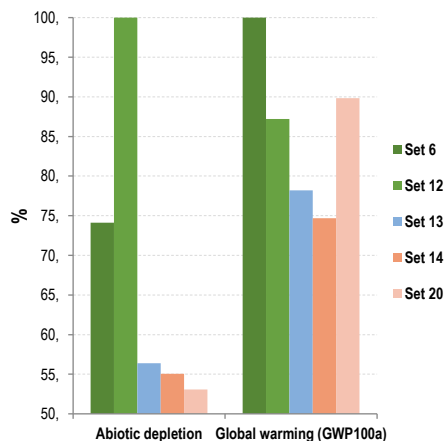


Figure 5.49. AD and GW relative impacts of the respective worst and best design sets (set 12 and 20 for AD; and set 6 and 14 for GW) contrasted with the AD and GW relative impacts of the referential design set (set 13).

As observed in figure 5.49, the referential set 13 has already an ecofriendly design, compared to the worst cases in both impact categories.

- In order to improve it and avoid further laborious redesign, designer should consider the alternative design of set 14, and replace only the current EEPROM memory component in set 13 (a TSSOP8-typed memory) by a UFDFPN-typed EEPROM memory (that one that shapes the design set 14).

Table 5.21 compares both components in the contexts of the studied physical attributes analyzed in previous sections.

Subparts	Materials or physical attributes	TSSOP8	UFDFPN8
Die	Die area ratio (mm ² / mg)	0,6975	0,4997
Package	Land pattern (Including standard IPC1753B in mm ²)	7,6 x 4,1	4,1 x 3,1
Die attach	Silver (mg)		1,108
Lead frame	Palladium (mg)	0,002	0,001
Coating	Gold (mg)	0,002	
Lead frame	Copper (mg)	14,147	2,918
Wires	Copper (mg)		0,018
	Gold (mg)	0,019	
	TOTAL Gold (mg)	0,021	0,000
	TOTAL Silver (mg)	0,000	1,108
	TOTAL Palladium (mg)	0,002	0,001
	TOTAL Copper (mg)	14,147	2,936
	IC weight (mg)	34,00	16,00

Table 5.21. Physical attributes of the TSSOP8- and the UFDFPN8-typed memories of the referential set 13 and alternative set 14 (both design sets are identical except from these components. For a detailed overview of both components, see annex 9a and 9b).

For the AD impact category, table 5.21 shows that benefits of the studied UFDFPN8-typed memory come from the null use of gold in its lead frame coat and wires. Also, it contains only half of palladium on its lead frame coat and almost a fifth of the copper content in its lead frame compared to the corresponding subparts of the TSSOP8-typed memory used in set 13. On the other hand, notice the exclusive presence of silver in the die attach subpart of the UFDFPN-typed memory; Designers should pay attention on this content since it could be penalizing in design alternatives pretty different from that of set 13 (i.e.; different microcontrollers or voltages detectors).

For the GW impact category, the benefits of the studied UFDFPN8-typed memory come from its reduced die area ratio compared to that one of the TSSOP8-typed memory and mainly from its reduced land pattern area (almost half of that one of the TSSOP8-typed memory). This later aspects leads to use a smaller PCB than that one used in the referential set 13 (685,55 mm² instead of 704 mm², according to annex 6). However, designer should also be cautious with the reduced packaging size of the UFDFPN8-typed memory, as it could be more difficult to separate it from the PCB in the EoL phase, as it was saw for similar-sized components in previous chapter.

➤ On the other hand, although there exists a clear advantage of set 20 over set 14 in the AD impact category (both with similar electronic design except from their microcontroller components), designers who would be considering replacing the microcontroller component of set 13 should avoid using the WLCSP-typed microcontroller used in set 20, as its internal die causes significant impacts in the GW category, as showed in figure 5.49. Alternatively, they should consider alternative components of this packaging technology, by evaluating several variations of their die area to mass ratio in order to see, for example, at what extend the die surface should reduce to compete with the enhanced design of set 14 in the GW category.

This later aspect leads to discriminatory strategies based on physical features of dissimilar packaging technology, depending on the designers' goals and especially when information is very limited. For example, while BGA-typed components usually use unfavorable materials such as gold and silver in wires and die attach subparts respectively (figure 5.50a), Chip Scale Package (CSP) typed components use advantageous materials such as copper in distinctive subparts (DRL and UBM subparts, figure 5.50b).

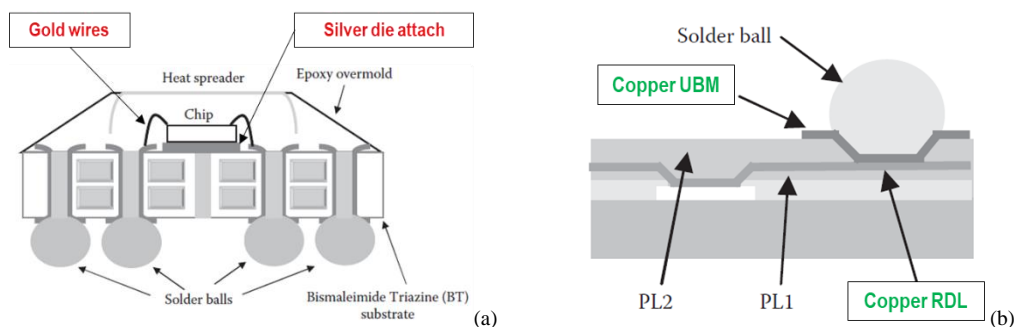


Figure 5.50. Cross section views showing the basic subparts of (a) a BGA-typed component, and (b) a CSP-typed component. Figures extracted and adapted from [176].

However, the CSP technology is also characterized by the dominant presence of the internal die, which usually covers more than 80% of the total packaging size (Figure 5.51).

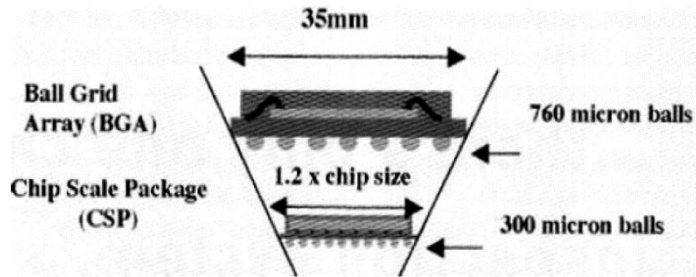


Figure 5.51. Cross section view of a BGA and CSP components. Both devices has the same die size, but the latter differs mainly in the reduced package size and weight, which implies that bigger die areas are needed per mass produced. Figure extracted from [177].

- thus, designers wanting to improve the environmental profile of a design in the AD impact category should consider not only replacing directly certain conflicting components by CSP-typed components, but also trying to reduce the GW impacts of other components; for example by trying to gains marginal benefits from reducing their gold and silver contents or by using their reduced land patterns, so that the final size of the PCB can be reduced.

In line with this later aspect, another recommendation would be optimizing the arrangement of electronic components according to more convenient IPC-standard versions, as it is showed in figure 5.52.

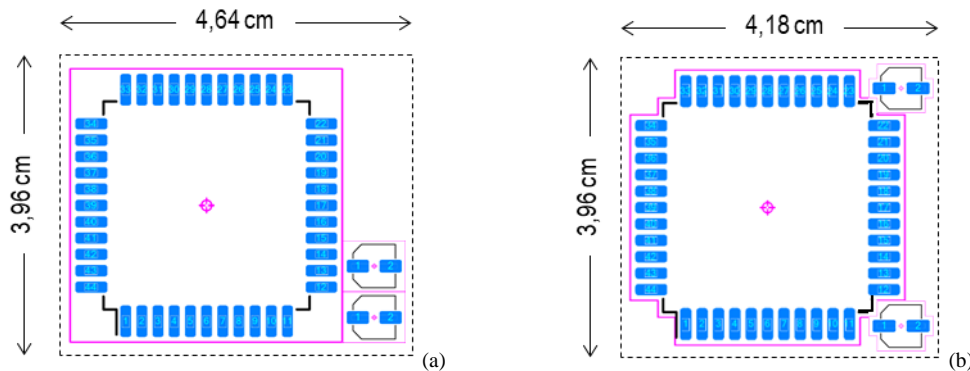


Figure 5.52. Arrangement of three SMD electronic components under the IPC1753B standard (a), and the IPC1753C standard (b). Notice that the particular perimeter of the latter gives more flexibility for reducing the final size of the PCB component of a design. Both figure are in scale 1:1.

In any case, designers should be cautious when using BGA-typed components in general, since high pin densities per mm^2 may lead to the necessity of using more PCB layers, as it was pointed out in the section 2.1 of the previous chapter.

2.1.4. Evaluation of electronic component alternatives through technical attributes

This section focuses on the endurance rate of EEPROM memories to illustrate the relevance of this technical feature to the eco-design of intermittent IoT devices. It considers the previous section 2.1.1 focused on the data and information design of the case study “Smart monitoring”, and the endurance rate (writing cycle per memory block) of NFC-EEPROM memories. Specifically, this section compares the life cycle (manufacturing, use and recycling phases (worst scenario)) of the NFC-memory-based version (referential design or set 13) with the life cycle of the alternative Bluetooth-based version presented in section 2.1.2; and determines the limits by which one could be better to the other, on the basis of an uncertainty analysis of the intensity use of the object. The functional unit is defined as “Monitoring the usage rate of an object (unspecified) during 300 hours (or $1,08 \times 10^6$ seconds)”.

For this, two essential aspects need to be explained: the writing cycling schema in the EEPROM memory for the NFC-memory-based version, and the energy consumption of the BLE module of the smartphone for the BLE-based version (energy consumption that considers only the discovering mode, as data application in this version is embedded in advertising BLE packets). For the first aspect, the reader should recall the data & information flow design presented in the previous section 2.1.1 (second alternative), and consider the memory block organization of the NFC-EEPROM memory component in figure 5.53b.

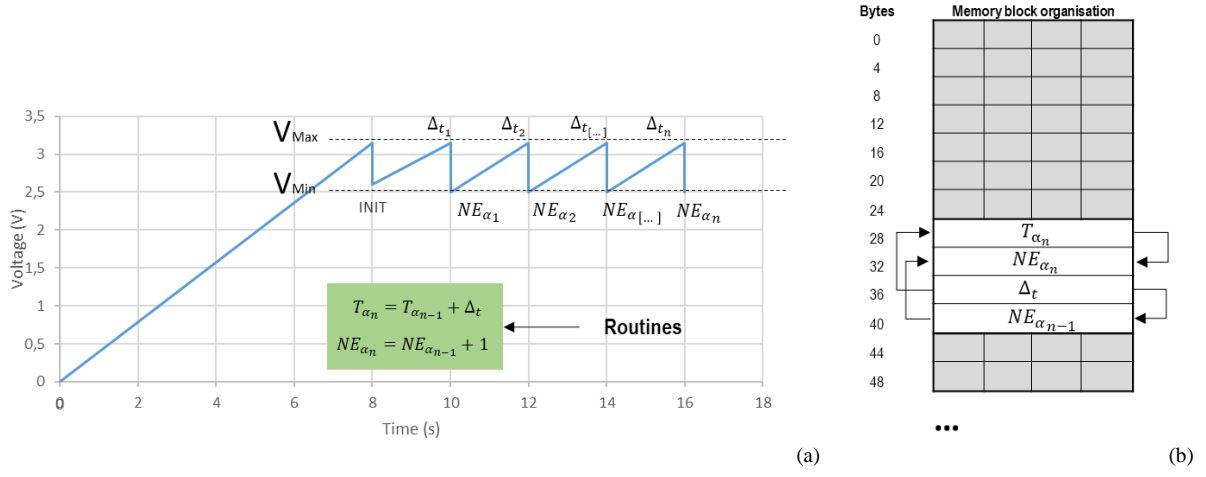


Figure 5.53. (a) Recalling of the intermittent routines (second alternative) for the NFC-memory-based version seen in section 2.1.1. (b) Actual organization of the memory blocks of the studied EEPROM memory used in set 13. Each block (line) is composed of 4 bytes; gray blocks contain fixed, referential data of the application (e.g., identifiers of the application) and white blocks represent the actual data of the application.

As observed, the memory-based version needs four memory blocks to work. Each memory block represents a variable of the main program (T_{α_n} , Δ_t , NE_{α_n} , and $NE_{\alpha_{n-1}}$), which is updated (rewritten) in every charging-discharging cycle of the sensor system, as is showed in figure 5.53b (whenever energy is sufficient, the program updates the differential of time variable (Δ_t) on the block of the 36th byte with a new value and later the value of $NE_{\alpha_{n-1}}$ on the block of the 40th byte, with the previous value of NE_{α_n} in the i th charging-discharging cycle; so that the microcontroller of the device calculates new values for T_{α_n} and NE_{α_n} by executing recursive routines, making use of the block of the 28th byte and the block of the 32nd byte sequentially, as showed by the right arrows in figure 5.53b).

In this sense, and by considering the functional unit defined above: “Monitoring the usage rate of an object (unspecified) during 300 hours (or $1,08 \times 10^6$ seconds)”, the number of writing cycles executed in a block of the EEPROM memory component of set 13 could be determined as follows:

$$WC_{Block} = \frac{W_r \times 1,08 \cdot 10^6 \text{ secs}}{4} \quad (5.14)$$

Where:

WC_{Block} = Writing cycles or number of times that a memory block is rewritten

W_r = frequency at which the system rewrites data in a memory block (in seconds)

For the second aspect, the energy required by the BLE module of the smartphone for accomplish the aforementioned functional unit could be calculated as follows:

$$E_{Rx(BLE)} = \left(\frac{P_{Rx} \times 300 \text{ hrs}}{B_p} \right) \times 1\% \quad (5.15)$$

Where:

$E_{Rx(BLE)}$ = Energy consumption of the BLE module of the smartphone in the discovering mode (in kWh)

P_{Rx} = Typical power consumption of a standard bluetooth module of a smartphone in the discovering mode (in kW)

B_p = Real power output of the battery of a smartphone assuming a discharging rate (in %)

Due to the lack of studies showing the energy consumption of the Bluetooth technology in its specific BLE version and in its different states, Equation 5.15 estimates the energy consumption of the BLE module of the smartphone ($E_{Rx(BLE)}$) by multiplying the typical power consumption of the classical Bluetooth technology in the discovering state ($P_{Rx} = 223 \text{ mW}$ or $2,23 \times 10^{-4} \text{ kW}$, according to Perrucci, G.P. [166]) with the reduced energy consumption rate of 1%, claimed in technical specifications of BLE [178]. Also, B_p consider only 95% of the power output of a Li-ion battery, as 5% would be lost due self-discharging, as suggested by Tarkoma, S. et al [179].

2.1.4.1. Influence of memory endurance on environmental design

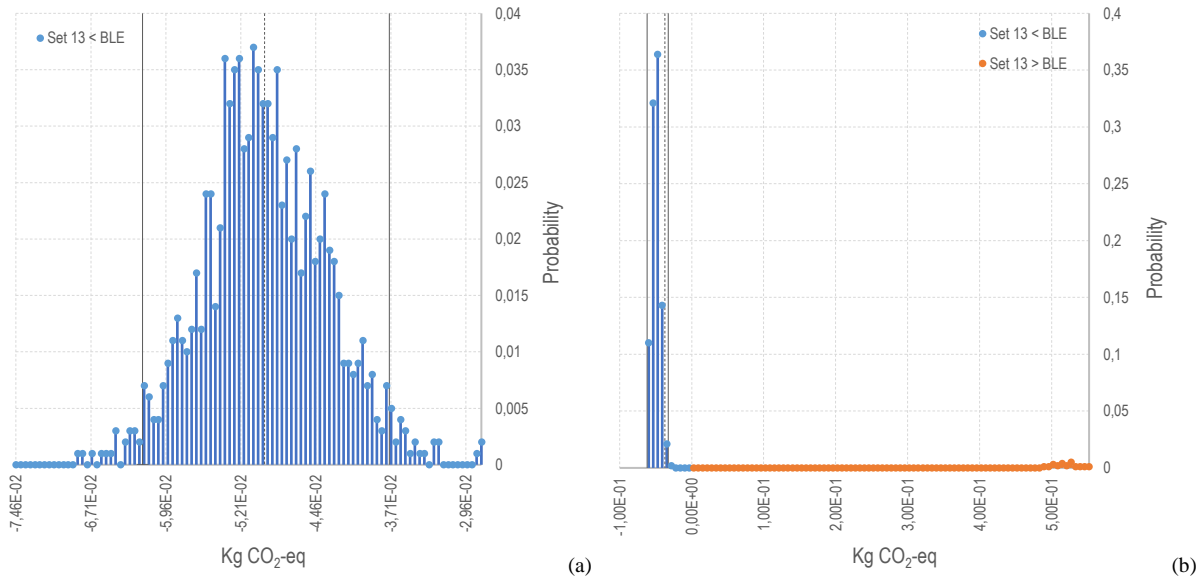
The uncertainty analysis for this section considers the life cycle of the NFC-memory- and BLE-based versions. Although several technical features may exist in the context of the case study, in this work, one focuses on the memory endurance as a critical feature that determines the lifetime of the whole prototype.

The use phases of both versions consider equation 5.14 and 5.15 respectively, and imposes a condition: if the writing cycles of a memory block (WC_{Block}) overcome the maximal writing cycles reported in the technical specifications of the memory component of set 13 (1MM of writing cycles, as reported in its datasheet [136]), before accomplishing the use period defined in the functional unit; it is assumed that this memory is no longer reliable, provoking the early replacement of the device. Thus, this section examines the variations of the writing frequency (W_r) of memory blocks for the referential design (set 13), according to empirical data of different use intensities of the object presented in table 5.22.

Use intensity	W_r (writings / Sec)				Variations (%)
	Minimum	Maximum	Mean	SD	
Very low	0,57	1,94	1,17	0,47	40,2%
Low	0,81	4,52	1,88	0,95	50,5%
Moderate	1,44	7,59	2,96	1,51	51,0%
High	2,59	7,96	3,6	1,29	35,8%

Table 5.22. Empirical writing rate values (W_r) obtained from different use intensities of the object (field tests under controlled environment). The proposed variations consider the typical writing frequency of different use intensity scenarios (mean) \pm the correspondent standard variation (SD).

Figure 5.54 presents the distribution of the GW impact difference of the BLE version (with an estimated energy consumption of the smartphone of $7,04 \times 10^{-04}$ kWh for 300 hrs) and the referential memory-based version (set 13) with a very low, low, moderate and high use intensity of the object (AD impact comparison shows similar behavior).



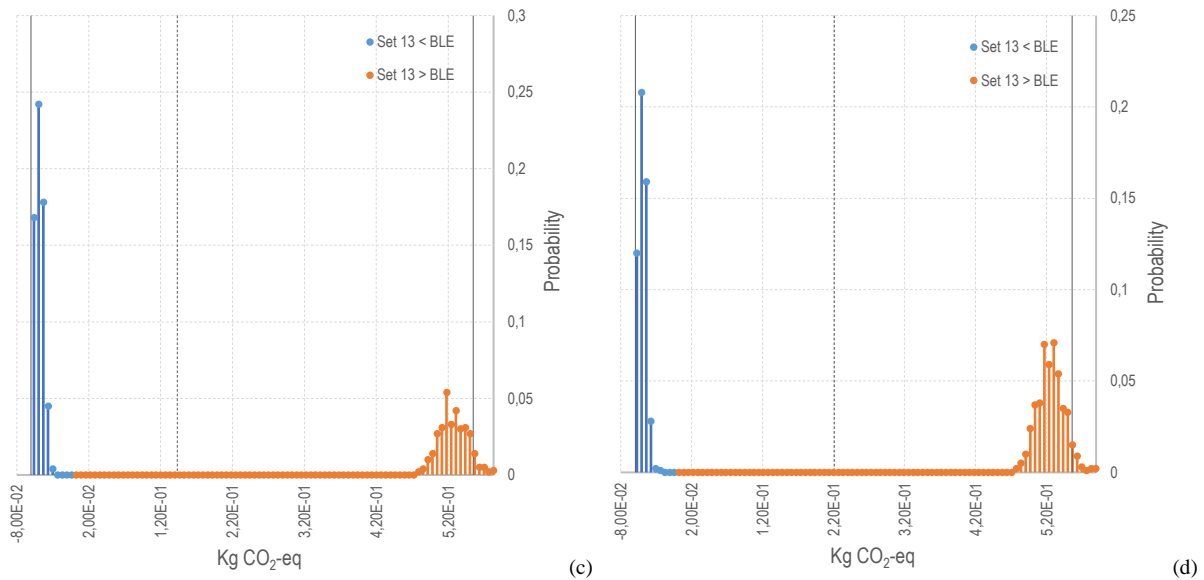


Figure 5.54. GW Impact distribution for the writing rate (W_r) variation of the referential design of set 13 with (a) very low use intensity of the object, (b) low use intensity, (c) moderate use intensity and (d) High use intensity. As explained in previous sections, the uncertainty analysis is based on Montecarlo test (10000 runs) that calculates the probability that the impact of the BLE version overcomes that one of referential set 13 (the blue area), or the contrary situation (orange area).

Figures 5.54b, 5.54c and 5.54d present bimodal impact distributions, as Monte Carlo runs test for two mutually exclusive events (the writing cycle of the memory of the set 13 (W_r) overcomes the writing cycles of a block (WC_{Block}) of its memory component or not). As observed in figure 5.54a, an increasing variation of more than 40% in the mean writing frequency of a very low use intensity scenario do not provoke the depletion of a memory block, and no further replacement of the device is required (with 95% of confidence). This is also the case for the low use intensity scenario, with the difference that — with a very low probability— a maximum value for the writing frequency (i.e.: 4,52 writings per second) would lead to an early depletion of a memory block. On the other hand, the variation of the writing frequency in a moderate use intensity scenario becomes relevant, especially if the typical writing frequency mean increase in 51%, as observed in figure 5.54c. Moreover, the probability that the impact of set 13 overcomes that one of the BLE version (that is, that the set 13 is replaced once) increase considerably, when the typical writing frequency mean in a high use intensity scenario increases in 35,8%, as observed in figure 5.54d.

Concretely, this means that under the data design flow showed in the previous section 2.1.1 (second alternative), and a constant energy consumption of $2,23 \times 10^{-04}$ kWh for discovering BLE messages in the smartphone; it is improbable that a typical very low, or low use intensity scenario of the object lead to the early replacement of the device and, consequently, that the impact of the NFC-memory-based version never overcomes that one of the BLE version. However, this conclusion should be adopted carefully, as combined use patterns (mixed low-high intensities) may occurs in reality.

2.1.4.2. Recommendations for the case study “Smart monitoring” in the context of technical attributes

The section above use on-field data to illustrate the relevance of data design for the referential flow of IoT systems in terms of technical features of EEPROM memories (writing cycle rates) and BLE modules (in this case, energy consumption of the BLE module of a smartphone in the discovery state).

- For a very low and low use intensities of the object, it is recommended keeping the NFC-memory-based version, and for a moderate intensity scenario, designer should consider advanced memory management, software-based routines such as Wear Leveling⁹, in order to benefit from unused memory blocks and assure the optimal functioning of the device within the use period of the object defined in the functional unit.
- For a high use intensity, it is recommended redesign the data flow of the IoT system, or switching to the BLE-version. In the case of adopting the BLE alternative, designers should

⁹ Wear-Leveling (WL) is a software-based technique that evenly distribute the burden of repeated writing cycles over a larger set of memory block [248].

consider redesign this version by focusing on its electronic design, since its relative impact (figure 5.55) is explained by few components (figure 5.56) and not by its energy needs in the use phase (less than 0,001% and 0,1% for the AD and GW impacts categories respectively).

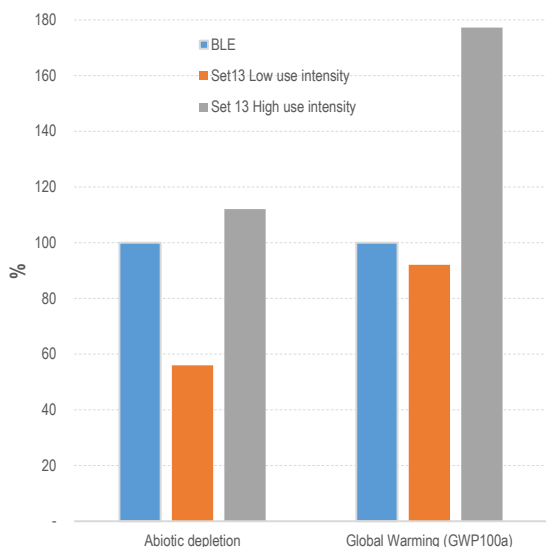


Figure 5.55. Relative impact of the life cycle of the BLE version (REF) and the memory-based version (set 13) with a low and high use intensities. In a high-use intensity scenario, the device under the referential design (set 13) is replaced once to fulfill the defined functional unit.

Indeed, with an absolute impact of $7,16 \times 10^{-05}$ Kg Sb-eq, attributed mainly to its BLE module (figure 5.56a), the relative AD impact of the BLE version almost doubles that one of the memory-based version (only with an absolute impact of $4,01 \times 10^{-05}$ Kg Sb-eq). By inspecting the big contributors of the BLE module (BlueNRG2) in figure 5.56b, a preliminary recommendation would be conducting a sensibility analysis on the silver and gold content shares of the respective die attach and wires subparts of the BLE SoC-QFN32 component, as both metals would be present in high quantities (5,51% in the case of silver and 1,32% in the case of gold, according to annex 11).

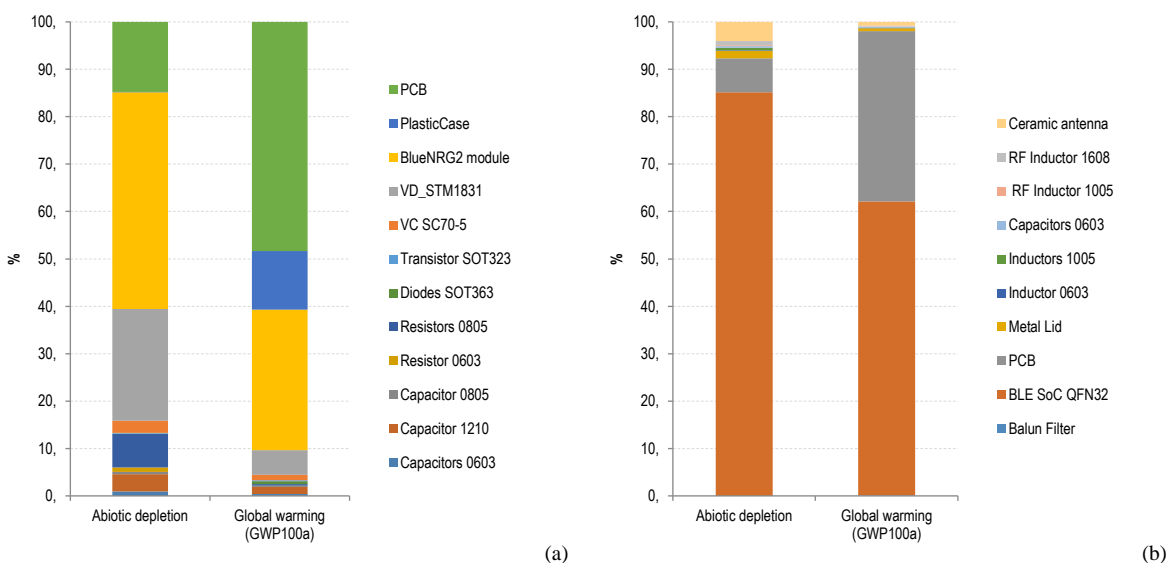


Figure 5.56. (a) AD and GW impact contributors of the BLE version. (b) Detailed impact contributors of the BLE module (BlueNRG2). The absolute impact of the BLE SoC QFN32 component amounts to $2,9 \times 10^{-05}$ Kg Sb-eq and 0,11 Kg CO₂-eq for the respective AD and GW categories.

On the other hand, with an absolute impact of 0,625 Kg CO₂-eq for the BLE version and 0,575 Kg CO₂-eq for the memory-based version, there is not big impact differences between both designs and little modifications in key features of the BLE version may lead to significant benefits in the GW category. For example, a preliminary recommendation would be conducting a sensibility analysis on the die surface ratio of the BLE SoC component as seen in section 2.1.3.2.1 and, simultaneously, another sensibility analysis on the gold content share of its wires and silver content share of its die attach, as it was proposed previously, to gain marginal benefits in the GW category.

2.1.5. Evaluation of electronic component alternatives through circularity attributes

To illustrate the relevance of certain features of electronic components to generate significant environmental savings (in this work, features that are known as “circularity features” or “circularity aspects”), an uncertainty analysis on the reusability and recyclability benefits and impacts of set 8 and set 20 is conducted. Specifically, this section contrasts the lifecycle of both sets (whose differ only in the microcontroller component) to study (1) the conditions that facilitates the successful separation and reuse of the studied TFBGA-typed microcontroller and (2) the benefits from three different recycling scenarios (on the basis of component sizes). These scenarios consist of a best scenario that includes mechanical separation before shredding (thermal separation), to maximize gold and silver recovery; a regular scenario, which applies a manual separation of the waste device before shredding (manual separation of the electronic card from the PCB); and a worst scenario, which involves shredding of the entire device without separation. Figure 5.57 recalls the waste flows of the regular and best recycling scenarios, together with the waste flow of the reuse scenario under the LCA implementation for the framework for eco design, presented in the previous chapter.

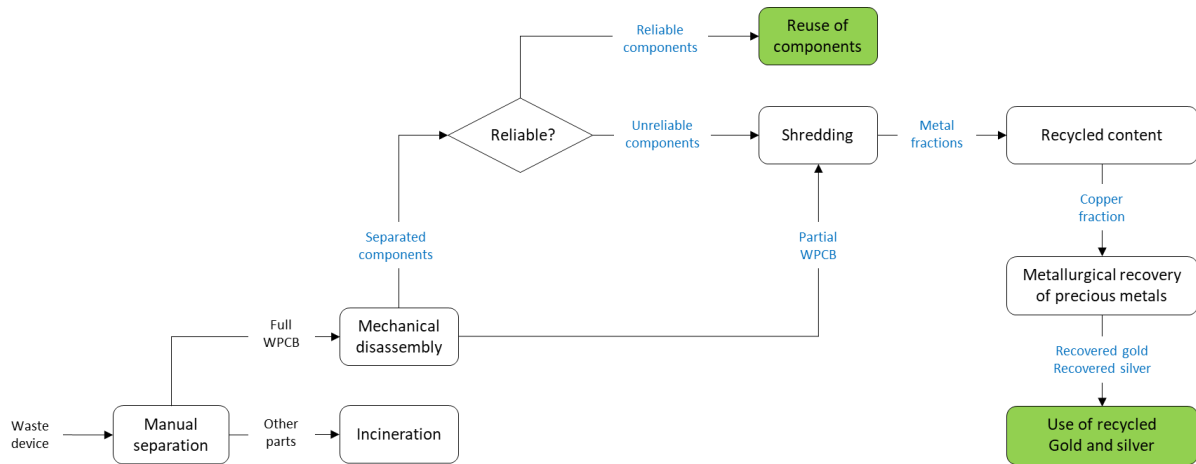


Figure 5.57. Recall of the EoL LCA modeling proposed in the framework for eco design. It is applied on the EoL phase modeling of set 8 and set 20. Each equipped with a TFBGA64- and a WLCSP36-typed microcontrollers respectively.

The motivation of considering worst, regular and best recycling scenarios in terms of separability comes from the importance of metal concentrations in electronic scraps, seen in the previous chapter (section 2.2.1); and the relevance of gold and silver, evidenced in the section 2.1.3 of this chapter. In this line, the thermal separation step (mechanical disassembly) considers the size of electronic components as the unique circularity feature facilitating successful separation. that is, components whose any side measure more than 3 mm are assumed to be separated successfully, adopting the posture of Chen, M. et al [127] (Electronic components below this threshold, would be considered as component melted with the PCB (partial WPCB waste flow). Annexes 12 and 13 provide the normalized quantities of the recycled contents for set 8 and Set 20 applied in this section.

2.1.5.1. Analysis of circularity features favoring electronic component reuse

To consider a separated TFBGA-type microcontroller as a reliable component to be reused, this section analyzes the limits within the bridging effect in its solder balls could be avoided in thermal separation, as it was described by equation 4.1 and 4.5 in the section 2.2.2 of the previous chapter (Here recalling them in the adapted equation 5.16 and 5.17, for the convenience of the reader).

$$W_{max} = 12 - 80,7 F1 + 9,529 F2 - 44,4 F3 + 88,7 F1F3 - 3,532 F2F3 - 0,92 F2F4 - 1,597 F1F2F3 \quad (5.16)$$

$$W_{crit} = Ball\ diameter \times \left(1 - \left(\frac{Ball\ diameter}{pitch}\right)^2\right) \quad (5.17)$$

Where:

W_{max} = Maximal warpage that a BGA component suffer, depending on its circularity features (F1 to F4)

W_{crit} = Critical warpage threshold above which bridging occurs

That is, by considering the ball diameter, the solder ball pitch (F1), the largest packaging size (F2), the compound thickness (F3) and the substrate thickness (F4) features of the TFBGA-typed MCU

component of set 8, one can say that its reuse is only possible only if its maximal warpage (W_{max}) does not overcome the critical warpage (W_{crit}) beyond of which, bridging occurs or, in other words, when the following condition is met:

$$W_{max} - W_{crit} \leq 0 \quad (5.18)$$

In this way, the equation 5.18 becomes a non-linear objective function composed of 5 variables that could be minimized to a value (zero) by a gradient method, to obtained the threshold values for F1, F2, F3, F4 and ball diameter below which bridging of the separated TFBGA64-typed microcontroller component is avoid (Table 5.23).

Environmental features	TFBGA-Typed MCU			Variation
	Current value (mm)	threshold value (mm) Eco design targets	SD	
Solder ball pitch (F1)	0,5	0,52751	0,027506112	5,214%
Largest sized side (F2)	5	4,43254	0,56745712	-12,802%
Compound thickness (F3)	0,6	0,62629	0,026285358	4,197%
Substrate thickness (F4)	0,2	0,20062	0,000619041	0,309%
Solder balls diameter	0,3	0,29998	2,4224E-05	-0,008%

Table 5.23. Current and threshold values of the studied circularity features of the TFBGA64-typed microcontroller with which bridging does not occur (they were obtained by the Gradient Reduced generalized method). For the uncertainty analysis, each of the studied features adopts a random variable of a normal distribution with its current value as the mean, and the absolute difference between the current value and its optimized value (threshold value) as the standard deviation. The current values of the circularity features of the studied component are available in its datasheet [171].

As observed, designers wanting to assure the reuse of the TFBGA-typed microcontroller of set 8 should make sure that the alternative components they consider be at least 12% small and have an increase of more than 5% in the solder ball pitch, with respect to the studied TFBGA-typed microcontroller. In this way, Monte Carlo tests are conducted, running two mutually exclusive events: a reuse-recycling event in which the TFBGA-typed MCU component of set 8 is reused, allowed by favorable variations of its solder balls diameter and circularity features F1-F4 (the rest of the device is recycled); or a full-recycling event, in which unfavorable variations of the aforementioned features of the component provokes either its unavailable separation or its unreliable reuse. Both events consider a best recycling scenario (optimal separation of the plastic case, electronic card and electronic components whose any side exceed 3 mm, as described in annexes 12 and 13) for a fair comparison with the lifecycle of set 20 (which also consider a best recycling scenario). Results are showed in figure 5.58.

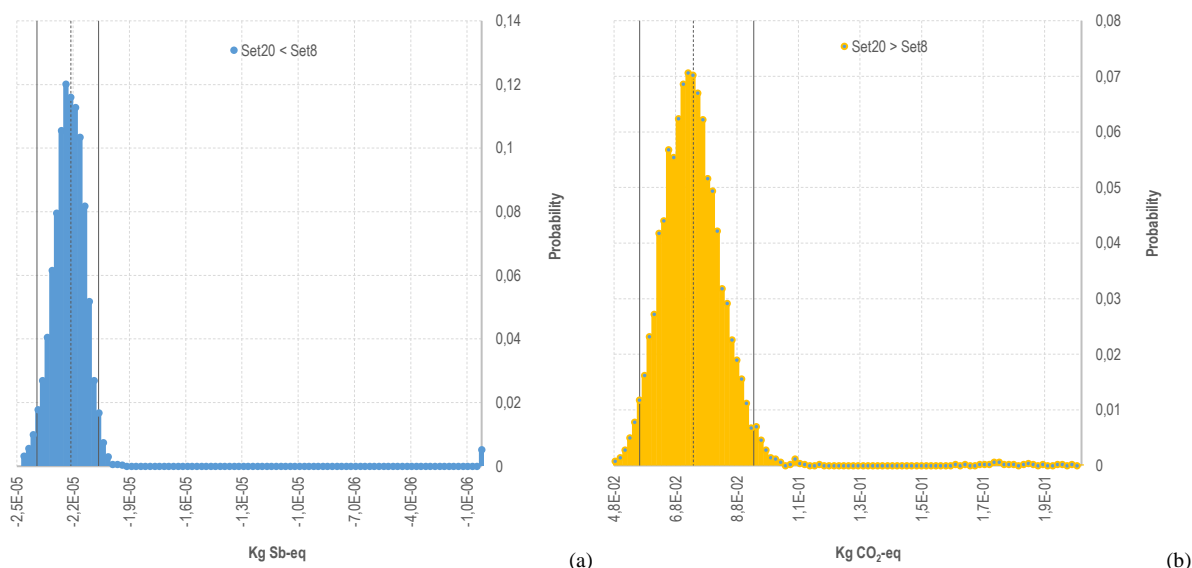


Figure 5.58. Impact distributions of the random values of the studied features showing the probability that the AD impact of the lifecycle of Set 8 is greater than that one of set 20 (a); and that the GW impacts of the lifecycle of set 20 is greater than that one of set 8 (b).

Although figure 5.58a shows an unfavorable result in the AD impact category for the lifecycle of set 8 in a reuse scenario, the reader should be cautious in his or her interpretations. Indeed, the reader should keep in mind that the uncertainty analysis calculates the probability that the impact of a lifecycle of a

design set is inferior or superior to another, but not at what extend. To explain this tricky aspect for eco-design, consider figure 5.59a-b.

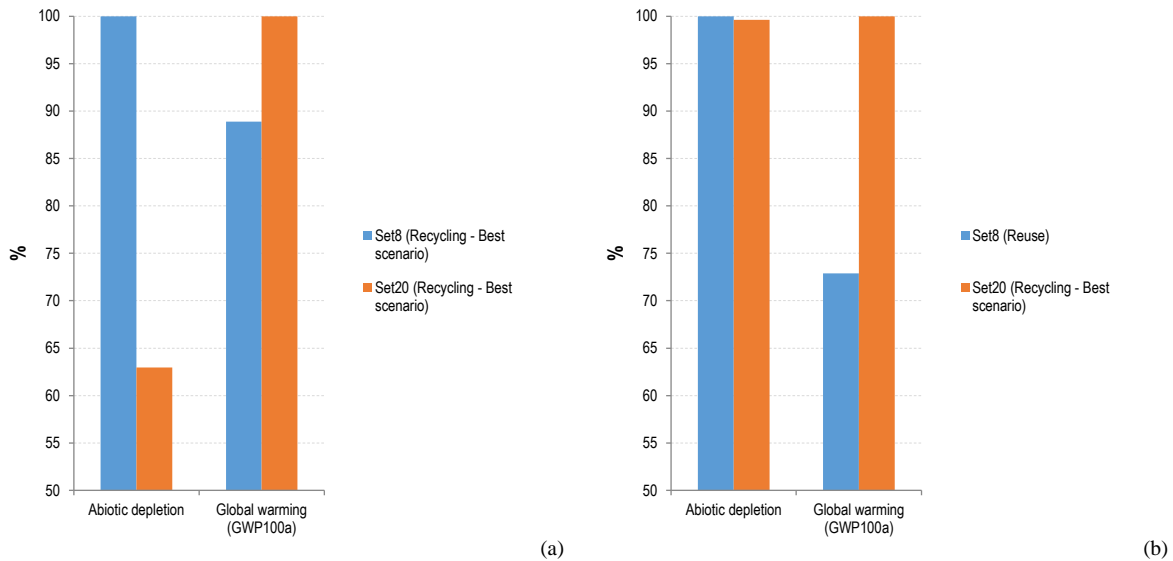


Figure 5.59. (a) Relative AD and GW impacts of set 8 and set 20, both with a best recycling scenario (unsuccessful separation and unsuccessful reuse). Here, the AD impact of set 20 is inferior to that one of set 8 (approximately in more than 35% of less damage or, in absolute terms, $2,21 \times 10^{-05}$ Kg Sb-eq less than a best recycling scenario of set 8 with an approximate 6×10^{-05} Kg Sb-eq). (b) Relative AD and GW impacts of set 8 with a reuse scenario and set 20 with a best recycling scenario. Here, the AD impact of set 20 is slightly inferior to that of set 8 (in less that 0,4%) and the relative GW impact of set 8 is significant reduced.

As observed, the relative environmental savings of reusing the TFBGA-typed MCU component of set 8 are evident for both AD and GW impact categories. However, for the AD impact category, the problem is that the significant benefits from reusing the TGBGA-type microcontroller component are not simply enough to allow design of set 8 overthrows that one of set 20 (as observed in the slightly difference between both sets in the AD impact category of figure 5.59b). Designers should bear in mind this methodological issue, whenever the use of similar Monte Carlo-based uncertainty analysis are planned.

2.1.5.2. Benefits from optimized separation according to component size

Table 5.24 and 5.25 presents the gold and silver recovery rates of set 8 and set 20 respectively, which consider the weight of waste flows and the recovered content from both design sets. These recovered quantities are obtained from the gold and silver content in shredded copper fractions (mg / kg of waste flow) as is detailed in annexes 12 and 13. The information of both tables is organized by the correspondent waste flows of the worst, regular and best recycling scenarios.

	Worst	Regular	Best		
Waste flow	Full device	WPCB	WPCB	Waste components	Total (best)
Waste flow weight (mg)	1,71E+04	1,27E+03	9,97E+02	2,75E+02	1,27E+03
Au recovery rate (mg / Kg waste flow)	2,91E-04	1,08E-03	6,79E-04	3,09E-03	
Ag recovery rate (mg / Kg waste flow)	3,50E-03	1,30E-02	8,17E-04	7,44E-02	
Au recovered from the device (mg)	4,96E+00	1,37E+00	6,77E-01	8,50E-01	1,53E+00
Ag recovered from the device (mg)	5,97E+01	1,65E+01	8,14E-01	2,05E+01	2,13E+01
Au recovery rate of the device (%)	0,029%	0,108%			0,120%
Ag recovery rate of the device (%)	0,350%	1,298%			1,673%

Table 5.24. Gold and silver recovery rates of the different recycling scenarios of set 8. For the Regular and the Best scenarios, the plastic case is separated manually from the PCB and incinerated without energy recovery, as is proposed in the LCA implementation of the framework for eco design (in chapter 4, section 4.1). The waste flow weight in the worst scenario includes the plastic case of the device.

	Worst	Regular	Best		
Waste flow	Full device	WPCB	WPCB	Waste components	Total (best)
Waste flow weight (mg)	1,66E+04	8,68E+02	6,57E+02	2,11E+02	8,68E+02
Au recovery rate (mg / Kg waste flow)	1,64E-04	8,29E-04	1,01E-03	0,00E+00	
Ag recovery rate (mg / Kg waste flow)	2,91E-03	1,47E-02	1,19E-03	7,60E-02	
Au recovered from the device (mg)	2,73E+00	7,20E-01	6,65E-01	0,00E+00	6,65E-01
Ag recovered from the device (mg)	4,84E+01	1,28E+01	7,82E-01	1,60E+01	1,68E+01
Au recovery rate of the device (%)	0,016%	0,083%			0,077%
Ag recovery rate of the device (%)	0,291%	1,472%			1,939%

Table 5.25. Gold and silver recovery rates of the different recycling scenarios of set 20. For the Regular and the Best scenarios, the plastic case is separated manually from the PCB and incinerated without energy recovery, as is proposed in the LCA implementation of the framework for eco design (in chapter 4, section 4.1). The waste flow weight in the worst scenario includes the plastic case of the device.

In both tables, the waste flow “Waste components” of the best scenario consider all the electronic components in the design set whose any side exceed 3 mm, according to the proposed LCA implementation of the framework for eco design, seen in previous chapter. Notice that the total weight of the waste flow in the best scenario is the same as the one of the regular scenario, but the gold and silver recovered contents and recovery rates are different, as thermal separation processes in the best scenario increases the metal concentration in the “WPCB” and “Waste components” waste flows. The benefits from this aspect can be observed by comparing the relative AD impacts of all recycling scenarios of set 8 in figure 5.60a, and set 20 in figure 5.60b.

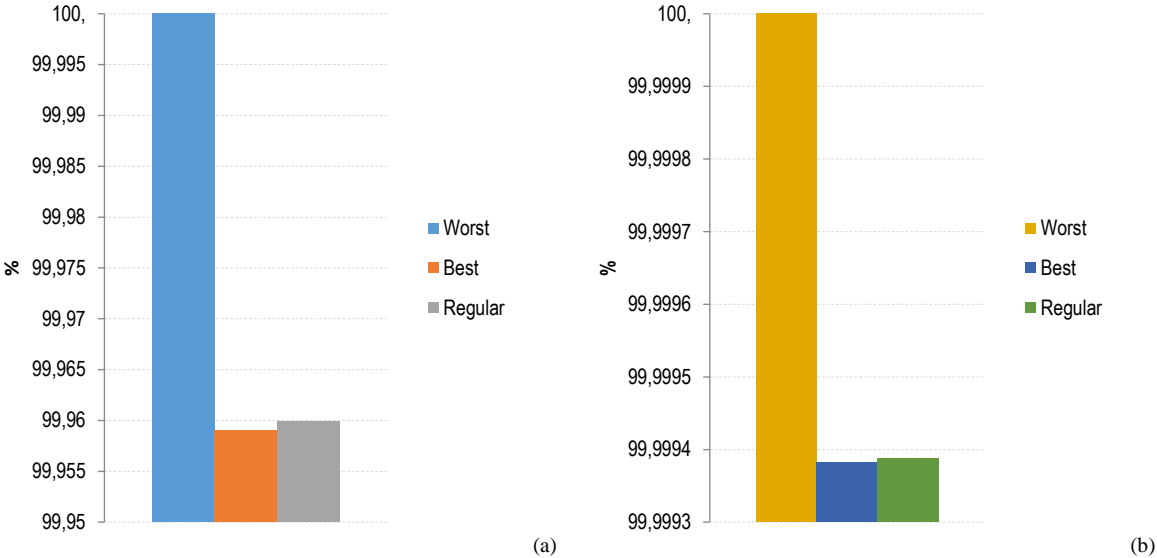


Figure 5.60. Relative AD Impact comparison of the worst, regular and best recycling scenarios of set 8 (a) and set 20 (b).

The slight benefits from manual separation is evidenced for both sets, as it can be observed impact differences between the worst scenario and the other two scenarios. On the other hand, with the small recovery rates described in table 5.24 and 5.25, one can barely glimpse the beneficial effects of thermal separation of big components. Indeed, although the TFBGA-typed MCU and UFDFPN-typed memory components of set 8 are separated successfully from WPCB (both, with packaging sides greater than 3 mm, as reported in their respective datasheets), the best scenario for this design set provides insignificant benefits, in relation to its regular scenario (in which the entire PCB is treated by a shredding process). This fact is also observed in set 20, with the difference that in this set, its MCU component (the studied WLCSP-typed component) is treated together with the waste PCB, and only its silver-richest UFDFPN-typed memory is separated and recycled independently.

On the other hand, the GW impact comparison of all the recycling scenarios for both sets in figure 5.61 shows that it is convenient recycling IoT devices in separated waste flows only when:

- Incineration of separated plastic casings (without energy recovery) does not occur.
- The relative contents of recycling target materials in separated components are significant.

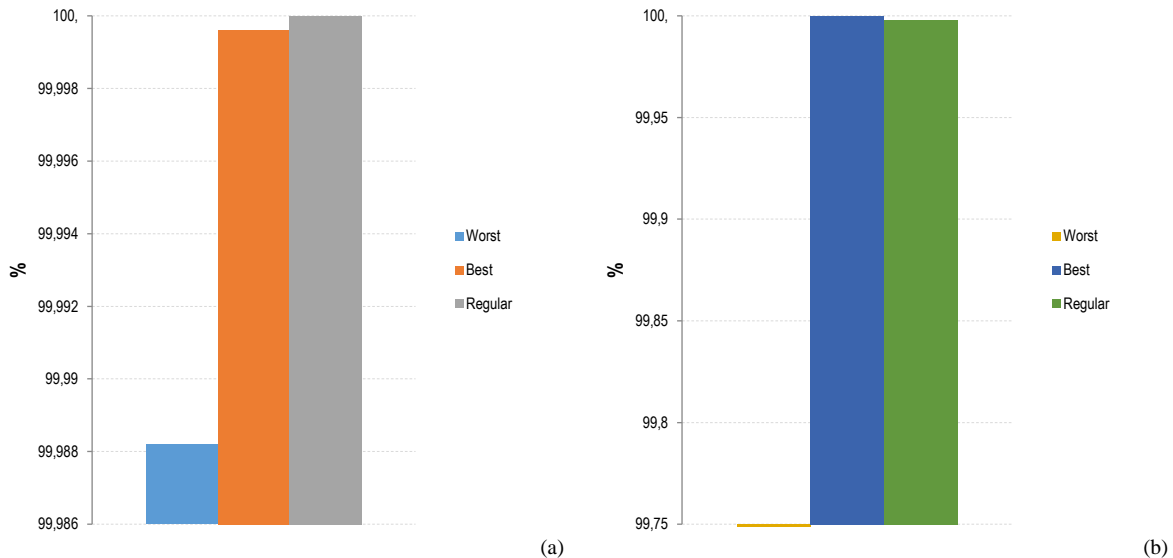


Figure 5.61. Relative GW Impacts of the worst, regular and best recycling scenarios of (a) set 8 and (b) set 20 (with an impact contribution of 99,017%, the relative impact of the worst scenario of set 20 practically does not appear). The gap between the worst and the other two recycling scenarios is explained by the fact that, in the latter, incineration of the plastic casing occurs, together with independent, metallurgical-recovery processes for every waste flow.

With respect of the first aspect, the incineration of the plastic parts after manual separation causes a significant impact of 0,0158 Kg CO₂-eq for both sets (with an impact contribution of more than 99% for the EoL phase). The second aspect is illustrated, for example, by comparing the waste flows and the metal recovery rates of the best recycling scenarios of set 8 and set 20. In the case of set 8, the waste flow “waste components” separates the gold- and silver-richest TFBGA-typed MCU and UFDFPN8-typed memory components from the waste PCB, increasing the recovered gold and silver per kg of waste flow ($3,09 \times 10^{-03}$ and $7,44 \times 10^{-02}$ mg / Kg for gold and silver respectively, according to table 5.24); on the contrary of the best scenario of set 20, whose separates only the UFDFPN-typed memory component, obtained null recovery rates of gold and moderate recovery rates for silver ($7,60 \times 10^{-02}$ mg / Kg of waste flow, as is showed in table 5.25). The results of this is that one can recovered more gold in the best scenario of set 8 (alleviating the additional impact from a separated, metallurgical process recovery for treating the waste flow “waste components” independently); but not in the best scenario of set 20. In this line, notice that treating the UFDFPN-typed memory component together with the waste PCB of set 20 (“WPCB” waste flow of the regular scenario in table 5.25) is very slight convenient than treating it separately, as it is showed in figure 5.61b.

2.1.5.3. Recommendations for the case study “Smart monitoring” in the context of circularity attributes

According to figure 5.59b, a design facilitating the reuse of the TFBGA component studied in this work would improve even more the environmental performance of set 8 against set 20 in the GW category, and reduce significantly the AD impact of the set 8, to such an extent that almost match the AD impacts of set 20, who uses the more advantageous MCUs component for the AD impact category. Thus, if designers want to improve the design of set 8 against set 20 by considering the reuse of similar TFBGA-typed MCU components, they should conduct a mixed uncertainty analysis consisting in two simultaneous parts.

- The first part would consider little variations for reduced gold, silver, palladium, tin or copper contents shares in other electronic components of set 8, as it was seen in section 2.1.3.1.1; for example resistors and voltage detectors (the former with a gold content share of more than 0,5% and the latter with 0,9% only in wires, according to annex 12).
- The second part would consider optimal variations of all the circularity features of TFBGA-type microcontrollers, as seen in section 2.1.5.1 (solder ball pitch and diameters; packaging sizes, and compound and substrate thickness) to find the limits at which, the separability and reliability of alternative wasted TFBGA-type MCU would be warranted.

On the other hand, a reliability analysis on WLCSP-typed microcontrollers, similar to that one presented in this work for evaluating reuse of waste components could be promising, if further research on key

feature predicting warpage and bridging effects in WLSCP-typed components is developed (the studied WLSCP component has great probabilities to be successfully separated, because one of its sides made almost 3 mm (2,9 mm, according to technical documentation)). However, for a recycling approach, the use of similar but bigger WLSCP-typed microcontroller components is not recommended, because the benefits from their poor silver recoveries from their solder balls would be immediately eclipsed by the additional impact of treating separated waste flows, as showed in section 2.1.5.2.

Finally, designer should also consider circular strategies for the plastic case in the all scenarios presented in this section, as its incineration generates significant damage in the GW category.

3. Guidelines

The design methodology proposed in chapter 4 helps fixing in mind the ancillary entities (devices, components, functions and capacities) and angles of analysis (physical, technical and circularity features) for the eco design of IoT systems or further design tools. These pillars must be translated in key aspects that have to be analyzed simultaneously, under the perspective of data that originates, flows, transforms and interprets throughout the local and mutualized infrastructure of an IoT system. In this chapter, this methodology was used in the context of some key aspects identified for the case studies “Smart metering” and “Smart monitoring” (e.g., materials, performance and endurance, package dimensions, etc.), to inspire the following hierarchical guidelines:

1. Consider several aspects of the operational context that may affect not only the efficiency of electronic components, but also the data flow design (and consequently the reference flow) of an IoT system. For example, in the context of LoRa-based IoT Systems, long distance ranges would force designers to consider energy intensive data preprocessing routines in a MCU, or change the planned sampling rate of a sensor component when designing an IoT prototype, to align the data volume generated in the acquisition stage to the low bitrate impose to its projected LoRa transceiver, working with ADR.
2. Study technical features under unfavorable contexts to see at what extend the environmental profile of a device, or an IoT system is guaranteed. For example, low endurances of memories may compromise the lifetime of intermittent devices under high use intensities; or extreme temperatures may affect differently the reliability of ceramic and tantalum capacitors, according to their Temperature Coefficient of Capacitance (TCC).
3. When estimating the reference flow of an IoT system for its (re)design, consider not only the energy that devices need in different states, but also other technical features (e.g., bitrate, data payloads, parameters of the transmission means such as frequency bandwidths, etc.) that can affect these energy requirements.
4. Consider technical features and capacities in a comprehensive way, so that to propose reasonable designs. For example, in the context of LoRa-based IoT systems, selecting communication interfaces with high bitrates makes sense only when the application type allows big data payloads (i.e.; in short-range transmissions).
5. The size of internal dies of IC components is of a paramount importance. If possible, apply X-ray techniques to determine the actual die surfaces, in order to have an initial idea of the GW impact of IC components. However, this estimation must be rethought, whenever information of the technology node of the internal die is available.
6. Apply variations on the internal die sizes of different IC components (whenever this information is available), to challenge the GW savings or impacts of heterogeneous electronic designs. Challenge your conclusions, when technical information of the technology node of the studied components is available.
7. When heterogeneous designs are confronted, and depending on the material quantities on their electronic components' subparts, apply little variation on material contents with high impact relevance; or big variations on material content with low impact relevance to challenge benefits or address unfavorable design.

8. When dissimilar packaging technology is compared, designer can analyze the impact of materials on the basis of total contents and not on the basis of subparts. In this sense, if there exist large gaps in relevant materials (gold and silver), designers can directly discriminate certain technologies. If there exist small or moderate gaps, designer need to conduct sensibility analysis.
9. A visual inspection of specific features may give and rough idea of the environmental impact of certain components. For example, electronic components with high pin densities could be consider as less convenient, as every pin is probably connected with a wire made in gold. However, first intuitions should be valid with an inspection of the material declaration of the studied components (wires of modern IC can be made in gold, silver or less often in copper).
10. When designing for Recyclability (DfR), make sure that high contents of target materials be concentrated in few electronic components, likely to be separated from WPCBs; so that benefits from recovery overcome impacts from treatment of independent waste flows. This guideline is not exclusive for high-impact materials (i.e.; gold or silver), but for all target materials depending on their quantities (for example substantial contents of copper in lead frames or substantial contents of tin in solder balls), and the available recycling technology.
11. When heterogeneous designs are confronted, and depending on the selected IPC-7351 standard, analyze small variations to the biggest electronic components ' sides; or big variations to the smallest electronic components' sides to observe at what extend the arrangement of land patterns and the PCB size can be optimized. Complete this analysis by considering different separation processes techniques in the EoL phase of the studied designs, bearing in mind that the packaging sizes may compromise the disassembly rate of the electronic card and/or the estimation of other critical physical features such as the internal die area ratio of electronic components.
12. When significant GW impacts from the PCB size of an electronic design, and significant GW impacts from the internal die of one or many irreplaceable ICs composing another electronic design are almost identical, consider possible variations on gold and silver content shares in other electronic components (e.g., passive components) to grant marginal and significant advantages to one alternative, in the GW and AD categories respectively.
13. A physical, technical or circularity feature can be beneficial for one life cycle phase, but unfavorable for another one. For example, Ferroelectric RAM memories (FeRAM) has high writing endurance (an advantage for the use phase), but they usually required platinum (a disadvantage for the manufacturing phase, in the AD impact category). This platinum content could just be lost, depending on its functional recyclability (a potential disadvantage for the EoL phase).
14. Different physical, technical or circularity features of an electronic component can be beneficial for one impact category, but unfavorable of another one. For example, copper-rich subparts of CSP-type components are beneficial for reducing impacts in the AD category, but the typical area to mass ratio of their dies performs bad for the GW impact category.
15. When invariable behavior characterizes an application (for example uniform water consumption, unchanging lighting in a household, etc.) information can be extrapolated from historical or redundant data in the cloud infrastructure so that massive local-to-cloud transmissions can be avoid.
16. The protocol overhead may be relevant, depending on the transmission frequency and the reliability requirement of an application. When low accuracy characterizes an IoT system, high frequency is not necessary and approximate computing can be applied.
17. When high transmission frequency is necessaire, consider connectionless protocols and reinforce end-to-end security (for example by using message authentication, rate throttling, robust encryption, etc.). However, evaluate simultaneously the additional energy requirements and find a balanced solution distributed over the sensing, edge and cloud layers.

18. When estimating the impact of an IoT device whose design documentation is not available, the presence of BGA components may indicate an elevated number of PCB layers, as high pin densities require complex circuitry.
19. When estimating the impacts of the use phase of an IoT system whose design documentation is unavailable, consider that additional communication between IoT layers may occur when the user accesses directly to cloud resources.
20. Designers should consider at least the AD and GW impact categories for essential LCA analysis and find optimal tradeoffs in these two categories.
21. Design efforts should be oriented to enable and guarantee circularity of plastic parts, if their content share in a device is significant.
22. Designers should privilege electronic components with full documentation (at least detailed material declarations (standard IPC-1752A), full technical notes such as datasheets and land pattern PCB design, and minimal documentation involved conformity with directives (Reach, RoHs, etc.)). They should also privilege manufacturers that usually provide this information.

For practicality purposes, every guideline of the list above focuses on one or at most two aspects. However, designers should adopt them with a global perspective, by trying to confront ones with others in the context of their own designs. In this sense, they should challenge this list, improve it, enlarge it, etc. through the continuous and simultaneous use of the design frameworks that shape the proposed methodology.

Conclusion

Overview

This last chapter provides a discussion on the main findings and limits of this work; and presents future research perspectives. It provides also final words that highlights the contributions of the proposed methodology, to answer to the main interrogation seen in the introduction section and solve the research questions stated in chapter 1.

1. Findings

The review of the literature, the construction of the methodology and its illustration through the case studies, all allow for the following findings.

- First, in most of the current environmental studies there is a strong emphasis on impacts from local devices and partial IoT systems. In these works, it is observed that such impacts are attributed to the energy consumption and the early replacement of devices. However, no more details for electronic design are given beyond these conclusions. This is unfortunate, as other studies within the perimeter of sensor systems would attribute significant impacts to certain electronic components. This work provides specific evidence that explains the negative contribution of different electronic components from different perspectives, which facilitates at the same time the practice of eco-design of prototypes.

Indeed, in this work a positive correlation between the global warming damage and the area of the electronic card of a design is found (which is explain mainly in term of the embodied energy per mm^2). In this line, one observes that the surface of the PCB is in turn directly affected by the land pattern of electronic components in a specific design. In addition, this work found a significant contribution of the internal chip in specific types of ICs (such as LQFP, SO, BGA and CSP); and a marginal contribution of different electronic components' subparts due to specific materials (mainly gold in wires and silver in die attaches). In this sense, it is observed that considering small reductions of gold and silver contents is capital in comparative-based eco design of heterogeneous electronic designs with almost similar impacts, where the replacement of one or more big-die ICs is restrictive. It is also noted that the use of CSP-type components could hamper the eco design of devices. That is, their high pin densities may provoke complex circuitry and increase the number of PCBs' layers on the one hand, and on the other hand, they may require considering several form factors with minimal area/mass ratio of internal dies, in the context of comparative analysis.

In the category of abiotic resource depletion, the LCA results obtained in this work show that a significant damage is generated from the presence of gold in the wires of specific types of electronic components (BGA-type microcontrollers and SOT23-type voltage comparators). On the other hand, other materials such as silver, tin, and copper would be concentrated in certain characteristic subparts of these components (die attaches, solder balls, and substrates) and would cause impacts at different levels. In this sense, it is observed that (1) very dissimilar packaging types can cause very different damages, depending on the relevance of the impact that each of the materials with which they are made, and (2) the amount of a material may or may not be relevant to the eco design of a device, depending on the impact relevance of this material to a specific impact category. Thus, this work found that small reductions in the content of materials with high relevance in the depletion of abiotic resources (gold and silver) and very small reductions in significant content of materials with little relevance (copper) allow both to improve the environmental profile of electronic components and consequently, the ecological design of electronic cards.

On the other hand, the review of the academic and technical literature suggests that the reliable performance of electronic components is strongly conditioned to operational and environmental contexts (e.g., temperature). With this in mind and based on field tests of a prototype, this work demonstrates that, under normal conditions of temperature and use, a very high frequency of overwriting can significantly degrade the blocks of EEPROM memories, shortening the lifetime of intermittent, self-powered devices. However, this mainly depends on the design of the data and information flow design of the IoT systems to which they belong.

Previous works also denounce the inefficiency of recovery of certain materials in recycling processes. This work produced results that complements this body of literature: firstly, it found that the manual separation of electronic cards from the plastic parts, and the mechanical separation of big components both offer interesting advantages, only when there is a correct treatment of non-electronic waste. Secondly, it found that Design-for-Recycling is convenient only when the amounts of target metals in the separated streams is significant (otherwise, more global warming damage is generated when treating separated parts in individual waste flows). On the other hand, the literature also reveals potential barriers to the reuse of specific electronic components, imposed because of certain physical attributes. In this sense, this work found that, to increase the probabilities of successfully separating and reusing BGA-type components, in the component selection stage it is necessary to prioritize small packages sizes, mainly; and big solder bump pitches, additionally. However, it is also noted that very small packages would potentially frustrate thermal separation.

- Secondly, in the LCA literature of sensors, sensor systems, partial and/or complete IoT systems, an absence or a vague definition of reference flows is evidenced. On the other hand, few emerging authors would suggest implicitly that such reference flows should be built on the basis of data circulating in local and mutualized infrastructure.

By considering this last aspect, this work affirms the central role of data and information for IoT systems. Specifically, this work built a framework and proposed an implementation for estimating theoretically and empirically the data traffic of a mature IoT system. Once this has been done, its reference flow and its long-term impact were calculated. During this process, it was found that the frequency at which the local infrastructure connects with the cloud infrastructure, the volume of data transmitted, and the protocol overhead of transmissions in regular and / or user-driver operations are all fundamental aspects that affect the reference flow, the impact and the eco design of full IoT systems.

It was also observed that the data and information flow managed by specific capacities of sensing and edge devices, under specific operational parameters (e.g., transmission bandwidths, spreading factors or distance range) are as relevant as the use time for environmental impact estimation. This finding challenges the conclusions of Malmudin, J. et al. [11] and Coroama, V. C. et al [249], who claim that for end-user ICT equipment, the use time is more relevant because the energy consumption and embodied carbon footprint is not to the same extent related to transmitted data volume.

On the other hand, the State-of-the-Art suggests that a detailed analysis of the data and information required by the applications facilitates effective eco-design strategies for sensor systems. From the pragmatic perspective applied to the development of prototypes, some works would show that this last aspect is essential, since it would allow not only the most appropriate and right-provisioned design of local devices, but also the most optimal allocation of all available and complementary resources. In this work, a preliminary analysis of the flow of data and information, adjusted to the main functions of an autonomous sensor system oriented to smart monitoring was applied. In this context, it was observed that simple modifications in the design of the data operational stages of an IoT system (for example transmitting data continuously rather than recording and transmitting it in batches) can generate different versions of prototypes, with very different environmental impacts.

2. Limits

The reader should consider that the impact analysis of the case studies presented in this work was limited to the AD and/or GW categories because of their opposing behavior evidenced in literature. However, although the other impact categories do not present this peculiarity, designers should be always conscious that some materials or substances might affect these categories significantly. Moreover, in this work relevance of materials was pointed-out only from the ecological point of view (nothing was said from the performance point of view).

Also, it should be clarified that some simplification were applied to the LCA implementation seen in this work. Firstly, the estimated AD damage calculated for all design instances of the case study “Smart

monitoring” considers only scarcity of materials; nothing was done for criticality. This is a weak of current LCIA methodologies; designers and LCA practitioners should include this aspect whenever new methodologies appears. Secondly, the LCA implementation assumes a collection rate of waste prototypes of 100%. In reality, this rate depends of inner factors such as the size of the device and / or external factors such as the price of raw materials. Thirdly, few materials and electronic components were excluded from the LCA implementation seen in chapter 5 because of different reasons. A detailed list of these reasons is provided in annex 14.

On the other hand, the interdependencies of some features of electronic components were explored rapidly (i.e.; interdependency of ICs’ land patterns and PCB sizes) and, unfortunately, potential changes in the number of layers of the PCB in the case study “Smart monitoring” were not explored. However, this later aspect does not penalize the obtained results, because not all pin outputs of the studied high pin-density components (TFBGA64-type and WLCSP microcontrollers) were used.

For illustration and simplicity, the analysis of the different attributes suggested for the case study “Smart monitoring” focuses on specific life cycle phases individually (manufacturing phase for the physical attributes, use phase for the technical attributes and EoL phase for circularity attributes). However, the idea of applying the framework for eco design of the proposed methodology is consider these and more attributes altogether in sensibility/uncertainty analysis along several life cycle phases, in order to avoid impact transfers and spot key aspects for sounding design of IoT systems. Bearing this in mind, further use of the proposed framework under the context of the case study “Smart monitoring” may produce even more findings, eco-design hints and/or sharp guidelines.

Finally, high order impacts of IoT systems were only analyzed in the context of the mutualized infrastructure and, disquieting aspects, such as rebound effects were not covered in this work.

3. Further research

With the aim of refine the proposed methodology, the following research perspectives could be considered.

Firstly, advance data manipulation techniques, such as approximate computing, need to be investigated in the context of IoT systems and specially, in the context of intermittent EH devices. Also, further work focusing on new approaches for improving the extraction of substantial information from minimal data (i.e.; information entropy) could be very beneficial, especially for upgrading the data-information-knowledge-based design approach presented in this work.

Secondly, more parameters in the context of (1) physical attributes, such as the technology node of integrated circuits; (2) technical attributes, such as right-provisioned microprocessors; and (3) circularity attributes, such as thermomechanical properties of materials need to be considered in further research. The in-depth analysis of the technology node feature of ICs will refine the impact estimation step in the GW category. What is more, the technology node may become a useful physical feature for eco-design, provided that this information is more accessible to designers. The study of right-provisioned microprocessors on the other hand, will permit not only evaluating more judiciously IoT prototypes, but also facilitate the component selection process according to sober data and information flow design. Lastly, analyzing the thermo-expansion mismatch of adjacent materials in IC packaging would help to anticipate potential barriers —beyond bridging— that difficult the reuse of waste components (for example, delamination).

Thirdly, particular aspects of emerging technologies and materials need to be further investigated under the lens of physical, technical and circularity properties. For example, shape-memory polymers of polyurethane used in electronics are stable and robust while in use, and they can be triggered to decompose when a device is to be taken apart for recycling [128]. This could be an obvious advantageous property for the circular design of IoT devices, whose electronic cards are embedded into their casing parts (specifically in active disassembly procedures, in which one aims to access electronic parts using an all-encompassing stimulus, rather than a fastener-specified tool or machine [128]). However, no studies show the advantages (or disadvantages) of these emerging materials in the physical dimension (e.g., embodied emissions) or technical dimensions (e.g., influence on performance or lifetime span).

Finally yet importantly, more research on criticality of materials in the context of electronics and IoT need to be done, and results from it need to be translated in terms of concrete attributes or capacities of electronic components.

4. Final words

In a context in which the accelerate adoption of the Internet of Things threatens our environment, promising solutions emerges, trying to alleviate the impacts of IoT systems from different perspectives. However, these initiatives fall short facing the paramount complexity of IoT systems, and the urge of a comprehensive, lifecycle-based design methodology for sustainable design becomes more and more evident.

On the other hand, the existing literature reveals disperse works oriented to the environmental assessment of IoT systems and devices; and the scarce contributions for eco-design suffer from several issues. In this context, the main interrogation “How can one estimate the potential impact of an IoT system and how can one minimize this impact by an efficient and practical design methodology?” emerges, and the specific research questions “How a designer can consider data flow within an IoT system in order to harmonize and reduce the potential impacts of promising initiatives?” and “How a designer can disclose, measure and integrate key environmental aspects to the typical design of sensor systems and edge devices (local devices) in a practical, efficient and comprehensive way?” are rapidly identified.

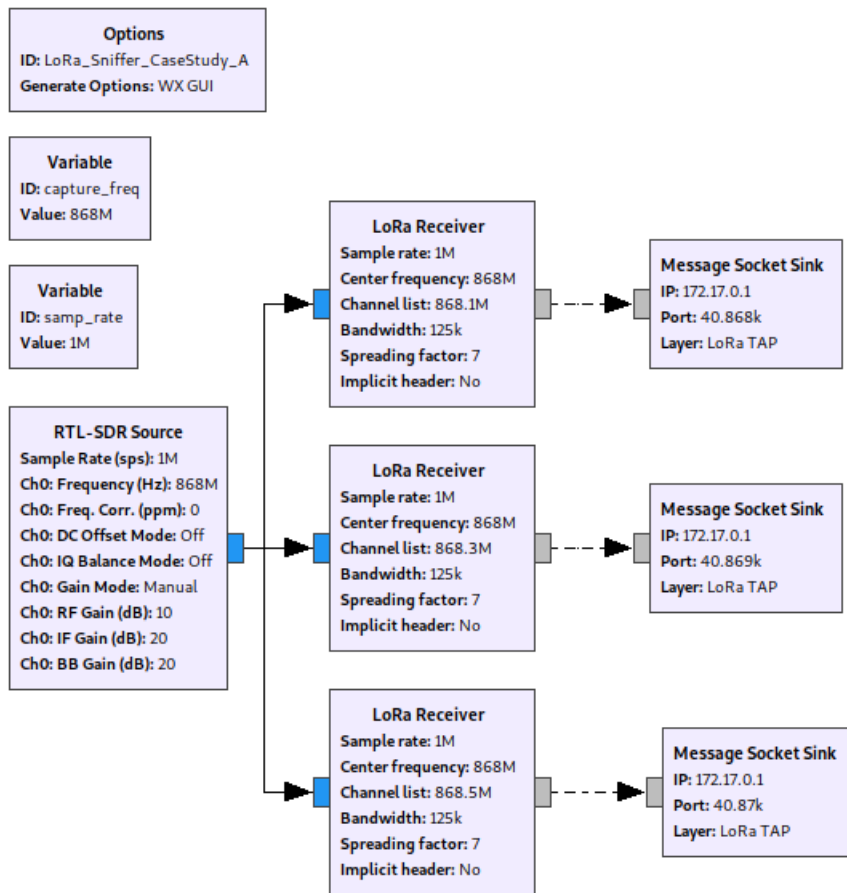
This thesis proposes a structured and efficient methodology oriented to (1) facilitate simple, yet more precise impact estimation of full IoT systems and (2) facilitate thoughtful design of sensor and edge devices from the available information that designers may have (i.e.; datasheets, material declarations, installation manuals, etc.), so that collateral damage in both local equipment and mutualized infrastructures can be avoided. Based on data and on the analysis and design of its further transformation into information within the sensing, edge and cloud resources of IoT systems, two framework are built. The first framework, unlike the device-centered literature; identifies the essential entities (devices, electronic component, functions and capacities) and their interrelations within full IoT systems, so that reference flows can be clearly identified and real damage can be easily calculated. The second framework, unlike the limited standards, generic guidelines and non-lifecycle methodologies found in previous works; proposes a lifecycle-based design procedure that discloses, evaluates and integrates key environmental aspects to the product development process of local devices (physical, technical and circularity features of electronic components). Such integration facilitates the decision-making process in early design and the identification of clear environmental targets.

Both frameworks were illustrated by two implementations applied on two case studies, showing their efficacy in impact estimation and eco-design and generating sharpening guidelines. Designers should apply both frameworks simultaneously in the context of their own projects, as a sort of roadmap that recall that every element (i.e.; data, information, knowledge, devices, components, functions, capacities; and physical, technical and circularity attributes) must be reviewed carefully.

Annexes

1. GNU-radio companion implementation for the Lora sniffer A

The GNU-radio companion implementation runs in a Docker instance and uses the RTL-SDR source block of the gr-lora repository [167]. This block is configured to work in the 868 MHz frequency and from it; three LoRa receiver blocks are created. Every of these blocks capture LoRa transmissions in three main channel frequency (channel list), under a 125 kHz bandwidth and a Spreading Factor of 7.



To analyze the captured packets, Message Socket Sink blocks are configured to warp up them in UDP packets, which are later transmitted to localhost through 40868, 40869 and 40870 ports. The localhost has the IP address 172.17.0.1 and runs Wireshark under Ubuntu 14. It is equipped with a RTL-RDS bundle connected by USB.

2. Data traffic in the local equipment of the case study “Smart metering”

The following table show an extract of the data traffic between the flowmeter and the gateway of case study “Smart metering”, obtained in the last hour of the experiment (from 21:06 to 22:06). The data traffic happens in the 868.1 frequency channel. The IP source 172.17.0.2 correspond to the Docker instance that runs the GNU-radio implementation seen in annex 1 and the IP destination 172.17.0.1 correspond to the IP addresses of the localhost that runs the Wireshark instance. For facilitating the visualization, a filter in the latter is applied, so that only UDP packets containing the data application of the case study “Smart metering” are showed. The actual data application (the LoRa packet less the UDP headers) is show in the “Info” column (Len = X bytes). The total size of LoRa messages is obtained from the sum of the individual packets in minute resolution. For example, the first two packets happening on 21:06:18 and 21:06:18 are consider a complete LoRa message whose size is 57 Bytes (28 Bytes + 29 Bytes). In this sense, the complete LoRa messages are highlighted in alternate tones.

capture time	Source	Destination	Protocol	Length	Info
21:06:18	172.17.0.2	172.17.0.1	UDP	70	34537 > 40868 Len=28
21:06:18	172.17.0.2	172.17.0.1	UDP	71	34537 > 40868 Len=29
21:09:14	172.17.0.2	172.17.0.1	UDP	70	34537 > 40868 Len=28
21:09:14	172.17.0.2	172.17.0.1	UDP	71	34537 > 40868 Len=29
21:12:12	172.17.0.2	172.17.0.1	UDP	70	34537 > 40868 Len=28
21:12:12	172.17.0.2	172.17.0.1	UDP	71	34537 > 40868 Len=29
21:15:17	172.17.0.2	172.17.0.1	UDP	72	34537 > 40868 Len=30
21:15:17	172.17.0.2	172.17.0.1	UDP	70	34537 > 40868 Len=28
21:15:17	172.17.0.2	172.17.0.1	UDP	85	34537 > 40868 Len=43
21:15:17	172.17.0.2	172.17.0.1	UDP	71	34537 > 40868 Len=29
21:18:15	172.17.0.2	172.17.0.1	UDP	70	34537 > 40868 Len=28
21:18:15	172.17.0.2	172.17.0.1	UDP	71	34537 > 40868 Len=29
21:21:19	172.17.0.2	172.17.0.1	UDP	71	34537 > 40868 Len=29
21:24:21	172.17.0.2	172.17.0.1	UDP	70	34537 > 40868 Len=28
21:24:21	172.17.0.2	172.17.0.1	UDP	71	34537 > 40868 Len=29
21:30:19	172.17.0.2	172.17.0.1	UDP	72	34537 > 40868 Len=30
21:30:19	172.17.0.2	172.17.0.1	UDP	70	34537 > 40868 Len=28
21:30:19	172.17.0.2	172.17.0.1	UDP	74	34537 > 40868 Len=32
21:30:19	172.17.0.2	172.17.0.1	UDP	85	34537 > 40868 Len=43
21:30:20	172.17.0.2	172.17.0.1	UDP	71	34537 > 40868 Len=29
21:33:23	172.17.0.2	172.17.0.1	UDP	70	34537 > 40868 Len=28
21:33:23	172.17.0.2	172.17.0.1	UDP	71	34537 > 40868 Len=29
21:36:19	172.17.0.2	172.17.0.1	UDP	70	34537 > 40868 Len=28
21:42:23	172.17.0.2	172.17.0.1	UDP	70	34537 > 40868 Len=28
21:45:20	172.17.0.2	172.17.0.1	UDP	72	34537 > 40868 Len=30
21:45:20	172.17.0.2	172.17.0.1	UDP	70	34537 > 40868 Len=28
21:45:21	172.17.0.2	172.17.0.1	UDP	85	34537 > 40868 Len=43
21:45:21	172.17.0.2	172.17.0.1	UDP	71	34537 > 40868 Len=29
21:48:18	172.17.0.2	172.17.0.1	UDP	71	34537 > 40868 Len=29
21:51:18	172.17.0.2	172.17.0.1	UDP	70	34537 > 40868 Len=28
21:51:18	172.17.0.2	172.17.0.1	UDP	71	34537 > 40868 Len=29
21:54:16	172.17.0.2	172.17.0.1	UDP	70	34537 > 40868 Len=28
21:54:16	172.17.0.2	172.17.0.1	UDP	71	34537 > 40868 Len=29
21:57:11	172.17.0.2	172.17.0.1	UDP	70	34537 > 40868 Len=28
22:00:08	172.17.0.2	172.17.0.1	UDP	72	34537 > 40868 Len=30
22:00:08	172.17.0.2	172.17.0.1	UDP	78	34537 > 40868 Len=36
22:00:09	172.17.0.2	172.17.0.1	UDP	85	34537 > 40868 Len=43
22:03:05	172.17.0.2	172.17.0.1	UDP	70	34537 > 40868 Len=28
22:03:05	172.17.0.2	172.17.0.1	UDP	71	34537 > 40868 Len=29
22:06:03	172.17.0.2	172.17.0.1	UDP	70	34537 > 40868 Len=28
22:06:03	172.17.0.2	172.17.0.1	UDP	71	34537 > 40868 Len=29

Notice that complete LoRa message happens once every 3 minutes, as stated by the manufacturer (with some exceptions, which are assumed as events in which LoRa messages were lost).

3. Data traffic between the local and mutualized infrastructure of the case study “Smart metering”

The following table show an extract of the data traffic between the gateway and the cloud server of the case study “Smart metering”, obtained in just under the last three minutes of the experiment (from 21:58:03 to 22:00:08). The main traffic type identified was DNS request from the gateway (IP address 192.168.137.47) to the IAP device (IP address 192.168.137.1) and roundtrip TCP and HTTP traffic between the gateway and the cloud server (www.mySolem.com). The green cells shows an instance of a regular transmission event for uploading the counts of the flow meter in the cloud server (HTTP post message in bold text). It start by a DNS request to obtain the IP address of the cloud server (www.mySolem.com) and finish by a TCP teardown routine (the table shows red frames to highlight this behavior). The red cells shows the mechanisms that are activated in the gateway and the cloud server when the user consults his or her water consumption (the three red sections shows the three peaks seen in the figure 5.21, presented in the section 1.3.3 of the chapter 5). It is assumed that the gateway send this information by the HTTP post messages (showed by the red bold text). Sometimes the IP source changes as the gateway reassign a new IP in the local network.

capture time	Source	Destination	Protocol	Length	Info
21:58:03	mysolem.com	192.168.137.47	HTTP	466	HTTP/1.1 408 Request Timeout
21:58:03	192.168.137.47	mysolem.com	TCP	54	33626 > 80 [ACK] Seq=147 Ack=413 Win=2508 Len=0
21:58:03	192.168.137.47	mysolem.com	TCP	54	33626 > 80 [FIN, ACK] Seq=147 Ack=413 Win=2508 Len=0
21:58:03	mysolem.com	192.168.137.47	TCP	54	80 > 33626 [FIN, ACK] Seq=413 Ack=148 Win=30016 Len=0
21:58:03	192.168.137.47	mysolem.com	TCP	54	33626 > 80 [RST, ACK] Seq=148 Ack=414 Win=2920 Len=0
21:58:04	192.168.137.47	192.168.137.1	DNS	71	Standard query 0xf6c7 A mysolem.com
21:58:04	192.168.137.1	192.168.137.47	DNS	87	Standard query response 0xf6c7 A mysolem.com A 51.159.17.150
21:58:04	192.168.137.47	mysolem.com	TCP	58	9167 > 80 [SYN] Seq=0 Win=2920 Len=0 MSS=1460
21:58:04	mysolem.com	192.168.137.47	TCP	58	80 > 9167 [SYN, ACK] Seq=0 Ack=1 Win=2920 Len=0 MSS=1460
21:58:04	192.168.137.47	mysolem.com	TCP	54	9167 > 80 [ACK] Seq=1 Ack=1 Win=2920 Len=0
21:58:04	192.168.137.47	mysolem.com	HTTP	200	POST /v2/periodic/0500000506F80001/ HTTP/1.1 (application/json)Continuation
21:58:04	mysolem.com	192.168.137.47	TCP	54	80 > 9167 [ACK] Seq=1 Ack=147 Win=30016 Len=0
21:58:22	mysolem.com	192.168.137.47	HTTP	466	HTTP/1.1 408 Request Timeout
21:58:22	192.168.137.47	mysolem.com	TCP	54	9167 > 80 [ACK] Seq=147 Ack=413 Win=2508 Len=0
21:58:22	192.168.137.47	mysolem.com	TCP	54	9167 > 80 [FIN, ACK] Seq=147 Ack=413 Win=2508 Len=0
21:58:22	mysolem.com	192.168.137.47	TCP	54	80 > 9167 [FIN, ACK] Seq=413 Ack=148 Win=30016 Len=0
21:58:22	192.168.137.47	mysolem.com	TCP	54	9167 > 80 [ACK] Seq=148 Ack=414 Win=2507 Len=0
21:58:23	192.168.137.47	192.168.137.1	DNS	71	Standard query 0x2555 A mysolem.com
21:58:23	192.168.137.1	192.168.137.47	DNS	87	Standard query response 0x2555 A mysolem.com A 51.159.17.150
21:58:23	192.168.137.47	mysolem.com	TCP	58	12306 > 80 [SYN] Seq=0 Win=2920 Len=0 MSS=1460
21:58:24	192.168.137.47	mysolem.com	TCP	58	[TCP Retransmission] 12306 > 80 [SYN] Seq=0 Win=2920 Len=0 MSS=1460
21:58:24	mysolem.com	192.168.137.47	TCP	58	80 > 12306 [SYN, ACK] Seq=0 Ack=1 Win=2920 Len=0 MSS=1460
21:58:24	192.168.137.47	mysolem.com	TCP	54	12306 > 80 [ACK] Seq=1 Ack=1 Win=2920 Len=0
21:58:24	192.168.137.47	mysolem.com	HTTP	200	POST /v2/periodic/0500000506F80001/ HTTP/1.1 (application/json)Continuation
21:58:24	mysolem.com	192.168.137.47	TCP	54	80 > 12306 [ACK] Seq=1 Ack=147 Win=30016 Len=0
21:58:42	mysolem.com	192.168.137.47	HTTP	468	HTTP/1.1 408 Request Timeout
21:58:42	192.168.137.47	mysolem.com	TCP	54	12306 > 80 [FIN, ACK] Seq=147 Ack=415 Win=2506 Len=0
21:58:42	mysolem.com	192.168.137.47	TCP	54	80 > 12306 [FIN, ACK] Seq=415 Ack=148 Win=30016 Len=0
21:58:42	192.168.137.47	mysolem.com	TCP	54	12306 > 80 [ACK] Seq=148 Ack=416 Win=2505 Len=0
21:58:43	192.168.137.47	192.168.137.1	DNS	71	Standard query 0x21d5 A mysolem.com
21:58:43	192.168.137.1	192.168.137.47	DNS	87	Standard query response 0x21d5 A mysolem.com A 51.159.17.150
21:58:43	192.168.137.47	mysolem.com	TCP	58	9468 > 80 [SYN] Seq=0 Win=2920 Len=0 MSS=1460
21:58:43	mysolem.com	192.168.137.47	TCP	58	80 > 9468 [SYN, ACK] Seq=0 Ack=1 Win=2920 Len=0 MSS=1460
21:58:43	192.168.137.47	mysolem.com	TCP	54	9468 > 80 [ACK] Seq=1 Ack=1 Win=2920 Len=0
21:58:43	192.168.137.47	mysolem.com	HTTP	200	POST /v2/periodic/0500000506F80001/ HTTP/1.1 (application/json)Continuation
21:58:43	mysolem.com	192.168.137.47	TCP	54	80 > 9468 [ACK] Seq=1 Ack=147 Win=30016 Len=0
21:59:01	mysolem.com	192.168.137.47	HTTP	466	HTTP/1.1 408 Request Timeout
21:59:01	192.168.137.47	mysolem.com	TCP	54	9468 > 80 [FIN, ACK] Seq=147 Ack=413 Win=2508 Len=0
21:59:01	mysolem.com	192.168.137.47	TCP	54	80 > 9468 [FIN, ACK] Seq=413 Ack=148 Win=30016 Len=0
21:59:01	192.168.137.47	mysolem.com	TCP	54	9468 > 80 [ACK] Seq=148 Ack=414 Win=2507 Len=0
21:59:02	192.168.137.47	192.168.137.1	DNS	71	Standard query 0xfa18 A mysolem.com
21:59:02	192.168.137.1	192.168.137.47	DNS	87	Standard query response 0xfa18 A mysolem.com A 51.159.17.150
21:59:02	192.168.137.47	mysolem.com	TCP	58	7695 > 80 [SYN] Seq=0 Win=2920 Len=0 MSS=1460
21:59:03	192.168.137.47	mysolem.com	TCP	58	[TCP Retransmission] 7695 > 80 [SYN] Seq=0 Win=2920 Len=0 MSS=1460
21:59:03	mysolem.com	192.168.137.47	TCP	58	80 > 7695 [SYN, ACK] Seq=0 Ack=1 Win=2920 Len=0 MSS=1460
21:59:03	192.168.137.47	mysolem.com	TCP	54	7695 > 80 [ACK] Seq=1 Ack=1 Win=2920 Len=0
21:59:03	192.168.137.47	mysolem.com	HTTP	200	POST /v2/periodic/0500000506F80001/ HTTP/1.1 (application/json)Continuation
21:59:03	mysolem.com	192.168.137.47	TCP	54	80 > 7695 [ACK] Seq=1 Ack=147 Win=30016 Len=0
21:59:13	mysolem.com	192.168.137.47	HTTP	551	HTTP/1.1 200 OK (application/json)
21:59:13	192.168.137.47	mysolem.com	TCP	54	7695 > 80 [ACK] Seq=147 Ack=498 Win=2423 Len=0
21:59:13	192.168.137.47	mysolem.com	HTTP	390	POST /v2/response/0500000506F80001/B0ACD6FAE59147DFBDE8ECD2B34085BB HTTP/1.1 (application/json)
21:59:13	mysolem.com	192.168.137.47	TCP	54	80 > 7695 [ACK] Seq=498 Ack=483 Win=31088 Len=0
21:59:13	mysolem.com	192.168.137.47	HTTP	420	HTTP/1.1 200 OK
21:59:13	192.168.137.47	mysolem.com	HTTP	200	POST /v2/periodic/0500000506F80001/ HTTP/1.1 (application/json)Continuation
21:59:13	mysolem.com	192.168.137.47	TCP	54	80 > 7695 [ACK] Seq=864 Ack=629 Win=32160 Len=0
21:59:16	mysolem.com	192.168.137.47	HTTP	570	HTTP/1.1 200 OK (application/json)
21:59:17	192.168.137.47	mysolem.com	TCP	54	7695 > 80 [ACK] Seq=629 Ack=1380 Win=1541 Len=0
21:59:17	192.168.137.47	mysolem.com	HTTP	346	POST /v2/response/0500000506F80001/CF5856A5567A4AA7B2E7DB0A9CAC8A60 HTTP/1.1 (application/json)
21:59:17	mysolem.com	192.168.137.47	TCP	54	80 > 7695 [ACK] Seq=1380 Ack=921 Win=33232 Len=0

21:59:17	mysolem.com	192.168.137.47	HTTP	420	HTTP/1.1 200 OK
21:59:17	192.168.137.47	mysolem.com	TCP	54	7695 > 80 [ACK] Seq=921 Ack=1746 Win=2920 Len=0
21:59:17	192.168.137.47	mysolem.com	HTTP	200	POST /v2/periodic/0500000506F80001/ HTTP/1.1 (application/json)Continuation
21:59:17	mysolem.com	192.168.137.47	HTTP	572	HTTP/1.1 200 OK (application/json)
21:59:17	192.168.137.47	mysolem.com	TCP	54	7695 > 80 [ACK] Seq=1067 Ack=2264 Win=2402 Len=0
21:59:17	192.168.137.47	mysolem.com	HTTP	787	POST /v2/response/0500000506F80001/74F9D612DF944AE3A97A6139602EBA7E HTTP/1.1 (application/json)
21:59:17	mysolem.com	192.168.137.47	HTTP	420	HTTP/1.1 200 OK
21:59:17	192.168.137.47	mysolem.com	TCP	54	7695 > 80 [ACK] Seq=1800 Ack=2630 Win=2036 Len=0
21:59:17	192.168.137.47	mysolem.com	HTTP	200	POST /v2/periodic/0500000506F80001/ HTTP/1.1 (application/json)Continuation
21:59:17	mysolem.com	192.168.137.47	TCP	54	80 > 7695 [ACK] Seq=2630 Ack=1946 Win=37383 Len=0
21:59:17	mysolem.com	192.168.137.47	HTTP	563	HTTP/1.1 200 OK (application/json)
21:59:17	192.168.137.47	mysolem.com	TCP	54	7695 > 80 [ACK] Seq=1946 Ack=3139 Win=1527 Len=0
21:59:17	192.168.137.47	mysolem.com	HTTP	398	POST /v2/response/0500000506F80001/50F7A8B843F4EC6A4FF8ECE619233DA HTTP/1.1 (application/json)
21:59:17	mysolem.com	192.168.137.47	TCP	54	80 > 7695 [ACK] Seq=3139 Ack=2290 Win=38849 Len=0
21:59:17	mysolem.com	192.168.137.47	HTTP	420	HTTP/1.1 200 OK
21:59:17	192.168.137.47	mysolem.com	TCP	54	7695 > 80 [ACK] Seq=2290 Ack=3505 Win=2920 Len=0
21:59:17	192.168.137.47	mysolem.com	HTTP	200	POST /v2/periodic/0500000506F80001/ HTTP/1.1 (application/json)Continuation
21:59:18	mysolem.com	192.168.137.47	TCP	54	80 > 7695 [ACK] Seq=3505 Ack=2436 Win=40315 Len=0
21:59:30	mysolem.com	192.168.137.47	HTTP	570	HTTP/1.1 200 OK (application/json)
21:59:30	192.168.137.47	mysolem.com	TCP	54	7695 > 80 [ACK] Seq=2436 Ack=4021 Win=2404 Len=0
21:59:30	192.168.137.47	mysolem.com	HTTP	346	POST /v2/response/0500000506F80001/57218E3BCDC74FDEA213E44AA1BDE558 HTTP/1.1 (application/json)
21:59:30	mysolem.com	192.168.137.47	TCP	54	80 > 7695 [ACK] Seq=4021 Ack=2728 Win=41781 Len=0
21:59:30	mysolem.com	192.168.137.47	HTTP	424	HTTP/1.1 200 OK
21:59:31	192.168.137.47	mysolem.com	HTTP	200	POST /v2/periodic/0500000506F80001/ HTTP/1.1 (application/json)Continuation
21:59:31	mysolem.com	192.168.137.47	HTTP	574	HTTP/1.1 200 OK (application/json)
21:59:31	192.168.137.47	mysolem.com	TCP	54	7695 > 80 [ACK] Seq=2874 Ack=4911 Win=1514 Len=0
21:59:31	192.168.137.47	mysolem.com	HTTP	787	POST /v2/response/0500000506F80001/0C572E37CA0148BA82BE9D4BD62BA48D HTTP/1.1 (application/json)
21:59:31	mysolem.com	192.168.137.47	HTTP	420	HTTP/1.1 200 OK
21:59:31	192.168.137.47	mysolem.com	TCP	54	7695 > 80 [ACK] Seq=3607 Ack=5277 Win=2920 Len=0
21:59:31	192.168.137.47	mysolem.com	HTTP	200	POST /v2/periodic/0500000506F80001/ HTTP/1.1 (application/json)Continuation
21:59:31	mysolem.com	192.168.137.47	TCP	54	80 > 7695 [ACK] Seq=5277 Ack=3753 Win=46179 Len=0
21:59:31	mysolem.com	192.168.137.47	HTTP	565	HTTP/1.1 200 OK (application/json)
21:59:31	192.168.137.47	mysolem.com	TCP	54	7695 > 80 [ACK] Seq=3753 Ack=5788 Win=2409 Len=0
21:59:31	192.168.137.47	mysolem.com	HTTP	398	POST /v2/response/0500000506F80001/618B4FB6FFA845F7A815CB3F095168FC HTTP/1.1 (application/json)
21:59:31	mysolem.com	192.168.137.47	TCP	54	80 > 7695 [ACK] Seq=5788 Ack=4097 Win=47645 Len=0
21:59:31	mysolem.com	192.168.137.47	HTTP	422	HTTP/1.1 200 OK
21:59:31	192.168.137.47	mysolem.com	TCP	54	7695 > 80 [ACK] Seq=4097 Ack=6156 Win=2041 Len=0
21:59:31	192.168.137.47	mysolem.com	HTTP	200	POST /v2/periodic/0500000506F80001/ HTTP/1.1 (application/json)Continuation
21:59:31	mysolem.com	192.168.137.47	TCP	54	80 > 7695 [ACK] Seq=6156 Ack=4243 Win=49111 Len=0
21:59:49	mysolem.com	192.168.137.47	HTTP	464	HTTP/1.1 408 Request Timeout
21:59:50	192.168.137.47	mysolem.com	TCP	54	7695 > 80 [ACK] Seq=4243 Ack=6566 Win=1631 Len=0
21:59:50	192.168.137.47	mysolem.com	TCP	54	7695 > 80 [FIN, ACK] Seq=4243 Ack=6566 Win=1631 Len=0
21:59:50	mysolem.com	192.168.137.47	TCP	54	80 > 7695 [FIN, ACK] Seq=6566 Ack=4244 Win=49111 Len=0
21:59:50	192.168.137.47	mysolem.com	TCP	54	7695 > 80 [ACK] Seq=4244 Ack=6567 Win=1630 Len=0
21:59:50	192.168.137.47	192.168.137.1	DNS	71	Standard query 0x4a0e A mysolem.com
21:59:50	192.168.137.1	192.168.137.47	DNS	87	Standard query response 0x4a0e A mysolem.com A 51.159.17.150
21:59:50	192.168.137.47	mysolem.com	TCP	58	47749 > 80 [SYN] Seq=0 Win=2920 Len=0 MSS=1460
21:59:50	mysolem.com	192.168.137.47	TCP	58	80 > 47749 [SYN, ACK] Seq=0 Ack=1 Win=2920 Len=0 MSS=1460
21:59:50	192.168.137.47	mysolem.com	TCP	54	47749 > 80 [ACK] Seq=1 Ack=1 Win=2920 Len=0
21:59:50	192.168.137.47	mysolem.com	HTTP	200	POST /v2/periodic/0500000506F80001/ HTTP/1.1 (application/json)Continuation
21:59:50	mysolem.com	192.168.137.47	TCP	54	80 > 47749 [ACK] Seq=1 Ack=147 Win=30016 Len=0
22:00:08	mysolem.com	192.168.137.47	HTTP	468	HTTP/1.1 408 Request Timeout

Notice that regular transmissions for uploading the data application happens every 18 seconds (with some exceptions, which are assumed as events in which messages were lost).

4. Bill of Materials of the EH sensor system in its memory-based version (referential design)

The following table shows the Bill of Materials of the referential electronic design of the memory-based version (set 13). The other sets vary only in the other electronic components studied in this work (voltage comparators, Microcontroller, NFC-EEPROM memory and PCB). They are marked in the blue cells and their technical and material declaration documentation are available in the reference section. The piezoelectric buzzer is excluded from the LCA analysis due to the lack of LCA data. All components have SMD-typed packages.

Quantity	Electronic component	Package type or material	Dimensions mm (L or Diameter x W x H)	Weight per component (g)	Total Weight per component type (g)	Number of pins or solder points
7	Ceramic capacitors	0402	1.10 x 0.6 x 0.6	0.0014	0,0098	2
1	Ceramic capacitor	1812	4.8 x 3.4 x 1.7	0.1952	0,1952	2
9	Resistors	0402	1.05 x 0.55 x 0.40	0.00108	0,00972	2
2	Schottky diodes	SOT666	1.7 x 1.3 x 0.6	0.0029	0,0058	6
1	Light Emitting Diode	0603	1.6 x 1.15 x 0.55	0.001	0,001	2
2	Transistors	SOT323	2.2 x 1.35 x 1.1	0.006	0,012	3
1	Voltage comparator [170] [180]	SC70-5	2.2 x 1.35 x 1	0.006	0,006	5
2	Voltage detectors [175] [189]	SOT23-5	2.9 x 1.6 x 1.3	0.0165	0,033	5
1	Microcontroller [171] [184]	UFQFPN32	5.1 x 5.1 x 0.6	0.04908	0,04908	32
1	NFC-EEPROM Memory [172] [186]	TSSOP8	4.5 x 3.1 x 1.05	0.034	0,034	8
2	Piezo electronic buzzers	n.a.	35 x 0.3	3,35	3,35	4
1	Plastic case	Acrylonitrile Butadiene Styrene (ABS)	83.5 x 48 x 7	15,78	15,78	n.a.
1	PCB	FR4 - 4 layers	32 x 22 x 1	1,1533	1,1533	n.a.
Total weight of the device (g)					20,6389	
Total weight of the electronic card (excluding the piezo electric buzzer) (g)					1,5089	

5. Bill of Materials of the EH sensor system in its BLE-based version

The following table shows the Bill of Materials of the electronic design of the BLE-Version. It includes a BLE module, which is described by its subcomponents (type and quantity). Non-conventional parts (e.g., Balun filter, metal lid, etc.) and special soldering types are presented with their material composition in percentages (xx,xxYY format, where xx,xx depicts the percentage share and YY the symbol element). To facilitate the LCA modeling of the SoC sub component of the BLE module, it is considered the unique available material declaration of an BlueNRG-2 SoC in a QFN32 package version [190] [191]. The piezoelectric buzzer is excluded from the LCA analysis due to the lack of LCA data. All components have SMD-typed packages. For the LCA modeling of the ceramic antenna, one uses a LCA data proxy (market of RF inductor (GLO)).

Quantity	Electronic component	Sub components	Package type or material	Dimensions mm (L or Diameter x W x H)	Weight per component (g)	Total Weight per component type (g)	Number of pins or solder points
5	Ceramic capacitors	n.a.	0603	1.6 x 0.8 x 0.9	0.0061	0,0305	2
1	Ceramic capacitor	n.a.	1210	3.2 x 2.5 x 1.7	0.1185	0,1185	2
1	Ceramic capacitor	n.a.	0805	2 x 1.25 x 1.3	0.0168	0,0168	2
1	Resistor	n.a.	0603	1.7 x 0.9 x 0.6	0.00183	0,00183	2
3	Resistors	n.a.	0805	2.1 x 1.35 x 0.65	0.00471	0,00471	2
2	Schottky diodes	n.a.	SC70-6	2.2 x 1.35 x 0.6	0.006	0,012	6
1	Transistor	n.a.	SOT323	2.2 x 1.35 x 1.1	0.006	0,006	3
1	Voltage comparator [170] [180]	n.a.	SC70-5	2.2 x 1.35 x 1	0.006	0,006	5
2	Voltage detectors [175] [189]	n.a.	SOT23-5	2.9 x 1.6 x 1.3	0.0165	0,033	5
1	BLE module [192]	1 Balun filter (100Si)	n.a.	n.a.	0.0032	0,0032	n.a.
		1 BlueNRG-2 SoC [190] [191]	QFN32	5 x 5 x 1	0.036	0,036	32
		1 PCB	n.a.	13.5 x 11.5 x 0.8	0.2484	0,2484	20
		1 Metal lid (64,08Cu18,82Zn17Ni0,1Mn)	n.a.	n.a.	0,198	0,198	n.a.
		Solder type 1 (95Sn5Sb)	n.a.	n.a.	0.015159	0,015159	n.a.
		Solder type 2 (Not specific)	n.a.	n.a.	0.0045	0,0045	n.a.
		1 Inductor	0603	0.6 x 0.3 x 0.3	0.0002	0,0002	2
		2 Inductors	1005	1 x 0.5 x 0.35	0.0004	0,0008	2
		14 Capacitors	0603	0.6 x 0.3 x 0.3	0.00033	0,00462	2
		2 Crystal oscillators	0805	2.05 x 1.2 x 0.55	0.005538	0,011076	2
		1 Inductor	1005	1 x 0.5 x 0.5	0.00098	0,00098	2
		1 Inductor	1608	1.6 x 0.8 x 0.8	0.004	0,004	2
		1 Ceramic Antenna	Undetermined	3.2 x 1.6 x 1.3	0.019791	0,019791	2
2	Piezo electric buzzers	n.a.	n.a.	35 x 0.3	3,35	3,35	4
1	Plastic case	n.a.	Acrylonitrile Butadiene Styrene (ABS)	83.5 x 48 x 7	15,78	15,78	n.a.
1	PCB	n.a.	FR4 - 4 layers	32 x 22 x 1	1,1533	1,1533	n.a.
Total weight of the device(g)						21,06	
Total weight of the electronic card (excluding the piezo electric buzzer) (g)						1,9294	

6. Variations of the PCB area according to the design sets of the memory-based version

The following table present the variations of the PCB surface of the memory-based version of the EH sensor system, with respect to the referential PCB size of set 13 (rightest column). One calculates these variations by adding to the referential PCB size (704 mm²), the difference of the aggregated land pattern area of the components that shapes a set with the aggregated land pattern area of the components that compose the referential set 13. The land pattern areas consider the IPC-7351 standard in its most penalizing version (0,5 mm), which add 1 mm to the length and width sides. The reference set is showed in gray; the smallest and the biggest PCB sizes appear in the green and red cells respectively.

	Components	Land patterns (mm)		Including the IPC-7351B standard (mm)		Land pattern areas (mm)	Aggregated land pattern area (mm)	PCB sizes (mm)
		L	W	L	W			
Set 1	VC SC70-5	2,2	2,4	3,2	3,4	10,88	146,08	770,83
	LQFP32	9,2	9,2	10,2	10,2	104,04		
	TSSOP8	6,6	3,1	7,6	4,1	31,16		
Set 2	VC SC70-5	2,2	2,4	3,2	3,4	10,88	127,63	752,38
	LQFP32	9,2	9,2	10,2	10,2	104,04		
	UFDFPN8	3,1	2,1	4,1	3,1	12,71		
Set 3	VC SC70-5	2,2	2,4	3,2	3,4	10,88	158,12	782,87
	LQFP32	9,2	9,2	10,2	10,2	104,04		
	SO8	6,2	5,0	7,2	6,0	43,20		
Set 4	VC SOT23-5	2,9	2,8	3,9	3,8	14,82	150,02	774,77
	LQFP32	9,2	9,2	10,2	10,2	104,04		
	TSSOP8	6,6	3,1	7,6	4,1	31,16		
Set 5	VC SOT23-5	2,9	2,8	3,9	3,8	14,82	131,57	756,32
	LQFP32	9,2	9,2	10,2	10,2	104,04		
	UFDFPN8	3,1	2,1	4,1	3,1	12,71		
Set 6	VC SOT23-5	2,9	2,8	3,9	3,8	14,82	162,06	786,81
	LQFP32	9,2	9,2	10,2	10,2	104,04		
	SO8	6,2	5,0	7,2	6,0	43,20		
Set 7	VC SC70-5	2,2	2,4	3,2	3,4	10,88	79,86	704,61
	TFBGA64	5,2	5,2	6,2	6,2	37,82		
	TSSOP8	6,6	3,1	7,6	4,1	31,16		
Set 8	VC SC70-5	2,2	2,4	3,2	3,4	10,88	61,41	686,16
	TFBGA64	5,2	5,2	6,2	6,2	37,82		
	UFDFPN8	3,1	2,1	4,1	3,1	12,71		
Set 9	VC SC70-5	2,2	2,4	3,2	3,4	10,88	91,90	716,65
	TFBGA64	5,2	5,2	6,2	6,2	37,82		
	SO8	6,2	5,0	7,2	6,0	43,20		
Set 10	VC SOT23-5	2,9	2,8	3,9	3,8	14,82	83,80	708,55
	TFBGA64	5,2	5,2	6,2	6,2	37,82		
	TSSOP8	6,6	3,1	7,6	4,1	31,16		
Set 11	VC SOT23-5	2,9	2,8	3,9	3,8	14,82	65,35	690,10
	TFBGA64	5,2	5,2	6,2	6,2	37,82		
	UFDFPN8	3,1	2,1	4,1	3,1	12,71		
Set 12	VC SOT23-5	2,9	2,8	3,9	3,8	14,82	95,84	720,59
	TFBGA64	5,2	5,2	6,2	6,2	37,82		
	SO8	6,2	5,0	7,2	6,0	43,20		
Set 13	VC SC70-5	2,2	2,4	3,2	3,4	10,88	79,25	704,00
	UFQFPN32	5,1	5,1	6,1	6,1	37,21		
	TSSOP8	6,6	3,1	7,6	4,1	31,16		
Set 14	VC SC70-5	2,2	2,4	3,2	3,4	10,88	60,80	685,55
	UFQFPN32	5,1	5,1	6,1	6,1	37,21		
	UFDFPN8	3,1	2,1	4,1	3,1	12,71		
Set 15	VC SC70-5	2,2	2,4	3,2	3,4	10,88	91,29	716,04
	UFQFPN32	5,1	5,1	6,1	6,1	37,21		
	SO8	6,2	5,0	7,2	6,0	43,20		
Set 16	VC SOT23-5	2,9	2,8	3,9	3,8	14,82	83,19	707,94
	UFQFPN32	5,1	5,1	6,1	6,1	37,21		
	TSSOP8	6,6	3,1	7,6	4,1	31,16		
Set 17	VC SOT23-5	2,9	2,8	3,9	3,8	14,82	64,74	689,49
	UFQFPN32	5,1	5,1	6,1	6,1	37,21		
	UFDFPN8	3,1	2,1	4,1	3,1	12,71		
Set 18	VC SOT23-5	2,9	2,8	3,9	3,8	14,82	95,23	719,98
	UFQFPN32	5,1	5,1	6,1	6,1	37,21		
	SO8	6,2	5,0	7,2	6,0	43,20		
Set 19	VC SC70-5	2,2	2,4	3,2	3,4	10,88	56,21	680,96
	WLCSP36	2,9	2,6	3,9	3,6	14,17		
	TSSOP8	6,6	3,1	7,6	4,1	31,16		
Set 20	VC SC70-5	2,2	2,4	3,2	3,4	10,88	37,76	662,51
	WLCSP36	2,9	2,6	3,9	3,6	14,17		
	UFDFPN8	3,1	2,1	4,1	3,1	12,71		
Set 21	VC SC70-5	2,2	2,4	3,2	3,4	10,88	68,25	693,00
	WLCSP36	2,9	2,6	3,9	3,6	14,17		
	SO8	6,2	5,0	7,2	6,0	43,20		
Set 22	VC SOT23-5	2,9	2,8	3,9	3,8	14,82	60,15	684,90
	WLCSP36	2,9	2,6	3,9	3,6	14,17		
	TSSOP8	6,6	3,1	7,6	4,1	31,16		
Set 23	VC SOT23-5	2,9	2,8	3,9	3,8	14,82	41,70	666,45
	WLCSP36	2,9	2,6	3,9	3,6	14,17		
	UFDFPN8	3,1	2,1	4,1	3,1	12,71		
Set 24	VC SOT23-5	2,9	2,8	3,9	3,8	14,82	72,19	696,94
	WLCSP36	2,9	2,6	3,9	3,6	14,17		
	SO8	6,2	5,0	7,2	6,0	43,20		

7. Material content shares of the studied voltage comparators

The following information is an adaptation of the Full Material Declaration (FMD) of the voltage comparators studied in this work. The values in the rightmost column “Content share in the IC” are considered as the typical material content shares used in the uncertainty analysis of section 2.1.3, seen in chapter 5. To obtain the internal die area ratio factor, one divides the product of the IC packaging surface and the die share with its total weight (following the Ecoinvent method described in [174], which is explained in section 4.1 of chapter 4). To obtain the die area of the component, one multiplies this factor with the total weight of the integrated circuit. For a detailed review, the reader can consult the FMD document provided by the manufacturer, which appears in the reference near to the name of the component.

a) Rail-to-rail 0.9 V nanopower comparator, SC70-5 type [180]

Subpart	mg	% subpart	Material	mg	Content share in the subpart	Content share in the IC
Die	0,178	2,967%	Die	0,178	100,000%	2,967%
Lead frame	2,954	49,233%	Iron (Fe)	0,067	2,268%	1,117%
			Copper (Cu)	2,829	95,768%	47,150%
			Phosphorus (P)	0,001	0,034%	0,017%
			Zinc (Zn)	0,004	0,135%	0,067%
			Nickel (Ni)	0,034	1,151%	0,567%
			Palladium (Pd)	0,003	0,102%	0,050%
			Silver (Ag)	0,016	0,542%	0,267%
Die attach	0,005	0,083%	Carbocyclic Acrylates	0,002	40,000%	0,033%
			Bismaleimide resin	0,002	40,000%	0,033%
			2-preponoic acid, 2-methyl	0,001	20,000%	0,017%
Bonding wires	0,033	0,550%	Gold (Au)	0,033	100,000%	0,550%
Encapsulation	2,830	47,167%	Epoxy Resin-1	0,056	1,979%	0,933%
			Epoxy Resin-2	0,056	1,979%	0,933%
			Epoxy Resin-3	0,056	1,979%	0,933%
			Phenol resin	0,114	4,028%	1,900%
			Silica	2,542	89,823%	42,367%
			Carbon black	0,006	0,212%	0,100%
TOTAL	6,000	100,000%				

Packaging Length (mm): 2,2
 Packaging Width (mm): 1,35
 Internal die area ratio (mm² / mg): 0,0147
 Internal die (mm²): 0,0881

b) Rail-to-rail 0.9 V nanopower comparator, SOT23-5 type [181]

Subpart	mg	% subpart	Material	mg	Content share in the subpart	Content share in the IC
Die	0,253	1,546%	Die	0,253	100,000%	1,546%
Lead frame	6,923	42,296%	Copper (Cu)	6,651	96,071%	40,634%
			Iron (Fe)	0,167	2,412%	1,020%
			Iron Phosphide (FeP)	0,002	0,029%	0,012%
			Zinc (Zn)	0,009	0,130%	0,055%
			Nickel (Ni)	0,086	1,242%	0,525%
			Palladium (Pd)	0,007	0,101%	0,043%
			Gold (Au)	0,001	0,014%	0,006%
			Silver (Ag)	0,057	72,152%	0,348%
Die attach	0,079	0,483%	methylene diacrylate	0,013	16,456%	0,079%
			Dicyclopentenyloxyethyl methacrylate	0,003	3,797%	0,018%
			Bismaleimide resin	0,003	3,797%	0,018%
			Palladium (Pd)	0,001	1,266%	0,006%
			Dicumyllyl peroxide	0,002	2,532%	0,012%
Bonding wire	0,157	0,959%	Gold (Au)	0,157	100,000%	0,959%
encapsulation	8,956	54,717%	Epoxy Resin	0,354	3,953%	2,163%
			Biphenyl epoxy resin	0,133	1,485%	0,813%
			Phenol resin	0,37	4,131%	2,261%
			Silica	7,179	80,159%	43,860%
			Carbon Black	0,017	0,190%	0,104%
			Zinc hydroxide	0,165	1,842%	1,008%
			VARIOUS NOT DECLARED	0,738	8,240%	4,509%
TOTAL	16,368	100,000%				

Packaging Length (mm): 2,9
 Packaging Width (mm): 1,6
 Internal die area ratio (mm² / mg): 0,0044
 Internal die (mm²): 0,0717

8. Material content shares of the studied microcontrollers

The following information is an adaptation of the Full Material Declaration (FMD) of the microcontrollers studied in this work. The values in the rightmost column “Content share in the IC” are considered as the typical material content shares used in the uncertainty analysis of section 2.1.3, seen in chapter 5. To obtain the internal die area ratio factor, one divides the product of the IC packaging surface and the die share with its total weight, following the Ecoinvent method described in [174], which is explained in section 4.1 of chapter 4). To obtain the die area of the component, one multiplies this factor with the total weight of the integrated circuit. For a detailed review, the reader can consult the FMD document provided by the manufacturer, which appears in the reference near to the name of the component.

a) Access line ultra-low-power 32-bit MCU Arm®-based Cortex®-M0+, LQFP32 type [182]

Subpart	mg	% subpart	Material	mg	Content share in the subpart	Content share in the IC
Die or dies	6,674	3,636%	Die	6,674	100,000%	3,636%
Die Attach Epoxy_ABLEBOND 3230_H	0,908	0,495%	Silver	0,643	70,813%	0,350%
			2,2-[Methylenebis(phenyleneoxymethylene)]	0,044	4,846%	0,024%
			Dihydro-3-(tetrapropenyl)furan-2,5-dione	0,044	4,846%	0,024%
			Epoxy resin	0,044	4,846%	0,024%
			Dodecyloxirane	0,044	4,846%	0,024%
			1,3-Isobenzofurandione, hexahydro-5-methyl-	0,044	4,846%	0,024%
			1,4-Bis(2,3-epoxypropoxy)butane	0,044	4,846%	0,024%
EMC_G631SHQ_Sumitomo (Encapsulation)	118,466	64,536%	Epoxy Resin A	2,488	2,100%	1,355%
			Epoxy Resin B	2,488	2,100%	1,355%
			Phenol Resin	6,634	5,600%	3,614%
			Silica(Amorphous)A	92,457	78,045%	50,367%
			Silica(Amorphous)B	13,662	11,532%	7,443%
			Carbon Black	0,738	0,623%	0,402%
BondingWire_Ag_MKE	0,301	0,164%	Silver	0,289	96,013%	0,157%
			Others	0,012	3,987%	0,007%
Anode Ball_Tin_Asahi	1,209	0,659%	Tin	1,209	100,000%	0,659%
Leadframe_C9+Ag_HDS	56,007	30,511%	Iron	1,225	2,187%	0,667%
			Phosphorus	0,041	0,073%	0,022%
			Zinc	0,063	0,112%	0,034%
			Copper	51,148	91,324%	27,864%
			Silver	3,528	6,299%	1,922%
			Lead	0,003	0,005%	0,002%
TOTAL	183,565	100,000%				

Packaging Length (mm): 7,2
 Packaging Width (mm): 7,2
 Internal die area ratio (mm² / mg): 0,0103
 Internal die (mm²): 1,8848

b) Access line ultra-low-power 32-bit MCU Arm®-based Cortex®-M0+, TFPGA64 type [183]

Subpart	mg	% subpart	Material	mg	Content share in the subpart	Content share in the IC			
Die or dies	4,675	7,305%	Silicon (Si)	4,675	100,000%	7,305%			
Substrate	17,112	26,738%	Bismaleimide (B)	0,774	4,523%	1,209%			
			Triazine (T)	0,774	4,523%	1,209%			
			Fiber glass	2,31	13,499%	3,609%			
			metal hydroxide	0,053	0,310%	0,083%			
			Zinc hydroxide	0,016	0,094%	0,025%			
			Thermosetting resin	1,297	7,579%	2,027%			
			Calcium sulfate	0,026	0,152%	0,041%			
			Baryum sulfate	0,243	1,420%	0,380%			
			(2-methoxymethylethoxy)propanol	0,04	0,234%	0,063%			
			Talc containing no asbestiform fibers	0,135	0,789%	0,211%			
			Quartz	0,135	0,789%	0,211%			
			Acrylates derivative	0,559	3,267%	0,873%			
			aromatic hydrocarbon	0,054	0,316%	0,084%			
			amine compound	0,008	0,047%	0,013%			
			Copper (Cu)	10,586	61,863%	16,541%			
			Nickel (Ni)	0,08	0,468%	0,125%			
			Gold (Au)	0,021	0,123%	0,033%			
			Die Attach	2,344	3,663%	Silver (Ag)	2,085	88,951%	3,258%
						Neopentyl glycol dimethacrylate	0,117	4,991%	0,183%
						2,6-Diglycidyl phenyl allyl ether	0,129	5,503%	0,202%
palmitic acid	0,002	0,085%				0,003%			
4-tert-butylcyclohexanol	0,007	0,299%				0,011%			
Hexamethyltetracosane-hexaene	0,002	0,085%				0,003%			
Fluorine trace	0,001	0,043%				0,002%			
Wires	0,351	0,548%	Gold (Au)	0,351	100,000%	0,548%			
Encapsulation	32,891	51,392%	Biphenyl epoxy resin	2,742	8,337%	4,284%			
			Phenol resin	1,371	4,168%	2,142%			
			Quartz	0,686	2,086%	1,072%			

			Silica, vitreous	27,818	84,576%	43,466%
			Carbon Black	0,247	0,751%	0,386%
			Magnesium dihydroxide	0,027	0,082%	0,042%
Solder Balls	6,627	10,355%	Tin (Sn)	6,513	98,280%	10,177%
			Silver (Ag)	0,08	1,207%	0,125%
			Copper (Cu)	0,033	0,498%	0,052%
			Nickel (Ni)	0,001	0,015%	0,002%
			Lead (Pb)	0,001	0,015%	0,002%
			TOTAL	64,000	100,000%	

Packaging Length (mm): 5,15
Packaging Width (mm): 5,15
Internal die area ratio (mm² / mg): 0,0303
Internal die (mm²): 1,9374

c) Access line ultra-low-power 32-bit MCU Arm®-based Cortex®-M0+, UFQFPN32 type [184]

Subpart	mg	% subpart	Material	mg	Content share in the subpart	Content share in the IC
Die or dies	2,881	5,870%	Die	2,881	100,000%	5,870%
Die Attach Epoxy _ABLEBOND 8290_	0,281	0,573%	Silver	0,198	70,463%	0,403%
			Bisphenol-F, epoxy resin	0,014	4,982%	0,029%
			Fatty acids, polymers with epichlorohydrin	0,014	4,982%	0,029%
			Gamma Butyrolactone	0,014	4,982%	0,029%
			Epoxy Resin	0,014	4,982%	0,029%
			Poly(Oxy(methyl-1, 2-ethanediyl)	0,014	4,982%	0,029%
			Copper Oxide	0,014	4,982%	0,029%
			1,4-Bis(2,3-epoxypropoxy) butane	0,001	0,356%	0,002%
Mold Compound_EME-G770_Sumito (Encapsulation)	17,061	34,763%	Epoxy Resin A	0,364	2,134%	0,742%
			Epoxy Resin B	0,364	2,134%	0,742%
			Phenol Resin A	0,364	2,134%	0,742%
			Phenol Resin B	0,364	2,134%	0,742%
			Silica(Amorphous)A	12,153	71,233%	24,761%
			Silica(Amorphous)B	2,986	17,502%	6,084%
			Metal Hydroxide	0,364	2,134%	0,742%
			Carbon Black	0,103	0,604%	0,210%
Bonding wire_WIRE Ag Si TYPE_MKE	0,196	0,399%	Silver	0,188	95,918%	0,383%
			Others	0,008	4,082%	0,016%
Anode Ball_Pure Tin_Nuonengda	1,659	3,380%	Tin	1,659	100,000%	3,380%
Lead frame_C7+Ag_HDS	27,000	55,014%	Nickel	0,793	2,937%	1,616%
			Silicon	0,176	0,652%	0,359%
			Magnesium	0,042	0,156%	0,086%
			Silver	1,701	6,300%	3,466%
			Copper	24,288	89,956%	49,486%
TOTAL	49,078	100,000%				

Packaging Length (mm): 5,10
Packaging Width (mm): 5,10
Internal die area ratio (mm² / mg): 0,0311
Internal die (mm²): 1,5269

d) Access line ultra-low-power 32-bit MCU Arm®-based Cortex®-M0+, WLCSP36 type [185]

Subpart	mg	% subpart	Material	mg	Content share in the subpart	Content share in the IC
Die or dies	4,411	74,147%	Die	4,411	100,000%	74,159%
RDL-Ti Target	0,001	0,017%	Titanium	0,001	100,000%	0,017%
RDL-Cu Target	0,003	0,050%	Copper	0,003	100,000%	0,050%
RDL-Cu Anode	0,062	1,042%	Copper	0,062	100,000%	1,042%
UBM-Cu Target	0,002	0,034%	Copper	0,002	100,000%	0,034%
UBM-Cu Anode	0,073	1,227%	Copper	0,073	100,000%	1,227%
SOLDER BALLS SACN125 0,23mm	1,179	19,818%	Tin	1,146	97,201%	19,267%
			Silver	0,014	1,187%	0,235%
			Copper	0,018	1,527%	0,303%
Backside Tape - LC2850	0,218	3,664%	Polyethylene terephthalate	0,154	70,642%	2,589%
			Silica	0,034	15,596%	0,572%
			Acrylic ester co-polymer	0,014	6,422%	0,235%
			Epoxy resin	0,014	6,422%	0,235%
			Carbon black	0,001	0,459%	0,017%
			Additive	0,001	0,459%	0,017%
TOTAL	5,949	100,000%				

Packaging Length (mm): 2,631
Packaging Width (mm): 2,903
Internal die area ratio (mm² / mg): 0,9520
Internal die (mm²): 5,6632

9. Material content shares of the studied NFC-EEPROM memories

The following information is an adaptation of the Full Material Declaration (FMD) of the memories studied in this work. The values in the rightmost column “Content share in the IC” are considered as the typical material content shares used in the uncertainty analysis of section 2.1.3, seen in chapter 5. To obtain the internal die area ratio factor, one divides the product of the IC packaging surface and the die share with its total weight, following the Ecoinvent method described in [174], which is explained in section 4.1 of chapter 4). To obtain the die area of the component, one multiplies this factor with the total weight of the integrated circuit. For a detailed review, the reader can consult the FMD document provided by the manufacturer, which appears in the reference near to the name of the component.

a) Dynamic NFC/RFID tag IC with 4-Kbit, 16-Kbit or 64-Kbit EEPROM, TSSOP8 type [186]

Subpart	mg	% subpart	Material	mg	Content share in the subpart	Content share in the IC
Die or dies	1,700	5,000%	Die	1,700	100,000%	5,000%
Lead-frame	14,517	42,696%	Copper (Cu)	14,147	97,451%	41,608%
			Iron (Fe)	0,341	2,349%	1,003%
			Zinc (Zn)	0,017	0,117%	0,050%
			Iron Phosphide (FeP)	0,012	0,083%	0,035%
Lead-frame Coating	0,062	0,182%	Nickel (Ni)	0,058	93,548%	0,171%
			Palladium (Pd)	0,002	3,226%	0,006%
			Gold (Au)	0,002	3,226%	0,006%
Die Attach	0,049	0,144%	Poly(tetrafluoroethylene)	0,025	51,020%	0,074%
			Synthetic resin	0,010	20,408%	0,029%
			Bismaleimide resin	0,010	20,408%	0,029%
			Titanium dioxide	0,002	4,082%	0,006%
			Silica, amorphous	0,002	4,082%	0,006%
Wires	0,019	0,056%	Gold (Au)	0,019	100,000%	0,056%
Encapsulation	17,653	51,919%	Epoxy Resin	1,434	8,123%	4,218%
			Phenol Resin	0,956	5,416%	2,812%
			Silica, vitreous	15,091	85,487%	44,384%
			Carbon black	0,096	0,544%	0,282%
			Bismuth (Bi)	0,076	0,431%	0,224%
Finishing	0,001	0,003%	Nickel (Ni)	0,001	100,000%	0,003%
Total	34,001	100,000%				

Packaging Length (mm): 4,5
 Packaging Width (mm): 3,1
 Internal die area ratio (mm² / mg): 0,0205
 Internal die (mm²): 0,6975

b) Dynamic NFC/RFID tag IC with 4-Kbit, 16-Kbit or 64-Kbit EEPROM, UFDFPN8 type [187]

Subpart	mg	% subpart	Material	mg	Content share in the subpart	Content share in the IC
Die or dies	1,228	7,675%	Die	1,228	100,000%	7,675%
Lead-frame	2,994	18,714%	Copper (Cu)	2,918	97,462%	18,236%
			Iron (Fe)	0,07	2,338%	0,437%
			Zinc (Zn)	0,004	0,134%	0,025%
			Iron Phosphide (FeP)	0,003	0,100%	0,019%
Lead-frame Coating	0,013	0,081%	Nickel (Ni)	0,012	92,308%	0,075%
			Palladium (Pd)	0,001	7,692%	0,006%
Die Attach	1,266	7,913%	Silver (Ag)	1,108	87,520%	6,925%
			polymer	0,101	7,978%	0,631%
			aniline	0,013	1,027%	0,081%
			Epoxy resin	0,038	3,002%	0,237%
			Epoxy resin molecular weight <= 700	0,006	0,474%	0,037%
Wires	0,018	0,113%	Copper (Cu)	0,018	100,000%	0,112%
Encapsulation	10,480	65,504%	Silica, vitreous	9,229	88,063%	57,678%
			Biphenyl epoxy resin	0,521	4,971%	3,256%
			Phenolic resin	0,407	3,884%	2,544%
			epoxy resin	0,209	1,994%	1,306%
			carbon black	0,021	0,200%	0,131%
			other	0,094	0,897%	0,587%
TOTAL	15,999	100,000%				

Packaging Length (mm): 2,1
 Packaging Width (mm): 3,1
 Internal die area ratio (mm² / mg): 0,0312
 Internal die (mm²): 0,4997

c) Dynamic NFC/RFID tag IC with 4-Kbit, 16-Kbit or 64-Kbit EEPROM, SO8 type [188]

Subpart	mg	% subpart	Material	mg	Content share in the subpart	Content share in the IC
Die or dies	1,700	2,125%	Die	1,700	100,000%	2,125%
Lead-frame	24,984	31,230%	Copper (Cu)	24,347	97,450%	30,434%
			Iron (Fe)	0,586	2,346%	0,733%
			Zinc (Zn)	0,030	0,120%	0,038%
			Iron Phosphide (FeP)	0,021	0,084%	0,026%
Lead-frame Coating	0,124	0,155%	Nickel (Ni)	0,114	91,935%	0,143%
			Palladium (Pd)	0,007	5,645%	0,009%
			Gold (Au)	0,003	2,419%	0,004%
Die Attach	1,027	1,284%	Silver (Ag)	0,925	90,068%	1,156%
			acrylate	0,062	6,037%	0,078%
			Methacrylate	0,039	3,797%	0,049%
			acrylate	0,002	0,195%	0,003%
Wires	0,062	0,078%	Gold (Au)	0,062	100,000%	0,078%
Encapsulation	52,101	65,127%	Epoxy Resin	3,938	7,558%	4,923%
			Phenol Resin	2,625	5,038%	3,281%
			Silica, vitreous	45,065	86,495%	56,331%
			Carbon-black	0,263	0,505%	0,329%
			Bismuth	0,210	0,403%	0,263%
Finishing	0,001	0,001%	Nickel (Ni)	0,001	100,000%	0,001%
TOTAL	79,999	100,000%				

Packaging Length (mm): 5,00
 Packaging Width (mm): 4,00
 Internal die area ratio (mm² / mg): 0,0053
 Internal die (mm²): 0,4250

10. Material content shares of the unique type of Voltage Detector

The following information is an adaptation of the Full Material Declaration (FMD) of the unique type of voltage detector presented in this work. This component type was modeled by the LCA implementation proposed in the section 8.1 of the chapter 4 because of its significant contribution to the AD impacts of all design sets and versions. To obtain the internal die area ratio factor, one divides the product of the IC packaging surface and the die share with its total weight, following the Ecoinvent method described in [174], which is explained in section 4.1 of chapter 4). To obtain the die area of the component, one multiplies this factor with the total weight of the integrated circuit. For a detailed review, the reader can consult the FMD document provided by the manufacturer, which appears in the reference near to the name of the component.

Voltage detector with sense input and external delay capacitor STM 1831, SOT23-5 type [189]

Subpart	mg	% subpart	Material	mg	Content share in the subpart	Content share in the IC
die	0,380	2,303%	Die	0,380	100,000%	2,303%
Lead-frame	7,200	43,636%	Copper (Cu)	6,936	96,333%	42,036%
			Iron (Fe)	0,162	2,250%	0,982%
			Phosphorus (P)	0,002	0,028%	0,012%
			Zinc (Zn)	0,009	0,125%	0,055%
			Nickel (Ni)	0,083	1,153%	0,503%
			Palladium (Pd)	0,007	0,097%	0,042%
			Gold (Au)	0,001	0,014%	0,006%
Die attach	0,070	0,424%	Aluminium oxide	0,021	30,000%	0,127%
			Diethylene glycol monoethyl ether acetate	0,028	40,000%	0,170%
			Epoxy resin	0,005	7,143%	0,030%
			Epoxy resin	0,014	20,000%	0,085%
			Aromatic amine	0,002	2,857%	0,012%
Bonding Wire	0,150	0,909%	Gold (Au)	0,150	100,000%	0,909%
encapsulation	8,700	52,727%	Silica, vitreous	7,421	85,299%	44,976%
			phenolic resin	0,305	3,506%	1,848%
			epoxy resin	0,348	4,000%	2,109%
			Biphenyl epoxy resin	0,174	2,000%	1,055%
			carbon black	0,017	0,195%	0,103%
			Zinc hydroxide	0,087	1,000%	0,527%
			Magnesium hydroxide	0,348	4,000%	2,109%
			TOTAL	16,500	100,000%	

Packaging Length (mm): 2,90
 Packaging Width (mm): 1,60
 Internal die area ratio (mm² / mg): 0,0065
 Internal die (mm²): 0,1069

11. Material content shares of the SoC component of the BLE module

The following information is an adaptation of the Full Material Declaration (FMD) of the BLE SoC component presented in this work. This component was modeled by the LCA implementation proposed in the section 8.1 of the chapter 4 because of its significant contribution to the AD and GW impacts of the BLE module of the BLE-based version. To obtain the internal die area ratio factor, one divides the product of the IC packaging surface and the die share with its total weight, following the Ecoinvent method described in [174], which is explained in section 4.1 of chapter 4). To obtain the die area of the component, one multiplies this factor with the total weight of the integrated circuit. For a detailed review, the reader can consult the FMD document provided by the manufacturer, which appears in the reference near to the name of the component.

Bluetooth® Low Energy wireless system-on-chip BlueNRG-2, QFN32 type [191]

Subpart	mg	% subpart	Material	mg	Content share in the subpart	Content share in the IC
Die	3,494	9,642%	Die	3,494	100,000%	9,642%
Leadframe	10,628	29,330%	Copper (Cu)	10,185	95,832%	28,107%
			Chromium (Cr)	0,028	0,263%	0,077%
			Tin (Sn)	0,026	0,245%	0,072%
			Zinc (Zn)	0,021	0,198%	0,058%
			Silver (Ag)	0,369	3,472%	1,018%
Die attach	2,452	6,767%	Silver (Ag)	1,998	81,485%	5,514%
			(Octahydro-4,7-methano-1 H-indenediyl)bis(m	0,147	5,995%	0,406%
			exo-1,7,7-trimethylbicyclo[2,2,1]hept-2-yl met	0,147	5,995%	0,406%
			Isobornyl acrylate	0,147	5,995%	0,406%
			2-(3,4-Epoxy cyclohexyl)ethyltrimethoxysilane	0,012	0,489%	0,033%
Bonding wires	0,482	1,330%	Gold (Au)	0,479	99,378%	1,322%
			Platinum (Pt)	0,003	0,622%	0,008%
			Palladium (Pd)	0,001	0,207%	0,003%
Encapsulation	17,020	46,970%	Epoxy Resin	0,851	5,000%	2,348%
			Phenol Resin	0,391	2,297%	1,079%
			Silica(Amorphous)A	14,467	85,000%	39,924%
			Silica(Amorphous)B	0,851	5,000%	2,348%
			Metal Hydroxide	0,391	2,297%	1,079%
			Carbon Black	0,068	0,400%	0,188%
connections coating	2,160	5,961%	Tin (Sn)	2,160	100,000%	5,961%
TOTAL	36,236	100,000%				

Packaging Length (mm): 5,00
 Packaging Width (mm): 5,00
 Internal die area ratio (mm² / mg): 0,0665
 Internal die (mm²): 2,4106

12. Recycled material content from waste flows of design set 8

The following information presents the normalization of the recoveries of copper, gold and silver in wastes flows of design set 8, which make part of the LCA implementation for the framework for eco design, presented in the section 8.1 of chapter 4. It considers the total content shares of aluminum, copper, Glass, plastic, silver, gold, lead and ferroelectric materials in specific waste flows of the EH sensor system device; and the transfer coefficients suggested by Huisman, J. [145]. The recycled material contents in respective scraps are obtained from the metals fractions output of shredding and separation processes, and serve as input for the metallurgical recovery of precious metals, as proposed in the LCA implementation of chapter 4. In this work, one focuses on gold and silver that can be recovered from copper metal fractions. For simplicity, the content shares for the waste flow “WPCB” of the regular scenario is not presented as it only differs from that one of the waste flow “Full device” in that the plastic case share does not exists (in the regular scenario, the plastic case is separated manually).

a) Recycled material content in the waste flow “Full device” (Worst recycling scenario)

Component type	Quantity	Weight (mg)	Total weight (mg)	% components type	Material	mg	Content share in the component type	Content share in the EH sensor system device
Capacitor 0402	7	1,4	9,8	0,057%	Copper (Cu)	0,0931	0,950%	0,000546%
					Nickel (Ni)	1,32986	13,570%	0,007799%
					Palladium (Pd)	0,00882	0,090%	0,000052%
					Silver (Ag)	0,2597	2,650%	0,001523%
					Tin (Sn)	0,1617	1,650%	0,000948%
					glass	0,0147	0,150%	0,000086%
					Titane dioxide (TiO2)	2,6969208	27,520%	0,015816%
					Barite	5,2351992	53,420%	0,030701%
Capacitor 1812	1	195,2	195,2	1,145%	Copper (Cu)	1,8544	0,950%	0,010875%
					Nickel (Ni)	26,48864	13,570%	0,155338%
					Palladium (Pd)	0,17568	0,090%	0,001030%
					Silver (Ag)	5,1728	2,650%	0,030335%
					Tin (Sn)	3,2208	1,650%	0,018888%
					glass	0,2928	0,150%	0,001717%
					Titane dioxide (TiO2)	53,7182592	27,520%	0,315022%
					Barite	104,2766208	53,420%	0,611514%
Resistors 0402	9	1,08	9,72	0,057%	Lead (Pb)	0,042768	0,440%	0,000251%
					Iron (Fe)	0,22842	2,350%	0,001340%
					Nickel (Ni)	0,16038	1,650%	0,000941%
					Copper (Cu)	0,035964	0,370%	0,000211%
					Tin (Sn)	0,113724	1,170%	0,000667%
					Chromium (Cr)	0,008748	0,090%	0,000051%
					Silicium (Si)	0,000972	0,010%	0,000006%
					Palladium (Pd)	0,013608	0,140%	0,000080%
					Silver (Ag)	0,0972	1,000%	0,000570%
					Gold (Au)	0,049572	0,510%	0,000291%
					Aluminium oxide (Al2O3)	6,79914	69,950%	0,039872%
					SiO2	1,945944	20,020%	0,011412%
					CaCO3	0,00486	0,050%	0,000029%
					Glass	0,064152	0,660%	0,000376%
					Epoxy resin	0,091368	0,940%	0,000536%
					Polyacrylate	0,062208	0,640%	0,000365%
Diode SOT666	2	2,9	5,8	0,034%	Lead (Pb)	0,09106	1,570%	0,000534%
					Iron (Fe)	2,51372	43,340%	0,014741%
					Copper (Cu)	1,31138	22,610%	0,007690%
					Nickel (Ni)	0,02146	0,370%	0,000126%
					Tin (Sn)	0,25926	4,470%	0,001520%
					Molybdenum (Mo)	0,11716	2,020%	0,000687%
					Glass	0,90596	15,620%	0,005313%
					Encapsulation insulator (SiO2)	0,55216	9,520%	0,003238%
					Epoxy resin	0,00058	0,010%	0,000003%
					Doted silica	0,0261	0,450%	0,000153%
					Diode 0603	1	1	1
Iron (Fe)	0,4334	43,340%	0,002542%					
Copper (Cu)	0,2261	22,610%	0,001326%					
Nickel (Ni)	0,0037	0,370%	0,000022%					
Tin (Sn)	0,0447	4,470%	0,000262%					
Molybdenum (Mo)	0,0202	2,020%	0,000118%					
Glass	0,1562	15,620%	0,000916%					
Encapsulation insulator (SiO2)	0,0952	9,520%	0,000558%					
Epoxy resin	0,0001	0,010%	0,000001%					
Doted silica	0,0045	0,450%	0,000026%					
Transistors SOT-323	2	6	12	0,070%				
					Iron (Fe)	0,1248	1,040%	0,000732%
					Copper (Cu)	4,356	36,300%	0,025545%
					Nickel (Ni)	0,096	0,800%	0,000563%
					Lead (Pb)	0,5292	4,410%	0,003103%
					Tin (Sn)	0,9132	7,610%	0,005355%
					Encapsulation insulator (SiO2)	5,8956	49,130%	0,034574%
					Doped silicium	0,0612	0,510%	0,000359%

PCB	1	919,688	919,688	5,393%	Copper (Cu)	530,3154382	57,663%	3,109952%
					Glass	349,2321178	37,973%	2,048017%
					Gold (Au)	0,028640729	0,003%	0,000168%
					Nickel (Ni)	0,143203646	0,016%	0,000840%
					Phenolic resin	39,35790634	4,279%	0,230808%
					Silver (Ag)	0,095161133	0,010%	0,000558%
Plastic case	1	15780	15780	92,539%	Tin (Sn)	0,515533126	0,056%	0,003023%
					AcrylonitrileButadieneStyrene (ABS)	15780	100,000%	92,539342%
Voltage Detectors SOT23-5 type	2	16,5	33	0,194%	Die	0,76	2,303%	0,004457%
					Copper (Cu)	13,872	42,036%	0,081350%
					Iron (Fe)	0,324	0,982%	0,001900%
					Phosphorus (P)	0,004	0,012%	0,000023%
					Zinc (Zn)	0,018	0,055%	0,000106%
					Nickel (Ni)	0,166	0,503%	0,000973%
					Palladium (Pd)	0,014	0,042%	0,000082%
					Gold (Au)	0,002	0,006%	0,000012%
					Aluminium oxide (Al2O3)	0,042	0,127%	0,000246%
					Diethylene glycol monoethyl ether acetate	0,056	0,170%	0,000328%
					Epoxy resin	0,01	0,030%	0,000059%
					Epoxy resin	0,028	0,085%	0,000164%
					Aromatic amine	0,004	0,012%	0,000023%
					Gold (Au)	0,3	0,909%	0,001759%
					Silica, vitreous	14,842	44,976%	0,087039%
					phenolic resin	0,61	1,848%	0,003577%
					epoxy resin	0,696	2,109%	0,004082%
					Biphenyl epoxy resin	0,348	1,055%	0,002041%
					Carbon black	0,034	0,103%	0,000199%
					Zinc hydroxide	0,174	0,527%	0,001020%
Magnesium hydroxide	0,696	2,109%	0,004082%					
Voltage comparator SC70-5 type	1	6	6	0,035%	Die	0,178	2,967%	0,001044%
					Iron (Fe)	0,067	1,117%	0,000393%
					Copper (Cu)	2,829	47,150%	0,016590%
					Phosphorus (P)	0,001	0,017%	0,000006%
					Zinc (Zn)	0,004	0,067%	0,000023%
					Nickel (Ni)	0,034	0,567%	0,000199%
					Palladium (Pd)	0,003	0,050%	0,000018%
					Silver (Ag)	0,016	0,267%	0,000094%
					Carbocyclic Acrylates	0,002	0,033%	0,000012%
					Bismaleimide resin	0,002	0,033%	0,000012%
					2-preponic acid, 2-methyl	0,001	0,017%	0,000006%
					Gold (Au)	0,033	0,550%	0,000194%
					Epoxy Resin-1	0,056	0,933%	0,000328%
					Epoxy Resin-2	0,056	0,933%	0,000328%
					Epoxy Resin-3	0,056	0,933%	0,000328%
					Phenol resin	0,114	1,900%	0,000669%
					Silica	2,542	42,367%	0,014907%
Carbon black	0,006	0,100%	0,000035%					
MCU TFBG464 type	1	64	64	0,375%	Die	4,675073048	7,305%	0,027416%
					Bismaleimide (B)	0,774012094	1,209%	0,004539%
					Triazine (T)	0,774012094	1,209%	0,004539%
					Fiber glass	2,310036094	3,609%	0,013547%
					metal hydroxide	0,053000828	0,083%	0,000311%
					Zinc hydroxide	0,01600025	0,025%	0,000094%
					Thermosetting resin	1,297020266	2,027%	0,007606%
					Calcium sulfate	0,026000406	0,041%	0,000152%
					Baryum sulfate	0,243003797	0,380%	0,001425%
					(2-methoxymethylethoxy)propanol	0,040000625	0,063%	0,000235%
					Talc containing no asbestiform fibers	0,135002109	0,211%	0,000792%
					Quartz	0,135002109	0,211%	0,000792%
					Acrylates derivative	0,559008735	0,873%	0,003278%
					aromatic hydrocarbon	0,054000844	0,084%	0,000317%
					amine compound	0,008000125	0,013%	0,000047%
					Copper (Cu)	10,58616541	16,541%	0,062081%
					Nickel (Ni)	0,08000125	0,125%	0,000469%
					Gold (Au)	0,021000328	0,033%	0,000123%
					Silver (Ag)	2,085032579	3,258%	0,012227%
					Neopentyl glycol dimethacrylate	0,117001828	0,183%	0,000686%
					2,6-Diglycidyl phenyl allyl ether	0,129002016	0,202%	0,000757%
					palmitic acid	0,002000031	0,003%	0,000012%
					4-tert-butylcyclohexanol	0,007000109	0,011%	0,000041%
					Hexamethyltetraacosa-hexaene	0,002000031	0,003%	0,000012%
					Fluorine trace	0,001000016	0,002%	0,000006%
					Gold (Au)	0,351005484	0,548%	0,002058%
					Biphenyl epoxy resin	2,742042844	4,284%	0,016080%
					Phenol resin	1,371021422	2,142%	0,008040%
					Quartz	0,686010719	1,072%	0,004023%
					Silica, vitreous	27,81843466	43,466%	0,163137%
					Carbon Black	0,247003859	0,386%	0,001449%
					Magnesium dihydroxide	0,027000422	0,042%	0,000158%
					Tin (Sn)	6,513101767	10,177%	0,038195%
Silver (Ag)	0,08000125	0,125%	0,000469%					
Copper (Cu)	0,033000516	0,052%	0,000194%					
Nickel (Ni)	0,001000016	0,002%	0,000006%					
Lead (Pb)	0,001000016	0,002%	0,000006%					

EEPROM memory UFDFPN8 type	1	16	16	0,094%	Die	1,227923255	7,675%	0,007201%
					Copper (Cu)	2,917817636	18,236%	0,017111%
					Iron (Fe)	0,069995625	0,437%	0,000410%
					Zinc (Zn)	0,00399975	0,025%	0,000023%
					Iron Phosphide (FeP)	0,002999813	0,019%	0,000018%
					Nickel (Ni)	0,01199925	0,075%	0,000070%
					Palladium (Pd)	0,000999938	0,006%	0,000006%
					Silver (Ag)	1,107930754	6,925%	0,006497%
					polymer	0,100993688	0,631%	0,000592%
					aniline	0,012999188	0,081%	0,000076%
					Epoxy resin	0,037997625	0,237%	0,000223%
					Epoxy resin molecular weight <= 700	0,005999625	0,037%	0,000035%
					Copper (Cu)	0,017998875	0,112%	0,000106%
					Silica, vitreous	9,228423224	57,678%	0,054119%
					Biphenyl epoxy resin	0,52096744	3,256%	0,003055%
					Phenolic resin	0,406974564	2,544%	0,002387%
					epoxy resin	0,208986938	1,306%	0,001226%
					carbon black	0,020998688	0,131%	0,000123%
					other	0,093994125	0,587%	0,000551%
					TOTAL		17052,208	100,000%

Materials that can be obtained from shredding and separation steps	Aggregated content shares	Metal fractions (per Kg of waste flow)			
		Ferro	Aluminum	Copper	Residue
Aluminium (Al)	0,040%	2,01E-06	3,33E-04	1,98E-05	4,83E-05
Copper (Cu)	3,334%	3,13E-04	1,67E-03	2,61E-02	5,28E-03
Ferro (Fe, Ni, Co)	0,189%	1,80E-03	1,89E-05	1,89E-05	5,68E-05
Glass	2,070%	1,16E-04	1,16E-04	2,07E-03	1,84E-02
Plastics (Thermosets, Thermoplastics)	92,827%	1,12E-02	4,64E-03	9,28E-02	8,20E-01
Silver (Ag)	0,052%	5,18E-06	5,18E-06	4,44E-04	6,85E-05
Gold (Au)	0,005%	4,56E-07	4,56E-07	3,68E-05	8,30E-06
Lead (Pb)	0,004%	4,70E-07	4,70E-07	3,19E-05	7,04E-06
Others	1,479%	1,02E-04	9,91E-05	5,22E-03	9,37E-03
TOTAL	100,000%	1,36E-02	6,88E-03	1,27E-01	8,53E-01

Recycled materials content in respective scraps (per Kg of metal fraction)		
In Ferro fraction	In Aluminium fraction	In Copper fraction
1,48E-04	4,83E-02	1,56E-04
2,31E-02	2,42E-01	2,06E-01
1,33E-01	2,75E-03	1,49E-04
8,54E-03	1,68E-02	1,63E-02
8,28E-01	6,75E-01	7,32E-01
3,81E-04	7,52E-04	3,50E-03
3,36E-05	6,63E-05	2,91E-04
3,47E-05	6,84E-05	2,52E-04
7,52E-03	1,44E-02	4,12E-02

b) Recycled material content in the waste flow "WPCB" (Regular recycling scenario)

Materials that can be obtained from shredding and separation steps	Aggregated content shares	Metal fractions (per Kg of waste flow)			
		Ferro	Aluminum	Copper	Residue
Aluminium (Al)	0,540%	2,70E-05	4,46E-03	2,66E-04	6,48E-04
Copper (Cu)	44,682%	4,20E-03	2,23E-02	3,49E-01	7,08E-02
Ferro (Fe, Ni, Co)	2,539%	2,41E-02	2,54E-04	2,54E-04	7,62E-04
Glass	27,745%	1,55E-03	1,55E-03	2,77E-02	2,47E-01
Plastics (Thermosets, Thermoplastics)	3,850%	4,66E-04	1,93E-04	3,85E-03	3,40E-02
Silver (Ag)	0,701%	6,94E-05	6,94E-05	5,95E-03	9,18E-04
Gold (Au)	0,062%	6,11E-06	6,11E-06	4,94E-04	1,11E-04
Lead (Pb)	0,053%	6,30E-06	6,30E-06	4,27E-04	9,43E-05
Others	19,828%	1,37E-03	1,33E-03	7,00E-02	1,26E-01
TOTAL	100,000%	3,18E-02	3,02E-02	4,58E-01	4,80E-01

Recycled materials content in respective scraps (per Kg of metal fraction)		
In Ferro fraction	In Aluminium fraction	In Copper fraction
8,48E-04	1,48E-01	5,79E-04
1,32E-01	7,40E-01	7,62E-01
7,58E-01	8,40E-03	5,54E-04
4,88E-02	5,14E-02	6,05E-02
1,46E-02	6,37E-03	8,40E-03
2,18E-03	2,30E-03	1,30E-02
1,92E-04	2,02E-04	1,08E-03
1,98E-04	2,09E-04	9,32E-04
4,30E-02	4,40E-02	1,53E-01

c) Recycled material content in the waste flow “WPCB” (Best recycling scenario)

Component type	Quantity	Weight (mg)	Total weight (mg)	% components type	Material	mg	Content share in the component type	Content share in the EH sensor system device
Capacitor 0402	7	1,4	9,8	0,983%	Copper (Cu)	0,0931	0,950%	0,009338%
					Nickel (Ni)	1,32986	13,570%	0,133385%
					Palladium (Pd)	0,00882	0,090%	0,000885%
					Silver (Ag)	0,2597	2,650%	0,026048%
					Tin (Sn)	0,1617	1,650%	0,016219%
					glass	0,0147	0,150%	0,001474%
					Titane dioxide (TiO2)	2,6969208	27,520%	0,270502%
					Barite	5,2351992	53,420%	0,525092%
Resistors 0402	9	1,08	9,72	0,975%	Lead (Pb)	0,042768	0,440%	0,004290%
					Iron (Fe)	0,22842	2,350%	0,022911%
					Nickel (Ni)	0,16038	1,650%	0,016086%
					Copper (Cu)	0,035964	0,370%	0,003607%
					Tin (Sn)	0,113724	1,170%	0,011407%
					Chromium (Cr)	0,008748	0,090%	0,000877%
					Silicium (Si)	0,000972	0,010%	0,000097%
					Palladium (Pd)	0,013608	0,140%	0,001365%
					Silver (Ag)	0,00972	1,000%	0,009749%
					Gold (Au)	0,049572	0,510%	0,004972%
					Aluminium oxide (Al2O3)	6,79914	69,950%	0,681955%
					SiO2	1,945944	20,020%	0,195179%
					CaCO3	0,00486	0,050%	0,000487%
					Glass	0,064152	0,660%	0,006434%
					Epoxy resin	0,091368	0,940%	0,009164%
					Polycrylate	0,062208	0,640%	0,006239%
Diode SOT666	2	2,9	5,8	0,582%	Lead (Pb)	0,09106	1,570%	0,009133%
					Iron (Fe)	2,51372	43,340%	0,252127%
					Copper (Cu)	1,31138	22,610%	0,131532%
					Nickel (Ni)	0,02146	0,370%	0,002152%
					Tin (Sn)	0,25926	4,470%	0,026004%
					Molybdenum (Mo)	0,11716	2,020%	0,011751%
					Glass	0,90596	15,620%	0,090868%
					Encapsulation insulator (SiO2)	0,55216	9,520%	0,055382%
					Epoxy resin	0,00058	0,010%	0,000058%
					Doted silica	0,0261	0,450%	0,002618%
Diode 0603	1	1	1	0,100%	Lead (Pb)	0,0157	1,570%	0,001575%
					Iron (Fe)	0,4334	43,340%	0,043470%
					Copper (Cu)	0,2261	22,610%	0,022678%
					Nickel (Ni)	0,0037	0,370%	0,000371%
					Tin (Sn)	0,0447	4,470%	0,004483%
					Molybdenum (Mo)	0,0202	2,020%	0,002026%
					Glass	0,1562	15,620%	0,015667%
					Encapsulation insulator (SiO2)	0,0952	9,520%	0,009549%
					Epoxy resin	0,0001	0,010%	0,000010%
					Doted silica	0,0045	0,450%	0,000451%
Transistors SOT-323	2	6	12	1,204%	Aluminium (Al)	0,0252	0,210%	0,002528%
					Iron (Fe)	0,1248	1,040%	0,012517%
					Copper (Cu)	4,356	36,300%	0,436908%
					Nickel (Ni)	0,096	0,800%	0,009629%
					Lead (Pb)	0,5292	4,410%	0,053079%
					Tin (Sn)	0,9132	7,610%	0,091594%
					Encapsulation insulator (SiO2)	5,8956	49,130%	0,591330%
					Doped silicium	0,0612	0,510%	0,006138%
					Copper (Cu)	530,3154382	57,663%	53,190751%
					Glass	349,2321178	37,973%	35,028055%
PCB	1	919,688	919,688	92,245%	Gold (Au)	0,028640729	0,003%	0,002873%
					Nickel (Ni)	0,143203646	0,016%	0,014363%
					Phenolic resin	39,35790534	4,279%	3,947606%
					Silver (Ag)	0,095161133	0,010%	0,009545%
					Tin (Sn)	0,515533126	0,056%	0,051708%
					Die	0,76	2,303%	0,076228%
					Copper (Cu)	13,872	42,036%	1,391365%
Voltage detectors SOT23-5 type	2	16,5	33	3,310%	Iron (Fe)	0,324	0,982%	0,032497%
					Phosphorus (P)	0,004	0,012%	0,000401%
					Zinc (Zn)	0,018	0,055%	0,001805%
					Nickel (Ni)	0,166	0,503%	0,016650%
					Palladium (Pd)	0,014	0,042%	0,001404%
					Gold (Au)	0,002	0,006%	0,000201%
					Aluminium oxide (Al2O3)	0,042	0,127%	0,004213%
					Diethylene glycol monoethyl ether acetate	0,056	0,170%	0,005617%
					Epoxy resin	0,01	0,030%	0,001003%
					Epoxy resin	0,028	0,085%	0,002808%
					Aromatic amine	0,004	0,012%	0,000401%
					Gold (Au)	0,3	0,909%	0,030090%
					Silica, vitreous	14,842	44,976%	1,488656%
					phenolic resin	0,61	1,848%	0,061183%
					epoxy resin	0,696	2,109%	0,069809%
					Biphenyl epoxy resin	0,348	1,055%	0,034904%

					Carbon black	0,034	0,103%	0,003410%
					Zinc hydroxide	0,174	0,527%	0,017452%
					Magnesium hydroxide	0,696	2,109%	0,069809%
					Die	0,178	2,967%	0,017853%
					Iron (Fe)	0,067	1,117%	0,006720%
					Copper (Cu)	2,829	47,150%	0,283749%
					Phosphorus (P)	0,001	0,017%	0,000100%
					Zinc (Zn)	0,004	0,067%	0,000401%
					Nickel (Ni)	0,034	0,567%	0,003410%
					Palladium (Pd)	0,003	0,050%	0,000301%
					Silver (Ag)	0,016	0,267%	0,001605%
					Carbocyclic Acrylates	0,002	0,033%	0,000201%
					Bismaleimide resin	0,002	0,033%	0,000201%
					2-preponic acid, 2-methyl	0,001	0,017%	0,000100%
					Gold (Au)	0,033	0,550%	0,003310%
					Epoxy Resin-1	0,056	0,933%	0,005617%
					Epoxy Resin-2	0,056	0,933%	0,005617%
					Epoxy Resin-3	0,056	0,933%	0,005617%
					Phenol resin	0,114	1,900%	0,011434%
					Silica	2,542	42,367%	0,254963%
					Carbon black	0,006	0,100%	0,000602%
					TOTAL	997,008		100,000%

Materials that can be obtained from shredding and separation steps	Aggregated content shares	Metal fractions (per Kg of waste flow)			
		Ferro	Aluminum	Copper	Residue
Aluminium (Al)	0,689%	3,44E-05	5,69E-03	3,39E-04	8,26E-04
Copper (Cu)	55,470%	5,21E-03	2,77E-02	4,34E-01	8,79E-02
Ferro (Fe, Ni, Co)	0,566%	5,38E-03	5,66E-05	5,66E-05	1,70E-04
Glass	35,142%	1,97E-03	1,97E-03	3,51E-02	3,12E-01
Plastics (Thermosets, Thermoplastics)	4,161%	5,04E-04	2,08E-04	4,16E-03	3,67E-02
Silver (Ag)	0,047%	4,65E-06	4,65E-06	3,99E-04	6,15E-05
Gold (Au)	0,041%	4,10E-06	4,10E-06	3,32E-04	7,47E-05
Lead (Pb)	0,068%	8,03E-06	8,03E-06	5,45E-04	1,20E-04
Others	3,815%	2,63E-04	2,56E-04	1,35E-02	2,42E-02
TOTAL	100,000%	1,34E-02	3,59E-02	4,88E-01	4,62E-01

Recycled materials content in respective scraps		
In Ferro fraction	In Aluminium fraction	In Copper fraction
2,57E-03	1,58E-01	6,94E-04
3,90E-01	7,72E-01	8,89E-01
4,02E-01	1,58E-03	1,16E-04
1,47E-01	5,48E-02	7,20E-02
3,76E-02	5,79E-03	8,52E-03
3,47E-04	1,29E-04	8,17E-04
3,07E-04	1,14E-04	6,79E-04
6,00E-04	2,24E-04	1,12E-03
1,97E-02	7,11E-03	2,76E-02

d) Recycled material content in the waste flow “Waste components” (Best recycling scenario)

Component type	Quantity	Weight (mg)	Total weight (mg)	% components type	Material	mg	Content share in the component type	Content share in the EH sensor system device
Capacitor 1812	1	195,2	195,2	70,930%	Copper (Cu)	1,8544	0,950%	0,673837%
					Nickel (Ni)	26,48864	13,570%	9,625233%
					Palladium (Pd)	0,17568	0,090%	0,063837%
					Silver (Ag)	5,1728	2,650%	1,879651%
					Tin (Sn)	3,2208	1,650%	1,170349%
					glass	0,2928	0,150%	0,106395%
					Titane dioxide (TiO2)	53,7182592	27,520%	19,519716%
MCU TF8GA64 type	1	64	64	23,256%	Barite	104,2766208	53,420%	37,891214%
					Die	4,675073048	7,305%	1,698791%
					Bismaleimide (B)	0,774012094	1,209%	0,281254%
					Triazine (T)	0,774012094	1,209%	0,281254%
					Fiber glass	2,310036094	3,609%	0,839403%
					metal hydroxide	0,053000828	0,083%	0,019259%
					Zinc hydroxide	0,01600025	0,025%	0,005814%
					Thermosetting resin	1,297020266	2,027%	0,471301%
					Calcium sulfate	0,026000406	0,041%	0,009448%
					Baryum sulfate	0,243003797	0,380%	0,088301%
					(2-methoxymethylethoxy)propanol	0,040000625	0,063%	0,014535%
					Talc containing no asbestiform fibers	0,135002109	0,211%	0,049056%
					Quartz	0,135002109	0,211%	0,049056%
					Acrylates derivative	0,559008735	0,873%	0,203128%
					aromatic hydrocarbon	0,054000844	0,084%	0,019622%
					amine compound	0,008000125	0,013%	0,002907%
Copper (Cu)	10,58616541	16,541%	3,846717%					

					Nickel (Ni)	0,08000125	0,125%	0,029070%
					Gold (Au)	0,021000328	0,033%	0,007631%
					Silver (Ag)	2,085032579	3,258%	0,757643%
					Neopentyl glycol dimethacrylate	0,117001828	0,183%	0,042515%
					2,6-Diglycidyl phenyl allyl ether	0,129002016	0,202%	0,046876%
					palmitic acid	0,002000031	0,003%	0,000727%
					4-tert-butylcyclohexanol	0,007000109	0,011%	0,002544%
					Hexamethyltetracosahexaene	0,002000031	0,003%	0,000727%
					Fluorine trace	0,001000016	0,002%	0,000363%
					Gold (Au)	0,351005484	0,548%	0,127546%
					Biphenyl epoxy resin	2,742042844	4,284%	0,996382%
					Phenol resin	1,371021422	2,142%	0,498191%
					Quartz	0,686010719	1,072%	0,249277%
					Silica, vitreous	27,81843466	43,466%	10,108443%
					Carbon Black	0,247003859	0,386%	0,089754%
					Magnesium dihydroxide	0,027000422	0,042%	0,009811%
					Tin (Sn)	6,513101767	10,177%	2,366679%
					Silver (Ag)	0,08000125	0,125%	0,029070%
					Copper (Cu)	0,033000516	0,052%	0,011991%
					Nickel (Ni)	0,001000016	0,002%	0,000363%
					Lead (Pb)	0,001000016	0,002%	0,000363%
					Die	1,227923255	7,675%	0,446193%
					Copper (Cu)	2,917817636	18,236%	1,060254%
					Iron (Fe)	0,069995625	0,437%	0,025434%
					Zinc (Zn)	0,00399975	0,025%	0,001453%
					Iron Phosphide (FeP)	0,002999813	0,019%	0,001090%
					Nickel (Ni)	0,01199925	0,075%	0,004360%
					Palladium (Pd)	0,000999938	0,006%	0,000363%
					Silver (Ag)	1,107930754	6,925%	0,402591%
					polymer	0,100993688	0,631%	0,036698%
					aniline	0,012999188	0,081%	0,004724%
					Epoxy resin	0,037997625	0,237%	0,013807%
					Epoxy resin molecular weight <= 700	0,005999625	0,037%	0,002180%
					Copper (Cu)	0,017998875	0,112%	0,006540%
					Silica, vitreous	9,228423224	57,678%	3,353351%
					Biphenyl epoxy resin	0,52096744	3,256%	0,189305%
					Phenolic resin	0,406974564	2,544%	0,147883%
					epoxy resin	0,208986938	1,306%	0,075940%
					carbon black	0,020998688	0,131%	0,007630%
					other	0,093994125	0,587%	0,034155%
					TOTAL	275,2	100,000%	
EEPROM memory UFDPPN8 type	1	16	16	5,814%				

Materials that can be obtained from shredding and separation steps	Aggregated content shares	Metal fractions (per Kg of waste flow)			
		Ferro	Aluminum	Copper	Residue
Aluminium (Al)	0,000%	0,00E+00	0,00E+00	0,00E+00	0,00E+00
Copper (Cu)	5,599%	5,26E-04	2,80E-03	4,38E-02	8,87E-03
Ferro (Fe, Ni, Co)	9,686%	9,20E-02	9,69E-04	9,69E-04	2,91E-03
Glass	0,946%	5,30E-05	5,30E-05	9,46E-04	8,41E-03
Plastics (Thermosets, Thermoplastics)	2,724%	3,30E-04	1,36E-04	2,72E-03	2,41E-02
Silver (Ag)	3,069%	3,04E-04	3,04E-04	2,61E-02	4,02E-03
Gold (Au)	0,135%	1,34E-05	1,34E-05	1,08E-03	2,44E-04
Lead (Pb)	0,000%	4,29E-08	4,29E-08	2,91E-06	6,41E-07
Others	77,841%	5,37E-03	5,22E-03	2,75E-01	4,93E-01
TOTAL	100,000%	9,86E-02	9,49E-03	3,50E-01	5,42E-01

Recycled materials content in respective scraps		
In Ferro fraction	In Aluminium fraction	In Copper fraction
0,00E+00	0,00E+00	0,00E+00
5,34E-03	2,95E-01	1,25E-01
9,33E-01	1,02E-01	2,77E-03
5,37E-04	5,58E-03	2,70E-03
3,34E-03	1,44E-02	7,78E-03
3,08E-03	3,20E-02	7,44E-02
1,36E-04	1,41E-03	3,09E-03
4,35E-07	4,52E-06	8,30E-06
5,45E-02	5,50E-01	7,84E-01

13. Recycled material content from waste flows of design set 20

The following information presents the normalization of the recoveries of copper, gold and silver in wastes flows of design set 20, which make part of the LCA implementation for the framework for eco design, presented in the section 8.1 of chapter 4. It considers the total content shares of aluminum, copper, Glass, plastic, silver, gold, lead and ferroelectric materials in specific waste flows of the EH sensor system device; and the transfer coefficient suggested by Huisman, J. [145]. The recycled material contents in respective scraps are obtained from the metals fractions output of shredding and separation processes, and serve as input for the metallurgical recovery of precious metals, as proposed in the LCA implementation of chapter 4. In this work, one focuses on gold and silver that can be recovered from copper metal fractions. For simplicity, the content shares for the waste flow “WPCB” of the regular scenario is not presented as it only differs from that one of the waste flow “Full device” in that the plastic case share does not exists (in the regular scenario, the plastic case is separated manually).

a) Recycled material content in the waste flow “Full device” (Worst recycling scenario)

Component type	Quantity	Weight (mg)	Total weight (mg)	% components type	Material	mg	Content share in the component type	Content share in the EH sensor system device
Capacitor 0402	7	1,4	9,8	0,059%	Copper (Cu)	0,0931	0,950%	0,000559%
					Nickel (Ni)	1,32986	13,570%	0,007988%
					Palladium (Pd)	0,00882	0,090%	0,000053%
					Silver (Ag)	0,2597	2,650%	0,001660%
					Tin (Sn)	0,1617	1,650%	0,000971%
					glass	0,0147	0,150%	0,000088%
					Titane dioxide (TiO2)	2,6969208	27,520%	0,016200%
					Barite	5,2351992	53,420%	0,031447%
Capacitor 1812	1	195,2	195,2	1,173%	Copper (Cu)	1,8544	0,950%	0,011139%
					Nickel (Ni)	26,48864	13,570%	0,159113%
					Palladium (Pd)	0,17568	0,090%	0,001055%
					Silver (Ag)	5,1728	2,650%	0,031072%
					Tin (Sn)	3,2208	1,650%	0,019347%
					glass	0,2928	0,150%	0,001759%
					Titane dioxide (TiO2)	53,7182592	27,520%	0,322677%
					Barite	104,2766208	53,420%	0,626373%
Resistors 0402	9	1,08	9,72	0,058%	Lead (Pb)	0,042768	0,440%	0,000257%
					Iron (Fe)	0,22842	2,350%	0,001372%
					Nickel (Ni)	0,16038	1,650%	0,000963%
					Copper (Cu)	0,035964	0,370%	0,000216%
					Tin (Sn)	0,113724	1,170%	0,000683%
					Chromium (Cr)	0,008748	0,090%	0,000053%
					Silicium (Si)	0,000972	0,010%	0,000006%
					Palladium (Pd)	0,013608	0,140%	0,000082%
					Silver (Ag)	0,0972	1,000%	0,000584%
					Gold (Au)	0,049572	0,510%	0,000298%
					Aluminium oxide (Al2O3)	6,79914	69,950%	0,040841%
					SiO2	1,945944	20,020%	0,011689%
					CaCO3	0,00486	0,050%	0,000029%
					Glass	0,064152	0,660%	0,000385%
					Epoxy resin	0,091368	0,940%	0,000549%
					Polyacrylate	0,062208	0,640%	0,000374%
Diode SOT666	2	2,9	5,8	0,035%	Lead (Pb)	0,09106	1,570%	0,000547%
					Iron (Fe)	2,51372	43,340%	0,015100%
					Copper (Cu)	1,31138	22,610%	0,007877%
					Nickel (Ni)	0,02146	0,370%	0,000129%
					Tin (Sn)	0,25926	4,470%	0,001557%
					Molybdenum (Mo)	0,11716	2,020%	0,000704%
					Glass	0,90596	15,620%	0,005442%
					Encapsulation insulator (SiO2)	0,55216	9,520%	0,003317%
Diode 0603	1	1	1	0,006%	Epoxy resin	0,00058	0,010%	0,000003%
					Doted silica	0,0261	0,450%	0,000157%
					Lead (Pb)	0,0157	1,570%	0,000094%
					Iron (Fe)	0,4334	43,340%	0,002603%
					Copper (Cu)	0,2261	22,610%	0,001358%
					Nickel (Ni)	0,0037	0,370%	0,000022%
					Tin (Sn)	0,0447	4,470%	0,000269%
					Molybdenum (Mo)	0,0202	2,020%	0,000121%
Transistors SOT-323	2	6	12	0,072%	Glass	0,1562	15,620%	0,000938%
					Encapsulation insulator (SiO2)	0,0952	9,520%	0,000572%
					Epoxy resin	0,0001	0,010%	0,000001%
					Doted silica	0,0045	0,450%	0,000027%
					Aluminium (Al)	0,0252	0,210%	0,000151%
					Iron (Fe)	0,1248	1,040%	0,000750%
					Copper (Cu)	4,356	36,300%	0,026166%
					Nickel (Ni)	0,096	0,800%	0,000577%
PCB	1	573,312	573,312	3,444%	Lead (Pb)	0,5292	4,410%	0,003179%
					Tin (Sn)	0,9132	7,610%	0,005485%
					Encapsulation insulator (SiO2)	5,8956	49,130%	0,035414%
					Doped silicium	0,0612	0,510%	0,000368%
					Copper (Cu)	330,5862472	57,663%	1,985779%

					Glass	217,7031384	37,973%	1,307708%					
					Gold (Au)	0,017853961	0,003%	0,000107%					
					Nickel (Ni)	0,089269805	0,016%	0,000536%					
					Phenolic resin	24,53479814	4,279%	0,147377%					
					Silver (Ag)	0,059321226	0,010%	0,000356%					
					Tin (Sn)	0,3213713	0,056%	0,001930%					
Plastic case	1	15780	15780	94,787%	AcrylonitrileButadieneStyrene (ABS)	15780	100,000%	94,787949%					
Voltage Detectors SOT23-5 type	2	16,5	33	0,198%	Die	0,76	2,303%	0,004565%					
					Copper (Cu)	13,872	42,036%	0,083327%					
					Iron (Fe)	0,324	0,982%	0,001946%					
					Phosphorus (P)	0,004	0,012%	0,000024%					
					Zinc (Zn)	0,018	0,055%	0,000108%					
					Nickel (Ni)	0,166	0,503%	0,000997%					
					Palladium (Pd)	0,014	0,042%	0,000084%					
					Gold (Au)	0,002	0,006%	0,000012%					
					Aluminium oxide (Al2O3)	0,042	0,127%	0,000252%					
					Diethylene glycol monoethyl ether acetate	0,056	0,170%	0,000336%					
					Epoxy resin	0,01	0,030%	0,000060%					
					Epoxy resin	0,028	0,085%	0,000168%					
					Aromatic amine	0,004	0,012%	0,000024%					
					Gold (Au)	0,3	0,909%	0,001802%					
					Silica, vitreous	14,842	44,976%	0,089154%					
					phenolic resin	0,61	1,848%	0,003664%					
					epoxy resin	0,696	2,109%	0,004181%					
					Biphenyl epoxy resin	0,348	1,055%	0,002090%					
					Carbon black	0,034	0,103%	0,000204%					
					Zinc hydroxide	0,174	0,527%	0,001045%					
Magnesium hydroxide	0,696	2,109%	0,004181%										
Voltage comparator SC70-5 type	1	6	6	0,036%	Die	0,178	2,967%	0,001069%					
					Iron (Fe)	0,067	1,117%	0,000402%					
					Copper (Cu)	2,829	47,150%	0,016993%					
					Phosphorus (P)	0,001	0,017%	0,000006%					
					Zinc (Zn)	0,004	0,067%	0,000024%					
					Nickel (Ni)	0,034	0,567%	0,000204%					
					Palladium (Pd)	0,003	0,050%	0,000018%					
					Silver (Ag)	0,016	0,267%	0,000096%					
					Carbocyclic Acrylates	0,002	0,033%	0,000012%					
					Bismaleimide resin	0,002	0,033%	0,000012%					
					2-preponic acid, 2-methyl	0,001	0,017%	0,000006%					
					Gold (Au)	0,033	0,550%	0,000198%					
					Epoxy Resin-1	0,056	0,933%	0,000336%					
					Epoxy Resin-2	0,056	0,933%	0,000336%					
					Epoxy Resin-3	0,056	0,933%	0,000336%					
					Phenol resin	0,114	1,900%	0,000685%					
					Silica	2,542	42,367%	0,015269%					
Carbon black	0,006	0,100%	0,000036%										
MCU WLCS36 type	1	5,949	5,949	0,036%	Die	4,411741594	74,159%	0,026501%					
					Titanium	0,001000168	0,017%	0,000006%					
					Copper	0,003000504	0,050%	0,000018%					
					Copper	0,062010424	1,042%	0,000372%					
					Copper	0,002000336	0,034%	0,000012%					
					Copper	0,073012273	1,227%	0,000439%					
					Tin	1,14619267	19,267%	0,006885%					
					Silver	0,014002354	0,235%	0,000084%					
					Copper	0,018003026	0,303%	0,000108%					
					Polyethylene terephthalate	0,154025891	2,589%	0,000925%					
					Silica	0,034005716	0,572%	0,000204%					
					Acrylic ester co-polymer	0,014002354	0,235%	0,000084%					
					Epoxy resin	0,014002354	0,235%	0,000084%					
					Carbon black	0,001000168	0,017%	0,000006%					
					Additive	0,001000168	0,017%	0,000006%					
					EEPROM memory UFDFPN8 type	1	16	16	0,096%	Die	1,227923255	7,675%	0,007376%
										Copper (Cu)	2,917817636	18,236%	0,017527%
Iron (Fe)	0,069995625	0,437%	0,000420%										
Zinc (Zn)	0,00399975	0,025%	0,000024%										
Iron Phosphide (FeP)	0,002999813	0,019%	0,000018%										
Nickel (Ni)	0,01199925	0,075%	0,000072%										
Palladium (Pd)	0,000999938	0,006%	0,000006%										
Silver (Ag)	1,107930754	6,925%	0,006655%										
polymer	0,100993688	0,631%	0,000607%										
aniline	0,012999188	0,081%	0,000078%										
Epoxy resin	0,037997625	0,237%	0,000228%										
Epoxy resin molecular weight <= 700	0,005999625	0,037%	0,000036%										
Copper (Cu)	0,017998875	0,112%	0,000108%										
Silica, vitreous	9,228423224	57,678%	0,055434%										
Biphenyl epoxy resin	0,52096744	3,256%	0,003129%										
Phenolic resin	0,406974564	2,544%	0,002445%										
epoxy resin	0,208986938	1,306%	0,001255%										
carbon black	0,020998688	0,131%	0,000126%										
other	0,093994125	0,587%	0,000665%										
TOTAL		16647,781	16647,781	100,000%									

Materials that can be obtained from shredding and speartion steps	Aggregated content shares	Metal fractions (per Kg of waste flow)			
		Ferro	Aluminum	Copper	Residue
Aluminium (Al)	0,041%	2,06E-06	3,41E-04	2,03E-05	4,95E-05
Copper (Cu)	2,152%	2,02E-04	1,08E-03	1,68E-02	3,41E-03
Ferro (Fe, Ni, Co)	0,193%	1,84E-03	1,93E-05	1,93E-05	5,80E-05
Glass	1,316%	7,37E-05	7,37E-05	1,32E-03	1,17E-02
Plastics (Thermosets, Thermoplastics)	94,957%	1,15E-02	4,75E-03	9,50E-02	8,38E-01
Silver (Ag)	0,040%	4,00E-06	4,00E-06	3,43E-04	5,29E-05
Gold (Au)	0,002%	2,39E-07	2,39E-07	1,93E-05	4,36E-06
Lead (Pb)	0,004%	4,81E-07	4,81E-07	3,26E-05	7,20E-06
Others	1,293%	8,93E-05	8,67E-05	4,57E-03	8,20E-03
TOTAL	100,000%	1,37E-02	6,35E-03	1,18E-01	8,62E-01

Recycled materials content in respective scraps (per Kg of metal fraction)		
In Ferro fraction	In Aluminium fraction	In Copper fraction
1,51E-04	5,36E-02	1,72E-04
1,48E-02	1,69E-01	1,43E-01
1,34E-01	3,04E-03	1,64E-04
5,38E-03	1,16E-02	1,11E-02
8,39E-01	7,48E-01	8,04E-01
2,92E-04	6,30E-04	2,91E-03
1,75E-05	3,77E-05	1,64E-04
3,51E-05	7,58E-05	2,76E-04
6,52E-03	1,37E-02	3,87E-02

b) Recycled material content in the waste flow “WPCB” (Regular recycling scenario)

Materials that can be obtained from shredding and speartion steps	Aggregated content shares	Metal fractions (per Kg of waste flow)			
		Ferro	Aluminum	Copper	Residue
Aluminium (Al)	0,791%	3,96E-05	6,53E-03	3,89E-04	9,50E-04
Copper (Cu)	41,289%	3,88E-03	2,06E-02	3,23E-01	6,54E-02
Ferro (Fe, Ni, Co)	3,707%	3,52E-02	3,71E-04	3,71E-04	1,11E-03
Glass	25,255%	1,41E-03	1,41E-03	2,53E-02	2,24E-01
Plastics (Thermosets, Thermoplastics)	3,242%	3,92E-04	1,62E-04	3,24E-03	2,86E-02
Silver (Ag)	0,775%	7,67E-05	7,67E-05	6,58E-03	1,02E-03
Gold (Au)	0,046%	4,59E-06	4,59E-06	3,71E-04	8,36E-05
Lead (Pb)	0,078%	9,23E-06	9,23E-06	6,26E-04	1,38E-04
Others	24,816%	1,71E-03	1,66E-03	8,76E-02	1,57E-01
TOTAL	100,000%	4,27E-02	3,09E-02	4,47E-01	4,79E-01

Recycled materials content in respective scraps (per Kg of metal fraction)		
In Ferro fraction	In Aluminium fraction	In Copper fraction
0,000925587	0,211619118	0,000870281
0,09079161	0,66852963	0,721817765
0,823830355	0,01200458	0,000828632
0,033084576	0,045799249	0,056452731
0,009176174	0,00524903	0,007246423
0,001795459	0,002485469	0,014716272
0,00010741	0,000148688	0,000829364
0,000215923	0,000298905	0,001398798
0,040072905	0,05386533	0,195839733

c) Recycled material content in the waste flow “WPCB” (Best recycling scenario)

Component type	Quantity	Weight (mg)	Total weight (mg)	% components type	Material	mg	Content share in the component type	Content share in the EH sensor system device
Capacitor 0402	7	1,4	9,8	1,493%	Copper (Cu)	0,0931	0,950%	0,014180%
					Nickel (Ni)	1,32966	13,570%	0,202544%
					Palladium (Pd)	0,00882	0,090%	0,001343%
					Silver (Ag)	0,2597	2,650%	0,039563%
					Tin (Sn)	0,1617	1,650%	0,024628%
					glass	0,0147	0,150%	0,002239%
					Titane dioxide (TiO2)	2,6969208	27,520%	0,410753%
Resistors 0402	9	1,08	9,72	1,480%	Barite	5,2351992	53,420%	0,797344%
					Lead (Pb)	0,042768	0,440%	0,006514%
					Iron (Fe)	0,22842	2,350%	0,034789%
					Nickel (Ni)	0,16038	1,650%	0,024427%
					Copper (Cu)	0,035964	0,370%	0,005477%

					Tin (Sn)	0.113724	1,170%	0.017321%
					Chromium (Cr)	0.006748	0,090%	0.001332%
					Silicium (Si)	0.000972	0,010%	0.000148%
					Palladium (Pd)	0.013608	0,140%	0.002073%
					Silver (Ag)	0.0972	1,000%	0.014804%
					Gold (Au)	0.049572	0,510%	0.007550%
					Aluminium oxide (Al2O3)	6.79914	69,950%	1,035539%
					SiO2	1.945944	20,020%	0.296376%
					CaCO3	0.00486	0,050%	0.000740%
					Glass	0.064152	0,660%	0.009771%
					Epoxy resin	0.091368	0,940%	0.013916%
					Polyacrylate	0.062208	0,640%	0.009475%
Diode SOT666	2	2,9	5,8	0,883%	Lead (Pb)	0.09106	1,570%	0.013869%
					Iron (Fe)	2.51372	43,340%	0.382851%
					Copper (Cu)	1.31138	22,610%	0.199729%
					Nickel (Ni)	0.02146	0,370%	0.003268%
					Tin (Sn)	0.25926	4,470%	0.039486%
					Molybdenum (Mo)	0.11716	2,020%	0.017844%
					Glass	0.90596	15,620%	0.137982%
					Encapsulation insulator (SiO2)	0.55216	9,520%	0.084096%
					Epoxy resin	0.00058	0,010%	0.000088%
					Doped silica	0.0261	0,450%	0.003975%
					Lead (Pb)	0.0157	1,570%	0.002391%
					Iron (Fe)	0.4334	43,340%	0.066009%
					Copper (Cu)	0.2261	22,610%	0.034436%
					Nickel (Ni)	0.0037	0,370%	0.000564%
					Tin (Sn)	0.0447	4,470%	0.006808%
					Molybdenum (Mo)	0.0202	2,020%	0.003077%
					Glass	0.1562	15,620%	0.023790%
					Encapsulation insulator (SiO2)	0.0952	9,520%	0.014499%
					Epoxy resin	0.0001	0,010%	0.000015%
					Doped silica	0.0045	0,450%	0.000685%
Transistors SOT-323	2	6	12	1,828%	Aluminium (Al)	0.0252	0,210%	0.003838%
					Iron (Fe)	0.1248	1,040%	0.019008%
					Copper (Cu)	4.356	36,300%	0.663438%
					Nickel (Ni)	0.096	0,800%	0.014621%
					Lead (Pb)	0.5292	4,410%	0.080599%
					Tin (Sn)	0.9132	7,610%	0.139084%
					Encapsulation insulator (SiO2)	5.8956	49,130%	0.897926%
					Doped silicium	0.0612	0,510%	0.009321%
PCB	1	573,312	573,312	87,318%	Copper (Cu)	330,5862472	57,663%	50,349739%
					Glass	217,7031384	37,973%	33,157145%
					Gold (Au)	0.017853961	0,003%	0.002719%
					Nickel (Ni)	0.089269805	0,016%	0.013596%
					Phenolic resin	24.53479814	4,279%	3,736758%
					Silver (Ag)	0.059321226	0,010%	0.009035%
					Tin (Sn)	0.3213713	0,056%	0.048946%
Voltage detectors SOT23-5 type	2	16,5	33	5,026%	Die	0.76	2,303%	0.115751%
					Copper (Cu)	13.872	42,036%	2,112767%
					Iron (Fe)	0.324	0,982%	0.049347%
					Phosphorus (P)	0.004	0,012%	0.000609%
					Zinc (Zn)	0.018	0,055%	0.002741%
					Nickel (Ni)	0.166	0,503%	0.025283%
					Palladium (Pd)	0.014	0,042%	0.002132%
					Gold (Au)	0.002	0,006%	0.000305%
					Aluminium oxide (Al2O3)	0.042	0,127%	0.006397%
					Diethylene glycol monoethyl ether acetate	0.056	0,170%	0.008529%
					Epoxy resin	0.01	0,030%	0.001523%
					Epoxy resin	0.028	0,085%	0.004265%
					Aromatic amine	0.004	0,012%	0.000609%
					Gold (Au)	0.3	0,909%	0.045691%
					Silica, vitreous	14.842	44,976%	2,260502%
					phenolic resin	0.61	1,848%	0.092906%
					epoxy resin	0.696	2,109%	0.106004%
					Biphenyl epoxy resin	0.348	1,055%	0.053002%
					Carbon black	0.034	0,103%	0.005178%
					Zinc hydroxide	0.174	0,527%	0.026501%
					Magnesium hydroxide	0.696	2,109%	0.106004%
Voltage comparator SC70-5 type	1	6	6	0,914%	Die	0.178	2,967%	0.027110%
					Iron (Fe)	0.067	1,117%	0.010204%
					Copper (Cu)	2.829	47,150%	0.430869%
					Phosphorus (P)	0.001	0,017%	0.000152%
					Zinc (Zn)	0.004	0,067%	0.000609%
					Nickel (Ni)	0.034	0,567%	0.005178%
					Palladium (Pd)	0.003	0,050%	0.000457%
					Silver (Ag)	0.016	0,267%	0.002437%
					Carboocyclic Acrylates	0.002	0,033%	0.000305%
					Bismaleimide resin	0.002	0,033%	0.000305%
					2-preponic acid, 2-methyl	0.001	0,017%	0.000152%
					Gold (Au)	0.033	0,550%	0.005026%
					Epoxy Resin-1	0.056	0,933%	0.008529%
					Epoxy Resin-2	0.056	0,933%	0.008529%
					Epoxy Resin-3	0.056	0,933%	0.008529%
					Phenol resin	0.114	1,900%	0.017363%

					Silica	2,542	42,367%	0,387158%
					Carbon black	0,006	0,100%	0,000914%
MCU WLCS36 type	1	5,949	5,949	0,906%	Die	4,411741594	74,159%	0,671928%
					Titanium	0,001000168	0,017%	0,000152%
					Copper	0,003000504	0,050%	0,000457%
					Copper	0,062010424	1,042%	0,009444%
					Copper	0,002000336	0,034%	0,000305%
					Copper	0,073012273	1,227%	0,011120%
					Tin	1,14619267	19,267%	0,174570%
					Silver	0,014002354	0,235%	0,002133%
					Copper	0,018003026	0,303%	0,002742%
					Polyethylene terephthalate	0,154025891	2,589%	0,023459%
					Silica	0,034005716	0,572%	0,005179%
					Acrylic ester co-polymer	0,014002354	0,235%	0,002133%
					Epoxy resin	0,014002354	0,235%	0,002133%
					Carbon black	0,001000168	0,017%	0,000152%
					Additive	0,001000168	0,017%	0,000152%
		TOTAL	656,581	100,000%				

Materials that can be obtained from shredding and separation steps	Aggregated content shares	Metal fractions (per Kg of waste flow)			
		Ferro	Aluminum	Copper	Residue
Aluminium (Al)	1,046%	5,23E-05	8,64E-03	5,15E-04	1,25E-03
Copper (Cu)	53,835%	5,06E-03	2,69E-02	4,21E-01	8,53E-02
Ferro (Fe, Ni, Co)	0,852%	8,09E-03	8,52E-05	8,52E-05	2,56E-04
Glass	33,331%	1,87E-03	1,87E-03	3,33E-02	2,96E-01
Plastics (Thermosets, Thermoplastics)	4,089%	4,95E-04	2,04E-04	4,09E-03	3,61E-02
Silver (Ag)	0,068%	6,73E-06	6,73E-06	5,77E-04	8,90E-05
Gold (Au)	0,061%	6,07E-06	6,07E-06	4,90E-04	1,10E-04
Lead (Pb)	0,103%	1,22E-05	1,22E-05	8,27E-04	1,82E-04
Others	6,615%	4,56E-04	4,43E-04	2,33E-02	4,19E-02
TOTAL	100,000%	1,60E-02	3,82E-02	4,84E-01	4,62E-01

Recycled materials content in respective scraps (per Kg of metal fraction)		
In Ferro fraction	In Aluminium fraction	In Copper fraction
3,26E-03	2,26E-01	1,06E-03
3,15E-01	7,05E-01	8,69E-01
5,04E-01	2,23E-03	1,76E-04
1,16E-01	4,89E-02	6,88E-02
3,08E-02	5,36E-03	8,44E-03
4,19E-04	1,76E-04	1,19E-03
3,78E-04	1,59E-04	1,01E-03
7,60E-04	3,20E-04	1,71E-03
2,84E-02	1,16E-02	4,82E-02

d) Recycled material content in the waste flow “Waste components” (Best recycling scenario)

Component type	Quantity	Weight (mg)	Total weight (mg)	% components type	Material	mg	Content share in the component type	Content share in the EH sensor system device
Capacitor 1812	1	195,2	195,2	92,424%	Copper (Cu)	1,8544	0,950%	0,878421%
					Nickel (Ni)	26,48864	13,570%	12,547554%
					Palladium (Pd)	0,17568	0,090%	0,083219%
					Silver (Ag)	5,1728	2,650%	2,450333%
					Tin (Sn)	3,2208	1,650%	1,525679%
					glass	0,2928	0,150%	0,138698%
					Titane dioxide (TiO2)	53,7182592	27,520%	25,446107%
					Barite	104,2766208	53,420%	49,395383%
EEPROM memory UDFPN8 type	1	16	16	7,576%	Die	1,227923255	7,675%	0,581662%
					Copper (Cu)	2,917817636	18,236%	1,382158%
					Iron (Fe)	0,069995625	0,437%	0,033157%
					Zinc (Zn)	0,00399975	0,025%	0,001895%
					Iron Phosphide (FeP)	0,002999813	0,019%	0,001421%
					Nickel (Ni)	0,01199925	0,075%	0,005684%
					Palladium (Pd)	0,000999938	0,006%	0,000474%
					Silver (Ag)	1,107930754	6,925%	0,524822%
					polymer	0,100993688	0,631%	0,047840%
					aniline	0,012999188	0,081%	0,006158%
					Epoxy resin	0,037997625	0,237%	0,017999%
					Epoxy resin molecular weight <= 700	0,005999625	0,037%	0,002842%
					Copper (Cu)	0,017998875	0,112%	0,008526%
					Silica, vitreous	9,228423224	57,678%	4,371464%
					Biphenyl epoxy resin	0,52096744	3,256%	0,246780%
Phenolic resin	0,406974564	2,544%	0,192782%					
epoxy resin	0,208986938	1,306%	0,098996%					

				carbon black	0,020998688	0,131%	0,009947%
				other	0,093994125	0,587%	0,044525%
		TOTAL	211,2	100,000%			

Materials that can be obtained from shredding and separation steps	Aggregated content shares	Metal fractions (per Kg of waste flow)			
		Ferro	Aluminium	Copper	Residue
Aluminium (Al)	0,000%	0,00E+00	0,00E+00	0,00E+00	0,00E+00
Copper (Cu)	2,269%	2,13E-04	1,13E-03	1,77E-02	3,59E-03
Ferro (Fe, Ni, Co)	12,588%	1,20E-01	1,26E-03	1,26E-03	3,77E-03
Glass	0,139%	7,76E-06	7,76E-06	1,39E-04	1,23E-03
Plastics (Thermosets, Thermoplastics)	0,607%	7,34E-05	3,03E-05	6,07E-04	5,36E-03
Silver (Ag)	2,975%	2,94E-04	2,94E-04	2,53E-02	3,90E-03
Gold (Au)	0,000%	0,00E+00	0,00E+00	0,00E+00	0,00E+00
Lead (Pb)	0,000%	0,00E+00	0,00E+00	0,00E+00	0,00E+00
Others	81,422%	5,62E-03	5,46E-03	2,87E-01	5,16E-01
TOTAL	100,000%	1,26E-01	8,18E-03	3,32E-01	5,34E-01

Recycled materials content in respective scraps		
In Ferro fraction	In Aluminium fraction	In Copper fraction
0,00E+00	0,00E+00	0,00E+00
1,70E-03	1,39E-01	5,34E-02
9,51E-01	1,54E-01	3,79E-03
6,17E-05	9,49E-04	4,17E-04
5,84E-04	3,71E-03	1,83E-03
2,34E-03	3,60E-02	7,60E-02
0,00E+00	0,00E+00	0,00E+00
0,00E+00	0,00E+00	0,00E+00
4,47E-02	6,67E-01	8,65E-01

14. Materials, components and other aspects excluded from the LCA implementation (case study “Smart monitoring”)

The following materials were excluded from the LCA implementation because of lack of LCA data or because of confidential reasons (Proprietary labels). Notice that a material is not taken into account **only if** it does not exist in Ecoinvent database **and** its relative quantity in the studied component is very low.

Missing materials	CAS number	Occurrence in component(s)
1,3-Isobenzofurandione, hexahydro-5-methyl-	19438-60-9	LQFP32
1,4-Bis(2,3-epoxypropoxy)butane	2425-79-8	LQFP32, UFQFPN32
2,2'-(Methylenebis(phenyleneoxymethylene))	39817-09-9	LQFP32
2,6-Diglycidyl phenyl allyl ether	EC 417-470-1	TFBGA64
2-preponic acid, 2-methyl	68586-19-6	VC_SC70-5
2-(3,4-Epoxy cyclohexyl)ethyltrimethoxysilane	3388-04-3	BlueNRG2 (SoC)
4-tert-butylcyclohexanol	98-52-2	TFBGA64
acrylate	Proprietary	SO8
Acrylates derivative	407-47-6	TFBGA64
Acrylic ester co-polymer	Proprietary	WLCSP36
amine compound	Proprietary	TFBGA64
Aromatic amine	Proprietary	VD_SOT23-5
aromatic hydrocarbon	Proprietary	TFBGA64
Bisphenol-F, epoxy resin	9003-36-5	UFQFPN32
Biphenyl epoxy resin	85954-11-6	UFDFPN8, TFBGA64, VD_SOT23-5
Bismaleimide (B)	13676-54-5	TFBGA64
Bismaleimide resin	35325-39-4	VC_SC70-5
Bismaleimide resin	Proprietary	VC_SOT23-5, TSSOP8
Bismuth	7440-69-9	SO8, TSSOP8
Carbocyclic Acrylates	Proprietary	VC_SC70-5
Dicumyl peroxide	80-43-3	VC_SOT23-5
Dicyclopentylloxyethyl methacrylate	68586-19-6	VC_SOT23-5
Dihydro-3-(tetrapropenyl)furan-2,5-dione	26544-38-7	LQFP32
Dodecylloxirane	3234-28-4	LQFP32
Epoxy resin molecular weight <= 700	Proprietary	UFDFPN8
exo-1,7,7-trimethylbicyclo[2,2,1]hept-2-yl met	7534-94-3	BlueNRG2 (SoC)
Fatty acids, polymers with epichlorohydrin	68475-94-5	UFQFPN32
Hexamethyltetracosane-hexaene	111-02-4	TFBGA64
Iron Phosphide (FeP)	26508-33-8	VC_SOT23-5, UFDFPN8, TSSOP8
Isobornyl acrylate	5888-33-5	BlueNRG2 (SoC)
Magnesium hydroxide	1309-42-8	VD_SOT23-5, TFBGA64
Metal Hydroxide	Proprietary	UFQFPN32, BlueNRG2 (SoC)
Methacrylate	Proprietary	SO8
methylene diacrylate OR (Octahydro-4,7-methano-1 H-indenediyl)bis(m	42594-17-2	VC_SOT23-5, BlueNRG2 (SoC)
Neopentyl glycol dimethacrylate	1985-51-9	TFBGA64
Phenolic resin	205830-20-2	UFDFPN8, TFBGA64
Poly(Oxy(methyl-1, 2-ethanediyl)	9046-10-0	UFQFPN32
Synthetic resin	Proprietary	TSSOP8
Talc containing no asbestiform fibers (Magnesium silicate monohydrate - talc)	14807-96-6	TFBGA64
Thermosetting resin	Proprietary	TFBGA64
Zinc hydroxide	20427-58-1	VC_SOT23-5, TFBGA64, VD_SOT23-5

Also, Because of their absence in Ecoinvent database, lack of data proxies, or the difficulty of modeling from specialized materials, the following components were excluded from the LCA implementation:

- 2 Piezoelectric buzzers (no LCA data nor proxy. lack of specialized material (piezoelectric ceramics)).
- 2 Crystal oscillators type 0805 (BLE module) (no LCA data nor proxy. Material declaration unavailable).

Finally, losses in the manufacturing phase of all PCB components were not taken into account.

15. Summary of LCA studies of sensors, sensor systems, partial IoT systems and full IoT systems

Title	Goal	Case study description	Functional unit	Reference flow	Results	Scope and limits	Eco-design strategies	Recommendations for the LCA study
Contributions to eco-design of machine-to-machine product service systems: the example of waste glass collection. Lelah, A. et al (2011) [51]	Identifying the main environmental impact contributors	An IoT system oriented to urban waste glass collection (composed of solar-based powered repeaters). It adapts the truck routes accordingly to containers' level [51]	centralized ten-year hourly provision of glass-level values for all the waste glass containers	not specified	Big contributors (baseline) PSS infrastructure (gateways, M2M platform and PC(end-user)) (60% GW, 47% RMD) Sensors (53% RMD, 14% WP)	The EoL phase is not taken into account The cloud servers, end-user devices and telecom infrastructures are included	1. Mutualize PSS infrastructure for similar services	Examine other M2M PSS cases Consider more advanced prototypes or cases of wide scale implantations.
An integrated method for environmental assessment and ecodesign of ICT-based optimization services. Bonvoisin, J. et al (2014) [10] And An environmental assessment method for wireless sensor networks. Bonvoisin, J. et al (2012) [61]	Impact estimation for determining the most influential parameters and suggest eco-design alternatives	An IoT system oriented to urban waste glass collection (composed of electricity-grid powered gateways). It adapts trucks routes accordingly to containers' level [10][61]	centralized ten-year hourly provision of glass-level values for all the waste glass containers	not specified	Big contributors (baseline) sensors (63% WE, 83% RMD) Repeaters (35% WE, 15% RMD)	The LCIA step does not consider the EoL Phase (It is considered by another assessment tool for EoL of electronics (reSICLED[78])) The cloud servers, end-user devices and the telecom infrastructures are excluded	1. Replacement of materials 2. Decrease energy consumption 3. Double battery capacity 4. A combination of alternatives 1, 2, and 3	1. The LCA scope should include mutualized infrastructure and end-user equipment. 2. uncertainty analysis should be taken into account
Life-cycle assessment of an intelligent lighting system using a distributed wireless mote network. Dubberley, M. et al. (2014) [73]	comparison of a smart lighting system versus a traditional system	An Intelligent Light System composed of a battery-based wireless sensor network (sensors include dimmable ballasts and housings cases) [73]	Meet the lighting needs of an office building of 5000 square feet for one year.	not specified	The impacts of the ILS are 18-344 smaller than those of conventional lighting systems Big contributors (sensors) PCB (82,8% E, 29,7% GW, 40,7% H, 70,8% P) Integrated circuit components (32,4% E, 49,1% FD) Lithium battery (37,8% A, 94,3% OD)	Edge and cloud infrastructure are excluded from the study	1. Replace the battery with a connection to the ballast 3. Reduce PCB and IC sizes (electronic redesign) 4. Limiting paint in ballasts and reduce plastic materials	Not specified
Life cycle assessment and eco-design of smart textiles: The importance of material selection demonstrated through e-textile product redesign. Van der Velden, N. M. et al (2015) [76]	Impact estimation	Self-care health sensors in the form of a garment, which invite the body to feel, move, and heal through vibration therapy [76]	Facilitates the self-care treatment of a woman—who is in need for vibration therapy—by means of the product, for a use period of one year; 5 times per week; 30 min per time	Not specified	Big Ecocost contributors Production phase (74% of the total impact), on which the electronic system accounts for a significant contribution (71%) (Due to the silver content of the conductive wire). The PCB contributes with 32%	The packaging process of the product is excluded.	1. Replace silver in wires with copper 2. Reduce wires content (may affected connectivity among components)	The development of smart textiles and PSS should be further included Relaunch a second LCA for estimating the eco-design alternatives

Life cycle assessment and eco-design of a textile-based large-area sensor system. Köhler, A. R. (2012) [60]	Impact estimation to support environmentally conscious decision-making in the course of product development	A textile-based sensing floor underlay with integrated microelectronic modules and capacitive proximity sensors [60]	Scenario 1: safety and energy management for an elderly person home for 20 years (sensing floor size 30m ²) Scenario 2: Presence monitoring system for a lecture room for 20 years (sensing floor size 4m ²)	not specified	The big ecocost contributor (for scenario 1 and scenario 2 respectively) is use phase (Energy consumption) (92,67% and 95,11%) Impacts in the sensing floor (for scenario 1 and scenario 2 respectively) Polyester base-layer (72,8% and 53,4%) Sensor modules (4 per m ²) (4,9% and 3,6%) Transceiver (3,2% and 17,8%)	It only consider the sensor network (modules) and transceiver (edge device)	1. Reduce spatial resolution (2 modules per m ² instead of 4) for avoiding power dissipation 2. Switch off the radio receiver (Rx) of sensor modules about 10 min after power up 3. Reduce sampling rate from 10Hz to 2Hz to prolong sleep phases (Two capacitance measurements per second are sufficient for both applications)	Improve the availability of comprehensive and well-updated secondary LCI datasets
Do home energy management systems make sense? Assessing their overall lifecycle impact. Van Dam, S. S. et al. (2013) [72]	LCA and CED comparison of three distinct types of products on the basis of energy invested and energy saved	Device 1: An energy monitor system (sensor, transmitting unit and a display) Device 2: A multifunctional HEMS (a touchscreen device and a thermostat) Device 3: An energy management system (plugs in a zigbee mesh network) [72]	Not specified	not specified	Ecocost calculations and CED results over 5 years (respectively) Energy monitor: 9€ and 765 MJ Multifunctional HEMS (old): 82€ and 7028 MJ Multifunctional HEMS (new): 49€ and 3852 MJ Energy management system: 48€ and 3924 MJ	The energy monitor system excludes the smart electricity meter (edge device) The multifunctional HEMS excludes edge devices (router and meters) The energy management system excludes edge devices (centralized PC)	1. Avoid design alternatives of HEMS with unnecessarily elaborate parts or functionalities. 2. minimize the own energy consumption of HEMS devices	Not specified
Advanced packaging for wireless sensor nodes in cyber-physical systems- impacts of multifunctionality and miniaturization on the environment. Wagner, E. et al. (2017) [26]	LCA comparison of three integration level versions of a sensor system	A sensor system for prognostic structure health monitoring [26] Version 0: Customized open source design (i.e.: Arduino) Version 1: A customized electronic design Version 2: Advanced packaging (wafer- and panel level integration)	Not specified	not specified	Version 0 has the most impacts (more than 15Kg CO ₂ eq) Version 1 and version 2 has moderate impacts (less than 5Kg CO ₂ eq)	It only includes the production phase of sensor systems	Not specified	Not specified
Streamlined assessment to assist in the design of Internet-of-Things (IoT) Enabled Products: a case study of the smart fridge. Dekoninck, E., & Barbaccia, F. (2019) [71]	LCA comparison of 4 use-scenarios. The paper aims to show how to include the user behavior and the service system in the impact estimation of IoT-enabled products	A typical fridge with a wider system versus a smart fridge with screen, cameras, speakers, internet connection and online delivery (service) [71] Scenario 1: normal use of a fridge Scenario 2: least use of a smart fridge Scenario 3: average use of a smart fridge Scenario 4: intensive use of a smart fridge	Not specified	not specified	Impacts over a period of 15 years Impact of scenario 1: 23100 Kg eq CO ₂ Impact of scenario 2: 23200 Kg eq CO ₂ Impact of scenario 3: 21700 Kg eq CO ₂ Impact of scenario 4: 20200 Kg eq CO ₂	it only consider the use phase (including impacts from mutualized infrastructure and transportation (grocery chopping or online delivery) use of apps, food wasted and waste energy from opening doors)	1. Understand how the internet-browsing feature can be used to replace other browsing rather than creating additional browsing for the household 2. Understand how the internet-browsing feature could reduce other impacts like "shopping miles" by enabling more efficient delivery-based shopping 3. Understand how the use-by-date tracking system can be designed to change user behavior around food stocking and cooking in order to reduce food waste	Not specified

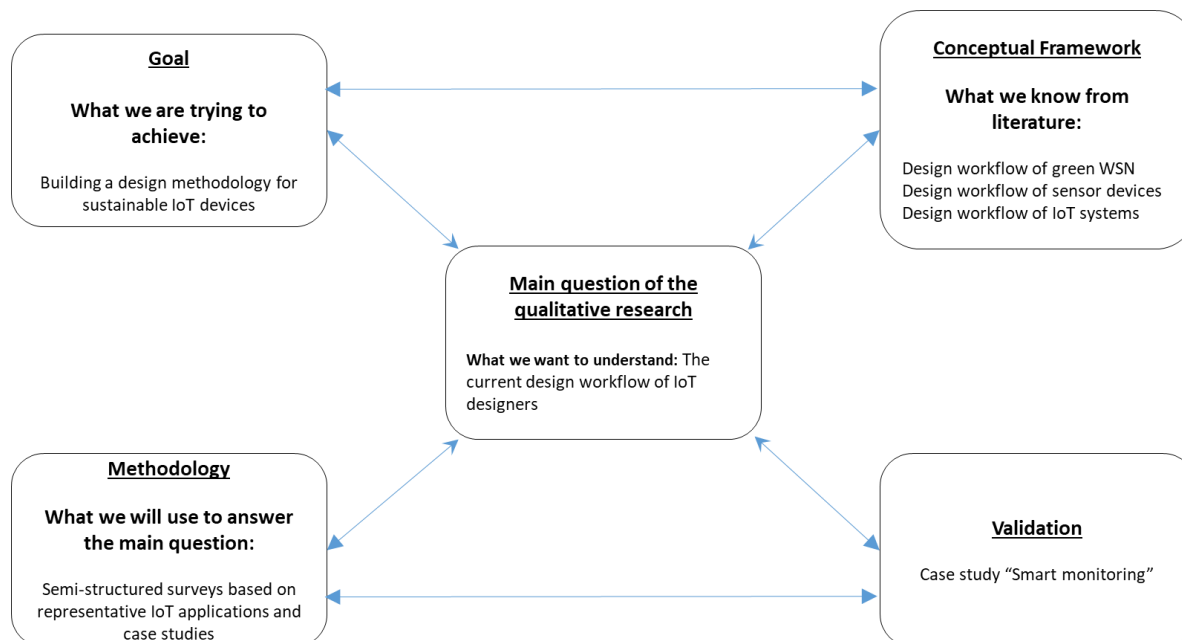
Material and manufacturing process selection for electronics eco-design: Case study on paper-based water quality sensors. Le Brun, G., & Raskin, J. P. (2020) [77]	LCA Comparison of two sensors in terms of materials and processes	A paper-based electrochemical device for bacteria detection (μ PEDs) versus A silicon-based biosensor [77]	1000 water quality measurements (Both sensor solutions are assumed to be single-use)	specified	Embodied energy for CNT- μ PEDs, Al- μ PEDs and Si-PDMS sensors exceed 1000, 5000 and 4500 MJ respectively. Carbon footprint for CNT- μ PEDs sensors amount to almost 50 Kg CO ₂ -eq while carbon footprint of Al- μ PEDs and Si-PDMS sensors exceed both 200 Kg CO ₂ -eq	It considers impacts of raw materials and manufacturing processes of sensors.	Not specified	Not specified
Assessing the embodied carbon footprint of IoT edge devices with a bottom-up life-cycle approach. Pirson, T., & Bol, D. (2021) [74]	Get a better understanding of the carbon footprint of the production of a wide range of IoT devices	Device 1: an occupancy sensor Device 2: a light-weight drone of less than 250 gr Device 3: a light-weight connected home assistant Device 4: a smart watch [74]	Production and transport to the use location of a single IoT device defined by its hardware profile	n.a.	Carbon footprint results Device 1: from 0.6 to 3.2 Kg CO ₂ eq Device 2: from 6.1 to 23.4 Kg CO ₂ eq Device 3: from 3.8 to 14.9 Kg CO ₂ eq Device 4: from 5.4 to 19.5 Kg CO ₂ eq	It consider raw material extraction, production and transportation of IoT devices (the use phase and the EoL phases are not taken into account)	Not specified	Take into account the use and EoL phases (including the mutualized infrastructure) Take into account more impact indicators
Quantifying the Net Environmental Impact of Using IoT to Support Circular Strategies—The Case of Heavy-Duty Truck Tires in Sweden. Ingemarsdotter, E. et al. (2021) [69]	Cost-Benefits LCA analysis to gain insights into when and how it makes sense to embed IoT hardware into products to support circularity	A tire-pressure-monitoring (TPM) IoT system composed of piezoelectric-based sensors systems and RFID tags [69]	Enabling a tractor/semi-trailer-typed truck to drive a distance of 2 * 10 ⁶ tire-Kms (assuming that tractor/semi-trailer-typed truck have 10 tires)	not specified	The TPM IoT system leads to a net impact reduction of approximately 4%	It consider the whole life cycle of tires (including maintenance and multiple use phases) as well as the fuel used by trucks. It also considers the production, use and disposal of sensor systems and the use phase of mutualized infrastructure. It excludes packaging.	Not specified	Not specified
Development of eco-efficient smart electronics for anticounterfeiting and shock detection based on printable inks. Glogic, E. et al. (2021) [75]	Impact estimation of two printable sensor systems	An anticounterfeit label (ACL) based on electrochromic display (device 1) and a Shock-detection tag (SDT) based on a piezoelectric sensor (device 2) [75]	Device 1: Producing at least 20 times visible chromacity change after receiving a 13.56 MHz signal (from the smartphone) over 2 years Device 2: Detecting and recording any frequency above 13.56 MHz in transportation operations, translating into a voltage signal readable by a smartphone	A single ACL device A single SDT device	The big contributors in both devices are NFC chip and the Radio-Frequency Identification antenna. Impacts of solvents, process energy, electrochromic display/piezoelectric sensor, Li-on battery and substrate are comparative small. In terms of global warming both devices embody around 0,23 Kg of CO ₂ -eq.	It only covers the production of sensor systems	1. Replace silver by copper-based nanoparticle ink 2. use flexography printing techniques	Not specified
Environmental impacts related to the commissioning and usage phase of an intelligent energy management system. Gangolells, M. et al. (2015) [240]	Impact estimation	An urban-scale intelligent energy management system composed of a core subsystem (edge devices for managing the other subsystems), a monitoring and controlling subsystems, and an environmental, energy and occupancy subsystems, (all composed by wireless sensor networks) [240]	Manufacturing and usage of the intelligent energy management system over a period of 5 years (scenario 1) and 10 years (scenario 2)	not specified	Single point impact Eco-indicator 99 for the 5-year and 10-year scenarios (respectively) Significant impacts attributed to the operational phase (53.93% and 69.9%) followed by the assembly phase (45.69% and 29.61%).	It consider the manufacturing phase (material extraction and assembly of all component devices), transport and functional lifespan (usage and maintenance). The mutualized infrastructure is excluded	Not specified	Not specified

16. Design methodology and questionnaires used in the qualitative research

The qualitative research presented in chapter 4 was conducted in two parts. the first part aims to reveal the current workflow of design teams and the second part aims to investigate the needs, expectations and attempts (if any) of designers and project leaders for integrating environmental aspects into their projects. This qualitative research was conducted at the System Division of CEA-Leti.

a. First part: current design workflow of IoT systems

The design of this part is composed of 5 elements (see figure below).



Design of the qualitative research oriented to acknowledge and understand the current design workflow of IoT systems (part I). This is an adaptation of the design methodology for qualitative research proposed by Maxwell, J. A. [241].

From the main goal of the thesis “Building a design methodology for sustainable IoT systems”, one derives the main question of the qualitative research that helps to achieve this goal: “what is the current design workflow of IoT designers”. Both aspects build the conceptual framework that contains key finding in the literature that partially answer this question (theoretical framework composed of the proposed design workflows seen in [10] and [107-108]).

The relevant aspects found in the conceptual framework are:

- Design workflow of sustainable WSN (according to Bonvoisin, J. et al [10]) would consist on defining the design goal on the basis of impact targets (step 1), designing the service which will be optimized by the WSN (step 2), estimating the impact of the equipment, infrastructure and application domain (step 3); redesigning the equipment, infrastructure or application domain (step 4), and restart the workflow if the established goal is not achieved (step 5).
- Design workflow of sensor devices and mechatronics (according to Heinis, T. et al [108]) would consist on analyzing the object that will benefit from an IoT application (step 1), analyzing the data operational stages of devices (step 2), and finally analyzing the added value of the IoT application according to types of users (step 3).
- Design workflow of IoT systems (according to Chakravarthi, V. S. [107]) would consist on analyzing the user requirements by specific questions (step 1), selecting the suitable technology according these requirements (step 2), selecting electronic components within these technologies (step 3), and software/hardware prototyping of devices (step 4).

From this, and by reconsidering the main question of the study, one determines the instruments for conducting the qualitative research, which consists of semi structured surveys oriented to acknowledge and understand the current design workflow of designers in 5 steps, assuming that that number of steps would cover sufficiently the design process from the analysis of the object, added value and customer requirements, to the development and redesign of IoT prototypes.

The construction of these surveys depends on three main sequential aspects: (1) identification of typical customer requirements and fundamental design challenges, (2) identification of representative applications including these user requirements and design challenges and (3) creation of fictive “IoT projects” based on these representative applications (case studies). The customer requirements and the design challenges identified in an exhaustive survey conducted by Asghari, P. et al. [242] were summarized here in service availability, readiness, energy consumption, cost and reliability. Because finding all these aspects in only one kind of application is impossible, the aforementioned authors propose a series of application types with a high probability of containing most of these aspects (table below).

Application types	Availability	Readiness	Energy	Cost	Reliability
Health care		✓	✓	✓	
Monitoring environment		✓		✓	✓
Smart cities		✓	✓		
Commercial applications	✓	✓		✓	

In this manner, 4 fictitious “IoT projects” around the themes of health care, monitoring environment, Smart cities and commercial applications were created. These projects were integrated into semi-structured surveys (shown below), which were distributed later among all members of design teams. The idea is that the designers describe the typical design flow that they would adopt in the context of these fictional projects (which they were presented as they would be presented to designers in reality).

a.1. Designed survey for the IoT application “Health care” (inspired by the case study presented by Jimenez, F., & Torres, R. [243] and Ding, Y. et al. [244]).

<p>Section-1-Objective¶ Identifying the cognitive process for conventional design of IoT systems.¶</p>	<p>Section-2-Instructions¶ a.→ The survey was designed on the basis of a client request (“business idea” or “IoT application” format). Read carefully section 3 and answer question(s) in section 4 by only using the provided region in subsections 4.a, 4.b, 4.c, 4.d, 4.e.¶ b.→ Length of the survey: 10—20 mins.¶</p>
<p>Section-3-IoT project «Hospital-at-home»¶ ¶ Client request: «...we want to commercialize an IoT system that allow efficient remote-monitoring and high dynamic medical care services for elder patients...».¶ ¶ Context: The system will be installed at patients’ homes and it must be operated and maintained by hospitals in mutual partnership. Consequently, its deployment and maintenance must be easy and low-cost. (The system must cover total patients-homes’ areas and it must permit the addition of new elder patients).¶ ¶ The system must be highly autonomous and it must not interfere with the patients’ activities or lifestyle.¶ ¶ Possible use case: Vital signals of a patient dramatically drop. The system detects this anomaly, send alerts and mobilize medical resources (Doctors, nurses or even ambulance services).¶ ¶ Related ideas or similar products:¶ https://www.youtube.com/watch?v=40oQFXGhfbQ¶ ¶ ¶</p>	<p>Section-4.a-Step 1: Cliquez ou appuyez ici pour entrer du texte.¶</p>
<p>Section 4. How can you design a rapid IoT prototype ready for demonstration in 5 steps?¶</p>	<p>Section-4.b-Step 2: Cliquez ou appuyez ici pour entrer du texte.¶</p>
	<p>Section-4.c-Step 3: Cliquez ou appuyez ici pour entrer du texte.¶</p>
	<p>Section-4.d-Step 4: Cliquez ou appuyez ici pour entrer du texte.¶</p>
	<p>Section-4.e-Step 5: Cliquez ou appuyez ici pour entrer du texte.¶</p>
	<p>Section-5-Participant information¶ a. → Name: Cliquez ou appuyez ici pour entrer du texte.¶ b. → Surname: Cliquez ou appuyez ici pour entrer du texte.¶ c. → Main fonction(s): Cliquez ou appuyez ici pour entrer du texte.¶ d. → Department: Cliquez ou appuyez ici pour entrer du texte.¶ e. → Date: Cliquez ou appuyez ici pour entrer du texte.¶</p>


a.2. Designed survey for the IoT application “Monitoring environment” (inspired by the case study presented by Li, H. et al. [245]).

<p>Section-1.Objective¶ Identifying-the-cognitive-process-for-conventional-design-of-IoT-systems.¶</p>	<p>Section-2.Instructions¶ c.→ The survey was designed on the basis of a client request (“business-idea” or “IoT-application”-format). Read-carefully-section-3-and-answer-question(s)-in-section-4-by-only-using-the-provided-region-in-subsections-4.a,-4.b,-4.c,-4.d,-4.e.¶ d.→ Length-of-the-survey:10–20-mins.¶</p>
<p>Section-3.IoT-project-«Smart-Poultry-farm»¶ ¶ Client request: «...we want to commercialize a high reliable, dynamic-monitoring-system-for-poultry-farms-that-avoid-chicken-diseases.The-system-must-be-compatible-with-modern-controlled-environment-systems-and-low-cost...».¶ ¶ Context:critical-indicators-for-chicken-health-are-temperature,-humidity,-CO₂-and-NH₃-concentrations.Any small variation on these parameters must be noticed-and-fixed-immediately.¶ ¶ Possible-use-case:a-little-variation-of-NH₃-concentrations-occurs-in-a-henhouse.The-system-detects-this-anomaly-and-automatically-alert-and-trigger-the-ventilation-system”-¶ ¶ Related-ideas-or-similar-products:¶ https://www.youtube.com/watch?v=-39rK06owl¶ (see-the-«Smart-poultry-farm-section»-from-4'46"-to-6'12")¶ ¶ ¶ ¶</p>	<p>Section-4.a.Step-1:Cliquez-ou-appuyez-ici-pour-entrer-du-texte.¶</p>
<p>Section-4.How-can-you-design-a-rapid-IoT-prototype-ready-for-demonstration-in-5-steps?¶</p>	<p>Section-4.b.Step-2:Cliquez-ou-appuyez-ici-pour-entrer-du-texte.¶</p>
	<p>Section-4.c.Step-3:Cliquez-ou-appuyez-ici-pour-entrer-du-texte.¶</p>
	<p>Section-4.d.Step-4:Cliquez-ou-appuyez-ici-pour-entrer-du-texte.¶</p>
	<p>Section-4.e.Step-5:Cliquez-ou-appuyez-ici-pour-entrer-du-texte.¶</p>
	<p>Section-5.Participant-information¶ f.→ Name:Cliquez-ou-appuyez-ici-pour-entrer-du-texte.¶ g.→ Surname:Cliquez-ou-appuyez-ici-pour-entrer-du-texte.¶ h.→ Main-fonction(s):Cliquez-ou-appuyez-ici-pour-entrer-du-texte.¶ i.→ Department:Cliquez-ou-appuyez-ici-pour-entrer-du-texte.¶ j.→ Date:Cliquez-ou-appuyez-ici-pour-entrer-du-texte.¶</p>

a.3. Designed survey for the IoT application “Smart cities” (inspired by the case study presented by Bonvoisin, J. et al. [10]).

<p>Section-1.-Objective¶ Identifying the cognitive process for conventional design of IoT systems. ¶</p>	<p>Section-2.-Instructions¶ e. → The survey was designed on the basis of a client request (“business idea” or “IoT application” format). Read carefully section 3 and answer question(s) in section 4 by only using the provided region in subsections 4.a, 4.b, 4.c, 4.d, 4.e. ¶ f. → Length of the survey: 10 → 20 mins. ¶</p>
<p>Section-3.-IoT project « Smart waste collection system » ¶ ¶ Client request: “...we want to deploy a dynamic system that manage the collecting circuit of our trash trucks based on the waste containers’ level deployed in our community”. ¶ ¶ Context: “...our waste containers are usually exposed to hostile environments (humidity, vandalism, etc.)...” ¶ ¶ “...Also, we have many waste containers. Our community is one of the most populated in the country; two waste containers per citizen are deployed in dense areas while one container per citizen is planned for the other areas. So any solution involved containers must last as long as possible”. ¶ ¶ “...Due to the high density of our population, waste containers tend to get full very quickly. The system must be dynamic enough to allow the efficient deployment of our trash trucks fleet...” ¶ ¶ Related ideas or similar products: ¶ https://www.youtube.com/watch?v=bazmkSKD5fk ¶ ¶ ¶</p>	<p>Section-4.a.-Step-1: Cliquez ou appuyez ici pour entrer du texte. ¶</p>
<p>Section-4.-How can you design a rapid IoT prototype ready for demonstration in 5 steps? ¶ ¶</p>	<p>Section-4.b.-Step-2: Cliquez ou appuyez ici pour entrer du texte. ¶</p>
	<p>Section-4.c.-Step-3: Cliquez ou appuyez ici pour entrer du texte. ¶</p>
	<p>Section-4.d.-Step-4: Cliquez ou appuyez ici pour entrer du texte. ¶</p>
	<p>Section-4.e.-Step-5: Cliquez ou appuyez ici pour entrer du texte. ¶</p>
	<p>Section-5.-Participant information¶ k. → Name: Cliquez ou appuyez ici pour entrer du texte. ¶ l. → Surname: Cliquez ou appuyez ici pour entrer du texte. ¶ m. → Main fonction(s): Cliquez ou appuyez ici pour entrer du texte. ¶ n. → Department: Cliquez ou appuyez ici pour entrer du texte. ¶ o. → Date: Cliquez ou appuyez ici pour entrer du texte. ¶</p>

a.4. Designed survey for the IoT application “Commercial applications” (inspired by the case study presented by Ishida, K. [50]).

<p>Section-1-Objective¶ Identifying the cognitive process for conventional design of IoT systems.¶</p>	<p>Section-2-Instructions¶ g.→ The survey was designed on the basis of a client request (“business idea” or “IoT application” format). Read carefully section 3 and answer question(s) in section 4 by only using the provided region in subsections 4.a, 4.b, 4.c, 4.d, 4.e.¶ h.→ Length of the survey: 10→20 mins.¶</p>
<p>Section-3-Business-idea-«Smart-Skateboarding-coach»¶ ¶ Client request: «...we want to commercialize an affordable, dynamic smart coaching system to facilitate learning skateboarding...».¶ ¶ Context: Skateboarding is a very complex discipline in which physics of human body and skateboard interact. (See the visual description of an «ollie» below (basic technique)).¶ ¶  <p>¶ Beginners know the principles of techniques and they can figure out movements by following youtube tutorials, but they are unable to track their progress...¶ ¶ Also, skateparks may not provide internet access and athletes may practice the discipline in isolated areas. The system must be ready to work offline when internet service is limited.¶ ¶ Possible use case: a skater tries an «ollie» and the system immediately compares his/her performance based on optimal parameters such as board inclination or feet position.¶</p> </p>	<p>Section-4.a-Step-1: Cliquez ou appuyez ici pour entrer du texte.¶</p>
<p>Section 4- How can you design a rapid IoT prototype ready for demonstration in 5 steps?¶</p>	<p>Section-4.b-Step-2: Cliquez ou appuyez ici pour entrer du texte.¶</p>
	<p>Section-4.c-Step-3: Cliquez ou appuyez ici pour entrer du texte.¶</p>
	<p>Section-4.d-Step-4: Cliquez ou appuyez ici pour entrer du texte.¶</p>
	<p>Section-4.e-Step-5: Cliquez ou appuyez ici pour entrer du texte.¶</p>
	<p>Section-5-Participant-information¶ p.→ Name: Cliquez ou appuyez ici pour entrer du texte.¶ q.→ Surname: Cliquez ou appuyez ici pour entrer du texte.¶ r.→ Main fonction(s): Cliquez ou appuyez ici pour entrer du texte.¶ s.→ Department: Cliquez ou appuyez ici pour entrer du texte.¶ t.→ Date: Cliquez ou appuyez ici pour entrer du texte.¶</p>

Finally, the replies of surveys were summarize in a manner to give an answer to the main question of the study (conclusions of the qualitative study, available in the section 1 of chapter 4). This is later validated by observing the design workflow adopted for developing the case study “Smart monitoring” of this thesis (section 2 of chapter 5). Unfortunately, only 2 kinds of the 4 IoT projects were considered by designers (Health care and commercial IoT)).

b. Second part: current knowledge of eco-design, attempts to integrate ecological aspects, and expectations of a design methodology for sustainable IoT systems

To know the current knowledge of IoT designers about eco-design, their attempts to integrate it into their projects, and their expectations about a design methodology, the second part of this qualitative research use an open survey model described below.

<p>Section-1.-Objective¶</p> <p>Identifying IoT designers’ knowledge, needs, expectations and main difficulties in terms of eco-design.¶</p>	<p>Section-2.-Instructions¶</p> <p>a. → Read carefully questions in section 3 and give your answers in section 4.¶</p> <p>b. → Length of the survey: 10—15 mins.¶</p>
<p>Section-3.-Open-Questions-¶</p> <p>a. → What is your knowledge of eco-design and/or eco-design strategies?¶</p> <p>b. → Did you tried to integrate an eco-design or sustainability analysis in your projects? If so, explain what were your initiatives and the main barriers that you faced; if not, pass to question c.¶</p> <p>c. → What do you expect from an eco-design tool and what would be the main barriers for its implementation in your department?¶</p>	
<p>Section-4.-Give-your-answer¶</p> <p>a. → Cliquez-ou-appuyez-ici-pour-entrer-du-texte.¶ ¶</p> <p>b. → Cliquez-ou-appuyez-ici-pour-entrer-du-texte.¶ ¶</p> <p>c. → Cliquez-ou-appuyez-ici-pour-entrer-du-texte.¶</p>	
<p>Section-5.-Participant-information¶</p> <p>a. → Name: Cliquez-ou-appuyez-ici-pour-entrer-du-texte.¶</p> <p>b. → Surname: Cliquez-ou-appuyez-ici-pour-entrer-du-texte.¶</p> <p>c. → Main function(s): Cliquez-ou-appuyez-ici-pour-entrer-du-texte.¶</p> <p>d. → Department: Cliquez-ou-appuyez-ici-pour-entrer-du-texte.¶</p> <p>e. → Date: Cliquez-ou-appuyez-ici-pour-entrer-du-texte.¶</p>	

References

- [1] James, M., Chui, M., Bisson, P., Woetzel, J., Dobbs, R., Bughin, J., & Aharon, D. (2015). The Internet of Things: Mapping the value beyond the hype. McKinsey Global Institute, 3.
- [2] Congressional Research Service of the American United States. 2020. The Internet of Things (IoT): An Overview. Updated report available on: <https://crsreports.congress.gov/product/pdf/IF/IF11239>. (Accessed on 06.04.2022).
- [3] Vidal, O. (2018). Ressources minérales, progrès technologique et croissance. *Temporalités. Revue de sciences sociales et humaines*, (28).
- [4] Marquet, K., Combaz, J., & Berthoud, F. (2019). Introduction aux impacts environnementaux du numérique.
- [5] Sinaeepourfard, A., Garcia, J., Masip-Bruin, X., Marín-Tordera, E., Cirera, J., Grau, G., & Casaus, F. (2016, June). Estimating Smart City sensors data generation. In 2016 Mediterranean Ad Hoc Networking Workshop (Med-Hoc-Net) (pp. 1-8). IEEE.
- [6] Belkhir, L., & Elmeligi, A. (2018). Assessing ICT global emissions footprint: Trends to 2040 & recommendations. *Journal of cleaner production*, 177, 448-463.
- [7] G. Lan, S. Khalifa, M. Hassan, and W. Hu, "Estimating calorie expenditure from output voltage of piezoelectric energy harvester— An experimental feasibility study," in Proc. 10th EAI Int. Conf. Body Area Netw., 2015, pp. 179–185.
- [8] Das, S., & Mao, E. (2020). The global energy footprint of information and communication technology electronics in connected Internet-of-Things devices. *Sustainable Energy, Grids and Networks*, 24, 100408.
- [9] Hilty, L. M., Aebischer, B., & Rizzoli, A. E. (2014). Modeling and evaluating the sustainability of smart solutions.
- [10] Bonvoisin, J., Lelah, A., Mathieux, F., & Brissaud, D. (2014). An integrated method for environmental assessment and ecodesign of ICT-based optimization services. *Journal of cleaner production*, 68, 144-154.
- [11] Malmodin, J., Lundén, D., Moberg, Å., Andersson, G., & Nilsson, M. (2014). Life cycle assessment of ICT: Carbon footprint and operational electricity use from the operator, national, and subscriber perspective in Sweden. *Journal of Industrial Ecology*, 18(6), 829-845.
- [12] Aslan, J., Mayers, K., Koomey, J. G., & France, C. (2018). Electricity intensity of Internet data transmission: Untangling the estimates. *Journal of Industrial Ecology*, 22(4), 785-798.
- [15] Köhler, A., & Erdmann, L. (2004). Expected environmental impacts of pervasive computing. *Human and Ecological Risk Assessment*, 10(5), 831-852.
- [16] Gossart, C. (2015). Rebound effects and ICT: a review of the literature. *ICT innovations for sustainability*, 435-448.
- [17] Zhu, C., Leung, V. C., Shu, L., & Ngai, E. C. H. (2015). Green internet of things for smart world. *IEEE access*, 3, 2151-2162.
- [18] Shaikh, F. K., Zeadally, S., & Exposito, E. (2015). Enabling technologies for green internet of things. *IEEE Systems Journal*, 11(2), 983-994.
- [19] Callebaut, G., Leenders, G., Van Mulders, J., Ottoy, G., De Strycker, L., & Van der Perre, L. (2021). The Art of Designing Remote IoT Devices—Technologies and Strategies for a Long Battery Life. *Sensors*, 21(3), 913.
- [20] Emilio, M. D. P. (2017). *Microelectronic circuit design for energy harvesting systems*. Berlin: Springer.
- [21] Umesh, S., & Mittal, S. (2021). A survey of techniques for intermittent computing. *Journal of Systems Architecture*, 112, 101859.
- [22] Wouters, E. H. (2019). *Secure Intermittent Computing*.
- [23] Ma, D., Lan, G., Hassan, M., Hu, W., & Das, S. K. (2019). Sensing, computing, and communications for energy harvesting IoTs: A survey. *IEEE Communications Surveys & Tutorials*, 22(2), 1222-1250.
- [24] Daulby, T., Savanth, A., Weddell, A. S., & Merrett, G. V. (2020, November). Comparing NVM Technologies through the Lens of Intermittent Computation. In *Proceedings of the 8th International Workshop on Energy Harvesting and Energy-Neutral Sensing Systems* (pp. 77-78).

- [26] Wagner, E., Böhme, C., Benecke, S., Nissen, N. N., & Lang, K. D. (2017, June). Advanced packaging for wireless sensor nodes in cyber-physical systems-impacts of multifunctionality and miniaturization on the environment. In 2017 IEEE International Conference on Prognostics and Health Management (ICPHM) (pp. 173-178). IEEE.
- [28] M. Proske, D. Sanchez, C. Clemm, S. Baur (2020). Life Cycle Assessment Of The Fairphone 3. Available on https://www.fairphone.com/wp-content/uploads/2020/07/Fairphone_3_LCA.pdf. (Accessed on 11.07.2022)
- [30] Samie, F., Bauer, L., & Henkel, J. (2016, October). IoT technologies for embedded computing: A survey. In 2016 International Conference on Hardware/Software Codesign and System Synthesis (CODES+ ISSS) (pp. 1-10). IEEE.
- [31] Taylor, H. R. (1997). Data acquisition for sensor systems (Vol. 5). Springer Science & Business Media.
- [32] POTTER, D., & Eren, H. (2011). Data Acquisition Fundamentals. In Instrument Engineers' Handbook: Process Software and Digital Networks (pp. 330-341). CRC Press (Taylor and Francis Group).
- [33] Tan, L., & Jiang, J. (2018). Digital signal processing: fundamentals and applications. Academic Press.
- [34] Lau, J. H. (2021). Advanced Packaging. In Semiconductor Advanced Packaging (pp. 1-25). Springer, Singapore.
- [35] Nowka, K. J., Carpenter, G. D., MacDonald, E. W., Ngo, H. C., Brock, B. C., Ishii, K. I., ... & Burns, J. L. (2002). A 32-bit PowerPC system-on-a-chip with support for dynamic voltage scaling and dynamic frequency scaling. IEEE Journal of Solid-State Circuits, 37(11), 1441-1447.
- [36] Prince, B., & Prince, D. (2018). Memories for the Intelligent Internet of Things. John Wiley & Sons.
- [37] Elkhodr, M., Shahrestani, S., & Cheung, H. (2016). Wireless enabling technologies for the Internet of things. In Innovative Research and Applications in Next-Generation High Performance Computing (pp. 368-396). IGI Global.
- [38] Adegbija, T., Lysecky, R., & Kumar, V. V. (2019, May). Right-provisioned IoT edge computing: An overview. In Proceedings of the 2019 on Great Lakes Symposium on VLSI (pp. 531-536).
- [39] Adegbija, T., Rogacs, A., Patel, C., & Gordon-Ross, A. (2015, November). Enabling right-provisioned microprocessor architectures for the internet of things. In ASME International Mechanical Engineering Congress and Exposition (Vol. 57571, p. V014T06A001). American Society of Mechanical Engineers.
- [40] Understanding bitrates in video files. Online: help.encoding.com/knowledge-base/article/understanding-bitrates-in-video-files, 2013.
- [41] Siantikos, G., Sgouropoulos, D., Giannakopoulos, T., & Spyrou, E. (2015, September). Fusing multiple audio sensors for acoustic event detection. In 2015 9th International Symposium on Image and Signal Processing and Analysis (ISPA) (pp. 265-269). IEEE.
- [42] Adegbija, T., Rogacs, A., Patel, C., & Gordon-Ross, A. (2017). Microprocessor optimizations for the internet of things: A survey. IEEE Transactions on Computer-Aided Design of Integrated Circuits and Systems, 37(1), 7-20.
- [43] Kyriazopoulou, C. (2015, May). Smart city technologies and architectures: A literature review. In 2015 International Conference on Smart Cities and Green ICT Systems (SMARTGREENS) (pp. 1-12). IEEE.
- [44] Sentilo website. Available on: <http://www.sentilo.io/wordpress/>. (Accessed on 11.07.2022).
- [45] Krishnamachari, L., Estrin, D., & Wicker, S. (2002, July). The impact of data aggregation in wireless sensor networks. In Proceedings 22nd international conference on distributed computing systems workshops (pp. 575-578). IEEE.
- [46] Jin Cui. Data aggregation in wireless sensor networks. Networking and Internet Architecture [cs.NI]. Université de Lyon, 2016. English. NNT: 2016LYSEI065. tel-01688566
- [47] Chippa, V. K., Venkataramani, S., Chakradhar, S. T., Roy, K., & Raghunathan, A. (2013, November). Approximate computing: An integrated hardware approach. In 2013 Asilomar conference on signals, systems and computers (pp. 111-117). IEEE.
- [49] Zins, C. (2007). Conceptual approaches for defining data, information, and knowledge. Journal of the American society for information science and technology, 58(4), 479-493.

- [50] Ishida, K. (2019, November). IoT application in sports to support skill acquisition and improvement. In 2019 IEEE 12th Conference on Service-Oriented Computing and Applications (SOCA) (pp. 184-189). IEEE.
- [51] Lelah, A., Mathieux, F., & Brissaud, D. (2011). Contributions to eco-design of machine-to-machine product service systems: the example of waste glass collection. *Journal of Cleaner Production*, 19(9-10), 1033-1044.
- [54] Chen, K. Y., & Sun, M. (1997). Improving energy expenditure estimation by using a triaxial accelerometer. *Journal of applied Physiology*, 83(6), 2112-2122.
- [55] STMicroelectronics. Sustainability Report 2013. Available on: https://www.st.com/content/st_com/en/about/st_approach_to_sustainability/sustainability-reports.html. (Accessed on 11.07.2022).
- [56] ISO 14040: Environmental Management – Life Cycle Assessment – Principles and Framework
- [57] Guinée, J. B., & Lindeijer, E. (Eds.). (2002). Handbook on life cycle assessment: operational guide to the ISO standards (Vol. 7). Springer Science & Business Media.
- [58] Forster, P., Ramaswamy, V., Artaxo, P., Berntsen, T., Betts, R., Fahey, D. W., ... & Van Dorland, R. (2007). Changes in atmospheric constituents and in radiative forcing. Chapter 2. In *Climate change 2007. The physical science basis*.
- [59] Myhre, G., D. Shindell, F.-M. Bréon, W. Collins, J. Fuglestedt, J. Huang, D. Koch, J.-F. Lamarque, D. Lee, B. Mendoza, T. Nakajima, A. Robock, G. Stephens, T. Takemura and H. Zhang, 2013: Anthropogenic and Natural Radiative Forcing. In: *Climate Change 2013: The Physical Science Basis. Contribution of Working Group I to the Fifth Assessment Report of the Intergovernmental Panel on Climate Change* [Stocker, T.F., D. Qin, G.-K. Plattner, M. Tignor, S.K. Allen, J. Boschung, A. Nauels, Y. Xia, V. Bex and P.M. Midgley (eds.)]. Cambridge University Press, Cambridge, United Kingdom and New York, NY, USA.
- [60] Köhler, A. R., Lauterbach, C., Steinhage, A., Buitter, J. C., & Techmer, A. (2012, September). Life cycle assessment and eco-design of a textile-based large-area sensor system. In *2012 Electronics Goes Green 2012+* (pp. 1-8). IEEE.
- [61] Bonvoisin, J., Lelah, A., Mathieux, F., & Brissaud, D. (2012). An environmental assessment method for wireless sensor networks. *Journal of Cleaner Production*, 33, 145-154.
- [62] Malmodin, J., Moberg, Å., Lundén, D., Finnveden, G., & Lövehagen, N. (2010). Greenhouse gas emissions and operational electricity use in the ICT and entertainment & media sectors. *Journal of Industrial Ecology*, 14(5), 770-790.
- [63] Engström, R., Wadeskog, A., & Finnveden, G. (2007). Environmental assessment of Swedish agriculture. *Ecological Economics*, 60(3), 550-563.
- [64] Seppälä, J., Koskela, S., Melanen, M., & Palperi, M. (2002). The Finnish metals industry and the environment. *Resources, Conservation and Recycling*, 35(1-2), 61-76.
- [65] Taylor, C., & Koomey, J. (2008). Estimating energy use and greenhouse gas emissions of internet advertising. *Network*.
- [66] Emmenegger, M. F., Frischknecht, R., Stutz, M., Guggisberg, M., Witschi, R., & Otto, T. (2006). Life cycle assessment of the mobile communication system UMTS: towards eco-efficient systems (12 pp). *The International Journal of Life Cycle Assessment*, 11(4), 265-276.
- [67] Pihkola, H., Hongisto, M., Apilo, O., & Lasanen, M. (2018). Evaluating the energy consumption of mobile data transfer—from technology development to consumer behaviour and life cycle thinking. *Sustainability*, 10(7), 2494.
- [68] Malmodin, J., Lundén, D., Nilsson, M., & Andersson, G. (2012, September). LCA of data transmission and IP core networks. In *2012 Electronics Goes Green 2012+* (pp. 1-6). IEEE.
- [69] Ingemarsdotter, E., Diener, D., Andersson, S., Jonasson, C., Mellquist, A. C., Nyström, T., ... & Balkenende, R. (2021). Quantifying the Net Environmental Impact of Using IoT to Support Circular Strategies—The Case of Heavy-Duty Truck Tires in Sweden. *Circular Economy and Sustainability*, 1-38.
- [70] Baliga BJ, Ayre RWA, Hinton K, Tucker RS (2010) Green cloud computing: balancing energy in processing, storage and transport. *Proc IEEE* 99:149–167. <https://doi.org/10.1109/JPROC.2010.2060451>.
- [71] Dekoninck, E., & Barbaccia, F. (2019, July). Streamlined assessment to assist in the design of Internet-of-Things (IoT) Enabled Products: a case study of the smart fridge. In *Proceedings of the Design Society: International Conference on Engineering Design* (Vol. 1, No. 1, pp. 3721-3730). Cambridge University Press.

- [72] Van Dam, S. S., Bakker, C. A., & Buiter, J. C. (2013). Do home energy management systems make sense? Assessing their overall lifecycle impact. *Energy Policy*, 63, 398-407.
- [73] Dubberley, M., Agogino, A. M., & Horvath, A. (2004, May). Life-cycle assessment of an intelligent lighting system using a distributed wireless mote network. In *IEEE International Symposium on Electronics and the Environment*, 2004. Conference Record. 2004 (pp. 122-127). IEEE.
- [74] Pirson, T., & Bol, D. (2021). Assessing the embodied carbon footprint of IoT edge devices with a bottom-up life-cycle approach. *Journal of Cleaner Production*, 322, 128966.
- [75] Glogic, E., Futsch, R., Thenot, V., Iglesias, A., Joyard-Pitiot, B., Depres, G., ... & Sonnemann, G. (2021). Development of eco-efficient smart electronics for anticounterfeiting and shock detection based on printable inks. *ACS Sustainable Chemistry & Engineering*, 9(35), 11691-11704.
- [76] Van der Velden, N. M., Kuusk, K., & Köhler, A. R. (2015). Life cycle assessment and eco-design of smart textiles: The importance of material selection demonstrated through e-textile product redesign. *Materials & Design*, 84, 313-324.
- [77] Le Brun, G., & Raskin, J. P. (2020). Material and manufacturing process selection for electronics eco-design: Case study on paper-based water quality sensors. *Procedia CIRP*, 90, 344-349.
- [78] Mathieux, F., Froelich, D., & Moszkowicz, P. (2008). ReSICLED: a new recovery-conscious design method for complex products based on a multicriteria assessment of the recoverability. *Journal of Cleaner Production*, 16(3), 277-298.
- [79] Finnveden, G., Hauschild, M. Z., Ekvall, T., Guinée, J., Heijungs, R., Hellweg, S., ... & Suh, S. (2009). Recent developments in life cycle assessment. *Journal of environmental management*, 91(1), 1-21.
- [80] ISO/TR 14062 (2002) Environmental management—integrating environmental aspects into product design and development.
- [81] ISO, I. (2006). ISO-14040 Environmental management—life cycle assessment—principles and framework: International Organization for Standardization.
- [82] Sector, I. T. S. (2012). Recommendation ITU-T Y. 2060: Overview of the Internet of things. Series Y: Global information infrastructure, internet protocol aspects and next-generation networks-Frameworks and functional architecture models.
- [83] SECTOR, S., & ITU, O. (2014). ITU-Tfg M2M.
- [84] Kafle, V. P., Fukushima, Y., & Harai, H. (2016). Internet of things standardization in ITU and prospective networking technologies. *IEEE Communications Magazine*, 54(9), 43-49.
- [85] "ITU-T Recommendation Y.4100", 2014-Common requirements of the Internet of Things.
- [86] Recommendation Y.4208 (01/20): Internet of Things Requirements for Support of Edge Computing. International Telecommunication Union.
- [87] Recommendation ITU-T Y.2067 (2014), "Common Requirements and Capabilities of a Gateway for Internet of Things Applications."
- [88] Recommendation ITU-T L.1370 (2020), "Sustainable and intelligent building services."
- [89] Gurova, O., Merritt, T. R., Papachristos, E., & Vaajakari, J. (2020). Sustainable Solutions for Wearable Technologies: Mapping the Product Development Life Cycle. *Sustainability*, 12(20), 8444.
- [90] Telenko, C.; Seepersad, C.C.; Webber, M.E. A Compilation of Design for Environment Principles and Guidelines. In *Proceedings of the International Design Engineering Technical Conferences and Computers and Information in Engineering Conference (IDETC/CIE2008)*, Brooklyn, NY, USA, 3–6 August 2008; pp. 289–301.
- [91] Gross, R.A.; Kalra, B. Biodegradable polymers for the environment. *Science* 2002, 297, 803–807.
- [92] Hunt, C.P.; Wickham, M.; Pittson, R.; Lewison, J. Reusable, Unzippable, Sustainable Electronics (ReUse) Interconnect System for the Circular Economy. Report for NPL, MAT 75. 2 February 2018.
- [93] EU Directive 2002/95/EC of the European Parliament and of the Council of 27 January 2003 on the restriction of the use of certain hazardous substances in electrical and electronic equipment. *O. J. Eur. Union* 2003, 13, 19–23.
- [94] US EPA. Identifying Greener Electronics. Overviews and Factsheets. Available online: <https://www.epa.gov/greenerproducts/identifying-greener-electronics>. (Accessed on 11.07.2022).

- [95] Bar-Cohen, A.; Iyengar, M. Design and optimization of air-cooled heat sinks for sustainable development. *Ieee Trans. Compon. Packag. Technol.* 2002, 25, 584–591.
- [96] Protolabs. Injection Moulding, Rapid Prototyping, 3D Printing, CNC. Available online: <https://www.protolabs.co.uk/>. (Accessed on 11.07.2022).
- [97] Graedel, T.E.; Harper, E.M.; Nassar, N.T.; Reck, B.K. On the materials basis of modern society. *Proc. Natl. Acad. Sci. USA* 2015, 112, 6295–6300.
- [98] Nivethitha, V., & Aghila, G. (2019). Survey on architectural design principles for edge oriented computing systems. *Journal of Computational and Theoretical Nanoscience*, 16(4), 1617-1624.
- [99] Arshad, R., Zahoor, S., Shah, M. A., Wahid, A., & Yu, H. (2017). Green IoT: An investigation on energy saving practices for 2020 and beyond. *IEEE Access*, 5, 15667-15681.
- [100] EnergyStar. The Simple Choice for Energy Efficiency. Available online: <https://www.energystar.gov/>. (Accessed on 11.07.2022).
- [101] Green Electronics Council. EPEAT for Manufacturers. Available online: <https://greenelectronicscouncil.org/epeat/manufacturers/>.
- [102] Pahl, C., Jamshidi, P., & Zimmermann, O. (2018). Architectural principles for cloud software. *ACM Transactions on Internet Technology (TOIT)*, 18(2), 1-23.
- [103] C. Karakus, A. C. Gurbuz, and B. Tavli, "Analysis of energy efficiency of compressive sensing in wireless sensor networks," *IEEE Sensors J.*, vol. 13, no. 5, pp. 1999-2008, May 2013.
- [104] Boothroyd, G.; Alting, L. Design for assembly and disassembly. *CIRP Ann. Manuf. Technol.* 1992, 41, 625–636.
- [105] Platcheck, E.R.; Schaeffer, L.; Kindlein, W.; Cândido, L.H.A. Methodology of ecodesign for the development of more sustainable electro-electronic equipments. *J. Clean. Prod.* 2008, 16, 75–86.
- [106] Cisco Systems, Inc. (2004). *Internetworking Technologies Handbook*. Cisco Press.
- [107] Chakravarthi, V. S. (2021). Internet of Things (IoT) Design Methodology. In *Internet of Things and M2M Communication Technologies* (pp. 19-46). Springer, Cham.
- [108] Heinis, T., Gomes Martinho, C., & Meboldt, M. (2017). Fundamental challenges in developing Internet of Things applications for engineers and product designers. In *DS 87-5 Proceedings of the 21st International Conference on Engineering Design (ICED 17) Vol 5: Design for X, Design to X*, Vancouver, Canada, 21-25.08. 2017 (pp. 279-288).
- [109] Huang, J., Meng, Y., Gong, X., Liu, Y., & Duan, Q. (2014). A novel deployment scheme for green internet of things. *IEEE Internet of Things Journal*, 1(2), 196-205.
- [110] Middendorf, A., Deyter, S., Gausemeier, J., Nissen, N. F., & Reichl, H. (2009, May). Integration of reliability and environmental aspects in early design stages of mechatronics. In *2009 IEEE International Symposium on Sustainable Systems and Technology* (pp. 1-6). IEEE.
- [111] Middendorf, A.; Nissen, N.; Reichl, H. et al. , "EE-Toolbox – A modular assessment system for the environmental optimization of electronics" in *IEEE International Symposium on Electronics and the Environment*, San Francisco, USA, 2000.
- [112] Söderman, M. L., & André, H. (2019). Effects of circular measures on scarce metals in complex products—Case studies of electrical and electronic equipment. *Resources, Conservation and Recycling*, 151, 104464.
- [113] Li, J., Zeng, X., & Stevels, A. (2015). Ecodesign in consumer electronics: Past, present, and future. *Critical Reviews in Environmental Science and Technology*, 45(8), 840-860.
- [114] Kasulaitis, B. V., Babbitt, C. W., Kahhat, R., Williams, E., & Ryen, E. G. (2015). Evolving materials, attributes, and functionality in consumer electronics: Case study of laptop computers. *Resources, conservation and recycling*, 100, 1-10.
- [115] Andrae, A. S., & Andersen, O. (2010). Life cycle assessments of consumer electronics—are they consistent?. *The International Journal of Life Cycle Assessment*, 15(8), 827-836.
- [116] Andrae, A. S., & Andersen, O. (2011). Life cycle assessment of integrated circuit packaging technologies. *The International Journal of Life Cycle Assessment*, 16(3), 258-267.

- [117] Kuo, C. H., Hu, A. H., Hung, L. H., Yang, K. T., & Wu, C. H. (2020). Life cycle impact assessment of semiconductor packaging technologies with emphasis on ball grid array. *Journal of Cleaner Production*, 276, 124301.
- [118] Würth elektronik (2018). HDI Design Guide. available on: https://www.wurth-elektronik.com/web/en/index.php/show/media/04_leiterplatte/2011_2/relaunch/produkte_5/microvia_hdi/180924_W_E_CBT_DesignGuide_HDI-12_EN_screen.pdf. (Accessed on 11.07.2022).
- [119] Bovea, M. D., Ibáñez-Forés, V., & Pérez-Belis, V. (2020). Repair vs. replacement: Selection of the best end-of-life scenario for small household electric and electronic equipment based on life cycle assessment. *Journal of environmental management*, 254, 109679.
- [120] Pini, M., Lolli, F., Balugani, E., Gamberini, R., Neri, P., Rimini, B., Ferrari, A.M., 2019. Preparation for reuse activity of waste electrical and electronic equipment: environmental performance, cost externality and job creation. *J. Clean. Prod.* 222, 77–89. <https://doi.org/10.1016/j.jclepro.2019.03.004>.
- [121] Lu, B., Song, X., Yang, J., Yang, D., 2017. Comparison on end-of-life strategies of WEEE in China based on LCA. *Front. Environ. Sci. Eng.* 11, 7. <https://doi.org/10.1007/s11783-017-0994-7>.
- [122] Sitek, J., Koscielski, M., Dawidowicz, P., Ciszewski, P., Khramova, M., Quang, D. N., & Martinez, S. (2017, September). Investigations of temperature resistance of memory BGA components during multi-reflow processes for Circular Economy applications. In 2017 21st European Microelectronics and Packaging Conference (EMPC) & Exhibition (pp. 1-7). IEEE.
- [123] IPC/JEDEC joint industry standard: J-STD-020D-01
- [124] Grossmann, G., & Zardini, C. (Eds.). (2011). *The ELFNET book on failure mechanisms, testing methods, and quality issues of lead-free solder interconnects*. Springer Science & Business Media.
- [125] Kang, J. S. (2020). Parametric study of warpage in PBGA packages. *The International Journal of Advanced Manufacturing Technology*, 107(9), 4213-4219.
- [126] Layiding, W., Dong, X., Peng, M., & Guanghong, D. (2005, May). Disassembling approaches and quality assurance of electronic components mounted on PCBs. In *Proceedings of the 2005 IEEE International Symposium on Electronics and the Environment*, 2005. (pp. 116-120). IEEE.
- [127] Chen, M., Wang, J., Chen, H., Ogunseitan, O. A., Zhang, M., Zang, H., & Hu, J. (2013). Electronic waste disassembly with industrial waste heat. *Environmental science & technology*, 47(21), 12409-12416.
- [128] Kaya, M. (2019). *Electronic waste and printed circuit board recycling technologies*. Springer.
- [129] Johnson, J., Harper, E. M., Lifset, R., & Graedel, T. E. (2007). Dining at the periodic table: Metals concentrations as they relate to recycling. *Environmental science & technology*, 41(5), 1759-1765.
- [130] Hagelüken, C. (2006). Recycling of electronic scrap at Umicore's integrated metals smelter and refinery. *Erzmetall*, 59(3), 152-161.
- [131] Bookhagen, B., Bastian, D., Buchholz, P., Faulstich, M., Opper, C., Irrgeher, J., ... & Koeberl, C. (2020). Metallic resources in smartphones. *Resources Policy*, 68, 101750.
- [132] Guinée, J. B., J. C. J. M. van den Bergh, J. Boelens, P. J. Fraanje, G. Huppes, P. P. A. A. H. Kandelaars, T. M. Lexmond, et al. 1999. Evaluation of risks of metal flows and accumulation in economy and environment. *Ecological Economics* 30: 47–65.
- [133] Graedel, T. E., Allwood, J., Birat, J. P., Buchert, M., Hagelüken, C., Reck, B. K., ... & Sonnemann, G. (2011). What do we know about metal recycling rates?. *Journal of Industrial Ecology*, 15(3), 355-366.
- [134] Lienig, J., & Bruemmer, H. (2017). *Fundamentals of electronic systems design* (p. 1). Cham: Springer International Publishing.
- [135] MIL-C-26655: Electronic Components - Capacitors Military Ordering Code.
- [136] AN5085 Application note. Cycling endurance and data retention of EEPROMs in ST25DVxxx products based on CMOS F8H process. Available on: https://www.st.com/resource/en/application_note/an5085-cycling-endurance-and-data-retention-of-eproms-in-products-of-the-st25dvi2c-series-based-on-the-cmos-f8h-process-stmicroelectronics.pdf. (Accessed on 26.03.2022).
- [137] Colin, A. (2018). *System Support for Intermittent Computing* (Doctoral dissertation, Carnegie Mellon University).

- [138] Balsamo, D., Weddell, A. S., Das, A., Arreola, A. R., Brunelli, D., Al-Hashimi, B. M., ... & Benini, L. (2016). Hibernus++: a self-calibrating and adaptive system for transiently-powered embedded devices. *IEEE Transactions on Computer-Aided Design of Integrated Circuits and Systems*, 35(12), 1968-1980.
- [139] Morin, E., Maman, M., Guizzetti, R., & Duda, A. (2017). Comparison of the device lifetime in wireless networks for the internet of things. *IEEE Access*, 5, 7097-7114.
- [140] Ashouri, M., Davidsson, P., Spalazzese, R., 2018. Cloud, edge, or both? Towards decision support for designing IoT applications. In: *Proceedings of the 2018 Fifth International Conference on Internet of Things: Systems, Management and Security*. IEEE, pp. 155–162.
- [141] Li, W., Santos, I., Delicato, F.C., Pires, P.F., Pirmez, L., Wei, W., Khan, S., 2017. System modelling and performance evaluation of a three-tier Cloud of Things. *Fut. Gen. Comput. Syst.* 70, 104–125.
- [142] Toczé, K., Nadjm-Tehrani, S., 2018. A taxonomy for management and optimization of multiple resources in edge computing. *Wirel. Commun. Mob. Comput.* 2018, 1–23.
- [143] Sarkar, S., Chatterjee, S., Misra, S., 2015. Assessment of the suitability of fog computing in the context of Internet of Things. *IEEE Trans. Cloud Comput.* 6 (1), 46–59.
- [144] Hischer, R., Classen, M., Lehmann, M., & Scharnhorst, W. (2007). Life cycle inventories of electric and electronic equipment: production, use and disposal. Final reportecoinvent Data v2. 0, 18.
- [145] Huisman, J. (2003). The QWERTY/EE concept, quantifying recyclability and eco-efficiency for end-of-life treatment of consumer electronic products.
- [146] Hischer, R., Classen, M., Lehmann, M., & Scharnhorst, W. (2007). Life cycle inventories of electric and electronic equipment: production, use and disposal. Part V: Disposal of Electric and Electronic Equipment (e-Waste). Final reportecoinvent Data v2. 0, 18.
- [147] Wellsandt, S., Nabati, E., Wuest, T., Hribernik, K.A., Thoben, K.D., 2016. A survey of product lifecycle models: towards complex products and service offers. *Int. J. Prod. Lifecycle Manag.* 9 (4), 353–390.
- [148] Bovea, M. D., & Pérez-Belis, V. (2012). A taxonomy of ecodesign tools for integrating environmental requirements into the product design process. *Journal of Cleaner Production*, 20(1), 61-71.
- [149] LR-FL. Flow meter module. Solem. Datasheet, notice and installation guide available on the attachments section of: <https://www.solem.fr/en/municipality-irrigation/16-lr-fl.html>. (Accessed on 23.03.2022).
- [150] IWM-PL3. Electronic pulse emitter module for multi jet meters with inductive interface. Bmeters. Datasheet, installation manual and declaration of conformity available on: <https://www.bmeters.com/en/products/iwm-pl3/>. (Accessed on 23.03.2022).
- [151] LR-MB. WiFi and LoRa gateway. Solem. Datasheet, notice and installation guide available on the attachment section of: <https://www.solem.fr/en/residential-watering/14-lr-mb-10.html>. (Accessed on 23.03.2022).
- [152] Lindblom, A. (2006). Inductive pulse generation (Doctoral dissertation, Acta Universitatis Upsaliensis).
- [153] Hanes, D., Salgueiro, G., Grossetete, P., Barton, R., & Henry, J. (2017). *IoT fundamentals: Networking technologies, protocols, and use cases for the internet of things*. Cisco Press.
- [154] Montagny, S. (2021). *LoRa – LoRaWAN and Internet of Things*. Université Savoie Mont Blanc. Available on: <https://www.univ-smb.fr/lorawan/en/free-book/>. (Accessed on 23.03.2022).
- [155] Semtech, A. (2019). Understanding the LoRa Adaptive Data Rate. Available on: <https://lora-developers.semtech.com/documentation/tech-papers-and-guides/understanding-adr/>. (Accessed on 23.03.2022).
- [156] Sanders, C. (2017). *Practical Packet Analysis, 3E: Using Wireshark to Solve Real-World Network Problems*. No Starch Press.
- [157] Loshin, P. (2003). *TCP/IP clearly explained*. Elsevier.
- [158] Fielding, R., Gettys, J., Mogul, J., Frystyk, H., Masinter, L., Leach, P., & Berners-Lee, T. (1999). RFC2616: Hypertext Transfer Protocol--HTTP/1.1.
- [159] Gast, M. (2005). *802.11 wireless networks: the definitive guide*. " O'Reilly Media, Inc."
- [160] Low-Power Long range LoRa Technology Transceiver Module. Microchip. Datasheet available on: <http://ww1.microchip.com/downloads/en/DeviceDoc/RN2483-Low-Power-Long-Range-LoRa-Technology-Transceiver-Module-Data-Sheet-DS50002346D.pdf>. (Accessed on 24.03.2022).

- [161] ESP-WROOM-S2 WiFi/WLAN module. Espressif. Datasheet available on: <https://www.espressif.com/en/producttype/esp-wroom-s2>. (Accessed on 24.03.2022).
- [162] BLEMOD BLE Solem Module Teardown. Solem. A view of the module is available on: <https://fccid.io/YWW-BLEMOD/Internal-Photos/Internal-Photos-3795789>. (Accessed on 224.03.2022).
- [163] Malmodin, J., Lundén, D., Moberg, Å., Andersson, G., & Nilsson, M. (2014). Life cycle assessment of ICT: Carbon footprint and operational electricity use from the operator, national, and subscriber perspective in Sweden. *Journal of Industrial Ecology*, 18(6), 829-845.
- [164] Krug, L., Shackleton, M., & Saffre, F. (2014, June). Understanding the environmental costs of fixed line networking. In *Proceedings of the 5th international conference on Future energy systems* (pp. 87-95).
- [165] Andrae, A. S., & Edler, T. (2015). On global electricity usage of communication technology: trends to 2030. *Challenges*, 6(1), 117-157.
- [166] Perrucci, G. P., Fitzek, F. H., & Widmer, J. (2011, May). Survey on energy consumption entities on the smartphone platform. In *2011 IEEE 73rd vehicular technology conference (VTC Spring)* (pp. 1-6). IEEE.
- [167] Pieter Robyns, Peter Quax, Wim Lamotte, William Thenaers. (2017). gr-lora: An efficient LoRa decoder for GNU Radio. Zenodo. 10.5281/zenodo.853201. Github repository an more details available on: <https://github.com/rpp0/gr-lora>. (Accessed on 24.03.2022).
- [168] Nooelec NESDR SMARTEE XTR Bundle - Premium RTL-SDR w/ Extended Tuning Range, Aluminum Enclosure, Bias Tee, 0.5PPM TCXO, SMA Input & 3 Antennas. More details in: <https://www.nooelec.com/store/sdr/sdr-receivers/nesdr/nesdr-smartee-xtr.html>. (Accessed on 24.03.2022).
- [169] Randerat, J. ., & Settington, R. E. (1974). *Piezoelectric ceramics*. London: Mullard.
- [170] Rail-to-rail 0.9 V nanopower comparator. STMicroelectronics. Datasheet available on: <https://www.st.com/resource/en/datasheet/ts881.pdf>. (Accessed on 25.03.2022).
- [171] Access line ultra-low-power 32-bit MCU Arm®-based Cortex®-M0+, up to 64 KB Flash, 8 KB SRAM, 2 KB EEPROM, ADC. STMicroelectronics. Datasheet available on: <https://www.st.com/resource/en/datasheet/stm32l051t6.pdf>. (Accessed on 25.03.2022).
- [172] Dynamic NFC/RFID tag IC with 4-Kbit, 16-Kbit or 64-Kbit EEPROM, and fast transfer mode capability. STMicroelectronics. Datasheet available on: <https://www.st.com/resource/en/datasheet/st25dv04k.pdf>. (Accessed on 25.03.2022).
- [173] Standard IPC-7351B: Generic Requirements for Surface Mount Design and Land Pattern Standard. Institute of Printed Circuit. 2010.
- [174] Hischer, R., Classen, M., Lehmann, M., & Scharnhorst, W. (2007). Life cycle inventories of electric and electronic equipment: production, use and disposal. Part I: Electronic components. Final report ecoinvent Data v2. 0, 18.
- [175] Voltage detector with sense input and external delay capacitor STM 1831. STMicroelectronics. Datasheet available on: <https://www.st.com/en/reset-and-supervisor-ics/stm1831.html>. (Accessed on 25.03.2022).
- [176] Chen, A., & Lo, R. H. Y. (2012). *Semiconductor packaging: materials interaction and reliability* (p. 216). Taylor & Francis.
- [177] Greig, W. (2007). *Integrated circuit packaging, assembly and interconnections*. Springer Science & Business Media.
- [178] <https://www.bluetooth.com/specifications/specs/>. (Accessed on 26.03.2022).
- [179] Tarkoma, S., Siekkinen, M., Lagerspetz, E., & Xiao, Y. (2014). *Smartphone energy consumption: modeling and optimization*. Cambridge University Press.
- [180] STMicroelectronics (2017). FMD of the SC70-5 typed voltage comparator. Available on: <https://www.st.com/en/amplifiers-and-comparators/ts881.html#quality-reliability>. (Accessed on 11.07.2022).
- [181] STMicroelectronics (2015). FMD of the SOT23-5 typed voltage comparator. Available on: <https://www.st.com/en/amplifiers-and-comparators/ts881.html#quality-reliability>. (Accessed on 11.07.2022).
- [182] STMicroelectronics (2018). FMD of the LQFP32-typed microcontroller STM32L051K6T6. Available on: <https://www.st.com/en/microcontrollers-microprocessors/stm32l051k6.html#quality-reliability>. (Accessed on 11.07.2022).

- [183] STMicroelectronics (2018). FMD of the TFBGA64-typed microcontroller STM32L051R6H6. Available on: <https://www.st.com/en/microcontrollers-microprocessors/stm32l051r6.html#quality-reliability>. (Accessed on 11.07.2022).
- [184] STMicroelectronics (2020). FMD of the UFQFPN32-typed microcontroller STM32L051K6U6. Available on: <https://www.st.com/en/microcontrollers-microprocessors/stm32l051k6.html#quality-reliability>. (Accessed on 11.07.2022).
- [185] STMicroelectronics (2018). FMD of the WLCSP36-typed microcontroller STM32L051T6Y6TR. Available on: <https://www.st.com/en/microcontrollers-microprocessors/stm32l051t6.html#quality-reliability>. (Accessed on 11.07.2022).
- [186] STMicroelectronics (2017). FMD of the TSSOP8-typed NFC-EEPROM memory ST25DV04K-IER6T3. Available on: <https://www.st.com/en/nfc/st25dv04k.html#quality-reliability>. (Accessed on 11.07.2022).
- [187] STMicroelectronics (2017). FMD of the UDFPN8-typed NFC-EEPROM memory ST25DV04K-IER6C3. Available on: <https://www.st.com/en/nfc/st25dv04k.html#quality-reliability>. (Accessed on 11.07.2022).
- [188] STMicroelectronics (2017). FMD of the SO8-typed NFC-EEPROM memory ST25DV04K-IER6S3. Available on: <https://www.st.com/en/nfc/st25dv04k.html#quality-reliability>. (Accessed on 11.07.2022).
- [189] STMicroelectronics (2013). FMD of the SOT23-5 typed voltage detector STM1831L24WY6F. Available on: <https://www.st.com/en/reset-and-supervisor-ics/stm1831.html#quality-reliability>. (Accessed on 11.07.2022).
- [190] STMicroelectronics (2020). FMD of the Bluetooth® Low Energy wireless system-on-chip BlueNRG-2 BLUENRG-M2SA. Available on: <https://www.st.com/en/wireless-connectivity/bluenrg-m2.html#quality-reliability>. (Accessed on 11.07.2022).
- [191] STMicroelectronics (2020). FMD of the SoC BlueNRG-2 BLUENRG-232. Available on: <https://www.st.com/en/wireless-connectivity/bluenrg-2.html#quality-reliability>. (Accessed on 11.07.2022).
- [192] STMicroelectronics (2021). Datasheet of the Bluetooth® Low Energy wireless system-on-chip BlueNRG-2. Available on: <https://www.st.com/en/wireless-connectivity/bluenrg-m2.html>. (Accessed on 11.07.2022).
- [193] World Economic Forum. January 2018. Internet of things Guidelines for sustainability. Description of the project available on: <https://widgets.weforum.org/iot4d/index.html>. (Accessed on 04.04.2022).
- [194] CISCO. 2020. CISCO Annual Internet Report (2018-2023). White Paper available on: <https://www.cisco.com/c/en/us/solutions/collateral/executive-perspectives/annual-internet-report/white-paper-c11-741490.html>. (Accessed on 04.04.2022).
- [195] C.P. Baldé, M. Wagner, G. Iattoni, R. Kuehr, In-depth Review of the WEEE Collection Rates and Targets in the EU-28, Norway, Switzerland, and Iceland, 2020, United Nations University (UNU) / United Nations Institute for Training and Research (UNITAR) – co-hosting the SCYCLE Programme, Bonn, Germany.
- [196] ADEME, Erwann FANGEAT. In Extenso Innovation Croissance, Alice DEPROUW, Marion JOVER, Mathilde BORIE, Océane TONSART. 2020. Rapport annuel du registre des déchets d'équipements électriques et électroniques. 102 pages.
- [197] Serpanos, D., & Wolf, M. (2017). Internet-of-things (IoT) systems: architectures, algorithms, methodologies. Springer.
- [198] McGrath, M. J., & Scanail, C. N. (2013). Sensor technologies: healthcare, wellness, and environmental applications (p. 336). Springer Nature.
- [199] International Platinum Group Metals Association. The Primary Production Of Platinum Group Metals. Available on https://ipa-news.com/assets/sustainability/Primary%20Production%20Fact%20Sheet_LR.pdf
- [200] International Platinum Group Metals Association. The Environmental Profile Of Platinum Group Metals. Available on <https://www.technology.matthey.com/article/61/2/111-121/>. (Accessed on 11.07.2022).
- [201] Palomino, A., Marty, J., Auffret, S., Joumard, I., Sousa, R. C., Prejbeanu, I. L., ... & Diény, B. (2021). Evaluating critical metals contained in spintronic memory with a particular focus on Pt substitution for improved sustainability. Sustainable Materials and Technologies, 28, e00270.
- [202] Ku, A. Y. (2018). Anticipating critical materials implications from the Internet of Things (IOT): Potential stress on future supply chains from emerging data storage technologies. Sustainable Materials and Technologies, 15, 27-32.

- [203] Lee, J. H., Chung, S. H., & Kim, W. S. (2019). Fog server deployment technique: An approach based on computing resource usage. *International Journal of Distributed Sensor Networks*, 15(1), 1550147718823994.
- [204] Mell, P., & Grance, T. (2011). The NIST definition of cloud computing.
- [205] European Commission, Study on the EU's list of Critical Raw Materials – Final Report (2020).
- [206] Ashton, K. (2009). That 'internet of things' thing. *RFID journal*, 22(7), 97-114.
- [207] Weiser, M. (1993). Hot topics-ubiquitous computing. *Computer*, 26(10), 71-72.
- [208] Weiser, M. (1999). The computer for the 21st century. *ACM SIGMOBILE mobile computing and communications review*, 3(3), 3-11.
- [209] Fink, Johannes Karl, "Mechanical Sensors," in *Polymeric Sensors and Actuators*, Hoboken, Massachusetts, Wiley-Scrivener, 2012, pp. 131–138.
- [210] Tanenbaum, A. S. (2002). *Computer networks*. Pearson Education India.
- [211] Akyildiz, I. F., Su, W., Sankarasubramaniam, Y., & Cayirci, E. (2002). Wireless sensor networks: a survey. *Computer networks*, 38(4), 393-422.
- [212] Adelstein, F., Gupta, S. K., Richard, G., & Schwiebert, L. (2005). *Fundamentals of mobile and pervasive computing (Vol. 1)*. New York: McGraw-Hill.
- [213] Shetty, D., & Kolk, R. A. (2010). *Mechatronics system design*. Cengage Learning.
- [214] Ghent, B.A. U.S. Patent 7,110,832. Washington, DC: U.S. Patent and Trademark Office (2006)
- [215] Ebling, M. R. (2016). Pervasive computing and the internet of things. *IEEE Pervasive Computing*, 15(1), 2-4.
- [216] Kiritsis, D. (2011), "Closed-loop PLM for intelligent products in the era of the Internet of things", *Computer Aided Design*, Vol. 43 No. 5, pp. 479–501.
- [217] Recommendation ITU-T Y.4113. Requirements of the network for the Internet of things.
- [218] Recommendation ITU-T Q.1742.11 (2014), IMT 2000 references (approved as of 31st December 2012) to ANSI-41-evolved core network with cdma2000 access network.
- [219] Passive component, what does passive component mean? Technopedia. Available on: <https://www.techopedia.com/definition/735/passive-component>. (Accessed on 18.04.2022).
- [220] Active component, what does active component mean? Technopedia. Available on: <https://www.techopedia.com/definition/726/active-component>. (Accessed 18.04.2022).
- [221] Graedel, T. E, Buckert, M., Reck, B. K., 2011. Assessing mineral resources in society. Metal stocks and recycling rates. UNEP, Paris. ISBN 978-92-807-3182-0
- [222] D. Reinsel, J. Gantz, J. Rydning, *Data Age 2025: The Evolution of Data to Lifecritical*. IDC White Paper, Seagate, <http://www.seagate.com/files/www-content/our-story/trends/files/Seagate-WP-DataAge2025-March-2017.pdf>, (2017).
- [223] The EINS Consortium. Overview Of ICT Energy consumption (D8.1). Report FP7--- 2888021. European Network Of Excellence In Internet Science. February 2013.
- [224] Van Heddeghem, W., Lambert, S., Lanoo, B., Colle, D., Pickavet, M., And Demeester, P. Trends In worldwide ICT Electricity consumption from 2007 To 2012. *Computer Communications* 50 (2014), 64---76.
- [225] Gelenbe, E., & Caseau, Y. (2015). The impact of information technology on energy consumption and carbon emissions. *ubiquity*, 2015(June), 1-15.
- [226] Masanet E, Shehabi A, Lei N, Smith S, Koomey J. Recalibrating global data center energy-use estimates. *Science* (80-) 2020;367:984–6. <https://doi.org/10.1126/science.aba3758>.
- [227] Koot, M., & Wijnhoven, F. (2021). Usage impact on data center electricity needs: A system dynamic forecasting model. *Applied Energy*, 291, 116798.
- [228] Andrae A, Edler T. On Global Electricity Usage of Communication Technology: Trends to 2030. *Challenges* 2015;6:117–57. <https://doi.org/10.3390/challe6010117>.

- [229] Andrae A. Comparison of several simplistic high-level approaches for estimating the global energy and electricity use of ICT networks and data centers. *Int J Green Technol* 2019;5:50–63.
- [230] Andrae A. Hypotheses for primary energy use, electricity use and CO2 emissions of global computing and its share of the total between 2020 and 2030. *WSEAS Trans Power Syst* 2020;15:50–9.
- [231] Andrae A. New perspectives on internet electricity use in 2030. *Eng Appl Sci Lett* 2020;3:19–31.
- [232] Stojčev, M. K., Kosanović, M. R., & Golubović, L. R. (2009, October). Power management and energy harvesting techniques for wireless sensor nodes. In 2009 9th International Conference on Telecommunication in Modern Satellite, Cable, and Broadcasting Services (pp. 65-72). IEEE.
- [233] LST Colbert de Tourcoing. Méthode d'analyse et cahier de charges fonctionel (CdCF).
- [234] European Commission, Joint Research Centre, & Institute for Environment and Sustainability. (2011). International reference life cycle data system (ILCD) handbook general guide for life cycle assessment: Provisions and action steps. Publications Office.
- [235] Oers, L. van, 2015. CML-IA database, characterisation and normalisation factors for midpoint impact category indicators. LCIA method available on: https://www.universiteitleiden.nl/en/science/environmental-sciences/tools-and-data#CML_IA. (Accessed on 05.05.2022).
- [236] Manz, O., Meyer, S., & Baumgartner, C. (2021, November). Life cycle assessment of an Internet of Things product: Environmental impact of an intelligent smoke detector. In 11th International Conference on the Internet of Things (pp. 72-79).
- [237] The Shift Project. 2018. 1byte Model available on <https://theshiftproject.org/wp-content/uploads/2018/10/Lean-ICTMaterials-1byte-Model-2018.xlsx>. (Accessed on 23.01.2021).
- [238] Boyd, S.B., 2012. Life-Cycle Assessment of Semiconductors. Springer, New York, NY doi: 10.1007/978-1-4419-9988-7.
- [239] B. K. Sovacool, “Valuing the greenhouse gas emissions from “nuclear power: A critical survey,” *Energy Policy*, vol. 36, no. 8, pp. 2950–2963, Aug. 2008.
- [240] Gangoellis, M., Casals, M., Forcada, N., Macarulla, M., & Giretti, A. (2015). Environmental impacts related to the commissioning and usage phase of an intelligent energy management system. *Applied energy*, 138, 216-223.
- [241] Maxwell, J. A. (2012). *Qualitative research design: An interactive approach*. Sage publications.
- [242] Asghari, P., Rahmani, A. M., & Javadi, H. H. S. (2019). Internet of Things applications: A systematic review. *Computer Networks*, 148, 241-261.
- [243] Jimenez, F., & Torres, R. (2015, November). Building an IoT-aware healthcare monitoring system. In 2015 34th International Conference of the Chilean Computer Science Society (SCCC) (pp. 1-4). IEEE.
- [244] Ding, Y., Gang, S., & Hong, J. (2015, November). The design of home monitoring system by remote mobile medical. In 2015 7th International Conference on Information Technology in Medicine and Education (ITME) (pp. 278-281). IEEE.
- [245] Li, H., Wang, H., Yin, W., Li, Y., Qian, Y., & Hu, F. (2015). Development of a remote monitoring system for henhouse environment based on IoT technology. *Future Internet*, 7(3), 329-341.
- [246] Andrae, A. S., & Vaija, M. S. (2014). To which degree does sector specific standardization make life cycle assessments comparable?—the case of global warming potential of smartphones. *Challenges*, 5(2), 409-429.
- [247] Andrae, A. S. (2015). Life-Cycle Assessment of Consumer Electronics: A review of methodological approaches. *IEEE consumer electronics magazine*, 5(1), 51-60.
- [248] Macronix International Co., LTD. (2014). *Wear Leveling in NAND Flash Memory*. Technical note.
- [249] Coroama, V. C., Schien, D., Preist, C., & Hilty, L. M. (2015). The energy intensity of the Internet: home and access networks. In *ICT Innovations for Sustainability* (pp. 137-155). Springer, Cham.